The Australian Craniofacial Unit

1975 – 1996

Being a submission
of selected published work
in fulfilment of the requirements for
the degree of Doctor of Medicine at the
University of Adelaide, South Australia.

Volume 2 of 2

David John David, AC
M.B.,B.S.(Adel), F.R.C.S.(Edin), F.R.C.S., F.R.A.C.S.
Department of Surgery
The University of Adelaide
January 1997

Chapter 4
Rare Craniofacial Clefts

Naturam expellas furca, tamen usque recurret.
(You may drive out nature with a pitchfork,
yet she'll be constantly running back.)

Horace

Rare Craniofacial Clefts

The craniofacial clefts comprise some of the rarest and most complex deformities of the craniofacial region. The ACFU manages a large series of cases which have been studied both clinically and with advanced radiology. Treatment protocols have been developed for the three sub groups:

(a) "Tessier" Clefts;

(b) Craniofacial Microsomia;

(c) Treacher Collins Syndrome.

The first two papers in this chapter A De-epithelialized Free Groin Flap for Facial Contour Restoration, 1978[1] and Microvascular Surgery in Maxillofacial Reconstruction, 1979[2] describe the value of the microsurgeon in the craniofacial team. At that time it was not well accepted that the two new developments in reconstructive surgery could or should be effectively combined. The association is now common place.

Some of the advances in three-dimensional computerised reconstruction were from the ACFU. Three-Dimensional Computerized Reconstruction of Craniofacial Clefts, 1985[3] provides an early description of the range of clefts using the new radiological tool.

Hairline Indicators of Craniofacial Clefts, 1988[4] presents some observations of developmental significance made only because of the large series of cases available for study.

The description of the Tessier Number 9 cleft, 1989[5] hitherto postulated but unreported also reflects the value of access to this large volume of case material.

The article Tessier Clefts Revisited with a Third Dimension, 1989[6] reported the completed series of facial clefts as postulated by Tessier with computed tomographic data and three dimensional

■

reconstruction of each variety. This analysis supports some but contradicts other hypotheses and speculations proffered by Tessier.

Rare Craniofacial Clefts: Principles and Management, 1991[7] and Soft Tissue Expansion in the Management of the Rare Craniofacial Clefts, 1992[8] describe the emphasis on management through the whole growth period, on the role of the soft tissues in facial clefts and on the use of soft tissue expansion — one of the modern tools of treatment.

Hemifacial Microsomia: a Multisystem Classification, 1987[9] presents an alpha-numeric classification of craniofacial microsomia which can be used to indicate and monitor treatment in this four dimensional problem.

Composite Free Flap Reconstruction for Severe Hemifacial Microsomia, 1985[10] demonstrates the role of microsurgery in end of growth reconstruction of these cases, building on the ideas of organisation and technical operation laid down a decade before.

Treacher Collins Syndrome, 1985[11] is a general description of the disease and sets out a treatment protocol based on the concept that it is a cleft condition requiring multidisciplinary management throughout growth.

The author's contribution to the Association of Treacher-Collins Syndrome and Translocation 6p21.31/16p13.11: Exclusion of the Locus from these Candidate Regions, 1991[12] is small but illustrates the value of a centralised multidisciplinary unit. A significant number of families with Treacher Collins Syndrome was managed by tailoring the investigations to include those able to be used in the gene mapping process.

Mandibular Lengthening by Distraction for Airway Obstruction in Treacher-Collins Syndrome, 1994[13] deals with a possible solution

to the potentially lethal problem of airway obstruction in the infant with a severe manifestation of this disease.

Intraorbital Tissue Expansion in the Management of Congenital Anophthalmos, 1996[14] shows how intraorbital tissue expansion can mould the bone during growth thus enhancing "growth-like" stimuli to obviate more major surgery.

Papers

1. David DJ, Tan E 1978 A De-Epithelialized Free Groin Flap for Facial Contour Restoration. Jnl Maxillofacial Surg 6(4):249–252

2. David DJ, Tan E 1979 Microvascular Surgery in Maxillofacial Reconstruction. Annals Academy of Med. 8(4):481–485

3. David DJ, Hemmy DC, Tessier P 1985 Three-Dimensional Computerized Reconstruction of Craniofacial Clefts. Proceedings of the First International Congress of The International Society of Cranio-Maxillo-Facial Surgery188–189

4. Moore MH, David DJ, Cooter RD 1988 Hairline Indicators of Craniofacial Clefts. Plast Reconstr Surg 82(4):589–593

5. David DJ, Moore MH, Cooter R, Chow SK 1989 The Tessier Number 9 Cleft. Plast Reconstr Surg, March 1989

6. David DJ, Moore MH Cooter RD 1989 Tessier Clefts Revisited with a Third Dimension. Cleft Palate Jnl 26(3):163–185

7. David DJ 1991 Rare Craniofacial Clefts: Principles of Management. Proceedings of 4th Int. Congress of The Int. Soc. of Cranio-Maxillo-Facial Surg 119–122

8. Moore MH, Trott JA, David DJ 1992 Soft Tissue Expansion in the Management of the Rare Craniofacial Clefts. Br J Plast Surg 45:155–159

9. David DJ, Mahatumarat C, Cooter RD 1987 Hemifacial Microsomia: A Multisystem Classification. Plast Reconstr Surg 80(4):525–533

10. David DJ, Tan E, Cooter RD 1985 Composite Free Flap Reconstruction for Severe Hemifacial Microsomia. Proceedings 1st Int Congr of the Int Soc of Cranio-Maxillo-Facial Surg 453–457

11. David DJ 1985 Treacher Collins Syndrome. In: Current Operative Surgery: Plast Reconstr Surg 103–118

12. Dixon M, Haan E, Baker E, David DJ, McKenzie N, Williamson R, Mulley J, Farrall M, Callan D 1991 Association of Treacher-Collins Syndrome and Translocation 6p21.31/ 16p13.11: exclusion of the locus from these candidate regions. Amer J of Human Genetics 48:274–280

13. Moore MH, Guzman-Stein G, Proudman TW, Abbott AH, Netherway DJ, David DJ 1994 Mandibular Lengthening by Distraction for Airway Obstruction in Treacher-Collins Syndrome. Jnl Craniofacial Surg 5(1):22–25

14. Dunaway DJ & David DJ 1996 Intraorbital Tissue Expansion in the Management of Congenital Anophthalmos. British Journal of Plastic Surgery 49, 529–535.

■

A De-Epithelialized Free Groin Flap for Facial Contour Restoration

David John David, Eugene Tan

The South Australian Cranio–Facial Surgical Unit (Head of Unit: D. J. David), and Plastic and Reconstructive Surgical Unit (Head: D. N. Robinson), Royal Adelaide Hospital, Australia

Summary

The transfer of de–epithelialized free groin flaps to restore facial contour after tumour resection and in hemifacial microsomia is described. The flap can be transferred in one stage and remodelled at a later minor operation. This provides an acceptable alternative to the other more difficult and often less successful methods of restoring soft tissue deficiencies of the face.

Key-Words: De–epithelialized free groin flap; Parotid tumour; Hemifacial microsomia.

Introduction

In contrast with the significant advances in techniques for correcting bony abnormalities associated with congenital and acquired facial deformities, reconstruction of soft tissue defects still presents major difficulties. Free dermo-fat grafts are unreliable; pedicle flaps are time consuming and produce unacceptable secondary defects; and subcutaneous silicone injections are not satisfactory for large deformities. *McGregor and Jackson* (1972) described the groin flap and with the development of free tissue transfer by microvascular anastomosis *(Taylor and Daniel* 1973) such axial pattern flaps became the obvious donor tissue. Soft tissue augmentation resulting from such conditions as cancer resection, progressive facial hemiatrophy (Romberg's disease) and hemifacial microsomia using microsurgical techniques became a reality. *Fujino et al.* (1975) described the microvascular transfer of a free deltopectoral dermal–fat flap for facial reconstruction. *Harashina et al.* (1977) used a free groin flap for reconstruction in a case of progressive facial hemiatrophy. This was followed by a similar case report from *Wells and Egerton* (1977). This communication describes the use of a free groin flap transfer to correct the contour defect resulting from, 1: a total conservative parotidectomy with excision of the ramus of the mandible for acinic cell carcinoma and, 2: left hemifacial microsomia.

FIG. 1. *Right facial contour defect resulting from total conservative parotidectomy and partial mandibulectomy*

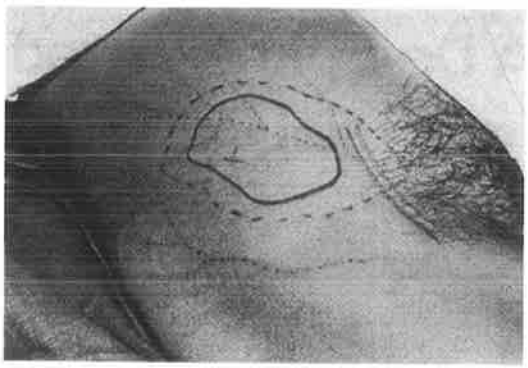

FIG. 2. *Right groin flap marked out on the skin.*

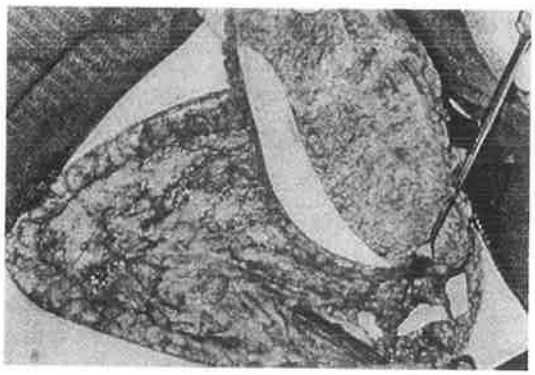

FIG. 3. *The partially de-epithelialized flap with skin gusset still attached to the superficial circumflex iliac artery.*

Case Report

1. A 54-year-old woman presented two years earlier with an acinic cell carcinoma in the deep lobe of the right parotid gland invading the ramus of the mandible. A total conservative parotidectomy with excision of the underlying bone was performed resulting in a severe contour deformity (Fig. 1). Having decided to use a free groin flap a mould of the shape and bulk of the deformity was prepared in acrylic and used to mark out the proposed flap on the right groin. The groin flap was based on the superficial circumflex iliac artery (Figs. 2 + 3). A skin flap was raised over the defect on the right side of the face, the incision extending from the zygomatic arch downwards, in front of the ear and into neck (Fig. 4). Using the methods described by *Harashina et al,* (1977) the upper part of the groin flap was de–epithelialized and a skin gusset left to be sutured into the skin of the submandibular wound. The superficial circumflex iliac artery was anastomosed to the right facial artery by a microsurgical technique. For the first three weeks the flap was very bulky (Fig. 5) but by the fifth week the swelling had partially subsided so the gusset was removed and the dermo–fat remodelled to give an acceptable facial contour (Fig. 6).

2. A 13–year–old boy with left hemifacial microsomia had both bony and soft tissue deficiencies, the latter being due to absence of the masseter and part of the temporalis muscles (Fig. 7). As described above, a de–epithelialized flap was removed from the left groin. The flap was inserted through a face–lift incision, which extended from the temple through the pre-auricular region to the neck. The superficial circumflex iliac artery was initially anastomosed to the facial artery, however the anastomosis thrombosed after 15 minutes. It was therefore resected and the vessels rejoined re–establishing the circulation, however within 5 minutes thrombosis recurred.

Careful examination under the microscope did not reveal any obvious intra or extra–luminal cause. Finally, a 7 cm cephalic vein graft was used to join the left superficial temporal artery to the abbreviated stump of the donor vessel, giving a satisfactory circulation (Fig. 8). At six weeks the gusset of skin was removed and the flap remodelled. The final result has been satisfactory (Fig. 9).

Discussion

The free flap is now an established weapon in the armamentarium of the reconstructive surgeon. Free dermo–fat flaps have been used where contour defects result from cancer resection, hemifacial microsomia and Romberg's disease. By this technique the major part of the operation can be performed in one stage. The tissue remains alive and can be sculptured or repositioned at a second minor operation. The donor site can be closed directly and in the two cases described, this was accomplished with an easily concealed linear groin scar. The skin gusset set into the facial incision not only allows easy closure of the wound with minimum tension, but provides an excellent, 'window' for monitoring flap survival. Without this, the flap in Case 2 would have been left to perish. We agree with *Harashina et al.* (1977) that the fat from the free flap should not be trimmed primarily as the flap vessels may lie very close to the flap margin.

FIG. 4.

FIG. 5.

FIG. 6.

FIG. 4. *The de–epithelialized flap being inserted under the facial incision.*
FIG. 5. *The bulky flap.*
FIG. 6. *The final result after resculpting the dermal fat and removing the skin gusset.*

FIG. 7.

FIG. 8.

FIG. 9.

FIG. 7. *Facial asymmetry in a boy with left hemifacial microsomia.*
FIG. 8. *The early post–operative result before removal of the skin gusset.*
FIG. 9. *The late post operative result after removal of the skin gusset and remodelling.*

Experience with these two cases has confirmed the usefulness of microsurgical techniques in reconstruction of the head and neck. Transferring tissue will only be consistently successful if the microsurgeon is fully capable of performing all the necessary micro–anastomotic techniques and dealing with all possible complications that may arise. The above cases demonstrated several particular points of technique. The skin gusset is vital for monitoring flap viability for the first few postoperative days. This can be done by observing the colour of the flap or by pricking the flap with a sterile needle to see if it bleeds.

Absence of circulation in the gusset is an indication for re–exploration of the anastomosis. The flap pedicle may not always lie comfortably adjacent to a suitable vessel in the neck in which case tension must be avoided at all cost and it may be necessary to insert a vein graft.

In the second case the facial artery anastomosis thrombosed twice for no apparent reason. This occurrence has raised the question about the suitability of this tortuous vessel which may have wide variations in perfusion pressure. The natural extension of this technique is the incorporation of viable bone from the iliac crest in a composite osseo-cutaneous free flap to further enlarge the scope of reconstruction in this difficult area. Since commencement of this paper, this has been achieved successfully in our hands and will be the subject of a further communication.

Conclusion

The free transfer of groin tissue to the face for contour restoration by micro–vascular anastomosis is a useful procedure. The addition of skin and tissue bulk to the depleted face dramatically broadens the options available to the reconstructive surgeon.

References

1 Fujino, T., R. Tanino, C. Sugimoto: Microvascular transfer of free delto-pectoral dermal–fat flap. Plast. Reconstr. Surg. 55 (1976) 428

2 Harashina, T., T. Nakajime, Y. Yoshimura: A free groin flap reconstruction for progressive facial hemiatrophy. Brit. J. Plast. Surg. 30 (1977) 14

3 McGregor, I. A., I. T. Jackson: The groin flap. Brit. J. Plast. Surg. 25 (1972) 3

4 Taylor, G. I., R. K. Daniel: The free flap; composite tissue transfer by vascular anastomoses. Australian and New Zealand J. Surg. 43 (1973) 1

5 Wells, J. H., M. T. Egerton: Correction of severe hemifacial atrophy with a free dermis–fat flap from the lower abdomen. Plast. Reconstr. Surg. 39 (1977) 223

D. J. David, M.B., F.R.C.S., F.R.C.S.E., F.R.A.C.S.,
326 South Terrace, Adelaide, South Australia, 5000

Microvascular Surgery in Maxillo–Facial Reconstruction

David John David,* MB, FRCSE, FRCS, FRACS
Eugene Tan,* MB, FRACS

Summary

The recent advances in microvascular surgery have been applied to maxillo-facial reconstruction in the area of the lower jaw and soft tissue of the face. Five cases are presented, demonstrating some of the techniques and results in patients suffering from congenital, post–traumatic and post-cancer resection deformities.

Keywords: Maxillo–facial Reconstruction; Microvascular Surgery

Introduction

The two major advances in plastic and reconstructive surgery in the last 20 years have been in the fields of microvascular surgery and cranio–facial surgery.

Paul Tessier[1] of Paris, first conceived of the concept of the craniofacial surgical team. By combining the techniques of plastic surgery and neurosurgery to expose the facial skeleton below and the cranial base above, the deformities of the orbito-cranial complex could be viewed directly and these bones could be sectioned and moved in three dimensions. Since its inception, the cranio–facial team has expanded to include other disciplines and the techniques of cranio–facial surgery have been applied to the wider field of maxillo-facial surgery; viz., congential, traumatic and post–tumour resection cases.

As the emphasis of microvascular surgery was transferred from reimplantation surgery to tissue transfer surgery, attention was focused on the various possible uses of free tissue transfer.[3,4,5] In 1975, Fugino et al[6] described a microvascular transfer of a free deltopectoral dermal-fat flap for facial reconstruction. Harashina et al[7] (1977) used a free groin flap for reconstruction in a case of progressive facial hemiatrophy. This was followed by a similar case report from Wells and Egerton,[8] (1977). Daniel[9] (1978) described mandibular reconstruction using free osteo–cutaneous groin flaps and free rib transfers in cases after tumour resection.

* South Australian Cranio–Facial Unit, Adelaide Children's Hospital, 72 King William Road, North Adelaide, SA 5006.
Address for Reprints D J David, 326 South Terrace, Adelaide, SA 5000.

Because modern society places such a high premium on facial appearance, it was inevitable that surgeons would look to combine these surgical advances to produce even better functional, psycho–social and aesthetic results for the benefit of affected individuals. This communication describes 5 cases in whom microvascular surgical techniques have been applied to maxillofacial reconstruction:

1. after a total conservative parotidectomy with excision of the ramus of the mandible for acinic cell carcinoma, using a de–epithelialised groin flap.

2. in a case of left hemifacial microsomia, using a de–epithelialised groin flap.

3. in a case of severe progressive hemifacial atrophy, using a de-epithelialised groin flap.

4. in a case of severe hemifacial microsomia, using a free osteo-cutaneous groin flap for mandibular reconstruction and soft tissue augmentation in association with mandibular osteotomy.

5. in a post-traumatic case, using a free osteocutaneous groin flap based on the deep circumflex vessels for reconstruction of the hemi–mandible, oral lining and facial skin.

Case Reports

Case I

A 54–year old woman presented two years earlier with an acinic cell carcinoma in the deep lobe of the right parotid gland invading the ramus of the mandible. A total conservative parotidectomy with excision of the underlying bone was performed resulting in a severe contour deformity. Having decided to use a free groin flap, a mould of the shape and bulk of the deformity was prepared in acrylic and used to mark out the flap on the right groin. The groin flap was based on the superficial circumflex iliac artery. A skin–flap was raised over the defect on the right side of the face and the excision extended from the zygomatic arch downwards, in front of the ear and into the neck. The upper part of the groin flap was de–epithelialised and a skin gusset was left to be sutured into the skin of the submandibular wound. The superficial circumflex iliac artery was anastomosed to the right facial artery by a microsurgical technique. For the first three weeks the flap was very bulky, but by the fifth week the swelling had partially subsided so the gusset was removed and the dermo–fat remodelled to give an acceptable facial contour.

FIG. 1. *A case of Romberg's disease, affecting left side of face.*

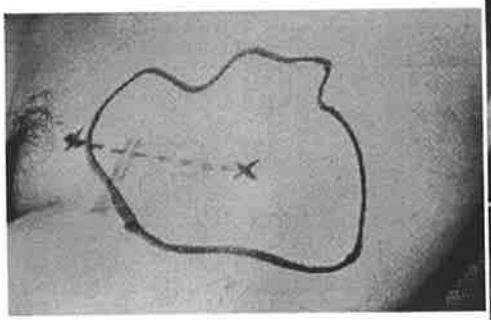

FIG. 2. *The pattern of the de–epithelialised groin flap is mapped out on the skin.*

FIG. 3. *The bed or recipient site into which the flap will be placed.*

Case II

A 13–year old boy with left hemifacial microsomia had both bony and soft tissue deficiencies, the latter being due to absence of the masseter and part of the temporalis muscles. As described above, a de–epithelialised flap was removed from the left groin. The flap was inserted through a face–lift incision, which extended from the temple through the pre-auricular region to the neck. The superficial circumflex iliac artery was initially anastomosed to the facial artery, however the anastomosis thrombosed after 15 minute.

It was therefore resected and the vessels rejoined, re–establishing the circulation. However, within 5 minutes thrombosis recurred. Careful examination under the microscope did not reveal any obvious intra or extraluminal cause. Finally, a 7 cm cephalic vein graft was used to join the left superficial temporal artery to the abbreviated stump of the donor vessel giving a satisfactory circulation. At six weeks the gusset of skin was removed and the flap remodelled. The final result has been satisfactory.

Case III

A 27–year old female medical graduate from Korea, presented with severe left hemifacial atrophy (Romberg's disease) which had been dormant for eight years. She had severe bony and soft tissue deformities which affected the left forehead, left maxilla and mandibular area (Fig. 1). At the first operation a groin flap was raised on the superficial circumflex iliac vessels, (Fig. 2). Using the techniques described in the previous cases a de-epithelialised flap was inserted under a large face–lift flap (Fig. 3) and the donor vessel was anastomosed to the facial artery on the left and the external jugular vein. Four weeks later the majority of the gusset was removed, the flap re–fashioned and the coup–de–sabre excised from her forehead. The postoperative result was acceptable (Fig. 4).

FIG. 4. *The early postoperative result.*

Case IV

A 17–year old girl with severe left hemifacial microsomia had absence of the left hemimandible, absence of the left malar arch and temperomandibular joint, absence of the left external ear, absent left masseter muscle and only a vestigial temporalis muscle (Fig. 5). At the first operation a zygomatic arch was fashioned out of rib and a new temperomandibular joint was fashioned out of costal cartilage. Three months later a sagittal split osteotomy to reposition the mandible was performed on the right. At the same time a large facelift incision, superficial to the facial nerve was performed and a dissection deep to the facial nerve established a tunnel between the mandibular stump and the newly fashioned temperomandibular joint. As osteocutaneous groin flap using the left iliac crest and the overlying dermo-fat placed on the superficial circumflex iliac vessels was used. The bone was introduced into the deep pocket below the facial nerve and the dermo–fat introduced under the facelift incision. Two months later the gusset was excised and the dermo-fat re–fashioned and some of the bone trimmed to give a very acceptable result, (Fig. 6).

FIG. 5. *A severe case of left hemifacial microsomia.*

FIG. 6. *The late result after transfer of a composite osteocutaeous groin flap and a mandibular osteotomy.*

Case V

A 43–year old man attempted suicide with a .303 rifle placed under his chin and succeeded only in disrupting the middle third of his face, and blowing apart his mandible, resulting eventually in a loss of left hemimandible, intra–oral lining and overlying skin. After initial debridgement and repair he was left with a small oral cavity, a remnant of left mandible, with a fused joint and absence of bone from the midline to the region of this remnant.

A year after the original trauma a reconstruction with a free osteocutaneous groin flap based on the deep circumflex vessels was performed to produce a combined mandibular, oral lining and facial skin reconstruction. Free tissue transfer is complete but the 'tidy-up' stages are yet lo be performed.

Discussion

Free tissue transfer of skin, dermo-fat and bone using microvascular surgical techniques to establish a blood supply to the transferred tissue, is now an established weapon in the armamentarium of the reconstructive surgeon. The routine use of these techniques for reconstruction after cancer surgery of the jaw and oral cavity should be questioned, as the patients are usually elderly alcoholic males with poor wound healing potential and there are very acceptable conventional reconstructive techniques available. So what type of patients do benefit from the application of microvascular techniques to facial deformities? We think that this type of reconstruction should only be carried out in post-traumatic or congenital deformity or after tumour resection in a young healthy person. A de-epithelialised free groin flap,[10] is the treatment of choice for severe soft tissue deformities of the face. This has the added advantage of being able to be combined with bone as a free osteocutaneous flap.

It may well be possible to incorporate in these flaps some of the attached abdominal musculature and its nerve supply, thus adding a functional component for facial reconstruction, especially in those cases of severe hemifacial microsomia where it is the altered functional matrix which so affects the result. To date it has not found a place in the more complex problems of orbito–cranial surgery, although the transfer of large segments of iliac bone based on the deep circumflex iliac system of vessels is a distinct possibility for the reconstruction of large defects in the calvarium, obviating the need for foreign material such as metal or acrylic. The future for this type of reconstructive surgery holds great promise and is full of possibilities.

Conclusion

Recent advances in microvascular surgery and craniofacial surgery have converged to focus on the problems of mandibular and soft tissue facial reconstruction where they have their most dramatic effect. It is to be hoped that these new techniques will be used with judgement and circumspection, not forgetting the well established modes of treatment so that with the careful selection of cases there will be a significant advance in the reconstruction and rehabilitation of the severely facially deformed.

References

1. Tessier P: The scope and Principles, dangers and limitations and the need for special training in orbitocranial surgery, Transactions of the V International Congress of Plast Reconst Surg, p 903, Butterworth, Melb, 1971.

2. Munro I R: Orbitocraniofacial surgery; the team approach. Plast Reconstr Surg, 55: 170–176, 1975.

3. Taylor G I and Daniel R K: The anatomy of several free flap donor sites. Plast Reconstr Surg, 56: 243, 1976.

4. Taylor G I, Miller G D H and Ham FJ: The free vascularised bone graft and the clinical extension of microvascular techniques. Plast Reconstr Surg, 55: 533, 1975.

5. Taylor G I and Watson W: The free osteocutaneous groin flap. Plast Reconstr Surg, 61: 494, 1978.

6. Fugino T. Tanino R and Sugimoto C: Microvascular transfer of a free deltopectoral dermo-fat flap. Plast Reconstr Surg, 55: 428, 1975.

7. Harashina T, Nakajima T and Yoshimura Y: A free groin flap reconstruction for progressive facial hemiatrophy. Brit J Plast Surg, 50: 14, 1977.

8. Wells J H and Egerton M T: Correction of severe hemifacial atrophy with a free dermo–fat flap from the lower abdomen. Plast Reconstr Surg, 59: 223, 1977.

9. Daniel R K: Mandibular Reconstruction with free tissue transfers. Annals of Plast Surg, 1: 546, 1978.

10. David DJ and Tan E: A de–epithelialized free groin flap for facial contour restoration of Maxillo–facial surgery, 6: 249, 1978.

Three-Dimensional Computerized Reconstruction of Craniofacial Clefts

David J. David (Adelaide), David C. Hemmy (Milwaukee), and Paul Tessier (Paris)

Introduction

Routine computed tomographic studies can be utilised as a substrate to provide an accurate three–dimensional representation of osseous abnormalities, which are faithfully reproduced. Using the programs 3D82 and 3D83 developed by the Section of Medical Imaging, Department of Radiology, University of Pennsylvania, we have been studying all craniofacial clefts presenting to the South Australian Craniofacial Unit since the beginning of 1982. As will be clearly seen, the beauty of this technique is the ability to inspect the bony anatomy completely from any angle, including inspection from within the cranial cavity.

History

In the 10 years since the inception of the South Australian Craniofacial Unit, we have assessed 45 craniofacial clefts and 31 frontonasal encephaloceles. The majority of these cases have had three-dimensional scanning performed, using the programs mentioned above. Studies of these scans have enabled more accurate diagnosis of the bony clefts to be performed. We have classified these clefts according to the Tessier system. We believe this classification is valuable as it sorts clefts into anatomical groups facilitating study. In turn, concepts of pathogenesis can be considered in the various anatomical groups. The breakdown of our experience using the Tessier classification has shown that we have seen most varieties of the classification, with the exception of T2 and T9 clefts. This is essentially similar to Tessier's own reported experience. When patients are studied within the various groups and other morphological anomalies in such patients are considered, clues to the pathogenesis become more obvious. For example, we have seen Tessier type 3 and type 5 clefts with evidence of amniotic band syndrome. Other clefts, e.g. Tessier types 6, 7 and 8, have been seen in light of the theory of failure of migration of neural crest mesenchyme. Another area highlighted by 3D imaging has been the concept of the frontonasal encephalocele as a "blowout" rather than a cleft. Evidence for this can be seen in the 3D scans showing significant lipping around exit foramina, multiplicity of exit foramina and depression of the ethmoid (without clefting) and elongation of the mid-face.

Two case examples are shown to illustrate the wealth of skeletal detail available from the 3D CT scan and the impact that this has on surgical management. The first case (Fig. 1) is a 5–year old girl. As can be seen from the photograph, there was a soft tissue Tessier type 7 cleft on the right side and a Tessier type 5 cleft on the left. However, examination of the 3D CT scans shows bilateral Tessier type 5 clefts, the most severe being on the left–hand side. Gross maxillary hypoplasia on the left–hand side can be seen, with profound depression of the left orbital floor. On each side, the infraorbital foramen is medial to the bony cleft. These findings were confirmed at operation, and there is no doubt that the three–dimensional visualisation of the facial skeleton pre–operatively facilitated both the soft tissue dissection of the clefts and bone grafting of the maxilla and orbital floor. The second case (Fig. 2) is an example of severe frontonasal dysplasia associated with a Tessier type 13 cleft and bilateral cleft of

lip and palate. There is gross mid-face hypoplasia, and on the 3D CT scan, clefting on nasal bones and crista galli can be visualised. At surgery, this anatomy was again confirmed and a wedge of dysplastic mid–line bone was removed, extending to an imaginary apex in the prolabial area. In this way the two halves of the face, including the orbits, were swung medially and stabilised together. Visualising the pathology on the 3D CT scan once again facilitated the performance of this surgery.

Many other cases might be presented to highlight the superb reproduction of the 3D82 and 3D83 program in these rare clefting syndromes. Certainly there are limitations to the technique: for example, the lack of a system of accurate measurement from these scans and the failure of scans to show craniofacial sutures, thin plates of bone and various bony foramina accurately. However, further technical improvements are already on the way. Nonetheless, the current state of this art, as shown in this presentation, allows the very vivid depiction of the craniofacial skeletal pathology of clefting syndromes and, coupled with the orderly Tessier classification system, is already allowing the surgeon to contribute to our understanding of the pathogenesis of this group of conditions.

FIG. 1. *Tessier type 5 bilateral clefting*

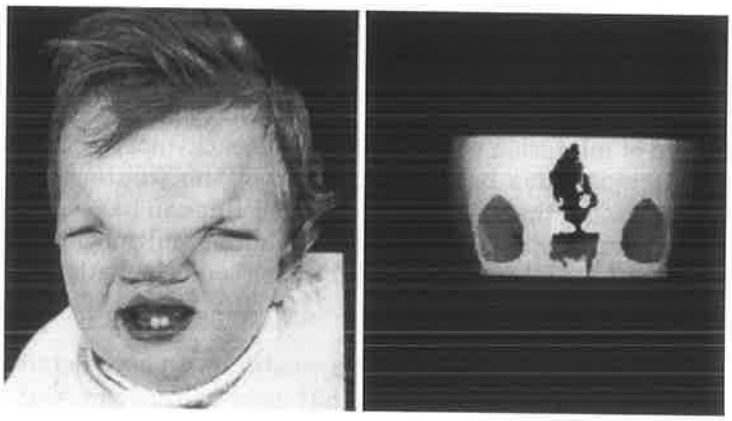

FIG.2. *Tessier type 13 mid–line cleft, with gross hypertelorism and repaired bilateral cleft lip*

Hairline Indicators of Craniofacial Clefts

Mark H. Moore, M.B., Ch.B., David J. David, F.R.C.S.(E), F.R.C.S., F.R.A.C.S., and Rodney D. Cooter, M.B., B.S.
North Adelaide, South Australia

The review of a complete series of Tessier craniofacial cleft patients presenting to the South Australian Craniofacial Unit has identified within the hairline a regular marker of clefting. Tongue-like projections of the temporal and frontal hairline pointing in the direction of their respective clefts have been identified for Tessier clefts numbered 7 to 14. No hairline indicator was revealed in "southbound" clefts numbered 0 to 6 without "northbound" extension. The hairline markers of laterally and superiorly bound clefts are a complementary element of the Tessier classification system.

The Tessier classification of rare craniofacial clefts evolved from the accurate and complete clinical, radiologic, and operative examination of 336 patients by a single surgeon.[1,2] Employing the orbit as the central focus, Tessier identified anatomic lines of soft tissue and bony disruption radiating "northbound" to the cranium and "southbound" to the face, thus enabling the clinician to categorise severe facial clefts numerically.

Whereas medially located clefts are characterised by more obvious soft-tissue disruption, laterally placed clefts have a predominance of skeletal disturbance. Beyond these general patterns of deformity, Tessier's description of the craniofacial clefts leaves some features, both superficial and deep, unrecorded.

From a review of a complete series of these clefts, a further regular marker of clefting has been identified within the hairline. We have focused on these hairline indicators of laterally and superiorly orientated clefts and consider them to be complementary extensions of the Tessier classification system.

Materials

Since 1975, 154 patients with rare craniofacial clefts have been clinically, radiologically, and surgically examined in the South Australian Craniofacial Unit. Examples of all 15 types of Tessier craniofacial clefts have been reviewed, with particular reference to those soft–tissue indicators that demarcate the axis of clefting.

Results

No disturbance in the frontal or temporal hairline was identified in any patient with a Tessier facial cleft numbered 0 to 6 without "northbound" extension. In each of the lateral and "northbound" clefts (numbers 7 to 14), examples were observed in which tongue-like projections of hair and hair-bearing scalp pointed across the temple or forehead toward the respective craniofacial cleft (Figs. 1 to 3). The length of the hairline projection varied from a minor irregularity in the frontal hairline to a long, narrow extension of the frontal hair-bearing scalp that was contiguous with the eyebrow (Fig. 2, *below, left).*

FIG. 1. *Bilateral Tessier number 7 clefts (nonsyndromal).*

As with other soft–tissue and bony markers of craniofacial clefts, the hairline indicator was not identified in every case of cleft numbers 7 to 14. In no case of frontoethmoidal meningoencephalocele, which Tessier includes within the craniofacial clefts, was a hairline indicator observed (Fig. 4).

FIG. 2. (Above, left) *Bilateral Tessier clefts numbered 6, 7, and 8 (Treacher Collins syndrome).* (Above, center) *Bilateral Tessier number 9 clefts. The hairline indicator is disrupted by postoperative scarring.* (Above, right) *Left Tessier number 10 cleft in a patient with bilateral craniofacial microsomia.* (Below, left) *Bilateral Tessier number 11 clefts and previously repaired midfacial clefts.* (Below, center) *Left Tessier cleft number 12 and left anophthalmia.* (Below, right) *Left Tessier number 13 cleft and paramedian clefts.*

Discussion

The Tessier classification of craniofacial clefts arose from the observation that there were consistent anatomic patterns of soft–tissue and bony disruption. Characteristically, medially placed clefts demonstrate more obvious soft–tissue disruption, while more laterally placed clefts are manifest by a predominance of skeletal disturbance.[1,2]

Extending clinical observation onto the forehead and drawing back the hair to observe the frontal and temporal hairline, an indicator of laterally and superiorly orientated clefts is revealed—the hairline indicator (Fig. 5).

Our review of a complete series of Tessier clefts has identified tongue-like projections of the hair–bearing scalp in clefts numbered 7 to 14. Although it is well recognised that patients with Treacher Collins syndrome who have bilateral Tessier number 6, 7, and 8 clefts have a projection of hair onto each cheek,[3] a patient in our series with bilateral number 6 clefts (Fig. 6) did not manifest such hairline disturbance, but it was present in another patient with bilateral number 7 clefts (Fig. 1).

FIG. 3. *Tessier number 14 cleft.*

FIG. 4. *Frontoethmoidal meningoencephalocele with no disturbance of the frontal hairline.*

The widow's peak, a V–shaped midline projection of frontal scalp hair, may be identified in a mild form in 3 percent and more distinctively in 0.1 percent of normal males.[4] While accepting that the midline widow's peak is seen in a small percentage of the normal population, these tongue-like projections of the frontal and temporal hairline are very real indicators of the "north" and laterally bound craniofacial clefts.

Indeed, a more pronounced widow's peak has been reported in 44 percent of patients with frontonasal dysplasia, which Tessier includes in the clefts numbered 0 to 14.[5] In an attempt to explain the etiology of the central hairline projections observed in patients with frontonasal dysplasia, Smith and Cohen postulated that the developing eye actually suppressed the local growth of hair.[4] Their hypothesis was formulated from the observation of a patient with alopecia surrounding an accessory optic remnant in the temporal region. Thus, in the orbital hypertelorism associated with frontonasal dysplasia, it was suggested

that a lower implantation of hair would occur in the midline with a resultant widow's peak V–shaped hairline. However, the demonstration of these hairline prolongation's not only in those clefts associated with orbital hypertelorism, but also where the orbit and eye are normally located, suggests that this embryologic hypothesis is untenable. Further evidence to support our rejection of this hypothesis is a patient with clefting and an ectopic optic remnant in the parietal region with obvious hair growth in close proximity (Fig. 7).

The failure to observe hairline indicators in any case of frontoethmoidal meningoencephalocele (Fig. 4) casts further doubts on inclusion of such disorders among the craniofacial clefts.[6]

In contrast to frontoethmoidal meningoencephaloceles, which herniate between the frontal and ethmoid bones at the site of the foramen caecum, those encephaloceles that are secondary to frontal bone clefting are associated with a hairline marker and are rightfully included in the craniofacial clefts (Figs. 1 to 3).

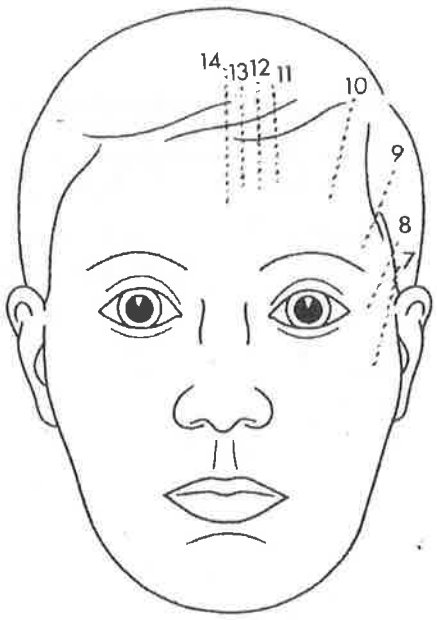

FIG. 5. *The hairline indicators are superior and lateral extensions of the Tessier craniofacial cleft classification.*

FIG. 6. *Bilateral Tessier number 6 clefts (nonsyndromal). No hairline disturbance is manifest.*

FIG. 7. *Ectopic optic remnant in parietal region with hair growth in close proximity.*

FIG. 8. *Bilateral facial microsomia. Note hairline indicator for associated Tessier number 11 cleft pointing toward eyebrow irregularity and coloboma of medial third of the upper eyelid.*

The identification of hairline markers of craniofacial clefts fulfills the views expressed by Tessier in his original description emphasising the importance of complete clinical observation and a complete examination of the whole face and cranium.[1] Indeed, clefts not previously suspected may be revealed by these hairline irregularities. One patient referred to the South Australian Craniofacial Unit with bilateral craniofacial microsomia and Goldenhar's syndrome also was shown to have a Tessier number 11 cleft after it was seen that his hairline indicator pointed in the direction of an eyebrow irregularity and a coloboma of the medial third of the upper eyelid (Fig. 8).

Conclusions

In the hairline of patients with laterally and superiorly orientated craniofacial clefts is a regular marker of the clefting process. These hairline indicators allow us to add further clinical features to those already described and thus better appreciate the extent of craniofacial clefting.

Mark H. Moore, M.B., Ch.B.
The South Australia Cranio-Facial Unit
Adelaide Children's Hospital
72 King William Road
North Adelaide 5006
South Australia

References

1. Tessier, P. Anatomical classification of facial, craniofacial, and laterofacial clefts. J. Maxillofac. Surg. 4: 69, 1976.

2. Tessier, P. Anatomical Classification of Facial, Craniofacial, and Laterofacial Clefts. In Symposium on Plastic Surgery in the Orbital Region. St. Louis: P. Tessier (Ed.), 1976.

3. Rogers, B. O. Berry-Treacher Collins syndrome: A review of 200 cases. Br. J. Plast. Surg. 17: 109, 1964.

4. Smith, D. W., and Cohen, M. M. Widow's peak scalp-hair anomaly and its relation to ocular hypertelorism. Lancet 2: 1127, 1973.

5. De Myer, W. The median cleft face syndrome: Differential diagnosis of cranium bifidum, occultum, hypertelorism, and median cleft nose, lip, and palate. Neurology 17: 961, 1967.

6. David, D. J., Sheffield, L., Simpson, D., and White, J. Frontoethmoidal meningoencephaloceles: Morphology and treatment. Br. J. Plast. Surg. 37: 271, 1984.

Case Report
The Tessier Number 9 Cleft

David J. David, F.R.C.S., F.R.C.S.(E), F.R.A.C.S., Mark H. Moore, M.B., Ch.B., Rodney D. Cooter, M.B., B.S., and Sik-Kuen Chow, M.D.
North Adelaide, South Australia, and Hong Kong

The anatomic classification of craniofacial clefts proposed by Tessier[1] involves a numbering system from 0 to 14 (Fig. 1). The number 9 cleft, the first of the cranial, or "northbound," clefts, was not personally observed by Tessier.[1] Indeed, the only records available to Tessier that such a cleft might have existed included a drawing by Morian,[2] an illustration in Sanvenero-Rosselli's book, and a personal communication from Hogeman.[1]

Clearly, the number 9 cleft is the rarest of these cleft deformities. It has been described as an upper lateral orbital cleft with the soft–tissue deformity involving the lateral third of the upper eyelid and the underlying bony disruption extending into the temporal fossa from the superolateral aspect of the orbit. [1,3]

Two patients with Tessier number 9 clefts have been surgically treated at the South Australian Cranio–Facial Unit. On the basis of the clinical, radiologic, and surgical examinations of these cases, we describe the soft–tissue and three dimensional skeletal anatomy of the number 9 cleft.

Case Reports

Case 1

A 9–year–old Chinese girl from Hong Kong was referred to the South Australian Cranio–Facial Unit with multiple craniofacial clefts. She was the product of a normal pregnancy, during which there was no known exposure to dangerous drugs, chemicals, or radiation. There was no reported history of craniofacial abnormalities in the extended family, and her Chinese parents (father 24 years old, mother 26 years old at time of patient's birth) are unrelated. She is the eldest of three children, and her intellectual development has been normal. Her siblings are normal and healthy.

At birth, her deformities included bilateral oro-ocular clefts and bilateral superolateral orbital clefts (Fig. 2). These were repaired at age 3 weeks. Subsequently, she underwent cleft palate repair, corrections of ectropion, repeated tarsorrahapies, and free and pedicled onlay bone grafting to both cheeks.

Clinical examination revealed oro–ocular clefts of the Tessier number 4 type on the right and the Tessier number 5 type on the left. Ectropion of the right upper lip and right lower eyelid and elevation of the right alar base reflect the uncorrected soft-tissue deficiency along the oro-ocular cleft margin. Similarly, the left lower eyelid ectropion remained uncorrected (Fig. 3).

From the South Australian Cranio-Facial Unit at the Adelaide Children's Hospital and the Royal Adelaide Hospital and the Plastic and Reconstructive Unit at Princess Margaret Hospital. Received for publication December 14, 1987; revised March 7, 1988.

There was a blind microphthalmic right eye with a mature cataract and signs of old endophthalmitis now proceeding to phthisis bulbi. The left eye showed signs of exposure keratitis. Absence of the upper lateral orbital wall had resulted in lateral displacement of the globe, more marked on the right side. The lateral third of the upper eyelid and lateral canthus remained distorted and did not appose the globe. No true upper eyelid colobomata were noted.

The lateral third of the eyebrow lay along the superior margin of a bony and soft-tissue furrow that radiated from the lateral canthal region superiorly and posteriorly across the temple into the temporoparietal hair–bearing scalp. The temporal hairline projected forward to border the scarred area which demarcated the cleft position. The soft-tissue distortion was bilateral but was more pronounced on the right side (Fig. 3). There was absent facial nerve function in the forehead and upper eyelids bilaterally.

Three–dimensional reconstructions of computed tomography well demonstrated the facial skeletal asymmetry. Bony clefting extended superiorly and posteriorly through the upper part of the greater wing of the sphenoid to the upper portion of the squamous temporal and adjacent parietal bones. The skeletal distortion was more marked on the right side, where an apparently separate full-thickness bone defect was noted in the upper temporal squama (Fig. 4). There was asymmetrical hypoplasia of the greater wing of the sphenoid and associated posterior and lateral rotation of the lateral orbital wall (Fig. 5). Sphenoid sinus pneumatization was normal, and the spheno-occipital synchondrosis was patent.

The zygomatic arch and body were normal in size, shape, and position. No abnormality was seen in the mandibular condyle, coronoid process, or ramus.

There was skull vault plagiocephaly, with relative bulging of the left parietal bone and flattening of the left occiput (Fig. 6). An apparent reduction in the anteroposterior dimension of the anterior and cranial fossae was noted; however, there were no obvious intracerebral anomalies. Mild cranial base asymmetry was reflected in the pterygoid plates, with the left pair being more laterally displaced from the midline.

The bilateral Tessier 9 clefts were best visualised after a bicoronal scalp flap had been raised and dissection of the orbits completed. Each orbit swept upward to become confluent with superolaterally directed furrows traversing the temporal fossae (Fig. 7). As expected from the pre-operative three–dimensional CT scans, this clefting was worse on the right side. No obvious distortion of the temporalis muscle was noted.

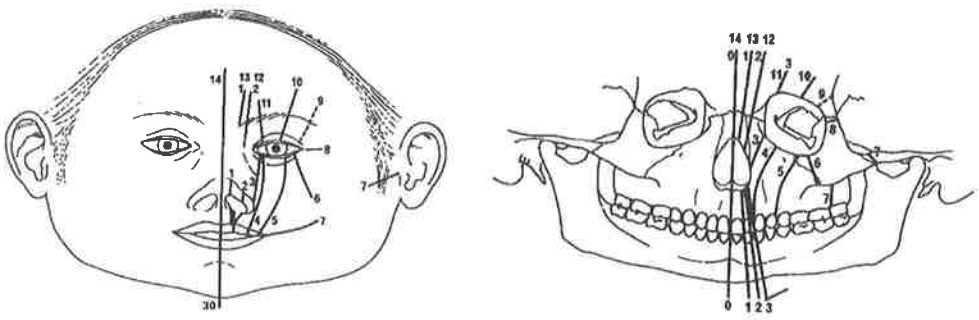

FIG. 1. *Tessier classification of craniofacial clefts.* (Left) *Soft tissue.* (Right) *Skeletal. (Reprinted with permission of the publishers of the* Journal of Maxillofacial Surgery, *George Thieme Verlag.)*

FIG. 2. *Unrepaired bilateral oro-ocular clefts with superolateral orbital extensions, the number 9 cleft.*

Case 2

An 8–year–old Indian boy from Malaysia was referred to the South Australian Cranio–Facial Unit for the surgical management of his craniofacial clefts. He was born to healthy, unrelated Tamil parents (father 25 years old, mother 21 years old at time of patient's birth) after a normal 40–week pregnancy and normal delivery. There was no family history of craniofacial deformities and no known exposure to dangerous drugs, chemicals, or radiation during the gestation. The patient has four healthy siblings and has achieved all physical and intellectual milestones appropriate to his age.

At birth, his deformities were obvious, but no previous attempts had been made to surgically correct them.

This patient's most striking deformity was the presence of a large right frontal encephalocele directed toward a broad coloboma of the middle third of the upper eyelid and scarred right cornea. The right palpebral fissure was grossly widened, and the amblyopic right eye was displaced laterally and downward with a right divergent squint. The right eyebrow was deficient medially, but the thinned out lateral two–thirds became contiguous with a broad downward and forward fronto-temporal hairline projection, suggesting the presence of a right Tessier number 9 cleft, in microform, in this patient with very obvious right Tessier number 10 and 2–12 clefts (Fig. 8).

Three–dimensional CT reconstructions demonstrated a large defect that involved the middle third of the right frontal bone, supraorbital rim, and orbital roof; this was consistent with a number 10 cleft. Medially, the frontal bone and frontal process of the maxilla was flattened, consistent with a number 12 cleft.

Lateral to the number 10 cleft, a distinctly separate minor notch existed in the lateral third of the supraorbital rim: the number 9 cleft (Fig. 9).

Subperiosteal dissection of the frontal bone confirmed the microform of the skeletal number 9 cleft through the superolateral orbital angle, quite distinct from the adjacent broad number 10 cleft (Fig. 10). No abnormality of the temporalis muscle was noted.

FIG. 3. *Severe soft–tissue scarring and distortion, age 9 years.*

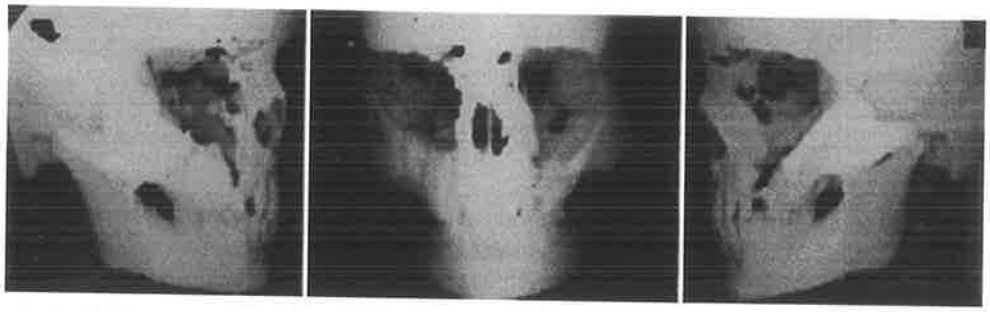

FIG. 4. *Three–dimensional CT views of the extensive bilateral superolateral orbital skeletal disruption.*

Discussion

The Tessier classification of rare craniofacial clefts evolved from one man's observations of consistent anatomic patterns of soft–tissue and bony disruption. The rarest craniofacial cleft, unseen by Tessier, is the number 9 cleft. The first case in this report manifested bilateral Tessier number 9 clefts, while the second case displayed an interesting unilateral microform of this recondite deformity.

The number 9 skeletal cleft produces complete absence of the superolateral orbital rim and wall. Bony deficiency extends superiorly and posteriorly through the upper part of the greater wing of the sphenoid to the upper portion of the squamous temporal and adjacent parietal bones with resultant temporal hollowing. The soft-tissue clefting commences at a distorted lateral third of the upper eyelid and lateral canthus before tracking through an almost absent lateral end of the eyebrow in an upward curve into the temporal scalp. As with other "northbound" and laterally orientated clefts, hairline projections point in the line of the cleft.[3]

Such clefts may be distinguished from the adjacent cleft numbers 8 and 10 by careful consideration of the disrupted anatomy. The number 8, or frontozygomatic, cleft may occur alone or in association with other clefts, as in the Treacher Collins and Goldenhar syndromes. Bony deformity takes the form of hypoplasia, rudimentary remnants or complete absence of the zygomatic bone, with the lateral orbital wall formed by the greater wing of the sphenoid developing forward and medially. Soft–tissue disruption includes lateral colobomata, dermatocoeles, and epibulbar cysts. The number 10 cleft, centered on the middle third of the supraorbital ridge and upper eyelid, is characterised by clefting of the orbital roof and frontal bone with an associated encephalocele and coloboma of the middle third of the upper eyelid.

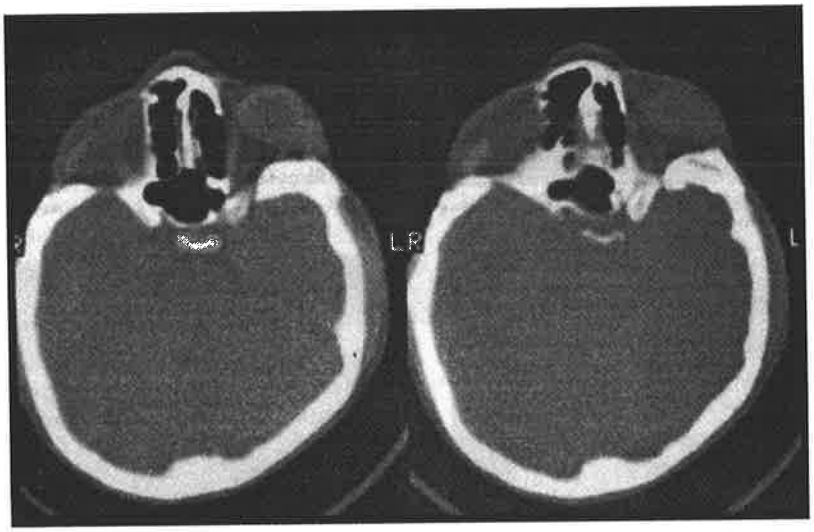

FIG. 5. *Two-dimensional CT view of the sphenoid hypoplasia and associated distortion of the lateral orbital walls.*

FIG. 6. *Two-dimensional CT view of the skull vault plagiocephaly.*

These two patients, representing both extremes of the clinical spectrum of the Tessier number 9 cleft, complete the morphologic classification system devised by Tessier. Neither patient demonstrated known predisposing nor any causative factors to account for their craniofacial deformity. Indeed, no convincing embryologic explanation is possible from the pattern of disruption observed in only two isolated patients— the step from morphologic observation to embryologic explanation requires extreme care!

Tessier recognised this when producing his "time zone" hypothesis; that "northbound" cranial and "southbound" facial clefts follow consistent patterns to form cranial and facial counterparts of the one cleft (with the numerical addition to number 14). Vascular compromise was speculated as an embryologic explanation of the apparent time zone pattern, but remains unproven.

These patients, like others examined at the South Australian Cranio-Facial Unit, do not always follow Tessier's time zone pattern; i.e., the number 9 cleft occurred with facial clefts other than the number 5.

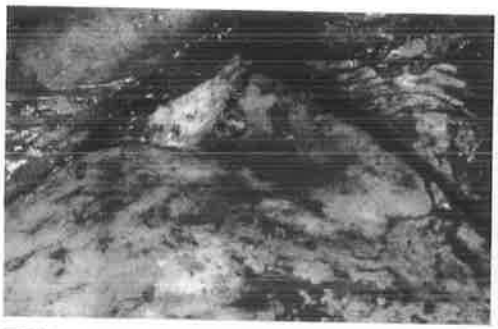

FIG. 7. *Operative view of the bony furrow radiating across the temporal fossa from the right superolateral orbital rim.*

FIG. 8. *Frontal encephalocele (number 10 cleft) with broad frontotemporal hairline projection indicating the number 9 and 10 clefts.*

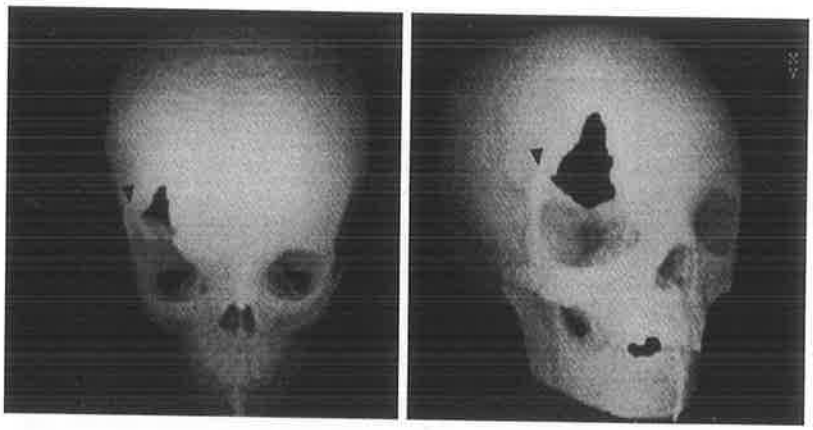

FIG. 9. *Three–dimensional CT view of the suprolateral orbital rim notching of the number 9 cleft separate from the larger frontal defect of the number 10 cleft.*

FIG. 10. *Operative view confirming the discretely separate microform number 9 and overt number 10 clefts with the broad frontal hollowing of the number 12 cleft more medially.*

Documenting the skeletal deformity of the number 9 cleft reveals the extreme bony deficiency which must be corrected to restore orbital position and contour. Indeed, where the Treacher Collins syndrome (Tessier cleft 6-7-8) manifests marked inferolateral orbital rim bony shortage, the number 9 cleft similarly presents an extraordinary degree of skeletal disruption requiring extensive bony reconstitution around the superolateral orbital rim.

Summary

The clinical, radiologic, and operative examination of two patients with the Tessier number 9 cleft has allowed the first complete description of this, the rarest of the rare craniofacial clefts. Soft–tissue disruption extends from the lateral third of the upper eyelid through a distorted lateral end of the eyebrow to the temporal scalp, with an associated hairline indicator. The skeletal disturbance similarly radiates superolaterally from the superolateral orbital rim across the greater wing of the splenoid to the upper squamous temporal. The three-dimensional extent of the bony disruption is associated with distortion of the cranial base and calvaria above.

Dr. Mark H. Moore
The South Australian Cranio-Facial Unit
Adelaide Children's Hospital
72 King William Road
North Adelaide, 5006
South Australia

References

1. Tessier, P. Anatomical classification of facial, craniofacial and laterofacial clefts. J. Maxillofac. Surg. 4: 69, 1976.

2. Morian, R. Uber die schrage Cesichtsspalte. Arch. Klin. Chir. 35: 245, 1887.

3. Kawamoto, H. K.,Jr. The kaleidoscopic world of rare craniofacial clefts: Order out of chaos (Tessier classification). Clin. Plast. Surg. 3: 529, 1976.

4. Moore, M. H., David, D.J., and Cooter, R. D. Hairline indicators of craniofacial clefts. Plast. Reconstr. Surg. 82: 589, 1988.

Tessier Clefts Revisited With a Third Dimension

David J. David, F.R.C.S., F.R.A.C.S.
Mark H. Moore, F.R.A.C.S.
Rodney D. Cooter, M.B., B.S.

The classification by Tessier of rare craniofacial clefts brought, for the surgeon, order to a previously confusing array of anatomic and developmental descriptions. An ordered two-dimensional categorisation of severe clefting malformations evolved from his clinical, radiologic, and surgical observations. The purpose of this paper is to report a complete series of facial clefts studied with computed tomography (CT) and three-dimensional reconstruction. The CT analysis supports some, but contradicts other, hypotheses and speculations presented by Tessier. The CT data reveal the scale of the reconstructive challenge and allow the assessment of our therapeutic interventions.

KEY WORDS: *cleft lip, cleft palate, craniofacial clefts, facial bones, maxillofacial development, hypertelorism, jaw abnormalities*

The rarity and large variety of craniofacial clefts have prevented the establishment of a concise, meaningful, and comprehensive classification system. Anatomic terms, eponyms, and attempts at developmental explanations have been applied (Morian, 1887; Sanvenero–Rosselli, 1953; Karfik, 1966). In 1976, Tessier proposed a classification of craniofacial clefts that has been widely accepted (Tessier, 1976a and 1976b; Kawamoto, 1976). Based on his personal experience, which included clinical, radiologic, and surgical observations of 336 patients, Tessier devised an ordered numbering system to identify the consistent anatomic pathways of soft tissue and skeletal clefts (Fig. 1). The appealing simplicity of the Tessier system has both improved communication between observers of craniofacial clefts and provided a better appreciation of the reconstructive surgery required to restore normality.

The recent application of three-dimensional reconstructions of high resolution CT data has enhanced our knowledge of the extent of the disordered craniofacial morphology of patients with facial clefts. The objective of the present study was to review, with the benefit of three dimensions, the clinical, radiologic, and surgical findings of a complete series of Tessier craniofacial clefts.

Methods

Since 1975, 253 patients with rare craniofacial clefts that could be classified by the Tessier system have been assessed at the Australian Cranio-Facial Unit (Table 1). All of these patients have had a complete clinical examination,

David J. David is Head of Unit, Mark H. Moore is Assistant Craniofacial Surgeon, and Rodney D. Cooter is Registrar, Australian CranioFacial Unit, Adelaide Children's Hospital, North Adelaide, South Australia.

Reprint requests: David J. David, Australian Cranio-Facial Unit, Adelaide Children's Hospital, 72 King William Road, North Adelaide, South Australia 5006.

photographic documentation, and radiologic investigation. Beginning in 1983, radiologic assessment included three–dimensional reconstructions from axial CT data (Marsh and Vannier, 1983). A General Electric GE8800 CT/T scanner generated the axial scans, and the three–dimensional reconstructions were produced with a 3D83 program developed by the Medical Imaging Processing Group, Department of Radiology, University of Pennsylvania.

Multiple examples of each of the Tessier clefts were available for review. From within this large series, representative cases were selected for each of the Tessier clefts (Number 0 to Number 14), and each was assessed with three–dimensional CT imaging. The clinical and CT features of each of these representative cases are presented with an initial brief summary of Tessier's original observations.

Case Presentations

Number 0

Tessier Description. A Number 0 Tessier cleft is a true median cleft lip with a broad columella and bifid nasal tip. The alveolar cleft is between the central incisors. The nasal septum may be thickened, duplicated, or absent. The nasal bridge is usually broad with associated orbital hypertelorism.

Soft Tissue Characteristics. The midline soft tissue anomaly may range from a mild broadening of the philtrum, as shown in Figure 2A, or there may be a true median cleft lip. The columella and nasal tip are typically bifid and broadened with a midline depression. The alae nasi are intact but laterally displaced. The nose appears shortened in the vertical dimension.

Skeletal Characteristics. Midline facial clefting produces a characteristic keel–shaped maxillary alveolus that slopes obliquely toward the alveolar cleft. There is usually an anterior open bite. Vertical hypoplasia in the region of the cleft and its margins produces a reduction in median and

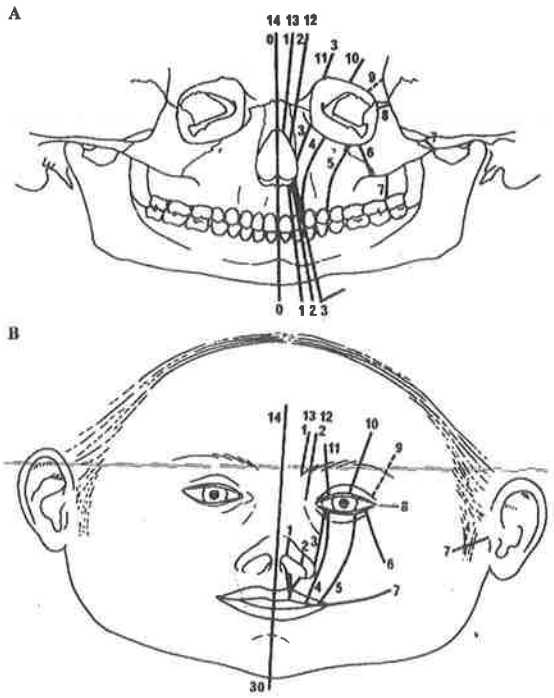

FIG. 1. *Tessier classification of craniofacial clefts.* **A.** *Soft tissue;* **B.** *skeletal. (From the* Journal of Maxillofacial Surgery, *Georg Thieme Verlag, Stuttgart.)*

paramedian midfacial height (Fig. 2B). The cartilaginous and bony nasal septum is thickened, and the nasal bones and nasal processes of the maxilla are broad, flattened, and displaced laterally from the midline (Fig. 2C). The midline cleft is manifested superiorly as enlargement and inferior prolapse of the ethmoidal and spenoidal sinuses, orbital hypertelorism, and symmetric widening of the anterior cranial fossae (Fig. 2D). The body of the spenoid is anatomically normal, although it is broadened with displacement of the pterygoid plates away from the midline. The extension of this cleft into the cranium constitutes a Number 14 cleft.

TABLE I

Population of Patients With Tessier Craniofacial Clefts Presenting to Australian Cranio–Facial Unit, 1975–1988

Hemifacial microsomia/Goldenhar	94
Treacher Collins syndrome	33
Rare craniofacial clefts (excluding those above)	71
Frontoethmoidal meningoencephaloceles	55
Total	253

Number 1

Tessier Description. As seen in a typical cleft lip, a cleft of the lip is found in the region of the cupid's bow. The nostril is cleft through the alar dome and extends above onto the nasal dorsum. It passes medial to a normal, but dystopic, medial canthus. There is an alveolar cleft between the central and lateral incisors that extends above through the pyriform margin lateral to the anterior nasal spine; the nasal septum is not involved. The bony cleft extends through the nasal bone or between the junction of the nasal bone and frontal process of the maxilla.

Soft Tissue Characteristics. Above the cleft lip, the clefting of the alar dome is associated with deviation to the opposite side of the shortened and broadened columella and nasal tip. Extension of the soft tissue cleft onto the nasal dorsum can be manifest as a series of vertical soft tissue furrows and ridges (Fig. 3A). Vertical inner canthal dystopia and severe telecanthus mark the superior aspect of the Number 1 facial cleft. A cranial soft tissue extension characterised by a tongue-like projection of the frontal hairline delineates the number 13 cleft.

Skeletal Characteristics. Skeletal clefting of the maxilla may extend posteriorly to form a complete cleft of the hard and soft palate. The maxilla is hypoplastic in all three dimensions. There is a keel–shaped alveolus and anterior open bite (Fig. 3B). Normal septation is preserved between the nasal cavity and the hypoplastic maxillary antrum on the affected side (Fig. 3C). Distortion of the nasal skeleton produces gross flattening of the nasal dorsum. There is asymmetry of the pterygoid plates, of the greater and lesses wings of the spenoid, and of the floor of the anterior cranial fossa (Fig. 3D). The distortion of the cranial base may result in a mild plagiocephaly.

Number 2

Tessier Description. As is typically seen in isolated cleft cases, a cleft of the lip is present. There is hypoplasia, but not true notching of the ala nasi with flattening of the lateral part of the nose. The nasal root is broadened, with lateral displacement of the inner canthus. The palpebral fissure and lacrimal drainage system are not disturbed. The alveolar cleft is through the lateral incisor area and extends to the pyriform aperture. There is normal septation between the nasal cavity and maxillary sinus. Notching at the junction between the nasal bone is present, as is a broad, flat frontal process of the maxilla. Transverse ethmoid enlargement produces orbital hypertelorism.

Soft Tissue Characteristics. Above the cleft of the lip and palate is a true broad cleft of the nostril that is medial to the intact, but laterally displaced, tail of the alar cartilage. A shallow soft tissue groove extends superiorly to the asymmetrically widened nasal root (Fig. 4A). The lacrimal system, palpebral fissures, and eyebrows remain intact.

Skeletal Characteristics. The alveolar cleft extends posteriorly as a complete unilateral cleft of the hard and soft palate. The nasal septum is intact but deviated to the opposite side. The nasal cavity remains separated from the normally pneumatized, although hypoplastic, maxilla on the cleft side (Figs. 4B, 4C). Above the nasomaxillary notching, the ethmoid sinus is less well developed, and there is no pneumatization of the frontal sinus on this side. Anterior rotation of the greater and lesser wings of the spenoid occurs on the cleft side in relation to the narrower orbit and smaller ethmoid sinus. There is mild asymmetry of the anterior cranial fossa. which is narrower on the cleft side (Fig 4D). The cranium is brachycephalic with marked occipital flattening.

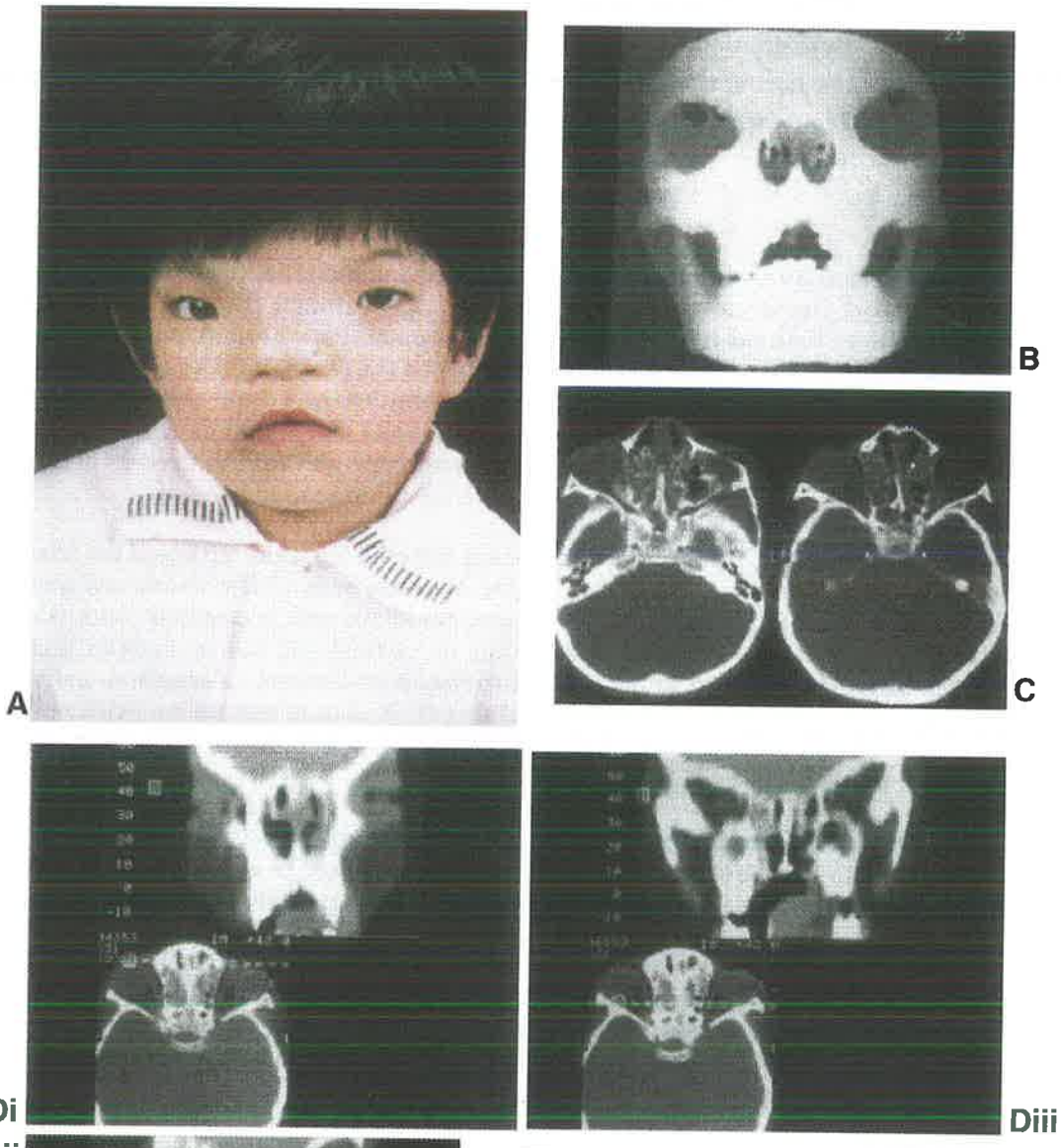

FIG. 2. A. *Five–year–old Chinese girl with untreated midline craniofacial clefts of the Tessier Number 0–14 type.* **B.** *CT reconstruction shows the keel–shaped maxilla and anterior open bite. Orbital hypertelorism is evident.* **C.** *Axial two–dimensional CT scan of the nasoethmoidal features of the Number 0 cleft.* **D.** *Sequential coronal two–dimensional CT reformats confirm the inferior prolapse and broadening of the ethmoids above and the thickened bifid nasal septum below* (i–iii).

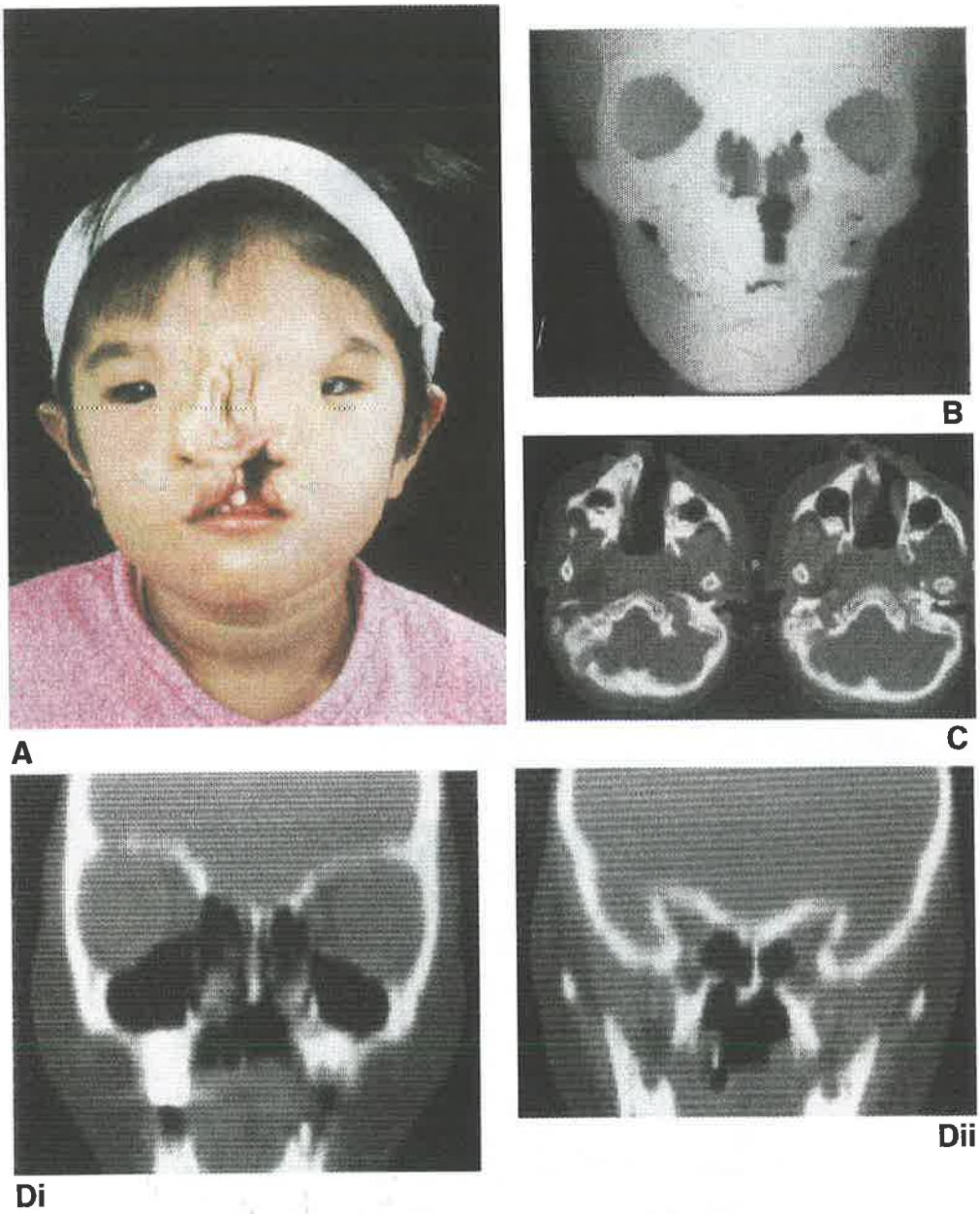

FIG. 3. A. *Four-year-old Malay Chinese girl with left-sided craniofacial clefts of the Tessier Number 1-13 type.* **B.** *Alveolar clefting between the central and lateral incisor extends into the pyriform margin.* **C.** *Normal septation between the nasal cavity and the hypoplastic cleft maxilla.* **D.** *Coronal two-dimensional CT reformats confirm cleft side maxillary hypoplasia, inferior orbital dislocation, pterygoid plate, and anterior and middle cranial fossa floor asymmetry* (i-ii).

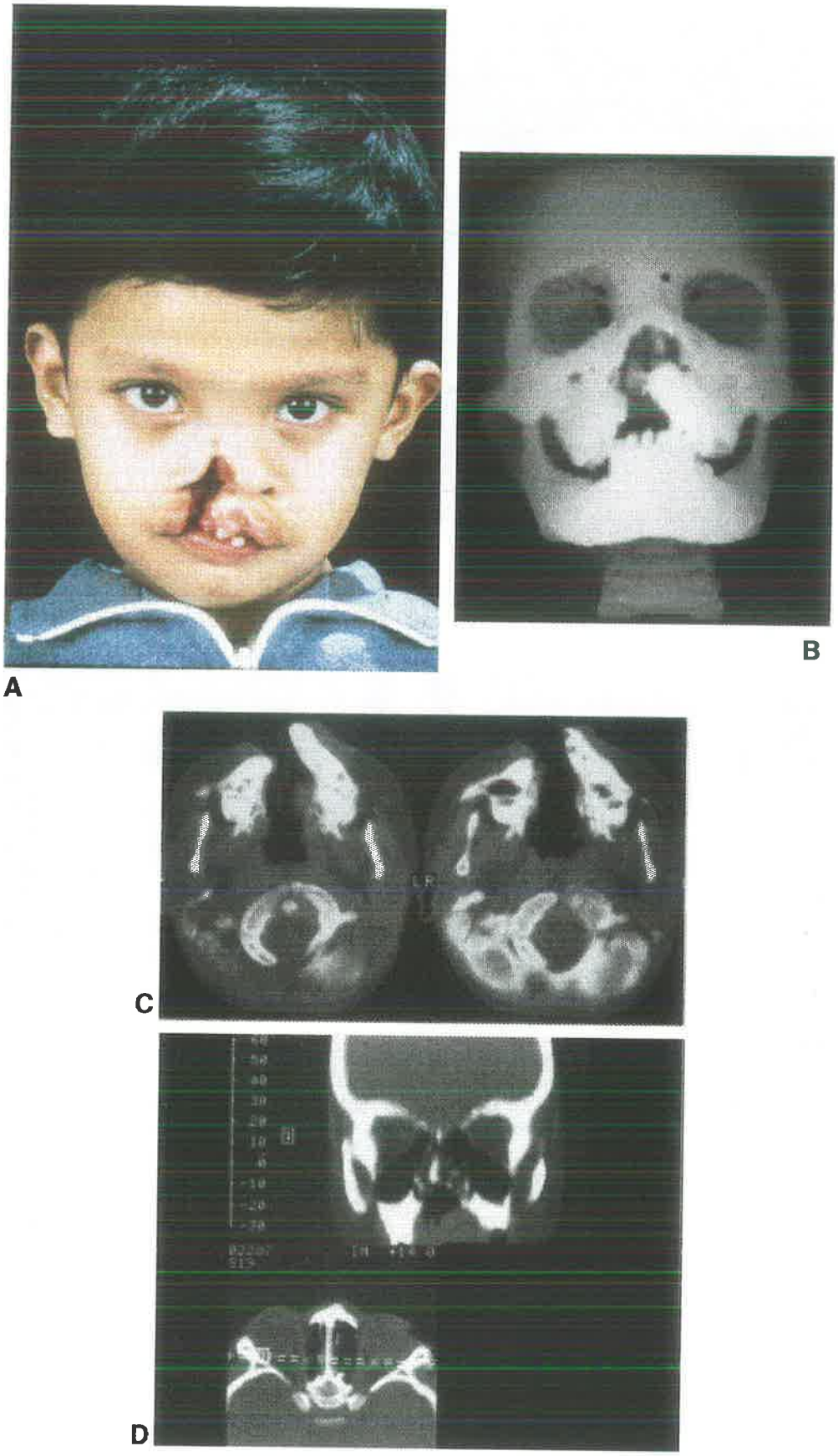

FIG. 4. A. *Four–year–old Malaysian boy with an unrepaired right–sided cleft of the Tessier Number 2 type.* **B.** *Cleft marginal hypoplasia produces a characteristic keel–shaped alveolus and hypoplastic maxilla.* **C.** *Axial two–dimensional CT scan shows the alveolar cleft and inferior displacement of the cleft side maxilla.* **D.** *Coronal two–dimensional CT reformat through the posterior orbits demonstrates the asymmetry extending from below in the maxilla, through the ethmoids, to the anterior cranial fossa.*

Number 3

Tessier Description. As in the Number 1 and Number 2 clefts, this cleft extends through the lip in the region of the typical cleft lip; however, it does not extend through the base. The cleft continues superiorly to involve the inner canthus and lower eyelid medial to the inferior lacrimal punctum, thereby disrupting the nasolacrimal system. Microphthalmia may be present. The alveolar cleft is between the lateral incisor and the canine. Absent septation between the nasal cavity and maxillary antrum, together with the distortion of the frontal process of the maxilla and lacrimal fossa, produces direct communication between the orbit, maxillary sinus, and nose.

Soft Tissue Characteristics. There is hypoplasia of the soft tissue margins of the cleft in the vertical dimension. This produces extreme soft tissue deficiency between the alar base and the cleft of the medial aspect of the lower eyelid (Fig. 5A). The inferior lacrimal punctum is evident at the lateral margin of the lower eyelid cleft. The lacrimal drainage system ends as an opening directly onto the cheek without communication into the nasal cavity. The globe is normal in size, but it is displaced inferiorly and laterally.

Skeletal Characteristics. The nasal septum shows the characteristic distortion seen in typical cleft lip and palate. There is absence of septation between the nasal cavity on the cleft side and the maxilla. The maxilla is hypoplastic in three dimensions, with a marked reduction in pneumatization (Figs. 5B, 5C).

Superior extension of the skeletal clefting into the medial portion of the orbital floor and into the inferior orbital rim in the region of the frontal process of the maxilla allows direct communication between the orbit above and the nasomaxillary region below. There is mild narrowing of the ethmoid sinus and of the body of the spenoid on the cleft side. The pterygoid process appears anatomically normal, but less displaced from the midline compared with that of the non–cleft side (Fig. 5D). Both the orbit and the floor of the anterior cranial fossa are inferiorly displaced.

Number 4

Tessier Description. The cleft lip is midway between the philtral ridge and the commissure of the mouth. The cleft is lateral to the normally shaped and placed nasal ala and passes onto the cheek. The cleft extends through the lower eyelid lateral to the punctum. The lacrimal system and inner canthus are normal. Microphthalmia may be present. The alveolar cleft passes between the lateral incisor and canine, as in the Number 3 cleft. The cleft passes around the pyriform aperture and continues through the portion of the maxillary sinus medial to the infraorbital foramen. The cleft terminates at the medial end of the inferior orbital rim.

Soft Tissue Characteristics. There is severe vertical soft tissue deficiency in a Number 4 cleft, with the medial margins of the cleft lip extending directly into the medially placed cleft of the lower eyelid (Fig. 6A). Within the medial segment of the right–sided cleft lip, muscle elements are apparently absent. Muscle bunching is noted in the ipsilateral lateral lip segment, as is seen in a typical unilateral cleft lip. The anatomically normal nasal ala is superiorly displaced in association with a severe deficiency in the overall nasal length. Marked dystopia of the right globe results in its inferior displacement into the medially deficient orbital floor and inferior rim. Both globes are otherwise normal.

Skeletal Characteristics. The complete palatal cleft passes through the maxilla medial to the infraorbital foramen and extends to the medial portion of the inferior orbital rim without evidence of an intact maxillary sinus (Figs. 6B,

6D). Bony septation persists medially, thereby separating the nasal cavity from the orbit, maxillary sinus, and mouth, which are contiguous. Marked midfacial hypoplasia is present. The cleft is manifest as asymmetry of the body of the spenoid; it is smaller on the right, with asymmetric placement of the pterygoid plates relative to the midline (Fig. 6C). The orbital floor cleft has no communication with the inferior orbital fissure. The cleft does not extend to the skull base, but there is marked facial asymmetry associated with plagiocephaly (Fig. 6E).

Number 5

Tessier Description. The cleft of the lip is just medial to the oral commissure and extends across the cheek as a furrow. It ends as a cleft at the junction of the middle and lateral third of the lower eyelid. Microphthalmia is frequently present. The alveolar cleft is through the premolar region and extends superiorly through the orbit at the inferolateral part of the rim and floor.

Soft Tissue Characteristics. There is a vertical soft tissue deficiency between the lateral portion of the lip and the lower eyelid cleft. The left side of the nose shows vertical shortening, and the left alar base is displaced superiorly (Fig. 7A).

Facial asymmetry secondary to the skeletal abnormality is reflected by a vertical orbital dystopia. However, both globes are normal, and there is no abnormality of the upper eyelids, eyebrow, forehead, or frontal hairline.

Skeletal Characteristics. The skeletal clefts vary, ranging from a narrow skeletal furrow that traverses the anterior maxillary wall as on the right (Fig. 7B) to a broad cleft of the maxilla lateral to the infraorbital foramen and maxillary sinus. This latter cleft enters the inferolateral orbital rim and floor without posterior communication with the inferior orbital fissure on the left side (Fig. 7B). Medial collapse of the lateral maxillary segments is present bilaterally, with reduction in the transverse dimensions of the maxillary arch. Manifestations of the skeletal disturbance in the spenoid include a shortening and thickening of the lateral orbital walls in the region of the greater wing and mild asymmetric placement of the pterygoid plates relative to the midline. The right-sided pterygoid plates are smaller and closer to the midline (Fig. 7C). There is minimal asymmetry of the cranial base and calvarium.

Number 6

Tessier Description. This zygomaticomaxillary cleft is similar to that typically found in Treacher Collins syndrome. The overlying tissue shows a vertical sclerodermic furrow radiating from the labial commissure or the angle of the mandible across the cheek to a coloboma of the lower eyelid between the middle and lateral one–third. Microphthalmia is not observed. The skeletal cleft is between the maxilla and zygoma; it passes through the inferolateral orbital rim to enter the inferior orbital fissure. No alveolar cleft is present. The zygomatic arch is intact.

Soft Tissue Characteristics. The soft tissue furrow, which is more apparent on the right, radiates from the oral commissure toward the lateral two-thirds of the lower eyelid. The antimongoloid obliquity of the palpebral fissures is associated with laterally placed lower eyelid clefts and some ectropion (Fig. 8A). A left–sided anophthalmia is accompanied by adjacent soft tissue hypoplasia and is reflected in a short palpebral fissure, enophthalmos, and minor ptosis of the eyebrow.

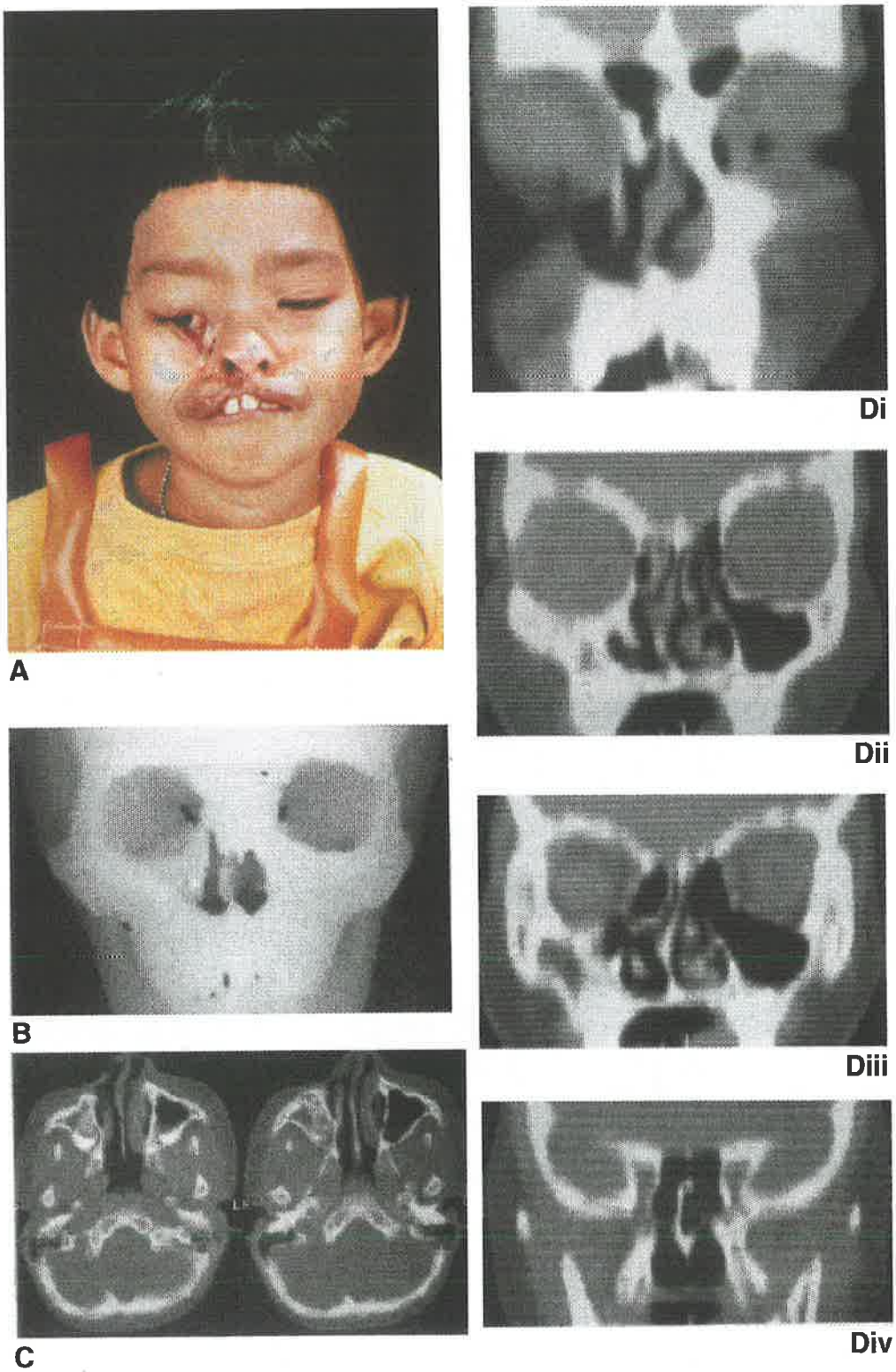

FIG. 5. A. *Seven-year-old Thai girl with an isolated unrepaired right-sided Tessier Number 3 cleft.* **B.** *Three-dimensional CT reconstruction shows the anatomy of the skeletal Number 3 cleft.* **C.** *Axial two-dimensional CT scan demonstrates the hypoplastic cleft right maxilla with associated relative absence of pneumatization.* **D.** *Sequential coronal two-dimensional CT reformats trace the clefting process through the anteroposterior extent of the midface* (i-iv).

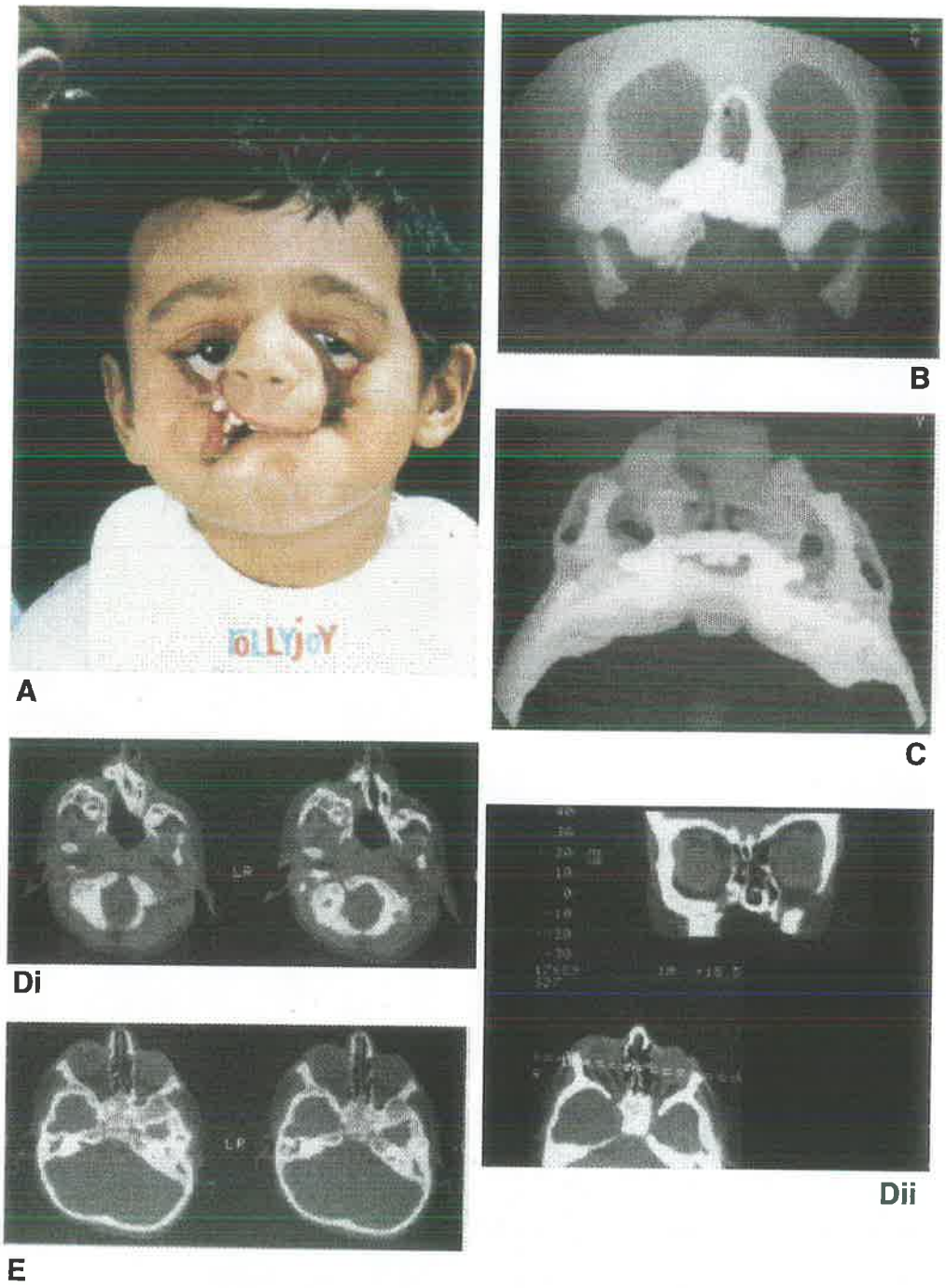

FIG. 6. A. *Two–year–old Malaysian boy of Indian descent with unrepaired clefts of the Tessier Number 4 type on the right and Number 5 cleft on the left.* **B.** *three–dimensional CT reconstruction exposes the asymmetric midfacial skeletal clefting.* **C.** *Three–dimensional CT reconstruction is tilted to view the pterygoid plates and posterior maxilla from behind. The marked cleft–induced asymmetry extends from the anterior maxilla (upper border) to the pterygoid plates and cranial base (lower border).* **D.** *Axial two-dimensional CT scan outlines the course and relation of the cleft through the lower midface* (i). *Coronal two–dimensional CT reformat emphasises the cleft extension into the medial portion of the orbit on the right Tessier Number 4* (ii). *E. Axial two–dimensional CT scan at the midorbit level confirms the asymmetry extending from the orbits anteriorly through the base of the skull and spenoid body to the occiput posteriorly.*

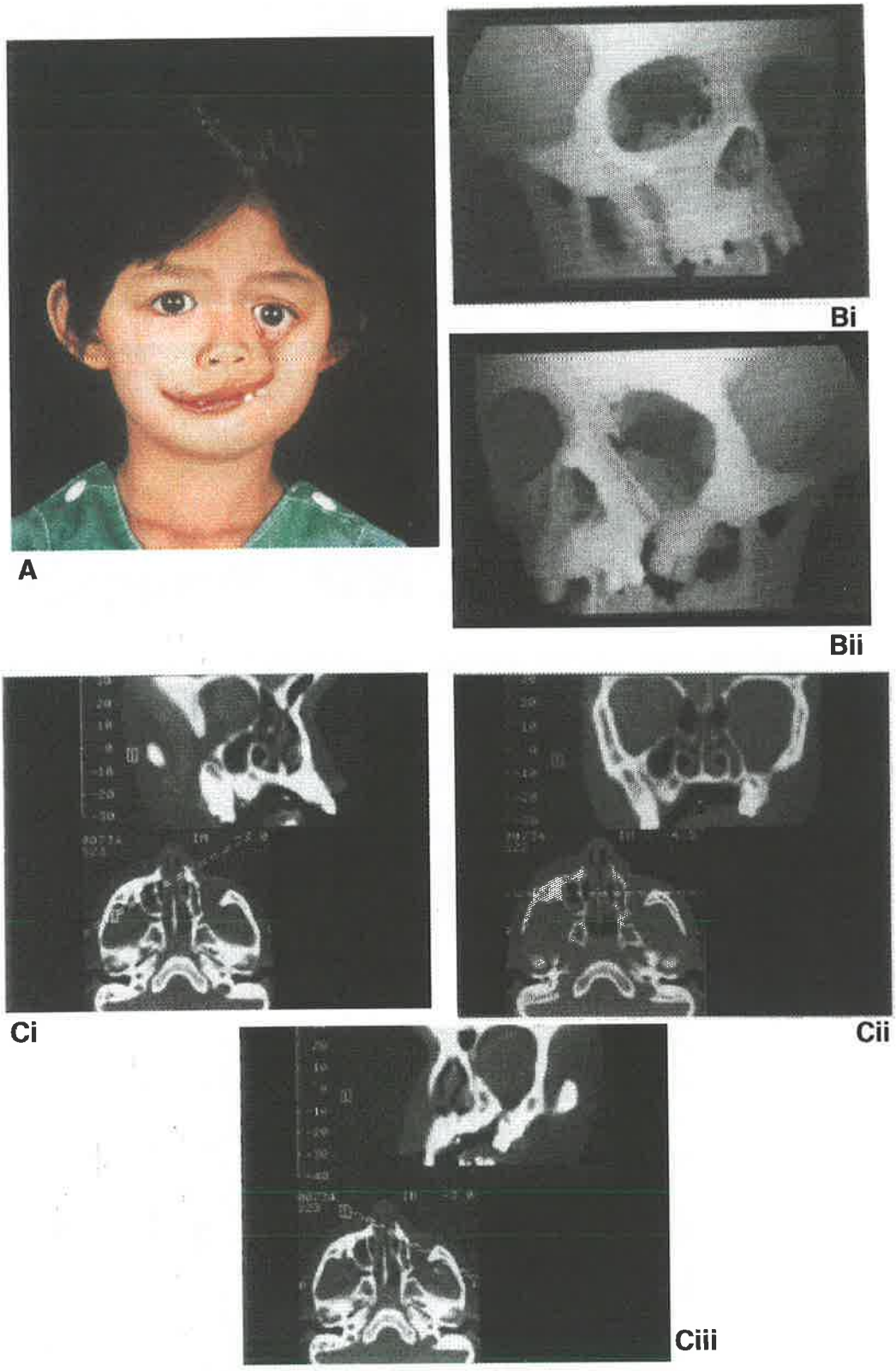

FIG. 7. A. *Five–year–old Malaysian boy with bilateral facial clefting of the Tessier Number 5 type, which is worse on the left side.* **B.** *Oblique three–dimensional CT reconstructions show the anterior boundaries of the bilateral Number 5 clefts from the premolar alveolar cleft below to the orbital floor above* (i-ii). **C.** *Oblique two–dimensional CT reformats demonstrate some of the techniques available for tracking the clefts posteriorly through the face* (i-iii).

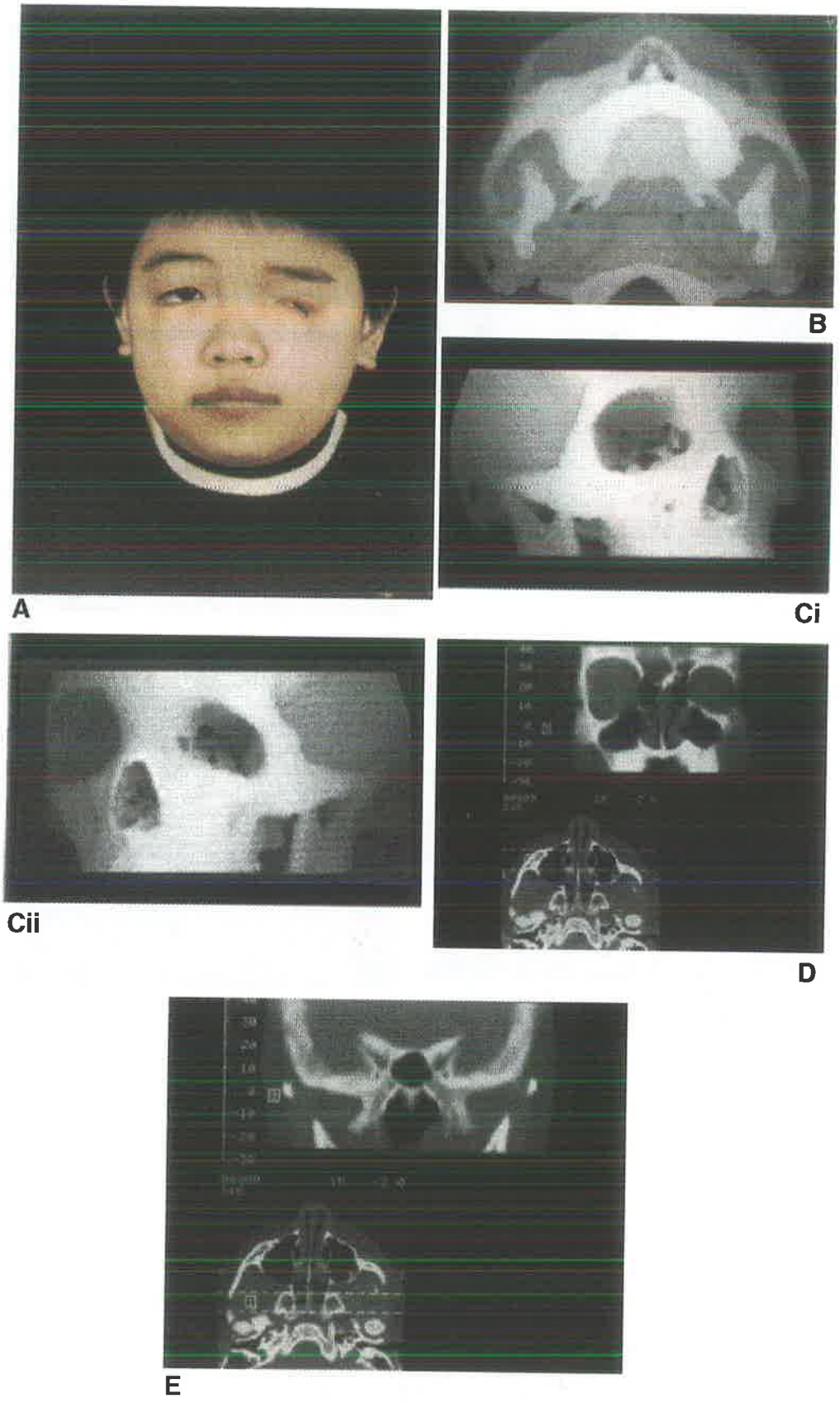

FIG. 8. A. *Eight–year–old Malaysian Chinese boy with bilateral Tessier Number 6 clefts.* **B.** *Worms–eye three–dimensional reconstruction demonstrates the skeletal hypoplasia in the region of the zygomaticomaxillary suture, which is more marked on the left side.* **C.** *Oblique three–dimensional CT reformats of the midface show the posterior maxillary and orbital hypoplasia* (i–ii). **D.** *Broad coronal two dimensional CT reformat exposes the posterior maxillary hypoplasia cleft extension into the lateral orbit.* **E.** *Coronal two–dimensional CT reformat visualises more posteriorly the mild middle cranial fossa asymmetry.*

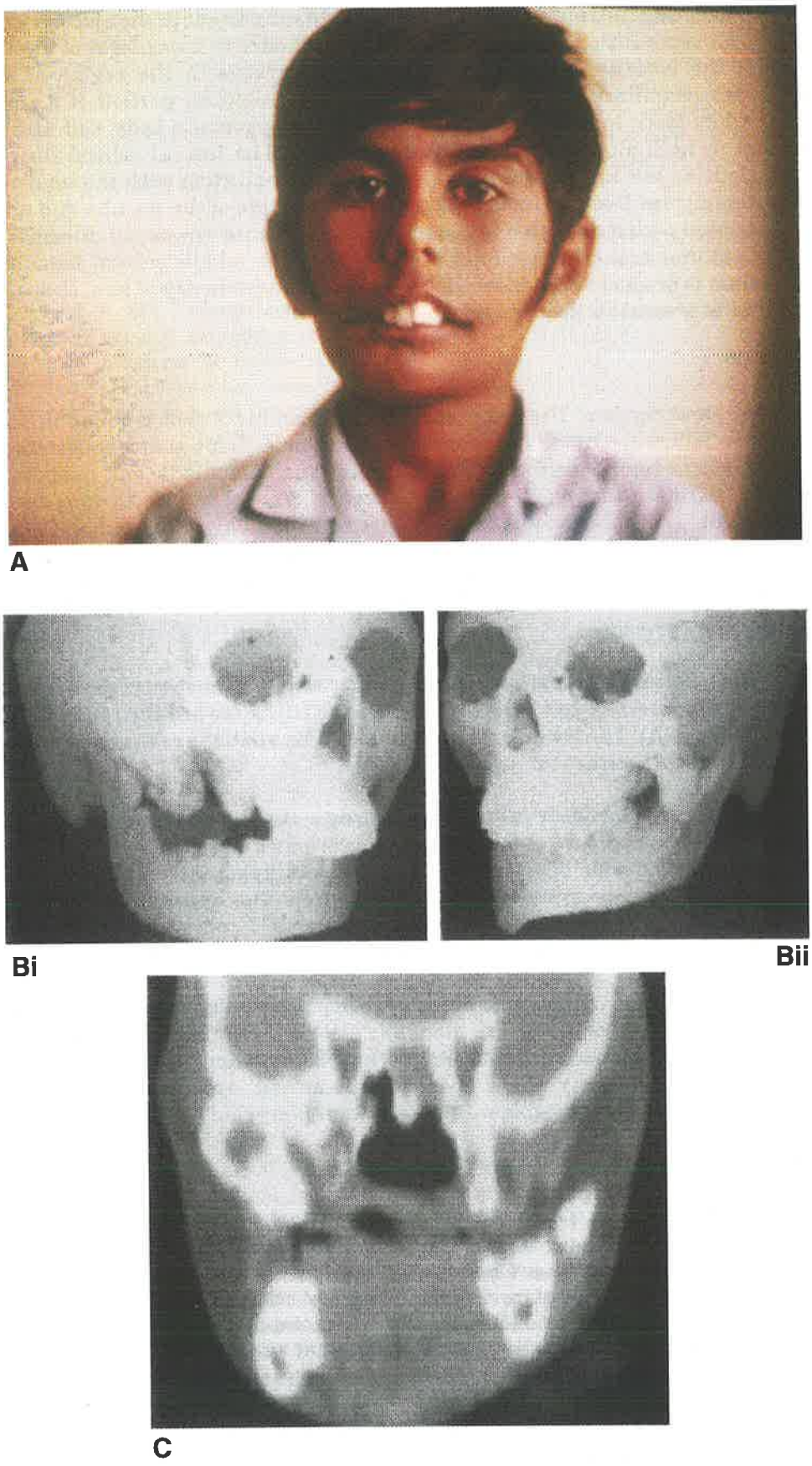

FIG. 9. A. *Thirteen year–old Fijian boy of Indian descent with isolated partially repaired bilateral Tessier Number 7 clefts.* **B.** *Oblique three–dimensional CT reconstructions confirm the gross skeletal disturbance in the pterygomaxillary region, zygomatic body and arch, and temporomandibular articulation (i–ii).* **C.** *Coronal two–dimensional CT reformat exposes the abnormal pterygoid plates, mandibular condyles, and tilt of both the cranial base above and mandible below.*

Skeletal Characteristics. No abnormality is present in the alveolar arch except for some tilting of the occlusal plane secondary to hypoplasia of the left side of the maxilla. There is a vertical bony groove in the region of the zygomaticomaxillary suture that ends in the inferolateral portion of a small bony orbit. More laterally, the remainder of the zygomatic body and arch is normal in both shape and dimension (Fig. 8B). The lateral orbital floor is downslanting but intact, and it lacks direct communication with the temporal or infratemporal fossae. The hypoplasia of the left side of the maxilla and orbit is associated with a reduction in the transverse and anteroposterior dimensions of the anterior cranial fossa; mild asymmetry of the middle cranial fossa and calvarium is present (Figs. 8C–8E). No significant asymmetry of size, shape, or position is present in the spenoid.

Number 7

Tessier Description. The temporozygomatic Number 7 cleft is found in both Treacher Collins syndrome and hemifacial microsomia. Soft tissue manifestations include macrostomia, malformations of the external and middle ear, temporalis muscle, variable involvement of the seventh cranial nerve (in hemifacial microsomia), and abnormalities of the preauricular hair in Treacher Collins syndrome. The skeletal cleft is through the pterygomaxillary junction, and vertical maxillary hypoplasia is present. In addition, abnormality of the mandibular ramus, coronoid, and condyle and absence of the zygomatic arch are typically present.

Soft Tissue Characteristics. A soft tissue furrow extends from the macrostomia laterally and superiorly across the cheek toward the preauricular hairline (Fig. 9A). The lower eyelids are intact. The anatomy of the external ear is normal, and there are no preauricular tags.

Skeletal Characteristics. Bony clefting is through the pterygomaxillary junction with hypoplasia of the alveolar process in the molar region, thereby producing a posterior open bite. The maxilla is hypoplastic, although the maxillary sinuses are symmetrically pneumatized. The hypoplastic zygomatic body arches upward, but then it takes a downward course and is severely malformed and displaced. The zygoma is continuous posteriorly with an apparently normal zygomatic process of the temporal bone (Fig. 9B). The mandibular condyle and coronoid process are hypoplastic and asymmetric. There is no antegonial notching of the mandible. Marked cranial base asymmetry, with tilting and asymmetric positioning of the temporomandibular articulations, is present. The anatomy of the spenoid is abnormal, especially on the right where there is no recognisable medial or lateral pterygoid plate (Fig. 9C).

Number 8

Tessier Description. The frontozygomatic or Number 8 cleft is found in both Treacher Collins syndrome and the Goldenhar variant of hemifacial microsomia. Skeletal defects are more prominent in Treacher Collins syndrome, whereas the soft tissue clefting is more typical in cases of "Goldenhar syndrome". Soft tissue clefting presents as a dermatocele, a true lateral eyelid coloboma with absence of the outer canthus, and anomalies of the globe itself, especially epibulbar cysts in patients with "Goldenhar syndrome." The frontozygomatic bony cleft produces absence of the lateral orbital rim; this border now is formed by the hypoplastic greater wing of the spenoid (Raulo and Tessier, 1981). The absence of bony support for the outer canthus produces lateral canthal dystopia and the characteristic antimongoloid slant of the palpebral fissures.

Soft Tissue Characteristics. The classical soft tissue deformities of the mouth, auricle, and periorbital tissues have been well described, as in the young girl with Treacher Collins syndrome shown in Figure 10A. Secondary to the bony deficiency in the lateral orbital wall and floor, there is soft tissue continuity between the orbit, temporal fossa, and infratemporal region. Preauricular hairline indicators delineate the Number 8 cleft as the first of the "northbound" clefts.

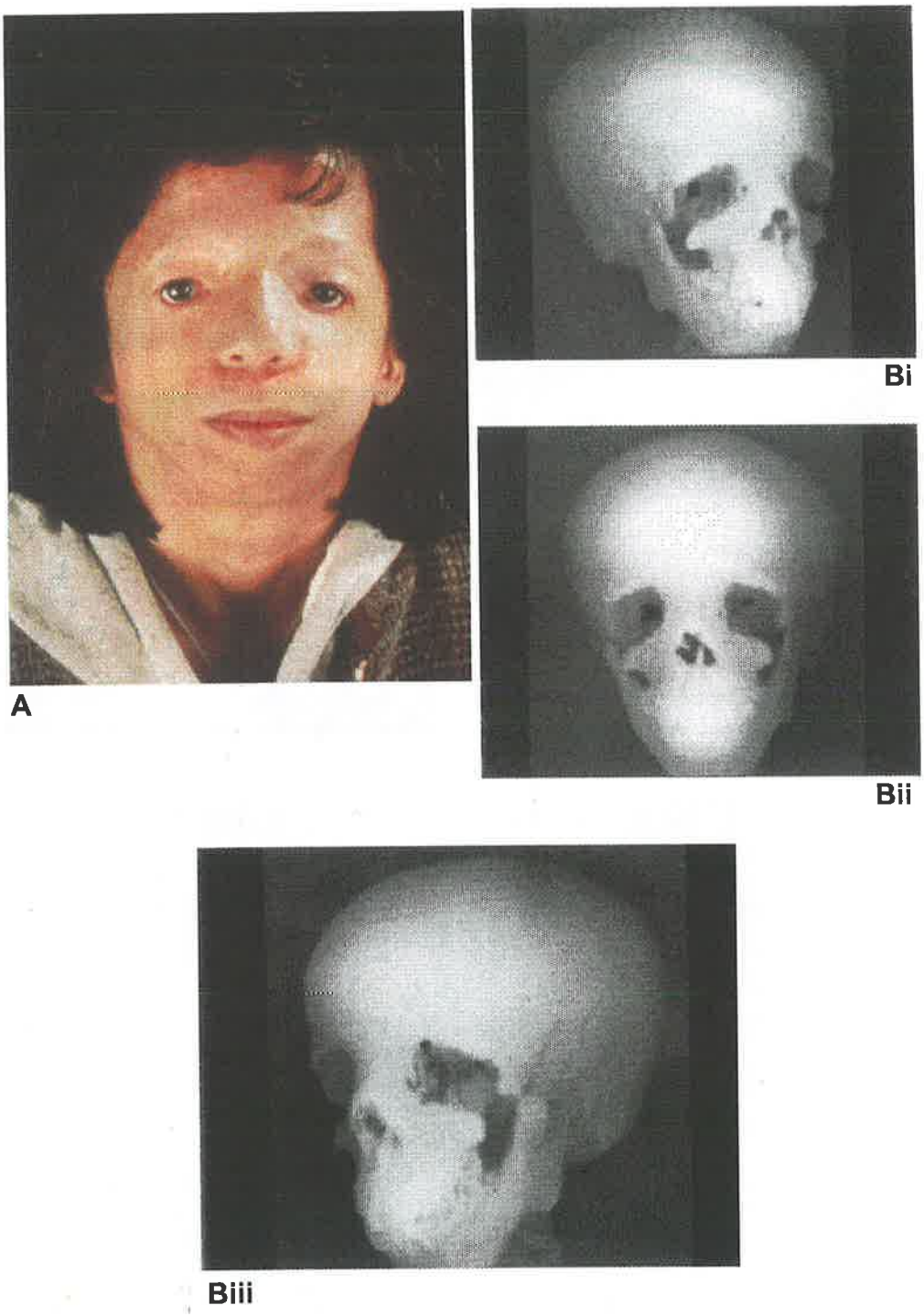

FIG. 10. A. *Twenty–nine–year–old Hong Kong Chinese woman with Treacher Collins syndrome (Tessier Number 6, 7, and 8 clefts).* **B.** *Three–dimensional CT reconstructions expose the true extent of the bony deficiency in the frontozygomatic region, the lateral orbital wall being formed by the hypoplastic greater wing of spenoid* (i–iii).

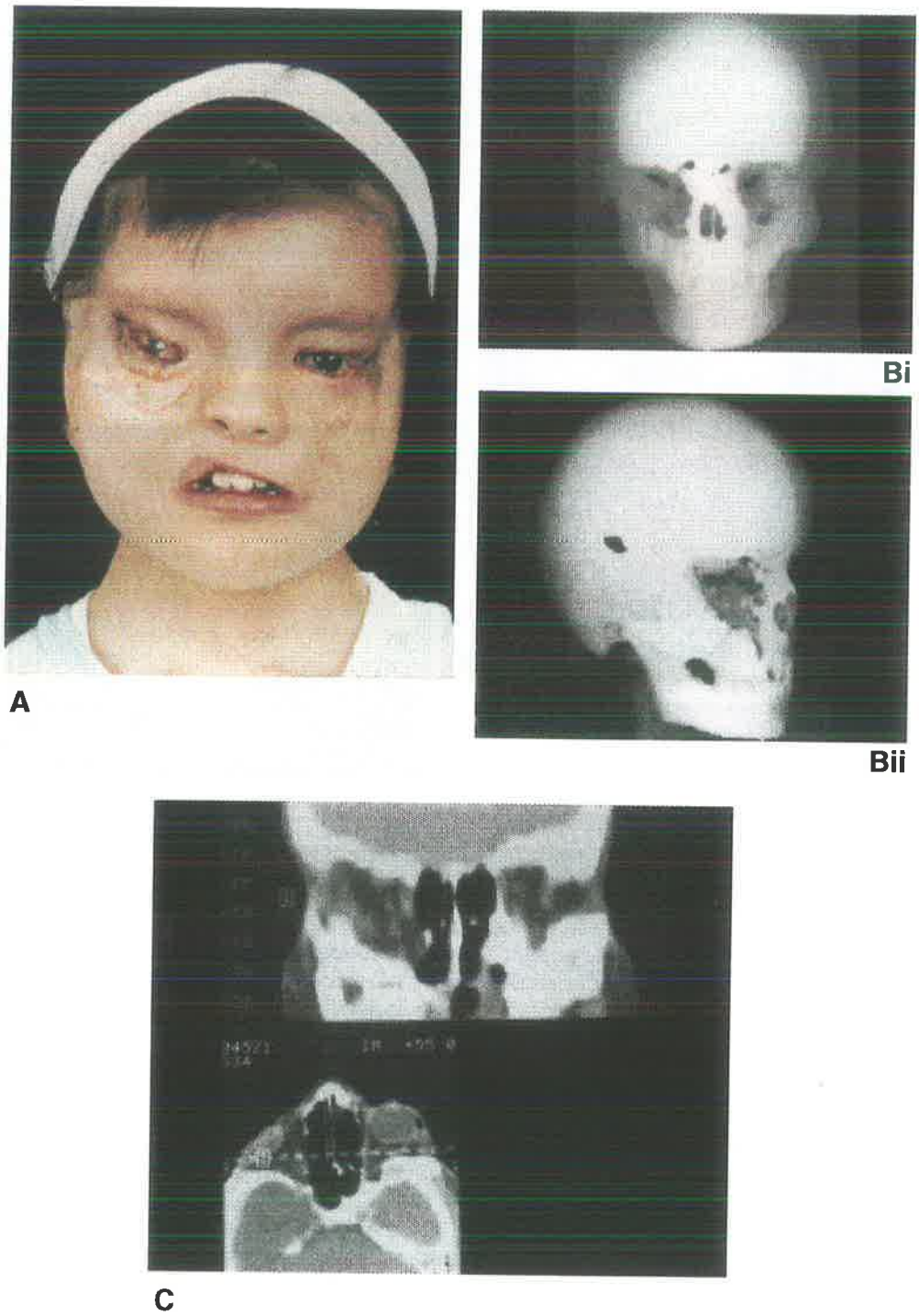

FIG. 11. A. *Nine–year–old Hong Kong Chinese girl with multiple repaired craniofacial clefts, including bilateral Tessier Number 9 clefts.* **B.** *Bony clefting radiates superiorly and posteriorly from the upper lateral orbit* (i-ii). **C.** *Gross bony deficiency in the region of the lateral orbital walls, with apparent posterior and lateral rotation of the axes of the orbits.*

Skeletal Characteristics. Complete absence of the bony lateral orbital wall and rim constitute the skeletal element of the Number 8 cleft. The lateral border of the orbit is formed by the greater wing of the spenoid from which small spicules of bone, which represent the rudimentary zygoma, may be found in Treacher Collins syndrome (Figs. 10B, 10C). The symmetry of the facial anomalies is reflected in the apparently normal symmetric anterior and middle cranial fossae.

Number 9

Tessier Description. This is an upper lateral orbital cleft. The soft tissue deformity is in the lateral one–third of the upper eyelid, and the bony cleft is through the superolateral orbital angle.

Soft Tissue Characteristics. Previous surgery obscures some of the clinical observations in the patient shown in Figure 11A. Microphthalmia is present. The superolateral bony deficiency of the orbits allows a lateral displacement of the globes. The lateral one-third of the upper eyelid and the outer canthus are distorted, thus preventing apposition to the globe. The upper eyelid does not have a true cleft. A soft tissue furrow radiates superiorly and posteriorly from the outer canthus into the temporoparietal hair–bearing scalp, which is bordered along its superior margin by the prolongation of the lateral one-third of the eyebrow. The temporal hairline projects forward bilaterally toward the scarred area of the repaired Number 9 clefts. There is no demonstrable facial nerve function in the forehead or upper eyelids.

Skeletal Characteristics. Skeletal clefting extends superiorly and posteriorly through the upper part of the greater wing of spenoid to the upper portion of the squamous temporal and adjacent parietal bones. The skeletal disturbance is more severe on the right side, where a bony defect is noted in the upper temporal squama (Fig. 11B). There is asymmetric hypoplasia of the greater wing of the spenoid with associated posterior and lateral rotation of the lateral orbital wall (Fig. 11C). Pneumatization of the body of the spenoid is symmetric and normal. Mild cranial base asymmetry is reflected in the pterygoid plates. The left pair is more laterally displaced from the midline. Skull vault plagiocephaly is evident with an apparent reduction in the anteroposterior dimension of the anterior cranial fossa.

Number 10

Tessier Description. In a Number 10 Tessier cleft there is an upper central orbital cleft with a cleft of the middle one-third of the upper eyelid, which often results in total ablepharia. The eyebrow is disrupted, being virtually absent medially, whereas the lateral portion angles upward toward the frontal hairline. There may be ocular anomalies, including colobomata of the iris. The skeletal cleft is through the midportion of the supraorbital rim, the adjacent frontal bone, and the orbital roof lateral to the supraorbital nerve. A frontal encephalocele frequently occupies the frontal bony cleft.

Soft Tissue Characteristics. The palpebral fissure is grossly elongated with an amblyopic eye displaced inferiorly and laterally. There is also a divergent squint of the right eye. The eyebrow is deficient medially and becomes thinned out laterally (Fig. 12A), where it is contiguous with a broad downward and forward projection of the frontotemporal hairline (this may be seen in both the Number 9 and 10 clefts.) A broad frontal encephalocele bulges forward from the middle one-third of the right forehead, supraorbital ridge, and orbital roof.

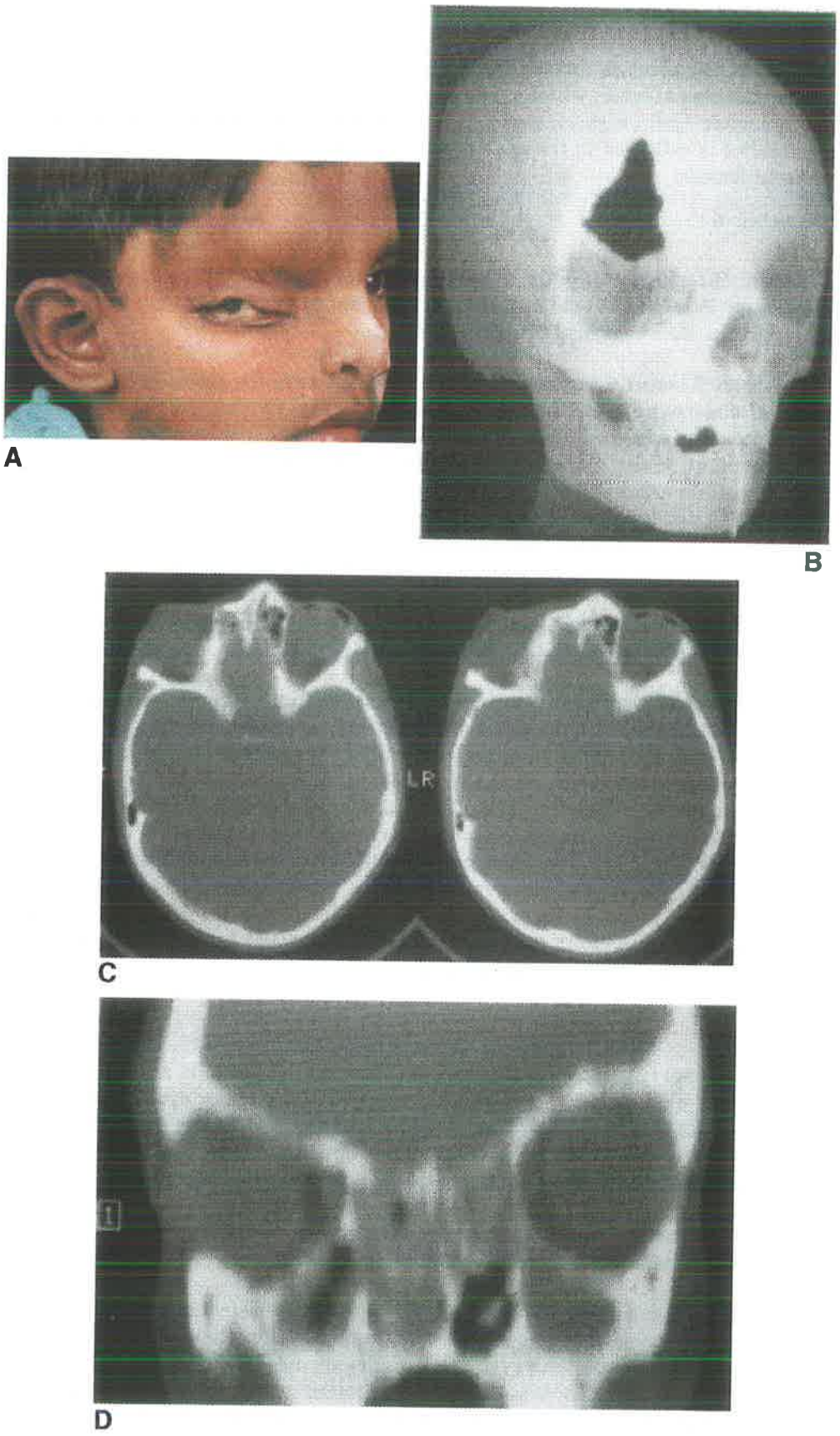

FIG. 12. A. *Eight–year–old Malaysian boy of Indian descent with multiple craniofacial clefts. including a Tessier Number 10 cleft on the right side.* **B.** *Frontal, supraorbital, and orbital roof bony cleft lateral to the supraorbital nerve.* **C.** *Axial two–dimensional CT scans through the orbits show the widening and lateral displacement of the cleft–side orbit.* **D.** *Asymmetry and inferior displacement of the cleft side orbit and anterior cranial fossa floor are evident on a coronal two–dimensional CT reformat.*

Skeletal Characteristics. The bony cleft, through which the frontal encephalocele presents, involves the anterior half of the orbital roof, the supraorbital rim, and two–thirds of the vertical height of the frontal bone lateral to the supraorbital nerve (Fig. 12B). The bony orbit is inferiorly displaced and widened with the lateral orbital wall shortened and laterally deviated (Fig. 12C). Similar distortion of the anterior cranial fossa is evident, being broader and more flattened on the affected side (Fig. 12D). The calvarium above the level of the cleft and the cranial base below is symmetric.

Number 11

Tessier Description. An upper medial orbital cleft produces a cleft of the medial one-third of the upper eyelid that extends through the eyebrow into the frontal hairline. The skeletal element of the cleft in the region of the frontal process of the maxilla may either pass lateral to the ethmoid, through the supraorbital rim, or it may pass through the ethmoidal labyrinth to produce orbital hypertelorism. This cleft usually accompanies the Number 3 cleft.

Soft Tissue Characteristics. The soft tissue features include a cleft of the medial portion of the upper eyelid, an irregularity in hair orientation at the medial end of the eyebrow, and a long tongue-like projection of the frontal hairline onto the forehead (Fig. 13A).

Skeletal Characteristics. There is a mild flattening of the frontal process of the maxilla and extensive pneumatization of both the ethmoidal and frontal sinuses, both of which are more prominent on the cleft side (Fig. 13B). No bony clefting of the supraorbital rim or frontal bone is evident. The cranial base and spenoid architecture, including the pterygoid processes, are symmetric and normal (Fig. 13C). No associated Number 3 cleft is found in this patient.

Number 12

Tessier Description. There is a soft tissue cleft medial to the inner canthus with a cleft of the root of the eyebrow. The frontal process of the maxilla is flat and broadened, and the ethmoid labyrinth is increased in transverse dimension, thereby producing orbital hypertelorism. The cribriform plate is of normal width. The frontal sinus is enlarged. Even though the frontal bone is flattened, bony clefts with encephalocele have not been observed.

Soft Tissue Characteristics. There is a lateral displacement of the inner canthus with a mild thinning, aplasia, or irregularity of the medial end of the eyebrow. There are no eyelid clefts (Fig. 14A). The soft tissue contour of the forehead is normal, with only a short downward prolongation of the paramedian frontal hairline to mark the superior extent of the soft tissue cleft.

Skeletal Characteristics. Flattening of the frontal process of the maxilla, an increase in the transverse dimension of the ethmoid sinus, and a laterally convex bowing of the medial orbital wall produce orbital hypertelorism (Fig. 14B). Superiorly there is a minor flattening of the frontal bone medially, and the nasofrontal angle is somewhat obtuse. The extensive pneumatization of the sinuses on the cleft side extends backward through the frontal and ethmoid sinuses and into the spenoid sinus. The anatomy of the spenoid, including the pterygoid processes, is otherwise normal. The anterior and middle cranial fossae floors are both broadened on the cleft side with minor widening of the cribriform plate.

A

B

C

FIG. 13. A. *Twenty–one–year–old Malaysian Indian man with bilateral facial microsomia and a left–sided Tessier Number 11 cleft.* **B.** *Slight paramedian flattening of the nasal root and supraorbital ridge with extensive frontal sinus pneumatization.* **C.** *Three–dimensional CT reformat view of the symmetric anterior cranial fossa floor.*

Number 13

Tessier Description. There is a paramedian frontal encephalocele and a soft tissue cleft that passes medial to an intact eyebrow. The frontal bone shows a paramedian bony cleft with an associated encephalocele. The olfactory groove, cribriform plate, and ethmoid sinus are all increased in transverse diameter, resulting in hypertelorism.

Soft Tissue Characteristics. The patient in Figure 15A shows a Number 1 facial cleft combined with a Number 13 cleft above. There is a large lipoma of the dorsum of the nose that extends onto the lower frontal bone above, and a characteristic hypertelorism is more marked on the cleft side. The cleft extends medially to the undisturbed eyebrow to end in a short paramedian frontal widow's peak.

Skeletal Characteristics. The bony cleft begins in the region of the nasal bone and extends superiorly through the full height of the frontal bone. Posteriorly, the cleft extends through the cribriform plate and ethmoid sinus as far as the lesser wing and body of the spenoid. The pterygoid processes are anatomically normal, but they are displaced laterally from the midline on the cleft side. There is orbital hypertelorism below and asymmetry of the floor of the anterior cranial fossa above (Fig. 15B).

Number 14

Tessier Description. This midline cranial cleft usually occurs with a midline facial cleft that completes a median craniofacial dysraphia. A broad nasal root and bifid nose are associated with orbital hypertelorism and a median frontal encephalocele. The frontal bone abnormality varies from a minor flattening to a large midline defect. There is an increased distance between the olfactory grooves. The crista galli is widened, duplicated, or in some cases absent. Marked inferior prolapse of the enlarged ethmoid bone occurs with orbital hypertelorism.

Soft Tissue Characteristics. The severe orbital hypertelorism is associated with a broad flattening of the glabella and extreme lateral displacement of the inner canthi. The periorbita, including the eyelids and eyebrows, are otherwise normal (Fig. 16A). A long midline projection of the frontal hairline marks the superior extent of the soft tissue features of this midline cranial cleft.

Skeletal Characteristics. The median frontal defect delineates the region through which the frontal encephalocele herniates. The lateral segments of the frontal bone sweep upward from the region of the intact glabella and are flattened laterally (Fig. 16B). No pneumatization of the frontal sinus is evident. The crista galli and the perpendicular plate of the ethmoid are bifid (Fig. 16C). Just as the ethmoid, including the cribriform plate, is widened and caudally displaced, the spenoid sinus is broadened and extensively, but symmetrically pneumatized. The lateral rotation of the greater and lesser wings of the spenoid results in a relative shortening of the anteroposterior dimension of the middle cranial fossa. The floor of the anterior cranial fossa is upslanting from its medial aspect to its lateral aspect, with a harlequin appearance on the coronal scan (Fig. 16D).

Discussion

The use of combinations of anatomic, embryologic, developmental, and eponymous terms has limited many attempts to classify congenital craniofacial clefting. The reports of Morian (1887), Harkins et al (1962), and Boo–Chai (1969) have not taken all variants into account. Attempts to correlate morphologic observations with embryologic and developmental disturbances have been made by Sanvenero–Rosselli (1953), Karfik (1966), Gorlin et al (1971), and Van der Meulen et al (1983).

In contrast, the Tessier classification of craniofacial clefts offers a numbering system that centers on the orbit and delineates consistent anatomic pathways for craniofacial clefts. The radiographic imaging techniques available to Tessier were far less sophisticated than those available today. His original assessments of the skeletal abnormalities were largely based upon clinical impression and two–dimensional radiographs. Computed three–dimensional imaging has now added a new tool for the anatomic description of craniofacial clefts.

The availability of two- and three–dimensional computed tomographic reconstructions of each cleft type has further defined the patterns of skeletal disturbance. As an adjunct to the standard three–dimensional images, serial coronal, oblique, and sagittal two-dimensional reformats prove a finer radiographic probe to "track" the cleft through the depth of the craniofacial skeleton. CT imaging allows the delineation of even marginal skeletal distortions and of any associated abnormalities within adjacent soft tissues.

The complete clinical documentation of a complete series of Tessier clefts has both confirmed and added to many of Tessier's descriptions. Among the superficial indicators of clefting were irregularities in the frontal and temporal hairline. These hairline indicators represented the superiormost markers of soft tissue disturbance in the lateral and superior cranial clefts (Numbers 7 through 14) (Moore et al, 1988). On occasion, as with the Number 11 cleft shown above (Fig. 13A), the hairline marker was the most prominent soft tissue finding.

As part of his numeric cleft classification, Tessier suggested that the anterior components of clefts that traverse both the cranium and the face occur along regular axes such that the sum of their designated numbers would total 14. Although some clefting patterns in our series conform to this rule, multiple clefts of the cranium and face were not uncommon. The extensive radiologic examination of this series not only demonstrated the three–dimensional extent of the clefts, but it also revealed a previously unsuspected spectrum of cleft combinations. Thus, the idea of "time zones," postulated vascular causation, and global absolutes such as the association of anophthalmia with particular clefts were not always confirmed in this series (Tessier, 1976a).

This review again distinguishes between the median and paramedian craniofacial clefts and the group of frontoethmoidal meningoencephaloceles. The latter is associated with a craniofacial skeleton that is normal in content but displaced in position by the soft tissue encephalocele. Craniofacial clefts associated with encephaloceles show skulls that are markedly deficient in three dimensions, both in their soft tissue and skeletal makeup (David et al, 1984). Frontoethmoidal meningoencephaloceles also lack the frontal hairline indicator seen with the midline cranial clefts (Moore et al, 1988).

In addition to the documentation of the superficial craniofacial skeletal distortion associated with craniofacial clefts, the two– and three–dimensional CT images reveal previously unrecognised associated cranial base dysmorphology. From the close examination of the spenoid, which is the "keystone" of the cranial base, the majority of facial clefts in our series were seen to have some distortion in the cranial base. These were manifest as asymmetries in the shape or size of the greater or lesser spenoid wings and frequently reflected in the pterygoid processes, which were often unequally displaced from the midline or asymmetric in their anatomy. The spenoid, and in particular its pterygoid processes, which collapse into or away from medially or laterally located clefts, may be the posterior extension of the cleft. Such medial or lateral displacement and distortion of the pterygoid plates could then be markers of the axis about which the clefts are centered. Correspondingly, asymmetries of the anterior and middle cranial fossae and calvarial distortions above could often be identified even in isolated facial clefts, without evidence of

associated cranial clefts. Tessier selected the orbit as the axis about which the numbering of clefts was centered. He speculated that all facial clefts had their origins in the cranial base (Tessier, 1976b). However, the speculation of such principles of embryologic causation based on small series is a tenuous position and could be open to criticism.

FIG. 14. A. *Eleven–year–old Malaysian boy with right–sided Tessier Number 2–12 clefts* **B.** *Worms–eye three–dimensional CT reformat shows the mild flattening and widening of the frontal process of the maxilla and underlying ethmoids on the cleft side.*

The data reported above demonstrate that the visible components of craniofacial clefts do not necessarily reflect their true extent. It is valuable to maximise the amount of diagnostic information available prior to operation if one is to attempt complete correction of the abnormality. In conjunction with a thorough assessment, radiologic studies that include two– and three–dimensional CT images help the reconstructive surgeon to predetermine the staging of operations, the placement of incisions, the requirements for soft tissue augmentation, the amount and placement of bone grafts, the pattern of osteotomies, and the site and type of skeletal fixation to be employed.

The volume of bone grafts required in the repair of such clefts is often surprisingly large. A more accurate pre–operative assessment of the skeletal distortion, bone graft requirements, and their optimal placement and fixation improves the precision of the surgical correction. Three–dimensional scans are also the easiest reference form of radiology in the operating room because they allow the surgeon to assimilate rapidly the pattern and extent of skeletal disruption.

A

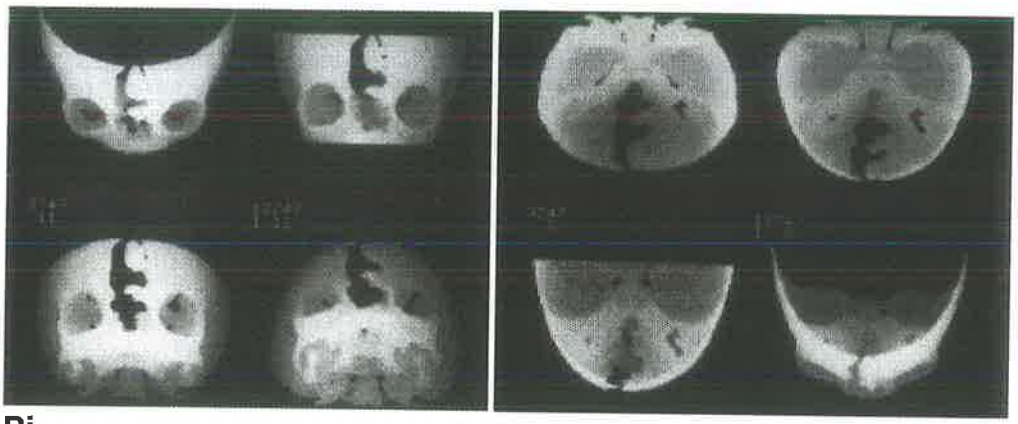

Bi Bii

FIG. 15. A. *Three–month–old Australian girl with right–sided Tessier Number 1–13 clefts.* **B.** *three–dimensional CT reformat sequence graphically demonstrates the superficial and deep dimensions of the Tessier Number 13 cleft* (i ii).

The rarity of severe craniofacial clefts has made the collection and complete anatomic documentation of a large series difficult. Preoperative and postoperative sequential CT scans with three–dimensional reconstructions of large series will provide the basis for quantitative analysis of surgical interventions and allow improved understanding of the growth dynamics of the severely malformed craniofacial skeleton. Only with complete radiologic and operative examination of these rare craniofacial malformations can we appreciate the enormity of the reconstructive challenge. The assessment of this understanding and of our therapeutic interventions will only come with the addition of a fourth dimension—time.

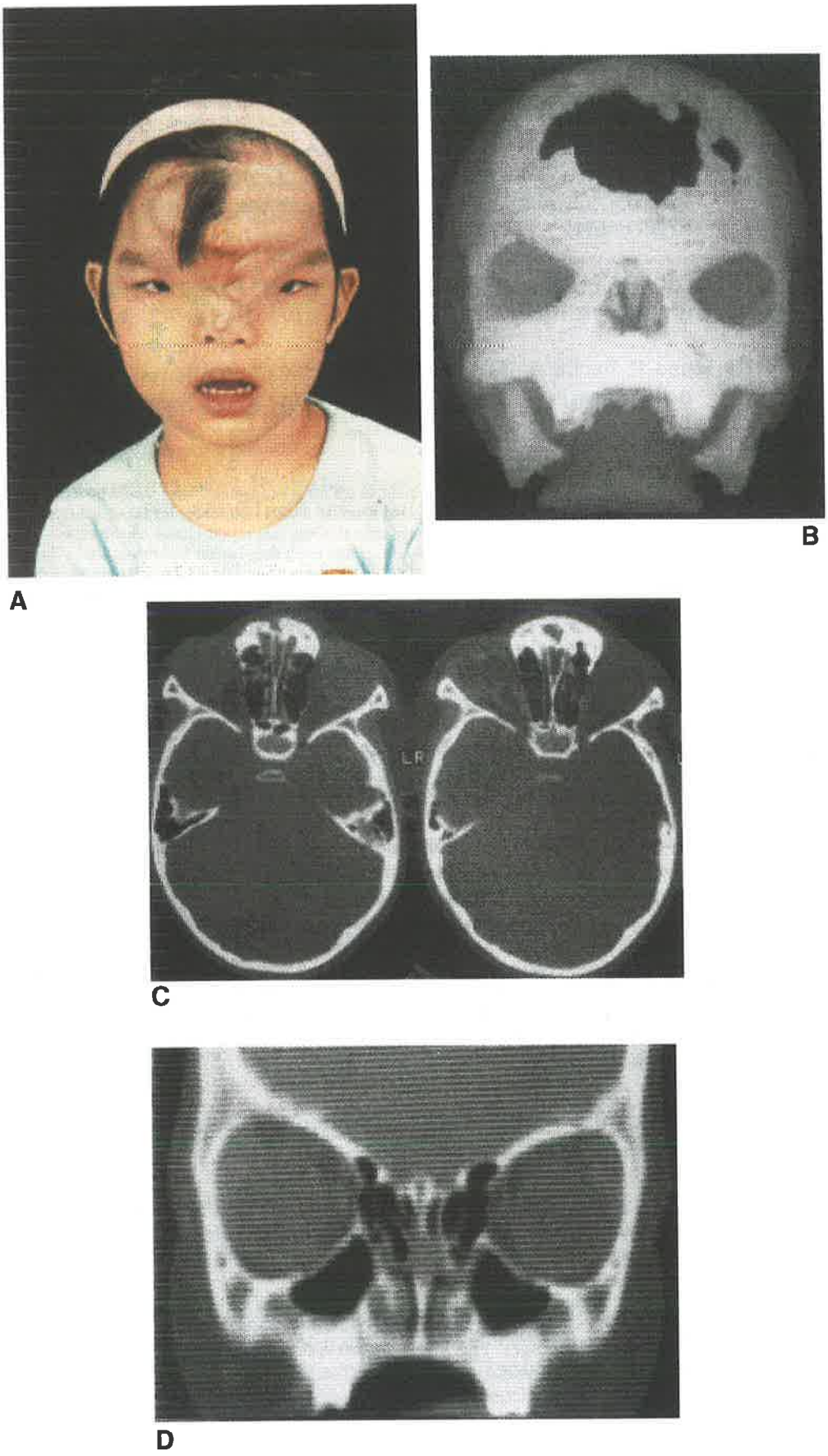

FIG. 16. A. *Four–year–old Malaysian girl with previously operated midline craniofacial clefts of the Tessier Number 0–14 type.* **B.** *Three–dimensional CT reconstruction reveals the orbital hypertelorism below and extensive median frontal defect above.* **C.** *Marked widening and extensive pneumatization of the ethmoid sinuses, with associated bifid perpendicular plate.* **D.** *Coronal two–dimensional CT reformat exposes the inferior prolapse of the widened ethmoid sinus with a characteristic harlequin appearance.*

References

1 Boo–Chai K. (1969). The transverse facial cleft: its repair. Br J Plast Surg 22:119–124.

2 David DJ, Sheffield L, Simpson D, White J. (1984). Frontoethmoidal meningoencephaloceles: morphology and treatment. Br J Plast Surg 37:271–284.

3 Gorlin RJ, Cervenka J, Pruzansky S. (1971). Facial clefting and its syndromes. Birth Defects Original Article Series 7(7):3–49.

4 Harktns CS, Berlin A, Harding RL, Longacre JJ, Snowrasse RM. (1962). A classification of cleft lip and cleft palate. Plast Reconstr Surg 29:3 1–39.

5 Karfik V. (1966). Proposed classification of rare congenital cleft malformations in the face. Acta Chir Plast 8:163–168.

6 Kawamoto HK. (1976). The kaleidoscopic world of rare craniofacial clefts: order out of chaos (Tessier classification). Clin Plast Surg 3:529–572

7 Marsh JL, Vannier MW. (1983). The third dimension in Craniofacial surgery. Plast Reconstr Surg 71:759–767.

8 Moore MH, David DJ, Cooter RD. (1988). Hairline indicators of craniofacial clefts. Plast Reconstr Surg 82:589–593.

9 Morian R. (1887). Ueber die schrage Gesichtsspalte. Arch Klin Chir 35:245.

10 Raulo Y. Tessier P. (1981). Mandibulo-facial dysostosis analysis: principles of surgery. Scand J Plast Reconstr Surg 15:251–256.

11 Sanvenero–Rosselli G. (1953). Developmental pathology of the face and the dystrophic syndrome—an essay of interpretation based on experimentally produced congenital defects. Plast Reconstr Surg 11:338.

12 Tessier P. (1976a). Anatomical classification of facial, cranio-facial and latero–facial clefts.. J Maxillofac Surg 4:69–92.

13 Tessier P. (1976b). Anatomical classification of facial, craniofacial, and laterofacial clefts. In: Tessier P. ed. Symposium on plastic surgery in the orbital region. St. Louis: CV Mosby:189–198.

14 Van Der Meulen IC, Mazzola R, Verney–Keers C, Stricker M, Raphael B. (1983). A morphogenetic classification of craniofacial malformations. Plast Reconstr Surg 71:560–572.

Rare Craniofacial Clefts: Principles of Management

D.J. David
Australian Craniofacial Unit
North Adelaide, South Australia (AUS)

Introduction

In the craniofacial region, the term cleft is used to imply two essential features:

— an absence of tissue, whether soft tissue or skeletal.

— hypoplasia of tissues at the margins of the cleft.

Clefting is not merely an extreme form of the hypoplasia spectrum, and not all forms of hypoplasia are associated with clefting; however, clefts, even in microform, always show hypoplasia.

The rarer and more complex clefts of the craniofacial soft tissue and skeleton are described by a confusing variety of eponymous, anatomical and embryological descriptions. Subgrouping to the anatomical location of deformity produces a clustering of patterns of deformity that aids clinical assessment and treatment planning. (Tessier). Thus clefting of the upper face is associated with cranial involvement and orbital dystopia; lateral facial clefting is predominantly a derangement of the skeleton with little soft tissue disturbance and medial facial clefting is predominantly soft tissue disruption with a lesser degree of bony deformity.

Material

The Australian Craniofacial Unit has since 1975 seen 300 patients which might be considered rare craniofacial clefts according to Tessier's classification. 24 of these were hemifacial microsomia, 33 Treacher Collins Syndrome, 82 fronto–ethmoidal meningo–encephaloceles and 91 rare craniofacial clefts. It is this group which demands a more intensive study.

Classification

The rarity and variety of presentations of the clefting disorders of the craniofacial region has long prevented the establishment of a meaningful and comprehensive yet manageable classification system. Many anatomical descriptions, eponymous terms and developmental explanations have been applied, but none are all–encompassing.

The most widely accepted classification scheme is that reported by Tessier (1976), who devised an orderly numbering system centred on the orbit identifying consistent anatomical pathways of soft tissue and skeletal disruption. Although this classification was largely a superficial and two dimensional descriptive classification, applications of 3D CT techniques, and more extensive surgical exposures have widened and enhanced knowledge of the extent of the disordered morphology in craniofacial clefting. (David et al., 1989).

Proceedings of 4th International Congress of The International Society of Cranio–Maxillo–Facial Surgery 119–122

Assessment

The very nature of these deformities, their rarity and the complexities of involvement of both facial form and function, of calvarium, cranial base, orbit and dental occlusion, demand the comprehensive multidisciplinary team approach as practised in modern craniofacial units. Complete clinical examination by the relevant medical and dental specialists is essential, with full assessment by a medical geneticist. Extensive photographic documentation with a detailed radiological examination incorporating cephalometric radiographs, axial and coronal 2D CT scans, with 3D reconstructions of the CT data, permits an objective analysis of the deformity. MRI, and complex manipulation of basic CT data, relate the soft tissue abnormalities to the underlying skeletal disturbances and will also detect associated brain malformations, such as cerebral hernias in the various cranial clefts.

By linking these complex clinical and radiological techniques of assessment to the timing of presentation of individual cases, a logical programme of treatment can be developed. Definitive surgical results are obtained only at the completion of facial growth; however separate regions of the facial skeleton undergo periods of rapid growth at differing times and it is necessary to establish an ordered approach to management of deformities of the forehead and orbits, midface and finally the mandible.

Treatment

Modern surgical techniques of wide exposure, craniofacial osteotomies and stable internal fixation permit the predictable correction of virtually any craniofacial deformity. Decision making revolves around the timing of the intervention in the developing and growing face. The severity of the deformity, the inherent growth potential of the disordered face and the various psychological influences, all influence the timing of intervention. The treatment programme must take into account the need to normalise skin, subcutaneous tissues, muscle and skeletal elements.

Surgery on the calvarium is ideally performed in the first two years of life to maximise the implements of the developing brain, whilst correcting the major disfiguring cranial abnormalities and minimizing any attendant psychological reactions.

Correction of orbital dystopia and hypertelorism is ideally done before the completion of the facial growth, with orbitofacial osteotomies carefully placed above the level of the developing secondary dentition, about five years of age. (Fig. 1).

Upper and lower jaw osteotomies, whilst occasionally requested for psychological reasons, are delayed until the completion of facial growth and the eruption of the secondary dentition. Early jaw surgery risks interference not only with the unerupted secondary dentition, but also interference with the inherent growth potential, and are likely to need revision because of subsequent facial growth.

By grouping together various clefts according to their common features a general treatment philosophy is possible.

FIG. 1. *Child born with Tessier 13 and 1 clefts. Preoperative and post-operative photograph.*

a) Cranial Clefts (Tessier 10–14)

The principle anatomical disturbance is orbital dystopia, including hypertelorism, with a wide range of frontal bone anomalies and defects. Dural herniations, median bony spurs embedded in the falx and abnormal venous channels are especially important from the neurosurgeons viewpoint.

The recommended treatment plan embodies early correction of the frontal bone defect with correction of hypertelorism to follow at approximately 5 years of age. The latter will invariably require medial and lateral canthopexies together with augmentation of the three dimensional hypoplastic nasal complex. Subsequent squint surgery is often required.

The results of hypertelorism correction in the cranial clefts are seldom aesthetically satisfactory. This is in contrast to the outcome of treatment of hypertelorism associated with fronto–ethmoidal meningo–encephaloceles. Frequent revision of both the facial skeleton and soft tissues is required to achieve the optimum result, often over a time span of a further 5-10 years.

Efforts are being made with the advent of tissue expansion to use this form of treatment to release some of the soft tissue tensions in the region of the zygomatic arch and the temporal fossa.

b) Lateral Facial Clefts (Tessier 6/7–9)

These clefts, though occasionally occurring in isolation, are most commonly manifest in Treacher Collins Syndrome and craniofacial microsomia. The treatment regime is that outlined for those conditions.

The Tessier number 9 cleft, although the rarest of all clefts, requires bony orbital surgery similar in nature, but more extensive in extent, than that for Treacher Collins Syndrome.

The principles of tissue expansion are applied to the anophthalmic orbit in an attempt to simulate the growth of the eye.

c) Median Facial Cleft (Tessier 0–6/7)

Early treatment is directed towards correcting the principle clinical disturbance — the soft issue deformities of the upper lip, nose and medial portion of the lower eyelid. Primary closure of the cleft lip deformity with reconstitution of the labial muscles is performed in concert with local flap repair of soft tissue nasal and lower eyelid defects. With further growth, frequent revisions and the addition of tissue expansion of colour-appropriate local skin are required. These, done in concert with inlay and onlay bone grafting of the maxillary alveolar and maxillary body defects, permit bony separation of oral cavity, nose and orbit, with good quality soft tissue cover — ideally timed at the eruption of the canine adjacent to the cleft at age 8-12 years. (Fig. 2) Subsequent combined orthodontic/orthognathic surgical management permits the production of appropriate facial aesthetics and function, at the completion of facial growth. Final revisionary nasal surgery completes most treatment protocols.

Conclusion

The basic biological problem is not solved by surgery at any stage. Multiple operations are necessary through the growing period of the patient. The definitive result is possible only when growth is complete.

FIG. 2. *Child born with Tessier 4 cleft on the right and Tessier 5 cleft on the left. Photograph shows following treatment with tissue expanders in order to facilitate bone grafting.*

References

1. Tessier P.: Anatomical classification of facial, craniofacial and laterofacial clefts J. Maxillofac. Surg. 1976a; 4: 69–92.

2. David D.J., Moore M.H., Cooter R.D.: Tessier clefts revisited with a third dimension Cleft Palate J 1989; 3: 163–185.

Soft tissue expansion in the management of the rare craniofacial clefts

M. H. Moore, J. A. Trott and D. J. David
Australian Cranio–Facial Unit, Adelaide Children's Hospital, North Adelaide, Australia

Summary

Management of the rare craniofacial clefts requires correction of both the soft tissue and skeletal hypoplasia. Tissue expansion of adjacent and distant soft tissue has been used to reconstruct these facial clefts with like quality tissue. Additionally, such soft tissue expansion permits tension free reconstruction of the skeletal clefts by osteotomy and bone graft.

The rare craniofacial clefts manifest the most extreme examples and variety of craniofacial dysmorphology. These clefts by definition may involve all soft tissue and skeletal elements and are attended by hypoplasia of the margins throughout the three–dimensional extent of the cleft (Tessier, 1976; David et al., 1989). Such tissue deficiency distorts the craniofacial growth potential and demands sequential therapeutic intervention to optimise the long-term functional and aesthetic outcome.

Where our understanding of the application and timing of craniofacial osteotomies and bone grafting in the rare clefts has progressed, long–term outcome is finally determined by the quality of the overlying soft tissues and skin.

The soft tissue and skin deficiency demands reconstruction ideally with tissue of like texture, consistency and, on the face most especially, colour. Tissue expansion is an evolving technique for reconstructing and resurfacing defects in head and neck and craniofacial surgery (Argenta and Vander Kolk, 1987; Antonyshyn et al., 1988).

This paper details our experience with tissue expansion in the management of rare craniofacial clefts, identifying potential roles for this technique in these four–dimensionally challenging deformations.

Subjects and methods

Since 1987, at the Australian Cranio-facial Unit, tissue expansion has been incorporated in the surgical management of 9 patients with rare craniofacial clefts. Many had undergone multiple previous surgical procedures—soft tissue and bony—both in this unit and elsewhere, but presented still requiring major soft tissue and skeletal reconstruction. No two cases were similar in either their cleft pattern or age of presentation.

Tissue expanders have been employed in this series of patients for a variety of reconstructive tasks outlined as follows.

The reconstruction and resurfacing of soft tissue structures deficient or absent through clefting

This conventional tissue expansion approach of stretching uninvolved adjacent skin permits reconstruction of a variety of structures and defects by simple advancement or transposition into the cleft area. In both cleft and non–cleft individuals, pre–expansion of the forehead provides sufficient extra colour–matched skin for major nasal reconstruction with primary closure of the donor site (Toth et al., 1990). In addition, application to multiply operated cleft cases permits excision of grossly scarred cleft soft tissues and resurfacing with soft tissues whose colour match, contour and vascularity is significantly improved.

Case IK. A 21–year–old Yugoslavian male presented with Tessier number 2, 3 and 12 clefts together with a left hemifacial microsomia, having undergone multiple previous soft tissue and skeletal operative procedures in his home country. There remained marked facial asymmetry, dystopia of the anophthalmic left orbit and absence of the left heminose (Fig. 1A).

Restoration of the skeletal symmetry was achieved via a transcranial orbital dystopia correction in concert with a Le Fort I osteotomy and bilateral mandibular ramus osteotomies to centralise the lower face. At the same procedure a 50 cc tissue expander was inserted over the stable right forehead— the transcranial orbital dissection having been performed via a left unifrontal bone flap. Two months later a Converse–type scalping nasal reconstruction was undertaken, extending the flap down through the relatively elongated eyebrow onto the upper eyelid. The forehead donor defect was closed directly without requirement for grafting. The flap was divided and inset at 2 weeks.

Two–year follow–up without revision shows preservation of nasal form, albeit less than the ideal that may have followed a series of minor revisions (Fig. 1B).

FIG. 1. A. *21–year–old with multiply operated Tessier number 2, 3, 6, 7, 8 and 12 clefts, requiring correction of the facial asymmetry and absent left heminose.* **B.** *2–year follow–up after heminose reconstruction with a pre–expanded Converse scalping flap allowing direct closure of the right forehead donor site.*

Provision of soft tissue coverage and increased vascularity for inlay and onlay bone grafting

Rare clefts, particularly the medial facial (Tessier numbers 0–6) or oro–naso–ocular clefts require for their ideal reconstruction combinations of inlay and onlay bone grafting. Inherent to such skeletal reconstruction is the provision of tension–free soft tissue cover of adequate vascularity (Sasaki and Pang, 1984).

Case SK This 7–year–old Malay Indian child with Tessier number 4 cleft on the right and Tessier number 5 cleft on the left returned for further bone grafting of the cleft maxillae and orbito–zygomatic complex. Despite bone grafting of the clefts on two previous occasions in concert with local cheek rotation flaps, he remained deficient in both skeletal and soft tissue elements (Fig. 2A, B).

Tissue expanders were inserted into both cheeks, under skin which had been raised as a rotation flap on two previous occasions (Fig. 2C). After satisfactory soft tissue expansion, iliac bone graft was employed as both inlay and onlay to correct the bony cleft deficiency, with tension–free soft tissue coverage, from further medial cheek rotation. This corrected the vertical soft tissue hypoplasia over the midface and symmetrically located the medial and lateral canthi (Fig. 2D, E).

Further soft tissue and skeletal growth is envisaged with subsequent mid and lower facial growth.

Release of soft tissue tractional forces restricting hypertelorism and orbital dystopia correction

Analysis of the rare median and paramedian cranial clefts associated with hypertelorism revealed that a major limiting factor and determinant of outcome after orbital osteotomy and medial translocation is the posterolateral traction of the temporo–zygomatic soft tissues on the orbital soft tissues and skeleton. In such cases there exists a relative foreshortening in the distance between the lateral canthus and the superior attachment of the external ear compared to the non–cleft side (Fig. 3A, C). Thus, although not inherently an element of the cleft, such distant soft tissue deficiency requires correction to facilitate ideal correction of hypertelorism. Subperiosteal expansion of the temporo–zygomatic soft tissues prior to orbital translocation releases those distorting laterally pulling soft tissues and permits stable, tension–free orbital skeletal and periorbital soft tissue correction.

Case KP. This Indian child with right-sided Tessier 3, 9, 10, 11 and 12 clefts presented initially to the Australian Craniofacial Unit at age 11 years, having previously only had his unilateral cleft lip and palate repaired (Fig. 3A, B, C).

Examination revealed a large right frontal encephalocele with extreme hypertelorism and right orbital vertical dystopia. The right eye was totally keratinised and the right palpebral fissure grossly elongated and inferolaterally displaced. The latter resulted in an apparent anteroposterior foreshortening of the temporo–zygomatic soft tissues.

At the initial surgery, via a coronal incision, a 70 cc expander was inserted subperiosteally in the region of the zygomatic arch and body (Fig. 3D). Six weeks later after expansion was completed, he underwent transcranial correction of the frontal clefts, hypertelorism and orbital dystopia. Orbital translocation was achieved without tension, allowing accurate localisation of the orbital soft tissues. Subsequently he underwent enucleation of the right eye with insertion of a prosthesis, together with a full thickness graft eyebrow reconstruction (Fig. 3E, F, G).

Further surgery is anticipated with ongoing facial growth.

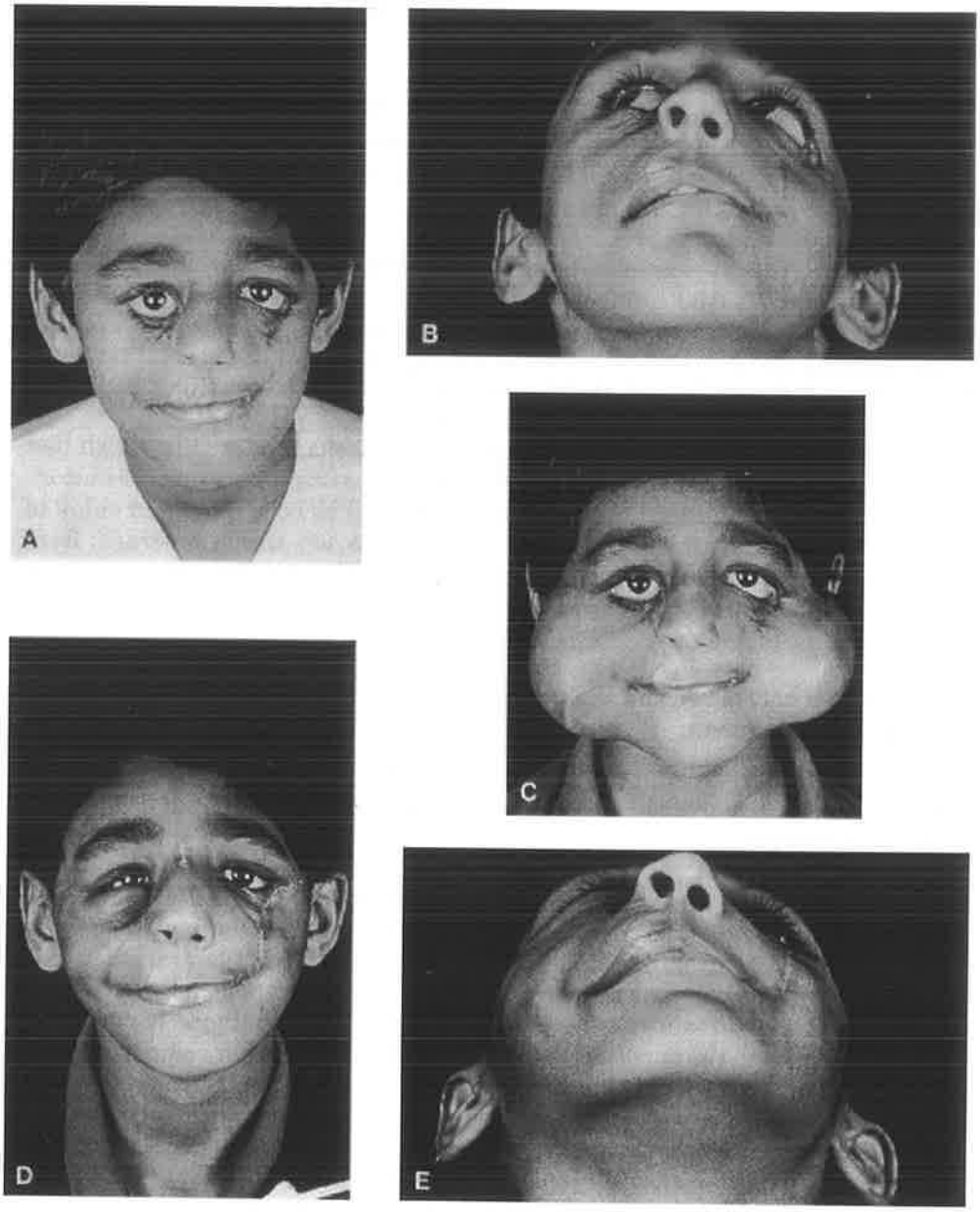

FIG. 2. A. B. *7-year-old child with right sided Tessier number 4 cleft and left sided Tessier number 5 cleft after multiple previous soft tissue revisions. Persistent soft tissue and skeletal deficiency of the midface and orbitozygomatic regions.* **C.** *Following insertion and expansion of tissue expanders in both cheeks.* **D. E.** *Early postoperative views after further bone grafting and rotation of expanded cheek flaps.*

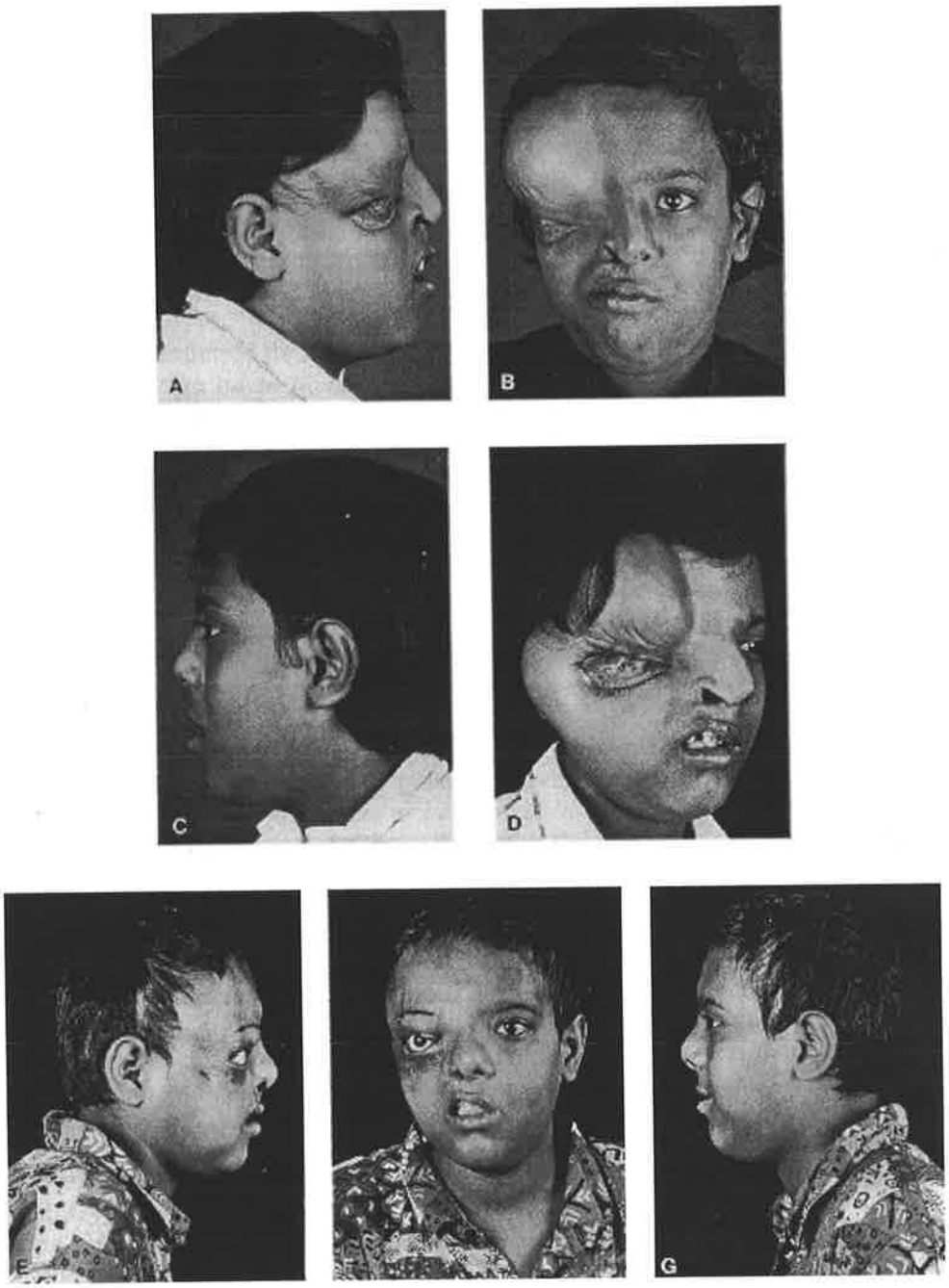

FIG. 3. A. B. C. *11–year–old with right sided Tessier 3, 9, 10, 11 and 12 clefts. Lateral views confirm the relative antero-posterior foreshortening of the temporo–zygomatic soft tissues on the involved side.* **D.** *Tissue expansion of the temporo–zygomatic soft tissues prior to hypertelorism correction.* **E. F. G.** *Early postoperative views confirm the tension free reconstruction of the right periorbital soft tissues after osteotomy and medial translocation of the right orbit.*

Discussion

The rare craniofacial clefts, by definition, may variably involve all the elements of skin, soft tissues and skeleton, with attendant hypoplasia of marginal tissues and a disturbance of growth potential throughout the three–dimensional extent of the cleft. The diagnosis, assessment and treatment of these cases is not then directed at a single–stage surgical correction, but demands a planned, staged, sequential approach to produce the ideal end–result at the completion of facial growth.

Reconstruction must consider the restoration of all elements—skin, soft tissue and skeleton, in a complex interrelated fashion at an age–appropriate time to optimise outcome. Osteotomy and bone grafting of the craniofacial skeleton with stable internal fixation can be performed with an acceptably predictable result, even in clefts. The timing of intervention and pattern of osteotomy is individualised for each of the rare cleft deformities, but logically involves orbital osteotomy early before age 5 years, with delay of midfacial and mandibular osteotomy until the completion of facial growth. The outcome, both functional and aesthetic, is however principally determined by the quantity, quality and redraping of the soft tissues. Reconstruction with soft tissues comparable in colour and consistency, and free from distorting tractional forces, idealises restoration of facial features and permits tension-free siting of vital soft tissue landmarks.

Where the cleft deformity is minimal or the soft tissue discrepancy small, local flaps will frequently suffice, albeit requiring revision in the face of subsequent facial growth. Tissue expansion of facial, neck or scalp soft tissues allows for the resurfacing of more extensive cleft deformities with colour appropriate skin.

To date, tissue expansion has been reported successfully used for soft tissue nasal reconstruction in clefts, just as for the non–cleft population, i.e. midline forehead rhinoplasty with pre–expansion of the forehead to allow primary closure (Toth et al., 1990). In this series, nasal reconstruction from tissue expanded forehead skin has been similarly performed, extending its versatility to pre-expansion of a Converse scalping forehead flap used for a heminasal reconstruction. Here, the expander was inserted at the same operation where a major cranio–orbital osteotomy was performed and rigidly fixed. The subsequent nasal reconstruction has not contracted significantly.

Rare clefts of the medial and lateral face almost uniformly require onlay and inlay bone grafting to restore the bony anatomy of the midface and orbitozygomatic region. Successful bone grafting demands an adequate surrounding vascularity and soft tissue envelope free from tension, conditions frequently deficient in the cleft tissues, whether multiply operated or not. Tissue expansion provides for both increased vascularity and a tension–free environment into which bone graft can be placed (Sasaki and Pang, 1984). Indeed, sequential tissue expansion may be the ideal adjunct to the required staged bone grafting and osteotomy in these cleft cases. Complex midfacial clefting, producing as it does three dimensional distortion of growth, demands repeated bone grafting and hence soft tissue augmentation during the periods of accelerated facial growth.

The versatility of tissue expansion is widened by use of tissues distant from the cleft to permit tension free orbito–facial skeletal osteotomy and translocation. In particular, the temporo–zygomatic soft tissues in cases of rare clefting with hypertelorism, whilst not an intrinsic feature of the clefting process, are foreshortened in the direction at right angles to the cleft orientation and become a significant limiting factor in medial translocation of the orbits. Preparatory expansion of these distant soft tissues, ideally in a subperiosteal plane, permits tension–free bony shift, the potential for accurate re–positioning of those important periorbital soft tissue landmarks (medial and lateral canthi)

and the production of an appropriately orientated and functional eyelid reconstruction. Long–term follow–up with subsequent facial growth is not available, but in the presence of an underlying stable facial skeleton, soft tissue contracture would not be anticipated.

Although dealing with cases which were complex in their pattern and combination of soft tissue and skeletal deformity, and additionally frequently multiply–operated upon, expander related complications were fortunately uncommon. Only in one patient have the expanders become exposed and the effective soft tissue gain become lost. In this case, whilst multiply operated and demonstrating multiple clefts, expander exposure was a consequence of technical error in placement.

With the collection together in tertiary referral centres of sufficient numbers of these rare and diverse cases, a coordinated, planned long–term approach to the management of the skeletal and soft tissue deformities is evolving. Tissue expansion, both immediately adjacent to and distant from the cleft, is one similarly evolving element of these rare cleft management programmes.

The Authors

Mark H. Moore, FRACS, Craniofacial Surgeon

James A. Trott, FRACS, Craniofacial Surgeon

David J. David, FRCS, FRACS, Head of Unit

Australian Cranio-Facial Unit, Adelaide Children's Hospital, 72 King William Road, North Adelaide, SA 5006.
Requests for reprints to M. H. Moore.
Paper received 22 August 1991. Accepted 18 September 1991, after revision.

References

1 Antonyshyn, O., Gruss, J. S., Zuker, R. and Mackinnon, S. E. (1988). Tissue expansion in head and neck reconstruction. Plastic and Reconstructive Surgery, 82, 58.

2 Argenta, L. C. and Vander Kolk, C. A. (1987) Tissue expansion in craniofacial surgery. Clinics in Plastic Surgery. 14, 143

3 David, D. J., Moore, M. H. and Cooter, R. D. (1989). Tessier clefts revisited with a third dimension. Cleft Palate Journal, 26, 163

4 Sasaki, G. H. and Pang, C. Y. (1984). Pathophysiology of skin flaps raised on expanded skin. Plastic and Reconstructive Surgery, 74, 59.

5 Tessier, P. (1976) Anatomical classification of facial, cranio-facial and latero-facial clefts. Journal of Maxillofacial Surgery, 4, 69.

6 Toth, B. A., Glafkides, M. C. and Wandel, A. (1990) The role of tissue expansion in the treatment of atypical facial clefting. Plastic and Reconstructive Surgery, 86, 119.

Hemifacial Microsomia: A Multisystem Classification

David J. David, F.R.C.S., F.R.C.S.(E), F.R.A.C.S., Charan Mahatumarat, M.D., and Rodney D. Cooter, M.B., B.S.
Adelaide, Australia

Variability of deformities in hemifacial microsomia has precluded the general acceptance of any classification based on one reference organ. We present a review of hemifacial microsomia classifications and propose a TNM-style multisystem classification.

This alphanumeric coding system, SAT, provides cohesion to existing hemifacial microsomia classifications The acronym SAT is derived as follows: S = skeletal, A = auricle, and T = soft tissue.

There are five levels of skeletal deformity (S_1 through S_5), four levels of auricular deformity (A_0 through A_3) and three levels of soft-tissue deformity (T_1 through T_3). Hence a patient with minimal deformity would be classified $S_1A_0T_1$, whereas a patient with the most severe deformity would be $S_5A_3T_3$.

Hemifacial microsomia is a term commonly used to describe variable underdevelopment of the craniofacial skeleton, external ear, and facial soft tissues. The deformity involves structures derived from the first and second branchial arches Hemifacial microsomia is now considered to be part of a continuous spectrum which includes Goldenhar syndrome.[1] In addition to underdevelopment of the components mentioned, Goldenhar syndrome is characterised by vertebral anomalies and epibulbar dermoids.[2]

The term *hemifacial microsomia* implies facial involvement only; however, anomalies in other organ systems may occur.[3] Both sides of the face may be involved. Facial asymmetry, phenotypic characteristics, and lack of inheritance patterns differentiate the bilateral form of facial microsomia from Treacher Collins syndrome.[4,5]

Reports of the incidence of hemifacial microsomia range from 1 in about 3500 live births[6] to 1 in 5642 births.[7] It is the second most common facial birth defect after cleft lip and palate.[8]

Severity ranges from minimal distortion requiring minor surgical input, if any, to severe hypoplasia needing reconstructive surgery. Accurate comparisons of surgical techniques and choice of appropriate treatment tailored to specific patient requirements are problems compounded by the lack of a generally accepted, uniform classification.

From the South Australian Cranio-facial Unit at the Adelaide Children's Hospital and the Department of Plastic and Reconstructive Surgery at the Royal Adelaide Hospital.
Received for publication June 17, 1986; revised December 5, 1986.
Presented, in part, at the International Workshop on Craniofacial Clefts, in Adelaide, Australia, on May 5 to 9, 1986.

Review Of Classification

Many attempts at classification of hemifacial microsomia deformities have been made. Some require that patients be classified according to their particular combination of deformities, whereas other classifications are based on the degree of deformity in one part only.

In their treatment planning, Longacre et al.[9] found it necessary to assess each patient individually, "since the prominent feature of these dysplasias of the first and second bronchial arch is their variability." While discussing the variants of the syndrome, Converse et al.[10] emphasize that "the deformity in hemifacial microsomia varies in extent and degree" and that it "is often difficult to classify the individual deformity." The complex interrelationship between affected structures has delayed the evolution of a "systematic and unified plan of treatment."[8]

Mixed-Deformity Classifications

Longacre et al.[9] divided a series of 44 patients with "first and second branchial arch syndromes" into two groups, 38 with unilateral microtia and 6 with bilateral microtia. Each group was then subdivided into four levels of facial deformity to assist treatment planning. However, the microtia was not graded, nor was the facial deformity clearly defined.

Grabb[7] made an evaluation of 102 patients and placed each into one of six groups. Each group contained patients with a cluster of deformities of varying degrees, but as Grabb cautioned, "the first and second bronchial arch syndrome is a spectrum of facial malformations which blend into one another, and there are no bold lines which delineate any of these six groups."

Converse et al.[11] found that the contiguity of the anatomic structures involved with the hemifacial microsomia deformity made difficult any attempt to provide an accurate method of classification. They therefore reviewed each deformity individually.

In 1974, Converse et al.[4] provided a classification system for bilateral facial microsomia, with 15 patients being subdivided into four groups. Allocation to groups 1, 2, and 3 was based on combinations of microtia and micrognathia. Group 4 patients, the most severely affected, included those with significant soft-tissue deficits and abnormalities of the auricles and facial skeleton. Each group reflected different combinations of deformity.

Edgerton and Marsh[12] reviewed 17 patients surgically treated for hemifacial microsomia. They produced four clinical groups and felt that their management was facilitated by dysplasia predominance grouping with the major functional deformity dictating the sequence of repair."

Skeletal Deformity Classifications

Pruzansky[13] described three grades of mandibular deformity:

Grade I: Mandible of smaller than normal size but with morphologic characteristics of the ramus being clearly present.

Grade II: Condyle, ramus, and sigmoid notch, while still identifiable, are grossly distorted, and the mandible is strikingly different in size and shape from normal.

Grade III: Mandible is severely malformed, ranging from poorly identifiable ramal components to complete agenesis of the ramus.

Swanson and Murray[14] used the mandible and temporomandibular joint as a center of reference in their description of three types of skeletal defects. In their classification, Lauritzen et al.[15] included malformations of the mandible, temporomandibular joint, zygomatic arch, and orbit. Although the classification of mandibular components was similar to Pruzansky's grade II and Swanson and Murray's type II classifications, Lauritzen et al.[15] restrict their type II category to those mandibles with the condylar head missing.

However, although it is accepted that a variety of craniofacial skeletal structures may be involved in hemifacial microsomia, "the mandibular deformity is assumed to be the abnormal keystone."[16]

Auricle Classifications

Meurman[17] reviewed 74 patients with microtic ears admitted to the Otolaryngological Hospital at Helsinki from 1951 to 1957. Subjects were divided into three grades of microtia:

Grade I: Malformed auricle of smaller than normal size but retaining characteristic features.

Grade II: Rudimentary auricle consisting of a low, oblong elevation hook formed at the cranial end corresponding to the helix.

Grade III: A more defective auricle with a malformed lobule and the rest of the pinna being totally absent.

Pruzansky[13] applied a modification of Meurman's system to include preauricular anomalies while grading 90 cases of hemifacial microsomia. This was in an attempt to grade the malformation severity of the external ear, temporal bone, and mandible to establish correlations between affected parts.

Figueroa and Pruzansky[18] used an otocentric approach to provide nine different combinations of deformity based on a three–level gradation of severity of mandibular and auricular malformations.

In 1975, Coccaro et al.[19] clearly demonstrated a patient with a normal ear and obvious underdevelopment of the face on the same side. A normal ear has been included by Murray et al.[8] in their classification of auricular structures ranging from normal to grade III.

Soft-Tissue Classifications

Figueroa and Pruzansky[18] labeled "simplistic" any attempt at hemifacial microsomia classification based solely on the external ear and mandible. They emphasized that a variety of other factors contributing to the syndrome would be excluded—one such factor being soft tissue.

Murray et al.[8] proposed a grading of soft–tissue deformities:

Mild: Minimal deficiency; no ear or cranial nerve involvement.

Moderate: Between mild and severe.

Severe: Major soft–tissue deficiency plus ear distortion, nerve deficits, and clefts of face or lips.

The SAT Multisystem Classification

Figueroa and Pruzansky[18] emphasised that analysis of the phenotypic heterogeneity of hemifacial microsomia needed delineating to provide a rational basis for treatment choice based on specific components. They suggested that "the ultimate analytical categorisation . . . will require a gradation system for each of the components and a cluster analysis based on the aggregation of specific components."

An alphanumeric coding system is proposed that is based on the universally accepted TNM classification of malignant tumors.[20,21] The derivation of SAT is as follows: S = *s*keletal, A = *a*uricle, and T = soft *t*issue. In this system, S has Five levels: S_1, S_2, and S_3 are adapted from the grades of mandibular deformity proposed by Pruzansky,[13] and patients with orbital involvement may be allocated to further levels S_4 and S_5 after Lauritzen et al.[15] (Fig. 1). A normal auricle represented by A_0, with A_1, A_2, and A_3 following the grades of microtia described by Meurman[17] (Fig. 2). The soft–tissue category has three levels, ranging from minimal deformity (T_1) to severe (T_3), similar to the grading of Murray et al.[8] (Fig. 3).

Skeletal Categories

S_1 = Small mandible with normal shape.

S_2 = Condyle, ramus, and sigmoid notch identifiable but grossly distorted; mandible strikingly different in size and shape from normal.

S_3 = Mandible severely malformed, ranging from poorly identifiable ramal components to complete agenesis of ramus.

S_4 = An S_3 mandible plus orbital involvement with gross posterior recession of lateral and inferior orbital rims.

S_5 = The S_4 defects plus orbital dystopia and frequently hypoplasia and asymmetrical neurocranium with a flat temporal fossa.

Auricle Categories

A_0 = Normal.

A_1 = Small, malformed auricle retaining characteristic features.

A_2 = Rudimentary auricle with hook at cranial end corresponding to the helix.

A_3 = Malformed lobule with rest of pinna absent.

Soft-Tissue Categories

T1 = Minimal contour defect with no cranial nerve involvement.

T2 = Moderate defect.

T3 = Major defect with obvious facial scoliosis, possibly severe hypoplasia of cranial nerves, parotid gland, muscles of mastication; eye involvement; clefts of face or lips.

Materials

From 1975 through 1985, the first 11 years of the South Australian Cranio–Facial Unit, 47 patients with deformities of the facial skeleton, auricle, and facial soft tissue were reviewed (Table I). This group included 34 patients with hemifacial microsomia, 4 patients with bilateral deformities (Table II), and 9 patients with Goldenhar syndrome.

Methods

S Category

Three–dimensional CT scans have greatly facilitated the analysis of skeletal deformity in hemifacial microsomia (Fig. 1). The need for sequential analysis, however, mandates the continued use of conventional techniques. Anteroposterior, lateral, and basal cephalometry and an Orthopantomogram are routinely used. CT scans with three–dimensional reformats are reserved for pre– and postoperative studies.

A Category

Auricular deformities are assessed by clinical examination and from bilateral photographic records (see Fig. 2).

T Category

Soft-tissue deformities are the most difficult to classify because their extent may not be revealed until operation. Clinical examination helps to assess muscle bulk and nerve deficits. Photographs are taken in routine positions (anteroposterior, lateral, oblique, chin–up, and occlusal views; see Fig. 3), and if indicated, photographic documentation is made of asymmetrical facial nerve function. All patients now have stereophotogrammetry.

Results

This range of deformities in our sample of 43 hemifacial microsomia (unilateral) patients is seen in the histogram (Fig. 4). The right side was predominant in both unilateral and bilateral forms of the syndrome. The male–to–female ratio in the 47 patients was 1.24:1.

Discussion

The need for a generally accepted, uniform classification of deformities of hemifacial microsomia is amplified by the review of attempts at classification. The mandible is the "keystone" to skeletal deformity levels S_1 to S_3, with extension into levels S_4 and S_5 for patients with orbital involvement. A prerequisite for inclusion into S_4 and S_5 levels is an S_3 mandible.

One patient with a severely hypoplastic left orbit (Fig. 5, *above left)* and ectopic eye remnants in the parietal region of the skull (Fig. 5, *above right)* was classified $S_1A_1T_2$. An Orthopantomogram shows a level S_1 type mandible on the left and a normal mandible on the right (Fig. 5, *below)*. This was the only patient who presented a challenge to the SAT coding system. The deformities were at marked variance to the patterns seen in other cases of hemifacial microsomia, thus raising the question of alternative diagnoses. The S_1 skeletal classification

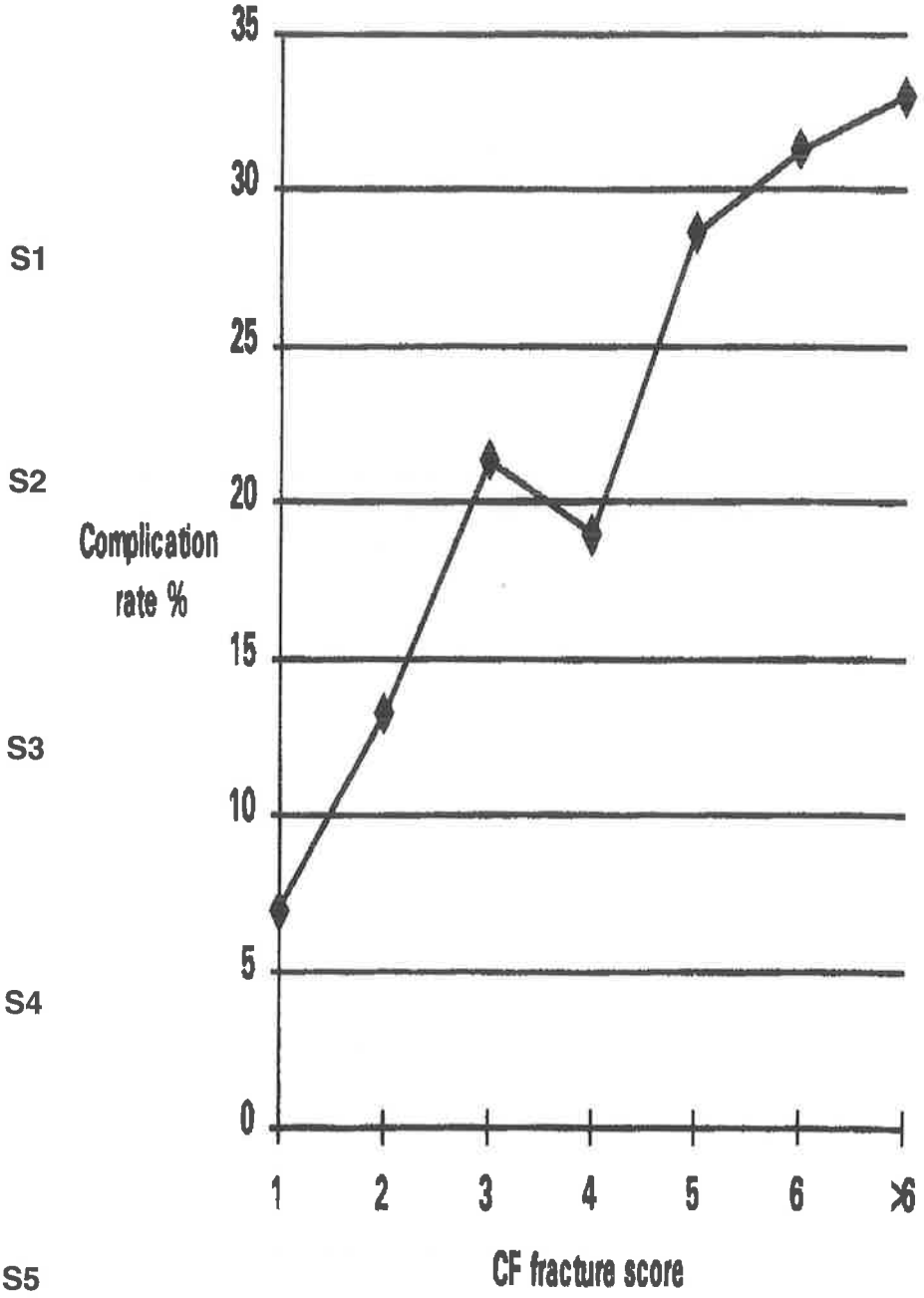

FIG. 1. *The S levels of skeletal deformity in the SAT system from the minimal deformity* S_1 *to the severe malformation of* S_5.

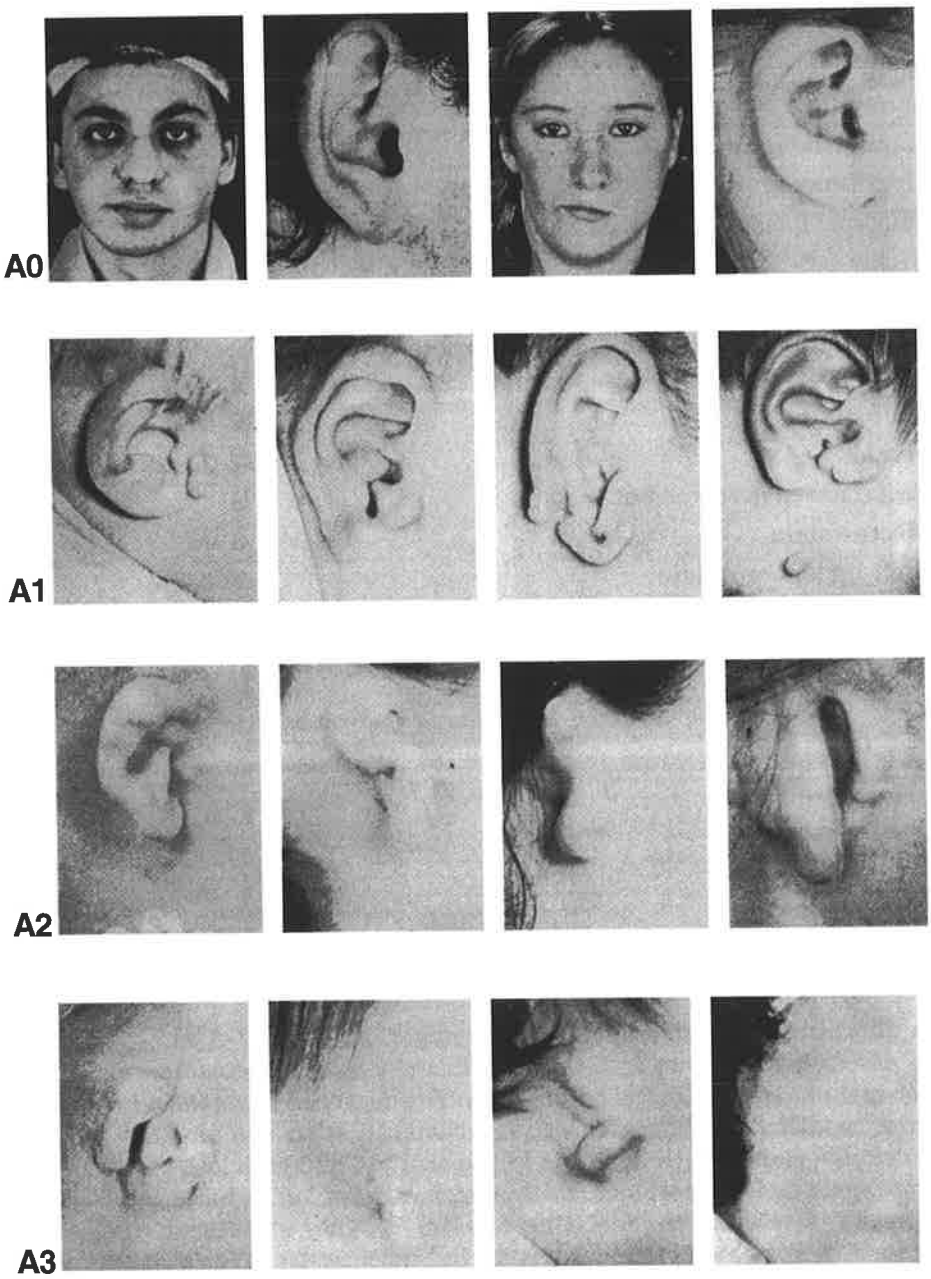

FIG. 2. *The A levels of auricular deformity in the SAT system ranging from a normal ear* $\mathbf{A_0}$. *to the severe deformity* $\mathbf{A_3}$.

reflects the minor mandibular deformity, but the hypoplastic orbit was treated as an S_5 deformity. Cohen[3] reported four cases of anophthalmia with hemifacial microsomia, similar to this patient, and suggested that such patients had a complex dysmorphogenetic syndrome rather than a bronchial arch dysplasia.

Allocating deformed auricles to relevant categories has been facilitated by Meurman's descriptions[17] of patients with microtia. Such is the variability of hemifacial microsomia that soft tissue and skeletal deformities may underlie a normal ear (see Fig. 2), and thus the level A_0 of the SAT system has been included.

TABLE I

Analysis of 47 Patients

Disorder	*No. of Patients*
Hemifacial microsomia	34
Goldenhar syndrome	9
Bilateral facial microsomia	4
Right	23
Left	20
Bilateral (right side being predominant in three patients)	4
Male	26
Female	21
Facial nerve involvement	8
Macrostomia	8
Cleft lip and/or palate	7

TABLE II

Bilateral Facial Microsomia Deformities

	Right	Left
Case 1	$S_2A_2T_2$	$S_2A_2T_2$
Case 2	$S_3A_3T_2$	$S_2A_2T_1$
Case 3	$S_3A_2T_3$	$S_1A_0T_1$
Case 4	$S_3A_1T_2$	$S_1A_0T_1$

In allocating patients to soft-tissue categories, Murray et al.[8] cautioned that the assessment of true soft–tissue deficiency may be possible only after correction of underlying skeletal deformities. The degree of hypoplasia involving muscles of mastication has a direct relationship with the severity of the mandibular deformity. With agenesis of the condyle and coronoid process, the lateral pterygoid and temporalis muscles may be absent[11] or reduced to a fibrous band, thereby increasing the facial asymmetry.[22] Other structures commonly involved include skin, subcutaneous tissue, and the muscles of facial expression.

Occasionally, the soft palate and ipsilateral side of the tongue are less developed. Branches of the facial nerve may be quite superficial if the parotid gland is hypoplastic, and in severe cases there may be facial nerve defects or it may have an abnormal course.[11] Although currently subjective, soft–tissue analysis is becoming more objective with the application of stereophotogrammetry and the development of techniques to take measurements from three-dimensional CT images.

The SAT coding system offers flexibility with time. A young patient can be reclassified as growth further aggravates facial scoliosis or, preferably, as successful treatment reduces the individual's coding toward normality (Fig. 6).

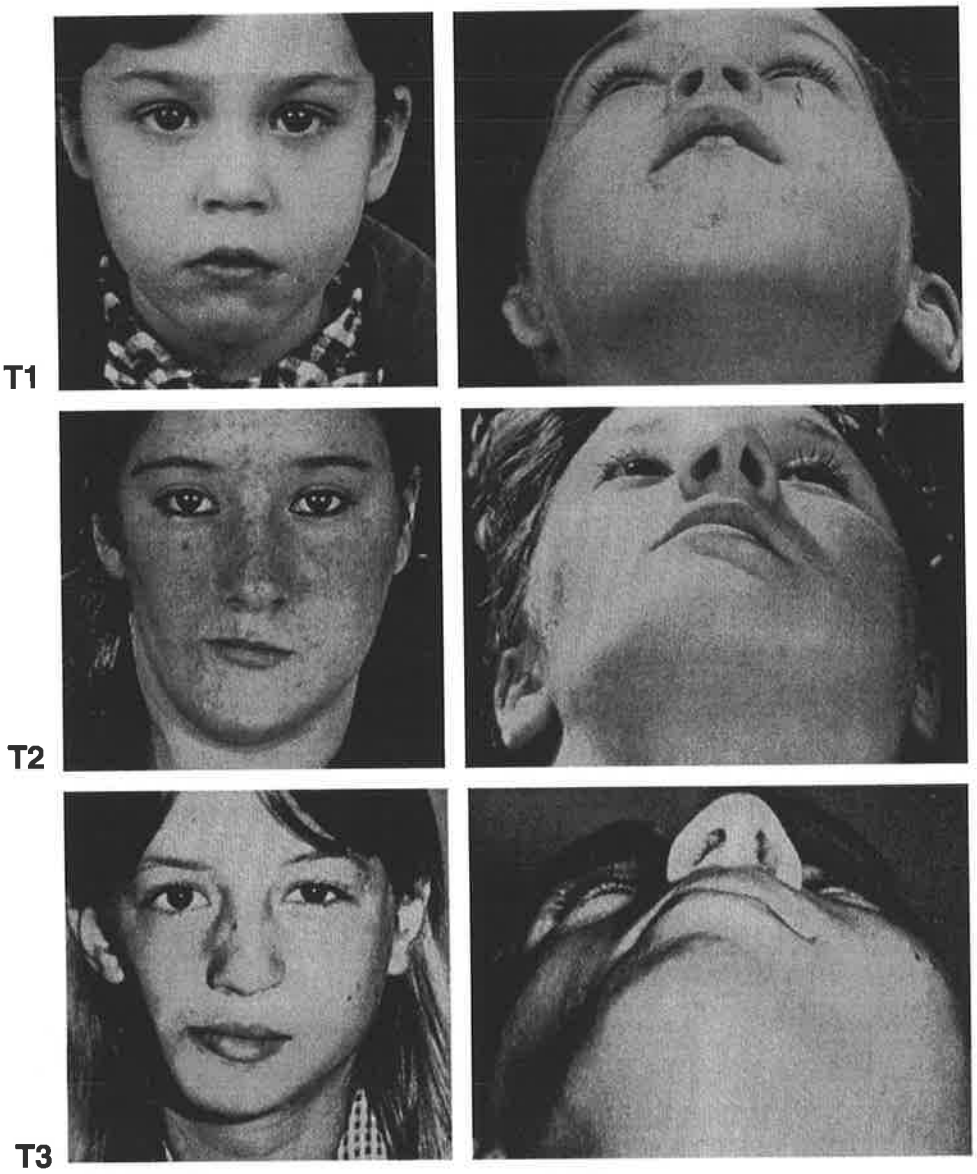

FIG. 3. *The T levels of soft–tissue deformity in the SAT system range from* T_1 *to* T_3.

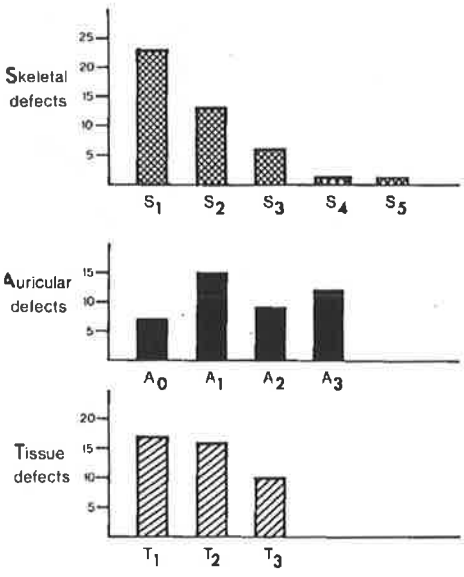

FIG. 4. *The histograms illustrate the range of deformities in our sample after applying the SAT classification to the 43 patients with unilateral defects.*

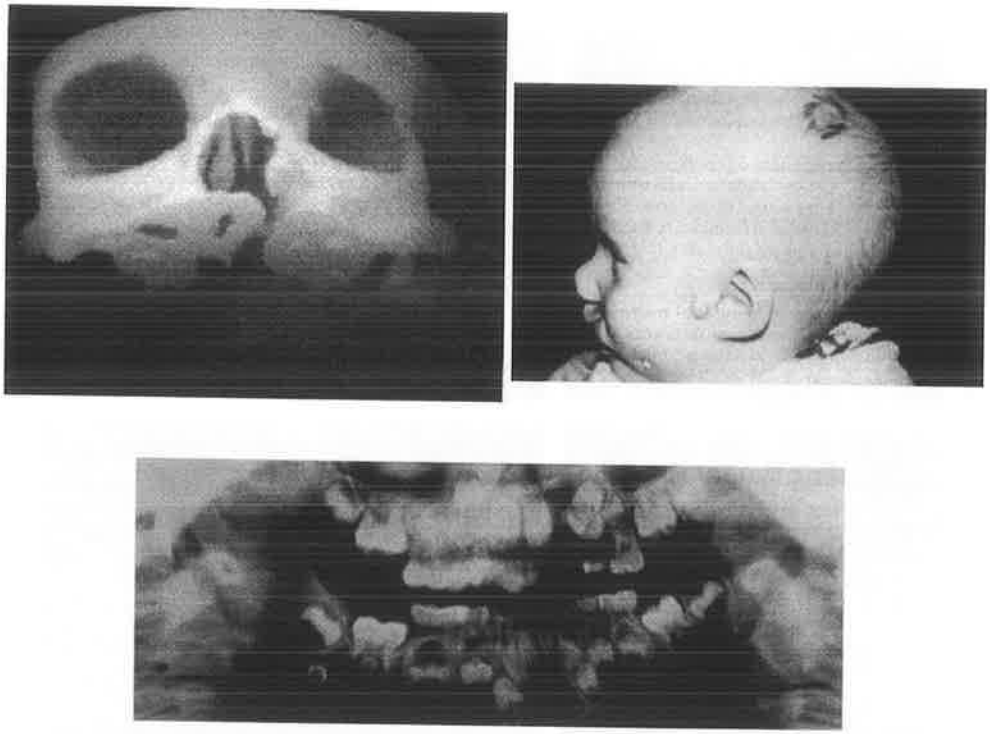

FIG. 5. (Above, left) *The three-dimensional CT scan shows left orbital hypoplasia. A left unilateral cleft is also seen.* (Above, *right) Ectopic eye remnants were found in the parietal region.* (Below) *The left mandibular ramus is short, but the condyle and coronoid process have normal shapes.*

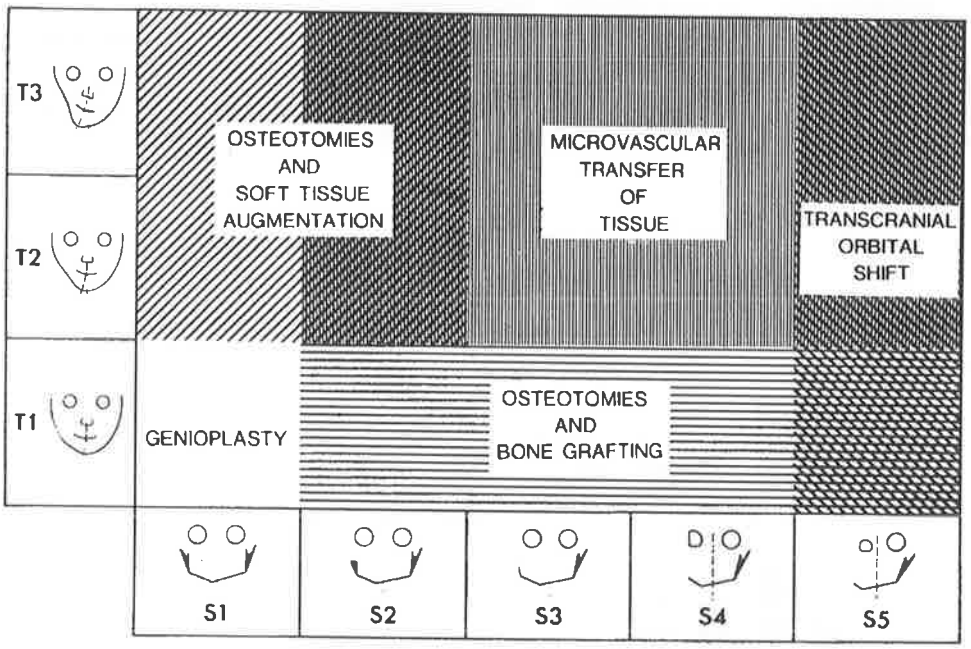

FIG. 6. *The surgical treatment plan based on skeletal and soft–tissue deformities.*

Conclusion

A review of the many hemifacial microsomia classifications suggests that a multisystem classification is justified for hemifacial microsomia with its inherent variability of deformities. The SAT alphanumeric coding system is simple and reproducible. It will facilitate communication while yielding meaningful information for treatment planning.

David J. David, F.R.C.S., F.R.C.S.(E), F.R.A.C.S. The South Australian Cranio-Facial Unit
Adelaide Children's Hospital and Royal Adelaide Hospital
72 King William Road
North Adelaide, South Australia 5006

References

1 Gorlin, R. J., Pindborg, J. J., and Cohen, M. M. *Syndromes of the Head and Neck,* 2d Ed. New York: McGraw–Hill, 1976.

2 Gorlin, R. J., Jue, K. L., Jacobsen, U., and Goldschmidt, E. Oculoauriculovertebral dysplasia. *J. Pediatr.* 63: 991, 1963.

3 Cohen, M. M. Variability versus "incidental findings" in the first and second branchial arch syndrome: Unilateral variants with anophthalmia. *Birth Defects* 7: 103, 1971.

4 Converse, J. M., Wood–Smith, D., McCarthy, J. G., Coccaro, P. J., and Becker, M. H. Bilateral facial microsomia: Diagnosis, classification, treatment. *Plast. Reconstr. Surg.* 54: 413, 1974.

5 David D. J. Treacher Collins Syndrome. In I.F.K. Muir (Ed.), *Current Operative Surgery: Plastic and Reconstructive.* East Sussex: Bailliere Tindall, 1985.

6 Poswillo, D. Otomandibular deformity: Pathogenesis as a guide to reconstruction. *J. Maxillofac. Surg.* 2: 64, 1974.

7 Grabb, W. C. The first and second branchial arch syndrome. *Plast. Reconstr. Surg.* 36: 485, 1965.

8 Murray, J. E., Kaban, L. B., and Mulliken, J. B. Analysis and treatment of hemifacial microsomia. *Plast. Reconstr. Surg.* 74: 186, 1984.

9 Longacre, J. J., De Stefano, G. A., and Holmstrand, K. E. The surgical management of first and second branchial arch syndromes. *Plast. Reconstr. Surg.* 31: 507, 1963.

10 Converse, J. M., McCarthy, J. G., Coccaro, P. J., and Wood–Smith, D. Clinical Aspects of Craniofacial Microsomia. In J. M. Converse, J. G. McCarthy, and D. Wood–Smith (Eds.), *Symposium on Diagnosis and Treatment of Craniofacial Anomalies.* St. Louis: Mosby, 1979. P. 461.

11 Converse, J. M., Coccaro, P.J., Becker, M., and Wood–Smith, D. On hemifacial microsomia. *Plast. Reconstructive Surgery* 51:268, 1973.

12 Edgerton, M. T., and Marsh, J. L. Surgical treatment of hemifacial microsomia. *Plast. Reconstr. Surg.* 59: 653, 1977.

13 Pruzansky, S. Not all dwarfed mandibles are alike. *Birth Defects* 2: 120, 1969.

14 Swanson, L. T., and Murray, J. E. Asymmetries of the Lower Part of the Face. In L. A. Whitaker, and P. Randall (Eds.), *Symposium on Reconstruction of Jaw Deformity.* St. Louis: Mosby, 1978. P. 171.

15 Lauritzen, C., Munro, I. R., and Ross, R. B. Classification and treatment of hemifacial microsomia. *Scand. J. Plast. Reconstr. Surg.* 19: 33, 1985.

16 Kaban, L. B., Mulliken, J. B., and Murray, J. E. Three–dimensional approach to analysis and treatment of hemifacial microsomia. *Cleft Palate J.* 18: 90, 1981.

17 Meurman, Y. Congenital microtia and meatal atresia. *Arch Otolaryngol.* 66: 443, 1957.

18 Figueroa, A. A., and Pruzansky, S. The external ear, mandible and other components of hemifacial microsomia. *J. Maxillofac. Surg.* 10: 200, 1982.

19 Coccaro, P. J., Becker, M. H., and Converse, J. M. Clinical and radiographic variations in hemifacial microsomia. *Birth Defects* 2: 314, 1975.

20 Copeland, M. M. American Joint Committee on Cancer Staging and End Results Reporting: Objectives and Progress. *Cancer* 18: 1637, 1965.

21 TNM-Atlas: Illustrated Guide to the Classification of Malignant Tumors. In B. Spiessl, O. Scheibe and G. Wagner (Eds.), *TNM Atlas.* Berlin: Springer–Verlag, 1982.

22 Ortiz–Monasterio, F. Early mandibular and maxillary osteotomies for the correction of hemifacial microsomia: A preliminary report. *Clin. Plast. Surg.* 9(4): 509, 1982.

Composite Free Flap Reconstruction for Severe Hemifacial Microsomia

David J. David, E. Tan, and Rodney D. Cooter (North Adelaide)

Introduction

Advances in microvascular surgery and craniofacial surgery have converged to focus on the problems of mandibular and soft tissue facial reconstruction for severe hemifacial microsomia.

The deformity in hemifacial microsomia involves structures derived from the first and second branchial arches. The spectrum of severity for each of the major phenotypic characteristics is highly variable (Figueroa and Pruzansky 1982). Many classifications have been proposed for hemifacial microsomia deformities. Pruzansky (1969) described three grades of mandibular deformity and also a gradation of deformities of the external ear. Swanson and Murray (1978) used the mandible and temporomandibular joint as a centre of reference in their description of three types of skeletal defects. An otocentric approach, in which the external ear formed the reference organ, was adopted by Figueroa and Pruzansky (1982). In their extended classification of five anatomical categories, Lauritzen et al. (1985) incorporated the extent of orbital involvement.

A type I skeleton has a normally shaped, but small, mandible on the affected side. Type II describes a functioning, but displaced, temporomandibular joint with an abnormal joint cavity and a short malformed ramus. In type III the temporomandibular joint, glenoid fossa and ramus are absent (Swanson and Murray 1978) or the ramal components are poorly identifiable (Pruzansky 1969).

When the mandibular ramus is missing, associated muscles are replaced by fibrous bands. This increases the facial asymmetry (Ortiz–Monasterio 1982). Analysis of soft tissue deficit is qualitative but may range from mild to severe (Murray et al. 1984). Severe hemifacial microsomia exists when skeletal deformity type II or III underlies major soft tissue deficiency involving skin and muscles of mastication.

Management Principles

In surgical management we follow the Gillies principle of recreating the defect. Facial structures are recentralized to establish a better three–dimensional relationship between skeletal and soft tissue components. This produces a defect, which can then be repaired with a free flap using microvascular techniques (Fujino et al. 1975; Harashina et al. 1977; Wells and Edgerton 1977; Daniel 1978; David and Tan 1978,1979; La Rossa et al. 1980).

Proceedings 1st International Congress of the International Society of Cranio-Maxillo-Facial Surgery 453–457

This approach is used as an adjunct to the more classical reconstruction of the zygoma and temporomandibular joint. Other authors are less enthusiastic about the need for soft tissue augmentation, adopting the principle "first the bone, rarely the soft tissue" (Munro 1980; Lauritzen et al. 1985).

Case Reports

Case I

Our initial use of this technique was in 1978 (David and Tan 1979). A 17-year-old girl presented with skeletal deformity type III and severe soft tissue deficiency. She had absence of the left hemimandible, absence of the left zygomatic arch and temporomandibular joint, absence of the left external ear, absence of the left masseter muscle and only a residual temporalis muscle (Fig. 1). Multiple operations had previously been performed.

The first operation consisted of zygomatic arch reconstruction from rib and a glenoid fossa from costal cartilage (Fig. 2). Three months later a right-sided sagittal split and a Le Fort I osteotomy were performed. At the same time an osteocutaneous groin flap, using the left iliac crest and the overlying dermofat placed on the superficial circumflex iliac vessels, was inserted (Figs.3, 4). The bone was introduced into a deep pocket below the facial nerve and the dermofat inserted below a facelift incision. The patient required subsequent minor surgery to recontour her face (Fig. 5).

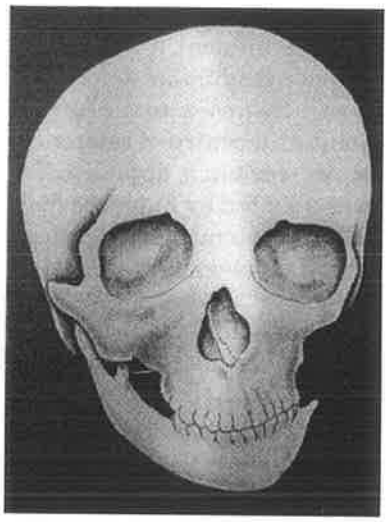

FIG. 1. *Case 1: Skeletal deformity type III*

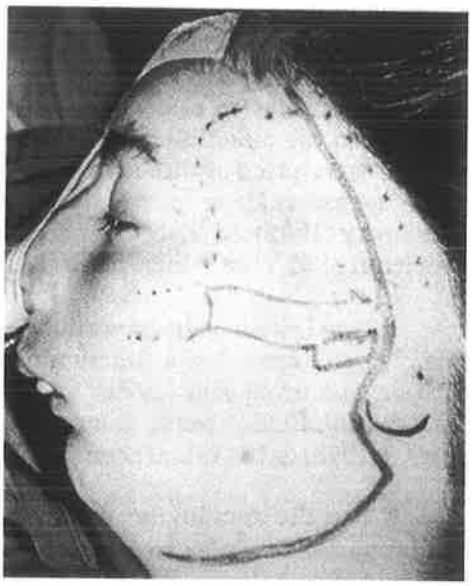

A

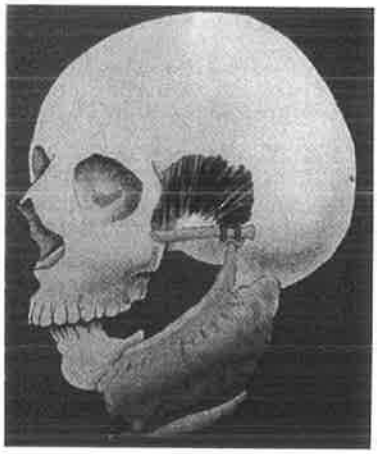

FIG. 3. *Insertion of an osteo–cutaneous groin flap*

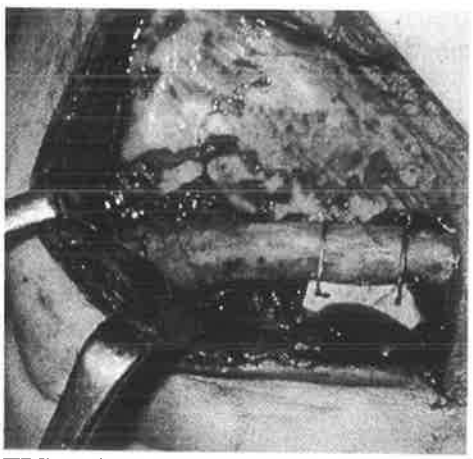

B

FIG. 2. A, B. *Reconstruction of zygomatic arch and glenoid fossa*

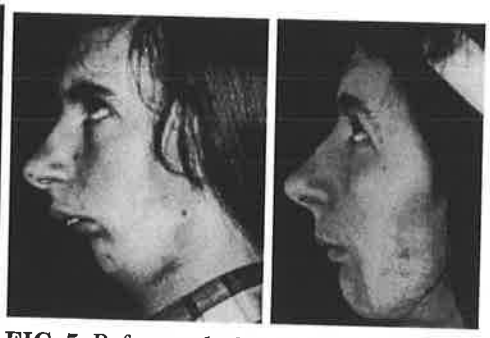

FIG. 5. *Before and after correction for type III deformity*

FIG. 4. *3D CT scan showing the reconstructed left hemimandible*

Case 2

A 14–year–old girl with skeletal deformity type II and severe soft tissue deficiency had previously undergone Le Fort I and subsigmoid osteotomies to lengthen her left mandibular ramus.

On this occasion, she had a Le Fort I osteotomy, rightsided sagittal split osteotomy and an angle osteotomy on the left (Fig.6). An inlay/onlay bone graft was harvested from the left ilium with soft tissue based on the deep circumflex iliac system (Fig.7). She required one second-stage sculpturing of the soft tissue (Fig. 8).

Case 3

A 12–year–old Chinese boy was referred from the Sultanate of Brunei. He had a right–sided cleft lip and palate and skeletal deformity type III (Goldenhar's syndrome) with severe soft tissue deficiency (Fig. 9).

Surgical management included a one-stage reconstruction of the zygomatic arch, right glenoid fossa, Le Fort I osteotomy in two pieces and a left vertical subsigmoid osteotomy. In the same procedure a microvascular composite bone and soft tissue reconstruction of his right facial defect was undertaken using the deep circumflex iliac system (Fig. 10). Le Fort I osteotomy stabilization was achieved with miniplates and the patient required one re-sculpturing operation and a sliding genioplasty (Figs.11, 12)

FIG. 6. *Osteotomies used to correct skeletal deformity type II in case 2*

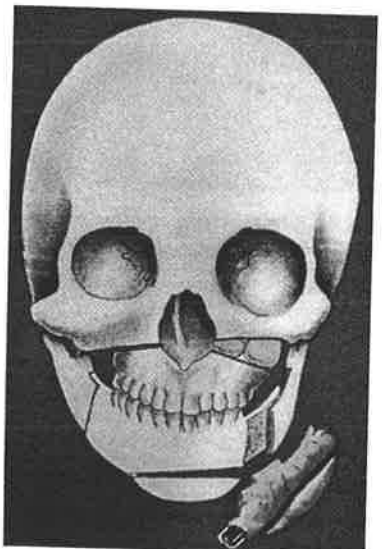

FIG. 7. *Composite free flap based on the deep circumflex iliac system*

FIG. 8. *Appearance of patient reported as case 2 (left) before and (centre) shortly after surgery, and (right) long-term result.*

FIG. 9. *Case 3: Skeletal deformity type III with severe soft tissue deficiency*

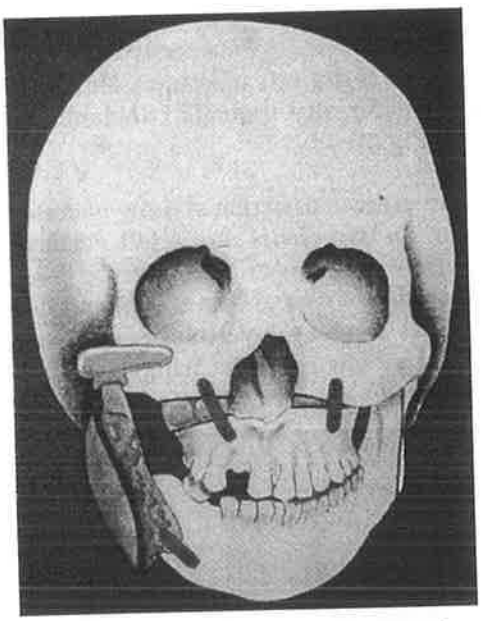

FIG. 10. *One-stage reconstruction including a microvascular composite free flap*

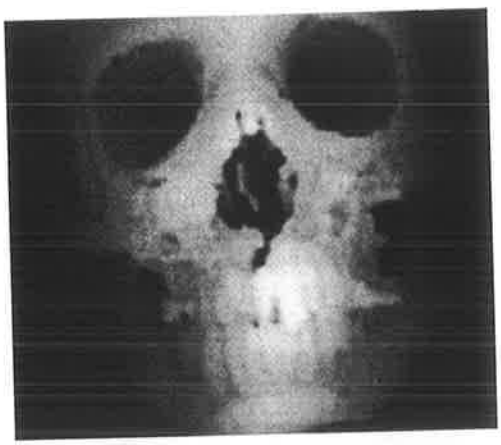

FIG. 11. *Postoperative 3D CT scan*

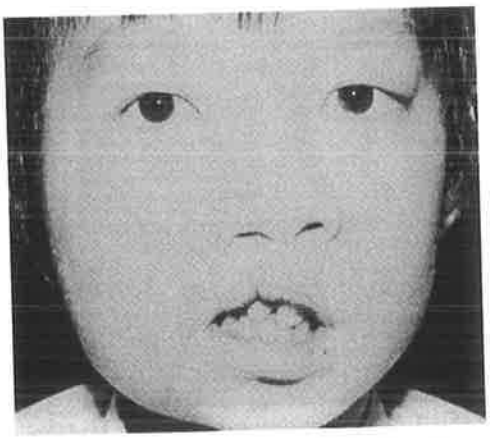

FIG. 12. *Postoperative result in case 3*

Discussion

The extreme variability of deformities encountered in hemifacial microsomia emphasizes that the treatment plan must be tailored to the specific needs of each patient (Figueroa and Pruzansky 1982).

Microvascular techniques make it possible to transfer combinations of tissue onto a bony framework provided by conventional reconstructive procedures. In addition to the benefits of soft tissue transfer it is our experience that bone transfer with microvascular anastomosis has been more successful than free bone grafting. Hence, simultaneous reconstruction of both soft and hard tissues may be achieved. Also, free flaps permit more accurate and predictable reconstruction (La Rossa et al. 1980).

Although microsurgical intervention may lengthen the procedure, most of the surgery can be accomplished in one operation.

Conclusion

Composite free tissue transfer plus appropriate arch and joint reconstruction, together with midface and mandibular osteotomies, comprises the treatment of choice for patients with hemifacial microsomia involving skeletal deformities type II and III and severe soft tissue deficiency.

This type of facial asymmetry is the ideal meeting ground for craniofacial and microsurgical techniques.

References

1 Daniel RK (1978) Mandibular reconstruction with free tissue transfers. Ann Plast Surg 1: 346

2 David DJ, Tan E (1978) A de-epithelialised free groin flap for facial contour restoration. J Maxillofac Surg 6: 249

3 David DJ, Tan E (1979) Microvascular surgery in maxillofacial reconstruction. Ann Acad Med 8: 481

4 Figueroa AA, Pruzansky S (1982) The external ear, mandible and other components of hemifacial microsomia. J Maxillofac Surg 10: 200

5 Fujino T, Tanino R, Sugimoto C (1975) Microvascular transfer of free deltopectoral dermal-fat flap. Plast Reconstr Surg 55: 428

6 Harashina T, Nakajima T, Yoshimura Y (1977) A free groin flap reconstruction for progressive facial hemiatrophy. Br J Plast Surg 30: 14

7 La Rossa D, Whitaker L, Dabb R, Mellissinoss E (1980) The use of Microvascular free flaps for soft tissue augmentation of the face in children with hemifacial microsomia. Cleft Palate J 17: 138

8 Lauritzen C, Munro IR, Ross RB (1985) Classification and treatment of hemifacial microsomia. Scand J Plast Surg 19: 33

9 Munro IR (1980) One-stage reconstruction of the temporomandibular joint in hemifacial microsomia. Plast Reconstr Surg 66: 699

10 Murray JE, Kaban LB, Mulliken JB (1984) Analysis and treatment of hemifacial microsomia. Plast Reconstr Surg 74: 186

11 Ortiz-Monasterio F (1982) Early mandibular and maxillary osteotomies for the correction of hemifacial microsomia. Clin Plast Surg 9: 509

12 Pruzansky S (1969) Not all dwarfed mandibles are alike. Birth Defects 5: 120

13 Swanson LT, Murray JE (1978) Asymmetries of the lower part of the face. In: Whitaker LA, Randal P (eds) Symposium on reconstruction of jaw deformities. Mosby, St. Louis, p 171

14 Wells JH, Edgerton MT (1977) Correction of severe hemifacial atrophy with a free flap from the lower abdomen. Plast Reconstr Surg 59: 223

Treacher Collins Syndrome

D. J. David

Introduction

Treacher Collins syndrome is also known by a number of other names: mandibulofacial dysostosis, Berry syndrome, Franceschetti–Zwahlen–Klein syndrome.

Sculptures from the pre-Columbian era have been found indicating the existence of the deformity and its familial incidence.[1] The first reference in the literature to mandibulofacial dysostosis was made by Berry in 1889.[2] Treacher Collins[3] emphasized the associated malar deformity in 1900. Franceschetti and his colleagues reviewed the syndrome in a series of papers in the 1940s, giving the name 'mandibulofacial dysostosis'[4,5] and describing the existence of the more complete forms of the syndrome as well as the minimal clinical manifestations that can occasionally be seen.

The syndrome is transmitted by autosomal dominant inheritance with a high, but variable, penetrance and expressivity, producing different degrees of involvement in affected members of the same family.

The patient with Treacher Collins syndrome exhibits abnormalities of the facial bones and soft tissues. The fully developed syndrome consists of the majority of the following features (Figure 6.1).

1. Antimongoloid slant of the palpebral fissures, which is reflected in the underlying slope of the bony orbit.

2. Notching or colobomata of the lateral portion of the lower lids in the majority of cases. Occasionally there is a coloboma of the upper lid. Absence of the eyelashes on the medial one–third of the lower lids is a common feature.

3. The typical bony configuration is in part produced by hypoplasia of the Facial bones, always bilateral, but frequently asymmetrical (Figure 6.2). Raulon and Tessier[7] give an excellent description of the orbital deformity, indicating that in the complete form there is total absence of the zygomatic bones and zygomatic arches, the latter being responsible for the lack of the lateral orbital rim. The lateral orbital wall is formed by the hypoplastic greater wing of the sphenoid and the inferior orbital fissure has no anterior boundary. Thus there is no separation between the orbital cavity, the temporal fossa and the infratemporal fossa. The inferior orbital rim is poorly defined and the infraorbital foramen is frequently absent, the infraorbital neurovascular bundle passing directly from the orbital cavity to the check. The overall shape of the orbit is characteristic. There is overhanging of the lateral part of the supraorbital ridge and a downward sloping orbital floor. The orbital contents appear to prolapse into the inferior orbital fissure.

The zygomatic arches are absent or much reduced, and as a result the aponeurosis of the hypoplastic temporalis muscle is directly continuous with the

aponeurosis of the masseter muscle. According to Tessier's classification of craniofacial clefts, Treacher Collins syndrome corresponds to clefts numbers 6, 7 and 8. [8] Cleft number 6 accounts for the eyelid coloboma. and the cleft between the maxilla and zygoma. Number 7 is the temporo–zygomatic cleft. accounting for absence of the zygomatic arch. Number 8 is a fronto–zygomatic cleft.

4. There is a typical hypoplasia of the mandible with an obtuse mandibular angle and the ramus may be deficient. The condylar process and the coronoid process may be flat or even aplastic. Kryzanski[9] believed that the antigonial notching is specific for the condition.

5. The external ears are frequently abnormal in shape, size and position and there are often anomalies of the middle and inner ears. There may be rudimentary ear tags, blind fistulae, or dimples between the ears and the angles of the mouth.

6. Macrostomia, a high arch palate, a receding chin and anterior open bite produce a very characteristic appearance to those affected by Treacher Collins syndrome. *Rarely the mandible is prognathic rather than retrognathic.*

7. In a number of cases, a tongue shaped process of hair projects onto the cheek in front of the tragus.

8. Other associated anomalies include cleft palate, and deformities of the radius, ulna, metacarpals and spine.

FIG. 6.1. *A child with a moderate degree of Treacher Collins syndrome exhibiting the abnormalities of the hard and soft tissues. The right external ear is malformed. The antimongoloid slant of the eyes is caused by the bony deficiency in the zygoma. The lower eyelid hypoplasia is combined with absence of lashes on the medial part of the lower lid. The nasal pyramid is prominent. There is an anterior open bite and the chin is retrognathic. The facial appearance is characteristic of the syndrome.*

Classification

Incomplete forms

The deformities are less severe and less extensive, but most of the anomalies are still present. The eyelids may be notched, the antimongoloid slant of the palpebral fissures less pronounced and the zygomatic bone present, but hypoplastic, or only partially absent. The external ears may be normal. but deafness is frequent.

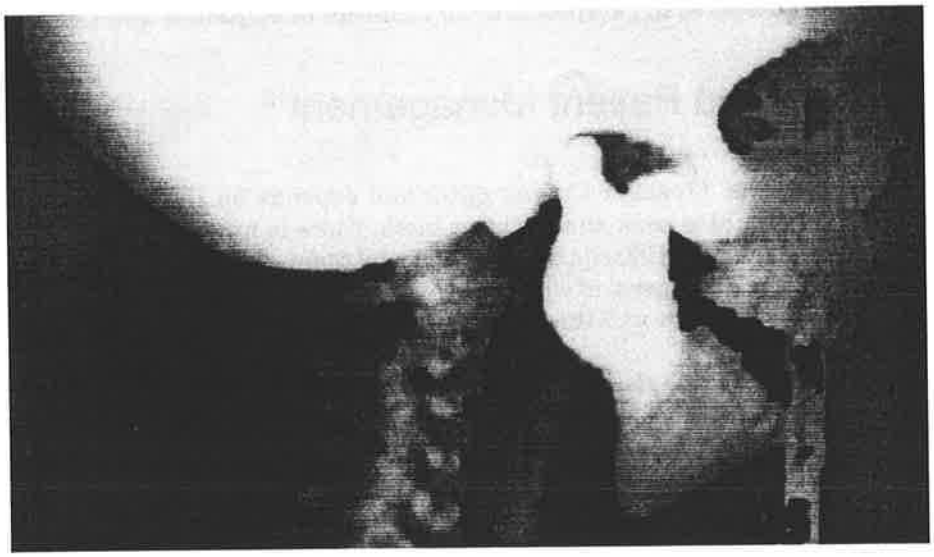

FIG. 6.2. *A three-dimensional reconstruction of the skull of a patient with Treacher Collins syndrome. The image is generated using computed tomography according to the method described by Hemmy, David & Hermann.[6] This right oblique view shows the distorted shape of the right orbit due to the hypoplastic right malar bone with absence of the zygomatic arch. The obtuse mandibular angle is well demonstrated, as is the flattening of the mandibular condylar process and coronoid process. The increased height and retrodisplacement of the chin are also apparent.*

Asymmetrical forms

The deformities are usually more pronounced on one side and external asymmetry is reflected in the orbital areas. It is doubtful if the deformity is ever completely one–sided; usually careful examination will reveal slight anomalies on the contralateral side.

Differential diagnosis

It is hard to confuse the complete form of Treacher Collins syndrome with anything else. The incomplete or asymmetrical forms should be distinguished from craniofacial microsomias, such as Goldenhar syndrome, with its epibulbar cysts and vertebral anomalies; or hemifacial microsomia, which shows severe asymmetrical deformities of the ramus and condyle of the mandible and the glenoid fossa. The rarer bilateral facial microsomias may sometimes be confused with the incomplete forms of Treacher Collins syndrome.

Aetiology

There is good evidence that the syndrome is inherited as an autosomal dominant, with incomplete penetrance and variable expressivity. The gene involved may have a lethal or sublethal effect, as many cases of miscarriage or early postnatal death have been recorded.[10]

Pathogenesis

Treacher Collins syndrome has been thought by some to result from delayed ossification of those facial bones derived from the first branchial arch.[5] Retardation of differentiation of maxillary mesoderm has also been suggested.[11] Poswillo's elegant work[1] indicated that the syndrome results from disorganisation of the pre–otic neural crest about the time of migration of cells to the first two branchial arches, the anomalies varying with alteration in the ratio of lateral plate mesoderm to neural crest mesoderm in the core of the formative branchial arches. He relates this thesis to the stapedial artery concept of McKenzie and Craig.[12]

Indications and Patient Management[13]

The management of Treacher Collins syndrome depends on the extent of the deformities. If a child is seen shortly after birth, there is much to be gained by early assessment by a multidisciplinary craniofacial team. Emphasis can be placed on 'total patient management' of which surgery is an important, but not the sole part, and both the patient and the parents will benefit by expert counselling.

Unfortunately, it is still unusual for an experienced team to be given the opportunity to intervene in the early period when the critical process of bonding between mother and child is taking place. Early involvement by a psychosocial team and genetic counselling are largely desirable. These patients often have distorted jaws, a large mouth and a cleft palate and early attention should be paid to the ability to feed. An experienced speech pathologist, who is capable of assisting with early feeding problems, is an invaluable adjunct to therapy. Early assessment of the auditory mechanism is essential to prevent developmental retardation from deafness.

Treacher Collins syndrome at its most severe is a complex craniofacial deformity which requires multidisciplinary medical and surgical management until the child is fully grown. This implies that a rational treatment plan should be developed to cater for the child and family over a long period of time.

Preoperative Care and Investigations

The basis of preoperative care is the multidisciplinary assessment. The *plastic surgeon* must be able to perform the bony surgery as well as correct the many difficult soft tissue problems associated with Treacher Collins syndrome.

The *ophthalmologist* and *orthoptist* produce a detailed preoperative and postoperative assessment of visual acuity, visual fields, eye positions and muscle functions, and deal with any ophthalmological complications which arise in the course of treatment.

The *ENT surgeon* should produce a complete report on the state of hearing, together with an analysis of the state of the external, middle and inner ears.

The *orthodontist* collects baseline cephalometric data for longitudinal growth studies necessary to plot the progress of this deformity with growth and after surgical intervention.

The *dental team* will attend to dental hygiene and any pre– or postoperative dental appliances that may be necessary. Prior to any definitive surgery on the jaws in adolescence, combined surgical-orthodontic assessment is necessary.

The *radiologist* is responsible for making and interpreting the radiographs. A detailed preoperative study consists of biplanar cephalometric radiographs; computed tomography, which is then subjected to the program 3D83 to produce a three dimensional reconstruction. The latter is invaluable for surgical planning.[6]

The *anaesthetist's* role in the management of Treacher Collins syndrome is vital. Of all craniofacial abnormalities, this is probably the most hazardous from the point of view of airway management. The relative protrusion of the upper jaw and the anterior teeth, together with a small mandible, tight suprahyoid muscles and a narrow nasal airway, makes intubation difficult and sometimes impossible even in the most experienced hands. Postoperative airway management has added risks for the same reasons.

Radiology

A thorough radiological assessment is essential before each operative stage.

Plain films. Routine plain film evaluation includes occipitomental, postero-anterior and lateral skull views. Use of the cephalostat and orthopantomograms is made when the patient is old enough.

Tomography. Routine polytomography has now been supplanted by computed tomography with two–dimensional reconstruction (Figure 6.3) and latterly three–dimensional reconstruction, using the program 3D83 (figure 6.2) which gives the most accurate model of the deformity seen from any angle, enabling bony reconstructive surgery to be accurately planned. Routine tomography may still be essential to assess the middle and inner ear deformities.

Timing Of Surgery

The timing of the surgical procedures must suit the severity of the deformity. In mild forms, the eyelid surgery and the reconstruction of the bony orbit can be done at the same time. The principal indications for such surgery are the psychological pressures on patient and family and such pressures may necessitate surgery at about four years of age, just prior to entering school. At the same time, the malar arches are reconstructed and the maxilla augmented. Due to resorption of bone graft, it is almost certain that the bony procedures will need to be repeated before facial growth is complete.

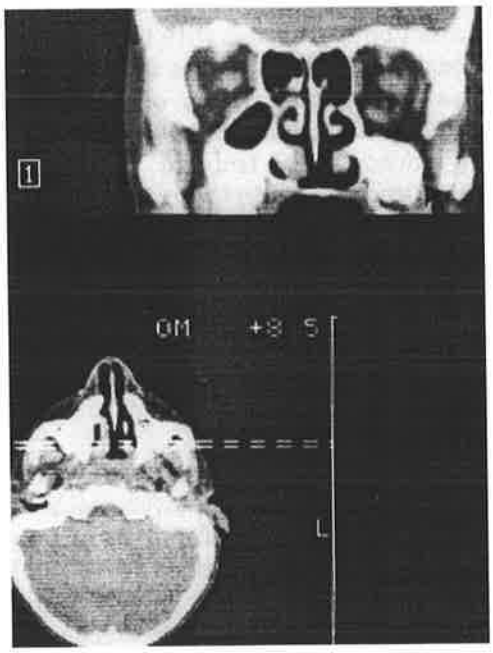

FIG. 6.3. *A computed tomogram with two–dimensional reconstruction at right angles to the slice through the marked plane. This view indicates the typical deficiency in the orbital floor and orbital rim, marked by an arrow on the left (the right of the picture)*

In the most severe cases, the eyelid coloboma and the soft tissue deficiencies must be corrected before the bony augmentation. The correction of the canthal dystopia is then done together with the bony augmentation, which gives support for the lateral canthal ligament and does not compromise the closure of the colobomata.

Correction of the mandibular and nasomaxillary deformities should wait until adolescence, when facial growth is sufficiently advanced.

Correction Of Eyelid Deformities

Tessier emphasises that the coloboma of the lower lid is not just a defect in the skin, but a deficiency affecting all layers of the lid, and attention should be paid to a multilayered repair.

Z-plasty with muscle flap (Figure 6.4)

This is one of the commonest forms of repair for the deformity, when there is marked tissue deficiency. The proposed Z–plasty is marked out on the lower lid and the two flaps raised from the underlying muscle. The lower lid margin of the coloboma, consisting of the tarsoconjunctival layer, is cut at right angles and sutured. The orbicularis muscle is elevated as a separate flap along the lid margin and by overlapping provides support for the lid margin. The skin flaps are then transposed and sutured into position.

Transposition of a musculocutaneous flap from the upper to lower lid (Figure 6.5)

Even more severe deformities may need transposition of a flap of upper lid skin and orbicularis muscle into an incision made in the lower lid. The ptosed lateral canthus is elevated by these incisions and can be placed upwards and fixed to a hole in the reconstructed lateral orbital margin (see below).

Transposition flap of full thickness upper eyelid to lower eyelid [14](Figure 6.6)

The coloboma is released both in its vertical and horizontal dimensions as described above, thus revealing the lower eyelid defects. A flap of upper eyelid is now raised using, instead of just skin and muscle, the full thickness of the lid, including enough tarsal plate and conjunctive to close the lower lid defect. The flap is based laterally and the inferior edge must be continuous with the incision on the lower lid. The tarsal plate and conjunctive are dissected as an island so that the levator mechanism, which attaches to the upper border of the tarsal plate, can be left intact in the upper lid. With the wide exposure thus provided at the lateral canthus, the lateral canthal ligament can be isolated. It is often hypoplastic and it may be transposed upwards and fixed into the reconstructed lateral orbital rim. The proponents of this technique maintain that it gives more support to the lower lid in the more severe deformities and that it is the conjunctive and tarsal plate which provide the most significant components of this support.

Orbitofacial Reconstruction

The orbits are reconstructed together with the malar bones and zygomatic arches. The reconstruction is achieved by bone grafting, with or without osteotomies of the deformed orbit. The surgical approach is made via a bicoronal scalp flap which gives access to the malar and orbital regions. If the eyelids have been satisfactorily repaired, further incisions can be avoided; however, if soft tissue deficiencies are still present, these can be corrected at the same operation as the bone grafting.

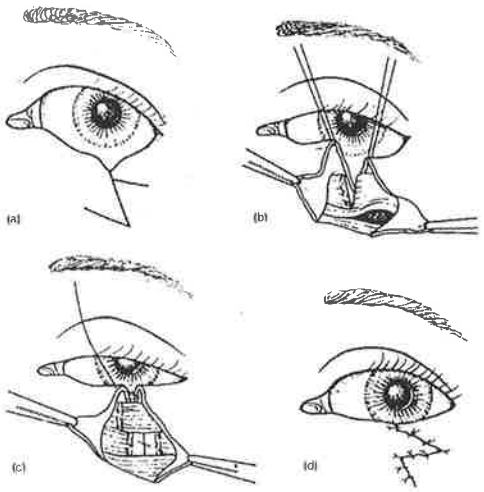

FIG. 6.4. a. *The proposed Z–plasty is marked out in the lower eyelid and the skin flaps are cut and elevated from the underlying muscle.* **b.** *The margins of the coloboma are then transected through all layers, tarsoconjunctival and muscle at right angles to the lower lid.* **c.** *The tarsoconjunctival layer is then sutured with a running pull–out nylon suture. The muscle layer is elevated as a separate layer and overlapped along the line of the bed margin, thus giving support for the lid.* **d.** *The skin flaps are transferred and sutured into position with fine interrupted sutures of 6/0 nylon.*

The bicoronal scalp flap (Figure 6.7)

This is the best approach to the craniofacial skeleton, providing wide exposure by dissecting in a plane deep to the periosteum. The incision extends across the top of the head from one ear to the other and may be continued inferiorly into the preauricular skin crease. Bleeding from the scalp is controlled by the appropriate neurosurgical clips. Dissection can be commenced by peeling the scalp forward in the subgaleal plane and dissection continued over the temporalis fascia to the level of the zygomatic arch. (Figure 6.8). The periosteum can then be divided at any convenient level above the orbital rims and raised as a separate layer. Alternatively the original scalp incision can be deepened through the periosteum and the scalp and periosteum raised as a single layer.

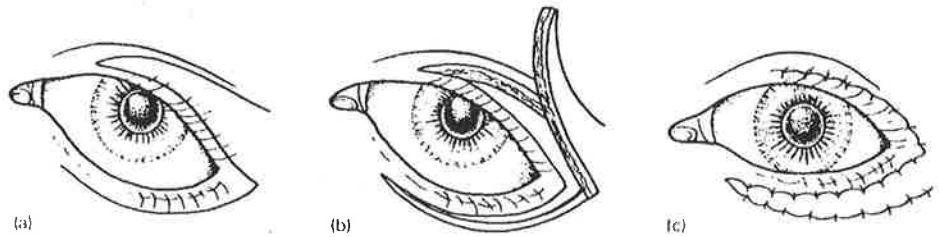

FIG. 6.5. a. *The upper eyelid is marked out, based laterally: the lateral canthus will be transposed upwards as this flap is transposed downwards.* **b.** *The lower eyelid is released horizontally through all but the tarsoconjunctival layers. If the eyelid is very depressed, the technique below should be used.* **c.** *The upper eyelid musculocutaneous flap is transposed into the lower lid defects created by the upward movement of the lateral canthus, which is fixed into a drill hole in the lateral orbital margin. The skin is sutured with fine 6/0 nylon.*

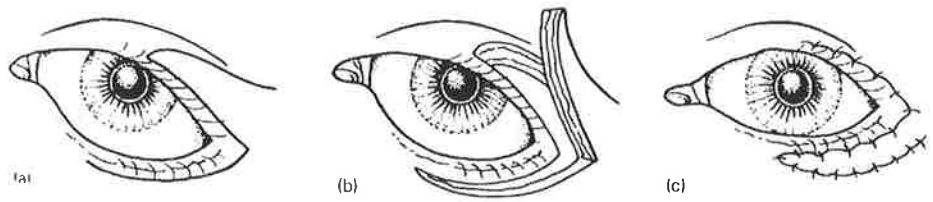

FIG. 6.6. a. *The upper eyelid is outlined, the superior position of the base of the flap being the point to which the lateral canthus will be elevated.* **b.** *Full thickness incision through the lower lid will reveal the tissue deficiency. The upper lid is of full thickness with a tarsal plate and conjunctival island on the musculocutaneous flap. Care is taken to leave a superior rim of tarsal plate with its attached levator mechanism.* **c.** *The defect in the tarsal plate is closed with 6/0 nylon. The lateral canthus is transposed upwards and fixed into the lateral orbital wall by a suture plane through one or two drill holes. The upper lid flap is now sutured in the lower lid defect in layers.*

Pericranial flaps (Figure 6.9)

The periosteum may be lifted attached to the temporalis muscle on each side and one or two flaps can be elevated with the muscle. This flap can be turned down along the lateral orbital wall and onto the face and used as a soft tissue augmentation to cover bone grafts. After dissection of these pericranial flaps, the subperiosteal stripping is continued around the orbital margins, dislocating the superior orbital nerve and vessels from their canal with a dissector (Figure 6.10). If there is a foramen, the outer edge can be removed with a fine osteotome and the neurovascular bundle dislocated. Dissection then continues within the bony orbit and the periorbital dissection can be taken back to within a centimetre of the orbital apex. Because of the deficiency of the malar bones and zygomatic arches, some difficulty may be found in establishing the plane of dissection over the cleft area. The small nubbin of arch is often hard to find posteriorly. Dissection can be extended medially over the orbital floor and inferior orbital rim to expose the bony deficiency in this region. Additional access can be gained through the eyelid if the eyelid repair is to be combined with the bony reconstruction of the orbit.

It is worth stating at this stage that when using the bicoronal scalp flap, at the completion of surgery. the temporalis muscle must he attached to the lateral orbital wall and as firmly as possible to the anterior part of the inferior temporal line to overcome the unsightly hollowing in this region that may otherwise occur. If necessary, the temporalis muscle can be divided vertically and the anterior portion rotated forward to achieve the necessary attachment to the lateral orbital wall. The scalp flap is usually closed in two layers with a running absorbable suture to the galea and a running nylon suture to the skin.

Bone grafting

Bone is harvested from the usual sites: ribs and iliac crests. However, these sites may be insufficient in children with severe defects. The cranial vault has become a favoured donor site and the technique has been described by Tessier. [15]

A full thickness 'bone flap' is removed from one or both parietal regions (Figure 6.11). It is always our practice to have this done by the craniofacial neurosurgeon. When the flap is detached, it is cut into strips and each of these strips is split with a power saw and/or an osteotome. After splitting, one half is replaced to repair the cranial defect and the remainder is used to reconstruct the face. Bone harvested from the calvarium is usually strong, appropriately curved and less subject to resorption than bone from other sites.

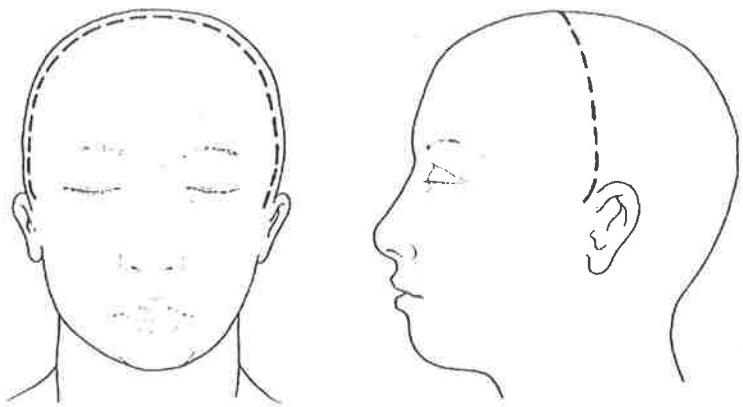

(a) (b)

FIG. 6.7. a. b. *The bicoronal scalp flap is the best and most versatile incision for exposure of the craniofacial skeleton, which may be dissected subperiosteally well down onto the maxilla. The incision passes transversely across the vertex from one preauricular skin crease to the other. Haemostasis is best achieved by rapid application of neurosurgical clips as the incision is made.*

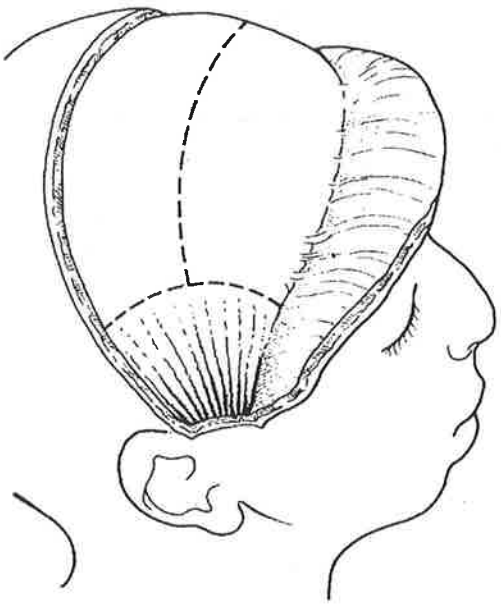

FIG. 6.8. *The dissection can be commenced by peeling the scalp forward in the subgaleal plane and dissection can be continued down over the temporalis fascia to the zygomatic arch. The periosteum can be divided at any level above the orbital rim and elevated using sharp instruments. The temporalis muscle is elevated from the underlying bone in a similar fashion.*

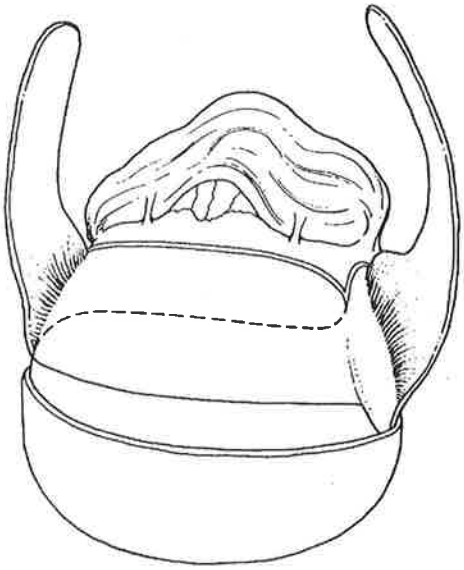

FIG. 6.9. *To fashion pericranial flaps, a strip of pericranium can be left attached to each temporalis muscle. Such a flap can be turned down along the lateral orbital wall and onto the face to act as soft tissue augmentation and to cover bone grafts with an additional layer.*

FIG. 6.10. *After dislocation of the supraorbital neurovascular bundle and subperiorbital dissection of the orbits, the dissection of the nasal bones can be extended onto the face to expose the medial part of the inferior orbital margin, the piriform margin and the anterior maxilla.*

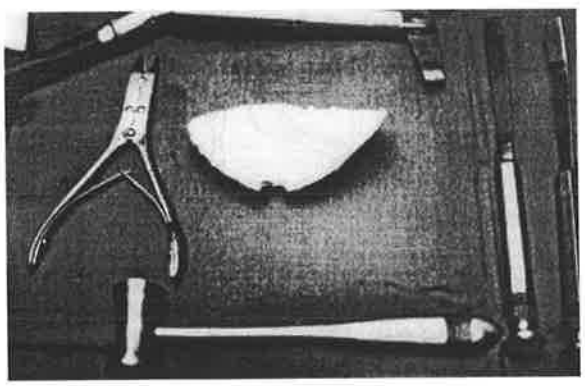

FIG. 6.11. *A full thickness bone flap has been removed from the parietal region of the skull. It is displayed with the instruments necessary to split it in the fashion described by Tessier.* [15] *After splitting, one half is used to repair the cranial defect and the remaining half to reconstruct the face.*

The Bony Reconstruction (Figures 6.12)

Reconstruction is achieved by a combination of onlay and inlay hone grafts, inserted through the combined lower eyelid and bicoronal scalp flap incisions. The superolateral margins are usually overhanging and should be reshaped by cutting away a crescent of bone which can be used in building up the inferior orbital defect. If the overhang is only slight, it can be reshaped with a large dental burr.

Bone is laid into the inferior orbital defect to build up the level of support for the globe. Strips of bone are then cut and shaped to augment the infraorbital margin, the lateral orbital margin and the lateral part of the superior orbital margin. These grafts are firmly secured with 26 or 28 gauge stainless steel wire. Next, an appropriately shaped piece of bone is used to reconstruct the zygomatic arch. Anteriorly the bone is wired to the malar and posteriorly is wedged into a notch made in the temporal bone.

Osteotomy plus bone graft (Figure 6.13)

In older patients, especially those with a more robust lateral orbital wall, an osteotomy of the lateral wall and part of the lateral superior orbital margin can be performed, the fragment advanced and the defect, thus created, filled with bone.

Calvarial bone flap (Figure 6.14)

Yet another, but significantly more complex, technique involves the transfer of donor calvarium on a musculo–periosteal pedicle.[16,21] In this case, the coronal incision is deepened to the subfollicular level only, the area of parieto–frontal bone to be moved is selected above the temporal line and left in continuity with the galea and the pericranium and temporalis muscle. The bony components can incorporate either partial or full thickness bone.

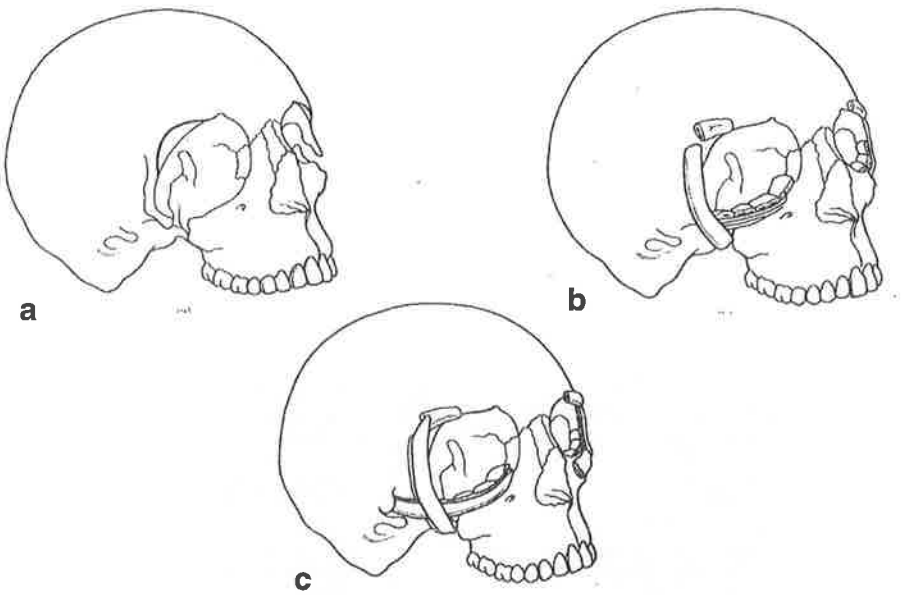

FIG. 6.12. a. *The supralateral orbital margins are usually overhanging and these can be reshaped by cutting a crescent of bone from this region, using an osteotome if the bone fragment is to be preserved and used elsewhere, or a dental burr if the deformity is slight.* **b.** *Bone is layered into the inferior orbital defect to build up the floor and thus the support for the globe. Layers of rib and/or calvarial bone can then be used to reconstruct the lateral orbital wall. Bone grafts should be securely wired into place.* **c.** *A groove is fashioned in the temporal bone into which the onlay arch graft is placed. Further strips can be layered on top of these basic elements if necessary.*

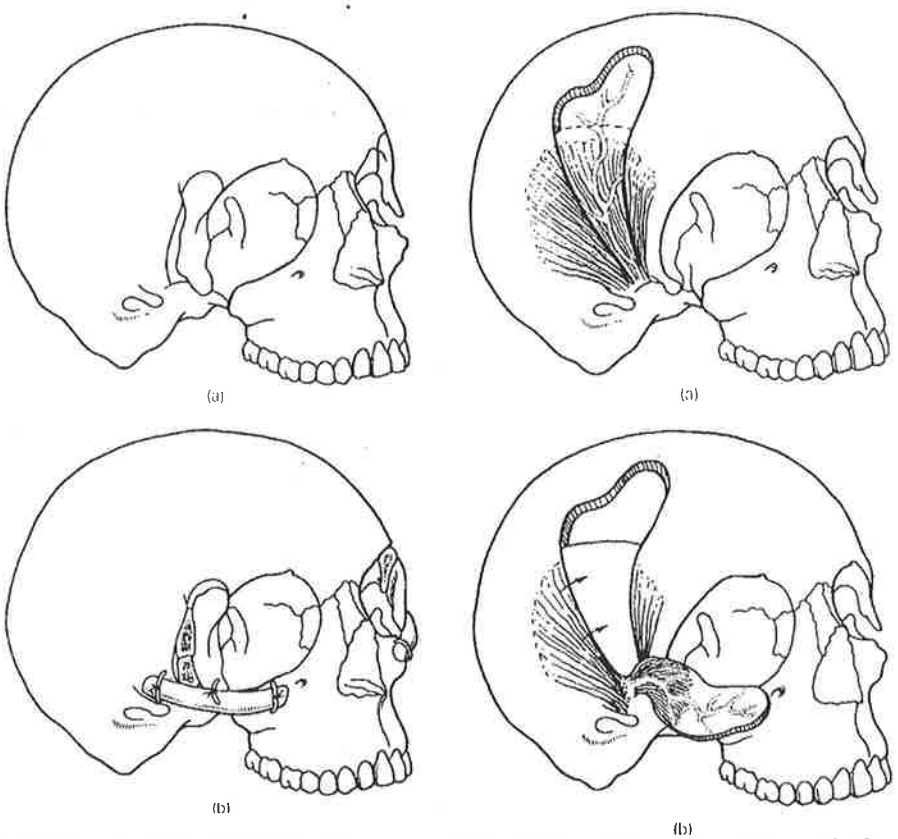

FIG. 6.13. a. *In older patients with a more robust lateral orbital wall, an osteotomy can be performed, care being taken not to enter the middle cranial fascia.* **b.** *The malar and orbital floor is reconstructed as previously described, and the gap created by the advanced lateral wall is filled with bone graft.*

FIG. 6.14. a. *The approach is made through the bicoronal scalp flap exposing the temporalis muscle, overlying galea in a plane just deep to the hair follicles. The area of calvarial bone to be used is marked out and included in the flap.* **b.** *The bone flap is raised in continuity with the central part of the temporalis muscle in which is included the main trunk of the superficial temporal vessels. The bony part of the flap can either be full thickness or partial thickness of the calvarium.*

The pedicle contains the main trunk of the superficial temporal vessels. The additional soft tissue transferred with the bone helps to augment the soft tissue of the cheek.

When the simpler bone grafting techniques have been used, additional soft tissue cover for the orbital region can be provided by the pericranial flaps already described. These flaps are passed down through the temporal fossa onto the cheek and layered over the bone grafted area. A few absorbable sutures are used to tack the pericranium into place. This soft tissue cover obviates the problem of thin skin stretched out over the bone graft. which may be both uncomfortable and unsightly.

Lower facial deformities

The correction of orthognathic problems, corrective rhinoplasty and genioplasty are usually deferred until adolescence. The choice of procedures depends on the severity of the disease.

In less severe cases where the dental occlusion is normal, the aim is to achieve a satisfactory profile by correction of the retrogenia and the usually excessive height of the chin, together with a corrective rhinoplasty. The latter

operation is not specific to the condition of Treacher Collins syndrome and will not be discussed further. The technique for genioplasty (Figure 6.15) consists of an osteotomy of the lower part of the mandibular symphysis and lower border of the body of the mandible. The surgical approach is through the lower buccal sulcus to give wide subperiosteal exposure of the bone, care being taken to observe and preserve the mental nerves.

The osteotomy cut is made beneath the level of the nerves and angled downwards and backwards. The fragment can be slid forwards and upwards, thus shortening and advancing the chin. Another variation is to transfer the fragment completely to the front of the remaining symphysis. In both cases, the fragment is secured by 26 gauge stainless steel wire.[7]

When the dental occlusion is abnormal, more complex osteotomies of the mandible and/or maxilla have to be used, often in conjunction with rhinoplasty and genioplasty. Such manoeuvres may require a tracheostomy and certainly will require complex multidisciplinary work–up and planning by surgeon, orthodontist and anaesthetist.

The steep mandibular plane and prominent antigonial notching together with shortening of the suprahyoid musculature, makes correction of the mandibular deformity difficult, with a high relapse rate. The mandibular osteotomy may be designed to suit the deformity, a sagittal splitting technique being used or an arching ramus osteotomy to correct the high mandibular plane type of skeletal morphology. Precise techniques of these procedures are beyond the scope of this chapter and reference should be made to more complex texts.[17]

The most complex combination of procedures to correct the severest dentofacial deformity combines a Le Fort II type of osteotomy of the middle third of the face to produce a downward rotation of the posterior dentition together with an osteotomy of the mandibular ramus of an L shape above the mandibular foramen. Wide subperiosteal dissection of the musculature must be performed. The mandibular body is then advanced and rotated to occlude with the previously positioned maxilla and the defects created in the mandible on each side are bone grafted (Tessier P. personal communication, 1984).

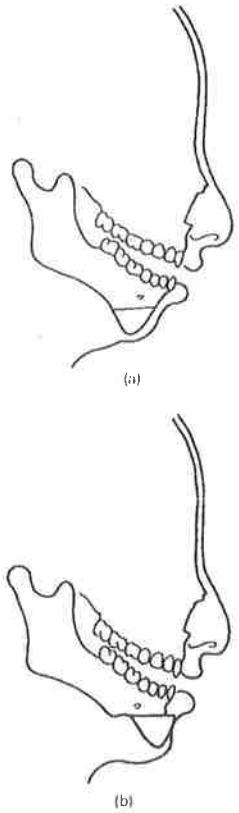

FIG. 6.15. *The osteotomy of the antero–inferior border of the mandible is made beneath the level of the nerves. If the cut is angled slightly inferiorly, the advancement will both advance and shorten the chin.*

Ear deformities

The *ear deformities* present a wide range of reconstructive problems that are not specific to Treacher Collins syndrome. Nevertheless, they represent some of the most taxing challenges to the reconstructive surgeon.[18–20]

Postoperative Care

Because of the distorted anatomy surrounding the upper airway, in cases of Teacher Collins syndrome, the single most important aspect of postoperative care is attention to the airway which should ideally be managed in an intensive care department in the early postoperative period. Where mandibular and/or maxillary surgery has been performed and intermaxillary fixation implemented, tracheostomy is usually performed because of the swelling and the varying degrees of choanal atresia which contribute to restriction of the airway.

The soft tissue surgery around the eyes requires meticulous eye toilet postoperatively. Sutures are removed on the fourth or fifth postoperative day.

Where the bicoronal scalp flap has been used, a subgaleal suction drain for the first 24 hours postoperatively is often helpful to prevent haematoma. Scalp sutures may be removed on the tenth postoperative day.

It is our practice to cover the surgery involving bone grafting with intravenous broad spectrum antibiotics during the procedure and for five days postoperatively. The intravenous regimen may be replaced by an oral regimen on the second or third day.

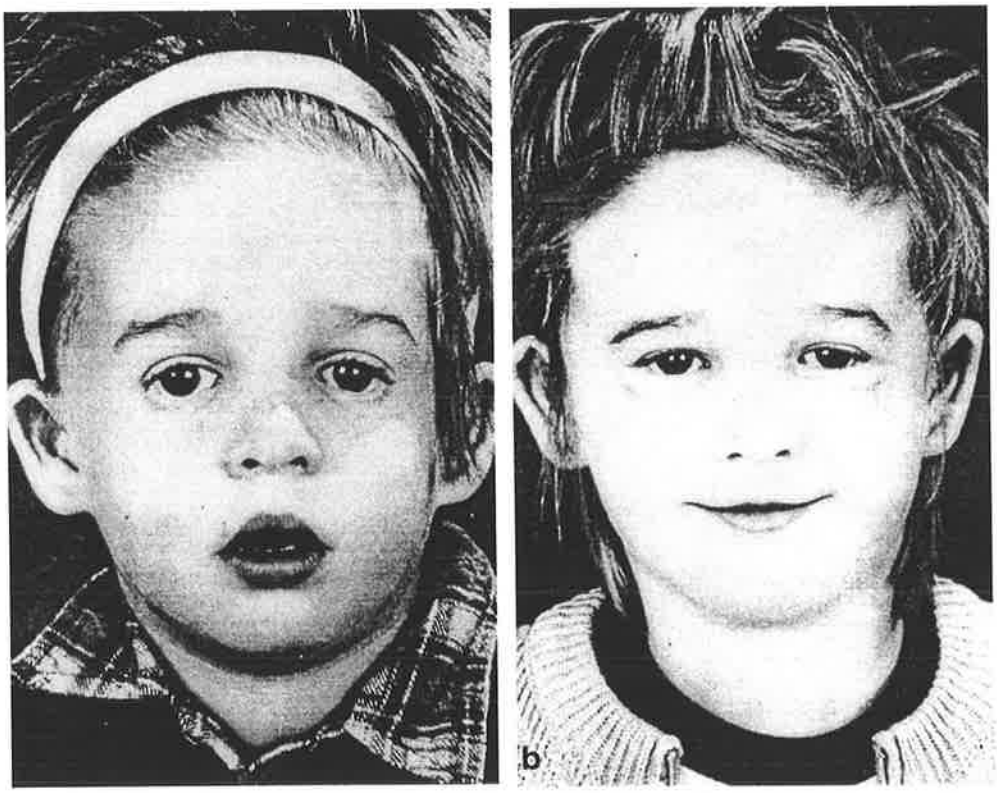

a

FIG. 6.16. a. *Relatively mild case of Treacher Collins syndrome pre-operatively.* **b.** *Same patient one year postoperatively. The surgery consisted of bony orbital reconstruction, covered with pericranial flaps, and lower lid augmentation by upper lid musculocutaneous flaps.*

Periorbital oedema is usually severe from the second to the seventh day, but begins to resolve by the tenth postoperative day. Some degree of swelling, ptosis and indeed ocular muscle imbalance, may persist for many months postoperatively, and it is important to have warned the patients and their families about this before surgery.

Where there has been wide periorbital dissection and bone grafting, it is our practice to check the vision in the early postoperative phase, as soon as possible. Regular ophthalmological follow-up is necessary.

Outcome: Long–term Complications and Results

It is obvious that the surgical approach to the deformities of Treacher Collins syndrome is complex.

The surgical procedures so far described can provide a considerable improvement to these patients, provided that these procedures are integrated into a rational plan for total patient care. It is not however always possible to remove all evidence of the deformity and optimal improvement can only be achieved after many operations over many years.

Bone grafting around the orbits in the young child may have to be repeated several times during growth because of partial absorption of bone grafts. It is our impression that cranial vault grafts are less susceptible to resorption than those from other sites, however, over the years, bone grafts may he needed from multiple sites — ribs and iliac crests as well as cranial vault.

The principal long-term complication of lower facial osteotomy is that of relapse. The deformed mandible in its new position is subjected to increased mechanical pull by the suprahyoid musculature, which tends to recreate the deformity. This tendency may be minimised by wide suprahyoid muscular dissection and, indeed, division together with careful choice of the osteotomy, however, this complication remains a continued problem.

a b

FIG. 6.17. a. *Preoperative photo of an adult who had had a previous rhinoplasty.* **b.** *One year after cheek augmentation with only bone graft and sliding genioplasty.*

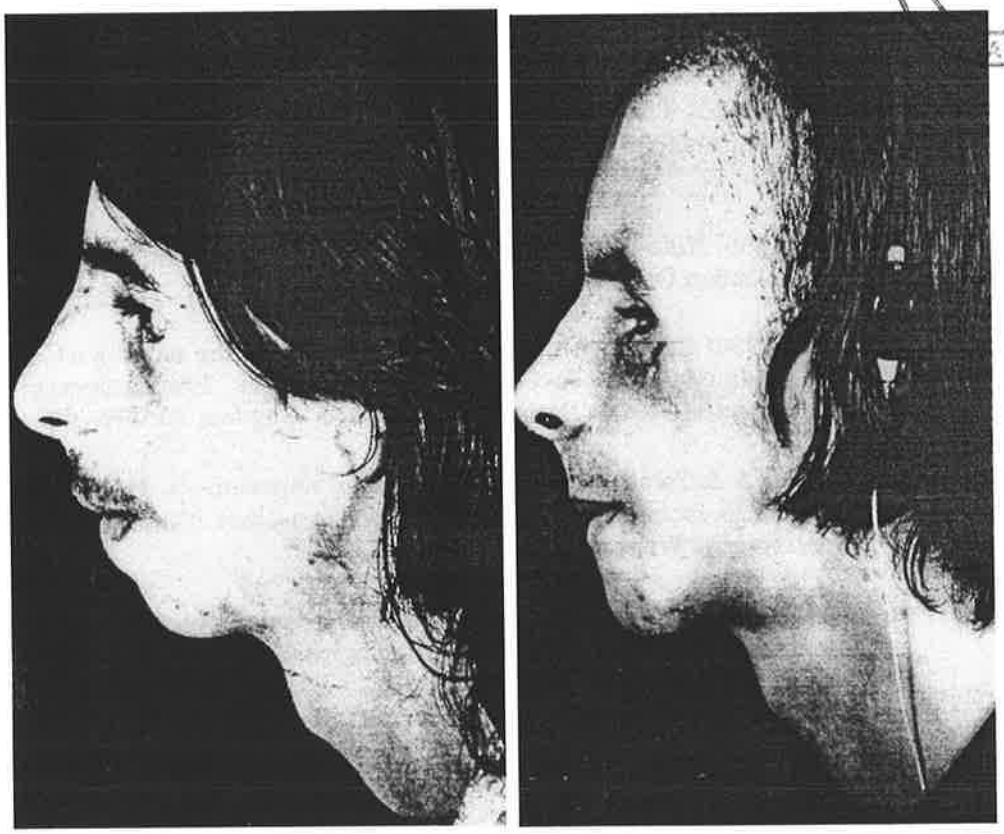

a b

FIG. 6.18. a. *Preoperative view of an adult with severe Treacher Collins syndrome.* **b.** *Early postoperative view after reconstruction of orbit eyelid, zygoma, reduction rhinoplasty and advancement genioplasty. Note the relative enophthalmos after surgery.*

Results

Figure 6.16 shows the results of correction of the orbital deformity in a relatively mild case in a child of six years. Figure 6.16b is taken one year post–surgery, which consisted of bicoronal scalp flap with bilateral pericranial flaps, and reconstruction of the lateral orbital walls, floor and zygoma with calvarial bone and reconstruction of the lower eyelid with an upper lid musculocutaneous flap.

Figure 6.17 shows the results of malar augmentation and sliding genioplasty in an adult female where the only previous surgery had been a rhinoplasty. The greater prominence of the cheek bone and chin point advancement is pleasing, but the lower eyelid deficiency remains noticeable.

Figure 6.18 demonstrates a severe case of Treacher Collins syndrome who has had orbitofacial reconstruction, reconstruction of the lower eyelid, rhinoplasty and sliding genioplasty. The early postoperative picture shows the line of the scalp flap and the significant change in facial contour, and highlights one of the problems, namely the production of a relative enophthalmos when the orbital reconstruction is complete.

References

1 Poswillo D (1975) The pathogenesis of Treacher Collins' syndrome (mandibulo–facial dysostosis). British Journal of Oral Surgery 13: 1–26.

2 Berry G A (1889) Note on a congenital defect (coloboma) of the lower lid. Royal London Ophthalmic Hospital Reports 12: 255.

3 Collins ET (1900) Cases with symmetrical notches in the outer part of each lid and defective development of malar bones. Transactions of the Ophthalmological Society of the United Kingdom 20: 190–192.

4 Franceschetti A & Zwahlen P (1944) Syndrome nouveau—la dysosteose mandibulo–faciale. Bulletin der Schweizerischen Akadamie der medezinische Wissenschaft 1: 60–66.

5 Francheschetti A & Clein D (1949) Mandibulo–facial dysostosis, new hereditary syndrome. Acta Ophthalmologica 27: 143–224.

6 Hemmy D, David DJ & Hermann D (1983) 3–Dimensional reconstruction of cranio–facial deformity using computed tomography. Neurosurgery 13: 534–541.

7 Raulo Y & Tessier P (1981) Mandibulo–facial dysostosis analysis; principles of surgery. Scandinavian Journal of Plastic & Reconstructive Surgery 15: 251–256.

8 Tessier P (1976) Anatomical classification of facial, cranio–facial and latero–facial clefts. Journal of Maxillofacial Surgery 4: 69.

9 Kryzanski S (1971) The challenge and opportunity in cranio–facial anomalies. Cleft Palate Journal 8: 239.

10 Gorlin RJ & Pindborg JJ (1964) Syndromes of the Head and Neck, p. 346. New York: McGraw–Hill.

11 Mann I (1943) Deficiency of the malar bones with defect of the lower lids (with notes of a similar case treated and suggestions by T. Pomfret Kilner). British Journal of Ophthalmology 27: 13.

12 McKenzie J & Craig J (1955) Mandibulo–facial dysostosis (Treacher Collins syndrome). Archives of Diseases in Childhood 30: 391.

13 David DJ, Poswillo D & Simpson D (1982) The Craniosynostoses: Causes, natural History and Management, p 290, Berlin, Heidelberg: Springer.

14 Jackson IT (1981) Plastic and Reconstructive Surgery 67: 365–367.

15 Tessier P (1982) Autogenous bone grafts taken from the calvarium for facial and cranial applications. Clinics in Plastic Surgery 9: 531–538.

16 McCarthy JG & Zide BM (1984) The spectrum of calvarial bone grafting: Introduction of vascularised calvarial bone flap. Plastic and Reconstructive Surgery 74: 10–18.

17 Epker B & Wolford LM (1980) Dentofacial Deformities: Surgical–Orthodontic Correction. Pp 41–94. St Louis: CV Mosby.

18 Tanzer RC (1971) Total reconstruction of the auricle, the evolution of a plan of treatment. Plastic and Reconstructive Surgery. 47: 523.

19 Brent B (1980) The correction of microtia with autogenous cartilage grafts. I. The classic deformity. Plastic and Reconstructive Surgery 66:1–12.

20 Brent B (1980) The correction of microtia with autogenous cartilage grafts. II. A typical and complex deformity. Plastic and Reconstructive Surgery 66: 13–21.

Association of Treacher Collins Syndrome and Translocation 6p21.31/16p13.11: Exclusion of the Locus from These Candidate Regions

M. J. Dixon,* E. Haan, † E. Baker, ‡ D. David, § N. McKenzie, ‖ R. Williamson,‖ J. Mulley,‡ M. Farrall,# and D. Callen‡
**Department of Cell and Structural Biology, University of Manchester, Manchester, England; †Department of Medical Genetics, ‡Cytogenetics Unit, and §Australian Craniofacial Unit, Adelaide Children's Hospital, North Adelaide; and ƒDepartment of Biochemistry and Molecular Genetics, Saint Mary's Hospital Medical School, and #Clinical Research Centre, Northwick Park Hospital, London*

Summary

Treacher Collins syndrome (TCS) is an autosomal dominant defect of craniofacial development which has not been chromosomally localized. We have identified a mother and two children who have TCS and also a balanced translocation t(6;16)(p21.31;p13.11), which suggested the possibility that the TCS locus might be located at one of the translocation breakpoints. These were defined by in-situ hybridisation as 6p21.31 (by using loci in the HLA complex defined by the probes p45.1DPbetaO03/HLA-DPB2 and pRS5.10/HLA class I chain) and 16p13.11 (by using probes pACHF1.3.2/D16S8 and VK45/D16S131). Pairwise and multipoint linkage analysis using localized chromosome 6 probes and chromosome 16 probes in 12 unrelated TCS families with multiple affected siblings excluded the TCS locus from proximity to both translocation breakpoints. These data were confirmed when a third affected child, who did not exhibit the translocation, was born to the mother.

Introduction

Treacher Collins syndrome (TCS) is an autosomal dominant defect of craniofacial development (Rovin et al. 1964; Frazen et al. 1967) which affects approximately 1/50,000 live births. Sixty percent of cases arise as new mutations. The features of TCS include (1) abnormalities of the pinnae which are frequently associated with atresia of the external auditory canals and anomalies of the middle–ear ossicles (bilateral conductive deafness is therefore common) (Phelps et al. 1981), (2) hypoplasia of the facial bones, particularly the mandible and the zygomatic

Received July 5, 1990; revision received September 21, 1990. Address for correspondence and reprints: Michael J. Dixon, Department of Cell and Structural Biology, Third Floor Stopford Building, University of Manchester, Oxford Road, Manchester M13 9PT, England.
 0002-9297/91/4802-0012$02.00

complex, (3) antimongoloid slanting of the eyes, with colobomata of the lower eyelids and a paucity of lid lashes medial to the defect, and (4) cleft palate. There is usually a reasonable degree of bilateral symmetry in these features. The expression of the gene is variable, and occasionally some individuals are so mildly affected that it is difficult to diagnose TCS. However, the gene is rarely nonpenetrant.

Since the tissues affected by TCS arise from the first and second bronchial arches during early embryonic development, it has been proposed that the condition may result from a neural crest cell abnormality. However, the underlying genetic defect is unknown.

Genetic linkage analysis has previously proved successful in identifying the chromosomal location of other craniofacial anomalies in which the underlying biochemical defect is not known (Moore et al. 1987; Brueton et al. 1988; Murray et al.1990). Cytogenetic abnormalities have been useful in directing attention to "candidate regions" in such studies (Tommerup and Nielson 1983; Bocian and Walker 1987).

We report here the identification of a mother and two children who exhibit concordance between TCS and a cytogenetically balanced translocation t(6;16)–(p21.31;p13.11). This suggests that the TCS locus might be at either of these chromosomal locations. Linkage analysis, however, excluded the TCS locus from both candidate regions. These findings were subsequently confirmed by the birth of a third child, who, despite being affected by TCS, did not exhibit the translocation.

Subjects and Methods

Families

The translocation family was identified by one of us (E. H.). The 12 families used for linkage analysis were identified by writing to consultant clinical geneticists throughout the United Kingdom and United States. All patients were examined by experienced clinicians and scored as affected if they presented with the clinical signs noted above. Venous blood samples for DNA preparation were taken from 100 individuals, 56 of whom were affected.

Cytogenetic and In-Situ Hybridization Analysis

Short-term lymphocyte cultures were established and synchronised using a thymidine block and deoxycytidine release for karyotyping (Wheater and Roberts 1987). Probes p45.1DPbeta003 (ATCC), a 1.7-kb unique fragment in pcDV1-pL2; pRS5.10 (supplied by Dr. J. Pan), a 700-bp unique fragment in pBR322; VK45, a 21.3-kb insert in lambda phage, and pACHF–1.3.2, a 2.2–kb unique fragment in pSP64, were tritium labeled to a specific activity of approximately 3.5×10^8 cpm/μg according to a method described elsewhere (Callen et al. 1988).

Each of the four probes was hybridised to metaphase chromosomes from the mother (II.6), at concentrations ranging from 0.05 to 0.2 μg/ml for periods of as long as 3 wk. Probe VK45 contained repeat elements and was preassociated to an excess of unlabeled DNA before hybridisation (Caller et al. 1988). All silver grains touching the chromosomes were counted to determine the pattern of hybridisation of each probe.

DNA Analysis

Genomic DNA was prepared from peripheral blood leucocytes (Kunkel et al. 1977). Five micrograms of DNA was digested with the restriction enzyme revealing the RFLP for the probe in question (table 1), according to the conditions specified by

the manufacturer. The digested DNA samples were fractionated by agarose gel electrophoresis in tris/acetate buffer by using 0.7%–1.0% gels, were transferred to Hybond–N+ membrane (Amersham) by standard methods (Sambrook et al. 1989), and were hybridised with DNA probes radiolabeled by the random primer method (Feinberg and Vogelstein 1983) at 65°C. Final membrane washes were in 0.2 × SSC at 65°C for 30 min. Autoradiography was performed at – 70°C with double intensifying screens for 1–4 d by using Fuji RX film.

Linkage Analysis

RFLPs were scored, and the data were coded in linkage format. Pairwise and multipoint linkage analyses were performed using the LINKAGE program (Lathrop et al. 1984). A gene frequency of .0001 was assumed for the mutant allele. Penetrance was taken to be 99%. Standard significance cutoff points were used. In the case of the chromosome 6 loci the results of the pairwise analyses were graphically interpolated, and the genetic distances corresponding to a lod score of – 2.0 were taken to be the extent of exclusion of the TCS mutation(s) around each locus.

TABLE 1

Description of Linkage Markers Ordered pter–cen

Probe	*Locus*[a]	*Polymorphic Enzyme(s)*	*Map Position*	*Reference*
Chromosome 6:				
F13a	F13AI	*Bam*HI, *Bcl*I	6p24–25	Zoghbi et al. 1988
HLA DQα	pDCHI	*Taq*I	6P21.3	Auffray et al. 1982
Chromosome 16:				
D16S8	CHFl.lA6	*Pvu*II	16p13.13-13.12	Kidd et al. 1989
D16S96	VK20A	*Taq*I, *Msp*I	16p13.12-13.11	Kidd et al. 1989
D16S96	VK20B	*Msp*I	16p13.12-13.11	Kidd et al. 1989
D16S79	36.1	*Taq*I, *Xmn*I,	16p13.12-13.11	Kidd et al. 1989
		*Hin*cII, *Bcl*I		Gedeon et al. 1989
D16S131	VK45C6	*Tag*I	16p13.11-12.3	Kidd et al. 1989
D16S75	R99.6	*Hin*dIII	16p13.12.3	Kidd et al. 1989

[a]*As detailed in the references, with the exceptions of R99.6 (D16S75), which is a 2-kb single-copy fragment of the CRI-R99 probe listed by Kidd et al. (1989) that is subcloned into the EcoRI / HindIII site of pBR322, and ACHFII.lA6, a 1.2-kb EcoRI / HindIII fragment of the phage ACHF1 listed by Kidd et al. (1989) that is subcloned into pUC18 (a 600-bp BstNI-BstNI single-copy fragment of the insert was used as the probe).*

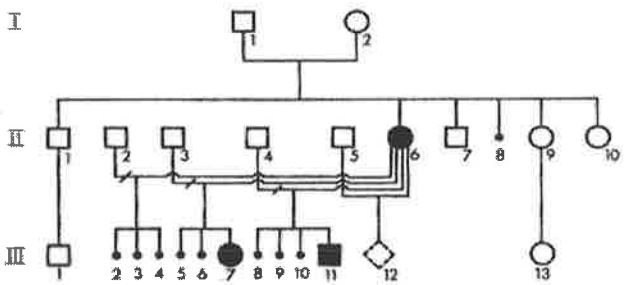

FIG. 1. *Pedigree of family. Individuals II.6, III.7, and III.11 have both Treacher Collins syndrome and a cytogenetically balanced translocation 6;16.*

Results

The pedigree of the family exhibiting the translocation is shown in figure 1. The proband, III.7 (figs. 2B and 2E), was diagnosed as having TCS at 6 wk of age. Her karyotype was 46,XX,t(6;16)(p21.31;p13.11). The proband's half-brother, III.11 (figs. 2C and 2F), was also diagnosed as being affected and exhibited the same translocation. The children's mother, II.6 (figs. 2A and 2D) appeared to have no features of TCS on clinical examination. However, orthopantomogram and occipitomental radiographs revealed hypoplasia of the zygomatic arches and prominent antegonial notching of the mandible (figs. 2G and 2H). Her karyotype, determined following the discovery of the translocation in her daughter, was also 46,XX,t(6;16)(p21.31:13.11) (fig.3A). Both the mother's parents, as confirmed by genetic testing, were unaffected and had normal karyotypes. It was not possible to contact either of the fathers of the affected children; however, from photographs both appeared clinically normal.

The translocation breakpoints at 6p21.31 and 16p13.11 were further localized by in–situ hybridization to metaphase chromosomes by using probes known to map to these two regions (table 2). The probe concentrations and times of exposure were chosen to maximize the signal on the translocated chromosomes, and this resulted in a high number of background grains on the remainder of the karyotype.

To define the breakpoint on chromosome 6 two probes were used: p45.1DPbeta003, which defines a class II DP chain at the proximal extremity of the HLA complex (Spence et al. 1989), and pRS5.10, which defines a class I chain at the proximal extremity of the HLA complex (Srivastava et al. 1987). Results from in-situ hybridizations with the p45.1DPbeta003 probe showed an excess of grains on the normal short arm of chromosome 6 and on the short arm of the der(6) t(6;16), while the number of grains on 16p and on the short arm of the der(16)t(6;16) were consistent with the background distribution of grains on the remainder of the chromosome complement. Results with probe pRS5.10 showed an excess of grains on the short arm of the normal chromosome 6 and on the der(16); that is, this probe was translocated to the derived chromosome 16. It can be concluded that the breakpoint on 6p lies between the chromosomal regions defined by these two probes, proximal to pRS5.10 but distal to p45.1DPbeta003.

To define the breakpoint on chromosome 16 two probes were used, VK45 (D16S131), which was not relocated by the translocation but remained on chromosome 16, and pACHF1.3.2 (D16S8) which was relocated onto chromosome 6 by the translocation. The breakpoint on chromosome 16 therefore lay between the chromosomal regions defined by these two probes.

Pairwise lod scores from families with TCS are summarized in table 3. The data in table 3A exclude the site of the TCS mutation from approximately 13 cM around the clotting factor 13A1 locus and from approximately 22 cM around the HLADQα locus. As these probes are within detectable linkage distance (25–35 cM) of one another, and as the length of the short arm of chromosome 6 is estimated at approximately 55 cM (Zoghbi et al. 1988), our data further exclude the TCS locus from most of 6p except for the telomere.

Similarly, we were able to exclude the TCS locus from close proximity to markers at 16p13.11 (table 3B). Multipoint linkage analysis was used to further exclude the TCS locus from approximately 30 cM round the translocation breakpoint at 16p 13.11 (fig.4).The anchor map was constructed using chromosome 16 RFLP typing from the CEPH reference pedigree panel. The linkage data were subsequently confirmed when the translocation mother gave birth to an affected child who was cytogenetically normal.

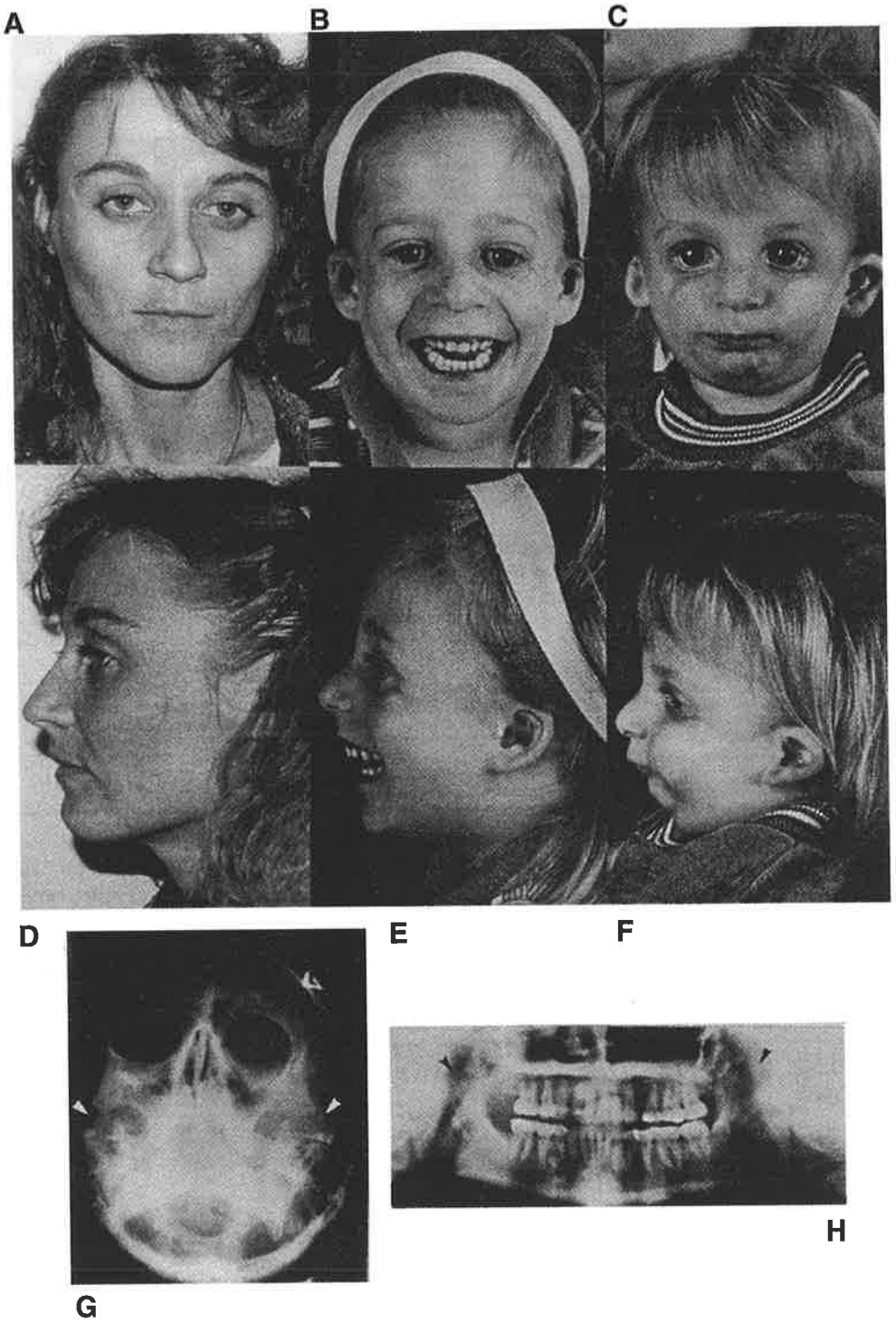

FIG. 2. *Photographs of family* **A.–F.** *and radiographs showing absence of zygomatic arches (arrowed) in mother, II.6* **G.** *and* **H.**

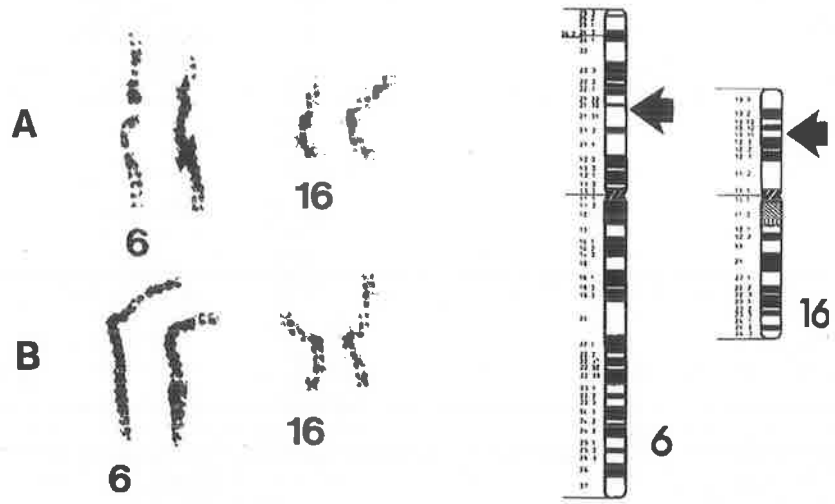

FIG. 3. *Partial karyotype of translocation. Shown are two partial karyotypes (***A.** *and* **B.***) which, from left to right, show normal 6, der(6), normal 16, and der(16). The ideogram is of the two normal chromosomes with breakpoints indicated by arrows.*

TABLE 2

In-Situ Hybridization of Probes to t(6:16)

PROBE	TOTAL No. OF GRAINS					
	Chromosomal Region					
	6p[a]	der6p[b]	16p[c]	der16p[d]	Remainder of Component[e]	No. OF METAPHASES
p45.1 DPbeta003	20	19	5	4	500	52
pRS5.10	21	7	5	25	465	79
VK45	10	6	26	44	852	37
pACHF1.3.2	2	12	10	1	184	17

[a] *Short arm of chromosome 6.*
[b] *16pter–16p13.11::6p21.31–6cen (der6p).*
[c] *Short arm of chromosome 16.*
[d] *6pter–6p21.31::16p13.11–16cen (der16p).*
[e] *Totaled over all metaphases scored.*

Discussion

The genetic mutation(s) responsible for TCS is extremely variable in expression. Some individuals are so mildly affected that detection of obligate carriers is at times difficult. Rarely, the defective gene is nonpenetrant, although in the great majority of cases careful examination of the obligate carrier will reveal minor stigmata of TCS. This was the case for the translocation mother, who on routine clinical examination did not appear to exhibit any features of this disorder. Radiographic examination, by revealing bilateral hypoplasia of the zygomatic arches, permitted the mother to be correctly diagnosed as affected. This demonstrated concordance, at that time, between TCS and the cytogenetically balanced translocation between, the short arms of chromosomes 6 and 16.

TABLE 3

TCS Linkage Values

A. TCS Linkage with 6p Markers								
	Recombination Fraction θ							
Locus	.00	.01	.05	.10	.15	.20	.30	.40
F13A1	- 19.15	- 9.49	–4.69	–2.69	–1.65	–1.02	–.36	–.10
HLADQα	-32.52	- 16.90	–8.82	–5.37	–3.55	–2.41	–1.13	–.47
B. TCS Linkage with 16p Markers								
	Recombination Fraction θ							
Locus	.00	.01	.05	.10	.15	.20	.30	.40
D16S8	–18.73	–11.12	–5.97	–3.65	–2.38	–1.56	–.63	–.18
D16S96	–17.74	–9.98	–4.80	–2.57	–1.44	–.78	–.15	.03
D16S79	–25.99	–13.81	–6.95	–3.88	–2.31	–1.39	–.49	–.20
D16S131	–1.49	–.92	–.13	.18	.29	.32	.24	.11
D16S75	–13.93	–5.84	–2.49	–1.17	–.55	–.23	–.01	–.01

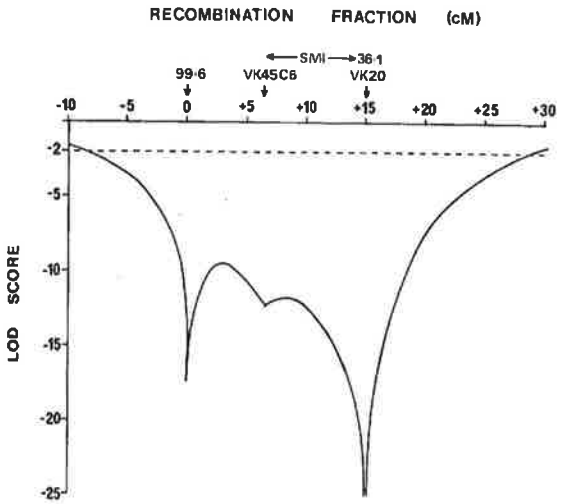

FIG. 4. *Location map of chromosome 16p probes, summarizing lod scores (log 10 odds ratio) calculated for TCS locus at various map positions in fixed marker map of R99.6 (D16S75) VK45C6 (D16S131), 36.1 (D16S79), and VK20 (D16S96). The relative genetic position of R99.6 (D16S75) has arbitrarily been placed at 0. The interval into which the 16p13.11 translocation breakpoint maps is indicated by SMI.*

The translocation breakpoints were defined, cytogenetically and by in–situ hybridisation,as 6p21.31 and 16p13.11.On chromosome 6 the p45.1DPbeta003 probe (HLA–DPB2) and the pRS5.10 probe (HLA class I chain) are at the opposite extremities of the HLA complex and are separated by approximately 4,000 kb. The chromosome 6 breakpoint must lie within this genetic distance (Spence et al. 1989).

We obtained DNA from an additional 12 families with TCS, none of whom had a visible chromosomal abnormality. Using the pDCH1 probe which defines a class 1I DQ alpha chain within the MHC complex, we were able to exclude the TCS mutation from the translocation breakpoint at 6p21.31. Moreover, as the factor 13A1 locus is within approximately 25–35 cM of the HLA complex, and as the length of 6p is estimated at 55 cM (Zoghbi et al. 1988), our data further exclude the TCS locus from most of 6p except for the telomere.

The probes on chromosome 16, pACHF1.1A6 (D16S8) and VK45C6 (D16S131) have been located in the vicinity of 16p13.11–p12.3 by a combination of in–situ hybridization and Southern analysis of mouse/human hybrid cell panels (Caller et al. 1989; Hyland et al. 1989). The chromosome 16 breakpoint was defined as lying between these probes. Both pairwise and multipoint linkage analysis in the additional 12 families excluded the site of the TCS mutation from this second candidate region.

We initially thought that there was a possibility that our data supported genetic heterogeneity, with a mutation at one of the chromosomal breakpoints causing TCS in the translocation family and with mutations at other loci being responsible in the other families. However, our exclusion data do not support this conclusion; no evidence of linkage was detected in any of the informative families studied (data not shown). The subsequent birth of a third child to the translocation mother, a child who, despite being affected, did not exhibit the translocation, confirmed the linkage findings.

We are now constructing a complete exclusion map for TCS by using highly informative markers and by continuing to study alternative candidate locations for the TCS locus, such as that at 5q 11 (Balestrazzi et al. 1983). We would welcome knowledge of other TCS families from which multiple affected individuals are available for study.

Acknowledgments

We thank the Treacher Collins families and the National Deaf Children's Society for their interest and cooperation, without which the present study would not have been possible. We should also like to thank those clinicians who collected samples on our behalf, particularly Drs. D. Donnai, A. Colley, and C. Benjamin (St. Mary's Hospital, Manchester), Dr. T. Hulse (Maidstone Hospital), and Dr. J. Raeburn (Western General Hospital, Edinburgh). Dr. J. Pan (pRS5.10) and Dr. U. Grundmann (F13a) supplied probes. The financial support of the Wellcome Trust, Medical Research Council, The Hearing Research Trust, The Royal Society, The Nuffield Foundation, and the Australian Cranio–Maxillo–Facial Foundation is gratefully acknowledged.

References

1 Auffray C, Korman AJ, Roux–Dosseto M, Bono R, Strominger JL (1982) cDNA clone for the heavy chain of the human B cell alloantigen DC1: strong sequence homology to the HLA-DR heavy chain. Proc Natl Acad Sci USA 79: 6337–6341

2 Balestrazzi P, Baeteman MA, Mattei MG, Mattei JF (1983) Franceshetti syndrome in a child with a de nova balanced translocation (5:13) (q11;p11) and significant decrease of hexosaminidase B. Hum Genet 64: 305–308

3 Bocian M, Walker AP (1987) Lip pits and deletion 1q32–41. Am J Med Genet 26: 437–443

4 Brueton L, Huson SM, Winter RM, Williamson R (1988) Chromosomal localization of a developmental gene in man: direct DNA analysis demonstrates that Greig cephalopolysyndactyly maps to 7p13. Am J Med Genet 31: 799–804

5 Callen DF, Hyland VJ, Baker EG, Fratini A, Gedeon AK, Mulley JC, Fernandez KEW, et al (1989) Mapping the short arm of human chromosome 16. Genomics 4: 348–354

6 Callen DF, Hyland VJ, Baker EG, Fratini A, Simmers RN, Mulley JC, Sutherland GR (1988) Fine mapping of gene probes and anonymous DNA fragments to the long arm of chromosome 16. Genomics 2: 144–153

7 Feinberg AP, Vogelstein B (1983) A technique for radiolabeling DNA restriction endonuclease fragments to high specific activity. Anal Biochem 132: 6–13

8 Frazen LE, Elmore J, Nadler HL (1967) Mandibulo–facial dysostosia (Treacher Collins syndrome). Am J Dis Child 113: 406–410

9 Gedeon AK, Mulley JC, Breuning MH (1989) XmnI, HincII and BclI RFLPs at D16S79. Nucleic Acids Res 17: 4905

10 Hyland VJ, Fernandez KEW, Callen DF, McKinnon RN, Baker EG, Friend K, Sutherland GR (1989) Assignment of anonymous DNA probes to specific intervals of human chromosomes 16 and X. Hum Genet 83: 61–66

11 Kidd KK, Bowcock AM, Schmidtke J, Track RK, Ricciuti F, Hutchings G, Bale A, et al (1989) Report of the DNA committee and catalogs of cloned and mapped genes and DNA polymorphisms. Cytogenet Cell Genet 51: 622–947

12 Kunkel LM, Smith KD, Boyer SH, Borgeonker DS, Wachtel SS, Miller OJ, Breg WR, et al (1977) Analysis of human Y–chromosome specific reiterated DNA in chromosome variants. Proc Natl Acad Sci USA 74: 1245–1249

13 Lathrop GM, Lalouel JM, Julier C, Ott J (1984) Strategies for multilocus linkage analysis in humans. Proc Natl Acad Sci USA 81: 3443–3446

14 Moore GE, Ivens A, Chambers J, Farrall M, Williamson R, Page DC, Bjornsson A, et al. (1987) Linkage of an X–chromosome cleft palate gene. Nature 326: 91–92

15 Murray JC, Nishimura DY, Buetow KH, Ardinger HH, Spence MA, Sparkes RS, Falk RE, et al (1990) Linkage of an autosomal dominant clefting syndrome (Van der Woude) to loci on chromosome 1q. Am J Hum Genet 46: 486–491

16 Phelps PD, Poswillo D, Lloyd GAS (1981) The ear deformities in mandibulofacial dysostosis. Clin otolaryngol 6: 15–28

17 Rovin S, Dachi SF, Borenstein DB, Cotter WB (1964) Mandibulofacial dystosis, a familial study of five generations J Pediatr 65:215-221

18 Sambrook J, Fritsch EF, Maniatis T (1989) Molecular cloning: a laboratory manual. Cold Spring Harbor Laboratory, Cold Spring Harbor, NY

19 Spence MA, Spurr MK, Field LL (1989) Report of the Committee on the Genetic Constitution of Chromosome 6 Human Gene Mapping 10. Cytogenet Cell Genet 51: 149–165

20 Srivastava R, Chorney MJ, Lawrance SJ, Pan J, Smith Z, Smith CL, Weissman SM (1987) Structure, expression, and molecular mapping of a divergent member of the class I HLA gene family. Proc Natl Acad Sci USA 84: 4224–4228

21 Tommerup N. Nielson F (1983) A familial reciprocal translocation t(3:7)(p21.1:p13) associated with the Greig polysyndactyly–craniofacial anomalies syndrome. Am J Med Genet 16: 313–321

22 Wheater RF, Roberts SH (1987) An improved lymphocyte culture technique: deoxycytidine release of a thymidine block and use of a constant humidity chamber for slide making. J Med Genet 24: 113–115

23 Zoghbi HY, Daiger SP, McCall A, O'Brien WE, Beaudet AL (1988) Extension DNA polymorphism at the factor XIIIa (F13A) locus and linkage to HLA. Am J Hum Genet 42: 877–883

Mandibular Lengthening by Distraction for Airway Obstruction in Treacher–Collins Syndrome

Mark H. Moore, FRACS
Gabriela Guzman–Stein, MD
Timothy W. Proudman, MB, BS
Amanda H. Abbott, PhD
David J. Netherway, PhD
David J. David, FRACS
North Adelaide, South Australia

Mandibular lengthening by distraction was performed in a 6–year–old tracheostomy–dependent Treacher–Collins syndrome patient. Detailed preoperative imaging revealed an occluded retrotongue base pharyngeal airway, which, following mandibular distraction, became patent and permitted tracheostomy removal. Mandibular distraction as a technique must be targeted toward clinical problems—management of upper–airway obstruction may be one such scenario.

KEY WORDS: *Airway obstruction, mandibular lengthening, Treacher–Collins syndrome.*

Mandibular lengthening by distraction has been reported in both laboratory and clinical situations [1–4]. Adapted from the technique employed in the upper and lower extremities, and popularized by Ilizarov [5], it is now possible to lengthen the mandible unilaterally and bilaterally. The clinical indications for and timing of such exercises in mandibular distraction have not yet been clearly elucidated.

Treacher–Collins syndrome (TCS)—in addition to its distinctive facial dysmorphology—is associated with frequent upper-airway abnormalities. Obstructive apnea occurred in 25% of TCS patients in one series [6]. The compromise of the upper airway has been related to cranial base anomalies, mandibular hypoplasia, and retrognathia, as well as to the complex interplay between mandibular position and the basicranium [7–9]. The possibility of early "skeletal surgery, including maxillary and mandibular advancements" to facilitate forward displacement of the occluding floor of mouth soft tissues and "enlarging the airway" has been raised [9]. The advent of techniques of mandibular lengthening by gradual distraction provides the opportunity to elongate the mandible, increase the size of the retrotongue base pharynx, and open the upper airway.

This report describes mandibular lengthening by distraction in a TCS patient who was tracheostomy dependent, where the surgery produced resolution of upper airway obstruction.

From the Australian Cranio–Facial Unit, Women's & Children's Hospital, North Adelaide, South Australia.
Address correspondence to Mr Moore, Australian Cranio-Facial Unit, 72 King William Road, North Adelaide,

Case Report

One patient, R. L., with severe TCS and cleft palate was 6 years 2 months of age when he underwent bilateral mandibular lengthening by distraction. Significant upper airway obstruction was noted from an early age and repeat tracheostomies were needed from age 10 months. Bilateral orbitozygomatic reconstruction with pedicled calvarial bone flaps were performed at age 4 years, and repair of the cleft palate at age 5 years.

Preoperative assessment confirmed typical, severe TCS facies (Fig 1). Total occlusion of the upper airway was documented on sleep studies and oximetry, and he remained tracheostomy dependent. Mandibular lengthening by distraction was achieved using a pair of standard external fixators with two double-pin holders, as described previously (Fig 2). A bolt arrangement at one end allowed controlled calibrated distraction.

An intraoral approach through the lower vestibule exposed the vertical ramus and angle of the mandible in a subperiosteal plane bilaterally. Corticotomy was performed in the region of the mandibular angle, the exact position and obliquity of the line being determined by the posterior teeth, both erupted and unerupted, and the amount of proximal bone in the abnormally short vertical ramus for placement of the pins. Two "half-pins" were placed percutaneously on either side of the corticotomy, the orientation producing downward and forward mandibular movement when distracted. Slight bony separation was produced at the corticotomy site after attachment of the external fixator and prior to wound closure.

Serial distraction of 1 mm per day was commenced after 5 days and continued for an additional 20 days. During this time, we became concerned that the right mandibular condyle had become dislocated proximally. Radiological investigation with oblique plain radiographs and computed tomography (CT) scans failed to confirm this. Following the active movement period, the fixators were maintained for another 6 weeks prior to removal. Subsequently the tracheostomy was occluded as a trial, and oximetry and formal sleep studies were repeated. These confirmed the clinical impression of complete resolution of airway obstruction and allowed removal and closure of the tracheostomy (Fig 3).

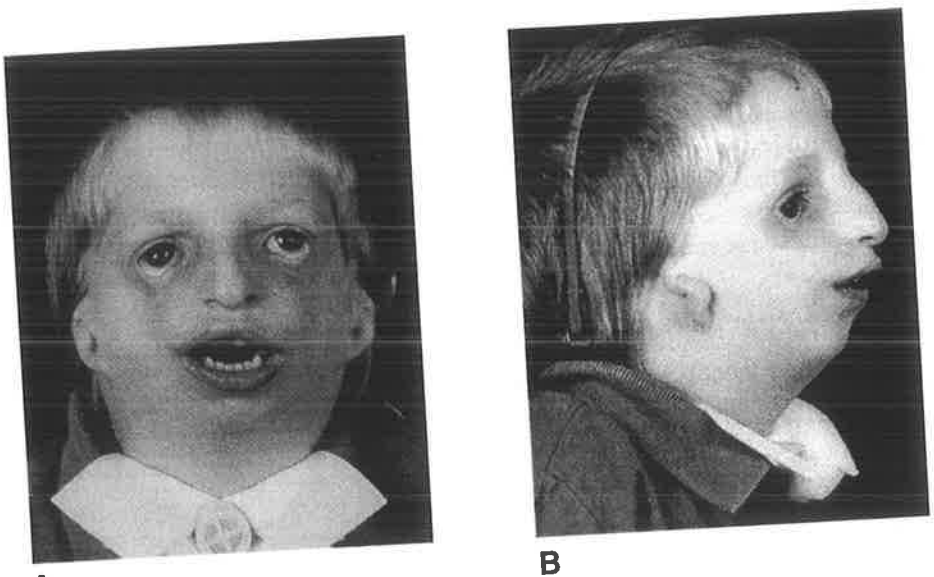

FIG. 1. A. B. *Preoperative frontal and right lateral view of a Treacher–Collins syndrome*

Detailed CT scan assessment of the craniofacial skeleton was performed immediately prior to placement of, and 2 weeks after removal of, the external fixators. This information provides the basis for the quantitative assessment of the skeletal changes induced by distraction and the secondary soft–tissue alterations that created a functional, nonoccluded upper airway.

The identification of known landmarks on the mandible [10] permitted the construction of wire–frame models and the assessment of the changes in shape and position of the mandible relative to the cranial base (Fig 4). CT scan views in the sagittal plane demonstrated the production of a patent airway in the retrotongue base region (Fig 5). Follow–up after 18 months showed maintenance of a safe retrotongue base airway.

Discussion

Although the soft tissue and skeletal anomalies of the Treacher–Collins facies are uniquely characteristic and demanding of staged surgical intervention for both functional and aesthetic reasons, recent reports have detailed the more immediately problematic occurrence of obstructive apnea in this condition. Those same skeletal features—short mandibular vertical ramus and body, mandibular symphyseal recession, and displaced maxilla—that characterise TCS appearance also contribute to the upper–airway compromise reported in 25% of these patients [6].

Acute angulation of the cranial base [7,8,11] progressive with time, medial narrowing of the medial pterygoids [8], and mandibular ramus and body deficiency all contribute to circumferential reduction in pharyngeal free air space [9]. To date, objective assessment and early management of the airway in TCS have received little attention, with a direct step to tracheostomy in those severe cases where airway compromise is lifethreatening.

FIG. 2. *Clinical appearance with distraction devices placed bilaterally.*

FIG. 3. A. B. *Frontal and right lateral views 8 months after fixator removal confirmed anterior displacement of the mandible and tracheostomy removal.*

Mandibular lengthening by distraction has been reported in hemifacial microsomia and Nager's syndrome [4]. The rationale for distraction in that study was to reduce the degree of skeletal abnormality, possibly altering the soft-tissue functional matrix, potentiating further growth and minimizing later skeletal surgery; however, these aims have not yet been fulfilled. This procedure does, however, leave the major floor of mouth and tongue skeletal attachments undisturbed and result in anterior translocation of these soft tissues with creation of a retrotongue base pharynx of increased dimension. In this case it was sufficient to remove all clinical evidence of airway obstruction and permit removal of a long–standing tracheostomy. This response, following mandibular distraction, suggests that the relative anteroposterior position of the mandible has a major influence on upper–airway mechanics in TCS at this age. The other areas of dysmorphology at higher levels, while contributory, were not the major source of obstructive apnea.

Although follow–up is limited—only 18 months in this case—the prolonged safe maintenance of a normal upper airway is anticipated. The tendency for subsequent skeletal remodeling and relapse is undoubtedly present, with possible progressive recurrence of airway obstructive symptoms. The encompassing soft–tissue functional matrix has been stretched and altered to a degree comparable to the skeletal changes. The underlying pathology is, however, of a clefting condition with inherent impaired growth potential, unaltered by skeletal distraction. The simultaneous placement of a tissue expander in the anterior neck may alter the superficial soft–tissue distorting forces and overcome the tendency for long–term relapse.

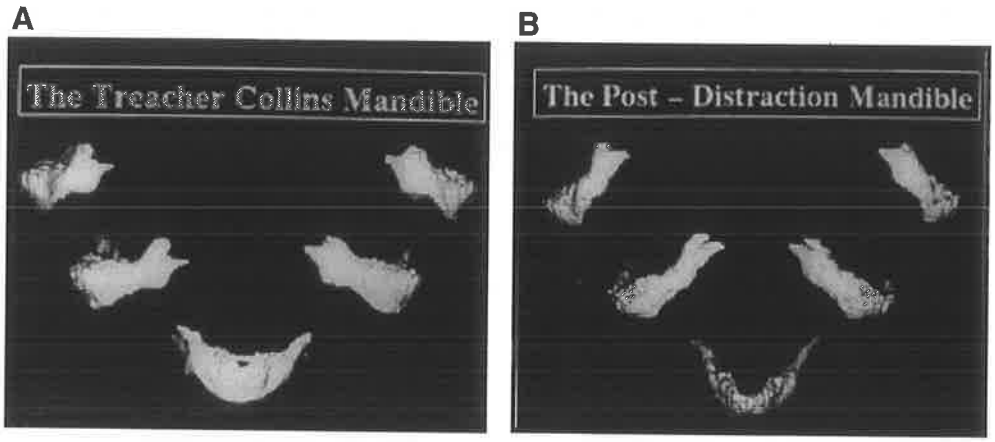

FIG. 4. A. *Preoperative three–dimensional computed tomography (CT) reconstructions of the mandible in this case.* **B.** *Postoperative three–dimensional CT reconstruction of the mandible identifies the lengthening primarily in the ascending ramus, with greater length achieved on the left side.*

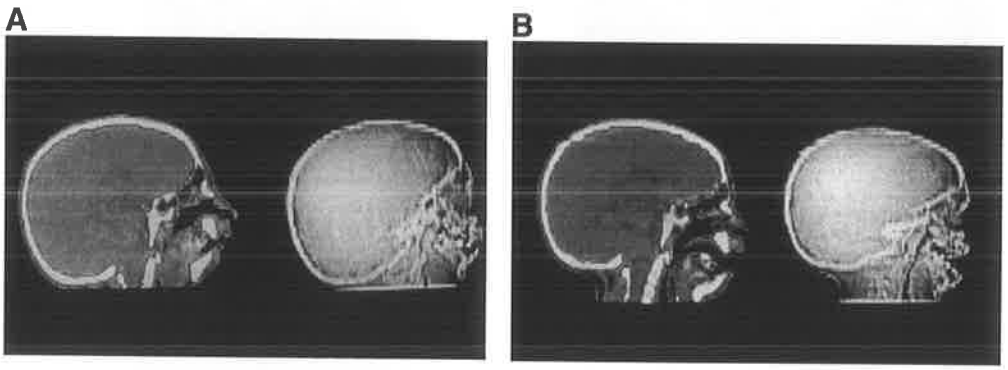

FIG. 5. A. *Preoperative sagittal two–dimensional computed tomography scan with outlining of the airway confirms obstruction of the retrotongue base pharynx.* **B.** *Comparable postoperative views identify the production of a patent retrotongue base pharyngeal airway.*

Mandibular distraction would appear to be of maximum value during the period of mixed dentition. Earlier than this, the bone is not sufficiently mineralised and the pins will cut through; if used later, definitive osteotomies would achieve more with greater predictability. Even at this time the available bone for pin placement is limited. The location of the corticotomy must leave sufficient bone substance on the proximal fragment (condyle and vertical ramus) for the siting of the two pins of the distraction device, and at the same time not be placed so distally as to damage the unerupted secondary dentition. Indeed, the relative lack of bone substance, as well as hypoplastic soft tissue and muscle envelope supporting the proximal fragment, risks proximal subluxation and even dislocation of the condylar head as distraction proceeds within the tight tissue envelope. A variable three–point fixator, with pins in the cranium, proximal fragment (vertical ramus), and mandibular body, may overcome this and provide a stable framework for complex, coordinated three–dimensional distraction. This needs to be explored to improve control of the degree of anterior, inferior, and lateral movement in these challenging deformities.

References

1. Snyder CC, Levine GA, Swanson HA, Browne EZ. Mandibular lengthening by gradual distraction. Plast Reconstr Surg 1973; 51: 506–508

2. Karp NS, Thorne CHM, McCarthy JG, Sissons HA. Bone lengthening the cranio–facial skeleton. Ann PlastSurg 1990;24: 231–237

3. Costantino PD, Shybut G, Eriedman CD, et al. Segmental mandibular regeneration by distraction osteogenesis. Arch Otolaryngol 1990; 116: 535–545

4. McCarthy JG, Schreiber J. Karp N. et al. Lengthening the human mandible by gradual distraction. Plast Reconstr Surg 1992;89: 1–8

5. Ilizarov GA. The principles of the Ilizarov method. Bull Hosp It Dis Orthop Inst 1988;48: 1–11

6. Sher AK, Shprintzen RJ, Thorpy MJ. Endoscopic observation of obstructive sleep apnoea in children with anomalous upper airway: predictive and therapeutic value. Int J Paediatr Otorhinolaryngol 1986; 11: 135–146

7. Shprintzen RJ, Croft C, Berkman MD, Rakoff SJ. Pharyngeal hypoplasia in Treacher–Collins syndrome. Arch Otolaryngol 1979; 105: 127–131

8. Shprintzen RJ. Palatal and pharyngeal anomalies in craniofacial syndromes. Birth Defects 1982;18: 53–78

9. Arvytas M, Shprintzen RJ. Craniofacial morphology in Treacher–Collins syndrome. Cleft Palate–Craniofac J 1991;28: 226–230

10. Abbott AH, Netherway DJ, David DJ, Brown T. Application and comparison of techniques for threeædimensional analysis of craniofacial anomalies. J Craniofac Surg 1990;1: 119–134

11. Peterson–Falsone SJ, Figueroa AA. Longitudinal changes in cranial base angulation in mandibulofacial dysostosis. Cleft Palate J 1989; 26: 31–35

Intraorbital Tissue Expansion in the Management of Congenital Anophthalmos

D. J. Dunaway and D. J. David
Australian Craniofacial Unit, Women's and Children's Hospital, North Adelaide, South Australia

SUMMARY

Seven cases of intraorbital tissue expansion for the treatment of congenital anophthalmos or microphthalmos are presented. The ages of the patients at insertion of the expander ranged from 4 months to 8 years. A 4ml spherical tissue expander with a remote injection port was inserted into the affected orbit via a bicoronal approach. Expansion periods ranged between 4 months and 3 years and are continuing in 2 patients. Results were assessed by clinical examination, comparison of photographs, 3D CT scans and orbital measurements taken from axial CT scans which were compared with established normal values.

Results confirmed enlargement of the orbit with expansion. Long–term expansion over several years established near normal bony growth patterns. Placement of the expander within the orbital soft tissue cone resulted in more symmetrical expansion than subperiosteal placement. An osteotomy releasing the lateral orbital wall in older children allows expansion of the orbit and may reduce the incidence of expander extrusion.

Although intraorbital tissue expansion successfully induces orbital growth, improvement in the form and size of the congenitally deficient eyelids is less marked.

The growing eye is an important stimulus for the development of the orbit and eyelids both before and after birth. It is also a stimulus to the growth of surrounding facial structures. This growth stimulus is absent in congenital anophthalmia and microphthalmia and results in a small orbital cavity, underdeveloped eyelids and often deficient growth of the midface on the affected side.

Traditional management of the anophthalmic or enucleated orbit in childhood involves the use of incrementally enlarged conformers which have been shown to enlarge the palpebral fissures and fornices, but have little effect on the bony orbit.[1,2] Alternatively, orbital enlargement may be achieved with expansion osteotomies[3–5] and the use of serial spherical implants postoperatively to encourage growth.

Three groups of workers[2,6,7] have shown that the use of gradually inflated intraorbital tissue expanders in anophthalmic cat orbits can induce normal orbital growth patterns. This technique has been used in humans, but has not been extensively reported. We present an account of seven cases of intraorbital tissue expansion carried out at the Australian Craniofacial Unit.

Patients and methods

Seven children, ranging in age from neonates to 8 years old, presenting between 1989 and 1992 with unilateral or bilateral congenital anophthalmia or microphthalmia were treated with intraorbital tissue expansion. The management of these cases falls into two broad categories:

1. Children in whom the expander remains in situ for a few months and is rapidly expanded to increase the size of an osteotomised orbit and eyelids before the insertion of a prosthesis.

2. Infants in whom the expander remains in situ throughout the orbital growth period and is gradually inflated to encourage a normal orbital growth rate.

All of the patients had an initial assessment which included axial 2D and 3D CT scans. The details of operative treatment varied slightly between patients. There follows an account of the most commonly used procedure and deviations from this procedure are detailed in the individual case reports that follow.

After raising a bicoronal scalp flap the periosteum is raised from the superior, lateral and inferior walls of the orbit. An incision is then made in the reflected orbital periosteum superiorly, through which a 4ml spherical tissue expander is placed within the orbital soft tissues. The tube to the filling port is then passed through a further small incision placed posteriorly and laterally in the orbital periosteum. From this point the tube passes through a small hole created in the lateral orbital wall into the temporal fossa and up onto the scalp (Fig. 1). Injection ports are placed subcutaneously in the temporoparietal region. A tarsorraphy is performed and 2 ml of saline injected into the expander. In patients over 2 years of age, expander placement is preceded by osteotomies through the frontozygomatic suture, lateral orbital wall, zygomatic bone and arch, lateral part of the orbital floor and inferior orbital rim.

Inflation of the tissue expanders generally starts 2 weeks postoperatively and continues at varying rates, as detailed in the individual case reports. Infants undergoing prolonged expansion during growth will have the expanders removed at the age of seven.

Assessment of the results of tissue expansion was by clinical observation, comparison of photographs and analysis of CT data. Orbital measurements were taken from axial CT scans as described by Waitzman et al.[8,9] and compared to the normal values they defined in their analysis of 542 axial CT scans from skeletally normal subjects.

In their study, Waitzman et al. used a laser guiding system to ensure that the axial films were in a plane parallel to the orbitomeatal plane. Orbital measurements were taken from a CT section that transected the lens of the globe, medial and lateral rectus muscles, optic nerve, ethmoid air cells, nasal bones and superior aspect of the frontal process of the zygomatic bones. The measurements they made that relate to this study are defined in Figure 2, with relevant numerical data given in Table 1.

In this study, scout films were studied to ensure that the CT axial investigation had been carried out at an angle closely approximating to the orbitomeatal plane. Films that did not fulfil this criteria were rejected. Waitzman's criteria were used to select the orbital slice to be measured using the normal side if present or using the features available in cases of bilateral anophthalmia. Measurements defined in Figure 2 were used to assess orbital growth with expansion and were compared to normal values. Subjective assessments of 2D and 3D CT scans were also used.

FIG. 1. *Placement of the expander. The expander can be seen sitting partially inflated within the orbit, with the injection port tubing emerging into the temporal fossa. An osteotomy cut at the zygomaticofrontal suture can also be seen.*

Case reports

The details of seven cases of the use of intraorbital tissue expansion are given Numerical data relating to the analysis of CT scans is given in Table 2.

Case 1

Female. Presented at 3 years of age. Diagnosis: bilateral anophthalmia. (Figs 3, 4).

At presentation, small orbits and hypoplastic eyelids with short palpebral fissures were noted. CT measurements demonstrated that orbital wall lengths and the lateral orbital distance were below the 95% confidence interval for normal 3-year-olds.

4 ml spherical tissue expanders were inserted into each orbit to lie within the soft tissues of the orbits. Orbital osteotomies as previously described were performed and the remote expander ports were brought through the lateral orbital wall to lie subcutaneously in the temporal region. 2 ml of saline was injected into each expander and postoperatively. 0.1 ml of saline was injected each week for a period of 20 weeks. Thereafter, expansion took place at a much slower rate and is ongoing. The expanders will remain in situ until the patient is 7 years of age. Expansion has progressed without complications. The initial increase in orbital size resulted from a decrease in the mid-interorbital distance as the medial orbital wall expanded.

Measurements taken 2.5 years after expander insertion show that orbital growth has occurred to an extent that the orbital wall lengths and lateral orbital distance now lie within the normal range. This is also shown by an increase in the lateral orbital wall angles. There has been no tendency for the expanders to displace anteriorly and a 3D CT scan shows bone growing across the anterior surface of the expander (Fig. 3). Whilst bony orbital growth has been demonstrated, the response of the soft tissues has been less favourable with the persistence of small eyelids and short palpebral fissures (Fig. 4).

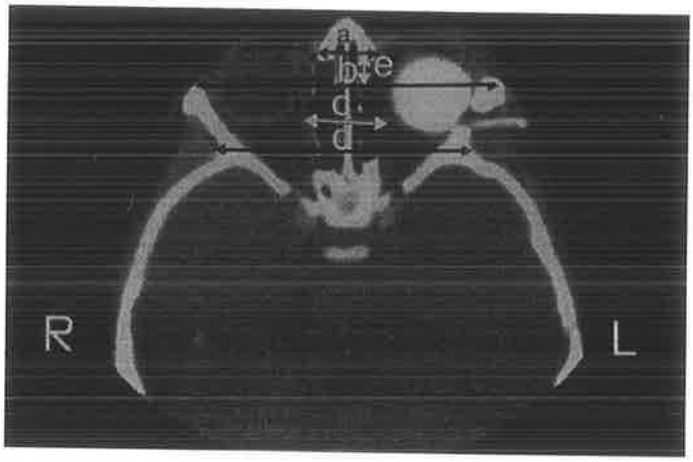

FIG. 2. *CT measurements in the orbital region. (after Waitzman et al.[9]). The parameters measured are demonstrated on axial CT scans from our series. A partially inflated expander can be seen in the left orbit with the injection port tubing emerging through a hole in the lateral orbital wall into the temporal fossa.*

Key	*Measurement*	*Description*
a	Anterior interorbital distance (AID)	The distance between a point on each lacrimal bone representing the anterior end of the medial orbital wall.
b	Lateral orbital distance	The distance between the most anterior tip of each lateral orbital wall.
c	Mid–interorbital distance (MID)	The distance between a point on each medial orbital wall midway between the lacrimal bone and the base of the optic strut.
d	Intertemporal distance (ITD)	The distance between the most medial aspect of each temporalis groove.
e	Medial orbital wall protrusion (MOWP)	The perpendicular distance between the most anterior tip of each lateral orbital wall and the lacrimal bone.
f	Medial orbital wall length (MOWL)	The distance between the lacrimal bone and the base of the optic strut.
g	Lateral orbital wall length (LOWL)	The distance between the most anterior tip of the lateral orbital wall and the base of the optic strut.
h	Lateral orbital wall angle (LOWA)	The angle formed between a line joining the anterior and posterior ends of the lateral orbital wall and the sagittal axis.

Case 2

Female. Presented at 5 years of age. Diagnosis: congenital left microphthalmia.

Before referral to the Australian Craniofacial unit an enucleation of the vestigial left eye had been performed with a lateral canthoplasty to aid retention of a prosthesis. On presentation the left orbit was clinically hypoplastic with blepharophimosis. Measurements from axial CT scans revealed a marginally

TABLE 1

Means and 95% confidence intervals in the orbital region (selected values from Waitzman et al.[9])

Age (months)	Anterior interorbital distance mean	95% CI	Lateral orbital distance mean	95% CI	Mid–interorbital distance mean	95% CI	Intertimporal distance mean	95% CI	Medial orbital wall length mean	95% CI	Lateral orbital length mean	95% CI	Medial orbital wall protrusion mean	95% CI
3	17.40	12.6–22.2	65.40	54.7–76.0	16.00	10.1–21.9	58.50	48.6–68.5	28.60	24.2–33.0	33.70	29.5–38.0	6.00	2.2–9.7
6	17.90	14.4–21.4	69.90	56.4–83.4	16.50	11.4–21.6	63.10	50.3–75.8	32.50	27.0–37.9	36.80	29.7–43.9	6.80	3.0–10.5
9	18.60	14.1–23.2	72.90	64.2–81.5	17.30	12.9–21.7	64.00	56.1–71.9	36.20	30.4–41.9	38.80	33.6–44.0	8.80	4.4–13.2
11	17.80	13.4–22.3	73.50	66.6–80.4	17.60	15.1–20.2	64.10	55.5–72.6	34.20	26.5–41.8	39.40	34.4–44.4	7.30	2.1–12.5
12	18.20	14.3–22.2	74.70	66.4–83.0	18.80	15.6–22.0	65.10	55.3–74.9	37.60	33.2–42.0	40.30	34.8–45.8	8.70	4.5–12.8
24	18.40	14.7–22.0	77.70	71.2–84.1	19.80	15.2–24.4	66.50	57.1–76.0	39.40	31.9–46.9	41.80	36.0–47.5	9.30	3.7–14.9
36	19.30	15.6–23.0	79.10	71.4–86.9	21.30	16.5–26.6	68.30	59.6–77.1	40.50	35.5–45.4	42.60	38.0–47.2	9.60	6.1–13.1
48	20.30	15.3–25.4	81.70	71.8–91.6	22.10	15.1–29.0	69.40	58.4–80.4	40.40	34.0–46.7	43.00	37.0–48.9	10.10	6.6–13.6
60	20.60	15.3–25.9	84.10	76.9–91.4	22.90	18.3–27.5	70.50	61.5–79.6	42.10	36.4–47.7	43.80	39.0–48.5	11.20	7.1–15.2
72	21.50	17.0–25.9	85.60	78.2–92.9	25.10	19.1–31.2	70.70	61.8–79.6	41.40	36.2–46.5	44.40	39.5–49.2	9.90	5.8–13.9
84	21.50	17.5–25.6	86.60	74.6–98.7	24.80	17.2–32.5	72.30	61.5–83.1	41.90	37.0–46.8	44.20	38.2–50.2	10.60	4.4–16.8
96	22.20	17.5–26.8	88.80	79.4–98.2	25.90	20.6–31.3	74.00	63.9–84.1	42.10	33.5–50.7	44.50	39.4–49.7	10.70	5.1–16.2
108	22.20	16.4–28.1	88.10	76.5–99.6	25.10	17.1–33.2	73.90	58.0–89.8	42.50	35.9–49.0	45.30	40.1–50.4	11.10	5.0–17.1
120	22.10	18.6–25.6	89.10	81.8–86.4	26.30	20.6–32.0	73.80	64.3–83.2	42.60	35.8–49.4	45.20	40.2–50.2	10.60	6.6–14.6
204	23.80	19.9–27.7	95.30	82.0–108.5	27.50	22.3–32.7	78.70	65.0–92.4	44.20	37.4–51.1	47.10	41.2–53.0	10.90	5.5–16.3

FIG. 3. *(Case 1). A 3D CT scan shows the intraorbital tissue expanders in place with tubing emerging through the right lateral orbital wall leading to an injection port in the temporoparietal region. A thin lip of bone arising from the superior orbital margin can be seen covering part of the superior surface of the expanders.*

smaller left orbit with a short lateral orbital wall length and reduced lateral orbital distance.

At 9 years of age, a 4 ml spherical tissue expander was inserted into the soft tissues of the orbit via a bicoronal approach and orbital and zygomatic osteotomies performed. 2ml of saline was injected into the expander intra–operatively. A further 5 ml of saline was injected into the expander in the following 5 months. At this stage the expander was removed, the orbit bone grafted with rib grafts and a new prosthesis constructed.

Clinically, significant improvement in soft tissue projection was noted following the tissue expansion which allowed an appropriate ocular prosthesis to be inserted. Orbital measurements taken from axial CT showed an increase in the lateral orbital distance slightly greater than that which would be expected from normal growth, coupled with an increase in lateral orbital angle on the affected side. In general, however, expansion over this 5–7 month period had a small effect on the orbital parameters measured.

Case 3

Female. Presented at 2 years of age. Diagnosis: congenital left microphthalmia.

Measurements from axial CT scans at presentation indicated that the left orbit was smaller than the right, but that both were within the 95% confidence interval for age–matched normal children.

A 4 ml tissue expander was inserted into the left orbit after performing orbital and zygomatic osteotomies. Expansion took place rapidly initially, achieving an 8 ml volume in 6 weeks. At this time, the expander cavity became mildly infected, resulting in removal of the expander. An orbital conformer was inserted.

Results of expansion of soft tissues were assessed as satisfactory with an apparent increase in orbital size. Some increase in ptosis of the left upper eyelid was noted. CT measurements confirmed a small increase in lateral orbital distance and lateral orbital wall length on the expanded side. There was also a decrease in the mid–interorbital distance. These changes, however, were small.

Results of expansion of soft tissues were assessed as satisfactory with an apparent increase in orbital size. Some increase in ptosis of the left upper eyelid

TABLE 2

Orbital measurements taken from axial CT films of the seven cases

Age (months)	*Months post–op*	*AID (mm)*	*LOD (mm)*	*MID (mm)*	*ITD (mm)*	*Right MOWL (mm)*	*Left MOWL (mm)*	*Right LOWL (mm)*	*Left LOWL (mm)*	*Right MOWP (mm)*	*Left MOWP (mm)*	*Right LOWA*	*Left LOWA*
Case 1													
41.0	–1.00	22.30	63.00	21.50	56.90	35.30	36.90	35.30	36.90	7.60	7.60	33.00	38.00
44.00	2.00	25.00	63.30	16.60	61.70	38.30	40.00	38.30	38.30	8.30	8.30	35.00	38.00
46.00	4.00	25.00	70.00	20.00	60.00	38.40	40.00	38.40	38.40	8.30	8.30	35.00	40.00
73.00	31.00	25.20	80.00	22.60	67.10	45.70	45.70	42.80	42.80	11.40	11.40	40.00	40.00
Case 2													
72.00	–12.00	23.30	83.30	21.70	71.70	40.00	40.00	40.00	39.20	1.30	1.30	46.00	45.00
108.0	–1.00	24.00	84.80	22.40	76.50	40.00	41.60	38.40	38.40	9.60	8.00	45.00	43.00
113.0	5.00	22.40	87.50	20.00	78.70	37.50	40.00	37.50	40.00	7.50	7.50	44.00	48.00
Case 3													
36.00	–3.00	16.70	76.70	18.30	70.00	45.00	40.00	41.70	38.30	10.00	10.00	45.00	39.00
41.00	2.00	16.60	78.30	16.60	70.00	40.00	41.70	40.00	41.70	10.00	10.00	44.00	40.00
Case 4													
1.00	–3.00	18.30	53.30	16.70	56.70	30.00	26.70	26.70	20.00	10.00	8.30	44.00	36.00
4.00	1.00	17.10	58.60	17.10	54.30	35.70	31.40	30.00	28.60	5.70	5.70	43.00	40.00
11.00	7.00	28.80	60.00	33.30	60.00	31.10	28.90	31.10	26.70	8.90	8.90	43.00	40.00
Case 5													
96.00	–3.00	22.50	80.00	22.50	70.00	37.50	40.00	40.00	40.00	6.20	7.50	43.00	46.00
Case 6													
0.00	–8.00	18.30	56.70	17.50	51.70	28.30	28.30	28.30	28.30	8.30	8.30	47.00	51.00
8.00	–1.00	21.70	68.40	19.10	65.00	38.30	35.00	40.00	36.70	8.30	8.30	45.00	45.00
23.00	15.00	24.20	88.50	24.30	74.30	42.90	45.70	42.90	45.70	11.40	11.40	49.00	49.00
Case 7													
1.00	–7.00	18.70	60.00	14.60	60.00	33.00	32.00	34.70	30.70	10.70	10.70	44.00	44.00
9.00	1.00	16.00	68.00	18.00	64.00	28.00	34.00	34.00	40.00	12.00	8.00	44.00	44.00

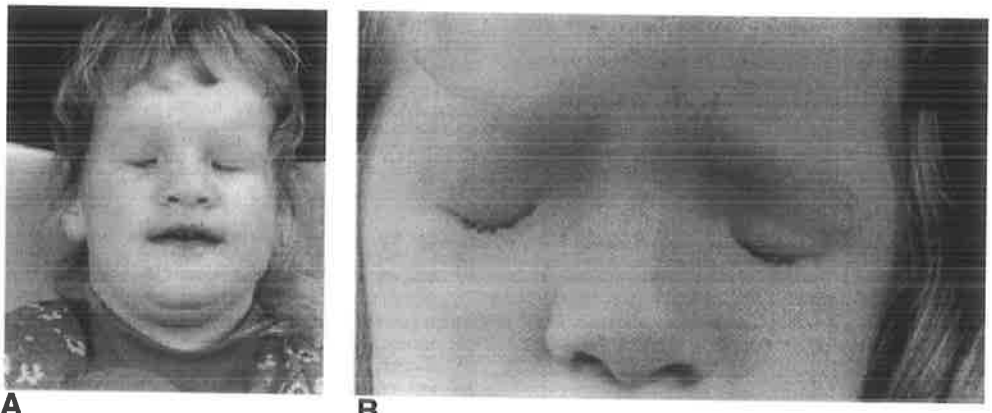

A B

FIG. 4. A. B. *(Case 1). Figure4B was taken 2.5 years after Figure4* **A.** *Although the orbits have enlarged, it can be seen that intraorbital tissue expansion has had little effect on the form of the eyelids.*

was noted. CT measurements confirmed a small increase in lateral orbital distance and lateral orbital wall length on the expanded side. There was also a decrease in the mid–interorbital distance. These changes, however, were small.

Case 4

Female. Presented at 2 weeks of age. Diagnosis: left hemifacial microsomia, left anophthalmos.

In this case, unilateral anophthalmia and marked blepharophimosis were associated with an ipsilateral left sided hemifacial microsomia including an absent left external auditory meatus and vestigal external ear, but mild facial asymmetry. Axial CT scans confirmed a small left orbit with a very short lateral orbital wall length and comparatively low lateral orbital wall angle.

At 4 months of age, a 4 ml tissue expander was inserted into the orbit as previously described. Expansion commenced at the rate of 0.1 ml per week. It soon became apparent that expansion was not occurring at the expected rate. Injection of larger volumes of fluid revealed there to be leakage of saline from the injection port at the time of injection. Expansion is continuing 4 years later despite this transient leak.

Expansion has clinically resulted in enlargement of the left orbit which has been maintained appropriately with growth. There has been little growth of the eyelids and the blepharophimosis remains marked. Axial CT measurements confirm an increase in size of the left orbital cavity. This was due to an initial increase in lateral orbital wall length and angle. The left and right orbits are now of a similar size. It should be noted that between 4 and 1 months of age there was an increase in the interorbital distance greater than would be expected with normal growth. The facial asymmetry from the hemifacial microsomia remains mild.

Case 5

Male. Presented at 8 years of age. Diagnosis: right microphthalmia.

This patient was referred from Thailand. There was a mildly contracted right eye socket with moderate orbital dystopia and ptosis. This deficiency in orbital size was reflected in the CT measurements only in a slightly decreased lateral orbital wall angle on the right with a low normal lateral orbital distance. CT also revealed a vestigial right eye.

A right orbital osteotomy with insertion of a tissue expander was undertaken as previously described. Expansion to a volume of 6.5 ml took place and the expander was removed and replaced with a conformer 5 months after

insertion. A reasonable alteration in orbital size was clinically obtained, but there was little enlargement of the eyelids. No postoperative CT data are available.

Case 6

Female. Presented at 7 months of age. Diagnosis: bilateral microphthalmia, Tessier 0,14 cleft, choanal atresia. (Fig. 5).

Axial CT measurements revealed that anterior and mid–interorbital distances were within normal limits as was the medial orbital wall length. However, the lateral orbital distance and lateral orbital wall length were below the 95% confidence interval for age–matched normal individuals.

4 ml expanders were inserted subperiosteally into both orbits via a bicoronal approach, developing a pocket beneath the periosteum of the orbital roof. Expansion was then started as detailed in previous cases. Three months after insertion the patient suffered a purulent discharge from the left orbit which was treated with antibiotics. At 5 months after insertion, there was evidence of leakage from the expanders and they were replaced.

Examination of axial CT scans revealed a marked increase in orbital size as expansion was commenced. By 15 months after insertion of the expanders the lateral orbital distance and lateral orbital wall length had increased to the upper range of normal for age–matched individuals. It was also noted that there had been thinning and marked superior displacement of the orbital roof on each side.

Case 7

Female. Presented at birth. Diagnosis: left microphthalmia. This patient presented at birth with a small left orbit secondary to microphthalmia. She had a 4ml expander inserted into the soft tissue cone of the left orbit via a bicoronal approach at 8 months of age. No orbital osteotomies were undertaken. Attempts at expansion caused a forward herniation of the expander. One month after insertion, the left orbit became infected. This was initially controlled with antibiotics but repeated infections prevented expansion and resulted in removal of the expander 4 months after insertion.

Discussion

The developing eye has a marked effect on the orbit, eyelids and surrounding skeletal structures. The globe triples in size between birth and adolescence with 70% of this increase occurring by four years of age and 90% by seven years. [10,11] According to Moss's functional matrix theory,[12] this capsular matrix will induce growth in surrounding structures. The loss of an eye early in life has been shown clinically to reduce growth of the orbit and surrounding areas,[13,14] the effect of which is more marked with enucleations at an earlier age.[15] Loss of an eye also induces compensatory changes, most notably the enlargement of the ipsilateral maxillary antrum and ethmoid air cells into the space that would have been occupied by the orbit.[14] However, some orbital growth does occur in the absence of an orbit and the CT measurements of Waitzman et al.[9] give some insight into the complexities of orbital growth. They note that the medial and lateral orbital wall lengths grew considerably in the first year of life and then changed little, whereas the lateral orbital and intertemporal distances sustained growth throughout childhood. This would be difficult to explain if the enlarging eye were the only source of orbital growth. It would seem therefore that adjacent functional matrices such as the enlarging brain and masticatory apparatus, which grow at different rates for variable lengths of time, have some effect on orbital growth. In any study of orbital expansion in childhood these other factors must be considered in interpreting the results. The cases reported in this study underwent expansion at different ages for variable periods and demonstrated different

coexisting pathologies. A detailed numerical analysis of orbital growth would therefore not be meaningful. However, it can be stated that expansion resulted in an increase in orbital wall length and lateral orbital distance. On average, orbital wall lengths increased by an amount 14% greater than that predicted by normal orbital growth and the increase in lateral orbital distance outstripped normal orbital growth by 11%. Slow expansion over a long period in younger subjects produces more marked bony orbital growth than rapid expansion later in childhood. This may be so because the influence of expansion is at a rate more closely mimicking the biological influence of the enlarging eye and because most orbital growth naturally occurs early in life. [10, 11]

Tissue expansion was noted to have a number of effects on the orbit. Early expansion often resulted in a decrease of interorbital distance. This was presumably due to a reversal of ethmoidal air cell enlargement that occurs in the absence of an eye.[14] Expansion also produced effective lengthening of the orbital walls and lateral orbital distance, whereas it had little effect on medial orbital wall protrusion. According to Waitzman et al.[9] this closely mimics the way in which a normal orbit grows.

Placement of the tissue expander within the orbit deserves consideration. In case 6 the expander was placed beneath the periosteum instead of within the orbital soft tissue cone as in the other cases. Orbital growth occurred in this case but in addition there was thinning of the orbital roof and deformation of the orbital cavity into space that would normally be occupied by the anterior cranial fossa. In their animal experiments, Lo et al.[6] used a subperiosteal expander but this was a custom-made device that fitted around the orbital rim. Placement of a spherical expander should probably be within the soft tissue cone of the eye. Previous attempts at tissue expansion in human orbits have been complicated by extrusion of the expanders.[16] This is in contrast to the generally successful experiments in cats. Eppley et al.[7] suggest that this is because the cat lateral orbital wall is thin and there is a natural discontinuity of the orbital rim which allows expansion to occur with relatively little resistance. They state that this is in contrast to the human orbit which has a thick continuous orbital rim. Gemperli et al.[17] reported a case in which the problem of extrusion was overcome during orbital expansion in a microphthalmic child by placing the expander within the vestigial scleral shell after enlargement with cadaveric scleral grafts. In our series, patients over the age of 2 years had lateral orbital osteotomies as previously described. This has the effect of reducing the resistance of the orbital wall to lateral expansion and may have prevented anterior extrusion of the expander. Further resistance to anterior displacement of the expander may be provided by tethering of the expander where the tubing to the injection port passes through the lateral orbital wall. Gemperli's[17] successful case of orbital expansion in a human subject also routed the tubing in this way. Very slow rates of expansion used in long-term treatment of young patients may also reduce anterior displacement of the expander by allowing bony expansion to occur with very low displacing forces. A 3D CT scan of case 1 (Fig. 3) shows a thin lip of bone growing over the anterior surface of the correctly positioned expanders 2.5 years after their insertion. Only one case in our series (case 7) demonstrated any degree of anterior herniation of the expander.

The effects of expansion on soft tissues were less predictable. Although some cases resulted in a moderate increase in the size of the eyelids, normal anatomy was not restored and blepharophimosis remained a problem. Animal studies on the use of expanders in the enucleated cat orbit,[6,7] however, report favourable growth of the eyelids. This may reflect a difference in the condition treated. In the animal experiments, a normal eye was enucleated leaving a normal overlying eyelid. In the anophthalmic children treated in our study the eyelids were small with short palpebral fissures at birth, reflecting the lack of influence of a developing globe in utero. Tissue expansion as used in our series does not adequately address this problem. This may indicate that this technique may be very much more effective in the management of early childhood enucleation where the eyelids are initially normal.

Conclusions

The placement of spherical tissue expanders within the orbits of congenitally anophthalmic or microphthalmic children can be effective in stimulating orbital growth or enlargement. Long–term expansion over several years allows the establishment of normal bony growth patterns. Subperiosteal placement of spherical expanders may induce asymmetrical growth and therefore placement of the expander within the orbital soft tissues is recommended. An osteotomy releasing the lateral orbital wall from the remaining orbit allows expansion of the orbit and may, combined with the tethering effect of passing the expander tubing through the lateral orbital wall, reduce the incidence of expander extrusion.

Although intraorbital tissue expansion successfully induces orbital growth, improvement in the form and size of the congenitally deficient eyelids has been less marked.

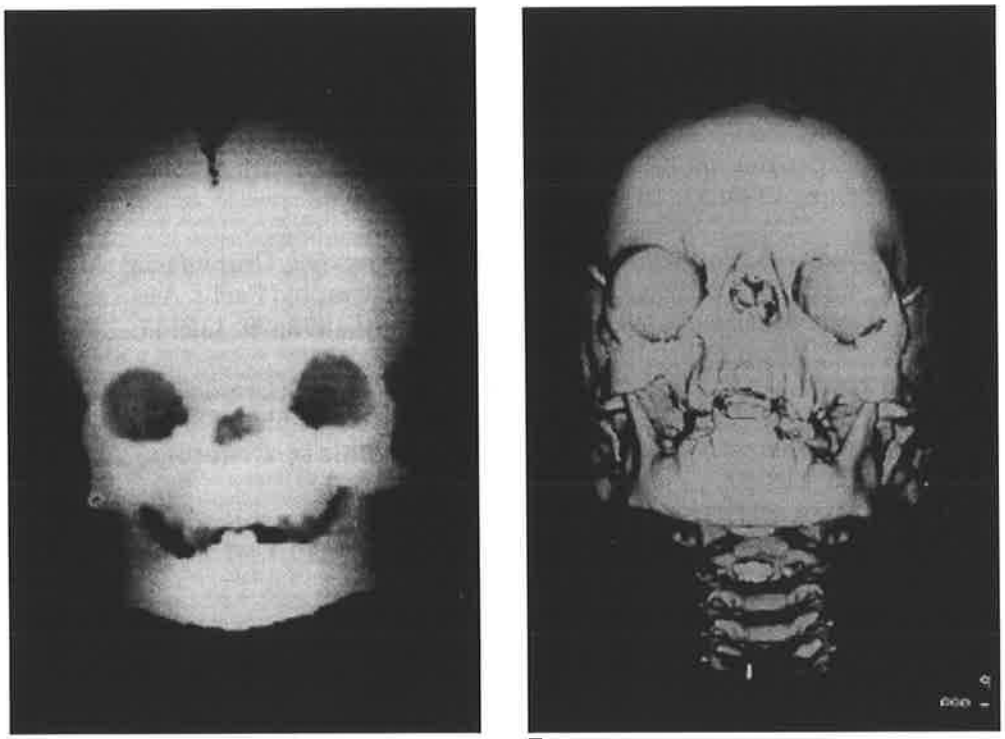

A B

FIG. 5. A. B. *(Case 6). ID CT Scans before insertion of tissue expanders* **A.** *and after two years of expansion* **B.** *Note the increase in size of the orbits. In this patient, the expanders were inserted subperiosteally and caused thinning and upward displacement of the orbital roofs, although this cannot be seen in these views.*

The Authors

David J. Dunaway MB ChB, BDS, FDSRCS, FRCS, Senior Registrar in Plastic and Craniofacial Surgery

David J. David AC, FRCS, FRCSEd, FRACS, Head of Unit, Australian Craniofacial Unit, Women's and Children's Hospital, 72 King William Road, North Adelaide, 5006, South Australia.

Correspondence to Mr D. J. Dunaway FDSRCS, FRCS, Senior Registrar in Plastic Surgery, Head and Neck Unit, Department of Plastic and Reconstructive Surgery, Newcastle General Hospital, Westgate Road, Newcastle upon Tyne, NE4 OBE, UK.

Paper received 13 March 1996.
Accepted 5 August 1996, after revision.

References

1. Lamb VR. An expandable conformer. Int Opthalmol Clin 1970; 10: 903–6.

2. Cepela MA, Nunery WR, Martin RT. Stimulation of orbital growth by the use of expandable implants in the anophthalmic cat orbit. Ophthal Plast Reconstr Surg 1992; 8: 157–67.

3. Marchac D, Cophignon J, Achard E, Dufourmentel C. Orbital expansion for anophthalmia and microorbitism. Plast Reconstr Surg 1977; 59: 486–94.

4. Tessier P. Traitement chirurgical des malformations orbitofaciales rarest J Genet Hum 1966; 15: Suppl: 322–55.

5. Elisevich K, Bite U, Colcleugh R. Microorbitism: a techniquc of orbital rim expansion. Plast Reconstr Surg 1991; 88: 609–12.

6. Lo AKM, Coleleugh RG, Allen L, Van Wyck A, Bite U. The role of tissue expanders in an anophthalmic animal model. Plast Reconstr Surg 1990; 86: 399–408.

7. Eppley BL, Holley S, Sadove AM. Experimental effects of intraorbital tissue expansion on orbitomaxillary growth in anophthalmos. Ann Plast Surg 1993; 31: 19–26.

8. Waitzman AA, Posnick JC, Armstrong DC, Pron GE. Craniofacial skeletal measurements based on computed tomography. Part I. Accuracy and reproducibility. Cleft Palate Craniofac J 1992; 29: 112–17.

9. Waitzman AA, Posnick JC, Armstrong DC, Pron GE. Craniofacial skeletal measurements based on computed tomography. Part II. Normal values and growth trends. Cleft Palate Craniofac J 1992; 29: 118–28.

10. Duke-Elder WS. System of ophthalmology, Vol 3, Part 1: Embryology. London: Henry Kimpton, 1963.

11. Todd TW, Beecher H, Williams D, et al The weight and growth of the human eyeball. Hum Biol 1940, 12: 1–15.

12. Moss ML. The primary role of functional matrices in facial growth. Am J Orthod 1969; 55: 566–77.

13. Taylor WOG. The effect of enucleation of one eye in childhood on subsequent development of the face. Trans Ophthalmol Soc UK 1939; 59: 361–7.

14. Osbourne D, Harden OB, Deeming LW. Orbital growth after childhood enucleation. Am J Opthalmol 1974; 77: 756–64.

15. Kennedy RE. The effect of early enucleation on the orbit in animals and humans. Trans Am Ophthalmol Soc 1964; 62: 277–306.

16. Anderson RL. Commentary on Cepela MA, Nunery WR, Martin RT. Stimulation of orbital growth by the use of expandable implants in the anophthalmic cat orbit. Ophthal Plast Reconstr Surg 1992; 8: 168–9.

17. Gemperli R, Cardim V, De Paula Schmid R, Manders EK. The use of tissue expanders for the induction of facial growth. J Craniofac Surg 1991; 2:42–6.

Chapter 5
Encephaloceles

It is the common wonder of all men,
How among so many millions of faces,
There should be none alike.

Sir Thomas Browne

Encephaloceles

Cephalocele is a general term that encompasses the more particular entities frontoethmoidal meningoencephalocele, basal encephalocele etc. Frontoethmoidal meningoencephaloceles represent a complex deformity of the craniofacial skeleton of indeterminate aetiology. There is an increased incidence throughout the Malay peninsula, parts of Indonesia, Burma, Bangladesh, Northern India and the southern part of the old Soviet Union.

Extension of the ACFU's services to the Asian region provided the author with the opportunity to treat and study this disease entity, which is important as a natural experiment in growth distortion.

In this area, ACFU gave regional leadership to neurosurgeons and others in developing countries, grappling with a poorly understood disease process.

The first paper Increased Paternal Age in Fronto-Nasal Encephalocele, 1984[1] is an early attempt to understand the aetiology of this mysterious condition.

Frontoethmoidal Meningoencephaloceles: Morphology and Treatment, 1984[2] describes the pathology and pathogenesis on which a treatment protocol can be established.

Cephaloceles: Treatment, Outcome, and Antenatal Diagnosis, 1984[3] and Skeletal Morphology of Anterior Encephaloceles Defined Through the use of Three-Dimensional Reconstruction of Computed Tomography, 1985-86[4] deal with the subject from a neurosurgical point of view and the latter article paid attention to the role of computed tomography in management.

The following three articles: Frontoethmoidal Meningoencephaloceles, 1987[5], Cephaloceles: Classification, Pathology, and Management, 1989[6], Meningoencephaloceles:

■

Classification, Pathology, and Management, 1989[7], deal with development of the early concepts of classification, pathology and management.

Frontoethmoidal Meningoencephalocele: Classification and Associated Features, 1991[8] deals with the mainly neurosurgical features associated with the craniofacial deformity.

Cephaloceles: Classification, Pathology and Management — A Review, 1993[9] and Frontoethmoidal Meningoencephalocele, 1994[10] are reviews which present the author's current thinking on the nature and management of this condition, particularly the thesis that it is not one of the rare craniofacial clefts as proposed by Tessier.

Papers

1. Sheffield LJ, Simpson DA, White J, David DJ 1984 Increased Paternal Age in Fronto-Nasal Encephalocele. Pathology: 106

2. David DJ Sheffield L, Simpson DA, White J 1984 Frontoethmoidal Meningoencephaloceles: Morphology and Treatment. Br J Plast Surg 37:271–284

3. Simpson DA, David DJ White J 1984 Cephaloceles: Treatment, Outcome, and Antenatal Diagnosis. Neurosurgery 15(1):14–21

4. Hemmy DC, David DJ 1985-86 Skeletal Morphology of Anterior Encephaloceles Defined Through the Use of Three — Dimensional Reconstruction of Computed Tomography. Paed Neurosurgery 12:18–22

5. David DJ, Simpson DA 1987 Frontoethmoidal Meningoencephaloceles. Clin Plastic Surg 14(1):83–89

6. David DJ, Proudman TW 1989 Cephaloceles: Classification, Pathology, and Management. World J Surg 13:349–357

7. David DJ, Simpson DA, Cooter RD 1989 Meningoencephaloceles: Classification, Pathology, and Management. Adv. in Plast and Recon Surg 5:85–108

8. Hanieh A, David DJ 1991 Fronto-Ethmoidal Meningoencephalocele: Classification and Associated Features. Proceedings 4th Int Congr Int Soc of Cranio — Maxillo-Facial Surg 127–130

9. David DJ 1993 Cephaloceles: Classification, Pathology and Management — A Review. Jnl Craniofacial Surg 4(4):192–201

10. David DJ, Harries RHC 1994 Frontoethmoidal Meningoencephalocele — Chapter 37. Mastery of Plastic and Reconstructive Surgery, Cohen 516–526

Increased Paternal Age In Fronto-Nasal Encephalocele

L. J. Sheffield, D. A. Simpson, J. White and D. J. David
Medical Genetics & Epidemiology Unit, Neurosurgery Department, S.A. Craniofacial Unit, Adelaide Children's Hospital

Fronto-nasal encephalocele is a rare congenital malformation in Australia but is relatively common in Southeast Asian countries such as Thailand and Malaysia. Fourteen patients referred from Malaysia for cranio-facial surgery with fronto-nasal encephalocele have been studied. There was no family history of this disorder in any of the cases but there appeared to be an increase in the paternal age and birth order. (Mean paternal age 37.5 yr, mean birth order 4.14). Comparison with population means for maternal age and birth order (Malaysia) and paternal age (South Australia) showed only paternal age to be statistically significantly different from the population figures. ($z=5.51$, $P<0.001$).

Although Malaysian paternal age data are required to conclusively show an increase in paternal age, the observations are very suggestive of an increased paternal age effect in fronto-nasal encephalocele. This is suggestive of a new autosomal dominant mutation which has important genetic counselling implications as well as being unique in the etiology of neural tube defects.

Fronto-ethmoidal meningoencephaloceles: morphology and treatment

D. J. David, L. Sheffield, D. Simpson and J. White
South Australian Cranio-Facial Unit, Adelaide Children's Hospital, Adelaide

Summary

Twenty-five cases of fronto-ethmoidal meningoencephaloceles have been studied. The relationship to other sincipital meningoencephaloceles is explored. In all cases the exit holes from the anterior cranial fossa are at the site of the foramen caecum. The facial component of the defect determines the sub-classification: naso-frontal, naso-ethmoidal and naso-orbital. The cranio-facial deformity may consist of hypertelorism, orbital dystopia, elongation of the face and dental malocclusion. These reflect the distorting influence of the extruded intracranial contents on facial growth. Early removal of the meningoencephalocele by the cranio-facial route is recommended to allow normal growth forces to be re-established. In older patients with established deformities translocation of the orbits may be necessary.

A congenital meningoencephalocele is a herniation of brain and meninges through a skull defect. The alternative name is cranium bifidum, giving the attractive but unproven assumption that these conditions are the cephalic equivalent of spina bifida. Spring (1854) wrote what was probably the first extensive monograph on the subject. He stated that LeDran (1740) introduced the term hernia cerebri; however, LeDran's case was probably a cephalhaematoma. Spring himself attempted to distinguish between meningocele and cerebral hernia, the latter being divided into encephalocele and hydrencephalocele when hydrocephalus was present. The term meningoencephalocele seems appropriate because it describes the contents of the hernia. We wish to discuss the sincipital meningoencephaloceles which, by definition, present in the front of the skull and are seen externally. We consider classification, morphology and treatment with some comments on epidemiology. Modern methods and investigation offered by a multi-disciplinary Cranio-Facial Unit enable these lesions to be studied more thoroughly and treated more effectively.

Classification

Meningoencephaloceles may be sub-divided into occipital, parietal, basal and sincipital. The latter group have been further classified by Suwanwela and Suwanwela (1972), based on a paper by Meyer (1890), into:

Fronto-ethmoidal —naso-frontal
—naso-ethmoidal
—naso-orbital

Inter-frontal

Cranio-facial clefts

The bony defects associated with sincipital meningoencephaloceles have been included in many attempts to classify cranio-facial clefts. Two of the most recent and significant endeavours are Tessier's (1976) anatomical classification and Mazzola's (1976) morphological classification based on embryological considerations. Tessier's classification describes clefts arranged around the orbit and numbered O to 14; as he has written, this system ". . . does not prevent a more sophisticated or detailed explanation, but rather it provides an immediate

reference to the exact location and character of what is being described". Included in Tessier's series and in subsequent article derived from his original paper (Kawamoto *et al.*, 1977), are cases of sincipital meningoencephalocele of the naso-ethmoidal type, and cases of inter-frontal meningoencephalocele, which may both be classed as Tessier type 14 clefts.

Mazzola uses the term fronto-nasal dysraphia, under which heading he makes a sharp distinction between the bifid nose and the midline fistulae. He has included in the sub-heading "bifid nose" teratomas, dermoid cysts, and encephaloceles. He considers that these arise spontaneously, noting however that Cohen *et al.* (1971) have shown that some are inherited as dominant genes. We wish to describe the bony and soft tissue morphology of fronto-ethmoidal meningoencephaloceles and to make a clear distinction between these and other facial clefts included in both Tessier's and Mazzola's classifications.

Material

Since 1977 the South Australian Cranio-Facial Unit has developed relationships with various South-East Asian countries, and in particular has treated patients referred from Malaysia. Twenty two cases of meningoencephalocele have been referred to the South Australian Cranio-Facial Unit; twenty were referred from

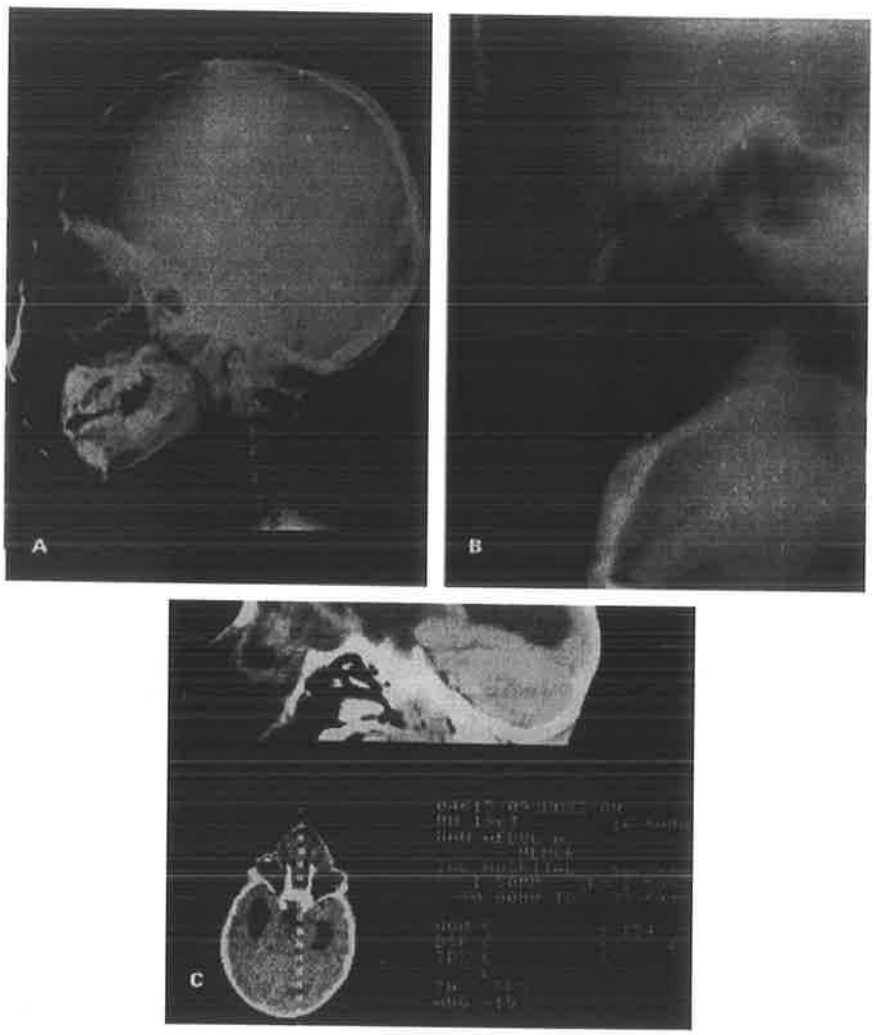

***FIG. 1.*—A** *Plain lateral radiograph showing a fronto-ethmoidal meningoencephalocele demonstrating the distortion at the root of the nose.* **B** *Sagittal tomogram giving a clearer definition of the relationship of the deformity to the face of skull and face.* **C** *Two-dimensional reconstruction from the computerised axial tomogram giving clearer definition of the deformity.*

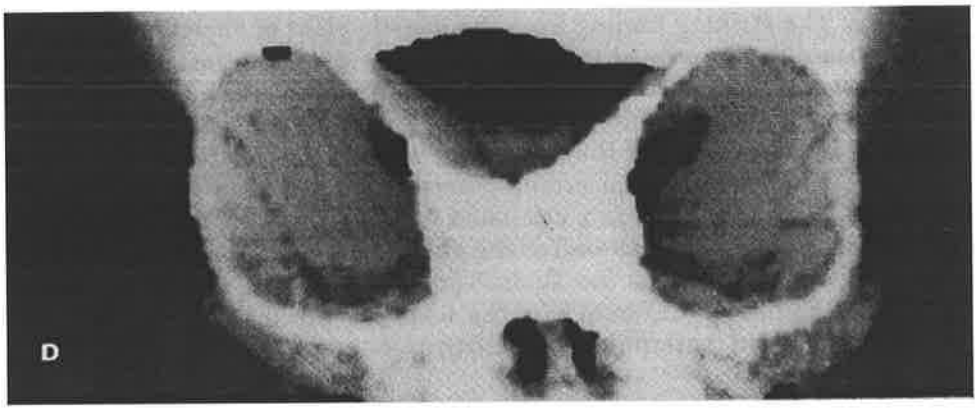

FIG. 1. —D Three dimensional reconstruction producing a vastly improved image.

Malaysia, one from Indonesia, one from Papua New Guinea and one was an Australian. All patients had been previously assessed by local neuro-surgeons and/or plastic surgeons for referral to the central Unit.

Factors involved in making this selection included whether the patient and family would benefit from complicated assessment and surgery. Patients with severe mental retardation and other associated problems rendering them unsuitable for surgery were thus eliminated. Three other patients were studied in Adelaide before the Cranio-Facial Unit was formed; two of these were Australian aboriginals and one an infant of European racial origin.

Investigations

All patients were admitted to the Unit at least one week prior to surgery and a routine cranio-facial work-up was performed, as described by us elsewhere, David *et al.* (1982). This period is needed to complete the cranio-facial mensuration, developmental assessment, neurological assessment, ophthalmological assessment and radiology which are essential in surgical planning. Since 1977 the latter mode of investigation has undergone considerable development (Fig. 1). Plain radiographs and standard tomography have been supplanted by computerised axial tomography. Two dimensional reconstruction has been added and, latterly, three dimensional reconstruction as described by Hemmy *et al.* (1983). Three dimensional reconstruction gives a very accurate picture of the defect and displays particularly well the nature of the anterior fossa deformity in relation to the orbits and face. Accurate pre-operative classification of the lesion is possible and surgical planning is facilitated.

Age, sex and race

The patients referred from South-East Asia were relatively old, the age range referral being 1½ to 19 years. The four cases born in Australia were seen much earlier, the age range being 2 weeks to 15 months. In the combined series 13 were boys and 12 girls. The racial origins of the parents, in so far as these can be determined, are set out in Table 1.

Genetic data

Consanguinity was found in two families and in a third the parents of the affected child were distantly related. However, there was no history of encephaloceles or any other neural tube defect in any siblings, parents, or other relatives of the

index cases. The striking finding from the genetic point of view, however, was that the paternal age seemed to be raised (Table 2). Statistical evidence of a raised paternal age is difficult to obtain: whilst Malaysian population figures are available for maternal age and birth order, there are no such statistics kept for paternal age. An estimate of the population distribution for paternal age has been made for this study by recording paternal age in 366 cases where births confined in the Penang hospitals are listed for the first 3 months of 1983. The mean paternal age obtained as well as the published population figures for 1979 in Malay births are shown in the Table. The mean paternal age of our cases is statistically significantly different from the mean paternal age in Penang ($P<.05$), whilst the population maternal age and birth order are not statistically different from that of our cases.

A raised paternal age suggests that the course of this type of meningoencephalocele may be due to an autosomal dominant mutation and, if this is confirmed, it would have important genetic counselling implications. The lack of familial cases and the geographic distribution of such meningoencephaloceles argue against dominant mutations as a cause. Further investigation is in progress and will be the subject of a separate report.

TABLE 1

Sincipital meningoencephaloceles: racial origins of parents

Racial origins	*Number of cases*
Malay (including Indonesia)	18
Indian (born in Malaysia)	2
Australian Aboriginal	3
Papuan	1
European	1
Total	25

TABLE 2

Parental ages and birth order in 17 Malay cases

Mean parental age and birth order	*Malay cases*	*Malay population Figures*
Paternal age	37.3	32.1
Maternal age	29.4	28.0
Birth order	3.8	3.4

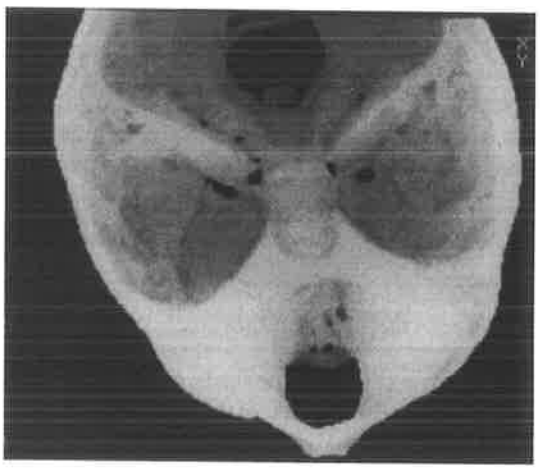

FIG. 2. *— Three dimensional reconstruction of the anterior cranial fossa showing the exit hole and the relationship of the cribriform plate and crista galli.*

Morphology of the bone defects

The description fronto-ethmoidal is most appropriate because it describes the site of the cranial end of the defect which is always in the position of the foramen caecum at the junction of the frontal and ethmoid bones (Fig. 2). The posterior margin of the defect is formed by the crista galli. This is often distorted and the cribriform plate is usually tilted downwards, as a deep central trough the anterior end of which is well below the plenum sphenoidale; the cribriform plate forms an angle of 45 to 50 degrees with the orbito-meatal plane. In our cases, the cranial exit holes varied in size and shape. All naso-frontal defects were round and central. All naso-orbital defects were bilobed (two patients from this group had been previously operated upon and one lobe of the exit hole had been obliterated by metal mesh). Two of the naso ethmoidal type were bilobed, while in one case the defect was lozenge-shaped and central; the remainder were round.

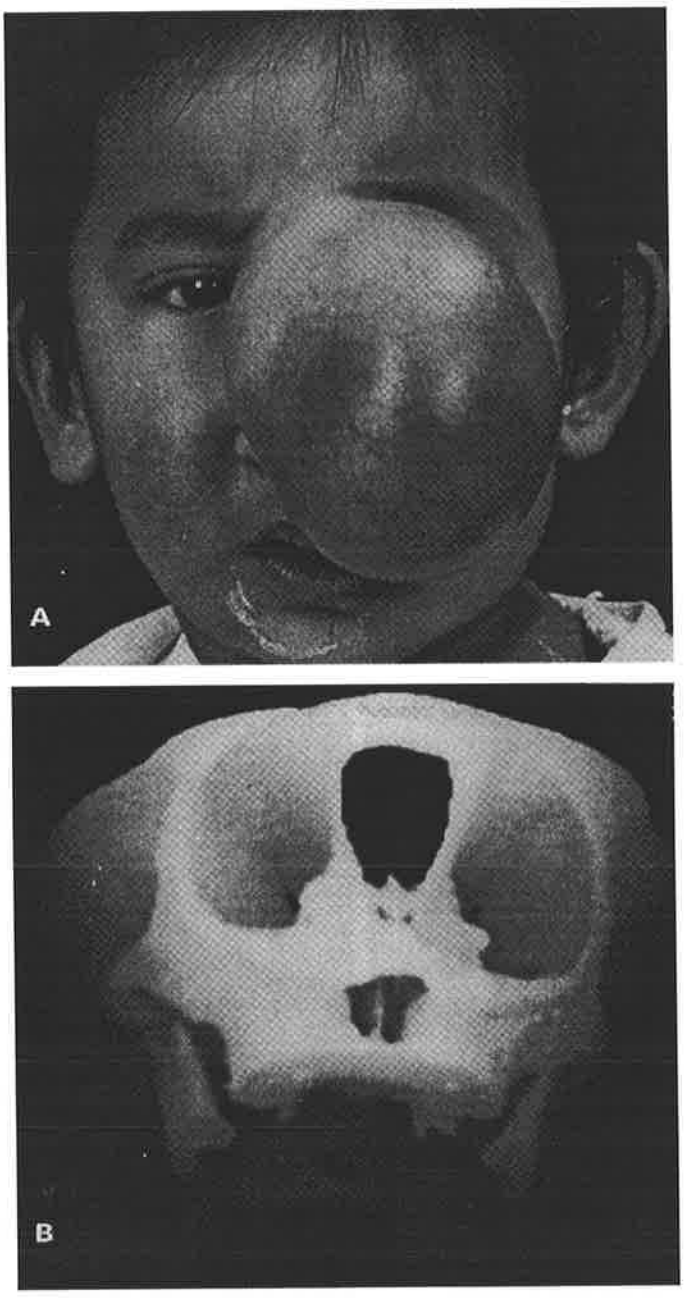

FIG. 3. *—**A** A massive fronto-ethmoidal meningoencephalocele of the naso-frontal type. **B** The three-dimensional reconstruction of the same patient shows the defect on the face with the frontal bone above and the nasal bones inferiorly.*

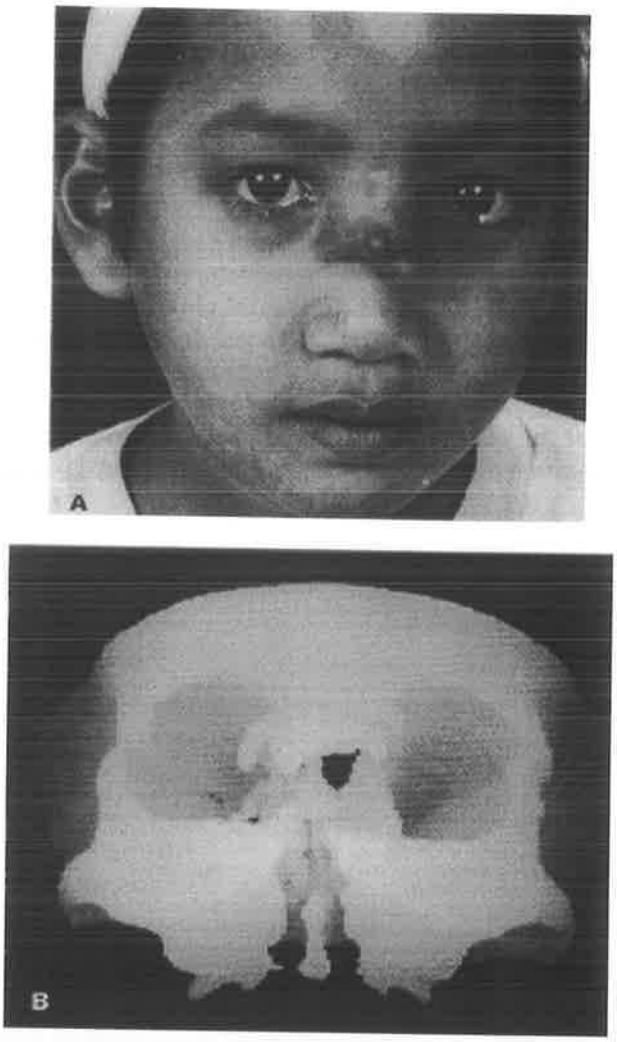

***FIG. 4.—A** A fronto-ethmoidal meningoencephalocele of the naso-ethmoidal type. **B** Three dimensional reconstruction of the same child showing the distorted nasal bones above the crescentic deformities in the medial orbital walls and the depressed pyriform aperture inferiorly.*

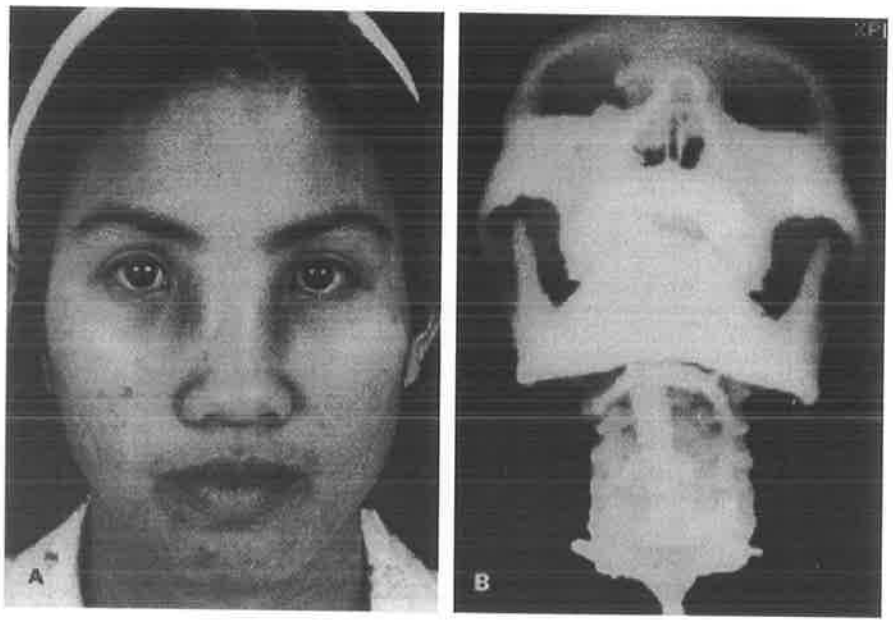

***FIG. 5.—A** A fronto-ethmoidal meningoencephalocele of the naso-orbital type. **B** The same patient showing the defect in the left medial orbital wall in the region of the frontal processes of the maxilla.*

The morphology of the facial bone defects showed more variation. In the naso-frontal type the holes were at the junction of the frontal and nasal bones (Fig. 3), the nasal bones being attached to the inferior margin of the defect which varied in shape.

In the naso-ethmoidal type, the facial defects lay between the nasal bones and the nasal cartilages (Fig. 4), the nasal bones being above and the nasal cartilages below. The nasal bones were deformed and often broadened, with crimped margins. The fronto-nasal angle was obliterated producing an over-hanging ledge. If the facial defect was confined to the nasal pyramid and was small and oval, the medial walls of the orbit were not involved. If, however, the meningoencephalocele was larger and the facial defect extended more laterally, then the anterior margins of the medial orbital walls were eroded and crescent-shaped.

The naso-orbital meningoencephaloceles present on the face through holes in the medial orbital wall (Fig. 5), in the frontal process of the maxilla and the lacrimal bones. In our cases the bony track was long and shaped like an inverted "Y". The inverted "Y" may be asymmetrical as in the case shown in Fig. 5. These encephaloceles come through the frontal process of the maxilla onto the face leaving the nasal bones intact anteriorly and the lacrimal bones and lateral plate of the ethmoid intact posteriorly. However, during the passage of the cerebral hernia through the substance of the ethmoid the lateral plate of that bone is pushed laterally, forming a bony tunnel.

General features of the face and facial skeleton

In all cases the faces appear to be longer than normal (Fig. 6) although this is hard to measure with ordinary cephalometric techniques because some of the bony land-marks, particularly in the glabellar region, are obliterated. The pyriform aperture and the nasal cartilages are misshapen; the aperture is shorter and broader than usual and displaced inferiorly. There was no evidence, however, in any case of a bifid nose or a midline nasal cleft. There was telecanthus in all cases with medial canthal dystopia in some and hypertelorism in most. As a rule the hypertelorism is not so severe as that associated with midline facial clefts; it is of the Tessier second degree variety with normal lateral canthal distance. Some patients had dental malocclusion which may be related to the deformity: the vertical plate of the ethmoid bone is attached to the tilted cribriform plate which is itself retro-displaced, presumably inducing secondary maxillary hypoplasia. The naso-ethmoidal type of encephalocele has a direct effect on the nasal septal cartilage pushing it downwards and backwards. It is as though the encephalocele has blown out onto the face through the weakened junction of the frontal and ethmoidal bones displacing the otherwise normal orbits and nasal capsule, widening the orbits and lengthening the face. In contrast with the clefts, which appear to have a deficiency of tissue at their margins, the defects of the fronto-ethmoidal meningoencephaloceles are like tunnels or blow-outs.

Neuropathology of the meningoencephalocele

The pathological constituents of the herniations varied. No patient had extension of the ventricular system into the defect. Some patients had viable brain at the neck of the encephalocele but distal to the defect in the dura mater, biopsies mostly consisted of glial tissue, often infiltrated with fibrous trabeculae. Nine patients had undergone previous surgery; seven had had intra-cranial operations only and two had intra-cranial operations plus attempts to excise the facial lesions. In those cases where the neck of the encephalocele had been divided at previous surgery, there was no significant spontaneous atrophy of the facial extension.

Histologically the glial masses did not look markedly atrophic, certainly they remained in sufficient bulk to produce a significant distortion of the face.

The soft tissue mass of the meningoencephalocele may extend into the orbits and fuse with the periorbitum making excision of the orbital component of the mass extremely difficult. The tumour may flow over the infra-orbital rim medially which then becomes indented and depressed. The overlying skin is usually of full thickness, but may be discoloured or scarred from previous ulceration and healing. The skin is often thickened and crusty. In only one case was the skin cover of the extruded cerebral tissue defective: in this neonate the cerebral hernia was covered only by a thin layer of epidermis.

FIG. 6.—The typical long face associated with frontoethmoidal meningoencephalocele.

Ocular problems

At presentation 4 patients had decreased visual acuity and 3 patients suffered from squint. In 11 patients lacrimal drainage dysfunction was demonstrated and there was orbital dystopia in 3 patients.

*FIG. 7.—**A** Pre-operative photograph of a child where both orbits have been translocated after transcranial removal of the meningoencephalocele. **B** Post-operative photograph.*

Neurological problems

Four patients showed developmental retardation. Six patients had hydrocephalus and in two there was previous history of epilepsy. In all patients capable of being assessed, there was no evidence of anosmia before or after surgery.

Treatment

In all 22 patients treated by the Cranio-Facial Unit, a combined approach was used. Access was gained by a bi-coronal scalp flap. Where there was a large soft tissue mass on the face requiring removal or where there was previous facial scarring, an additional nasal incision was made. The first step was wide sub-periosteal exposure of the craniofacial skeleton to outline the facial exit holes of the encephalocele. The planned osteotomies were then marked out on the skeleton with marking pencil and in many cases the sub-cranial bone cuts were made at this stage. The neurosurgeon then performed a frontal craniotomy removing the frontal bone as a free graft. If this was thick enough it was split according to the techniques described by Tessier (1982) and the inner table was used for grafting; otherwise two or even three ribs were harvested, one with a small cap of costal cartilage to use as a bone-graft for the nose. Where there was hypertelorism affecting both orbits, the orbits were translocated medially to move the globes of the eyes. Thirteen patients required translocation of both orbits, four patients required movement of one orbit only and five patients had osteotomy of the medial orbital walls, canthopexy and bonegrafting of the nasal defect.

Before these orbital translocations were attempted, the neurosurgical dissection of the anterior cranial fossa was undertaken. The roofs of the orbits and the dural neck of the meningoencephalocele were exposed extra-durally as far as the cranial bony defect; additional exposure was often obtained by excising a rectangle of bone from the glabellar region which could be replaced if there was no hypertelorism to correct. The dura was then opened on each side. The cerebral herniation was then inspected and as much as possible conserved; the neck of the encephalocele was then transected and the dural defect repaired, usually with a piece of temporalis fascia. The remaining orbital cuts were then made.

FIG. 8.—A Pre-operative photograph of a patient where one orbit has been moved. B Post-operative photograph.

In the naso-ethmoidal type of deformity, the medial orbital walls were often found to be defective and the angle of the cribriform plate so steep that the translocated orbits came to overlie the cribriform plate. The soft tissue mass was often very vascular and required careful dissection from the overlying skin and from the orbit where it was often closely adherent to the periorbitum. Care was taken not to remove too much skin from the midline over the nose as the soft tissue in this area has the capacity to "take up" in the first few months post-operatively.

The presence of hydrocephalus need not contraindicate definitive cranio-facial surgery. If possible, we prefer to avoid a pre-operative shunt. In three cases, preliminary external ventricular drainage was needed and was continued for 48 hours after operation; in two of these, the child's state worsened post-operatively when the drain was removed and a subsequent vetriculo-peritoneal shunt was necessary.

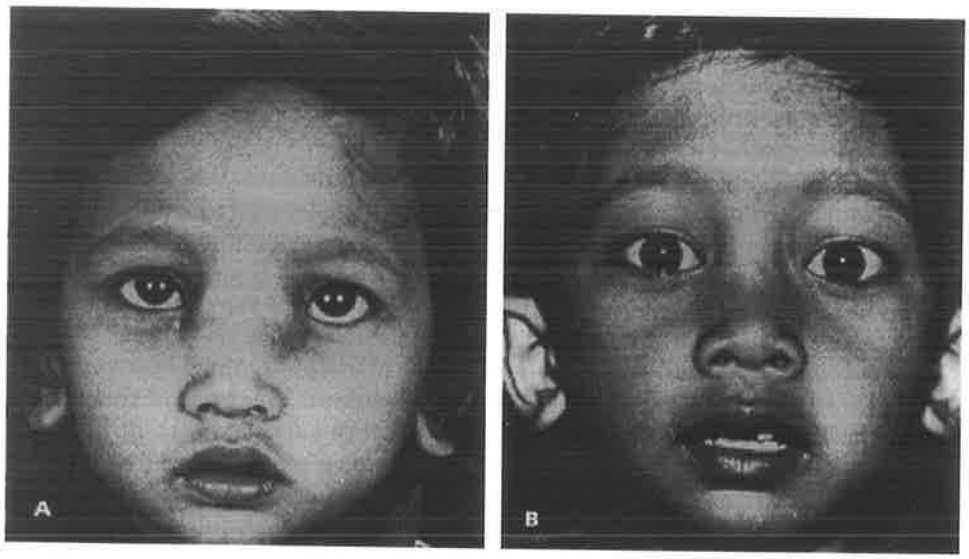

***FIG. 9.—A** Pre-operative photograph where medial orbital wall osteotomies, trans-nasal canthopexies and nasal bone-grafts were performed after removal of the meningoencephalocele. **B** Post-operative photograph.*

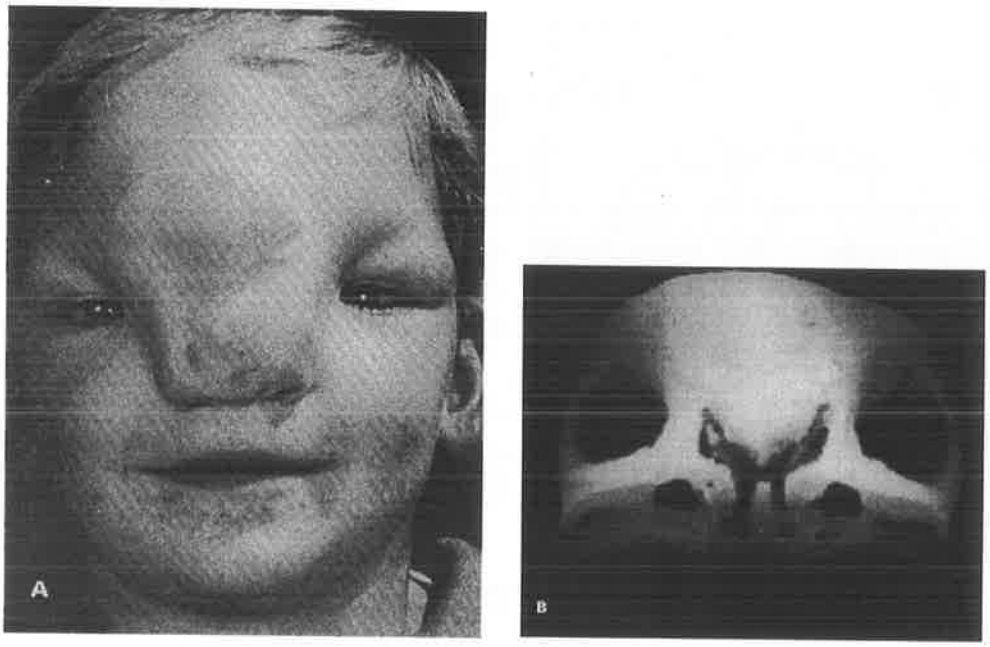

***FIG. 10.—A** a patient with facial clefting and severe hypertelorism with a short face. **B** The three dimensional reconstruction of this patient's skull. Compare with Fig. 4 (A) and (B).*

Operative results

All patients undergoing trans-cranial correction for fronto-ethmoidal meningoencephalocele survived the surgery. Surgery was usually accomplished between 4 and 8 hours and complications, apart from the acute post-operative hydrocephalus in two patients mentioned above, were minimal. Three patients had CSF rhinorrhoea which ceased spontaneously. Several patients had squints postoperatively, in all but two of these the problem resolved spontaneously, however in two patients the squints were of sufficient severity to warrant further surgical correction. Fig. 7 shows pre- and post-operative results of a patient requiring translocation of both orbits. Fig. 8 shows the results of a patient requiring one orbit to be translocated medially and Fig. 9 shows a case of a younger child requiring removal of the meningoencephalocele, osteotomies of the medial orbital walls and nasal bone-grafting.

Discussion

We suggest that fronto-ethmoidal meningoencephaloceles are fundamentally different in origin from the midline clefts. The meningoencephalocele is a "blow-out" of the intra-cranial contents, through a midline tunnel from the anterior cranial fossa into the facial skeleton. The skeletal deformities relate to the space occupying effect of the hernia of extruded brain and are not intrinsic to the tissues themselves. If this view is correct, early complete surgery should allow the developing brain and eyes to mould the orbital skeleton and the forces generated by the nasal airway, speech and mastication will remodel the facial deformity (Naim-Ur-Rahman 1979). The midline clefts of the nose on the other hand have a deficiency of tissue; the abnormality being intrinsic to the tissues themselves and early surgery of these cases would not be expected to help.

It has been suggested that meningoencephaloceles are one of the neural tube defects, to be considered with anencephaly and myelomeningocele as a varying expression of a single developmental aberration. Sincipital encephaloceles pose difficulties however in that they do not have the circumstantial supporting evidence of sibling affection. Suwanwela *et al.* (1971) of Bangkok have studied a large number of sincipital encephaloceles and found no record of siblings with other congenital neurological malformation. This has been the case in our 25 patients. There are also extraordinary geographic peculiarities in the distribution of fronto-ethmoidal meningoencephaloceles: these malformations are common in Malaysia, Thailand and Burma, but rare in Europe, North America, Australia as well as in Japan and China. There is also some evidence that sincipital lesions are common in some parts of Russia (Barrow and Simpson 1966). The high incidence in Thailand and apparently also in Malaysia seems definite, and in both countries it is the Thais and Malays, not the Chinese who are affected, despite the presence in these countries of large Chinese ethnic minorities. Thus in their epidemiology the sincipital fronto-ethmoidal meningoencephaloceles show remarkable peculiarities and in the present state of knowledge it seems unwise to include them with other neural tube defects. They may indeed result from some unknown environmental agent, perhaps dietetic. Our findings of an apparent increase in paternal age of the patients suggests that an autosomal dominant gene mutation may account for the occurrence of the lesion but this requires further investigation of cases and population norms.

Until recently, fronto-ethmoidal meningoencephaloceles were initially treated by neurosurgeons, plastic surgeons being as a rule consulted secondarily to deal with established deformities. The advent of cranio-facial surgery allows definitive correction of the deformity at a single stage. Division of the neck of the encephalocele is not enough to wither the distal component of the extruded tissue, or to prevent distortion of the developing facial skeleton. Cranio-facial surgery is

recommended with removal of the extruded brain and repair of the aura and anterior cranial fossa and the appropriate osteotomy and bone-grafts, preferably in the first 3 months of life in the hope that the airway will establish normal growth forces of the cranio-facial skeleton and allow the face to assume more normal proportions. The simplest operation, namely the moving of the medial orbital walls with bone-grafting and canthopexies is the operation of choice in the first years of life (Fig. 11). In the older patient, however, the displaced orbits can be reconstructed in three dimensions if necessary.

FIG. 11.—A Pre-surgical photograph of an Australian Aboriginal child with a naso-frontal type of meningoencephalocele where the operation was performed at 4 months of age. *B* Post-operative photograph at one year of age.

Acknowledgments

The authors wish to express their thanks to Mr Lal Kumar and Dr Chandran Arianayagam, Department of Plastic Surgery at the General Hospital, Kuala Lumpur and Dato Arumugasamy of the Department of Neurosurgery, Kuala Lumpur for their part in referring cases to the South Australian Cranio-Facial Unit and in the continuing management of these patients. Professor Harvey Carey of the Universiti Sains Malaysia kindly arranged to study the parental ages of babies delivered at the Penang Hospital. We wish also to thank Miss Gael Philips of Department of Histopathology of the Adelaide Children's Hospital for her contribution to the histopathology of fronto-ethmoidal meningoencephaloceles.

References

1 Barrow N. and Simpson, D. A. (1966). Cranium bifidum: investigation, prognosis and management. Australian Paediatric Journal, 2, 20.

2 Cohen, M. M. Jr., Sedano, H. O., Gorlan, R. J. and Jirasek,J. E. (1971). Fronto-nasal dysplasia (median cleft face syndrome): comments on etiology and pathogenesis. Birth Defects 7(7), 117.

3 David, D. J., Poswillo, D. and Simpson, D. A. (1982). The Craniosynostoses: Causes, Natural History and Management. Berlin: Springer Verlag.

4 Hemmy, D. C., Herman, G. T. and David, D. J. (1983). Three-dimensional reconstruction of the skull and facial bones utilising computed tomography in cranio-facial surgery. Transactions of the VIII International Congress of Plastic Surgery, Montreal.

5 Kawamoto, H. K., Wang, M. K. H. and Macomber, W. B. (1977). Rare cranio-facial clefts in J. M. Converse, Ed. Reconstructive Plastic Surgery, 2nd Edition, Philadelphia: W. B. Saunders.

6 LeDran, H. F. (1740). Observations in Surgery, London: James Hodges.

7 Mazzola, R. F. (1976). Congenital malformations in the fronto-nasal areas; their pathogenesis and classification. Clinics in Plastic Surgery, 3, 573.

8 Meyer von, E. (1890). Über Eine Basale Hirnhernie In der Gegend der Lamina Cribrosa. Virchows Archiv (Pathologische Anatomie) 120, 309.

9 Naim-Ur-Rahman (1979). Naso-encephalocele: treatment by transcranial operation. Journal of the Neurological Sciences, 42,73.

10 Spring, A. (1854). Monographie de la hernie du cerveau et de quelques lésions voisines. Mémoires de L'Académie Royale de Medecine de Bélgique.

11 Suwanwela, C., Sukabote, C. and Suwanwela, N. (1971). Fronto-ethmoidal encephalomeningoceles. Surgery, 69, 617.

12 Suwanwela, C. and Suwanwela, N. (1972). A morphological classification of sincipital encephalomeningoceles. Journal of Neurosurgery, 36, 201.

13 Tessier, P. (1976). Anatomical classification of facial, craniofacial and latero-facial clefts. Journal of Maxillo-facial Surgery, 4, 69.

14 Tessier, P. (1982). Autogenous bone grafts taken from the calvarium for facial and cranial applications. Clinics in Plastic Surgery, 9, 531.

The Authors

David J. David, MB, FRCS(Ed), FRCS, FRACS, Head of the South Australian Cranio-Facial Unit, Adelaide Children's Hospital.

Leslie Sheffield, FRACP, MSc, DCH, BMedSc, Medical Geneticist, Adelaide Children's Hospital.

Donald Simpson, MS, FRCS, FRACS, Director of Neurosurgery, Adelaide Children's Hospital.

Julian White, MB, BS, Registrar, South Australian CranioFacial Unit, Adelaide Children's Hospital.

Requests for reprints to: David J. David, MB, FRCS(Ed), FRCS, FRACS, South Australian Cranio-Facial Unit, Adelaide Children's Hospital, King William Road, North Adelaide, South Australia 5006.

Cephaloceles: Treatment, Outcome, and Antenatal Diagnosis

Donald A. Simpson, M.S., F.R.A.C.S., David J. David, F.R.A.C.S., and Julian White, M.B., B.S.
South Australian Craniofacial Unit, Adelaide Children's Hospital, Adelaide, South Australia

A series of 74 cephaloceles (17 cranial meningoceles and 57 meningoencephaloceles) is reported. Infants born with large meningoencephaloceles containing recognisable cerebral tissue usually did badly despite endeavours to conserve brain function by expanding the cranial capacity (5 cases) or decompressing hydrocephalic ventricles (9 cases). Infants with cranial meningoceles almost all did well, even when there was associated hydrocephalus. The etiological diversity of cephaloceles is emphasised. Frontoethmoidal meningoencephaloceles, which occur with noteworthy frequency in South and Southeast Asia, require separate consideration in both genetic counselling and treatment; the associated facial deformities (hypertelorism and orbital dystopia) can be corrected with a one-stage craniofacial reconstruction. Antenatal diagnosis by ultrasound is now often possible and was achieved in 4 cases; we suggest that neurosurgeons should participate in such antenatal evaluations. (*Neurosurgery* 15:14–21, 1984)

Key words: Cranial capacity expansion, Cranial meningocele, Craniofacial reconstruction, Facial deformity, Frontoethmoidal meningoencephalocele, Genetic counselling, Hydrocephalic ventricle decompression

A cephalocele is a congenital herniation of intracranial contents through a cranial defect (17). When the herniation contains brain tissue, it is an encephalocele or more precisely a meningoencephalocele; the absence of recognisable brain tissue characterises a cranial meningocele. These developmental anomalies are well known, and their neurosurgical management has been ably discussed by Matson (15), Mealy et al. (18), and others. However, recent advances in two unrelated fields have made it necessary for neurosurgeons to reconsider their philosophies of management. Reconstructive craniofacial surgery is now an established discipline; craniofacial operative techniques have much to offer in the treatment of certain types of cephalocele. More fundamentally, antenatal diagnosis of cephaloceles is now often possible; this offers the option of termination of pregnancy before term and, if this is to be considered, the likely prognosis of the malformation is of crucial importance.

Material and Classification

From 1955 through 1983, 51 infants and young children were referred to the Adelaide Children's Hospital for the management of cephaloceles of various types. With 1 exception the children had all been born in Australia. From 1975 through 1983,22 other children and adolescents were referred to the South Australian Craniofacial Unit with sincipital (frontoethmoidal) meningoencephaloceles; with 2 exceptions, all came from Southeast Asia (Malaysia or Indonesia). As 1 patient had two separate lesions (a parietomeningoencephalocele and an occipital meningocele), there were 74 cephaloceles in the combined series.

The patients were studied according to a protocol for developmental anomalies established in 1963. For the present purpose, chief importance is attached to the data on pathology and on major long term disabilities. The protocol identifies disabilities in mobility, vision, personality, and mentality. Mentality is categorised as normal, retarded but educable, and ineducable. Normal mentality is defined as the ability to cope with mainstream education; for preschool children, psychological tests and developmental assessments were used to forecast ability. Epilepsy is defined as the occurrence of more than one well-attested epileptic seizure. Air encephalography and latterly computed tomography (CT scanning) were used routinely to assess the cerebral anatomy, recently, three-dimensional CT scanning has been used to delineate the craniofacial skeleton (9). In neonates, B-Mode ultrasonography was used to delineate the ventricular and cisternal anatomy.

Encephaloceles are conveniently classified according to the anatomical site of the cranial defect (24). We class a cephalocele as occipital when the defect lies between the lambda and the foramen magnum (Fig. 1). If the cephalocele occupies a defect in the occipital bone and in the posterior arch of one or more cervical vertebrae, it is classed as occipitocervical. Parietal cephaloceles (16) are associated with midline bone defects at some point between the bregma and the lambda (Fig. 2). Sincipital or frontal cephaloceles are sited at some point between the bregma and the anterior margin of the ethmoid bone. The majority extend into the root of the nose (Figs. 3 and 4) and are called frontoethmoidal meningoencephaloceles by Suwanwela and Suwanwela (24), who have further subclassified them according to the direction of the herniation (Fig. 5). We follow their system, with minor modifications (Table 1). We have seen no case of lateral or temporal cephalocele (14) and no verified case of basal (intranasal) cephalocele (2, 15). We excluded from this series cases of so-called nasal glioma, although these probably originate as cephaloceles, and we also excluded cases of congenital interfrontal bulging associated with hydrocephalus or craniosynostosis.

Incidence and epidemiology

In Australia, cephaloceles are seen much less frequently than meningomyeloceles (1). Reliable South Australian birth data are available for the period 1966-1970, during these years, eight cephaloceles were reported, giving a ratio of I to 12.75 with respect to spina bifida cystica and an incidence of 0.08/1000 total births.

The sex ratios differed in the main anatomical groups: the male:female ratio was 1:2 for occipital cephaloceles, 1:0.63 for parietal cephaloceles, and 1:0.67 for sincipital cephaloceles. There were also striking differences in ethnicity (Table 2). Among Australians of European extraction, the large majority (66.7%) of cephaloceles were in the occipital site sincipital cephaloceles were rare (2.2%). This was not so in the small group of Australians of the aboriginal race, in which 3 of 6 cephaloceles were sincipital. The cases referred from Malaysia and Indonesia were selected by their need for craniofacial surgery; all had sincipital lesions. The large majority were of the Malay race and apparently none were Chinese, although in Malaya, the chief country of origin, people of Chinese stock comprise some 35% of the population.

FIG. 1. *Occipital meningoencephalocele containing cerebral tissue, with associated hydrocephalus. This infant of the aboriginal race was born in Australia.*

FIG. 2. *Parietal meningoencephalocele containing cerebral tissue, with associated hydrocephalus and gross dysplasia of the hemispheres. This infant of European descent was born in Australia.*

FIG. 3. *Frontoethmoidal meningoencephalocele containing cerebral tissue, with associated hydrocephalus. This 2-year-old boy was born in Malaysia, of the Malay race.*

FIG. 4. *Frontoethmoidal meningoencephalocele three-dimensional computed tomographic (CT) reconstruction shows the defect in the anterior cranial fossa (arrows).*

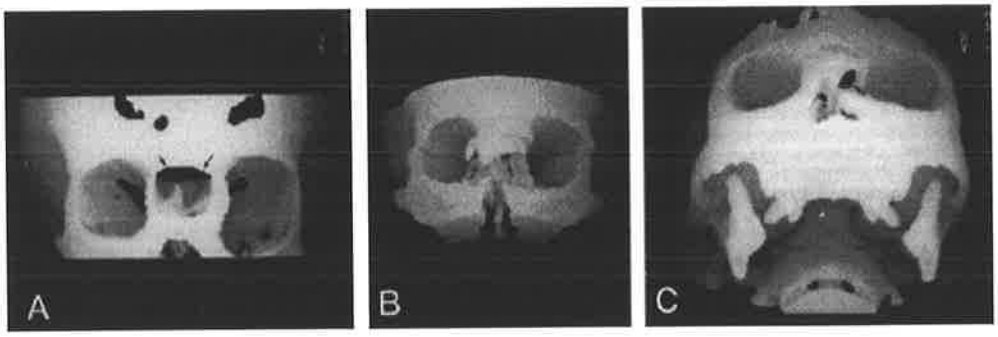

FIG. 5. *Three-dimensional CT reconstructions of frontoethmoidal cephaloceles, showing the exit foramina (arrows) in the facial skeleton:* ***A*** *nasofrontal;* ***B*** *nasoethmoidal;* ***C*** *nasoorbital.*

TABLE 1

Cephaloceles Classified According to the Anatomical Site of the Bone Defect

Type		Total No.
Occipital[a]		34
Occipitocervical		2
Parietal[a]		13
Sincipital		25
Nasofrontal	4	
Nasoethmoidal	9	
Nasoorbital	10	
Uncertain	2	
Total		74

[a]*one patient had two separate lesions.*

TABLE 2

Ethnic Origins of Parents of Patients with Cephaloceles[a]

Anatomical Site	Ethnic Group				
	European Australian	Aboriginal Australian	Malay	Indian	Other
Occipital	30[b]	3	—	—	1
Occipitocervical	2	—	—	—	—
Parietal	13	—	—	—	—
Sincipital	1	3	18	2	1
Total	45	6	18	2	2

[a]*The designation European Australian includes native-born parents as well as recent migrants; the designation Indian refers to parents of the Indian race domiciled in Malaysia. Mixed racial origin was recorded in two Malay families (Iban-Chinese and Malay-Iban).*

[b] *One infant had two lesions.*

TABLE 3

Pathology of Cephaloceles

Site	No. Meningoceles	No. Meningoencephaloceles	Total No.
Occipital	13	21	34
Occipitocervical	2	—	2
Parietal	3	10	13
Sincipital	—	25	25
Total	18	56	74

Two infants with occipital encephaloceles each had one sibling with a neural tube defect (NTD); in one this was an occipital meningoencephalocele, and in the other it was anencephaly. Two other infants with occipital cephaloceles themselves had coexisting NTDs—diastematomyelia in one and a spinal meningocele and a parietal meningoencephalocele in the other. No association with a NTD was found in cases of sincipital meningoencephalocele, but two patients came from the same aboriginal tribe and are cousins.

Pathology

In 18 cases, the lesions were meningoceles, in the remaining 56, the extrusion included some cerebral tissue (Table 3). As 9 of the sincipital lesions had earlier been operated elsewhere, there is some doubt about their original contents, but our operative findings suggested that all were meningoencephaloceles.

The meningoceles were occasionally associated with other cerebral anomalies. In 2 patients, there was significant hydrocephalus, which was due to a Dandy-Walker anomaly (Fig. 6) in 1 and an aqueduct stricture in the other. Two others had posterior fossa cysts.

The meningoencephaloceles were much more often associated with serious cerebral dysplasias. In the occipital group (21 cases), there were 11 with recognisable cerebral cortex within the herniation; in 4 of these, there was also cerebellum or 4th ventricle. One occipital meningoencephalocele contained only cerebellar tissue, 7 contained nodules of glia or other neural tissue, and 2 were not adequately examined. There was significant hydrocephalus in 7 and microcephaly in 5.

The parietal meningoencephaloceles were also usually associated with gross dysplasias. In 6, the herniations contained parietal cortex, 3 contained only small glial nodules, and 1 was not adequately examined. Varying degrees of holoprosencephaly ranging from partial agenesis of the corpus calamus to lobar holoprosencephaly (20) were seen in 4 cases of parietal meningoencephalocele, and 3 of these exhibited progressive hydrocephalus. Two other parietal lesions were associated with microcephaly. The prognosis for patients with sincipital meningoencephaloceles was in general more favourable, however, there were progressive hydrocephalus in 7 cases and other cerebral dysplasias in 4.

No case in this series exhibited such major extracranial anomalies as to justify a diagnosis of a specific syndrome (3); however, associated cleft palate (two cases), tracheoesophageal fistula, microphthalmia, and corneal opacity (one case each) were recorded. In five cephaloceles, dermoid cysts were included in the herniation.

Treatment

Occipital cephaloceles. Six patients with occipital meningoencephaloceles were treated expectantly: 5 died, and 1 is alive after 25 years, profoundly retarded and totally dependent. Twenty-seven patients underwent simple excision of the cephalocele and dural closure 2 of these later required cranioplasty to cover large pulsatile defects. One underwent conservative closure; seemingly well-formed cerebral tissue was preserved, and the cranial capacity was enlarged by duraplasty. Five of the 34 infants underwent shunting for progressive hydrocephalus.

Occipitocervical meningoceles. In one case, bilocular meningoceles were excised; in the other, the meningocele did not seem to need excision and with time became inconspicuous.

Parietal cephaloceles. One patient was treated expectantly and died. Seven parietal cephaloceles were excised. Four were treated by conservative closure and duraplasty. Duraplasty was more difficult when the sagittal sinus was in close relation to the dural defect or was represented by circumferential venous channels (Fig. 7); in one case, the division of a seemingly unimportant sinus, done to enlarge the cranial capacity, was followed by seizures apparently due to cortical venous infarction. Two of these 13 infants required shunts for hydrocephalus.

Sincipital meningoencephaloceles. Three infants, referred before the formation of the South Australian Craniofacial Unit, underwent primary neurosurgical treatment: frontal craniotomy, transection of the neck of the meningoencephalocele, and intracranial repair of the bone defects. In the 22 more recent cases, neurosurgical treatment was combined with definitive correction of the associated facial deformities. The operative techniques are reported in detail elsewhere (4). The meningoencephaloceles were explored by bifrontal craniotomy, and cerebral tissue of possible functional value was preserved. The encephalocele was then transected as far distally as possible. The dural defect was repaired with a fascial graft. The craniofacial surgeon then corrected the associated hypertelorism and orbital dystopia by orbital osteotomies designed to mobilise the walls of the orbits. In 13 cases, bilateral orbital translocation was done (Fig. 8). In 4, only one orbit was moved, and in 5 only the medial orbital walls were relocated. Canthopexy and rhinoplasty completed the facial reconstruction. Shunts were inserted before or after operation in 4 cases.

Outcome

The adequacy and duration of follow-up have varied. Nine patients were still under 2 years old when last assessed. Twenty-six patients returned to homes in distant places; although we have tried to follow them by letter or by personal visits, the assessments, especially of intellectual function, are somewhat questionable, and we have excluded 5 of these patients from consideration here. Nevertheless, we believe that the results of treatment are worth discussion (Table 4).

Eleven (16%) children died. Five of these had undergone operation, but succumbed after living in states of total dependency for periods of up to 5 years. There were no early postoperative deaths. Five others are alive, but totally dependent.

Of the remaining 52 cases, 38 have either no detectable disabilities or minor disabilities (slow learning, clumsiness, squints) that do not prevent normal schooling and acceptable social life. Eight have serious intellectual impairments, 3 of these attend special schools and are classified as mildly or moderately retarded, and 5 came from distant places and their mental states have not been assessed fully. Six others were under 2 years of age when last seen, all seemed to be developing normally. In the entire series, only 10 infants (15%) are recorded as having had epilepsy.

The functional capacities can be related to the nature and size of the herniations and to the coexisting cerebral dysplasias. Patients with cranial meningoceles (17 cases; 25%) have done well; in two instances, shunts were needed, but these children show no major disabilities. Patients with meningoencephaloceles containing only small nodules of structureless glial or neuronal tissue (9 cases) have also as a rule done well. The finding of masses of occipital or parietal cortex (20 cases) was usually most ominous: 15 of these patients died or live in total dependency, and 2 have severe intellectual disabilities. Holoprosencephaly and microcephaly were also very adverse findings. Hydrocephalus may be less serious, if treated appropriately; however, of 9 patients with meningoencephaloceles treated by shunts, 5 have serious degrees of retardation and a 6th treated recently shows ominous behavioural traits.

The size of the herniation also correlated with prognosis, at least in the occipital, occipitocervical, and parietal groups. In these categories, the diameters of the cephaloceles were recorded in 46 cases: 26 measured less than 5 cm and 20 measured more than 5 cm. Of the 26 patients with small lesions, only 2 have done badly. Of the 20 patients with large lesions, only 5 have done well (2 of these lesions were meningoceles). Correlation of outcome with cephalocele size was not possible with the sincipital lesions; with these, the most important prognostic indicators were the associated cerebral dysplasias.

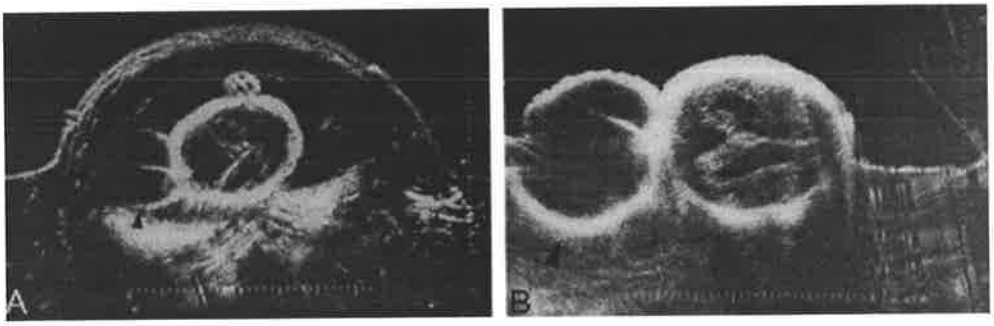

FIG. 6. *Ultrasonic scans of an occipital meningocele (arrowheads) associated with a Dandy-Walker anomaly:* ***A*** *antenatal (28 weeks of gestation);* ***B*** *postnatal.*

The aesthetic results of craniofacial reconstructions are reported elsewhere (4). In summary, the correction of hypertelorism and orbital dystopia has been maintained in all cases. This is probably because the hypertelorism was usually not severe, with minimal involvement of the lateral orbital walls. Nasal bone grafts in younger children have often been replaced as there was some resorption in all cases. The facial appearance was improved in all cases, especially where skin incisions in the frontonasal region were avoided. The scars in this region, however, have been remarkably inconspicuous, with little or no tendency to become hypertrophic. The initial distortion of the nasal cartilages has always resolved when the distorting influence of the cephalocele has been removed.

FIG. 7. *venous anatomy in an infant with a large parietal meningoencephalocele (see Fig. 2). The sagittal sinus divides into two channels around the neck of the cephalocele.*

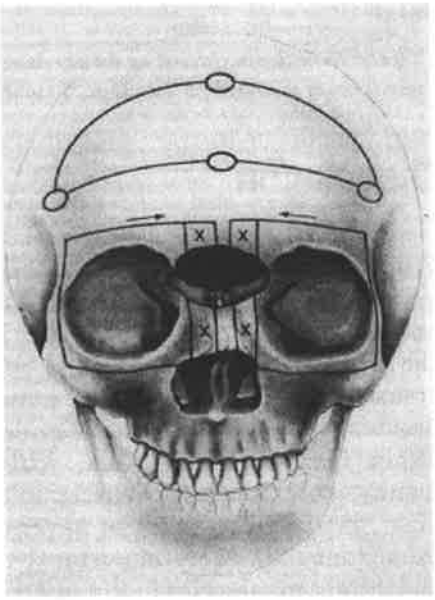

FIG. 8. *Transcranial correction of hypertelorism associated with fronto-ethmoidal meningoencephalocele: after excision of bone blocks (×) from the margins of the central defect, the orbits are translocated medially in the directions of the arrows.*

Antenatal Diagnosis

During the period 1975-1983, antenatal screening for neural tube defects by estimation of the serum and (where indicated) amniotic fluid -ᾳfetoprotein content was available in Adelaide, and some 25% of all babies born were actually screened. No cases of encephalocele were diagnosed by this method, and three cases in our series were investigated with negative results. Antenatal ultrasonic examinations were also used in obstetric canters, although not as part of a systematic screening program; two large encephaloceles (one parietal and one occipital) were diagnosed (Fig. 6). In both cases, the pregnancy went to term and a live infant was delivered. Both children survive, one with gross retardation and the other with a Dandy-Walker anomaly necessitating a shunt. During the same period, two occipital cephaloceles were diagnosed by ultrasound at 22 weeks of gestation; the pregnancies were terminated, and the diagnosis of encephalocele was confirmed by autopsy.

TABLE 4

Disabilities in Relation to Site and Pathology of Cephaloceles in 68 Patients[a]

Site	Pathology	Normal or Slight Disability	Uncertain	Significant Mental Defect	Totally Dependent
Occipital	Meningocele	11	1	—	—
	Meningoencephalocele	10	1	1	9
Occipitocervical	Meningocele	1	—	1	—
Parietal	Meningocele	3	—	—	—
	Meningoencephalocele	1	2	1	6
Sincipital	Meningoencephalocele	12	2	5	1
Total		38	6	8	16

[a]*Of the 16 patients classed as totally dependent, 11 have since died. The statistics exclude 5 recent cases followed for less than 6 months.*

Discussion

From the etiological viewpoint, cephaloceles are certainly not a homogeneous group. It is usual to consider these malformations as part of the spectrum of neural tube defects (6, 7). This view is probably valid for the occipital cephaloceles; the increased incidence of spina bifida and anencephaly in siblings (12) and the occasional finding of spinal or cranial defects elsewhere in the same individual provide strong circumstantial evidence. There is further support in the effects of experimental teratogens, which may induce either anencephaly or meningoencephalocele in susceptible animals (11). However, occipital cephaloceles may also occur as part of several syndromes showing autosomal-recessive inheritance (3). More importantly, there is little, if any, evidence to place the sincipital cephaloceles in the category of neural tube defects. The careful familial studies of Suwanwela in Thailand (23) and Kyu in Burma (personal communication) and our own less extensive experiences have not shown a significant incidence of central nervous system anomalies in siblings or offspring of those with sincipital cephaloceles. Sincipital encephaloceles are disproportionately frequent in Pakistan (19), India, Burma, Thailand, and Malaysia (21); our small series suggests the possibility that there is also an increased incidence among Australian aboriginals. This remarkable geographical predilection in peoples of such diverse racial stocks suggests an environmental cause. Be this as it may, the different empiric risks for future pregnancies should be remembered when one counsels the parents of an infant with a cephalocele.

Our experience illustrates the clinical diversity of cephaloceles; each new case requires full neurological assessment and evaluation by CT scanning or

ultrasound. Patients with meningoencephaloceles containing only small nests of neural tissue and cranial meningoceles are likely to do well (13, 18). Large meningoencephaloceles containing masses of recognisable cerebral cortex carry a bad prognosis, especially if there is associated holoprosencephaly or other major cerebral dysplasia. We have hoped to minimise the ultimate disability by the liberal use of shunts and by more conservative operative procedures; five parietal and occipital meningoencephaloceles were treated by operations planned to avoid or minimise the ablation of cortical tissue and to expand the cranial capacity by duraplasty. Thus far, the results have been very disappointing. The sincipital encephaloceles offer more scope for improvement in the results of operation. These patients often suffer ostracism and psychological damage because of the grotesque facial deformities (18). Early one-stage craniofacial operations, as performed by Dhawan and Tandon (5) and ourselves, allow preservation of at least some of the extruded frontal cortical tissue and immediate correction of the orbi-nasal deformity insofar as this is due to hypertelorism or orbital dystopia. We cannot confirm Naim-ur-Rahman's claim that early excision of the frontoethmoidal herniation is alone sufficient to restore normal facial growth (19). However, it is our belief that this procedure, combined with translocation of at least the medial orbital walls and resection of redundant bone in the glabellar area, gives a better esthetic result if done at 3 months of age than when done during later childhood. In older children, established deformities (hypertelorism, orbital dystopia) must be corrected by full orbital translocation.

However treated, many patients with meningoencephalocele will have serious mental and physical disabilities. In our series, the total mortality was 16%; another 18% are totally or severely incapacitated. Even among the larger number (56%) classed as having slight or no disability, there are patients with significant complaints. Mealey et al. reported that, among 40 patients with operated occipital lesions, 15 (38%) died and 11 (28%) were physically or mentally disabled (18). In the large series of meningoencephaloceles reported by Lorber and Schofield, nearly half of the patients died and 74% of the survivors were retarded (12). If our figures look better, it is in part because of the inclusion of the sincipital encephaloceles, which are a selected group.

The high incidence of major disability clearly calls for concern, especially as most of the infants who died lived for periods of up to 5 years, with much consequent distress to their parents. Many cephaloceles can now be diagnosed by B-mode and real time ultrasonography (8, 10, 22), and this offers the possibility of termination of pregnancy. We studied 4 cases in which large cephaloceles were visualised antenatally; in 2, pregnancy was terminated, 1 lives in a state of total incapacity, and 1 is well but shunt-dependent. There is a significant risk of long term disability when the cephalocele is large. For the ultrasonographer, we suggest that a cephalocele is large when its longest diameter exceeds half of the longest diameter of the fetal skull. The likelihood of an adverse outcome is greater if the cephalocele contains echogenic material and is still greater when there is holoprosencephaly or microcephaly. Care must be taken to distinguish cephaloceles from less serious mass lesions, such as cervical lymphangiomas and other hamartomas. The evaluation of cerebral malformations diagnosed in utero is not easy, and we urge that neurosurgeons collaborate with specialists in obstetrical ultrasonography to share experience and to develop more exact prognostic criteria.

Acknowledgements

We thank Drs. R. Sweet and P. W. Verco of the Queen Victoria Maternity Hospital, S.A., and Dr. B. R. Pridmore of the Queen Elizabeth Hospital, S.A., for their invaluable help in the antenatal diagnosis of cases reported in this paper. We also thank Professor D. C. Hemmy of the University of Wisconsin Medical School for much assistance in the application of his method of three-dimensional computed tomographic reconstruction (9) to the investigation of sincipital cephaloceles.

Received for publication, November 28, 1983; accepted, March 3 1984.
Reprint requests: Donald A. Simpson, South Australian Craniofacial Unit, Adelaide Children's Hospital, South Australia.

References

1. Barrow N, Simpson DA: Cranium bifidum: Investigation, prognosis and management. Aust Paediatr J 2: 20–26, 1966.

2. Choudhury AR, Taylor JC: Primary intranasal encephalocele: Report of four cases. J Neurosurg 57: 5520–555, 1982.

3. Cohen MM Jr, Lemire RJ: Syndromes with cephaloceles. Teratology 25:161–172, 1982.

4. David DJ, Sheffield L, Simpson D, White J: Fronto-ethmoidal meningo–encephaloceles: Morphology and treatment. Br J Plast Surg (in press).

5. Dhawan IK, Tandon PN: Excision, repair and corrective surgery for fronto-ethmoidal meningocele. Childs Brain 9: 126–136,1982.

6. Elwood JH, Nevin NC: Anencephalus and spina bifida in Belfast (1964–1968). Ulster Med J 42: 213–222, 1973.

7. Field B: Neural tube defects in New South Wales, Australia. J Med Genet 15: 329–338, 1978.

8. Fiske CE, Filly RA: Ultrasound evaluation of the normal and abnormal fetal neural axis. Radiol Clin North Am 20: 285–296 1982.

9. Hemmy DC, David DJ, Herman GT: Three–dimensional reconstruction of craniofacial deformity using computed tomography. Neurosurgery 13: 534–541, 1983.

10. Hidalgo H, Bowie J, Rosenberg ER, Ram PC, Ford K, Lipsit E: In utero sonographic diagnosis of fetal cerebral anomalies. AJR 139:143–148, 1982.

11. Lemire RJ, Beckwith JB, Warkany J: Anencephaly. New York, Raven Press, 1978, pp 90–99.

12. Lorber J, Schofield JK: The prognosis of occipital encephalocele. Z Kinderchir 28: 347–351, 1979.

13. Man DWK, Forrest DM: The prognosis of occipital encephalocele: Experience of 46 cases. Z Kinderchir 37: 158–160, 1982.

14. Martinez-Lage JF, Gonzalez–Tortos J, Poza M: Meningocele of the asterion. Childs Brain 9: 53–59, 1982.

15. Matson DD: Neurosurgery of Infancy and Childhood. Springfield Charles C Thomas, 1969, ed 2, pp 61–75.

16. McLaurin RL: Parietal cephaloceles. Neurology (Minneap) 14:764–772, 1964.

17. McLaurin RL: Cranium bifidum and cranial cephaloceles, in Vinken PJ, Bruyn GW (eds): Handbook of Clinical Neurology, vol 30, Congenital Malformations of the Brain and Skull, part 1. Amsterdam, North-Holland Publishing Co, 1977, pp 209–218.

18. Mealy J Jr, Dzenitis AJ, Hockey AA: The prognosis of encephaloceles. J Neurosurg 32: 209–218, 1970.

19. Naim–ur–Rahman: Nasal encephalocele: Treatment by transo–cranial operation. J Neurol Sci 42: 73–85, 1979.

20. Probst FP: The Prosencephalies: Morphology, Neuroradiological Appearances and Differential Diagnosis. Berlin, Springer–Verlag, 1979, pp 29–34.

21. Rapport RL II, Dunn RC Jr, Alhady F: Anterior encephalocele. J Neurosurg 54: 213–219, 1981.

22. Robinson HP, Hood VD, Adam AH, Gidson AAM, Ferguson–Smith MA: Diagnostic ultrasound: Earlier detection of fetal neural tube defects. Obstet Gynecol 56: 705–710, 1980.

23. Suwanwela C: Geographical distribution of frontoethmoidal encephalomeningocele. Br J Prev Soc Med 26: 193–198, 1972.

24. Suwanwela C, Suwanwela N: A morphological classification of sincipital encephalomeningoceles. J Neurosurg 36: 201–211 1972.

Skeletal Morphology of Anterior Encephaloceles Defined through the Use of Three-Dimensional Reconstruction of Computed Tomography

David C. Hemmy, David J. David FRACS.
Medical College of Wisconsin, Milwaukee, Wisc., USA, and South Australian Craniofacial Unit, Adelaide, South Australia

Abstract

We have used three-dimensional reconstruction of computed tomography to study the morphology of anterior encephaloceles. The findings based on living patients rather than cadaver specimens confirm previous findings suggesting 'blow out' defects which displace otherwise normal osseous structures.

Key words. Encephalocele - Computed tomography

The congenital meningoencephalocele is a herniation of brain and meninges through a skull defect. This entity has also been given the attractive alternate name of cranium bifida, an unproven assumption.

Meningoencephaloceles may be anatomically subdivided into occipital, parietal, basal and sincipital. The last group has been classified by *Suwanwela and Suwanwela* [7] based on a paper by *von Meyer* [9] into the following subgroups: (1) Frontoethmoidal: (A) nasofrontal: (B) nasoethmoidal: (C) Nasoorbital: (2) Interfrontal, and (3) craniofacial clefts.

The defects associated with sincipital meningoencephaloceles have been included in many classifications of craniofacial clefts [1,4,8]. The anatomical classification of *Tessier* [8] arranges clefts around the orbit through a numbering system of 0-14. This system 'provides an immediate reference to the exact location and character of what is being described' and 'does not preclude a more sophisticated or detailed explanation' [8]. *Tessier* includes cases of sincipital meningoencephaloceles of the nasoethmoidal type which he classifies as Tessier type 14 clefts.

We wish to discuss the morphology of frontoethmoidal meningoencephalocele as demonstrated through the use of three-dimensional reconstruction of computed tomography [2,3,5].

Materials and Methods

In 1980, we began to study patients from the Southwest Pacific region referred to the South Australian Craniofacial Unit with three-dimensional reconstruction of computed tomography prior to definitive surgical treatment. Some of the initial scans were conducted in Hobart, Tasmania, with three-dimensional processing completed in Milwaukee or in Buffalo, N.Y., at the State University of New York

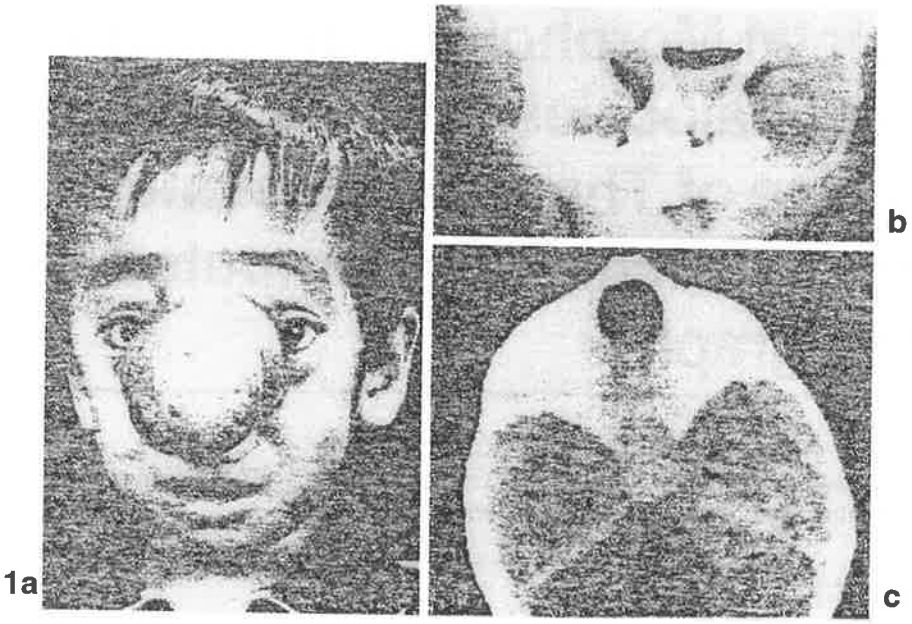

FIG. 1. ***a*** *Child with nasofrontal meningoencephalocele.* ***b*** *Facial presentation at the junction of the nasal and frontal bones displacing the nose inferiorly. Note the downward angulation of the crista galli and the cribriform plate well below the level of the planum sphenoidale.* ***c*** *Site of intracranial exit at the foramen caecum.*

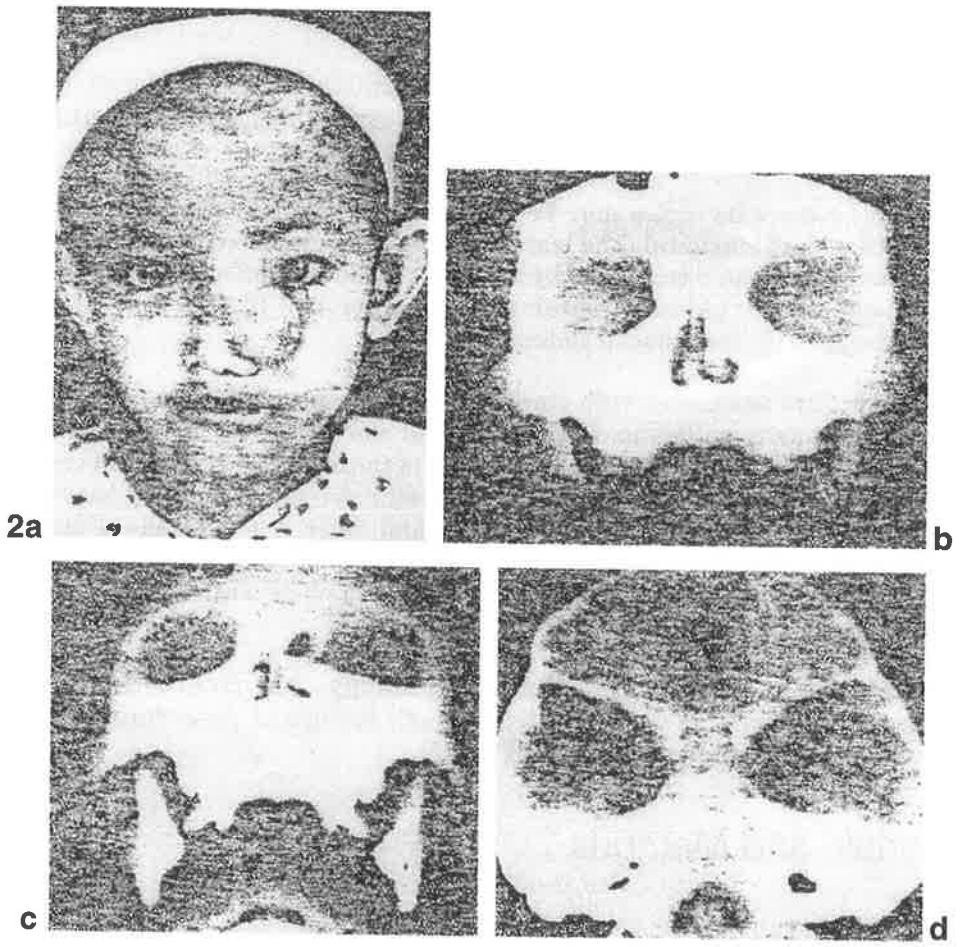

FIG. 2 ***a, b, c, d.*** *Nasoethmoidal meningoencephalocele. Notice reduction in frontonasal angle and splaying of nasal bones. There is some erosion of the anteromedial orbit and elongation of the face. Previous craniotomy with amputation of cerebral herniation was unsuccessful as a treatment of deformity.*

under the supervision of one of the authors (D.C.H.). More recently, a simplified acquisition protocol and a similar processing program called 3D83 (developed by the Medical Imaging Section of the University of Pennsylvania. GE Medical Systems. New Berlin. Wisc.) has permitted the entire study to be conducted at the Adelaide Children's Hospital.

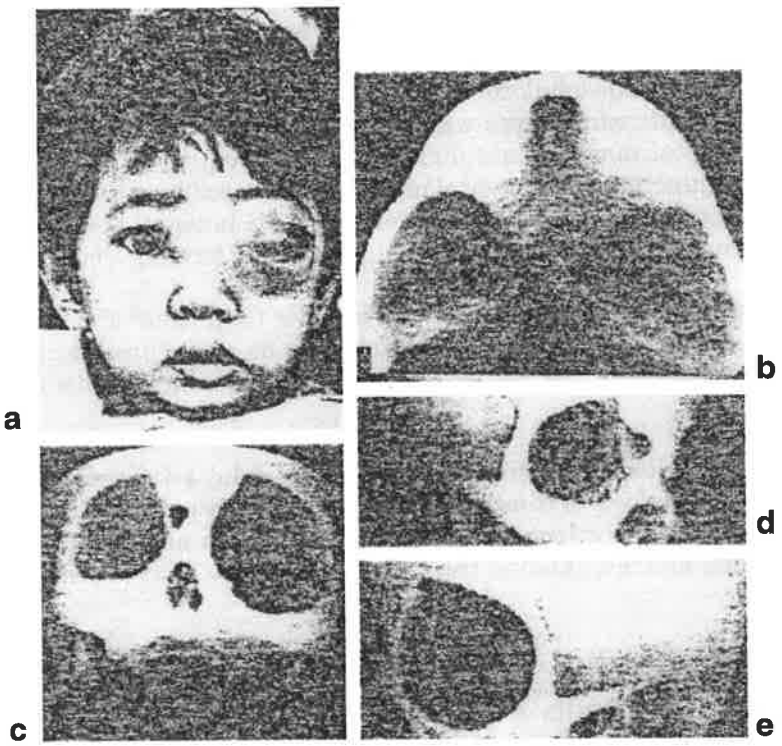

FIG. 3. a, b, c, d, e, Nasoorbital Meningoencephalocele. Notice bilateral bilobed presentation.

All the patients except 2 in this study were from Southeast Asia and were Malay or Asiatic Indian. The remaining 2 were Australian, one Aboriginal and one Caucasian. The deformity was divided among the three subcategories as follows; nasofrontal(9), nasoethmoidal(11), and nasoorbital(16).

All patients were administered a general anesthetic during the CT scan in order to prevent motion as the reconstruction program does permit motion. Scans were obtained using the GE CT/T 8800 scanner. Abutting slices of 1.5mm thickness were used. If cerebral detail was desired (usually during the first scan), standard scanning technique was used. When only osseous detail was required, a low mA dynamic technique was employed.

Results

Intracranial Morphology

The site of the cranial end of the defect was always in the position of the foramen cecum at the junction of the frontal and ethmoidal bones, therefore making the term frontoethmoidal the most appropriate (fig, 1,2,3). The posterior margin of the defect was formed by the crista galli. which was often distorted together with the cribriform plate, which was usually tilted downward, the anterior end lying well below the planum sphenoidale. The cribriform plate formed an angle of approximately 45^0 with the orbitomeatal plane. The holes of departure from the cranium varied in both size and shape. The nasofrontal defects were all round and central. The nasoorbital defects were all bilobed while the nasoethmoidal defects were either single and central or bilobed.

Facial Morphology

The nasofrontal defect was characterized by a defect at the junction of the nasal and frontal bones, the defect being the variable in shape with the nasal bone attached to inferior margin (fig. 1). The nasoethmoidal variety was comprised of a defect between the nasal bones and the nasal cartilages (fig.2). The deformed nasal bones lay above the defect, nasal cartilage below. The nasal bones were splayed and the frontonasal angle was reduced or obliterated. Larger nasoethmoidal meningoencephaloceles tended to erode the anterior margins of the medial orbital walls while there was no orbital involvement in the smaller types. The nasoorbital meningoencephaloceles presented trough holes in the medial wall at the junction of the frontal process of the maxilla and the lacrimal bones leaving the nasal bones intact anteriorly and the lacrimal bones and the lateral plate of the ethmoid was generally pushed laterally forming a bony tunnel.

The piriform aperture was shorter and broader than usual and displaced inferiorly. There was no evidence of a bifid nose or a midline nasal cleft. Hypertelorism was present but not as severe as that associated with midline clefts.

In contradistinction to craniofacial clefts, which display a deficiency of tissue at their margins, the defects of frontoethmoidal meningoencephaloceles are like 'blowout' defects which displace otherwise normal orbits and nasal capsule widening the orbits and lengthening the face.

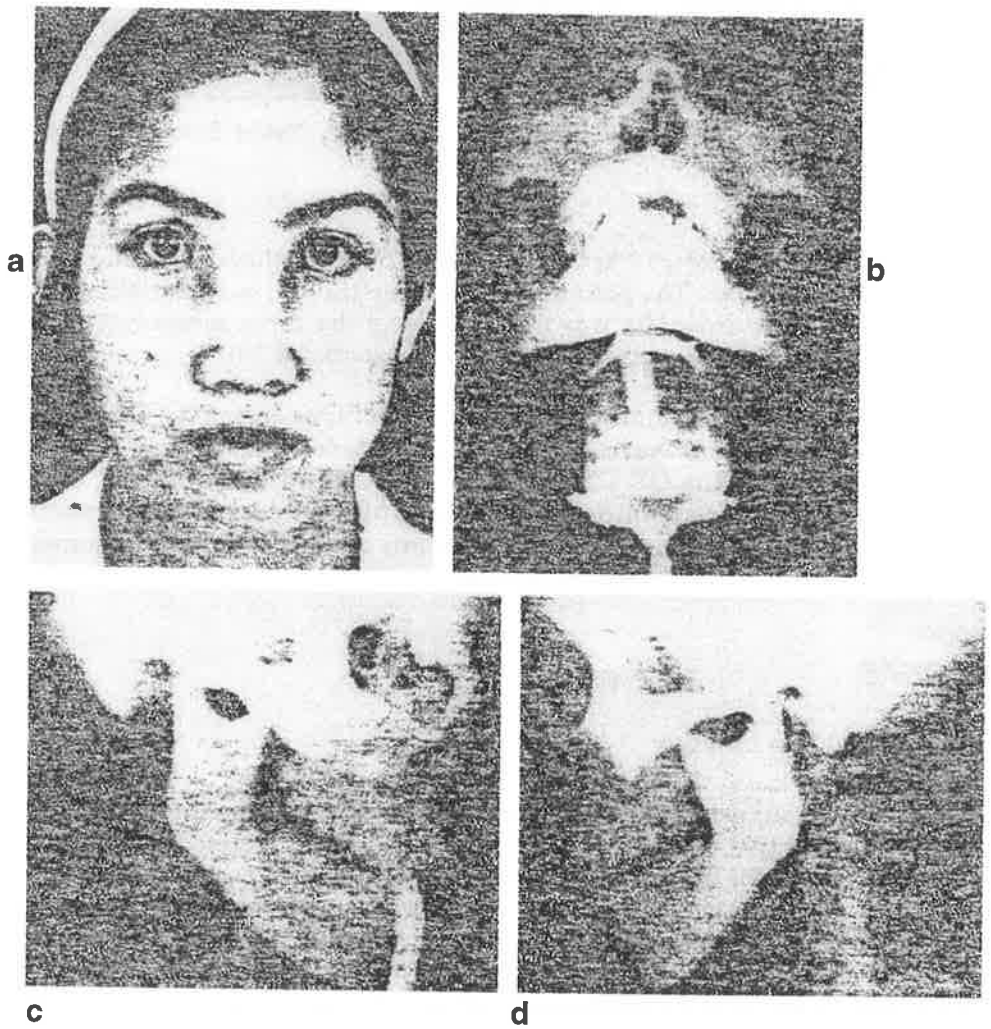

FIG. 4. a, b, c, d *Classic facial presentation of nasoorbital meningoencephalocele. Endotracheal tube in place.*

Discussion

We feel that frontoethmoidal meningoencephaloceles differ fundamentally from midline craniofacial clefts. The meningoencephalocele is a 'blowout' of the developing brain at the site of the anterior neuropore from the anterior cranial fossa into the facial skeleton. The skeleton features which result in meningoencephalocele are related to the space-occupying effect of the brain herniation with the defect occuring at the junction of bones rather than in an area marked by the absence of tissue.

The results of these investigations confirm the postmortem investigations reported by *Suwanwela and Suwanwela* [7] which indicated that three fundamental subtypes of the frontoethmoidal meningoencephalocele exist depending upon the position of presentation in the face. Furthermore, this method if investigation provides a rather accurate description of the type of meningoencephalocele prior to surgical repair facilitating preoperative planning.

References

1 Gundlach, K.H.; Pfiefer, G.: Classification of facial malformations. Int. J. oral Surg. 10:suppl. 1,pp.267–272 (1981).

2 Hemmy, D.C.; David, D.J.: Herman, G.T.; Three–dimensional reconstruction of cranial deformity using computed tomography. Neurosurgery 13: 534–541 (1983).

3 Hemmy, D.C.; Tessier, P.L: Accuracy of 3-dimensional reconstruction of CT data based on and compared to dry skulls with craniofacial deformities. Radiology (in press 1985)

4 Mazzola, R.A.; Congenital malformations in the frontonasal area: their pathogenesis and classification. Clin. Plast. Surg. 3: 573–608 (1976).

5 Salvolini, U.; Cabanis, E.A.; Iba–Zizen, M.T.; DeNicola, M.; Hemmy, D.C.: Apport diagnostique de la reconstruction tri–dimensionnelle en scanner rx: coupes et surfaces de l'anatomie céphalique. Ann. Chir. Plast. Esthet. 29: 339–357 (1984)

6 Simpson, D.A.; David, D.J.; White. J.; Cephaloceles: treatment, outcome, and antenatal diagnosis. Neurosurgery 15:14-21 (1984).

7 Suwanwela, C.; Suwanwela N.; A morphological classification of sincipital encephalomeningoeceles. J Neurosurg. 36: 201–211 (1972)

8 Tessier, P.: Anatomical classification of facial–cranio and latero–facial clefts. J. Max. Fac. Surg. 4: 69–92 (1976).

9 von Meyer, E.: Über eine basale Hirnhernie in der Gegend der Lamina cribrosa. Virchows Arch. path. Anat. Physiol. 120: 309–320 (1890)

David C. Hemmy, MD.,
Medical college of Wisconsin,
Milwaukee, Wisc. (USA)

Frontoethmoidal Meningoencephaloceles

D. J. David* and D. A. Simpson†

A *cephalocele* is a congenital herniation of intracranial contents through a cranial defect;[7] when the herniation is formed of meningeal and cerebral tissue, it is termed a *meningoencephalocele*. Cephaloceles are conveniently classified according to the site of the defect–occipital, parietal, sincipital (frontal), and basal. Spring (1854) wrote what was probably the first extensive monograph on the subject. He stated that Le Dran (1740) introduced the term "hernia cerebri"; however, Le Dran's case was probably a cephalhematoma. Spring himself attempted to distinguish between *meningocele* and *cerebral hernia,* the latter being divided into encephalocele and hydrencephalocele when hydrocephalus was present.

The sincipital meningoencephaloceles are sited at some point between the bregma and the anterior margin of the ethmoid bone; the majority extend into the root of the nose and have been termed "frontoethmoidal meningoencephaloceles" by Suwanwela and Suwanwela,[10] who have greatly expanded our knowledge of the epidemiology and morphology of this type of cephalocele. Unlike the basal meningoencephaloceles, which are purely intranasal and sometimes inconspicuous, frontoethmoidal meningoencephaloceles are obvious at birth as a facial disfigurement, often very gross, and sometimes associated with ocular and neurologic disability of various types (Fig. 1).

Etiology

In Western Europe, North America, Japan, and Australia, these lesions are relatively rare, occipital cephaloceles being much more prevalent, in South East Asia frontoethmoidal meningoencephaloceles are by far the commonest type of cephalocele,[1,9] and this appears to be the case in parts of the Indian subcontinent and in Southern Russia.

Many authors include cephaloceles in the general category of neural tube defects and accord them the same significance in genetic counseling. For frontoethmoidal meningoencephaloceles, this view appears to be incorrect; siblings and offspring do not show any increased incidence of anencephaly or myelodysplasia, and even in high risk areas it is very unusual to find more than one case of frontoethmoidal meningoencephalocele in the same family. Parents can be reassured accordingly.

Material and Classification

Since 1977 the South Australian Cranio–Facial Unit has developed relationships with various South East Asian countries, and in particular has treated patients referred from Malaysia and Indonesia. Thirty–seven cases of frontoethmoidal meningoencephalocele have been referred to the South Australian Cranio–Facial Unit, together with 1 case of interfrontal meningoencephalocele and 15 cases of small cranial meningoceles associated with midline facial clefts. These have been

*Head, The South Australian Cranio–Facial Unit, Adelaide Children's Hospital and Royal Adelaide Hospital, North Adelaide, South Australia

†Neurosurgeon, The South Australian Cranio–Facial Unit, Adelaide Children's Hospital and Royal Adelaide Hospital, North Adelaide, South Australia

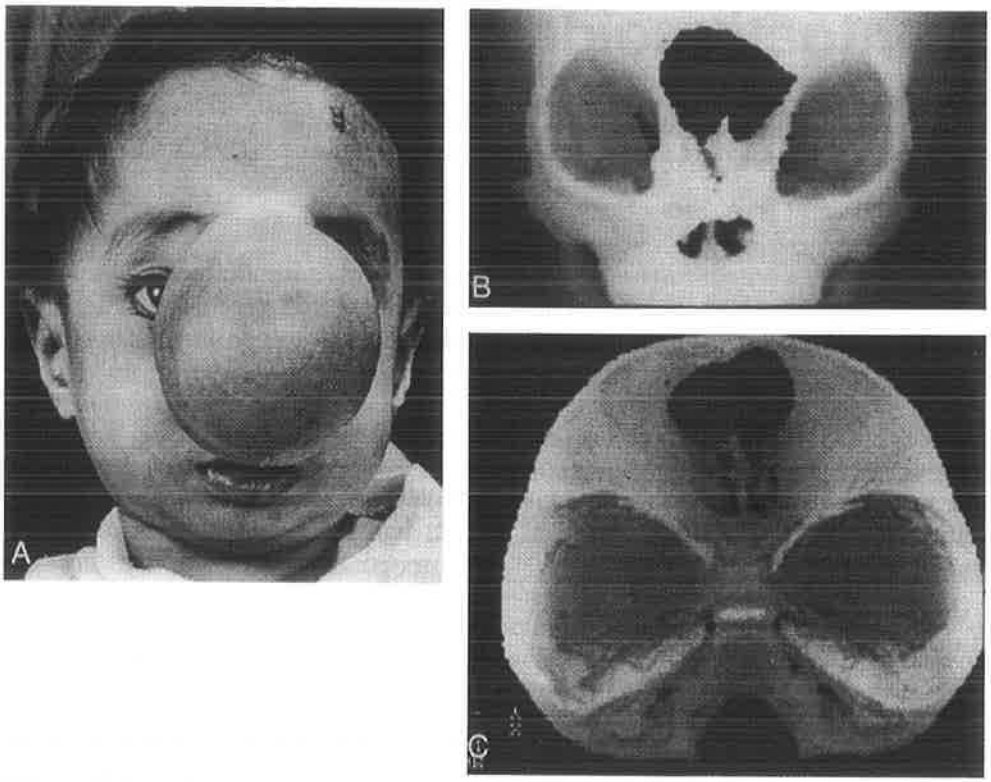

*FIG. 1. **A** A child with frontoethmoidal meningoencephalocele of the nasofrontal type. **B** The facial defect is at the junction of the nasal and frontal bones displacing the nose inferiorly. Note the inferior position of the crista galli and the cribriform plate, well below the level of the plenum sphenoidale. **C** Site of the intracranial exit at the foramen caecum.*

grouped according to Suwanwela and Suwanwela's classification[10] which was based on a paper by Meyer.[5] This subdivided sincipital meningoencephaloceles into frontoethmoidal (nasofrontal, nasoethmoidal, or nasoorbital), interfrontal, and craniofacial clefts.

Pathology

The External Mass. Most are smooth sessile masses, bilateral or unilateral, and often asymmetric; pedunculated mases are also seen. The diameter varies from 1 (Fig. 2) to 10 cm or more (see Fig. 1). The meningoencephalocele is usually covered with normal hairless skin, sometimes scarred or abnormally pigmented; rarely, the extruded brain may have no dermal covering at birth, and then it soon becomes ulcerated and infected.

The Internal Skull Defect. This is usually central and almost always located at the junction of the frontal and ethmoidal bones, at the site of the foramen caecum (Figs. 1*C*, 2*C*, and 3*C);* the crista galli lies behind the defect and is usually flattened and distorted. The cribriform plate is usually tilted downward, as a deep central trough, the anterior end of which is well below the plenum sphenoidale; the cribriform plate forms an angle of 45 to 50 degrees with the orbitomeatal plane. The exit holes vary in size and shape. All of the nasofrontal defects are round. The naso–orbital defects are usually bilobed. The nasoethmoidal type are bilobed, lozenge–shaped, or round.

The External Skull Defect. In the nasofrontal type, the defect replaces the normal root of nose, the nasal bones being displaced inferiorly. In our experience, this is the least common type (see Fig. 1*B*). In the nasoethmoidal type, the defect is between the nasal bones and the nasal cartilages (see Fig. 2*B*); the septal cartilage is displaced downward and backward, the nasal bones are usually deformed and broadened. The frontonasal angle is obliterated, producing

an overhanging ledge. If the facial defect is confined to the nasal pyramid and is small and oval, the medial walls of the orbit are not involved. If, however, the meningoencephalocele is larger and the facial defect extends more laterally, then the anterior margins of the medial walls are eroded and crescent–shaped. In our experience, this is the most common type. In the naso–orbital type, the midline frontal and nasal elements are normally related, but there are defects in the medial orbital walls (see Fig. 3*B*), which come through in the frontal process of the maxilla and lacrimal bones. The bony track is long and shaped like an inverted "Y." which may be asymmetric. During the passage of the cerebral hernia through the substance of the ethmoid, the lateral plate of that bone is pushed laterally, forming a bony tunnel. The naso–orbital lesions are intermediate in frequency in our material.

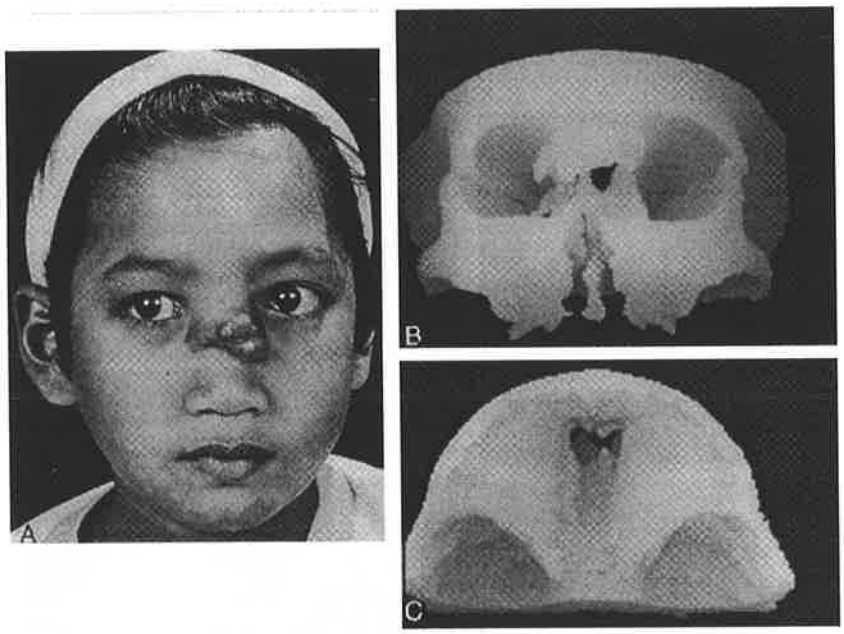

***FIG. 2. A** Nasoethmoidal frontoethmoidal meningoencephalocele with a small facial mass, but a very long face. **B** The exit hole on the face is below the nasal bones, which are subsequently deformed. **C** The view from the anterior fossa demonstrates a bilobed exit hole at the site of the foramen caecum.*

Facial Dysmorphology. The face is longer than normal (see Fig. 2*A*). This elongation is hard to measure with ordinary cephalometric techniques because some of the bony landmarks, particularly in the glabella region, are absent. The piriform aperture and the nasal cartilages are mis–shaped; the aperture is shorter and broader than usual and is displaced inferiorly. There is telecanthus in all cases, with medial canthal dystopia in some and telorbitism in most. As a rule, the telorbitism is not as severe as that associated with midline facial clefts; it is of the Tessier second degree variety[11] with normal lateral canthal distance. There may be expansion of the bony orbit in some of the naso–orbital varieties, where the orbital contents have been massively increased by the cephalocele. Some patients have dental malocclusion that may be related to the deformity; the vertical plate of the ethmoid bone is attached to the tilted cribriform plate, which is itself retrodisplaced, presumably inducing secondary maxillary hypoplasia. The nasoethmoidal type of cephalocele has a direct effect on the nasal septal cartilage, pushing it downward and backward. It is as though the cephalocele has blown out onto the face through the weakened junction of the frontal and ethmoidal bones displacing the otherwise normal orbits and nasal capsule, widening and often distorting the orbits and lengthening the face.

Cerebral Anomalies. The cerebral component of the meningoencephalocele is usually composed of the tips of both frontal lobes; rarely, there is also a diverticulum of the lateral ventricle, and Suwanwela et al.[8] have described cases in which the herniation contains large masses of frontal lobe tissue; in one case, nearly half the entire cerebrum was affected. In most cases,

the extruded cerebral tissue is gliotic and presumably not functional; there may be a clear demarcation band between normal and abnormal cerebral cortex, corresponding with the external skull defect.

Associated cerebral malformations of clinical importance were present in about half our cases these included hydrocephalus, arachnoid cysts, and various other dysplasias. Our cases were selected by referral for specialized treatment, and it is likely that the incidence of hydrocephalus and of more serious malformations, such as holoprosencephaly and microcephaly, would be higher if all newborn cases were fully studied. However, it is important to emphasise that, in many cases, the cerebral ventricular anatomy is grossly normal. When hydrocephalus is present, it is not necessarily progressive and may not require treatment.

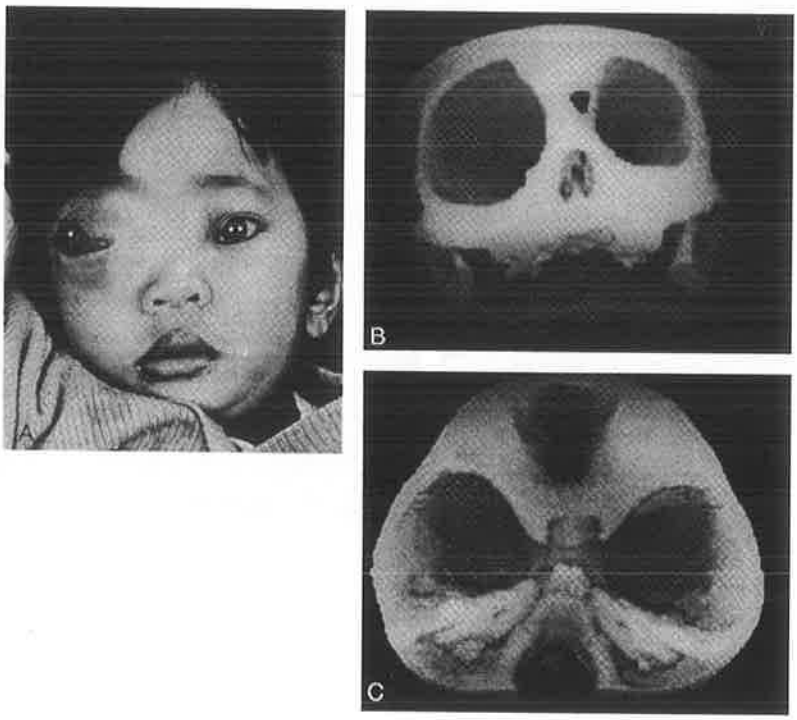

FIG. 3. A *Naso–orbital frontoethmoidal meningoencephalocele with massive expansion of the right orbit.* ***B*** *The right orbit is seen to be grossly enlarged and there is a smaller exit hole into the left orbit.* ***C*** *The view from the anterior cranial fossa shows the exit hole in the usual situation through the site of the foramen caecum and the much–depressed cribriform plate.*

Ocular Anomalies. Microphthalmia has been recorded; a number of patients have decreased visual acuity and some suffer from squints. All patients in our series have lacrimal drainage dysfunction.

Other Anomalies. Extracranial malformations are rare; in particular, frontoethmoidal meningoencephaloceles are rarely associated with myelodysplasias, unlike interfrontal cephaloceles, which appear to have a different pathogenesis, being typically associated with severe hydrocephalus and myelomeningocele.

Complications. Meningitis may occur, presumably from spread of nasal or cutaneous microorganisms to the meninges; this is especially likely to happen if the cephalocele becomes ulcerated.

Clinical Presentation

Because the lesions are obvious at birth, early referral to a neurosurgeon is the usual practice in developed countries, and until recently management was initially along neurosurgical lines, with subsequent referral to a plastic surgeon. In contrast with the small cephaloceles associated with clefts, which are usually associated with severe hypertelorism and short faces, we believe that combined one–stage management of the frontoethmoidal meningoencephalocele in infancy by a craniofacial team is ideal.[2] In developing countries, children are often referred late for cosmetic correction of established deformities.

Investigations

Investigations should include craniofacial mensuration, developmental and intellectual assessment, a full neurologic examination, and radiologic investigation both of the skeletal lesions and of the cerebral anatomy by computerized tomography (CT); three–dimensional CT scanning has been very helpful.[3,4]
Vision must be assessed fully, as well as the sense of smell; surprisingly, the latter is often intact.

Operative Treatment

Operative treatment has three main aims: (1) to conserve cerebral function, (2) to prevent infection, and (3) to make the facial appearance socially acceptable. The first aim is less easily achieved than one would wish: The herniated cerebral tissue within the cephalocele is usually too adherent to be extricated, and distal to the dural constriction, it is likely to be gliotic and dysplastic. The second aim, prevention of cerebral infection by occluding the congenital craniofacial fistula, is relatively easy. The third aim can be difficult to realise, especially when there is marked telorbitism and orbitofacial deformity.

The basis of surgical planning is the radiologic assessment, which consists above all of computerized axial tomography with reconstruction in three dimensions. There are two key principles of surgery.

(1) The operation should be performed by the transcranial approach so that the defect can be isolated intracranially and possibly intradurally, with careful repair of the dura. The surgeon should, if possible, repair the bony and soft–tissue deformities at one sitting.

(2) Complete bony reconstruction of the orbits and, if necessary, translocation of the orbits should be performed where necessary. Access is gained by a bicoronal scalp flap. Where there is a large soft–tissue mass on the face, or where there is previous facial scarring, an additional nasal incision is made to allow removal of the facial mass and trimming of the facial skin. The first step is wide subperiosteal exposure to outline the facial exit holes of the meningoencephalocele. Planned osteotomies are then marked out on the skull and, in many cases, the subcranial aspects of the bony reconstruction are made at this stage. This may involve osteotomies or bone grafts. The neurosurgeon then performs a small bifrontal craniotomy, exposing both frontal lobes, and the frontal bone is temporarily removed as a free graft. If this is thick enough, it is split and the inner table is used for grafting; otherwise, two or even three ribs are harvested, one with a small cap of costal cartilage to use as a bone graft for the nose.

Before the bony orbital surgery is undertaken, the neurosurgical dissection of the anterior fossa is performed. The roofs of the orbits and the dural neck of the meningoencephalocele are exposed extradurally as far as the cranial bone

defect; additional exposure is often obtained by excising a rectangle of bone from the glabella region, which is replaced if there is no hypertelorism to correct. The dural sac of the meningoencephalocele is opened on both sides; cerebral herniation is inspected and, as much as possible, is conserved. The neck of the encephalocele is then transected and the dural defect repaired, usually with a piece of temporalis fascia. The remaining orbital osteotomies are then made. In the nasoethmoidal type of meningoencephalocele, the medial orbital walls are often found to be defective and the angle of the cribriform plate is so steep that the translocated orbits come to overlie the cribriform plate. In some naso–orbital lesions, one or both orbits may be grossly expanded by the increased soft–tissue volume. Osteotomies need to be designed to decrease the orbital size and may need to be supplemented by bone grafting of the orbital roofs, floor, and medial and lateral walls. Where there is significant telorbitism affecting both orbits, the orbits are translocated medially to move the eyes. Less severe deformities may require movement of one orbit only or osteotomy of only the medial orbital walls. Canthopexy and bone grafting of the nasal defect are final procedures.

Before external dissection of the soft–tissue mass, it is our custom to cannulate the inferior lower lid canaliculus and inject dye into the nasolacrimal drainage apparatus. The soft–tissue mass is often very vascular, and careful dissection is required to separate it from the overlying skin; the canaliculi and nasolacrimal apparatus are often stretched and distorted. Care must be taken not to remove excessive skin from the midline over the nose, because the soft tissue in this area has the capacity to "take up" in the first few months postoperatively.

This operative program[2] was devised for cases presenting later in childhood with established deformities. We have a limited experience of operations undertaken in infancy (1 to 3 months) and believe that this is the ideal time to intervene, both to promote parental acceptance and ultimate psychologic well–being and also in the hope, expressed by Naim–Ur–Rahman,[6] that facial deformity will be avoided. The rationale for this hope is the concept that the skeletal deformities relate to the space occupying the effect of the hernia of extruded brain and not to some intrinsic deformity in the facial structures. If this view is correct, early complete surgery should allow the developing brain and eyes to mold the orbital skeleton, and the forces generated by the nasal airway, speech, and mastication will remodel the facial deformity. When operations are done in infancy, we believe it is necessary only to translocate and reconstruct the medial orbital walls with canthopexy and insertion of a nasal bone graft, in addition to removing the contents of the meningoencephalocele. However, long–term studies are needed to validate this belief (Fig. 4).

As has been noted, frontoethmoidal meningoencephaloceles are often associated with hydrocephalus. If this is severe and progressive, a ventriculoperitoneal or ventriculoatrial shunt may be required. However, we usually defer this operation until the completion of the one-stage transcranial operation for the cephalocele, controlling intracranial pressure intra-operatively by draining the dilated ventricles through a separate bur-hole incision. This strategy allows regulation of intracranial pressure during operation and for 2 or 3 days thereafter, avoiding the occasional complications (postoperative extradural hemorrhage, infection) sometimes associated with an internal shunt. The hydrocephalus associated with cephaloceles sometimes arrests spontaneously, even when quite severe. However, if the hydrocephalus is clearly progressive and the postoperative intracranial pressure is high, there should be no delay in performing a shunt; we prefer ventriculoperitoneal drainage.

***FIG. 4. A** Patient with an encephalocele prior to surgery. **B** Same patient a few years after transcranial correction.*

Summary

Frontoethmoidal meningoencephaloceles constitute a well–defined clinical entity with remarkable epidemiologic peculiarities, being very prevalent in South East and Southern Asia, but relatively rare in Western Europe, Japan, Australia, and North America. They do not show an increased risk of recurrence in siblings and offspring, unlike other cephaloceles and neural tube defects generally, from which they should be distinguished. Combined craniofacial and neurosurgical operative treatment permits one–stage correction of the whole deformity, the associated hypertelorism being reduced by selective orbital translocation and the nasal deformity by rhinoplasty. In planning these procedures, three–dimensional CT scanning is very helpful. Although our experience is chiefly with cases referred in childhood, we have some experience with operations done in infancy and believe this to be the ideal age.

References

1. Aung Thu, Hta Kyu (1984): Epidemiology of frontoethmoidal encephalomeningocele in Burma. J Epidemiol Commun Health 38: 89–98, 1984.

2. David DJ, Sheffield L, Simpson D, et al: Frontoethmoidal meningoencephaloceles: Morphology and treatment. Brit J Plast Surg 37: 271–284, 1984.

3. Hemmy DC, David DJ, Herman GT: Three–dimensional reconstruction of craniofacial deformity using computed tomography. Neurosurgery 13: 534–541, 1983.

4. Hemmy DC, David DJ: Skeletal morphology of anterior encephalocele defined through the use of three–dimensional reconstruction of computed tomography. Paediatr Neurosci 12: 18–22, 1985.

5. Meyer E von: Über eine basale Hirnhernie in der Gegund der Lamina Cribosa. Virchows Arch (Pathol Anat) 120: 309, 1890.

6. Naim–Ur–Rahman: Nasal encephalocele: Treatment by transcranial operation. J Neurol Sci 42: 73–85, 1979.

7. Simpson DA, David DJ, White J: Cephaloceles: Treatment, outcome and antenatal diagnosis. Neurosurgery 15: 14–21, 1984.

8. Suwanwela C, Sukabote C, Suwanwela N: Frontoethmoidal encephalomeningocele. Surgery 69: 617–625,

9. Suwanwela C: Geographic distribution of frontoethmoidal encephalomeningocele. Br J Prev Soc Med 26: 193–198, 1972.

10. Suwanwela C, Suwanwela N: A morphological classification of sincipital encephaloceles. J Neurosurg 36: 201–211, 1972.

11. Tessier P: Orbital hypertelorism: 1. Successive surgical attempts. 2. Material and methods. 3. Causes and mechanisms. Scand J Plast Reconstr Surg 6: 135–155, 1972.

The South Australian Cranio–Facial Unit
Adelaide Children's Hospital
72 King William Road
North Adelaide 5006
South Australia

Cephaloceles: Classification, Pathology, and Management

David J. David, A.C., F.R.C.S., F.R.C.S.(E), F.R.A.C.S, and Timothy W. Proudman, M.B.B.S.
Australian Craniofacial Unit, Adelaide Children's Hospital, Royal Adelaide Hospital, Adelaide, South Australia

A cephalocele is defined as a herniation of cranial contents through a defect in the skull. Cephaloceles are classified according to their contents and location. We have reviewed a total of 112 patients with cephaloceles, 51 of whom had sincipital meningoencephaloceles (fronto-ethmoidal meningoencephaloceles). This group is distinctive in its demographic distribution, in the effect on growth of other facial structures, and in the combined Craniofacial approach needed to treat them. This review is based on the sincipital encephaloceles with the other cephaloceles included for completeness. Despite many theories, the cause of congenital cephalocele is not known. Preoperative work-up includes 3-dimensional computed tomography scan of the facial skeleton, and surgical management is multidisciplinary in nature. The aim is to remove the lesion before the deformity has time to greatly distort facial growth, which appears to realign itself after surgery. The 50 patients who underwent surgery for fronto-ethmoidal encephalocele all survived with minimal complications.

A herniation of cranial contents through a defect in the skull is termed a cephalocele and, like hernias in other parts of the body, the contents may vary. When the hernia consists of brain and meninges, it is called a meningoencephalocele; the absence of brain tissue characterises a meningocele.

The traditional neurosurgical management of cephaloceles is well documented [1-4]. The advent of reconstructive craniofacial surgery has meant that there is more to offer in the treatment of certain types of cephalocele. This relatively new discipline has also thrown some light on the relationship between the congenital herniations of intracranial contents affecting facial shape and their relationships to Craniofacial clefts [5-8]. This article deals principally with the classification of this condition together with more detailed attention to the morphology and treatment of those lesions that affect the Craniofacial skeleton, namely, the sincipital hernias, the basal hernias, and those associated with Craniofacial clefts as well as the traumatic meningoceles.

Material

A total of 112 patients have been reviewed who were referred to the Adelaide Children's Hospital Neurosurgery Department and the South Australian Craniofacial unit between 1955 and 1988. Since the South Australian Craniofacial Unit (renamed Australian Craniofacial Unit in 1988) was founded in 1975, a total of 48 sincipital and 3 basal encephaloceles have been treated. Two patients have had surgery in their own countries when our department was undertaking overseas clinics. The sincipital cephaloceles make up the largest group of patients, with all but 3 coming from Southeast Asia. Three patients were seen with secondary encephaloceles related to Craniofacial clefts and 3 following Craniofacial surgery, one with Apert's Syndrome. Clinical examination was incomplete in detecting anosmia and assessing intellectual ability in some

Reprint requests: Mr. D.J. David, Australian Craniofacial Unit, Adelaide Children's Hospital, King William Road, North Adelaide 5006, South Australia.

preschool children and in all infants. Psychological and developmental tests were used to assist in evaluating neurological function. Mental ability was broadly divided into 3 categories: normal, moderate mental retardation (retarded but educable), and severe mental retardation (ineducable) [6]. The diagnosis of epilepsy required more than 1 witnessed seizure. In the case of sincipital encephaloceles, all patients underwent review by an ophthalmologist, and, in infants, visual status was determined by defining the refractive error. Lacrimal dysfunction, when suspected, was determined by contrast studies. The main method of investigation of the extracranial mass was by air encephalography, more recently replaced by computed tomography (CT) scan [9, 10]. In infants, B-mode ultrasonography was also of use to determine the status of the ventricles and cisterns pre– and postoperatively. Three-dimensional CT scanning has been a major recent improvement in investigation since it is particularly useful in delineating the Craniofacial skeleton [9, 10].

Classification

Meningoencephaloceles are classically divided into groups based on the anatomic site of the cranial bony defect to which they are related. They can also be classified as primary, where the meningoencephalocele is responsible for the cranial defect (a blow–out phenomenon), or secondary, where there has been a preceding event such as surgery, trauma, or a facial cleft. In 1972. Suwanwela and Suwanwela [11] extended the classification of this sincipital group into its present recognised form based on a paper by von Meyer [12], written in 1890. In 1976, Tessier [13] included sincipital encephaloceles in his anatomical classification of Craniofacial clefts, and in the same year, Mazzola [14] published a morphological classification of facial clefts on embryological grounds. In 1979, Gerhardt and associates [15] recognised 5 types of basal encephaloceles. In Table 1, we list a composite classification of encephaloceles and provide a description of them as well as the number of patients we have seen. Examples of the various types are seen in Figs. 1-6.

TABLE 1.

Encephaloceles

Type of encephalocele	*Cranial defect*	*No. of patients*
Primary		
Occipital	Between lambda and foramen magnum	39
Parietal	Between bregma and lambda	13
Sincipital	At junction of frontal and ethmoidal bones	51
Naso-frontal		18
Naso-ethmoidal		12
Naso-orbital		5
Combined		16
Basal	At junction of spenoid and ethmoid bones	3
Trans-ethmoidal		3
Spheno-ethmoidal		0
Spheno-orbital		0
Spheno-maxillary		0
Trans-sphenoidal		0
Secondary		6
Craniofacial cleft		3
Trauma		0
Surgery		3
Total		112

FIG. 1. *Occipital encephalocele.*

FIG. 2. *Parietal encephalocele. Reprinted with permission of publisher [8]*

Incidence and Epidemiology

Cephaloceles are reported to occur with an incidence of 0.08 per 1,000 total births in Australia [8]. They occur much less frequently than meningomyeloceles [16], at a ratio of 1:12.75, with respect to spina bifida cystica. In our series, occipital meningoencephaloceles were more common in females (2:1) compared with the other main anatomic groups where males were slightly more common (1:0.63) for the parietal group and (1:0.67) for the occipital group.

Perhaps the most striking differences are found on a racial basis. In Australians of European descent, occipital encephaloceles were the most common, occurring in approximately two-thirds of patients; however, sincipital encephaloceles were infrequent. occurring in just over 4% of patients. All patients from Southeast Asia treated by the Australian Craniofacial Unit had sincipital encephaloceles, as did 3 of the 6 patients who were Australian aboriginals. This type of encephalocele is most prevalent in Malaysia [17], Thailand, Indonesia, Burma [18], and parts of Russia [16]. It occurs with much greater frequency than other encephaloceles in these countries. It is reported to be between 5 and 12 times more common where often the reverse is true in Europe, the United States of America, Australia, and other parts of Asia [8, 16-18]. Thirty-three of the 36 families from Malaysia were of Malay origin. The Chinese and Indian immigrants to Southeast Asia were not affected with the same frequency, despite making up large minority groups in those countries. Consanguinity was reported in 4 families where cousins had married and another family where the parents were distant relatives. There was no family history in any of the parents, but the average paternal age was higher (36.6 years) than the average (32.1 years) in the Malaysian population [7]. The maternal age was unremarkable. There was no patient history nor family history of other encephaloceles or any neural tube defect.

Pathology

Sincipital Meningoencephaloceles

The term fronto–ethmoidal meningoencephalocele is descriptive of the bony defect at the foramen cecum where the frontal and ethmoid bones meet (Fig. 7). The

FIG. 3. *Sincipital encephalocele.*

crista galli forms the posterior margin of the defect and the cribriform plate is tilted downward by the mass up to 45 degrees or more [8]. The sense of smell is not interfered with. Histopathological data revealed variations in contents. Some patients had viable brain tissue at the neck of the encephalocele, but distal to the dural defect, there was mostly glial tissue with infiltration of fibrous trabeculae. Arachnoid cysts were reported on several occasions and 1 of these communicated with the ventricular system. Fronto–ethmoidal masses extending into the orbits were often fused with the periorbital tissue, making them difficult to excise. The skin coverage was complete in the majority of cases. In the remainder, there was superficial ulceration or scarring and, in some cases, there was thickening of the skin. One patient had only a thin layer of epidermis covering the encephalocele. Fronto–ethmoidal meningoencephaloceles emerge through the facial skeleton in any of 3 positions and the further classification is descriptive of this [11]. In the naso–frontal type, the bony defect is at the junction of the nasal and frontal bones with the nasal bones attached inferiorly. The fronto–ethmoidal defect is between the nasal bone and nasal cartilages and, consequently, the nasal bones form an overhanging ledge. When this type is large, it may extend the facial defect to include the anterior margins of the medial orbital walls. The naso–orbital bony defect is in the medial orbital wall between the frontal process of the maxilla and the lacrimal bones. The lateral plate of the ethmoid is pushed laterally and a bony tunnel is formed (Fig. 8).

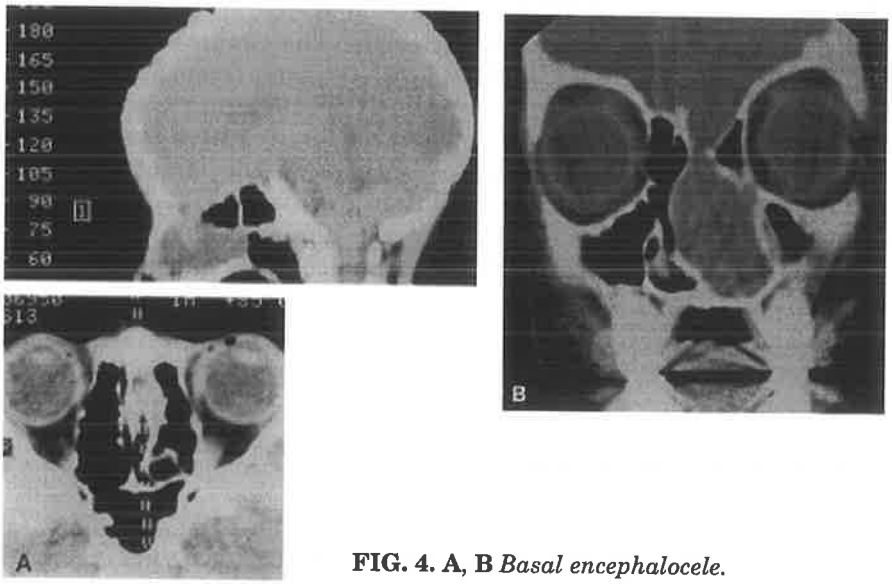

FIG. 4. A, B *Basal encephalocele.*

The subsequent displacement of other structures in the face and their disturbances in function can be well demonstrated in the older patients from Southeast Asia. There is an impression of lengthening of the face to provide room for the lesion. It is virtually impossible to take relevant measurements due to distortion of the landmarks, but the effect may be profound enough to interfere with dental occlusion. The eyes may be proptosed, dystopic, or even absent. Dystopia is a predominant feature of the naso–orbital type. Telecanthus is a feature which is characteristic to the patients with the diagnosis of sincipital encephalocele. Most patients were found to have a medial intercanthal distance far greater than the 97th percentile while the remainder had borderline high normal distances approximately equal to the 97th percentile. The extent of hypertelorism appears to be dependent on the type of encephalocele (naso–ethmoidal intercanthal distance being greater than that of the naso–frontal type) and the actual size of the encephalocele. The lateral canthal distance is often within normal limits. Lacrimal drainage dysfunction was the most common ocular problem, occurring in 17 patients. The lacrimal sac and drainage system were found to be elongated, distorted, and non-functioning. Ten patients had a squint and 12 had decreased visual acuity in 1 or both eyes.

FIG. 5. *Encephalocele associated with craniofacial cleft.*

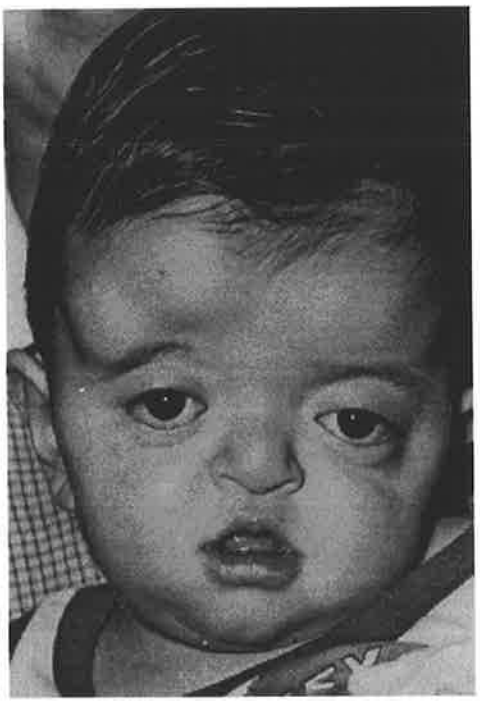

FIG. 6. *Encephalocele associated with Apert's Syndrome.*

Occipital Meningoencephaloceles

Patients in the occipital group were characterised by a midline bony defect. The sizes and shapes were variable; however, one association was noted. Large defects were associated with meningoencephaloceles of largely neural tissue. Small defects, 1–2 cm in diameter, usually contained small nodules of neural tissue and predominantly cerebrospinal fluid. About half of the occipital encephaloceles contained recognisable cerebral cortex and 4 included cerebellum or 4th ventricle. One contained only cerebellar tissue and the remainder, nodules of nondescript neural tissue. The facial skeleton was never affected; however, there was microcephaly in 5 patients and significant hydrocephalus in 7.

Parietal Meningoencephaloceles

The same bony defects and associated neural tissue were present in these patients as for the patients with occipital meningoencephaloceles. Half of these contained parts of the parietal cortex and a third of the cases had varying degrees of holoprosencephaly, often associated with progressive hydrocephalus. The parietal lesions also did not affect the facial skeleton: however, on 2 occasions they were associated with microcephaly.

Basal Meningoencephaloceles

The cases seen in the Australian Craniofacial Unit were of the trans–ethmoidal variety, as the bony canal extended through the cribriform plate into the nasal cavity. One patient had a past history of cerebrospinal fluid (CSF) rhinorrhea and meningitis. Although the meningoencephaloceles were of moderate size on some occasions, they did not appear to significantly distort the facial skeleton.

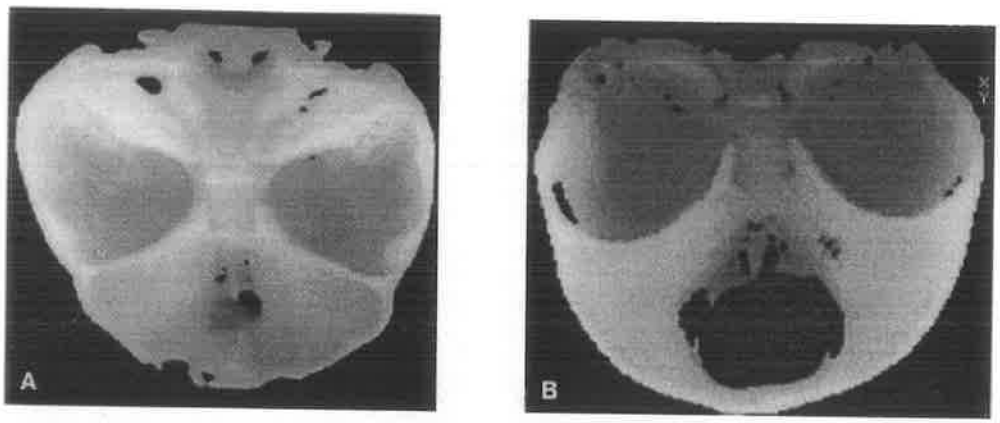

FIG. 7. *Three–dimensional computed tomography scan of exit holes of sincipital encephaloceles from the anterior cranial fossa between the frontal and ethmoid bones.* **A** *Naso–orbital encephalocele.* **B** *Naso–frontal encephalocele.*

Neurological Problems

Sincipital Meningoencephaloceles

There was a wide range of neurological problems associated with these meningoencephaloceles, with hydrocephalus and delayed development being the most common. Hydrocephalus was present in 9 patients, which was non–progressive in the majority of cases. There may have been absence of normal neural tissue in the cranial cavity and, consequently, mental retardation and delayed development has occurred in 9 cases. Epilepsy was reported in 4 instances. Anosmia is not a feature of this condition; however, due to the relatively unprotected neural tissue on the face, infection is a potential problem. One patient who presented had a cerebral abscess. Two other patients had also had previous meningitic infections.

Occipital Meningoencephaloceles

Neurological abnormality is related to the degree of cerebral or cerebellar dysplasia associated with the deformity or to other abnormalities such as holoprosencephaly or hydrocephalus. Approximately two–thirds of the patients showed little or no disability whereas the others were markedly disabled. The follow–up on some patients has been incomplete.

Parietal Meningoencephaloceles

Severe neurological disability and retardation was slightly more common in this group as 7 of 13 cephaloceles had marked problems.

Management

Sincipital Meningoencephaloceles

Investigation and work–up commences with a multidisciplinary craniofacial approach, which involves examination by the plastic surgeon, the neurosurgeon, the ENT surgeon, and the ophthalmologist and an interview with the social worker. Other members of the team, including the speech pathologist, orthodontist, neurologist, geneticist, and cardiologist are available to assist in assessment. Routine radiology is performed including cephalometric studies, 3–dimensional CT scan [19], a brain scan, and, in infants, ultrasonography. Following these investigations, 1 patient was precluded from surgery due to severe mental retardation and failure to thrive. Surgery is planned around the individual in question. Factors involved include the age of the patient, the site of the mass, the extent of the mental ability, and the degree of facial deformity. The principles of treatment are to remove the encephalocele after transecting the neck and closing the dura intracranially. In older patients, this is followed by transcranial bone grafting and, depending on the deformity, correction of orbital hypertelorism or dystopia. In younger patients capable of remodelling the facial structures, management aims to reconstruct using calvarial bone graft, canthopexy, and reconstruction of the medial orbital walls. After planning the operation and the facial reconstruction required, a combined plastic surgical and neurosurgical approach is undertaken. Surgical incisions include a bicoronal scalp flap, giving wide exposure of the craniofacial skeleton. In addition, a nasal incision is utilised in areas of previous scarring or where the soft tissue mass was large. The facial outlet holes are exposed by wide subperiosteal dissection and the planned osteotomies are marked on the skeleton. In many cases, the subcranial bone cuts are made prior to the craniotomy. The frontal craniotomy is performed and the frontal bone removed as a free graft by the neurosurgeon. Dissection of the anterior cranial fossa is extradural, exposing the cranial bony defect beyond the roof of the orbits to the dural neck of the meningoencephalocele. Excising a piece of rectangular bone from the glabella improves exposure and this can be replaced if there is no hypertelorism to correct. The dura is then opened and the cerebral herniation inspected. As much as possible is conserved and then the neck of the encephalocele is transected. The aural defect is usually repaired with temporalis fascia. Following neurosurgical transection of the encephalocele, it is removed and the orbital translocations or bone grafting is performed. In cases where the calvarium is thick enough, it is split through the diploe and the inner table is used as bone grafts to the bony defects. On other occasions, 2-3 ribs have been used, often with 1 incorporating a small cap of costal cartilage for the nasal bone graft.

Where hypertelorism affects both orbits, osteotomies are performed to translocate the orbit medially. This occurred in 22 cases and was most common in the naso-ethmoidal type encephalocele and in older patients. Translocation of 1 orbit was most common where the deformity was predominantly unilateral. The extent of orbital shifts varied from 6 mm to a total shift, in a bilateral case, of 2.5 cm. Osteotomy of the medial orbital wall, canthopexy, and bone graft to the nasal defect was performed where the defect was minor and the encephalocele was not massive. It was also performed in 2 patients with mental retardation where the results did not need to be maximally cosmetic.

Hydrocephalus was managed by external ventricular drainage and this was performed on 7 occasions. This was continued for 48 hours postoperatively and was then removed: however, in 3 cases, the patients' state worsened and subsequent ventriculoperitoneal shunt was necessary. One patient was managed by sequential lumbar puncture over several days and a permanent shunt avoided.

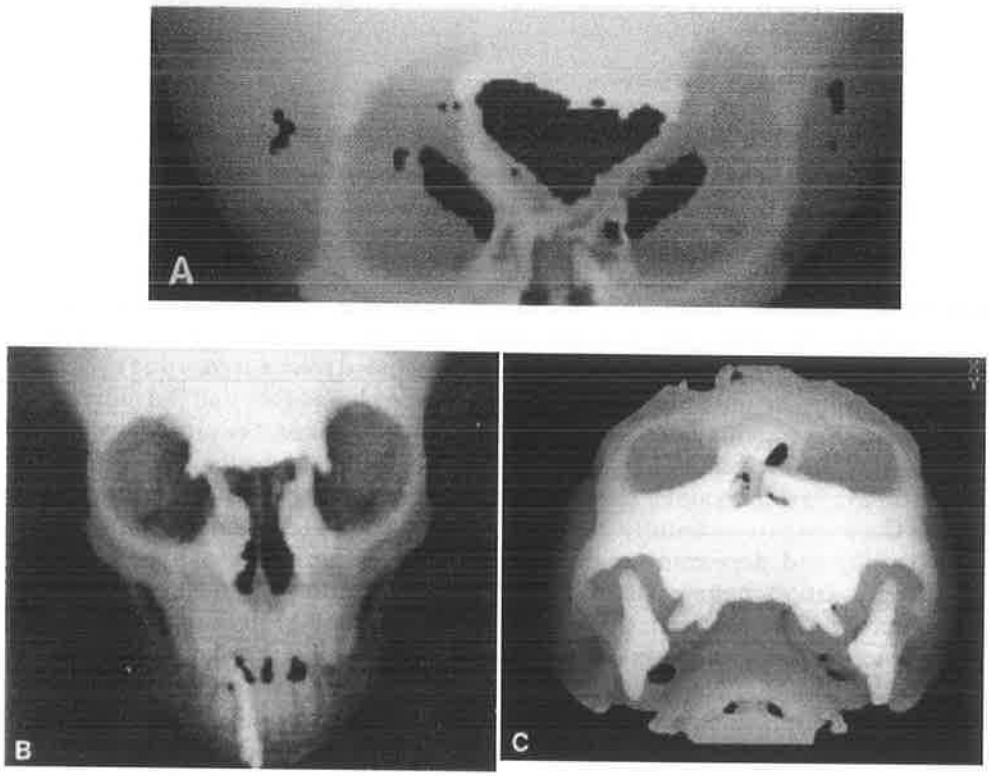

FIG. 8. *Three-dimensional computed tomography scan of facial defects associated with sincipital encephaloceles.* **A** *Naso-frontal type.* **B** *Naso-ethmoidal type.* **C** *Naso-orbital type.*

Basal Meningoencephaloceles

A similar approach was used for the basal meningoencephaloceles with preoperative investigation and planning. In all 3 cases, a bicoronal scalp flap and frontal craniotomy was performed. The anterior cranial fossa was dissected to reveal the exit hole of the encephalocele. In 2 cases, the encephalocele sac was returned to the anterior fossa from the ethmoid sinus. It was ligated intact where it exited through the body of the cribriform plate. The dural defect was repaired and the bony defect closed with a small bone graft. The encephalocele in the third patient was much larger and the mass was ligated at the exit hole in the anterior fossa and the mass removed subcranially after removing the nasal bone and dissecting it out.

Parietal and Occipital Meningoencephaloceles

These cephaloceles are treated by neurosurgeons alone and do not involve the craniofacial team as such, but are mentioned here for completeness. The surgical incision and closure has emphasis on conserving any viable brain tissue, the other main problem requiring attention is the control of hydrocephalus [8].

Results

Sincipital Meningoencephaloceles

All 50 patients who underwent transcranial correction of a fronto-ethmoidal meningoencephalocele survived the operation. The majority of operations were performed between 4 and 8 hours. The surgery performed included permanent shunting in 3 patients. Six patients had a CSF leak that settled spontaneously. We have had 2 patients who have had secondary encephaloceles related to raised intracranial pressure and inadequate reconstruction of the defect. One occurred in the early postoperative phase and was in the medial orbital wall. which resulted in proptosis. The second had a slowly developing secondary encephalocele in the frontal region, which was repaired 1 year after the initial surgery. Three patients required surgical correction of their squint although several other patients had transient postoperative strabismus which settled spontaneously. Nasolacrimal dysfunction, as well as being a major preoperative problem, usually persisted postoperatively. The ducts, despite being patent, were remarkably tortuous and failed to function. One patient required removal of a nasal bone fragment which had sequestered and other patients who have been under review have had removal of the canthopexy wires and further touch-up surgery. Examples of the 3 types of encephaloceles and the postoperative results are shown in Fig. 9.

FIG. 9. *Patients with fronto-ethmoidal meningoencephaloceles. Preoperative:* $\mathbf{A}_1$, $\mathbf{B}_1$, $\mathbf{C}_1$. *Postoperative* $\mathbf{A}_2$, $\mathbf{B}_2$, $\mathbf{C}_2$. **A**: *Naso-frontal,* **B**: *Naso-ethmoidal,* **C**: *Naso-orbital.*

Discussion

The approach to a patient with a fronto-ethmoidal meningoencephalocele is multidisciplinary and is an approach favored by craniofacial surgeons and supported by this group. The occipital and parietal meningoencephaloceles are of little interest to the craniofacial plastic surgeon and consequently, have not been emphasised in this article. Surgery is planned after there has been appropriate examination of the patient and study of ancillary investigations. particularly the 3-dimensional CT scan. This enables the defect to be visualised and, subsequently, the pre-planning of surgery for the specific deformity that exists.

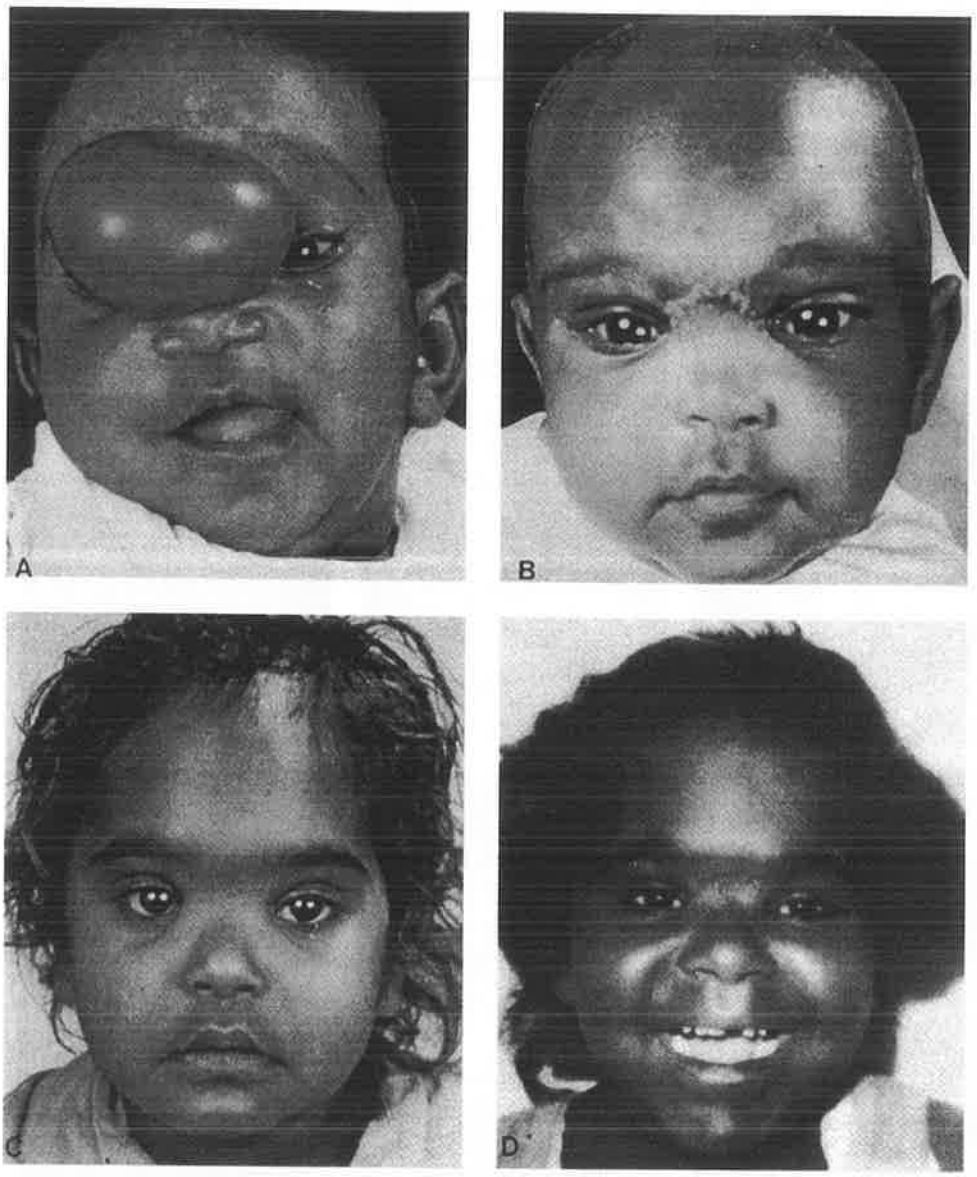

FIG. 10. *Facial growth after removal of fronto-ethmoidal meningoencephalocele.* **A** *Preoperatively, at 3 months of age.* **B** *Immediately postoperatively.* **C** *At 3 years of age.* **D** *At 6 years of age. Parts A and C are reprinted with permission of publisher [9]*

Investigation and surgery have led us to support the suggestion that sincipital encephaloceles have a different developmental pathology from the midline clefts. The facial cleft is a failure of development of intervening structures, allowing herniation of contents of the anterior cranial cavity. The sincipital encephalocele is a blow-out phenomenon [6]. It involves cranial cavity contents that have tunnelled through the midline facial skeleton. The orbital walls, frontal and nasal bones, and even the maxilla are distorted by this space-occupying lesion. The aim of treatment is to remove the lesion before the deformity has time to greatly distort the facial growth. This will allow growth to occur under normal circumstances. The brain, eyes, nasal airway, speech, and mastication will remodel the cranial, orbital, and facial skeleton. Facial growth has been observed to realign itself after surgery in infancy, as described by Naim-ur-Rahman [20]. Cephalometric data over several years is currently being collected by our clinic to attempt to substantiate what is only an impression (Fig. 10). Older children and adults may have a lengthening of the face, especially in the nasoethmoidal type. Complex facial osteotomies to correct this deformity [21] have not been needed in our series, with slight facial lengthening being considered acceptable.

The precise cause of cephaloceles is unclear. They have been postulated to belong to the family of neural tube defects, but unlike them, do not have an increased incidence of affected siblings. There is an interesting geographic and racial distribution of fronto-ethmoidal encephaloceles with prevalence in Southeast Asia. No familial cases have been reported in the literature nor any children affected of known subjects' and we have a similar experience. Suwanwela [17] described a pair of identical twins where 1 twin was not affected, concluding that a genetic mechanism was not the primary cause. Other theories have included a simple vitamin deficiency [17]; however, Kyu and Thu [18], in a large series in Burma, revealed that over half of the mothers of affected children were on vitamins during their pregnancy. They also found no difference in either maternal or paternal ages at the time of birth; however, they noted an increase in time between the birth of the affected child and that of the previous child than there was for other children in the family. They also found a high prevalence among rural and peasant farmers and, in particular, those who grew rice. About three-quarters of the patients were conceived during the wet season, compared with one-third of the controls. They concluded that a series of environmental factors, possibly even fungal agents, may be responsible. The precise cause of frontoethmoidal meningoencephaloceles is still in doubt and, although many theories have been postulated, it would appear that both genetic and environmental factors are implicated.

Résumé

Les encéphalocèles se définissent comme des hernies du contenu de la boite crânienne à travers un défect du crâne. On les classe selon leur contenu et selon l'endroit où elles se produisent. Nous avons passé en revue un total de 112 patients présentant une encéphalocèle dont 51 présentaient des méningo-encéphalocèles sincipitales (méningoencéphalocèles fronto-ethmoïdales). Ce groupe se caractérise par sa répartition démographique, son effet sur la croissance des autres structures de la face et son approche opératoire craniofaciale combinée. Cet article est centré sur les encéphalocèles sincipitales. Malgré le grand nombre de théories proposées, la cause des encéphalocèles congénitales reste inconnue. Le bilan préoératoire nécessite la tomodensitométrie en trois dimensions du squelette de la face; le traitement chirurgical est multidisciplinaire. Le but de cette chirurgie est d'enlever la lésion avant que la malformation ait eu le temps de perturber la croissance de la face; celle-ci se corrige après la chirurgie. Les 50 patients qui ont subi cette chirurgie ont tous survécu avec un minimum de complications.

Resumen

Se define el cefalocele como una herniación del contenido a través de un defecto en el cráneo. Los cefaloceles son clasificados de acuerdo a su contenido y a su ubicación. Hemos revisado un total de 112 pacientes con cefaloceles, 51 de los cuales presentaban meningoencefaloceles sincipitales (meningoencefaloceles frontoetmoidales). Este grupo se distingue en cuanto a su distribucidn demográfica, al efecto sobre el crecimiento de otras estructuras faciales, y al abordaje cráneofacial combinado que debe emplearse en su tratamiento. La revisión se basa en los encefaloceles sincipitales; el resto de los encefaloceles ha sido incluido con mires a una revisión más comprensiva. A pesar de la existencia de diversas teorías, la causa del encefalocele congénito es desconocida. La valoración preoperatoria incluye la escanografiá tridimensional computadorizada del esqueleto facial; el manejo quirúrgico es de naturaleza interdisciplinaria. El propósito es la remoción de la lesión antes de que la deformidad tenga tiempo de distorsionar grandemente el crecimiento facial, el cual parece realinearse después de la cirugía. Los 50 pacientes que fueron sometidos a cirugía por encefalocele frontoetmoidal sobrevivieron todos con mínimas complicaciones.

References

1. McLaurin, R.L.: Cranium bifidum and cranial cephaloceles. In Handbook of Clinical Neurology, P.J. Vinken, G.W. Bruyn, editors, vol. 30, ch. 7, Congenital malformations of the brain and skull, Part 1, Amsterdam. North–Holland Publishing Co., 1977, pp. 209–218

2. Spring, A.: Monographie de la hernie du cerveau et de quelques lesions voisines. Memoires de L'Academie Royale de Medecine de Belgique, 1954

3. LeDran, H.F.: Observations in Surgery, London, James Hodges, 1740

4. Matson, D.D.: Neurosurgery of Infancy and Childhood, Springfield, Charles C. Thomas, 1969, pp. 61–75

5. David, D.J.: New perspectives in the management of cranio-facial deformity. Ann. R. Coll. Surg. Engl. 66: 270, 1984

6. David, D.J., Sheffield, L., Simpson, D., White, J.: Fronto-ethmoidal meningoencephaloceles: Morphology and treatment. Br. J. Plast. Surg. 37: 271, 1984

7. David, D.J., Simpson, D.A.: Fronto-ethmoidal meningoencephaloceles. Clin. Plast. Surg. 14: 83, 1987

8. Simpson, D.A., David, D.J., White, J.: Cephaloceles: Treatment, outcome and antenatal diagnosis. Neurosurgery 15:14, 1984

9. David, D.J., Simpson, D.A., Cooter, R.D.: Meningoencephaloceles: Classification and management. In Advances in Plastic and Reconstructive Surgery, vol. 5, Chicago, Year Book Medical Publishers *(in press)*

10. Hemmy, D.C., David, D.J.: Skeletal morphology of anterior encephaloceles defined through the use of three–dimensional reconstruction of computed tomography. Pediatr. Neurosci. 12: 18, 1986

11. Suwanwela, C., Suwanwela, N.: A morphological classification of sincipital encephaloceles. J. Neurosurg. 36: 201, 1972

12. von Meyer, E.: Uber Basale Hirnhernie In Der Gegend Der Lamina Cibrosa. Virchows Archiv. (Pathologische Anatomie) 120: 309, 1890

13. Tessier, P.: Anatomical classification of facial, craniofacial and latero-facial clefts. J. Maxillofac. Surg. 4: 69, 1976

14. Mazzola, R.A.: Congenital malformations in the frontonasal area: Their pathogenesis and classification. Clin. Plast. Surg. 3: 573, 1976

15. Gerhardt, H.J., Muhler, G., Szdzuy, D., Biedermanm, F.: Zur Therapie problematik bei Sphenodthmoidalen Maningozelen. Zentralbl. Neurochir. 40: 85, 1979

16. Barrow, N., Simpson, D.A.: Cranium bifidum: Investigation, prognosis and management. Aust. Paediatr. J. 2: 20, 1966

17. Suwanwela, C.: Geographical distribution of fronto-ethmoidal encephaloceles. Br. J. Preventative Med. 26: 193, 1972

18. Thu, H., Kyu, H.: Epidemiology of fronto-ethmoidal encephalomeningocele in Burma. J. Epidemiol. Community Health 38: 89, 1984

19. Hemmy, D.C., David, D.J., Herman, G.T.: Three–dimensional reconstruction of cranial deformity using computed tomography. Neurosurgery 13: 534, 1983

20. Naim-ur-Rahman: Nasal encephalocele: Treatment by transcranial operation. J. Neurol. Sci. 42: 73, 1979

21. Jackson, I.T., Tanner, N.S., Hide, T.A.: Frontonasal encephalocele—"long nose hypertelorism." Ann. Plast. Surg. 11:490, 1983

Meningoencephaloceles: Classification, Pathology, and Management

David J. David, F.R.C.S., F.R.C.S.(E.), F.R.A.C.S.
South Australian Cranio-Facial Unit, Adelaide Children's Hospital, Royal Adelaide Hospital, Adelaide, South Australia
Donald A. Simpson, A.M., D.Univ., F.R.C.S., F.R.A.C.S.
South Australian Cranio-Facial Unit, Adelaide Children's Hospital, Royal Adelaide Hospital, Adelaide, South Australia
Rodney D. Cooter, M.B., B.S.
South Australian Cranio-Facial Unit, Adelaide Children's Hospital, Royal Adelaide Hospital, Adelaide, South Australia

A cephalocele is a congenital herniation of intracranial contents through a cranial defect[1]. When the herniation contains brain and meninges, it is termed a meningoencephalocele.

Spring[2] (1854) wrote what was probably the first extensive monograph on the subject. He stated that Le Dran[3] (1740) introduced the term "hernia-cerebri;" however, Le Dran's case was probably a cephalhematoma. Spring himself attempted to distinguish between meningocele and cerebral hernia, the latter being divided into encephalocele and hydranencephalocele when hydrocephalus was present.

The term "meningoencephalocele" seems appropriate because it describes the contents of the hernia: meninges and brain tissue. These developmental anomalies are well known, and their neurosurgical management has been ably discussed.[4,5] Recent plastic surgery literature has focused on the management of the craniofacial deformities produced by some of these lesions.[6-8] Reconstructive craniofacial operative techniques have much to offer in the treatment of certain types of meningoencephalocele.

Material

Our experience is set out in Table 1. Of our 92 cases, 51 were infants and young children referred to the Adelaide Children's Hospital for the management of cephaloceles of various types in the period 1955-1983. With one exception, the children had all been born in Australia. From 1975 through 1986, 41 other children and adolescents were referred to the South Australian Cranio-Facial Unit with sincipital meningoencephaloceles. In addition, two basal encephaloceles have been treated. Two patients have been managed with encephaloceles secondary to craniofacial clefts or to craniofacial surgery: these lesions are usually small meningeal or encephalomeningeal herniations.

Air encephalography, and lately computed tomography (CT scanning), were used routinely to assess the cerebral anatomy; recently, three-dimensional CT scanning has been used to delineate the craniofacial skeleton.[9] In neonates, B-mode ultrasonography was used to delineate ventricular and cisternal anatomy.

In this series, interest centered chiefly on the pathology and on the major long-term disabilities.

Mentality has been categorised as normal, retarded but educable, and ineducable. Normal mentality has been defined as the ability to cope with mainstream education; for preschool children, psychological tests and developmental assessments were used to forecast intellectual ability.

Epilepsy is defined as the occurrence of more than one well-attested epileptic seizure.

TABLE 1.

Cephaloceles Classified According to Anatomical Site of Bone Defect

Type		*Total No.*
Sincipital		41
Nasofrontal	13	
Nasoethmoidal	8	
Naso-orbital	5	
Mixed	13	
Associated with cleft	2	
Parietal		13
Occipital		36
Basal		2
Total		92

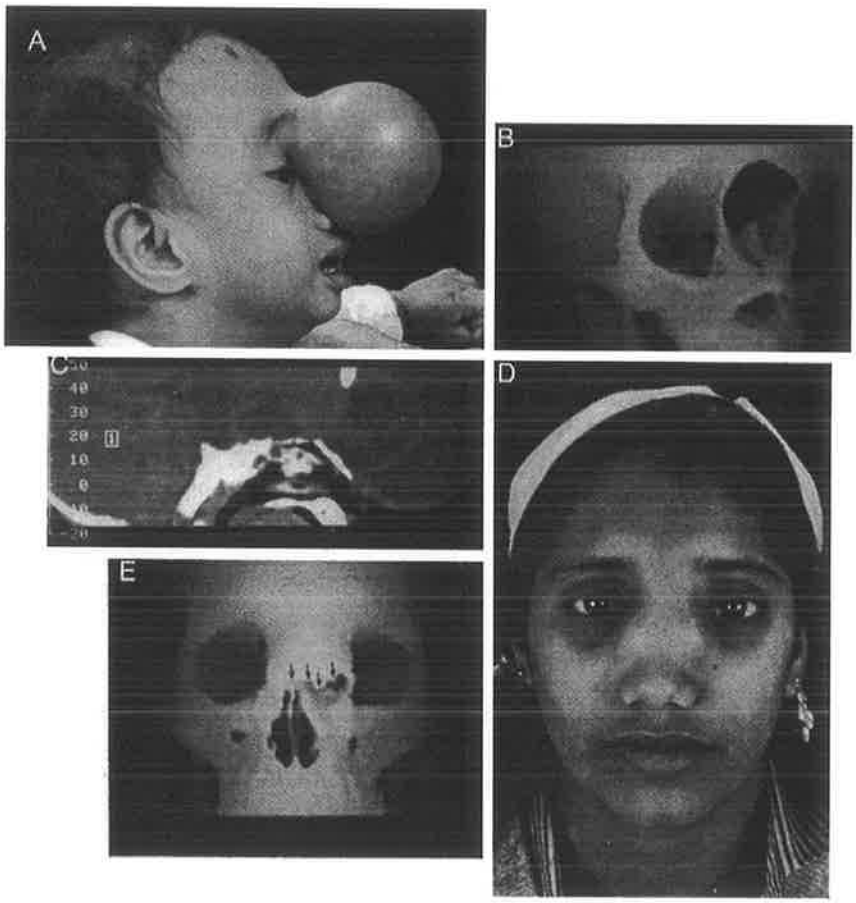

FIG 1. A—C, *a large nasofrontal type of frontoethmoidal meningoencephalocele. Three-dimensional CT reconstruction shows the facial defect with the nasal bones inferiorly. The sagittal section demonstrates the depressed cribriform plate at the base of the bony defect.* **D** *and* **E,** *a nasoethmoidal type of frontoethmoidal meningoencephalocele. The distorted nasal bones can be seen in the three-dimensional CT reconstruction.* (Continued.)

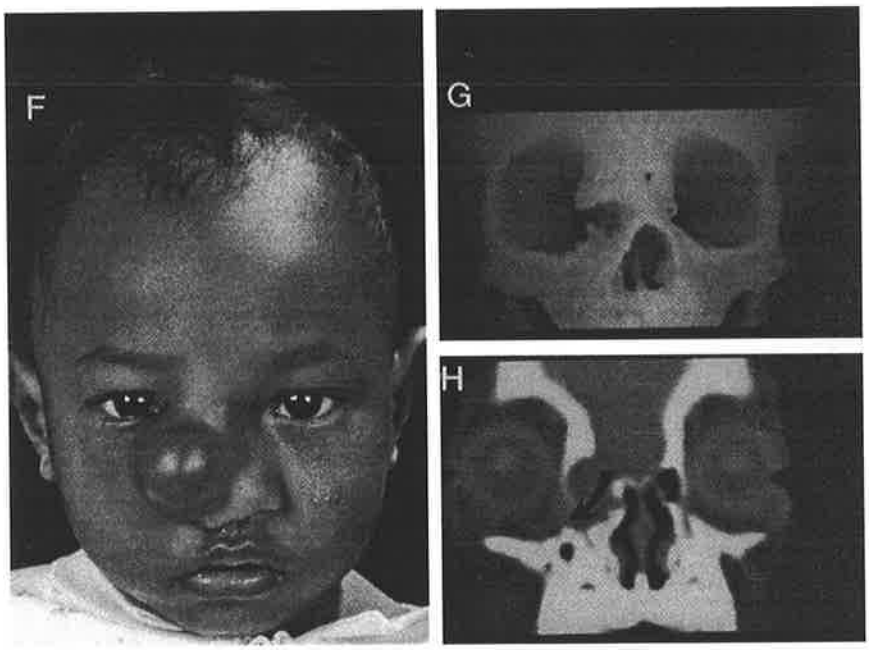

FIG. 1. ***(cont.).*** **F—H,** *a nasoorbital type of frontoethmoidal meningoencephalocele. The defect in the right medial orbital wall is demonstrated with the three-dimensional CT reconstruction. The coronal section shows the encephalocele's path into the right orbit.*

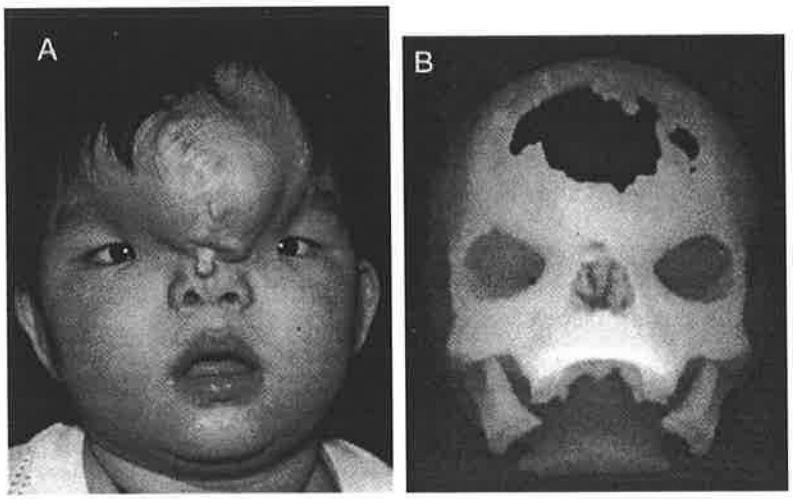

FIG. 2. A *a meningoencephalocele associated with a severe midline craniofacial cleft.* **B** *the bony defect is well seen in the three–dimensional CT reconstruction.*

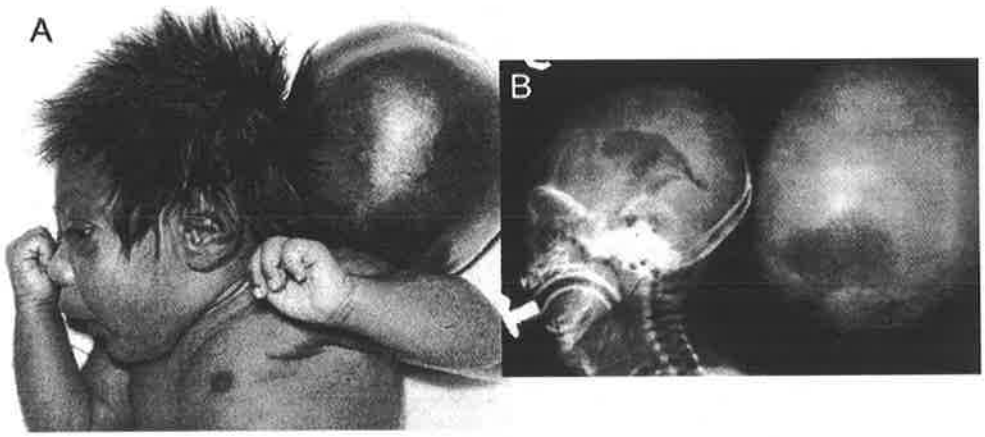

FIG. 3. A *and* **B** *occipital meningoencephalocele containing cerebral tissue.*

Classification

Meningoencephaloceles may be subdivided into four anatomical groups according to the site of the herniation:

1. Sincipital (Figs 1,A-C, and 2)
2. Parietal
3. Occipital (Fig 3)
4. Basal (Fig 4)

Further consideration may be given to etiology; although the majority are congenital, some are secondary to trauma or surgery.

Suwanwela and Suwanwela,[10] based on a paper by Meyer,[11] further classified the sincipital group into:

Frontoethmoidal

- Nasofrontal
- Nasoethmoidal
- Nasoorbital

Interfrontal

Associated with craniofacial cleft

The bony defects associated with sincipital meningoencephaloceles have been included in many attempts to classify craniofacial clefts. Two of the most recent and significant endeavors are Tessier's[12] anatomical classification and Mazzola's[13] morphological classification based on embryologic considerations.

David et al.[6] pointed out that there is a fundamental difference between the etiology and pathology of frontoethmoidal meningoencephaloceles and meningoencephaloceles associated with facial clefts.

Basal encephaloceles were classified by Gerhardt et al.,[14] who recognized five types:

1. Transethmoidal
2. Sphenoethmoidal
3. Spheno-orbital
4. Sphenomaxillary
5. Transsphenoidal

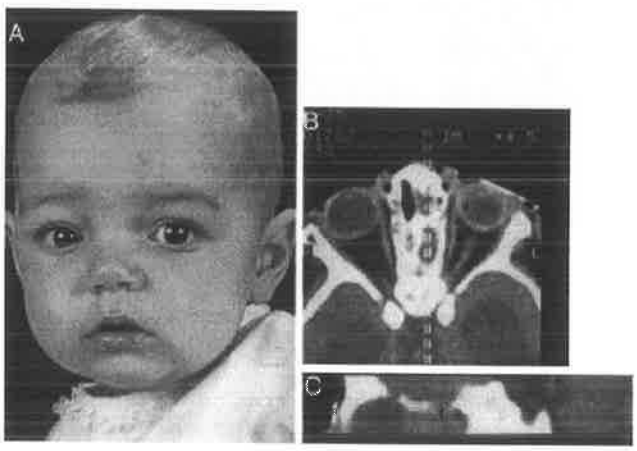

FIG. 4. A—C, *patient with a basal meningoencephalocele of the transethmoid variety. A CT sagittal reconstruction through the cribriform region shows the exit hole (arrow).*

Incidence and Epidemiology

In Australia cephaloceles are seen much less frequently than meningomyeloceles.[8,15] Reliable South Australian birth data are available for the period 1966-1970; during these years eight encephaloceles were reported, giving a ratio of 1:12.75 with respect to spina bifida cystica and an incidence of 0.08/1,000 total births.

The sex ratios differed in the main anatomical groups: the male:female ratio was 1:2 for occipital cephaloceles, 1:0.63 for parietal cephaloceles and 1:0.67 for sincipital encephaloceles. There were also striking differences in ethnicity. Among Australians of European extraction, the large majority (66.7%) of cephaloceles were in the occipital site; sincipital cephaloceles were rare (2.2%). This was not so in the small group of Australians of aboriginal race in which three of six cephaloceles were sincipital. The cases referred from Malaysia and Indonesia were selected by their need for craniofacial surgery, and all had sincipital lesions. The large majority of these were of the Malay race, and apparently none was Chinese, although in Malaysia, the chief country of origin, people of Chinese stock compose some 35% of the population.

Since 1977, the South Australian Cranio-Facial Unit has developed relationships with various Southeast Asian countries, and in particular has treated patients referred from Malaysia. Forty-one cases of sincipital meningoencephalocele have been referred to the South Australian Cranio-Facial Unit; 26 were referred from Malaysia, 3 from Indonesia, 2 from Papua New Guinea, and 1 was an Australian. All patients had been previously assessed by local neurosurgeons and/or plastic surgeons for referral to the central Unit. Three other patients with similar lesions were studied in Adelaide before the Cranio-Facial Unit was formed; two of these were Australian aboriginals, and one was an infant of European racial origin.

The cases from Southeast Asia are a selected series; the paramount consideration was whether the patient and family would benefit from complicated assessment and surgery. Patients with severe mental retardation and other associated problems rendering them unsuitable for surgery were thus eliminated. Of those patients referred with frontoethmoidal meningoencephalocele, the age range was from 0.5 to 22 years. The four cases born in Australia were seen much earlier, the age range being 2 weeks to 15 months. In the combined series, 18 were boys and 23 were girls. The racial origins of the parents, as far as can be determined, are set out in Table 2.

The genetic data collected on these patients indicated consanguinity in two families, and in a third, the parents of the affected child were distantly related. However, there was no history of encephaloceles or any other neural defect in the siblings, parents, or other relatives of the index cases. The striking finding from the genetic viewpoint, however, was that the paternal age seemed to be raised (Table 3). Statistical evidence of a raised paternal age is difficult to obtain: while Malaysian population figures are available for maternal age and birth order, there are no such statistics kept for paternal age. An estimate of population distribution for paternal age has been made for this study by recording the paternal age in 366 cases where births confined in the Penang hospitals are listed for the first three months of 1983. The mean paternal age obtained as well as the published population figures for 1979 in Malay births is shown in Table 3. The mean paternal age for our cases is statistically significantly different from the mean paternal age in Penang ($p<.05$), while the population maternal age and birth order are not significantly different from that of our cases.

The raised paternal age suggests that the course of this type of meningoencephalocele may be due to an autosomal dominant mutation, and if this is confirmed, it would have important genetic counseling implications. However, the lack of familial cases and the geographical distribution of the meningoencephaloceles argue strongly against dominant mutation as a cause.

TABLE 2.

Sincipital Meningoencephaloceles: Racial Origins of Parents

Malay	26
Indonesian	3
Papuan	2
Indian	2
Chinese*	2
Australian aborigine	3
European	1
Filipino	2
Total	41

**This includes one couple living in Malaysia with mixed racial origin (Iban-Chinese) and another couple living in Hong Kong.*

TABLE 3.

*Parental Ages and Birth Order in 17 Malay Cases**

	Malay Cases (n = 17)	Malay Population Figures
Paternal age	37.3	32.1
Maternal age	29.4	28.0
Birth order	3.8	3.4

**From David DJ, Simpson DA: Fronto-ethmoidal meningoencephaloceles.* Clin Plast Surg *1987; 14:83-89. Used by permission.*

Morphology of the Bone Defects

For the most common type of sincipital meningoencephalocele, the description frontoethmoidal is most appropriate, because it describes the site of the cranial end of the bone defect, which is always in the position of the foramen cecum at the junction of the frontal and ethmoidal bones (Fig 5). The posterior margin of the defect is formed by the crista galli. This is often distorted, and the cribriform plate is usually tilted downward as a deep central trough, the anterior end of which is well below the planum sphenoidale; the cribriform plate forms an angle of 45°-50° with the orbitomeatal plane (see Fig 1,A). In our cases, the cranial exit holes varied in size and shape. All nasofrontal defects were round and central, and all naso-orbital defects were bilobed (see Fig 5). Two of the nasoethmoidal type were bilobed, while in one case the defect was lozenge shaped and central. The remainder were round.

The morphology of the facial bone defects showed more variation. In the nasofrontal type, the holes were at the junction of the frontal and nasal bones (see Fig 1,A), the nasal bones being attached to the inferior margin of the defect, which varied in shape.

In the nasoethmoidal type, the facial defects lay between the nasal bones and the nasal cartilage (see Fig 1,B), the nasal bones being above and the nasal cartilages below. The nasal bones were deformed and often broadened, with distorted margins. The frontonasal angle was obliterated, producing an

overhanging ledge. If the facial defect was confined to the nasal pyramid and was small and oval, the medial walls of the orbit were not involved. If, however, the meningoencephalocele was larger and the facial defect extended more laterally, then the anterior margins of the medial orbital walls were eroded and crescent shaped.

The naso-orbital meningoencephaloceles present onto the face through holes in the medial orbital wall (see Fig 1,C), in the frontal process of the maxilla and lacrimal bones. In our cases the bony track was long and shaped like an inverted "Y." The inverted Y was sometimes asymmetrical. These meningoencephaloceles came through the frontal process of the maxilla onto the face leaving the nasal bones intact anteriorly, and the lacrimal bones and lateral plate of the ethmoid intact posteriorly. However, during the passage of the cerebral hernia through the substance of the ethmoid, the lateral plate of that bone may be pushed laterally, forming a bony tunnel. The developing orbits may be grossly expanded by the meningoencephalocele.

The parietal and occipital cephaloceles showed midline bone defects of various sizes and shapes; when the extruded contents included masses of well-formed brain, the bone defects were larger, while herniations containing large volumes of cerebrospinal fluid (CSF) and/or small nodules of neural tissue were usually associated with bone defects only 1-2 cm in largest diameter.

The two cases of basal meningoencephalocele showed bony canals through the body of the cribriform plate into the nasal cavity and are classified as transethmoidal in the system reported by Gerhardt et al.[14]

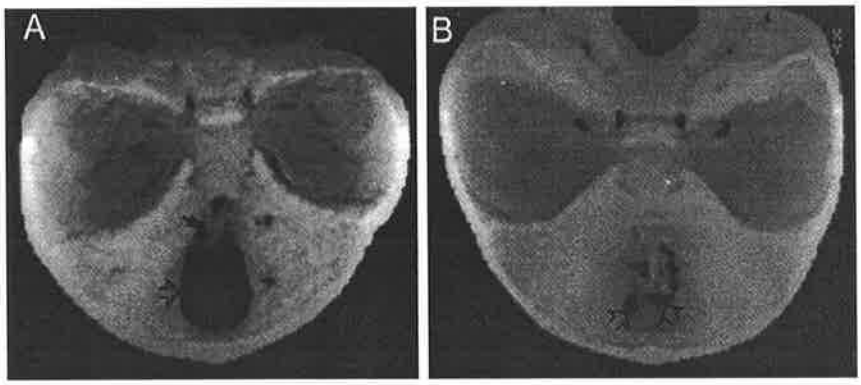

FIG. 5. *Three-dimensional reconstructions of the anterior cranial fossa showing the exit holes.* **A** *nasofrontal types have round central cranial defects with the crista galli seen in the posterior margin* (small arrow). **B** *naso-orbital types often have bilobed exit holes from the anterior cranial fossa.*

General Features of the Face and Facial Skeleton

Sincipital meningoencephaloceles are usually grotesque deformities associated with gross facial disfigurement. In most of our cases of frontoethmoidal meningoencephaloceles, the face appeared to be longer than normal (Fig 6), although this is hard to measure with ordinary cephalometric techniques, because some of the bony landmarks, particularly in the glabella region, are obliterated. The piriform aperture and the nasal cartilages were misshapen; the aperture was shorter and broader than usual and displaced inferiorly. No case has shown a bifid nose or a midline nasal cleft. There was telecanthus in all cases, with medial canthal dystopia in some and hypertelorism in most. As a rule the hypertelorism was not so severe as that associated with midline facial clefts; it was usually of a Tessier second-degree variety with normal lateral canthal distance[16]. Some patients had dental malocclusion, which may be related to the deformity: the vertical plate of the ethmoid bone is attached to the tilted cribriform plate which is itself retrodisplaced, presumably inducing secondary maxillary

hypoplasia. The nasoethmoidal type of encephalocele has a direct effect on the nasal septal cartilage, pushing it downward and backward. It is as though the encephalocele had blown out onto the face through the weakened junction of the frontal and ethmoidal bones, displacing the otherwise normal orbits and nasal capsule, widening the orbits and lengthening the face. In contrast with the clefts, which appear to have a deficiency of tissue at their margins[12], the defects of the fronto-ethmoidal meningoencephaloceles are like tunnels or blowouts. A wide variety of deformities are seen which are related to the volume and position of the displaced dysplastic brain and its coverings.

FIG. 6. *The typical long face of an adult patient with a frontoethmoidal meningoencephalocele.*

The more posteriorly situated meningoencephaloceles do not show characteristic facial deformities; the lesions, if large, are themselves disfiguring, and in some cases there is obvious microcephaly.

Facial deformities associated with the rare basal meningoceles are less marked. Associated anomalies such as cleft lip and palate[14, 17] presumably show the facial deformities typical of these conditions.

Neuropathology

Sincipital Meningoencephaloceles

The pathologic constituents of the herniations varied. Two patients had extension of the ventricular system into the defect. Most patients had viable brain at the neck of the encephalocele but distal to the defect in the dura mater, biopsies mostly consisted of glial tissue, often infiltrated with fibrous trabeculae. Eighteen patients had undergone previous surgery; 8 patients had had intracranial operations only, and 5 had had intracranial operations plus attempts to excise the facial lesions, and 5 others had had operations on the facial lesion only. In those cases where the neck of the encephalocele had been divided at previous surgery, there was no significant spontaneous atrophy of the facial extension. Histologically the glial mass did not look markedly atrophic; certainly they remained in sufficient bulk to produce a distortion of the face.

The soft tissue mass of the meningoencephalocele may extend into the orbits and fuse with the periorbitum, making excision of the orbital component of the mass extremely difficult. The tumor may flow over the infraorbital rim medially, which then becomes indented and depressed. Wherever the nasal skeleton was impinged on by the extruded brain and its coverings, it was distorted. The overlying skin is usually of full thickness, but may be discolored or scarred

from previous ulceration and healing. The skin is often thickened and crusty (Fig 7). In only one case was the skin cover of the extruded cerebral tissue defective: in this neonate the cerebral hernia was covered only by a thin layer of epidermis.

Parietal Meningoencephaloceles

These were usually associated with gross dysplasia. In 6, the herniations contained parietal cortex; 3 contained only small glial nodules; and 1 was not adequately examined. Varying degrees of holoprosencephaly ranging from partial agenesis of the corpus callosum to lobar holoprosencephaly were seen in four cases of parietal meningoencephalocele, and three of these exhibited progressive hydrocephalus. Two other parietal lesions were associated with microcephaly.

Occipital Meningoencephaloceles

In the occipital group (21 cases), there were 11 with recognisable cerebral cortex within the herniation; in four of these, there was also cerebellum or 4th ventricle. One occipital meningoencephalocele contained only cerebellar tissue, seven contained nodules of glia or other nondescript neural tissue, and two were not adequately examined. There was significant hydrocephalus in seven and microcephaly in five.

Ocular Problems

These were numerous among patients with sincipital lesions. One patient had microphthalmia resulting from massive extrusion of the hernia into the orbit. Eight patients had decreased visual acuity from ulceration and scarring of the cornea. Five patients suffered from squint.

The most common deformity was lacrimal drainage dysfunction. Injection of the puncta at operation frequently demonstrated a patent but elongated and tortuous drainage system which was not functioning before surgery and which failed to do so after surgery.

Orbital expansion and/or dystopia was present in all patients with the naso-orbital type of deformity.

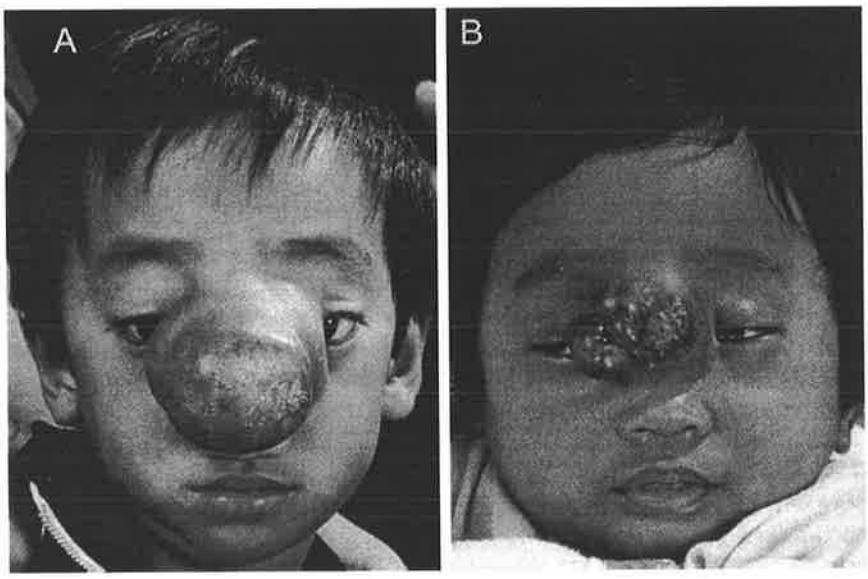

FIG. 7. A *and* **B** *the skin overlying frontoethmoidal meningoencephaloceles is often abnormal.*

Neurologic Problems

Sincipital Meningoencephaloceles

Ten patients showed developmental retardation. Seven patients had hydrocephalus, and in four there was a previous history of epilepsy. In all patients capable of being assessed, there was no evidence of anosmia before or after surgery.

Parietal Meningoencephaloceles

In our series of 13 cephaloceles, six showed gross neurologic disabilities and developmental retardation. One other, though trainable, is severely retarded and epileptic. Only four have slight or no disabilities. Two required shunt operations for hydrocephalus.

Occipital Meningoencephaloceles

These patients may or may not exhibit developmental retardation and other neurologic abnormalities, according to the degree of cerebral or cerebellar dysplasia associated with the herniation and the presence or absence of other anomalies, such as holoprosencephaly and hydrocephalus. In our cephalocele series, 22 of 36 cases showed little or no disability; the others were severely or totally disabled (10 cases) or incompletely followed.

Treatment

Sincipital Meningoencephaloceles

Treatment is based on a plan resulting from a detailed study of the clinical data, supplemented by CT scanning with two-dimensional and three–dimensional reconstruction.[19]

In all 41 cases of frontoethmoidal meningoencephalocele treated by the Cranio–Facial Unit, a combined approach was used. Access was gained by a bicoronal scalp flap. Where there was a large soft tissue mass on the face requiring removal, or where there was previous facial scarring, an additional nasal incision was made. The first step was wide subperiosteal exposure of the craniofacial skeleton to outline the facial exit holes of the meningoencephalocele. The planned osteotomies were then marked out on the skeleton, and in many cases subcranial bone cuts were made at this stage. The neurosurgeon then performed a frontal craniotomy, removing the frontal bone as a free graft. If it was thick enough, it was split and the inner table was used for grafting. Otherwise, two or even three ribs were harvested. The reconstructive maneuvers were based on the assessment made at the time of surgical planning.

The soft tissue mass is dissected with great care, as it often blends with the nasolacrimal apparatus and the periorbitum. When this has been completed, the neurosurgeon is presented with a craniofacial mass that can be disconnected at the level of the exit hole if necessary. This is done by transection of the neck of the meningoencephalocele and intracranial repair of the dural defect. All cerebral tissue of possible functional value is preserved. The dural defect is repaired with a fascial graft and after this has been completed, any craniofacial bony surgical maneuvers can be performed; at the end of the operation, the bone defect can be closed with a free graft.

Where there is hypertelorism affecting both orbits, the orbits are translocated medially to move the globes of the eyes. If only one orbit is displaced, then only one orbit is moved. An expanded orbit can be contracted, both by

osteotomies and by bone grafting. Where there is telecanthus only, and destruction and distortion of the medial canthal region, then reconstruction of the medial orbital walls, bone grafting of the lateral orbital walls, canthopexy and bone grafting of the nasal defect are all that is indicated.

In the nasoethmoidal type of deformity the medial orbital walls were often found to be defective and the angle of the cribriform plate so steep that the translocated orbits came to overlie the cribriform plate. Care was taken not to remove too much skin from the midline over the nose, as the soft tissue in this area has the capacity to "take up" in the first few months postoperatively.

The presence of hydrocephalus need not contraindicate definitive craniofacial surgery. If possible, we prefer to employ a preoperative shunt. In three cases, preliminary external ventricular drainage was needed, and it was continued for 48 hours after operation; in two of these the child's state worsened postoperatively when the drain was removed, and ventriculoperitoneal shunts were inserted.

In all instances in infants in the first year of life, bony facial osteotomies were kept to a minimum, working on the thesis that the bony facial skeleton will reorganize itself once the abnormal brain has been removed.[20] (Fig 8).

In the older patients, particularly those of the nasoethmoidal variety with the longer faces, we have not found it necessary to be involved with the more complex face shortening operations as described by Jackson et al.[21]

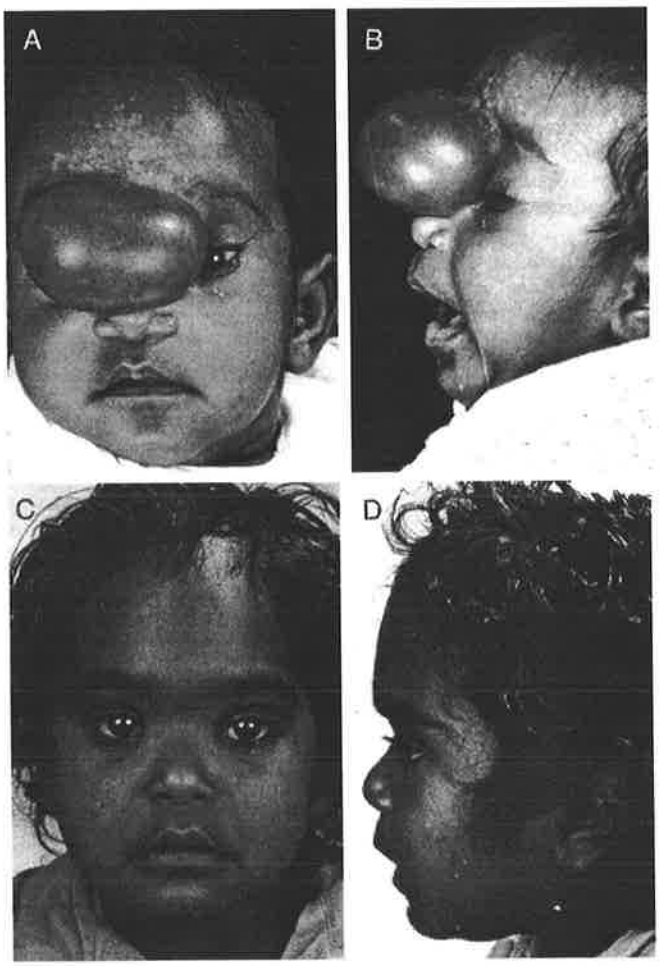

FIG. 8. *Facial reorganization after removal of a frontoethmoidal meningoencephalocele.* **A** *and* **B.** *preoperatively.* **C** *and* **D,** *3 years after removal of meningoencephalocele.*

Parietal and Occipital Meningoencephaloceles

These lesions require neurosurgical excision and closure, with special attention to conservation of potentially viable brain and control of hydrocephalus.[8] The principles of neurosurgical management are well described by McLaurin.[22] For the plastic surgeon, these lesions present no special interest, as there is always sufficient skin to allow tension-free closure.

Basal Meningoencephaloceles

In the two patients with basal encephaloceles, the approach was made through a bicoronal scalp flap and frontal craniotomy. Dissection of the anterior cranial fossa exposed the exit hole of the encephalocele, which was through the body of the cribriform plate. In both our cases the encephalocele sac could be delivered into the anterior fossa intact from the ethmoid sinus, ligated, the dural defect repaired, and the bony defect closed with a small portion of calvarial bone.

Operative Results

Sincipital

All patients undergoing transcranial correction for frontoethmoidal meningoencephaloceles survived the surgery. Surgery was usually accomplished in between four and eight hours. Complications included 2 patients with acute postoperative hydrocephalus; 3 patients had CSF rhinorrhea, which ceased spontaneously, and 1 patient had a secondary encephalocele in the frontal region as a result of raised intracranial pressure and inadequate reconstruction of the frontal bone, requiring secondary surgery. The same patient also had an infection of the left medial canthal region, which settled with antibiotics. Several patients had squints postoperatively, but all but two of these resolved spontaneously. In two patients the squints were of sufficient severity to warrant further surgical correction. The most significant long-term problem is epiphora resulting from nasolacrimal apparatus malfunction. Even in those cases where the nasolacrimal apparatus has been demonstrated to be intact, it is often so deformed that the tortuous ducts fail to function. A number of patients have required the removal of their transnasal canthopexy wire and minor secondary bone grafting to the nose and cheeks. As far as facial growth is concerned, the results in those patients who underwent operation in infancy appear to confirm the proposition that the facial skeleton will readjust itself to the normal growth forces after removal of the displaced dysplastic brain (see Fig 8). However, we have not yet validated this impression with long–term craniometric data. Various results have been demonstrated in Figure 9.

Discussion

We have confined our major discussion to the management of frontoethmoidal meningoencephaloceles, because meningoencephaloceles associated with clefts, or secondary to other surgery, do not have particular associated problems that complicate the otherwise documented craniofacial management of those deformities, and the meningoencephaloceles situated in the parietal and occipital regions have, as a rule, no special interest for craniofacial surgeons. We suggest that frontoethmoidal meningoencephaloceles are fundamentally different in origin from midline clefts. These sincipital lesions are a blowout of the intracranial contents through a midline tunnel from the anterior cranial fossa into the facial skeleton. The skeletal deformities relate to the space-occupying effect of the hernia of extruded brain and are not intrinsic to the tissues themselves. If this view is correct, early complete surgery should allow the developing brain and eyes to

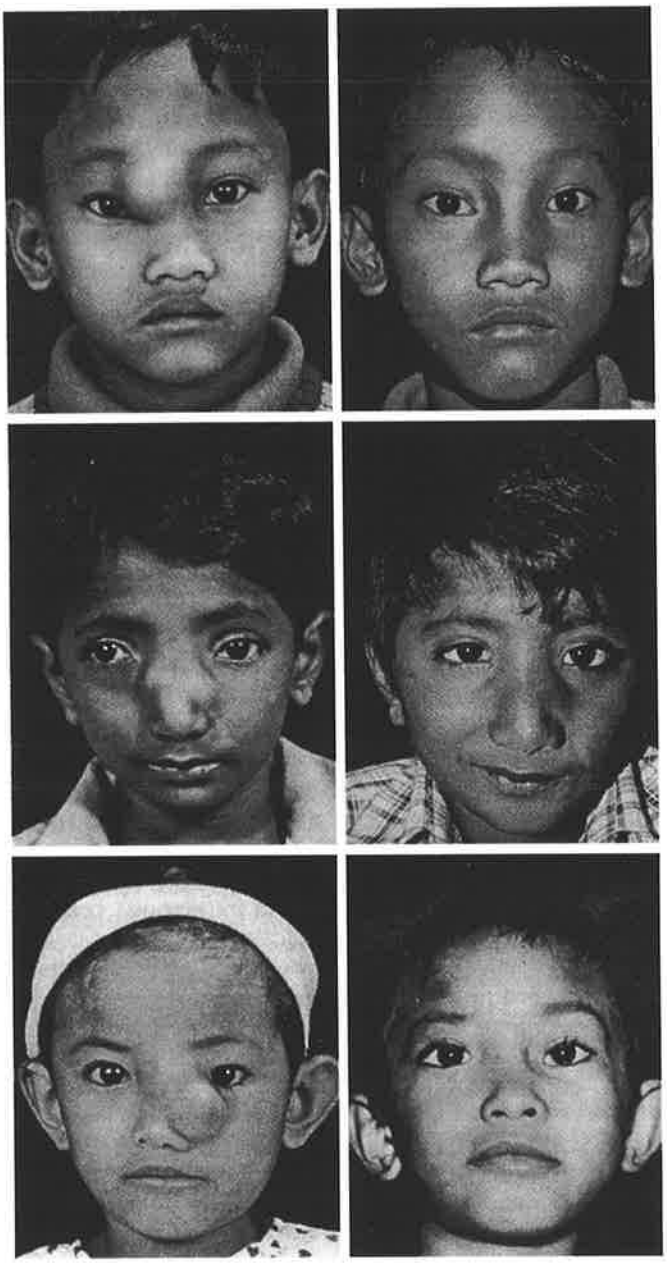

FIG. 9. *Preoperative and postoperative photographs of patients with frontoethmoidal meningoencephaloceles.*

mold the orbital skeleton, and the forces generated by the nasal airway, speech, and mastication will remodel the facial deformity. Naimur-Rahman[20] has suggested this to be the case, but we cannot confirm his claim that early excision of the frontoethmoidal herniation alone is sufficient to restore normal facial growth. The midline clefts of the nose, on the other hand, have a deficiency of tissue, the abnormality being intrinsic to the tissues themselves. Early surgery of these clefts would not be expected to help the skeletal deformity.

It has been suggested that the frontoethmoidal meningoencephaloceles are one of the neural tube defects to be considered with anencephaly and myelomeningocele as a varying expression of a single developmental aberration. The sincipital lesions pose difficulties, however, because they are not associated with circumstantial supporting evidence such as affected siblings. Suwanwela et al.[23] of Bangkok have studied a large number of these lesions and found no record of siblings with other congenital neurologic malformation. This has been the case in our 41 cases.

There are also extraordinary geographical peculiarities in the distribution of frontoethmoidal meningoencephaloceles; these malformations are common in Malaysia, Thailand, and Burma, but rare in Europe, North America, and Australia, as well as Japan and China. There is also some evidence that sincipital lesions are common in some parts of Russia.[15] The high incidence in Thailand and apparently also in Malaysia seems definite, and in both countries, it is the Thais and Malays, not Chinese, who are affected, despite the presence in these countries of large Chinese ethnic minorities. Thus, in their epidemiology the sincipital frontoethmoidal meningoencephaloceles show remarkable peculiarities. In the present state of knowledge it seems unwise to include them in other neural tube defects. They may indeed result from some unknown environmental agent, perhaps dietetic. Our finding of significantly increased paternal age of the patients suggests that an autosomal dominant gene mutation may account for the occurrence of the lesion, but this requires further investigation of cases and of population norms.

Until recently, frontoethmoidal meningoencephaloceles were initially treated by neurosurgeons; plastic surgeons being, as a rule, consulted secondarily to deal with established deformities. The advent of craniofacial surgery allows definitive correction of the deformity at a single stage. Division of the neck of the encephalocele is not enough to wither the distal component of the extruded tissue or to prevent distortion of the developing skeleton. Craniofacial surgery is recommended with removal of the extruded brain and repair of the dura and anterior cranial fossa and the appropriate osteotomies and bone grafts, preferably in the first three months of life, in the hope that the airway will establish normal growth forces of the craniofacial skeleton and allow the face to assume more normal proportions. The simplest operation, namely that of moving the medial orbital walls with bone grafting and canthopexies, is the operation of choice in the early years of life. In the older patient, however, the displaced orbits can be reconstructed in three dimensions if necessary.

We have not attempted to describe the details of each operation because in these days of the well–established craniofacial unit, it is now an accepted principle of this extension of plastic surgery that the details of each operation should be designed to fit the specific deformities present. The advent of CT scanning techniques giving accurate three-dimensional images has allowed the surgical team the opportunity to preplan such surgical maneuvers, tailoring each operation to each individual deformity.

Acknowledgements

We thank Deirdre Marshall, Visiting Medical Student from Stanford Medical Center, California, for reviewing the files of patients with meningoencephaloceles at the South Australian Cranio-Facial Unit.

References

1 McLaurin RL: Cranium bifidum and cranial cephaloceles, in Vinken PJ, Bruyn GW (eds): Handbook of Clinical Neurology. Congenital Malformations of the Brain and Skull, Part I. Amsterdam, North-Holland Publishing Co, 1977, vol 30, pp 209–218.

2 Spring A: Monographie de la herni du cerveau et de quelques lesions voisines. Memoires de L'Academie Royale de Medecine de Belgique, 1854.

3 Le Dran HF: Observations in Surgery. London, James Hodges, 1740.

4 Matson DD: Neurosurgery of Infancy and Childhood. Springfield, ILL, Charles C Thomas, Publishers, 1969, pp 61–75.

5 Mealy J Jr, Dzenitis AJ, Hockey AA: The prognosis of encephaloceles. J Neurosurg 1970; 32:209–218.

6 David DJ, Sheffield L, Simpson D, et al: Fronto–ethmoidal meningoencephaloceles: Morphology and treatment. BrJ Plast Surg 1984; 37:271–284.

7 David DJ, Simpson DA: Fronto-ethmoidal meningoencephaloceles. Clin Plast Surg 1987; 14:83–89.

8 Simpson DA, David DJ, White J: Cephaloceles: Treatment, outcome and antenatal diagnosis. Neurosurgery 1984; 15:14–21.

9 Hemmy DC, David DJ: Skeletal morphology of anterior encephaloceles defined through the use of three-dimensional reconstruction of computed tomography. Pediatr Neurosci 1986; 12:18–22.

10 Suwanwela C, Suwanwela N: A morphological classification of sincipital encephalomeningoceles. J Neurosurg 1972; 36:201–211.

11 Meyer von E: Uber Eine Basale Hirnhernie In Der Gegend Der Lamina Cribrosa. Virchows Archiv [A] 1890; 120:309–320.

12 Tessier P: Anatomical classification of facial, craniofacial and latero-facial clefts. J Maxillofac Surg 1976; 4:69–92.

13 Mazzola RA: Congenital malformations in the frontonasal area: Their pathogenesis and classification. Clin Plast Surg 1976; 3:573–608.

14 Gerhardt HM, Muhler G, Szdzuy D, et al: Zur Therapie problematik bei Sphenoethmoidalen Meningozelen. Zbl Neurochir 1979; 40:85–94.

15 Barrow N, Simpson DA: Cranium bifidum: Investigation, prognosis and management. Aust Paediatr J 1966, 2:20–26.

16 Tessier P: Orbital hypertelorism, in Symposium on Plastic Surgery in Orbital Region. St Louis, CV Mosby Co, 1976, vol 12.

17 Sakoda K, Ishikawa S, Uozumi T, et al: Sphenoethmoidal meningoencephalocele associated with agenesis of corpus callosum

and median cleft lip and palate: Case report. J Neurosurg 1979; 51:397–401.

18 Probst FP: The Prosencephalies: Morphology, Neuroradiological Appearances and Differential Diagnosis. Berlin, Springer-Verlag, 1979, pp 29–34.

19 Hemmy DC, David DJ, Herman GT: Three-dimensional reconstruction of cranial deformity using computed tomography. Neurosurgery 1983; 13:534–541.

20 Naim-ur-Rahman N: Nasal encephalocele: Treatment by transcranial operation. J Neurol Sci 1979; 42:73–85.

21 Jackson IT, Tanner NS, Hide TA: Frontonasal encephalocele— "long nose hypertelorism." Ann Plast Surg 1983; 11:490–500.

22 McLaurin RL: Encephalocele and related anomalies, in Hoffman HJ, Epstein F (eds): Disorders of the Developing Nervous System. Oxford, Blackwell, 1986.

23 Suwanwela C, Sukabote C, Suwanwela N: Frontoethmoidal encephalomeningocele. Surgery 1971; 69:617–625.

Fronto-Ethmoidal Meningoencephalocele Classification and Associated Features

A. HANIEH and D.J. DAVID
Australian Cranio-Facial Unit,
Adelaide Children's Hospital, Adelaide, South Australia (AUS)

Definition

Encephalocele is a protrusion of cranial contents beyond the normal confines of the skull. In fronto-ethmoidal meningoencephalocele (Fig. 1) the protrusion of the cranial content is through a congenitally enlarged foramen caecum. This point of exit is constant and interestingly it is a point of junction between desmocranium or membranous skull and chondrocranium or cartilaginous skull.

Classification

As mentioned, the cranial exit is constant, this led to the appropriate name of fronto-ethmoidal encephalocele, which means a protrusion between the ethmoid and the frontal bones. On the other hand, the point of the facial exit varies, the fronto-ethmoidal meningoencephalocele is classified according to the relation of this point of exit to the nasal bones.

Based on this, the fronto-ethmoidal meningoencephalocele is classified into the following:

1. Naso-frontal: (Fig. 2) The meningoencephalocele emerges between the frontal bone and the nasal bone.

2. Naso-ethmoidal: (Fig. 3) The meningoencephalocele emerges inferior to the nasal bone, between it and the nasal cartilage.

3. Naso-orbital: (Fig. 4) In this type the bulk of the meningoencephalocele is in the orbit, it passes through the medial wall of the orbit, either in the frontal process of the maxilla or through the lacrimal bone.

This type is often mixed, often partly intraorbital and partly facial, and often bilobar passing into both orbits.

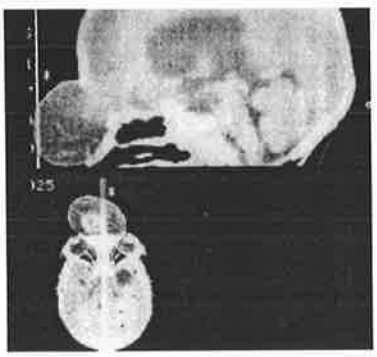

FIG. 1.

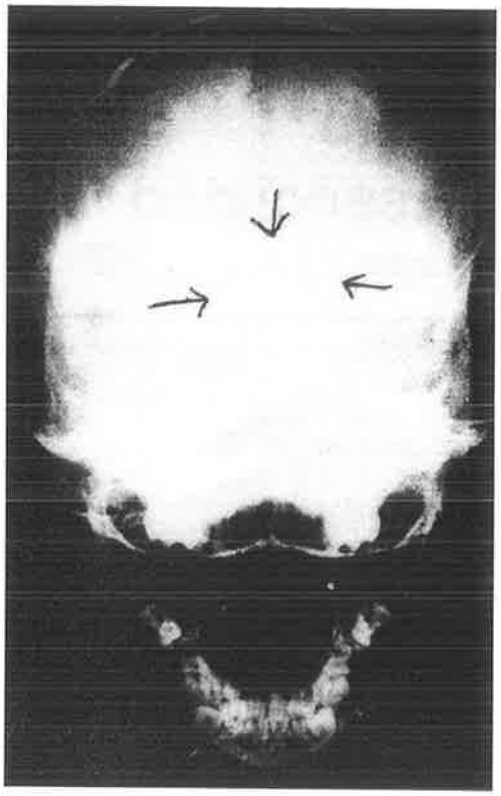

FIG. 2.

FIG. 3.

FIG. 4.

Material

We reviewed 32 cases of fronto-ethmoidal meningoencephalocele which were managed at the Australian Cranio-Facial Unit.

The records and imaging of these cases were examined.

Out of 32 cases there were three nasofrontal, 16 naso-ethmoidal and 13 naso-orbital (Fig. 5).

Classification 32 Cases of FEME	
Naso–Frontal	3
Naso–Ethmoidal	16
Naso–Orbital	13

FIG. 5.

Associated Features

In our study of the 32 cases, we found that there are several features commonly seen in association with the fronto-ethmoidal meningoencephalocele. Some of these features would modify or change the management of these cases, also it could affect the outcome of treatment.

A. Skull Changes

1. Anterior Cranial Fossa: It slants down towards the foramen caecum in 45° to the meato-orbital plane. It forms a deep trough which makes surgical exposure and repair of the neck of the encephalocele difficult. This feature is present in most cases. To overcome this difficulty we usually remove the inter orbital bone to improve access to the neck of the sac and its repair.

2. Long Face: (Fig. 6) This is a common feature. The encephalocele is interposed between the forehead and the nose, pushing the nasal structure downwards, producing long faces. This was seen in most cases.

3. Hypertelorism: (Fig. 7) This was assessed by measuring the inter pupillary distance. This distance usually varies with age and race. We found that this measurement gives the most reliable reflection of the position of the orbits.

The chart used is that of Feingold and Bossert, Birth Defects, 1974. Significant hypertelorism was present in 16 out of the 32 cases, 50%.

Hypertelorism is corrected at the same time of repair of meningoencephalocele.

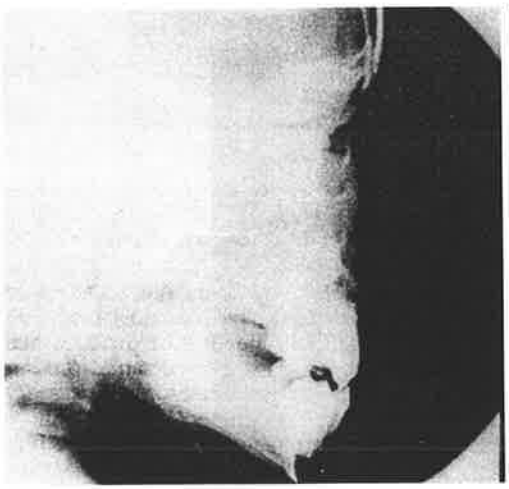

FIG. 6.

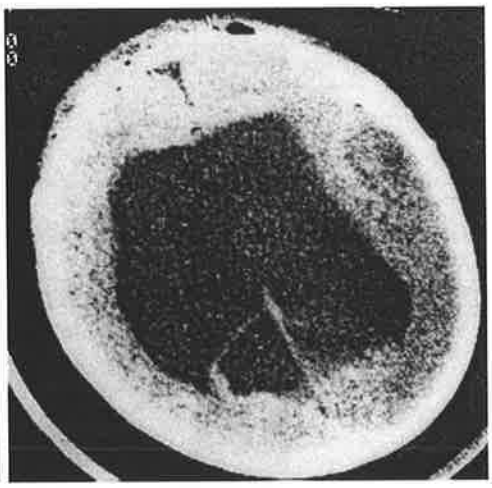

FIG. 8.

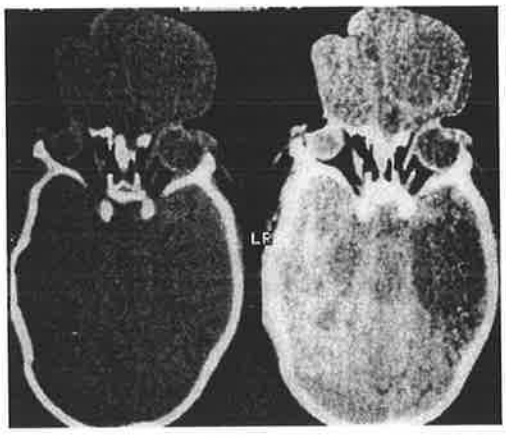

FIG. 7.

FIG. 9.

B. Hydrocephalus (Fig. 8)

Ventricular dilatation was present in five cases. The degree of dilation varies from severe to moderate. The ventricular size did not change after excision of the sac, neither there has been any need for shunting procedure.

C. Agenesis of corpus callosum (Fig. 9)

This is an interesting and unexpected finding.

Agenesis of corpus callosum is often associated with some degree of mental retardation. This was seen in five cases.

D. Holoprosencephaly (Fig. 10)

In this condition one cavity ventricle is seen.

This was seen in one case.

E. Arachnoid cyst

This was seen in one case, it was a temporal arachnoid cyst.

F. Dilated CSF spaces

This was seen in three cases. Two were in the frontal region and one in the parietal region.

G. Poorly developed brain

This was seen in two cases.

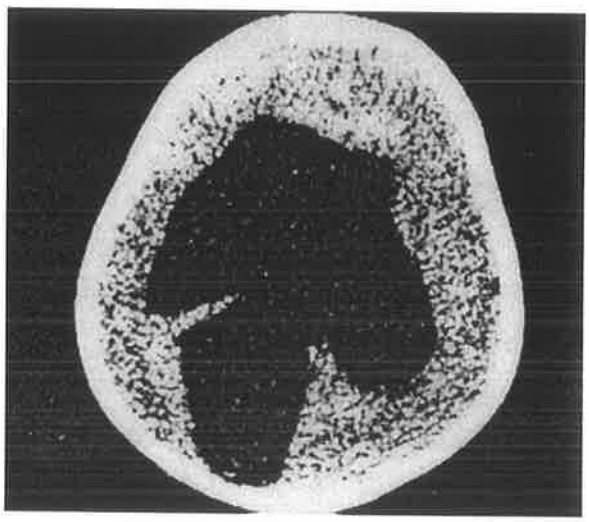

FIG. 10.

Discussion

It is not clear why a part of the central nervous system would be located outside the cranium. The factors needed to produce such an abnormality are raised intracranial pressure and weak point in the cranium. In cases of fronto-ethmoidal encephalocele the point of exit is the foramen caecum, which is the junction between two different parts of the skull; the chrondrocranium and the desmocranium. At six to eight weeks gestation a hydrocephalic stage exists, we can postulate that the protrusion occurs at this stage and it passes through a weak junction point which is the foramen caecum.

Cephaloceles: Classification, Pathology, and Management — A Review

David J. David, AC, FRCS, FRCSE, FRACS
North Adelaide, South Australia

The spectrum of diseases that give rise to cephaloceles is reviewed with particular reference to conditions encountered by Craniofacial teams. The broad term *cephalocele* contains the more focused term *meningoencephalocele,* which is most commonly used by Craniofacial surgeons. The interesting pathology of frontoethmoidal meningoencephaloceles is described with reference to the experience of the Australian Craniofacial Unit from 1975 to 1993. Further observations supporting the uniqueness of this entity are made. Although the meningoencephalocele associated with Craniofacial clefts does not in itself affect treatment, the management of frontoethmoidal meningoencephaloceles is dependent on a knowledge of their unique natural history. Long-term follow-up has allowed a number of conclusions to be reached in the light of treatment. Basal and posttraumatic encephaloceles are described with respect to their place in the classification system as well as the principles of treatment.

Key Words: Cephalocele, classification, cleft, craniofacial

Recent publications in *The journal of Craniofacial Surgery* [1] and also in this issue prompted an article that reviewed aspects of classification, pathology, and management of the interesting conditions that give rise to this pathological entity. This review draws on the experience of the Australian Craniofacial Unit from 1975 to 1993 and is encapsulated in a series of articles [2-10].

Definition and Classification

Definition and classification are intimately bound together, and there has been a lot of confusion about names and disease entities. A *cephalocele* is a congenital herniation of the intracranial contents through a cranial defect [11]. When the herniation contains brain and/or meninges it is called a *meningoencephalocele.* In 1854, Spring [12] wrote an excellent monograph on the subject, which was probably the first major work about this condition. He spent some time attempting to distinguish between a meningocele and a cerebral hernia, the latter being divided into encephalocele and hydranencephalocele when a hydrocephalus was present. The term meningoencephalocele seems appropriate for almost all of the conditions with which craniofacial surgeons are familiar because it describes the contents of the hernia— meninges and brain tissue.

From the Women's and Children's Hospital and the Royal Adelaide Hospital, North Adelaide, South Australia. Address correspondence to Dr David, The Australian Craniofacial Unit, Women's and Children's Hospital, 72 King William Road, North Adelaide, South Australia 5006.

Classification

Meningoencephaloceles may be subdivided into four anatomical groups according to the site of herniation: sincipital, parietal, occipital, and basal (Table). These, as well as meningoencephaloceles associated with craniofacial clefts, comprise the primary conditions. Secondary conditions are those that result from trauma and surgical intervention.

Meningoencephaloceles of primary interest to craniofacial surgeons are the sincipital group, the basal group, those associated with craniofacial clefts and trauma, and those of iatrogenic origin. Sincipital meningoencephaloceles were classified by Suwanwela and Suwanwela [13] based on a paper by van Meyer [14] on frontoethmoidal (nasofrontal, nasoethmoidal, nasoorbital) (Figs 1-3), interfrontal, and craniofacial-associated clefts. With these classifications we must recognize a number of different etiologies. The frontoethmoidal meningoencephalocele, with its three variants, is one disease entity. Those associated with craniofacial clefts are a distinct disease entity. The interfrontal condition, as described by the original authors, is probably closer to an anencephalic condition. Those associated with trauma, surgery, or otherwise have a different natural history altogether.

Meningoencephaloceles

Type of Encephalocele	*Cranial Defect*
Primary	
Occipital	Between lambda and foramen magnum
Parietal	Between bregma and lambda
Sincipital	At junction of frontal and ethmoidal bones
Nasofrontal	
Nasoethmoidal	
Nasoorbital	
Combined	
Craniofacial cleft	
Basal	At junction of sphenoid and ethmoidal bones
Transethmoidal	
Sphenoethmoidal	
Sphenoorbital	
Sphenomaxillary	
Transphenoidal	
Secondary	
Trauma	
Surgery	

The bony defects associated with sincipital meningoencephaloceles have been included in many attempts to classify craniofacial clefts. Two of the most recent and significant endeavours are Tessier's [15] anatomical classification and Mazzola's [16] morphological classification based on embryological considerations. David and co-authors [17] pointed out that there is a fundamental difference between the etiology and pathology of frontoethmoidal meningoencephaloceles and meningoencephaloceles associated with facial clefts. The differences have been well documented by the Australian Craniofacial Unit [2-10]. Continuing studies using three-dimensional imaging have confirmed this difference [18]. Basal encephaloceles have been classified by Gerhardt and colleagues [19], who recognize five types: transethmoidal, sphenoethmoidal, sphenoorbital, sphenomaxillary, and transsphenoidal.

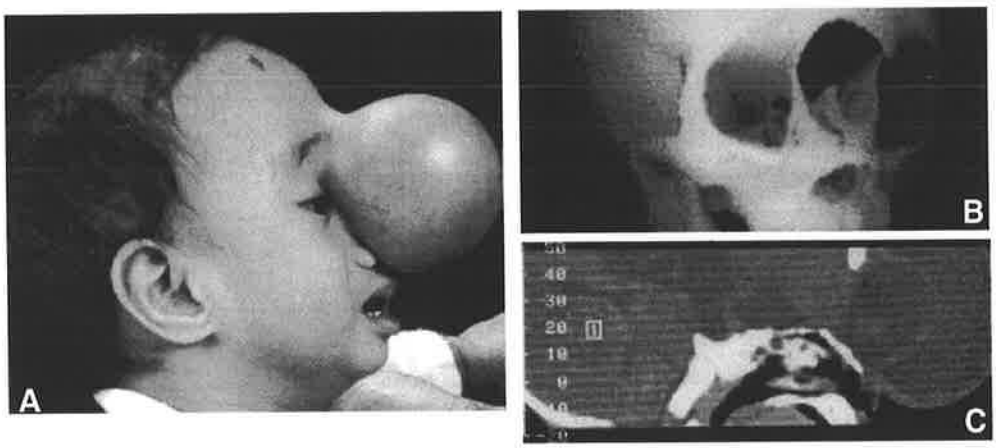

FIG. 1. A. *A large nasofrontal variety of frontoethmoidal meningoencephalocele.* **B.** *A three-dimensional reconstruction of the CT scan shows the facial defect with the nasal bones inferiorly.* **C.** *A sagittal section demonstrates the depressed cribriform plate at the base of the bony defect.*

In summary, cephalocele is the more correct and general term which encompasses the term meningoencephalocele, which in turn reflects the contents of the hernia. Broad classification refers to the sites of the exit holes in the cranial skeleton. The primary congenital conditions have varying etiologies, of which the frontoethmoidal meningoencephalocele is a unique pathological entity. Those conditions associated with craniofacial clefts have a different natural history. Basal meningoencephaloceles are different also.

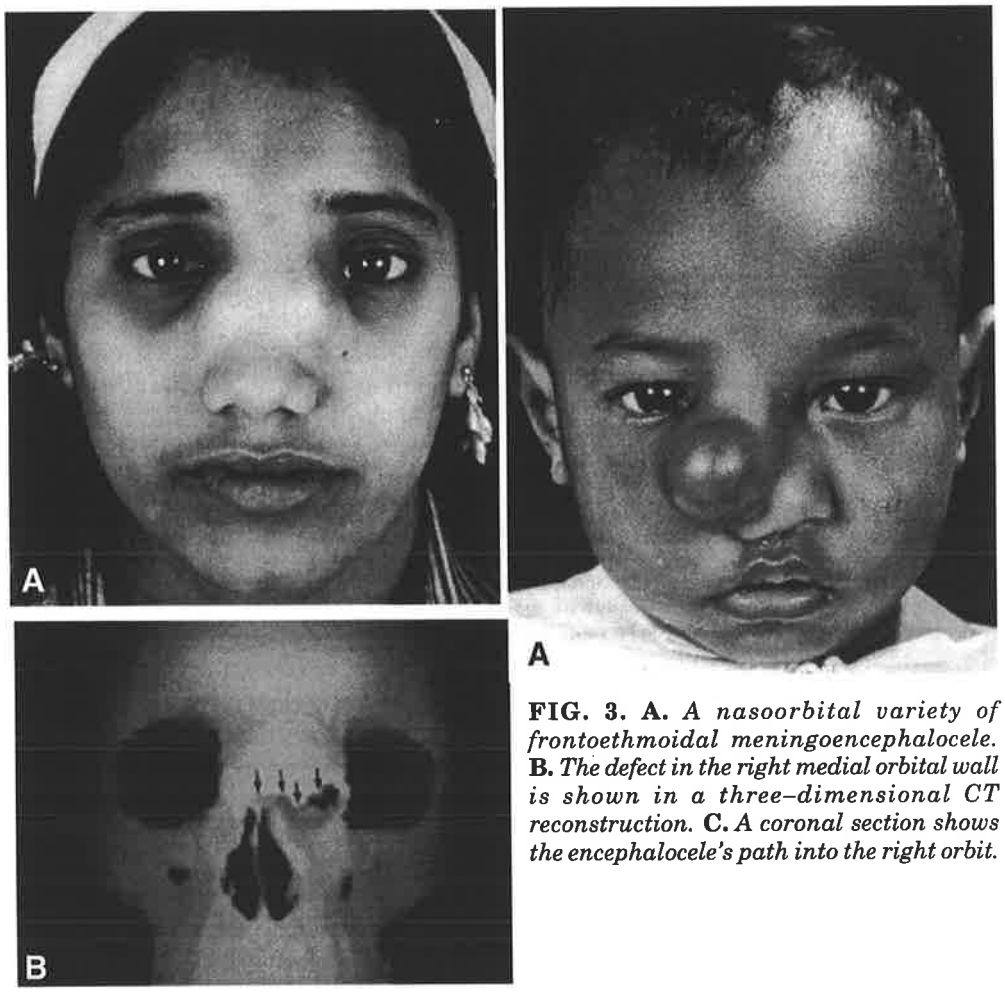

FIG. 2. A. B. *A nasoethmoidal variety of frontoethmoidal meningoencephalocele. The distorted nasal bones can be seen above the defect.*

FIG. 3. A. *A nasoorbital variety of frontoethmoidal meningoencephalocele.* **B.** *The defect in the right medial orbital wall is shown in a three-dimensional CT reconstruction.* **C.** *A coronal section shows the encephalocele's path into the right orbit.*

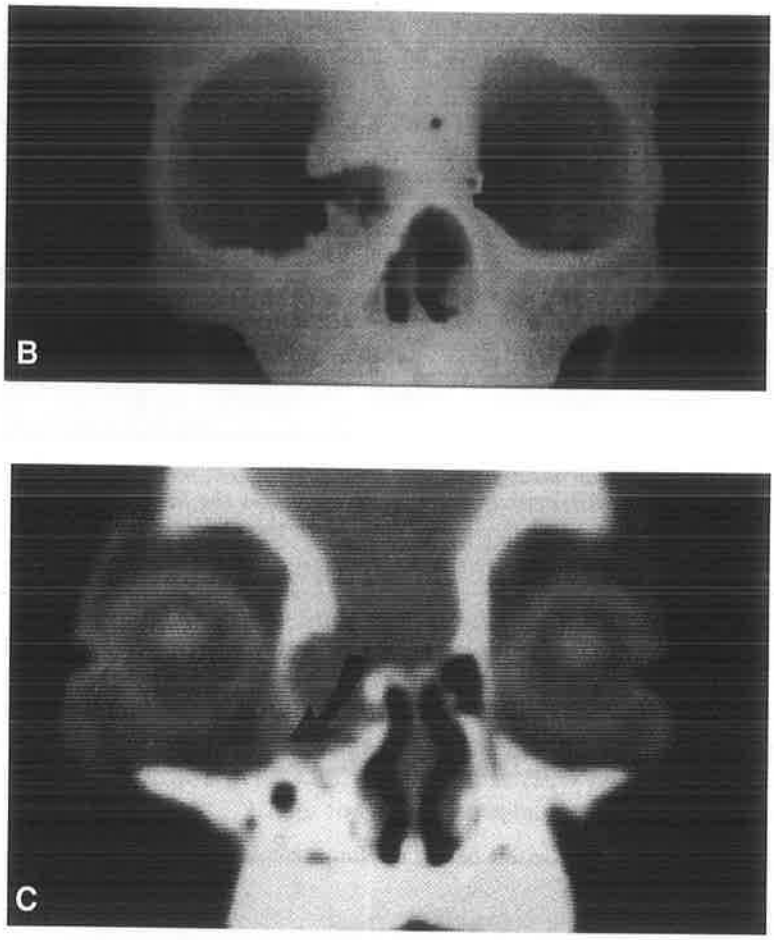

FIG. 3. *(continued)*

Instance and Epidemiology

In Australia, occipital cephaloceles are commonly found in the European population. However, sincipital encephaloceles are infrequently encountered. All of the patients, with the exception of one Australian Aborigine, have been of Southeast Asian origin [4,9]. This type of cephalocele is most prevalent in Malaysia [20], Thailand, Indonesia, Burma [21], and parts of Russia [22], and occurs with much greater frequency than other cephaloceles in these countries. It has been reported to be between 5 and 12 times more common, where often the reverse is true in Europe, the United States, and Australia. Chinese and Indian immigrants to Southeast Asia were not affected with the same frequency despite the fact that they made up large majority groups in those countries. There is no association with patient history, family history, other cephaloceles, or any neural tube defects. This clearly excludes frontoethmoidal meningoencephaloceles as a separate disease entity. Rare craniofacial clefts [8,15,17] can be associated with the meningoencephalocele if the cleft extends into the midline of the frontal bone (Fig 4). The larger no. 10 craniofacial cleft, where the meningoencephalocele is in the frontal bone and extends into the orbital roof and base of the skull and is part of the no. 9 cleft, is described by David and co–authors [23] (Fig 5).

Pathology

Frontoethmoidal Meningoencephaloceles

This term is descriptive of the bony defects of the foramen cecum where the frontal and ethmoid bones meet. The crista galli forms the posterior margin of the defect and the cribriform plate is tilted downward 45° or more by the mass. In transcranial passage of the mass through the skull, the sense of smell is not interrupted. The passage contains the neck of the encephalocele, but distal to the dural defect there is mostly glial tissue with infiltration of fibrous trabeculae. Arachnoid cysts, which may communicate with the ventricular system, have been found on several occasions. Frontoethmoidal masses extending into the orbits often fuse with the periorbital tissue making them difficult to excise. The skin coverage in the cases managed at our Craniofacial Unit has been complete in all cases; however, one can often see where there has been ulceration and healing and, as a result, there may be altered, thickened skin.

Frontoethmoidal meningoencephaloceles can emerge through the facial skeleton in any of three positions: (1) In the nasofrontal type the bony defect is at the junction of the nasal and frontal bones with the nasal bones attached inferiorly. Facial length in this type of deformity may be unaffected. (2) The nasoethmoidal defect is between the nasal bones and nasal cartilages and, consequently, the nasal bones form an overhanging ledge and the vertical plate of the ethmoid is tilted backward. The facial defect may extend into the anterior margins of the medial orbital walls, and in these patients the face is long; there may also be class III malocclusion in older patients, reflecting the effect of the retrodisplaced nasal septum on midfacial growth. (3) The nasoorbital bony defect is in the medial orbital wall and between the frontal process of the maxilla and the lacrimal bones. The lateral plate of the ethmoid is pushed laterally and a bony tunnel is formed.

FIG. 4. A. *A meningoencephalocele associated with a severe midline craniofacial cleft.* **B.** *The bony defect is seen in a three-dimensional CT reconstruction.*

The bony defects clearly reflect the size and distribution of the dysplastic tissue as it pours from its tunnel and onto the face. Orbits may be expanded, faces may be long, or there may be horizontal or vertical orbital dystopia. Telecanthus is characteristic of patients with this diagnosis. Most of these patients were found to have a medial intercanthal distance far greater than the 97th percentile, while the rest of the patients had borderline high to normal distances approximately equal to the 97th percentile. Interpupillary distances and lateral canthal distances, however, usually approached normal. Lacrimal drainage

dysfunction is the most common ocular problem. The lacrimal sac and drainage system are elongated, distorted, and often non–functioning.

Although the intracranial contents may be normal, they can be disorganised to some extent. Hanieh and David [10] have described the percentage of intracranial anomalies; however, this percentage is actually much higher because preselection for surgery was the basis for examining these patients and only those patients at initial examination thought suitable for surgical intervention were included.

Basal Meningoencephaloceles

In my experience I have encountered transethmoidal and sphenoethmoidal bone defects, through which meningoencephaloceles have presented in the nasopharynx and one of which was associated with clefting. The bony canal extended through the base of the skull in the cribriform plate area into the nasal cavity. The transethmoidal defects did not distort the face and were associated with a well-defined cranial base defect. One patient presented with meningitis. The sphenoethmoidal defect consisted of the contents of the third ventricle and of the adjacent brain structures. It was a much larger defect and appeared to be part of the wider clefting syndrome (Fig 6).

FIG. 5. *A no. 9 craniofacial cleft with defects in the temporoparietal regions on both sides.*

Meningoencephaloceles Associated with Craniofacial Clefts

These defects are most common with midline craniofacial clefts where the meningoencephalocele goes through the frontal bone, or almost invariably with the no. 10 cleft (Fig 7) where it goes through the frontal bone and the roof of the orbit. The former is associated with hypertelorism and the latter with generally severe orbital dystopia. I have seen it also in the no. 9 cleft [23] with severe disruption of the lateral orbit and temporal bone. In these cases it is the cleft that is the primary pathology; the meningoencephalocele is merely a secondary deformity and management of the case is the same as for that of the clefting syndrome. I do not believe that removing the encephalocele or blocking the exit

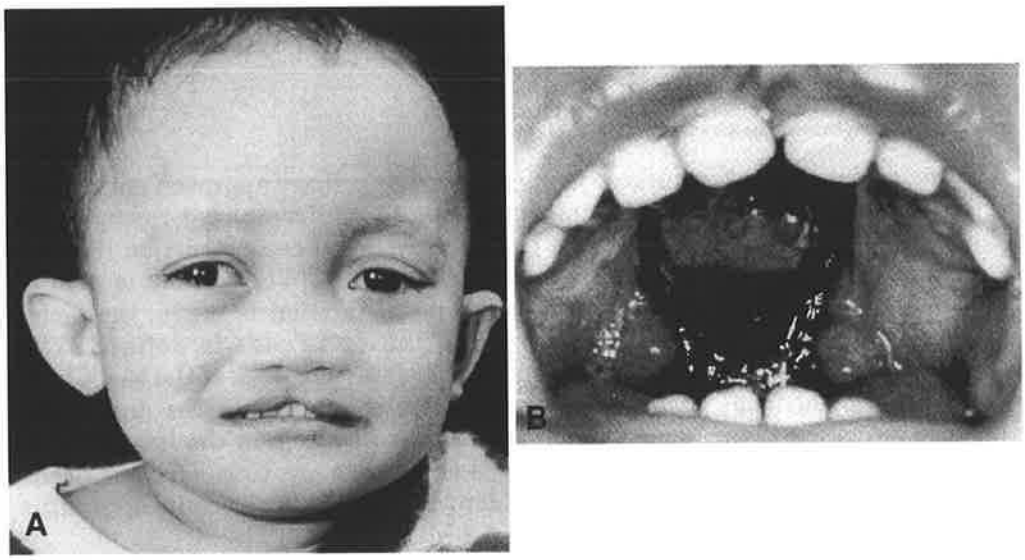

FIG. 6. A. B. *A large meningoencephalocele presenting through a sphenoethmoidal defect.*

hole would in any way solve the problem of the clefting syndrome, which continues to manifest itself throughout growth. The bony components need to be treated by the appropriate osteotomies, which can be carried out in cases of hypertelorism and orbital dystopia after 5 years of age, when most orbital growth is complete and the teeth have cleared the upper maxilla.

Meningoencephaloceles Secondary to Trauma or Surgery

Under these circumstances (Fig 8) the lesion is invariably associated with damage to the dura and will not spontaneously heal until the dura has been adequately repaired and the bone defect grafted.

FIG. 7. *Meningoencephalocele associated with a no. 10 craniofacial cleft.*

FIG. 8. *Meningoencephalocele associated with Apert's syndrome (postsurgery) where the dura has been damaged above the right orbit.*

Treatment Strategies In Light Of The Pathology

Frontoethmoidal Meningoencephaloceles

The treatment plan is formulated using a multidisciplinary approach and after a detailed study of the clinical data supplemented by computed tomography scanning with two–dimensional and three-dimensional reconstruction [6]. The transcranial access via the bicoronal approach is used. Where there is a large soft-tissue mass on the face, an additional nasal incision is made, the facial component is isolated, and the margin of the exit holes is defined. The neurosurgeon performs a frontal craniotomy; isolates the neck of the sac, which is then removed from above and below; grafts the defect in the dura after transection of the encephalocele; and then closes any hole in the bony cranial base either by the appropriate osteotomies or by bone grafting. The soft tissue mass is dissected carefully since it often blends with the nasolacrimal apparatus and the periorbitum.

Where there is genuine hypertelorism affecting both orbits, the orbits are translocated medially to move the globes of the eyes—although this is rare. Most frequently the surgical intervention consists of reconstruction of the medial orbital walls, possibly some bone grafting of the lateral orbital wall to move the globe a little medially, and nasal bone grafting and bone grafting of the orbital floor. All of this bone graft can be obtained from the calvarium, or the rib as a second choice. In the nasoorbital defect often there is an expanded orbit, which can be contracted both by osteotomies and bone grafting.

It is my belief that the cause of the deformity is directly related to the quality and quantity of the extruded brain tissue. If this is removed in the first few months of life with minimal surgery, then the functional matrix will restore the bony architecture as growth proceeds. In the more established cases, definitive surgery needs to be performed. I have found it quite possible to perform a Le Fort I osteotomy to shorten the face in patients with a nasoethmoidal defect, where there may be a long face combined sometimes with a class III malocclusion, others have designed more elaborate operations [24]. I recognize that there may be as many operative designs as there are deformities and that in the past operations were performed in two stages. Although this may be the only possible way in some treatment centers, I believe the combined craniofacial approach is the most desirable because it allows complete correction of the deformity with good visualisation in one stage.

Meningoencephaloceles Associated with Craniofacial Clefts

It is my belief that the clefting deformity continues to manifest itself throughout growth. The prominent meningoencephaloceles that may occur with the lateral craniofacial clefts—nos. 9 and 10—may need to be repaired in infancy as a matter of urgency [23]. Definitive surgery on the eye sockets, however, needs to be delayed until most of the growth is complete after 5 years of age and the presence of a meningoencephalocele does not play a major role in altering the strategies for correction of hypertelorism or orbital dystopia. If the dura is absent, however, extensive repair and grafting may be necessary, and it is my experience that this is more safe if done as a separate procedure from the definitive orbital surgery.

Basal Meningoencephaloceles

Where the lesion presents in the mouth and adequate access can be gained through the mouth, a combined approach is made by the transoral route and the bicoronal scalp flap and frontal craniotomy. Dissection of the anterior cranial fossa exposes the exit hole of the meningoencephalocele, and very delicate dissection of the sac from below after elevating the pharyngeal mucosa enables it to be delivered into the anterior fossa intact. The neck can then be ligated, the dural defect repaired,

and the bony defect closed with some calvarial bone, usually with adequate covering of the mucosa. In more extensive tumors and defects I have used the facial bi–partition technique essentially a subcranial Le Fort III osteotomy divided by hinging the maxillary segments laterally to give wide access to the clivus while the frontal craniotomy exposes the anterior fossa (Fig 9). This pathology is repaired as soon as the patient has been worked up, usually because of the risk of damage to the extruded contents and possible infection.

Traumatic and Iatrogenic Meningoencephaloceles

These cephaloceles are treated on an individual basis, and the treatment strategy is to repair the underlying dura effectively and to apply a bone graft to the defect.

Discussion

The major discussion on management in this paper has been that of the frontoethmoidal meningoencephalocele because the meningoencephaloceles associated with clefts or secondary to other surgery do not have the associated problems that complicate the otherwise–documented management of craniofacial deformities. It is the thesis emanating from the Australian Craniofacial Unit that frontoethmoidal meningoencephaloceles are fundamentally different in origin from midline clefts. These sincipital lesions are blowouts of the intracranial contents through a midline tunnel and the anterior cranial fossae of the facial skeleton. The resulting space-occupying lesions distort the craniofacial skeleton in a unique way in each case. So I can logically suggest that while there are some treatment principles and strategies, operations should be designed on an individual basis. Upon reviewing my work I have formed the following conclusions:

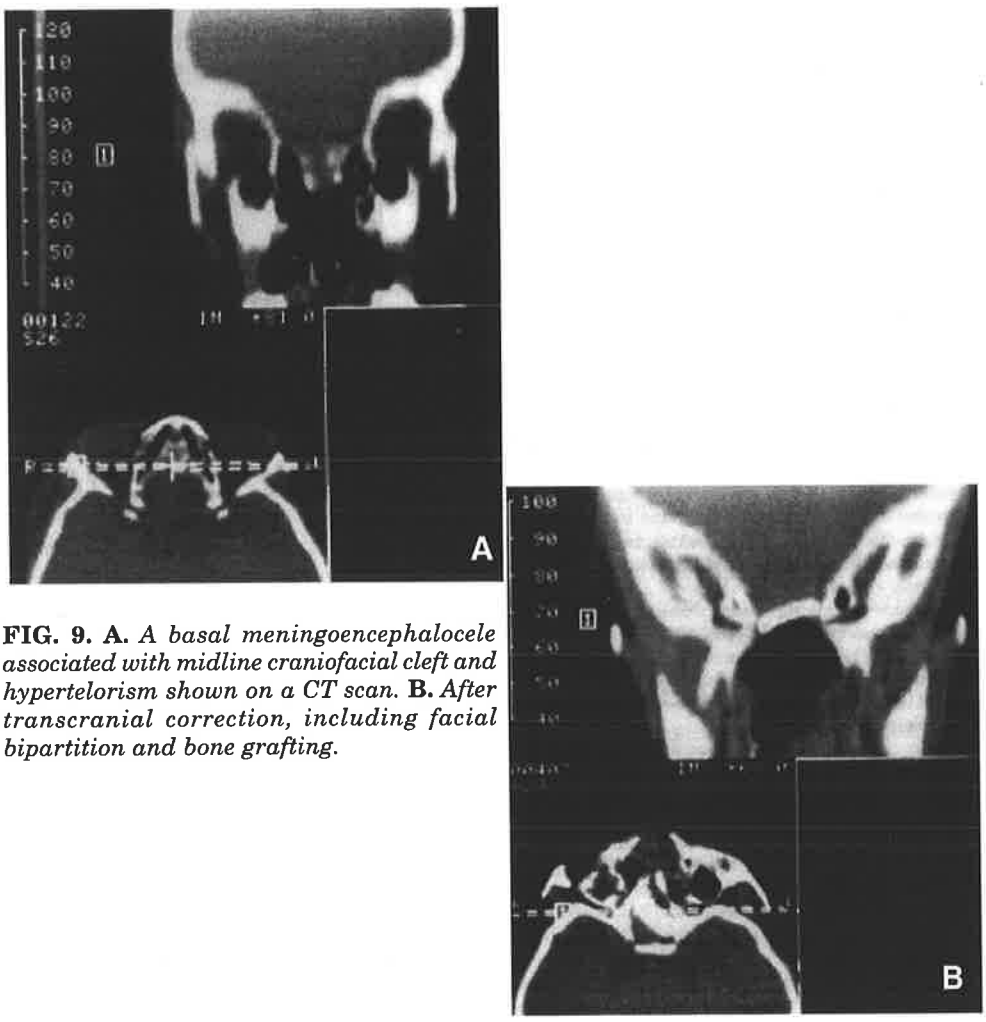

FIG. 9. A. *A basal meningoencephalocele associated with midline craniofacial cleft and hypertelorism shown on a CT scan.* **B.** *After transcranial correction, including facial bipartition and bone grafting.*

FIG. 10. A. *A large frontoethmoidal meningoencephalocele in an infant.* **B.** *Three years postoperatively.* **C.** *Six years postoperatively, indicating restoration of facial contour with growth.*

1. In frontoethmoidal meningoencephaloceles complete surgery early on should allow the developing brain and eyes to mold the orbital skeleton and the forces generated by the nasal airway, speech, and mastication to remodel the facial deformity. Follow-up of some cases for over a decade has tended to confirm this view (Fig 10).

2. Frontoethmoidal meningoencephaloceles are associated with a high percentage of intracranial abnormalities.

3. Frontoethmoidal meningoencephaloceles differ from other neural tube defects such as anencephaly and myelomeningocele. The evidence for this is their lack of affected siblings and the extraordinary geographical peculiarities.

4. Meningoencephaloceles are best treated by the craniofacial approach, although other approaches can be used. This methodology is considered superior because it allows a wide exposure and complete treatment in one stage.

5. The established craniofacial deformity in frontoethmoidal meningoencephaloceles in the mature individual can be effectively treated with craniofacial osteotomies, including maxillary advancement and shortening.

6. In the majority of cases of frontoethmoidal meningoencephalocele the interpupillary and lateral canthal distances are within normal limits. The abnormal measurement is the intercanthal distance.

7. Long-term follow-up after surgery has shown that the region of the frontal sinus is often deficient and flat and needs further bone grafting. Nasal bone grafts frequently need to be replaced. Initial watering of the eyes due to incompetence of the nasolacrimal apparatus usually disappears but may not show up for 3 or 4 years (Fig 11).

8. Craniofacial clefts have a deficiency of tissue at the margins of the cleft; this abnormality is intrinsic to the tissues themselves and early surgery of these clefts would not be expected to help the skeletal deformity. Treatment of these clefts can only be complete after growth is complete.

9. Basal encephaloceles have been associated with craniofacial clefts or as isolated entities. They need to be treated early to prevent damage and infection.

10. In severe cases of basal encephalocele the surgery is taxing and the craniofacial approach is helped by facial bipartition.

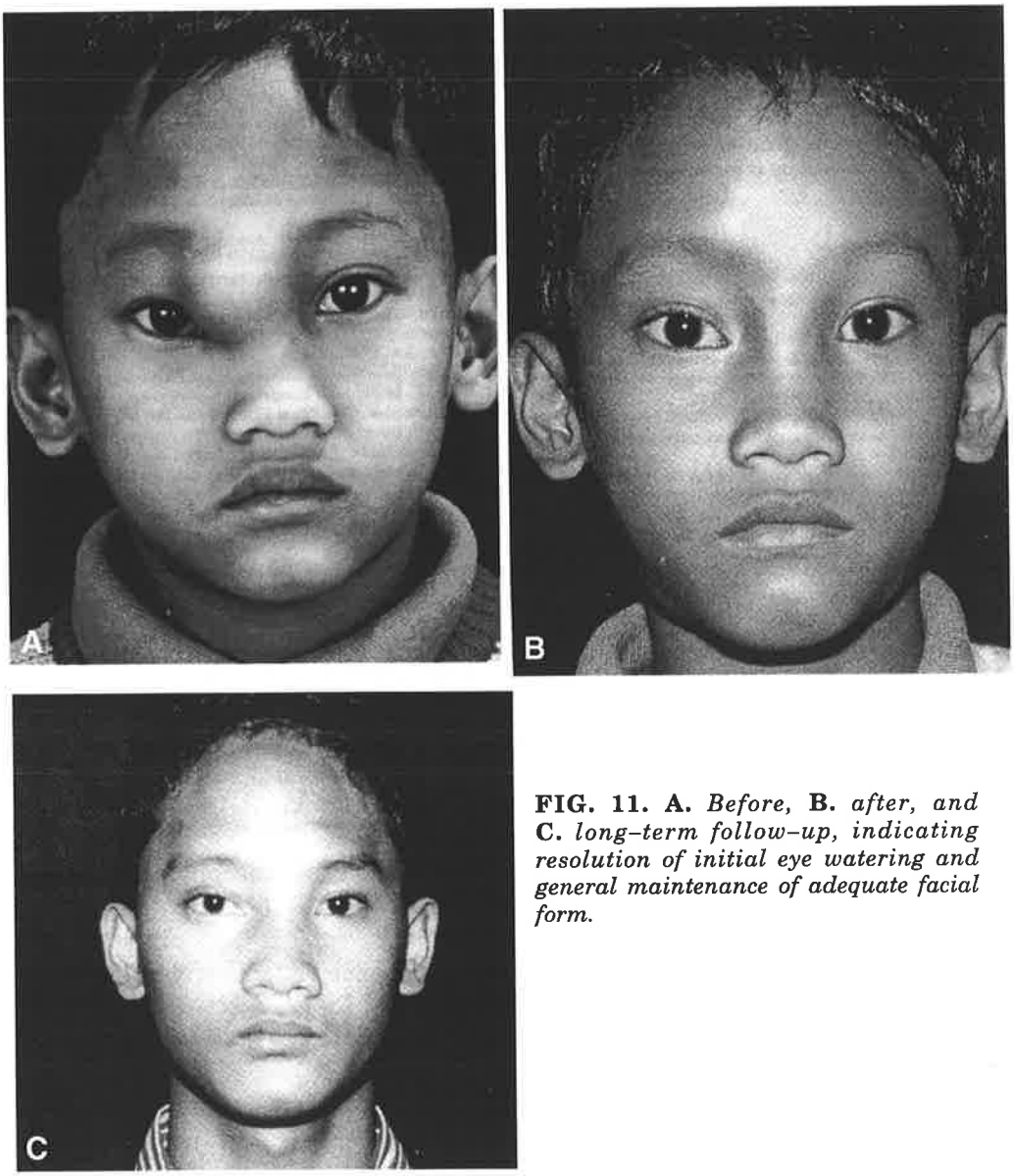

FIG. 11. A. *Before,* **B.** *after, and* **C.** *long–term follow–up, indicating resolution of initial eye watering and general maintenance of adequate facial form.*

Conclusion

Treatment must be based on a knowledge of the natural history of the disease, ideally managed by a multidisciplinary team approach, and operated on using craniofacial techniques. The design of each operation should fit the specific deformities presenting in each case. Long-term follow–up is essential.

References

1. Clauser L, Baciliero H, Nordera P, et al. Frontoethmoidal meningoencephalocele: a one–stage correction, reconstruction and plating by means of the microsystem. J Craniofac Surg 1991;2: 2–8

2. David DJ, Simpson DA, White J. Frontonasal encephaloceles: morphology and treatment. Proceedings of the 8th International Congress of Plastic and Reconstructive Surgery, Montreal, June–July 1983: 311–313

3. David DJ, Sheffield L, Simpson DA, White J. Frontoethmoidal meningoencephaloceles: morphology and treatment. Br J Plast Surg 1984;37: 271–284

4. Simpson DA, David DJ, White J. Cephaloceles: treatment, outcome and antenatal diagnosis. Neurosurgery 1984;15: 14–21

5. David DJ. New perspectives in the management of severe craniofacial deformities. Ann R Coll Surg Engl 1984;66: 270–279

6. Hemmy DC, David DJ. Skeletal morphology of anterior encephaloceles defined through the use of three–dimensional reconstruction of computed tomography. Pediatr Neurosci 1985;12: 18–22

7. David DJ, Simpson DA. Frontoethmoidal meningoencephaloceles. Clin Plast Surg 1987;14: 83–9

8. David DJ, Simpson DA, Cooter RD. Meningoencephaloceles: classification, pathology and management. In: Habal M, ed, Advances in plastic and reconstructive surgery. Mosby–Year Book, 1989;5: 85–108

9. David DJ, Proudman TW. Cephaloceles: classification, pathology and management. World J Surg 1989;13: 349–357

10. Hanieh A, David DJ. Frontoethmoidal meningoencephalocele: classification and associated features. In: Montoya AG, ed, Proceedings of the 4th International Congress of the International Society of Cranio–Maxillo–Facial Surgery, Santiago de Compostela, Spain, 1991: 127–130

11. McLaurin RL. Cranium bifidum and cranial cephaloceles. In: Vinken PJ, Bruyn GW, eds, Handbook of clinical neurology: congenital malformations of the brain and skull, part 1. Amsterdam: North–Holland Publishing, 1977;30: 209–218

12. Spring A. Monographie de la hernie du cerveau et des quelques lesions voisines. Memoires de L'Academie Royale de Medecine de Belgique, 1854

13. Suwanwela C, Suwanwela N. A morphological classification of sincipital encephaloceles. J Neurosurg 1972;36: 201–211

14. von Meyer E. Uber Eine Basale Hirnhernie in der Gegend der Lamina Cibrosa. Virchows Arch [A] 1890;120: 309–320

15. Tessier P. Anatomical classification of facial, craniofacial and latero-facial clefts. J Maxillofac Surg 1976;4: 69–92

16. Mazzola RA. Congenital malformations in the frontonasal area: their pathogenesis and classification. Clin Plast Surg 1976;3: 573–608

17. David DJ, Moore MH, Cooter RD. Tessier clefts revisited with a third dimension. Cleft Palate J 1989;26: 163–184

18. Lodge ML, David DJ, Moore MH, et al. Three–dimensional analysis of frontoethmoidal meningoencephaloceles and Tessier clefts with orbital hypertelorism: comparison and contrast. M.S. Thesis, Univ of Adelaide, 1993.

19. Gerhardt HJ, Muhler G, Szdzuy D, Biedermann F. Zur Therapie problematik bei Sphenoethmoidalen Meningozelen. Zbl Neurochir 1979;40: 85–94

20. Suwanwela C. Geographical distribution of frontoethmoidal encephalomeningocele. Br J Prev Soc Med 1972;26: 193–198

21. Thu H, Kyu H. Epidemiology of frontoethmoidal encephalomeningocele in Burma. J Epidemiol Community Health 1984;38: 89

22. Barrow N, Simpson DA. Cranium bifidum: investigation, prognosis and management. Aust Paediatr J 1966;2: 20–26

23. David DJ, Moore MH, Cooter RD. The Tessier number 9 cleft. Plast Reconstr Surg 1989;83: 520–525

24. Jackson IT, Tanner NS, Hyde TA. Frontonasal encephalocele — "long nose hypertelorism." Ann Plast Surg 1983;11: 490–500

Frontoethmoidal Meningoencephalocele

David J. David, Richard H. C. Harries

A *cephalocele* is a congenital herniation of intracranial contents through a cranial defect. When the herniation contains brain and meninges, it is termed a *meningoencephalocele.* Spring in 1854 wrote what was probably the first extensive monograph on the subject. He stated that Le Dran introduced the term *hernia cerebri* in 1740; however, Le Dran's patient probably had a cephalhematoma. Spring himself tried to distinguish between meningocele and cerebral hernia, the latter being divided into encephalocele and hydroencephalocele when hydrocephalus was present. The term *meningoencephalocele* seems appropriate because it describes the contents of the hernia. This chapter discusses frontoethmoidal meningoencephaloceles, which, by definition, present on the front of the skull and are seen externally. Modern methods and investigation offered by a multidisciplinary craniofacial unit enable these lesions to be studied more thoroughly and treated more effectively than in the past.

Etiology

In western Europe, North America, Japan, and Australia, these lesions are relatively rare; occipital cephaloceles are much more prevalent. In Southeast Asia frontoethmoidal meningoencephaloceles are by far the most common type of cephalocele, and this appears to be the case in parts of the Indian subcontinent and in southern Russia. For frontoethmoidal meningoencephaloceles, siblings and offspring do not show any increased incidence of anencephaly or myelodysplasia, and even in high-risk areas it is unusual to find more than one frontoethmoidal meningoencephalocele in the same family. Parents can be reassured accordingly. Recent work by the Australian Cranio-Facial Unit with Southeast Asian patients revealed that frontoethmoidal meningoencephalocele may have a genetic basis. It was found that advanced parental age was frequent in instances of this defect, suggesting that an autosomal dominant mutation may be involved, and this, if confirmed, would have important implications in genetic counseling. However, the lack of familial instances and geographic distribution of meningoencephalocele argues strongly against dominant mutation as a cause.

Classification

Meningoencephaloceles may be subdivided into occipital, parietal, basal, and sincipital types. The last group was further classified by Suwanwela and Suwanwela in 1972, based on a paper by Meyer published in 1890, into the following categories:

- Frontoethmoidal
  - Nasofrontal
  - Nasoethmoidal
  - Naso–orbital
- Interfrontal
- Craniofacial clefts

The bony defects associated with sincipital meningoencephaloceles have been included in many attempts to classify craniofacial clefts. Two of the most recent and important endeavors are Tessier's anatomic classification and Mazzola's morphologic classification based on embryologic considerations. However, it is important to note that there is a fundamental difference between the etiology and pathology of frontoethmoidal meningoencephaloceles and of meningoencephaloceles associated with facial clefts.

Pathology

To appropriately treat patients with frontoethmoidal meningoencephalocele, it is vital that the underlying pathology be clearly understood.

The term *frontoethmoidal meningoencephalocele* describes the site of the cranial end of the bony defect, which is always in the position of the foramen cecum at the junction of the frontal and ethmoidal bones. The posterior margin of the defect is formed by the crista galli. This margin is often distorted, and the cribriform plate is usually tilted downward as a deep central trough, the anterior end of which is well below the planum sphenoidale. The cribriform plate forms an angle of 45° to 50° with the orbitomeatal plane.

The cranial exit holes vary in size and shape. All nasofrontal defects appear round and central, whereas nave–orbital defects are usually bilobed. Nasoethmoidal meningoencephaloceles are particularly variable in the shape of the bony defect. The morphology of the defects of the facial bone shows even more variation.

In the nasofrontal type, the exit holes are at the junction of the frontal and nasal bones, the nasal bones being attached to the inferior margin of the defect (Fig. 37-1). In the nasoethmoidal type, the facial defects lie between the nasal bones and the nasal cartilage, the nasal bones being above and the nasal cartilages below. The nasal bones are deformed and often broadened with distorted margins. The nasal septal cartilage is pushed downward and backward. The frontonasal angle is obliterated, producing an overhanging ledge (Fig. 37-2). When the facial defect is confined to the nasal pyramid, the exit hole is small and oval and the medial walls of the orbit are not involved. If, however, the meningoencephalocele is larger, the facial defect extends more laterally and the anterior margins of the medial orbital walls are eroded and become crescent shaped. It is as though the meningoencephalocele had blown out onto the face through the weakened junction of the frontal and ethmoidal bones, displacing the otherwise normal orbits and nasal capsule, widening the orbits, and lengthening the face. In contrast, midfacial clefts appear to have a deficiency of tissue at their margins.

Naso–orbital meningoencephaloceles present onto the face through exit holes in the medial orbital wall, in the frontal process of the maxilla and lacrimal bones (Fig. 37–3). The bony tract is usually long and shaped like an inverted Y. The inverted Y is sometimes asymmetric. These meningoencephaloceles come through the frontal process of the maxilla onto the face, leaving the nasal bones intact anteriorly and the lacrimal bones and the lateral plate of the ethmoid bone intact posteriorly. A bony tunnel is thus formed through the substance of the ethmoid bone. The developing orbits may be grossly expanded by the meningoencephaloceles (Fig. 37–4).

Viable neural tissue is often seen at the neck of the meningoencephalocele, but tissue distal to the exit hole consists mostly of glial tissue infiltrated with fibrous trabeculae (Fig. 37–5). When the soft tissue mass of the meningoencephalocele extends into the orbits, it often fuses with periosteum, making excision of the orbital component of the mass extremely difficult.

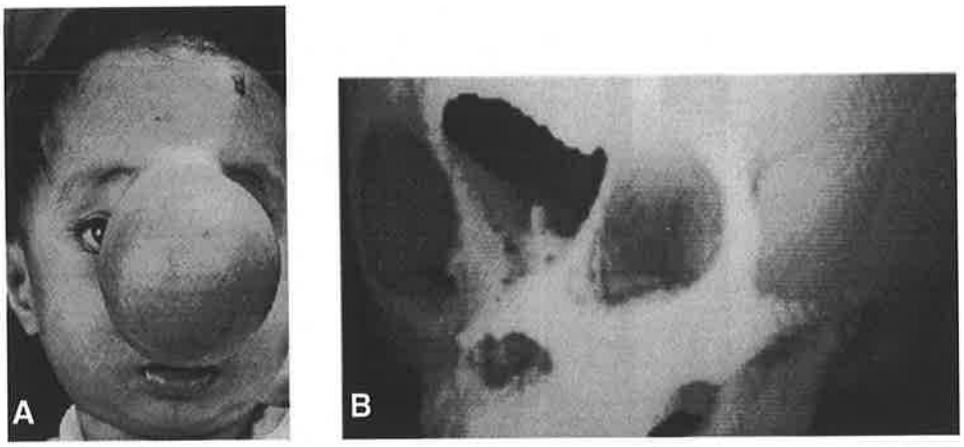

FIG. 37-1 A. *A large nasofrontal type of frontoethmoidal meningoencephalocele.* **B.** *Three-dimensional computed tomogram demonstrates the downward tilted cribriform plate with the crista galli forming the posterior margin of the cranial defect and the nasal bone forming the inferior margin of the facial defect. (From D. David et al. Meningoencephaloceles: Classification, pathology, and management. Adv. Plast. Reconstr. Surg. 5:85, 1989. Reproduced with permission.)*

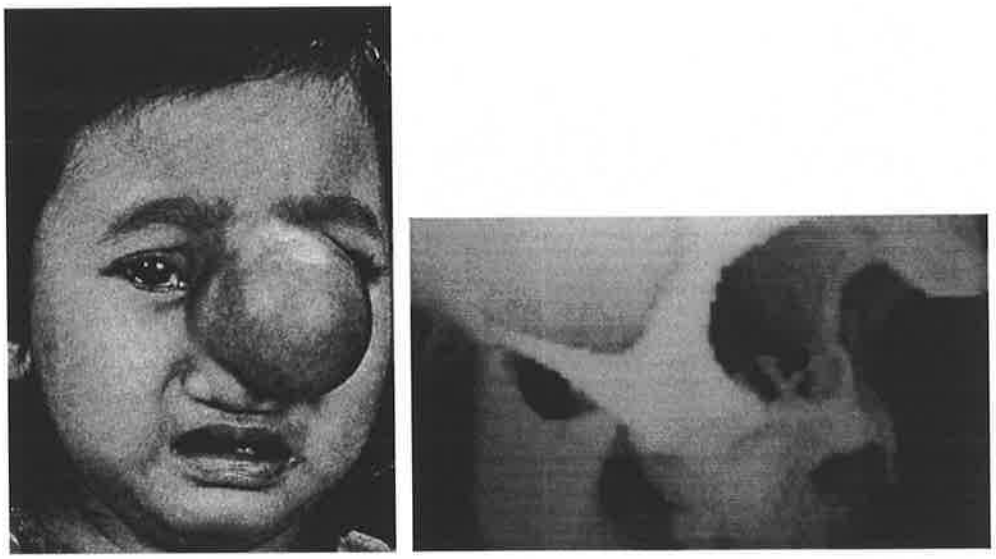

FIG. 37-2. *A nasoethmoidal frontoethmoidal meningoencephalocele. Note the deformed nasal structures secondary to the facial exit holes, The frontonasal angle is obliterated.*

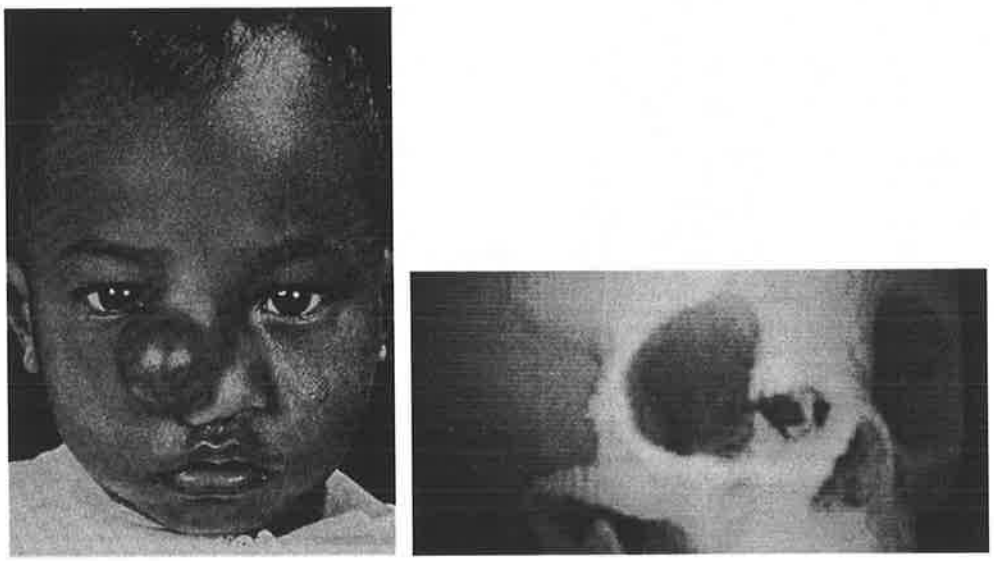

FIG. 37-3. *A naso–orbital frontoethmoidal encephalocele. A bony tunnel through the ethmoid bone exits onto the face through the frontal process of the maxilla, leaving the nasal bones intact anteriorly. (From D. David et al.: Classification, pathology, and management. Adv. Plast. Reconstr. Surg. 5:85, 1989, Reproduced with permission.)*

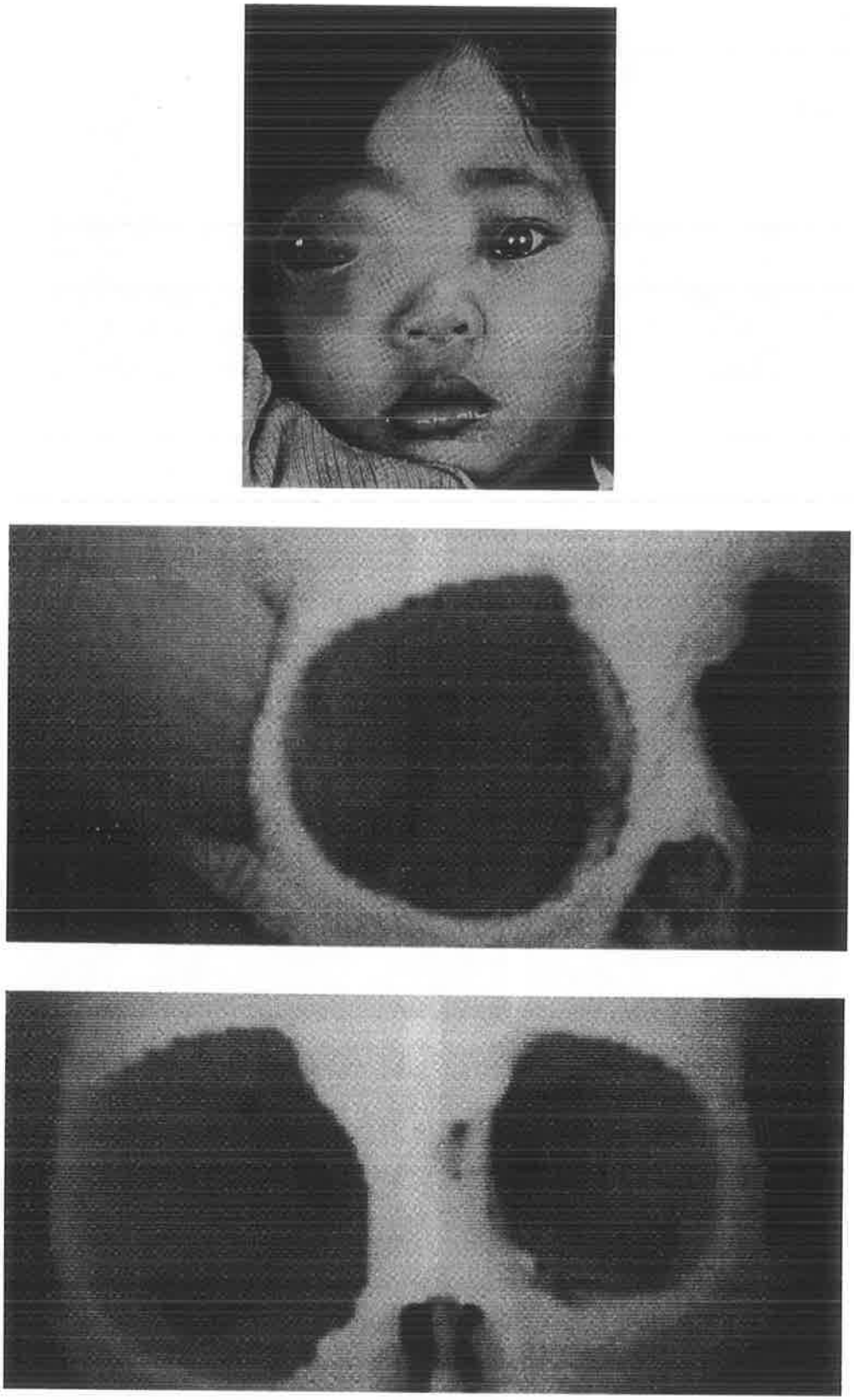

FIG. 37-4. *A naso–orbital frontoethmoidal encephalocele. The massive orbital expansion is well demonstrated. (From D. David, et al. Frontal Meningoencephaloceles. Clin. Plast. Surg. 14:83, 1987, Reproduced with permission.)*

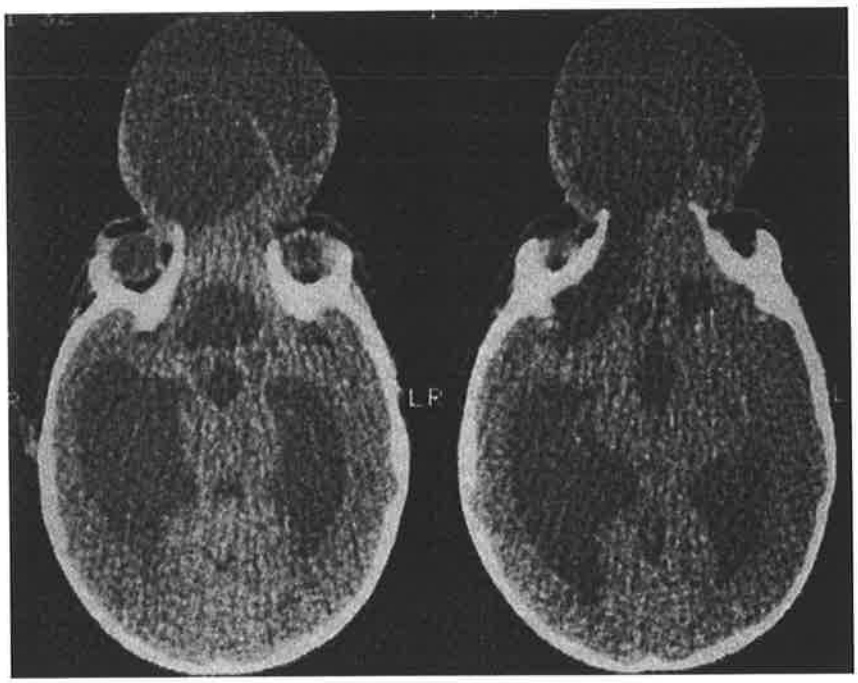

FIG. 37-5. *Viable neural tissue is often seen at the neck of the meningoencephalocele, but tissue distal to that is largely glial tissue with fibrous trabeculae.*

FIG. 37-6. *A typical long face of an adult patient with a frontoethmoidal meningoencephalocele. (From D. David, et al. Frontoethmoidal meningoencephaloceles: Morphology and treatment. Br. J. Plast. Surg. 37:271,1984. Reproduced with permission.)*

FIG. 37-7. *The skin overlying a frontoethmoidal meningoencephalocele, if involved, is full-thickness but dysplastic. (From D. David, et al. Meningoencephaloceles: Classification, pathology, and management. Adv. Plast. Reconstr. Surg. 5:85, 1989. Reproduced with permission.)*

Clinical Features

Frontoethmoidal meningoencephaloceles are usually grotesque deformities associated with gross facial disfigurement. The face appears to be longer than normal (Fig. 37–6), although this is hard to measure with ordinary cephalometric techniques, because some of the bony landmarks, particularly in the glabellar region, are obliterated. The pyriform aperture and nasal cartilages are misshapen, the aperture being shorter and broader than usual and displaced inferiorly. The Australian Cranio-Facial Unit has not seen a bifid nose or a midline nasal cleft in any of its patients. Telecanthus is an invariable feature; medial canthal dystopia is less common. Hypertelorism is a frequent finding (see Fig. 37–16A), but it is less severe than that seen with midline facial clefts. Some patients have dental malocclusion, which may be related to the attachment of the vertical plate of the ethmoid bone to the titled cribriform plate. The cribriform plate is retrodisplaced, presumably inducing secondary maxillary hypoplasia. Whenever it is involved, the nasal skeleton is distorted; the over lying skin is of full thickness but often discolored or ulcerated (Fig. 37–7).

Ocular problems are not uncommon. Micro–ophthalmia can occur, resulting from massive extrusion of the hernia into the orbit. Decreased visual activity is common if the globe is displaced, causing traumatic corneal ulceration. The most common ophthalmologic finding is lacrimal drainage dysfunction (see Fig. 37–16A). The function of the elongated and often tortuous drainage system is rarely corrected after the operation. Orbital expansion or dystopia (see Fig. 37–4) is present in all patients with naso-orbital meningoencephaloceles. Developmental retardation, hydrocephalus, and epilepsy are less frequently seen, and, perhaps surprisingly, anosmia is unusual.

Diagnostic Testing

Patients with frontoethmoidal meningoencephaloceles are best investigated using the team approach so successfully adopted by craniofacial units. The plastic surgeon, neurosurgeon, otorhinolaryngologic surgeon, ophthalmologist, radiologist, dentist, psychologist, and social worker are all involved before the operation. A full neurologic examination is of utmost importance. Delineating developmental and intellectual parameters as well as visual acuity and sense of smell is an important facet of the preoperative evaluation. Radiographic assessment of both the skeletal lesions and the cerebral anatomy using plain roentgenograms and computed tomography (CT), including three-dimensional CT is vital when investigating these patients. Antenatal diagnosis by B-mode ultrasonography is now possible. Alpha-fetoprotein assay is not useful because the meningoencephalocele is fully epithelized with normal or dysplastic skin.

Operative Treatment

Operative treatment has three main aims: (1) to conserve cerebral function, (2) to prevent infection, and (3) to make facial appearance acceptable. The first aim is less easily achieved than one would wish because the herniated cerebral tissue within the cephalocele is usually too adherent to be extricated, and distal to the dural constriction it is likely to be gliotic and dysplastic. The second aim, prevention of cerebral infection by occluding the congenital craniofacial fistula, is relatively easy. The third aim can be difficult to realize, especially when there is marked teleorbitism and orbitofacial deformity.

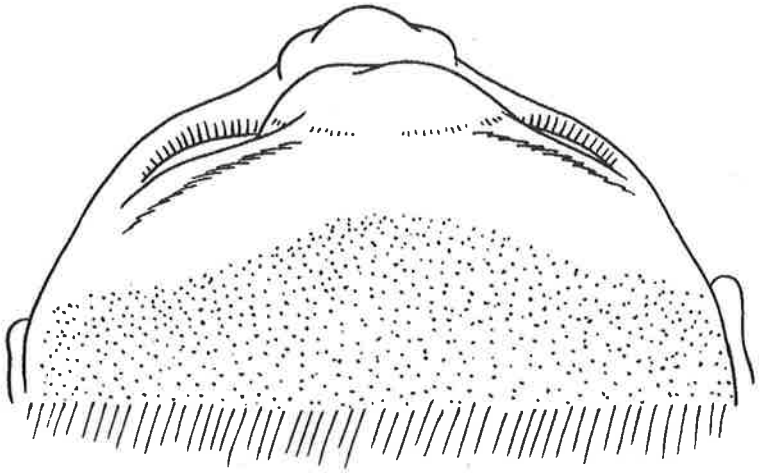

FIG. 37-8. *The operation begins with shaving of the patient's scalp in preparation for raising the bicoronal scalp flap. Patient has already undergone orotracheal intubation and insertion of central and arterial lines.*

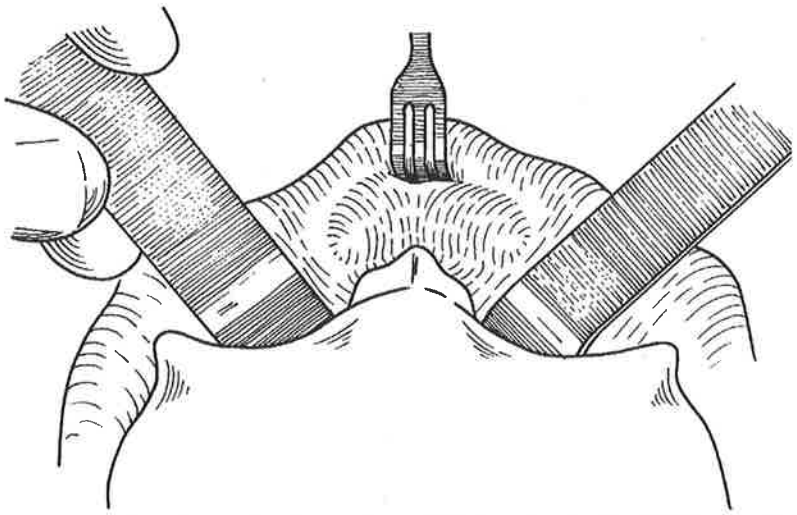

FIG. 37-9. *Subperiosteal dissection reveals the neck of the frontoethmoidal meningoencephalocele emerging from its facial exit hole.*

The basis of surgical planning is the radiographic assessment, which consists above all of CT with reconstruction in three dimensions. This is particularly important because the nature of deformity in frontoethmoidal meningoencephalocele is so variable that each operation must be specifically tailored to the deformity. There is *no* standard operation for frontoethmoidal meningoencephalocele. After radiographic analysis the deformity can be assessed and the correction planned with a combination of osteotomies, bone grafts, and soft tissue operations.

There are two key principles of surgical treatment:

1. The operation should be performed by the transcranial approach so that the defect can be isolated intracranially and possibly intradurally with careful repair of the dura.

2. Complete bony reconstruction of the orbits and, if necessary, translocation of the orbits should be performed when required. The surgeon should, if possible, repair the bony and soft tissue deformities at the same fume.

The patient is prepared for the operation by orotracheal intubation and insertion of central and arterial lines (Fig. 37–8). Access is gained by a bicoronal scalp flap. When there is a large soft tissue mass on the face, or when there is previous facial scarring, an additional nasal incision is made to allow removal of

the facial mass and trimming of the facial skin. The first step is wide subperiosteal exposure to outline the facial exit holes of the meningoencephalocele (Fig. 37–9). Planned osteotomies are marked out on the skull. In many instances the subcranial aspects of the bony reconstruction are made at this stage (Fig. 37–10), possibly involving osteotomies or bone grafts. The neurosurgeon performs a small bifrontal craniotomy, exposing both frontal lobes, and the frontal bone is temporarily removed as a free graft (Fig. 37–11). If the bone removed is thick enough, it is split and the inner table is used for grafting; otherwise, two or even three ribs are harvested, one with a small cap of costal cartilage for use as a bone graft for the nose.

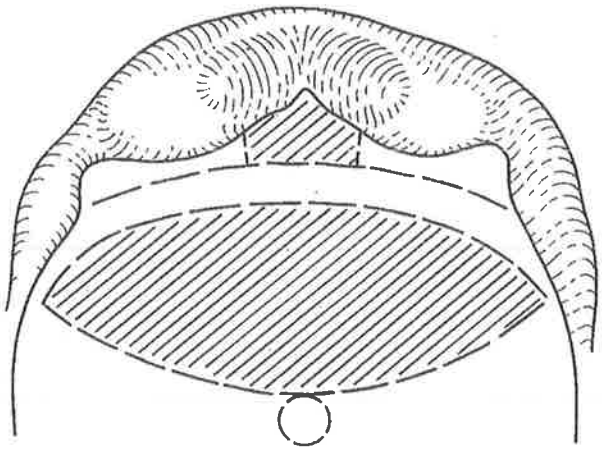

FIG. 37-10. *The proposed osteotomies. Operatively these orbital and frontal osteotomies are marked out. The central nasal segment is removed, and not replaced, if hypertelorism is to be corrected.*

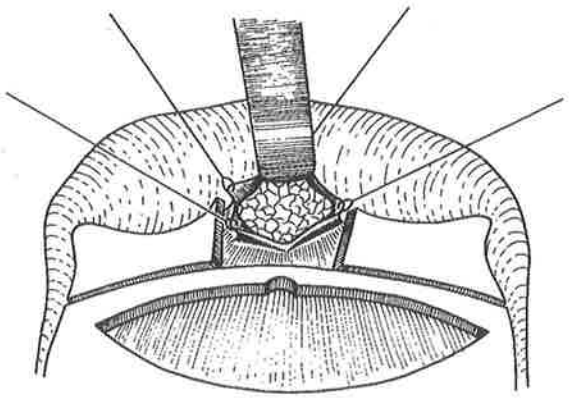

FIG. 37-11. *Dura overlying neck of meningoencephalocele is opened and the contents are dissected out. Free frontal bone graft has been removed to assist with cutting or orbital osteotomies and removal of meningoencephalocele.*

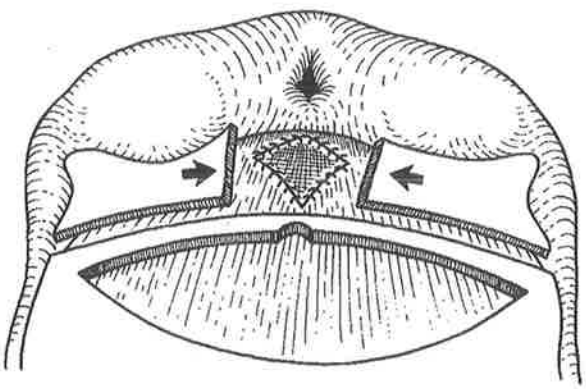

FIG. 37-12. *Meningoencephalocele has been removed and the dural defect repaired using temporal fascia. Orbits sectioned with the osteotome are moved medially as required. Nasal skin defect is closed in layers.*

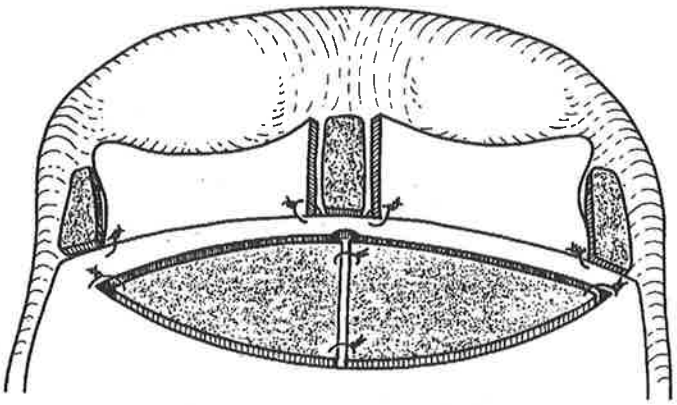

FIG. 37-13. *Hypertelorism has been corrected. Osteotomies are fixed with interosseous wires. The remaining bony defects of the nose are bone grafted if required using split calvarium and rib. Bicoronal scalp flap is replaced and closed in layers.*

Before the bony orbital part of the operation is undertaken, the neurosurgical dissection of the anterior fossa is performed. The roofs of the orbits and the dural neck of the meningoencephalocele are exposed extradurally as far as the cranial bone defect. Additional exposure is often obtained by excising a rectangle of bone from the glabellar region; this is replaced if there is no hypertelorism to correct. The dural sac of the meningoencephalocele is opened on both sides (see Fig. 37–11); cerebral herniation is inspected and, as much as possible, is conserved. The neck of the encephalocele is transected and the dural defect repaired, usually with a piece of temporalis fascia (Fig. 37–12). The remaining orbital osteotomies are made. In the nasoethmoidal type of meningoencephalocele, the medial orbital walls often are found to be defective and the angle of the cribriform plate is so steep that the translocated orbits come to overlie the cribriform plate. In some naso–orbital lesions, one or both orbits may be grossly expanded by the increased soft tissue volume. Osteotomies need to be designed to decrease the orbital size and may need to be supplemented by bone grafting of the orbital roofs, floor, and medial and lateral walls. When there is clinically significant teleorbitism affecting both orbits, the orbits are translocated medially to move the eyes (Fig. 37–13). Less severe deformities may require movement of one orbit only or osteotomy of only the medial orbital walls. Canthopexy and bone grafting of the nasal defect are final procedures.

Before external dissection of the soft tissue mass, it is our custom to cannulate the inferior lower lid canaliculus and inject dye into the nasolacrimal drainage apparatus. The soft tissue mass is often very vascular, and careful dissection is required to separate it from the overlying skin; the canaliculi and nasolacrimal apparatus often are stretched and distorted. Care must be taken not to remove excessive skin from the midline over the nose, because the soft tissue in this area has the capacity to "take up" in the first few months postoperatively.

Frontoethmoidal meningoencephaloceles often are associated with hydrocephalus. If this is severe and progressive, a ventriculoperitoneal or ventriculoatrial shunt may be required. However, we usually defer this operation until the completion of the one–stage transcranial operation for the cephalocele, controlling intracranial pressure intraoperatively by draining the dilated ventricles through a separate burhole incision. This strategy allows regulation of intracranial pressure during the operation and for 2 or 3 days thereafter, avoiding the occasional complications (postoperative extradural hemorrhage, infections) sometimes associated with an internal shunt. The hydrocephalus associated with cephaloceles sometimes arrests spontaneously, even when quite severe. However, if the hydrocephalus is clearly progressive and the postoperative intracranial pressure is high, there should be no delay in performing a shunt. We prefer ventriculoperitoneal drainage.

In older patients, particularly those with meningoencephaloceles of the nasoethmoidal variety with longer faces, we have not found it necessary to use the more complex face-shortening operations described by Jackson and associates. The operative program we use was devised for established deformities presenting later in childhood. We have limited experience with operations undertaken in patients in their infancy (1 to 3 months), but we believe that this is the ideal time to intervene, both to promote parental acceptance and ultimate psychological well-being and in the hope, as expressed by Naim–Ur–Rahman, that facial deformity will be avoided. The rationale for this hope is the concept that the skeletal deformities relate to the space–occupying effect of the hernia of extruded brain and not to some intrinsic deformity in the facial structures. If this view is correct, early complete surgical intervention should allow the developing brain and eyes to mold the orbital skeleton and the forces generated by the nasal airway, speech, and mastication to remodel the facial deformity. In operations on infants, it is necessary only to translocate and reconstruct the medial orbital walls with canthopexy and insertion of a nasal bone graft in addition to removing the contents of the meningoencephalocele. However, long–term studies are needed to validate this belief.

A B

FIG. 37-14. *Facial growth can approach normality after early removal of frontoethmoidal meningoencephaloceles. Child preoperatively at 4 months of age* **A.** *and postoperatively at 3 years of age* **B.** *(From D. David, et al. Meningoencephaloceles: Classification, pathology, and management. Adv. Plast. Reconstr. Surg. 5:85, 1989. Reproduced with permission.)*

A B

FIG. 37-15. *Preoperative* **A.** *and postoperative* **B.** *views of patient whose left orbit only was moved after removal of meningoencephalocele. (From D. David, et al. Frontoethmoidal meningoencephaloceles: Morphology and treatment. Br. J. Plast. Surg. 37:271, 1984. Reproduced with permission.)*

Operative Complications

All patients undergoing transcranial correction of frontoethmoidal meningoencephaloceles by the Australian Cranio–Facial Unit so far have survived the operation. The operation is usually accomplished in 2 to 4 hours. Complications have included two instances of acute postoperative hydrocephalus; three instances of rhinorrhea, which cleared spontaneously; and one secondary encephalocele in the frontal region as a result of raised intracranial pressure and inadequate reconstruction of the frontal bone, which necessitated a secondary operation. The same patient also had an infection of the left medial canthal region, which settled with antibiotics. Several patients squinted postoperatively, but in all but two of these patients the squinting resolved spontaneously. In these two patients the squinting was of sufficient severity to warrant further surgical correction. The most serious long-term problem is epiphora resulting from malfunction of the nasolacrimal apparatus. Even in patients in whom the nasolacrimal apparatus has been demonstrated to be intact, it is often so deformed that the tortuous ducts fail to function. Postoperative follow-up study over many years has shown that in almost all instances the condition settles down eventually. The explanation for this is obscure.

A number of patients have required the removal of their transnasal canthopexy wire and minor secondary bone grafting to the nose and cheeks. As far as facial growth is concerned, the results in patients who underwent the operation in infancy appear to confirm the proposition that the facial skeleton readjusts itself to the normal growth forces after removal of the displaced dysplastic brain (Fig. 37–14). However, we have not yet validated this impression with long–term craniometric data. It should be realised that cosmetically suboptimal results are often unavoidable when the meningoencephalocele is large and has dysplastic overlying skin. Various results are demonstrated in Figures 37–15 to 37–17.

FIG. 37-16. *Preoperative* **A.** *and postoperative* **B.** *views of a child in whom both orbits were translocated after transcranial removal of the meningoencephalocele. Note the resolution of epiphora. (From D. David, et al. Frontoethmoidal meningoencephaloceles: Morphology and treatment.Br.J. Plast. Surg. 37:271, 1984. Reproduced with permission.)*

FIG. 37-17. *Preoperative* **A.** *and postoperative* **B.** *views of a child in whom medial wall osteotomies, transnasal canthopexies, and nasal bone grafts were performed after removal of the meningoencephalocele. (From D. David, et al. Frontoethmoidal meningoencephaloceles: Morphology and treatment. Br. J. Plast. Surg. 37:271, 1984. Reproduced with permission.)*

Conclusion

Until recently, frontoethmoidal meningoencephaloceles were initially treated by neurosurgeons; plastic surgeons were, as a rule, consulted secondarily to deal with established deformities. The advent of craniofacial surgery allows definitive correction of the deformity in a single stage. Division of the neck of the encephalocele is not enough to wither the distal component of the extruded tissue or to prevent distortion of the developing skeleton. Craniofacial surgery is recommended with removal of the extruded brain, repair of the dura and anterior cranial fossa, and the appropriate osteotomies and bone grafts, preferably in the first 3 months of life; the hope is that the soft tissues will establish normal growth forces of the craniofacial skeleton and allow the face to assume more normal proportions. The simplest operation, namely moving the medial orbital walls with bone grafting and canthopexies, is the operation of choice in the early years of life. In older patients, however, the displaced orbits can be reconstructed in three dimensions if necessary.

We have not attempted to describe the details of each operation because in these days of the well–established craniofacial unit, it is now an accepted principle that the details of each operation be designed to fit the specific deformities present. The advent of CT techniques that give accurate three–dimensional images has allowed the surgical team the opportunity to plan surgical maneuvers, tailoring each operation to each deformity. It is important to realize that careful selection of patients should be practiced so that only those sufficiently able to benefit from the operation undergo it.

Suggested Reading

1 Aung, T., and Hta, K. Epidemiology of frontoethmoidal encephalomeningocele in Burma. J. Epidemiol. Community Health 38: 89, 1984.

2 David, D.J., et al. Fronto–ethmoidal meningoencephaloceles: Morphology and treatment. Br. J. Plast. Surg. 37: 271, 1984.

3 David, D.J., Simpson, D.A., and Cooter, R.D. Meningoencephaloceles: Classification, Pathology, and Management. Adv. Plast. Reconstr. Surg. 5: 85, 1989.

4 Hemmy, D.C., and David, D.J. Skeletal morphology of anterior encephaloceles defined through the use of three dimensional reconstruction of computerised tomography. Paediatr. Neurosci. 12:18, 1986.

5 Jackson, I.T., Tanner, N.S., and Hide, T.A. Frontonasal encephalocele: "Long nose hypertelorism." Ann. Plast. Surg. 11: 490, 1983.

6 Le Dran, H.F. Observations in Surgery. London: James Hodges, 1740.

7 Mazzola, R.A. Congenital malformations in the fronto-nasal area: Their pathogenesis and classification. Clin. Plast. Surg. 3: 573, 1976.

8 McLaurin, R.L. Cranium Bifidum and Cranial Cephaloceles. In P.J. Vinken and G.W. Bruyn (Eds.), Handbook of Clinical Neurology: Part 1. Congenital Malformations of the Brain and Skull. Amsterdam: North Holland Publishing, 1977. Vol. 30, Pp. 209–218.

9 Naim-Ur-Rahman, N. Nasal encephalocele: Treatment by transcranial operation. J. Neurol. Sci. 42: 73, 1979.

10 Simpson, D.A., David, D.J., and White, J. Cephaloceles: Treatment, outcome, and antenatal diagnosis. Neurosurgery 15: 14, 1984.

11 Spring, A. Monographic de la hernie de cerveau et do quelques lesions voisines. Memoires de L'Academie Royale de Medicene de Belgiques, 1854.

12 Suwanwela, C. Geographic distribution of fronto-ethmoidal encephalomeningocele. Br. J. Prev. Soc. Med. 26:193, 1972.

13 Suwanwela, C., and Suwanwela, N. A morphological classification of sincipital encephalomeningocele. J. Neurosurg. 36:201, 1972.

14 Tessier, P. Anatomical classification of facial, craniofacial, and laterofacial clefts. J. Maxillofac. Surg. 4:69, 1976.

15 von Meyers, E. Uber Eine Basale Hirnhernie In Der Gregend Der Lamina Cribrosa. Virchows Arch. [Pathol. Anat.] 120:309, 1890.

Chapter 6
Craniofacial Tumours

A desperate disease requires a dangerous remedy.
Guy Fawkes

6. Craniofacial Tumours

Tumour surgery of the head and neck has always been part of the ACFU's clinical activity. The team has applied itself to problems of cancer of the oral cavity and facial bones as well as those tumours primarily affecting the cranial base. The nature and severity of the pathology often obliterates any territorial distinction.

The first paper Use of an Innervated Deltopectoral Flap for Intraoral Reconstruction, 1977[1], reflects the focus at that time on preserving function when reconstructing the face.

The publications Psychosocial Aspects of Head and Neck Cancer Surgery, 1977[2] and Psychosocial Implications of Surgery for Head and Neck Cancer, 1982[3], present the philosophies in practice with respect to this aspect of patient care.

The condition described in Malignant Schwannoma of the Inferior Dental Nerve, 1978[4] does indeed transgress the cranial base. Modern investigative techniques have made the protocol of investigation presented in this paper obsolete. However at the time it involved the application of the new craniofacial approach to a difficult clinical problem.

Experience with Surgery for Head and Neck Cancer in a Geriatric Population, 1982[5] expressed a view, not ubiquitously held at that time, that age is not a limitation to major surgery of the head and neck.

Technical Aspects of the Craniofacial Approach to Tumours of the Orbit and Skull Base, 1988[6], presents the range of approaches used at the time by the ACFU to deal with tumours of this area.

Mandibular Reconstruction with Vascularized Iliac Crest: A 10-year Experience, 1988[7], documents the author's philosophy and the results of use of this reconstructive tool. Reference to Chapter 2,

Articles 16 and 17 shows the wider and more up to date use of this form of reconstruction.

The effects of benign tumours on the craniofacial skeleton during growth are dealt with in Craniofacial Deformation in Cystic Hygroma, 1990[8].

The uses of modern imaging and the transfacial approach to the base of skull are demonstrated in Basal Encephaloceles: Imaging and Exposing the Hernia, 1993[9].

Papers

1. David DJ 1977 Use of an Innervated Deltopectoral Flap for Intraoral Reconstruction. Plast Reconstr Surg 60(3):377–380

2. David DJ, Barritt JA 1977 Psychosocial Aspects of Head and Neck Cancer Surgery. Aust N.Z. J Surg 47(5):584–589

3. David DJ, Barritt JA 1982 Psychosocial Implications of Surgery for Head and Neck Cancer. Clin Plastic Surg 9(3):327–336

4. David DJ, Speculand B, Vernon-Roberts B, Sach RP 1978 Malignant Schwannoma of the Inferior Dental Nerve. Br J Plastic Surg 323–333

5. Trott JA, David DJ, Edwards RM 1982 Experience with Surgery for Head and Neck Cancer in a Geriatric Population. Aust N.Z. J Surg 52(2):149–153

6. David DJ, Simpson DA, Henrikkson TG, Moore MH 1988 Technical Aspects of the Craniofacial Approach to Tumours of the Orbit and Skull Base. Aust NZ J Surg 58:315–320

7. David DJ, Tan E, Katsaros J, Sheen R 1988 Mandibular Reconstruction with Vascularized Iliac Crest: A 10-Year Experience. Plast Reconstr Surg 82(5):792–803

8. Moore MH, David DJ 1990 Craniofacial Deformation in Cystic Hygroma. Jnl Craniofacial Surg 1(2):97–102

9. Moore MH, Lodge ML, David DJ 1993 Basal Encephalocele: Imaging and Exposing the Hernia. Br J Plastic Surg 46:497–502

Use of an innervated deltopectoral flap for intraoral reconstruction

David J. David, F.R.C.S.
Adelaide, South Australia

The radical surgical excision of tumors usually requires a flap reconstruction. At best, the flaps that have been so used result in a gross repair of this delicate and complex system of anatomy and physiology. In a recent study from this department[1], it was confirmed that a significant number of the problems with rehabilitation in these patients are traceable to flap insensitivity and flap bulk. The innervated deltopectoral flap has been designed to help overcome some of these difficulties.

Anatomy

Sensation to the deltopectoral flap area is supplied by the supraclavicular nerves, which arise by a common trunk from the third and fourth cervical nerves.[3] This trunk emerges from the posterior border of the sternocleidomastoid muscle and descends under cover of the platysma and the deep fascia, then divides into medial, intermediate, and lateral branches— which diverge from one another and pierce the deep fascia a little above the clavicle (Fig. 1). The intermediate and lateral branches, in particular, supply that part of the flap which usually goes to form the intraoral reconstruction.

We have found it possible to isolate the nerve supply of this flap at its origin, trace the nerves distally into the flap, and raise the flap with its nerve supply intact. The division of the nerve into its 3 branches may be low or high. One or more of the branches may pierce the clavicle, in which case that branch needs to be sacrificed.

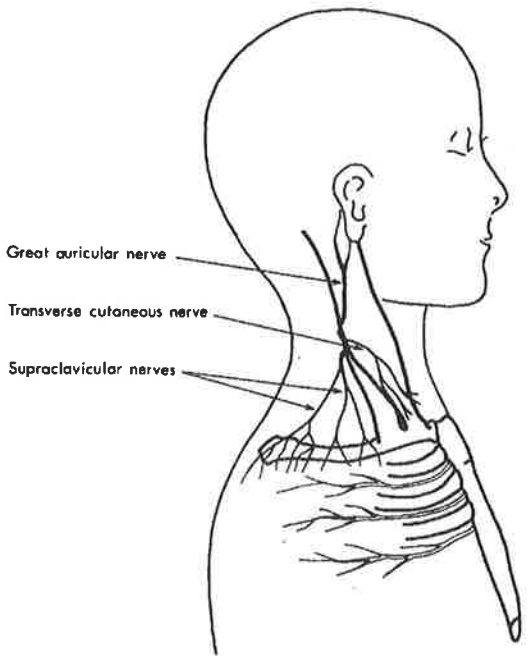

FIG. 1. *The relationship of the supraclavicular nerves to the deltopectoral flap.*

Preoperative Planning

With the patient awake and seated in a chair, the nerves may often be felt as they cross the clavicle, especially if the patient is thin. Having drawn out the deltopectoral flap on the skin, an injection of 10 cc of a local anesthetic solution is made just superficial to the periosteum, along the line of the clavicle. After 10 minutes, the area of the flap thus anesthetized can be mapped out. It is an advantage to leave these markings on the patient until he arrives in the operating room (Fig. 2, *left).*

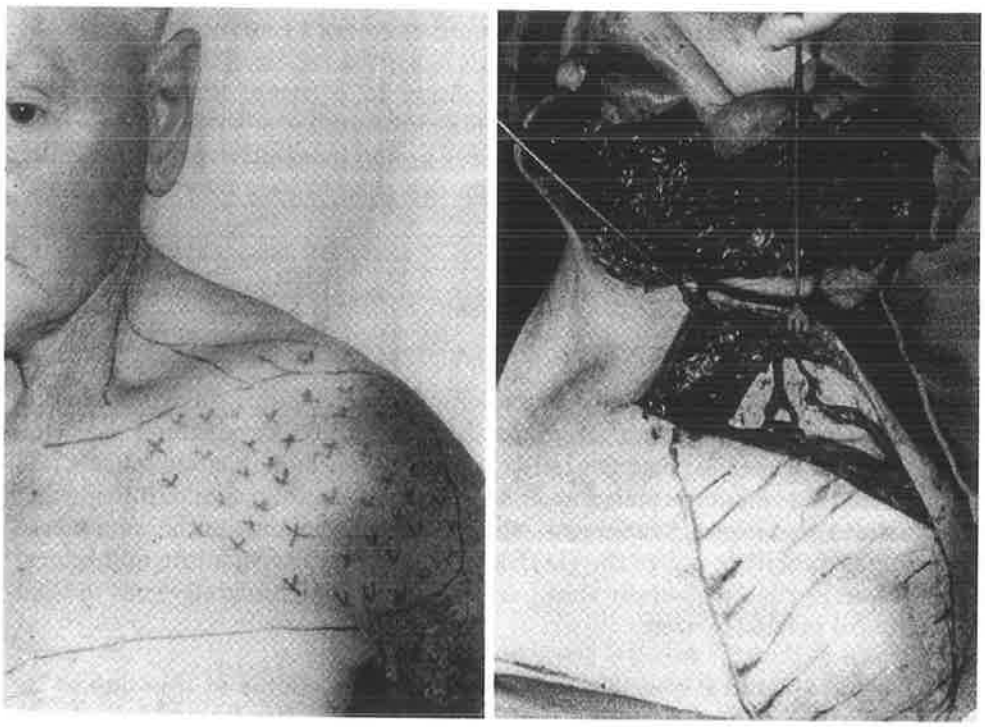

FIG. 2. (left) *The anesthetic area of the deltopectoral flap, produced by blocking the supraclavicular nerves as they pass over the clavicle.* (right) *The dissected nerve trunks in continuity with the flap.*

Operative Procedure

After the intraoral defect has been created, if it has not already been done, a transverse bi-pedicled neck flap is raised after the fashion described by MacFee.[4] The supraclavicular nerve trunk is found as it emerges from behind the sternocleidomastoid muscle at its midpoint. (The great auricular nerve is the best landmark, as it is easily found over the sternomastoid muscle and traced to the point where it emerges with the other cutaneous branches of the cervical plexus from the posterior border of that muscle.) The supraclavicular nerve trunk is then dissected distally, particular care being taken as it becomes more superficial, first piercing the deep fascia, then the platysma, and finally flowing over the clavicle into the flap (Fig. 2, *right).*

At this stage an accurate pattern of the intraoral defect can be made, and an outline can be drawn on the innervated deltopectoral flap. Those nerve branches that do not enter this area of the flap can be divided. The chest wall flap can now be completely raised and passed subcutaneously under the transverse neck flap into the oral cavity. The part of the flap that will remain subcutaneous is delineated, the design of the intraoral portion is checked, and the flap is returned to the chest wall. A thorough deepithelialization is done of the carrier portion which will remain subcutaneous.

Two possibilities exist with respect to the supraclavicular nerves. They can be left intact at their origin, or they can be disconnected and anastomosed by microsurgical techniques to the appropriate sensory nerves in the mouth—namely the inferior dental nerve or the lingual nerve, depending on the type of surgical excision performed (Figs. 3, 4).

The flap is then sutured into position. The neck wound is closed and the donor site is skin grafted, thus effecting a cosmetically acceptable repair without a fistula, in one stage.

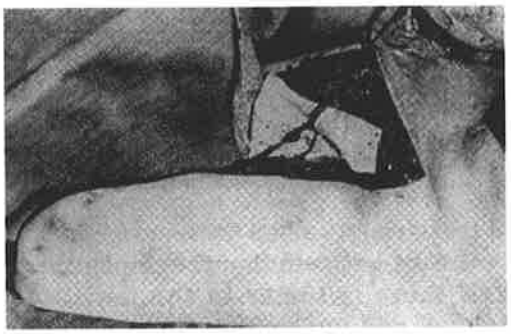

FIG. 3. *An innervated flap, with the nerves intact.*

FIG. 4. *After the supraclavicular nerve trunk has been anastomosed to the severed lingual nerve.*

Discussion

To date, 4 of our patients have had an intraoral reconstruction by this technique. Two of them had the supraclavicular nerves left intact at their origin, and two had the nerve disconnected in the neck and a microsurgical anastomosis performed (one case with the severed end of the lingual nerve, the other with the severed end of the inferior dental nerve). Two of our cases were for squamous cell carcinoma of the floor of the mouth, one was for squamous cell carcinoma of the tonsillo-lingual sulcus, and one case was for severe osteoradionecrosis of the mandible and the floor of the mouth.

In the two cases where the nerves remained in continuity, there is excellent sensation. In one case, this is still referred to the shoulder tip but in the other case, the cerebral readjustment has been made. At this stage, the two patients in whom the nerves were anastomosed have not had sufficient time to innervate the flaps.

Advantages

Converting the deltopectoral flap into one with a narrow and permanent pedicle achieves the required contour in one stage without lengthy and difficult subsequent operations. Prevention of the orocutaneous fistula makes the patient more comfortable postoperatively, and the nursing is less arduous. If so desired, the pedicle can be divided after 3 weeks and a portion of the flap returned to the shoulder.

The advantages of a sensitive intraoral lining are obvious to those who have been involved in the long-term rehabilitation of patients requiring intraoral reconstruction. The quality of speech, swallowing, and oral hygiene all depend to some degree on the quality of sensation inside the mouth. To date it has been determined that the sensitive skin Rap can be transferred into the mouth, but a further analysis of the quality of this sensation is yet to be made.

Disadvantages

Isolating the supraclavicular nerves and preparing the flap for transfer to the oral cavity adds time to the operation. Care must be taken that the principles of cancer surgery are not transgressed. If there is tumor in the neck, the supraclavicular nerves should be divided low and anastomosed to a suitable sensory nerve in the mouth. (A superficial tumor in the neck and in close proximity to the trunk would be a contraindication to the use of this technique.)

When a decision has been made to return the carrier portion of the flap to the chest wall, this remnant will be much smaller, thus leaving a larger chest and shoulder scar or skin graft.

Summary

The technique for the transfer of sensitive skin into the mouth for intraoral reconstruction is described. This procedure may be performed at one or two operative stages. Supraclavicular nerves supply sensation to the tip of the standard deltopectoral flap — which may be swung up with the nerves left in continuity, or the nerves may be divided and anastomosed to an appropriate sensory nerve in the mouth.

David J. David, F.R.C.S.
326 South Terrace
Adelaide 5000, South Australia

Mr. David is a Senior Visiting Plastic Surgeon in the Plastic and Maxillo-Facial Unit of the Royal Adelaide Hospital.

Acknowledgments

I thank Mr. G. 1. Taylor for his advice about innervated flaps, Mrs. Alison Bagnall of the Department of Speech Therapy of Royal Adelaide Hospital for her constructive suggestions, Mr. Eugene Tan for his help in the planning and execution of the surgery, and Dr. R. Edwards for his constructive criticisms.

References

1. David, D. J.: Function and intraoral flaps. Cancer Forum (In press).

2. Bakamjian, V.Y.: A two stage method for pharyngoesophageal reconstruction with a primary pectoral skin flap. Plast. & Reconstr. Surg., 36: 173, 1965.

3. Davies, D. V., and Davies, F.: Gray's Anatomy, Descriptive and Applied. Longmans, London, 1964.

4. MacFee, W. F.: Transverse incisions for neck dissection. Ann. Surg., 151: 280, 1960.

Psychosocial Aspects of Head and Neck Cancer Surgery

D. J. David[1] and J. A. Barritt[2]
Plastic and Maxillo–Facial Unit, Royal Adelaide Hospital

Thirty–six patients who underwent major surgical excision and reconstruction for head and neck cancer were subjected to a psychosocial assessment in hospital and, later, in their home environments. The information gained from the survey is discussed, with particular reference to those factors which can be used by the head and neck surgical team to improve the quality of the patients' existence.

The care of patients suffering from head and neck cancer, who need major surgical excision and reconstruction should be bases on the knowledge of the "whole patient". The loss if function and form of the face and oral cavity has far–reaching manifestations for both the patient and his family. The study of all the aspects affecting the patient necessitates a team of medical and paramedical personnel (Figure 1). The information gained contributes to the knowledge of the whole pattern of psychological problems in these patients.

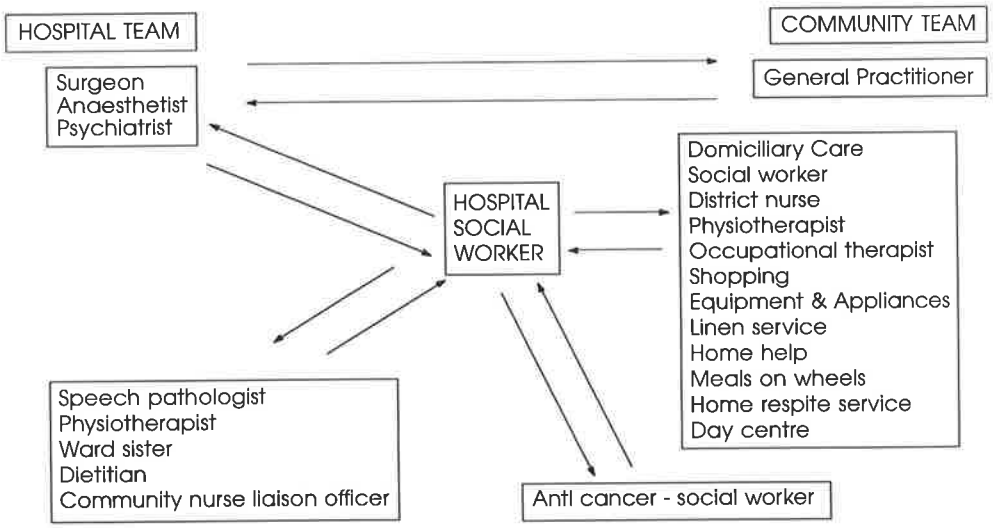

FIG. 1. *Head and neck cancer team.*

[1]Senior Visiting Plastic Surgeon.
[2]Social Worker.

Patients and Methods

Thirty–six patients suffering from head and neck cancer, who required major reconstructive surgery, were subjected to a psychosocial assessment: (i) before operation and (ii) three months after discharge from hospital. Further assessments were made subsequently (Tables 1 and 2).

TABLE 1

Assessment Procedure

Preoperative Interview
1. Eating difficulties
2. Ambulation
3. Sleeping habits
4. Social aspects
   (a) Environmental
   (b) Socioeconomic
   (c) Recreational
   (d) Accessibility to public institutions
   (e) Accessibility to local amenities
5. Sexual Functioning
6. Interests and hobbies
7. Use of domiciliary services
8. Type of work followed
   (a) Occupation and income
   (b) Motivation
   (c) Attitude of patient
   (d) Standard achieved
   (e) Attitude of employer to worker
9. Inter-relationships
   (a) Family
      (i) Role
      (ii) Status
      (iii) Personality and attitudes
   (b) Relatives
   (c) Friends, community groups
10. Spiritual
11. Emotional reaction to medical problem
    Fear, anxiety, anger, resentment, depression
    Level of acceptance

TABLE 2

Postoperative Interview at Three Months

1. Eating, drinking and speech difficulties
2. Environmental problems pertaining to medical problems
3. Employment situation
4. Maintenance of interest and hobbies
5. Emotional adjustment

The interviews were done by the Plastic and Mazillo–Facial Unit social worker, who met with the patients and their families independently of the surgeon, so as to make the findings as objective as possible. The study was aided by information gained by other members of the team. both at the hospital and the community level. Tables 3, 4, and 5 show and analysis of the patients for the point of view of the operation performed, their age, sex, and survival time. They have been divided into three groups because of the different psycho–social problems associated with each set: (i) those potentially cured: (ii) those alive with disease: and (iii) those who have died.

Results

The preoperative interview is the key to the successful progression of the patient and his family through the hospitalization and rehabilitation phases. Patients need to have the opportunity to understand fully and ask questions about the operation, hospitalization, and prognosis. Concepts of pathology that have taken medical students many years to absorb,, are placed before an often frightened and confused person, and he is expected to absorb them in minutes! The social work function is to interpret the illness in lay terms, and this is supplemented in the team approach by the anaesthetist, physiotherapist, speech pathologist., and ward sister, Such an approach necessitates a close liaison between members of the team, who feed back relevant information to the surgeon, so that he can allay the patient's anxieties. It is also important at this stage that the patient meets with people who will be looking after him after operation.

TABLE 3

Patients Potentially cured

	Age (years)	Sex	Operation	Postoperative survival	
				Years	Months
1	68	F	Composite resection with flap	3	9
2	75	F	Composite resection with flap	2	10
3	66	M	Mandibular resection with flap	2	9
4	77	F	Composite resection	2	
5	56	M	Composite resection with flap	1	10
6	45	M	Composite resection with flap	1	6
7	66	M	Total glossectomy, bilateral arch disection with flap	1	6
8	55	F	Composite resection with flap	1	
9	73	M	Total parotidectomy with flap	3	3
10	59	M	Maxillectomy with prosthesis	1	3
11	59	M	Mandibulectomy with flap	1	
12	59	M	Composite resection with flap	1	
13	54	M	Composite resection with flap		9
14	59	M	Resection, of lip and cheek with flap	1	

TABLE 4

Patients alive with Recurrent Disease

	Age (years)	Sex	Operation	Postoperative survival	
				Years	Months
15	43	M	Composite resection (bilateral) with flap	2	9
16	89	F	Total parotidectomy with flap	2	
17	64	F	Resection of lip and floor of mouth, bilateral neck dis-section with flap	1	6
18	38	M	Maxillectomy with flap	1	4
19	57	M	Composite resection with flap	1	
20	68	M	Composite resection	1	
21	55	M	Composite resection		9
22	83	M	Total parotidectomy with flap	2	
23	64	M	Bilateral neck dissection	2	6
24	38	M	Total parotidectomy neck dissection with flap	3	9

TABLE 5

Patients Dead

	Age (years)	Sex	Operation	Postoperative survival	
				Years	Months
25	76	M	Composite resection with flap	1	9
26	67	M	Composite resection with flap	2	9*
27	64	F	Composite resection with flap		9
28	48	M	Composite resection with flap	2	
29	34	M	Composite resection with flap		9
30	68	M	Composite resection with flap	1	
31	54	M	Composite resection with flap	1	3
32	50	M	Cheek resection with flap	3	
33	58	M	Maxillectomy with flap	1	6
34	83	F	Resection of floor of mouth with flap	1	2*
35	46	M	Composite resection with flap		11
36	48	M	Composite resection with flap and prosthesis	2	

A. Information Gained at the Preoperative Interview

This is of value in predicting certain difficulties during the rehabilitation period. These are as follows.

(i) Eating and drinking. — Nineteen out of 36 patients had an alcohol problem which presented its own particular medical and social difficulties. Seventeen of these patients were males, who had their major form of socialization in hotel, to the exclusion of their wives and families. Postoperative support by the wife meant disruption of her own separate will–established social pattern. To aviod the inherent conflicts in this situation, a wide social readjustment had to be made, involving relations, friends, and domiciliary services.

(ii) Social aspects and inter-relationships. — The home environment usually needs too be closely related to specific community services during the long-term rehabilitation. The patient's proximity to supporting relatives is of great importance. Three patients in the series had to move house for this reason. Knowledge of the role and status of the patient within the family group, with relatives, and with friends, will enable the team to predict some of the difficulties that will be encountered when certain aspects of the relationship are changed after operation.

(iii) Occupation and employment. — Major head and neck surgery invariably means a change in the patient's working habits. It was found that the greatest readjustments had to be made by heavy manual workers. Efforts to prepare the patient for this eventuality can be limited at the preoperative interview.

(iv) Spiritual and emotional factors. — Preoperative assessment of coping mechanisms gives n indication of how the patient will deal with the current crisis. An assessment of each patient's tendency to endogenous depression provides a baseline for postoperative comparison, and influences subsequent management of the depression. Two patients in the series required psychiatric intervention. A knowledge of the patient's spiritual philosophy enables the appropriate assistance to be obtained when and if necessary.

B. Findings in the Early Postoperative Phase

The first three postoperative weeks were found to be the most stressful for the patients because of: (a) The inability to communicate, especially in those patients with tracheostomy; (b) The presence of intravenous and nasogastric tubes: and (c) frequent lengthy dressing periods necessary to care for wounds flaps, and skin grafts.

This stage was characterized by a severe reactive depression in all patients, which was made more destressing by lack of sleep due to unavoidable nursing-staff intervention. During this time, all patients were seen in display antisocial reaction and become irritable. Management was based on the preoperative counselling which attempted to explain the finite period of this stage, together with intensive support from all members of the team. The technique is of reassurance, with constant reference to previous discussions of problems that the patients are now experiencing. The greatest single fear was that the communication barriers produced a feeling of emotional isolation from the members of the medical and nursing staffs. There was no place for the treatment of the reactive depression by drug therapy. Where there was an endogenous element, a psychiatrist was involved n the management. The watershed in this postoperative phase was when the patient saw progress being made in virtue of the division and inset of flaps. All patients made considerable progress at this time. The team needed to encourage support by the immediate family members, and this was eventually extended to the wider family and friends as the patient recovered.

The problems occurring in the later postoperative phase were: (a) the emerging awareness of a change in body image (Figure 2): (b) problems with swallowing and dribbling: and (c) problems with speech.

The withdrawal of intensive nursing facilities as the patient recovered was often associated with a feeling of rejection, because of the established dependence on these services. At he same time, parallel efforts to prepare the home to receive the patient were made. During this period the immediate family have to become aware of the need for changes necessitating another stage of intense counselling and recognition. Patients must be reassured that they can cope an relatives must be made aware of the problems that would present themselves. Community services may be needed for their assistance. Twelve patients in the series had involvement with community services.

FIG. 2. *Change in facial appearance after excision of the anterior mandible, bilateral neck dissection and forehead flap repair.*

C. Factors Emerging from the Postoperative Home Interview

This was conducted approximately three months after the patient had been discharged from hospital.

(1) Eating and drinking habits. — One of the most significant changes at this stage was related to eating habits. The problems referred to in the previous stage prior to discharge became more significant whin the patient was removed from the protective environment of the hospital into the home. Because of the increased time required for feeding, the messiness, and the need for special preparation, the patient's pattern of eating became socially unacceptable, causing loss of self–esteem and personal humiliation. In particular, eight patients from high socioeconomic income groups found that this altered their way of life completely, thus effecting a long-term anxiety problem.

Oral sphineter incompetence resulting in dribbling was a major retarding force to rehabilitation in ten paticnts. Swallowing problems were seen as mild, intermediate, and severe. All patients who had composite resections and intraoral flaps required an altered diet because of inability to chew, and the changed physiology of the oral cavity, Those patients who were fitted with tooth-bearing prothesis supported on flaps found them cosmetically acceptable, but functionally inadequate, and they tended not to use them at all except when they visited the doctor in hospital. Those patients who needed a prosthesis for obturating a palatal fistula found their appliances useful in every case.

(2) Speech therapy. — Twelve patients required some form of postoperative speech therapy. Five of these had severe difficulties with swallowing, and required long-term management by the speech pathologist.

(3) Ambulation and physiotherapy. — After three months, all patients studied still required rest periods during ht e day, and showed an overall reduction in their activities. Patients who had neck dissections and/or deltopectoral flaps showed reduction in neck movements and limitation of shoulder movement. Ten patients were treated for these problems by a physiotherapist, half of these requiring treatment for longer than three months. Two additional patients required long-term physiotherapy for chronic lung disease.

(4) Environmental problems. — In all of the patients studied these problems were solved by the ability of the wider family to provide support and temporary accommodation. Tow patients (vide supra) found it necessary to move from a country to a city environment.

(5) Sexual adjustment.-Where it was applicable, the information gained in this area was not considered reliable.

(6) Employment and income. — Twenty of the male patients had been working when they developed their cancer; eight of these returned to their former occupation. However, all of these were working in a reduced capacity/ Patients included in the series admitted to being never quite the same, in that they had decreased capacity for physical endurance and required daily rest periods. All patients who returned to work required the personal intervention of the surgeon to manipulate the work situation so that they could be accepted back. Employers preferred to sack patients with facial cancer, or have them pensioned off. Most patients suffered a degree of financial hardship because of their cancer.

(7) Domiciliary services. — Twelve patients were referred for long–term involvement with domiciliary care centres, which included social worker, district nurse physiotherapist, occupational therapist, shopping, equipment and appliances linen service, home help, Meals on Wheels, home respite service, and the day centre.

(8) Interests and hobbies. — Eleven patients replaced former leisure activities with new or modified activities.

(9) Inter-relationships. — There was a change of role within the family structure in 15 of the 36 patients; 13 of these were male, and two were female. The change was interpreted by these people as a loss of status.

(10) Emotional adjustment. — Those patients in the series who suffered a recurrence of their disease had associated chronic depression. All patients demonstrated a cycle of denial, anger, resentment, and acceptance. Because of this cycle, it was difficult to assess the actual level of acceptance in the patients studied. Loss of body image was one of the biggest problems encountered. In those patients with forehead flaps, the female coped better than the males because they were able to cover the defect with hair styling.

All patients were initially worried about the forehead defect, but quite rapidly adjusted to it: it did not therefore become a significant long-term problem.

The condition of 12 patients in the series became terminal between nine and 15 months after their surgery. This produced all the problems associated with the dying process for the patient and his family. The head ad neck team provided support for these patients and their families during this terminal phase. Of the 14 patients requesting spiritual assistance, six made their first request during the terminal phase.

Discussion

Because this is a complex problem affecting complicated human beings and their families, it is a time-consuming and arduous task to provide the total support required to assist them through what is surely a major crises on their lives. This study has shown that it is not enough to do an adequate operation and reconstruction, even though successful from the functional point of view, without attending to the social and emotional adjustment of the patient and his environment. The problems surrounding head and neck cancer excision and reconstruction are the more complex because of the nature of the parts involved. The patient who will readily accept a major operation on his intestine will face the prospect of a composite resection and reconstruction with considerable fear.

Epsteen (1958), in his article entitled "The Psychological Impact of Facial Deformities", said: "The psychological reactions to deformities due to injury or disease occurring in adults are often much more severe than those that would follow congenital disfigurements. Time has taught the congenitally deformed person to make some adjustments which are often sufficiently artful to hide the unhappiness they harbour in disguise. Acquired deformities, particularly those contracted during adult life, present serious problems. Their sudden unexpected occurrence brings a mental shock which is so acute that adjustments are quite often impossible."

Surgery for cancer of this region is performed to cure the disease, or to palliate the patient. In both these situations, the surgeon needs to base his decision on an understanding of the natural history of the disease, and a complex knowledge of the potential effects of therapy on the patient as a whole person and on his family. This study has indicated the complexity of the situation and has attempted to analyse some of the problems. Success of the therapy can only be measured in therms of patient satisfaction, not solely in terms of survival rate. To provide complete patient care under these circumstances means the use of the team approach to cater for the function and psychosocial rehabilitation of the patient.

Conclusions

1. The surgeon heads the team because he has the ultimate responsibility for patient care. The team provides a coordinated service to their patient by feeding back information to the surgeon, who makes the final decisions on management. The team's efforts should be aimed at reinforcing the doctor–patient relationship.

2. Members of the team need to collect and relay this information.

3. It must be emphasized that subsequent problems can often be traced back to inadequate presurgical work–up. Those patients who are not well informed become resentful.

4. Many of the social difficulties encountered recur regularly, so that their occurrence can often be expected and watched for as in the patient with an alcohol problem.

5. In view of the tendency of employers to reject patients who have suffered facial disfigurement as a result of their head and neck surgery, a concentrated effort needs to be made to educate the community, and to manipulate the environment to accept these people back to work where possible.

6. Proper care may merge into chronic patient dependence. This aspect of rehabilitation needs to be handled sympathetically but firmly by building on the positive aspects of each individual.

7. Patients who expected a recurrence of their cancer have an associated loss of confidence in the surgical team, and a recurrence of their depression.

8. Those patients whose condition becomes terminal need to have supported to the end by the head and neck cancer team.

9. The results of this study have been incorporated in the ongoing management of patients by the Royal Adelaide Hospital team.

The psychosocial aspects of head and neck cancer surgery are complex and significant. It is not enough to do this sort of surgery with the preamble "just leave it to me". The true worth of the procedure must be measured in terms of quality as well as quantity of survival and this is best done by a team that extends its influence into the patient's own environment.

Acknowledgements

We wish to thank Mrs. A Bagnall, Speech Pathologist; Mrs Cruden, Physiotherapist; Dr R. Edwards, Anaesthetist; and Mr D. N. Robinson, Head of the Plastic and Maxillo–Facial Unit at the Royal Adelaide Hospital, for their help in the preparation of this paper.

Psychosocial Implications of Surgery for Head and Neck Cancer

David John David, M.B., F.R.C.S.E., F.R.C.S., F.R.A.C.S.,* and Jeanette A. Barritt, Dip. Soc. Sci. A.U.A.†

Symposium on Social and Psychological Considerations in Plastic Surgery

Most of the functions associated with human interaction are centered around the head and neck. Speech, subtleties of expression controlled by facial muscles, and the ability to eat and drink in a socially acceptable fashion with one's family and friends are vitally important.[4] When people are confronted with a diagnosis of cancer they are shocked and fearful. To face the prospect of this dreaded disease and a treatment that produces a dramatic change in facial form and function is devastating.

In modern society, one of the many social factors that tends to operate to the disadvantage of the facially deformed is the high social premium placed on physical appeal.[5] This cultural bias is not only detrimental to anybody whose face is badly disfigured but may serve to turn even a slight defect into a social and economic handicap—since he looks different, he must be different.[4] Such an attitude is often applied to the patient who suffers from head and neck cancer and has undergone surgical excision and reconstruction.

A number of observations have been made concerning cancer of the head and neck, particularly squamous carcinoma: (1) Surprisingly few cases of cancer of the oral cavity and paranasal sinuses are diagnosed early. (2) The majority of patients who die from head and neck cancer do so from local disease in the head and neck. Distant metastases are relatively unusual.

Management of the patient is based on a knowledge of the natural history of the disease. Equally as important are the social and psychological aspects that will ultimately affect the ability to cope with the change in his or her internal and external environments. It is important to have information about patients who are (a) potentially cured, (b) alive and functioning, but with recurrent disease, or (c) terminal.

Analysis of the Patient Group

Included in this study were 151 patients undergoing surgery for head and neck cancer at the Plastic and Reconstructive Surgery Unit at the Royal Adelaide Hospital. Ninety–three suffered from oral cancer, 24 from cancer of the skin, 11 from cancer of the salivary glands, seven from cancer of the paranasal sinuses, and 16 had other cancers of head and neck. Patients with laryngeal and pharyngeal cancer were excluded from this study.

There were 112 males, and 39 females. The ages at presentation ranged from 20 to 88 years, with an average age of 60 years. The peak incidence of

*Senior Visiting Plastic Surgeon, Royal Adelaide Hospital and Adelaide Children's Hospital; Head, South Australian Cranio-Facial Unit, Adelaide, South Australia
†Social Worker, Royal Adelaide Hospital; Social Worker, South Australian Cranio-Facial Unit, Adelaide, South Australia

presentation occurred in the sixth decade. At the time of this study, 83 patients were alive and 68 patients were dead. Of the living, three were alive with recurrent disease but were not terminal, and three were terminal.

The Team Approach

Loss of function and form of the face and oral cavity has far-reaching manifestations for both patient and family. To study all of the factors affecting this group, a team of medical and paramedical personnel should be assembled (Fig. 1). The Royal Adelaide Hospital Group set up such an organisation and reported its initial findings in 1977.[1]

The value of this team approach in caring for the patient and collecting important information has been reaffirmed. At the present time, the team has both hospital and community arms. The hospital social worker acts as a coordinator and relates data pertaining to the psychosocial management of the patient to the various members of the team. All patients undergoing major head and neck reconstructive surgery are subject to a psychosocial assessment both before surgery and three months after discharge from the hospital. Further follow–up assessments are made.

In the Australian community, it is usual for the surgeon to be head of the team, as the patients expect the person who is operating upon them to be in charge of their total management and have ultimate responsibility for their care. The team provides a coordinated service to the patient and feeds back information to the surgeon, who makes the final decisions on management. The team's efforts should be aimed at reinforcing a good doctor/patient relationship. The relationship between the hospital team and community team is strengthened by the liaison work of the hospital social worker and the continuing relationship between the medical members and the local medical practitioner. There is an educative element also in this type of organisation, as new avenues of problem solving can be opened up.

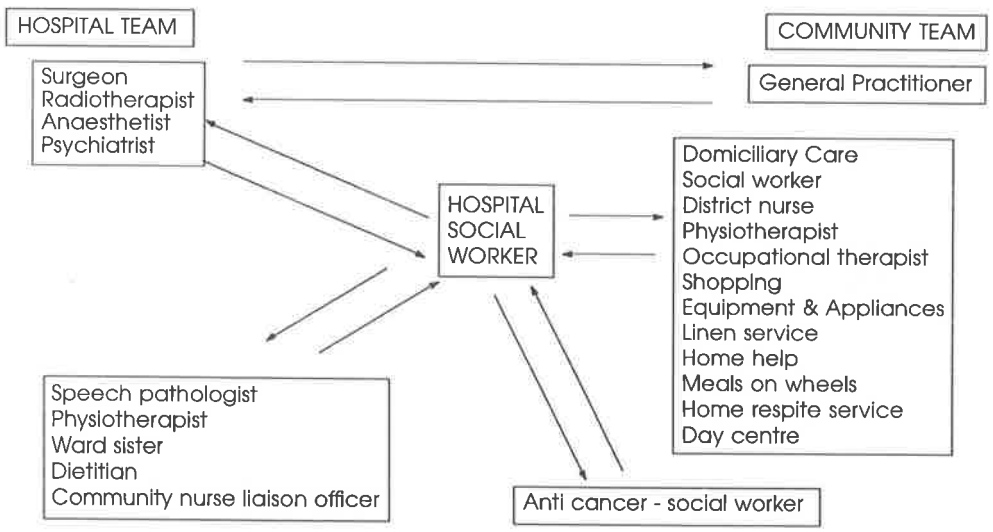

FIG. 1. *Head and neck cancer team*

Patient Management

The preoperative management is the key to the successful progression of the patient and his family through the hospitalisation and rehabilitation phases. After the initial sharing of the diagnosis and agreed treatment, patients must be given frequent opportunities to ask questions, so that they understand fully about the operation, hospitalisation, and prognosis. Concepts of pathology that have taken medical students many years to absorb are placed before an often frightened, confused person, who is expected to absorb them in minutes.

The initial preoperative interview is, wherever possible, conducted jointly by the surgeon and the social worker, who makes the patient aware of the emotional and practical support he or she can provide. As in any crisis situation, the initial reaction of the patient and family is one of shock, and there may be a range of emotional responses exhibited at this stage. However, it is important to understand, that very little specific information is taken in by the patient or the family at this interview. It then becomes necessary for a rapid follow–up and frequent interpretation in lay terms by the social worker, which is supplemented in the team approach by the anesthetists, physiotherapists, speech pathologists and nurses.

Immediately prior to surgery, the patient and family meet with the intensive care and postoperative ward teams who will be caring for the patient during and after surgery. There is a sense of urgency to treat the cancer; therefore, a limited time is available between crisis intervention and surgical management.

During this brief preoperative period, information is gathered about the patient's strengths and weaknesses. This will assist the team in determining the patient's ability to cope and will highlight any areas that will require extra support. Such information gained at the preoperative assessment is of value in predicting certain particular difficulties.

Socioeconomic Data. The patient population was divided between city dwellers (81) and country town dwellers (70). The total population of the area was 1,585,000. The economic status of the patients was as follows: upper income group, ten males and two females; middle income group, 43 males and 16 females; and lower income group, 59 males and 18 females.

Information about the home environment is important, as many adjustments may have to be made. The planning of long–term rehabilitation should commence from the beginning. This task is made very difficult for more than half of the patients who live in country centers and are not adequately serviced to meet their specific needs after the surgery.

Drinking Habits. Alcohol consumption is an etiologic factor in oral cancer. ninety-three patients in this study presented with carcinoma of the oral cavity. At the time of presentation, 57 males gave a history of heavy alcohol consumption, compared with eight females. Eighteen males and ten females had minimal or no intake of alcohol. Of the 57 male alcoholics who were operated upon, ten males ceased drinking, as did two of the eight females. No patients increased their alcohol consumption as a result of surgery. Alcohol problems present their own medical and social difficulties. If a patient has had his major form of social life in bars and hotels outside the home, to the exclusion of the family, postoperative support by the family may mean disruption of their own separate, well-established pattern.

Interrelationships. Knowledge of the role and status of the patient within the family group will enable the team to predict some of the difficulties that result from the changes that occur after surgery.

Spiritual and Emotional Factors. Preoperative assessment of coping mechanisms gives an indication as to how the patient will deal with the current crisis. It is important during this phase to diagnose those patients who have an endogenous element to their depression, as they may require psychiatric intervention. The inevitable reactive depression can usually be handled by supportive methods. Knowledge of the patient's religious or spiritual predilection enables the appropriate assistance to be obtained when and if necessary. The chaplain is a very valuable member of the head and neck cancer team. Members of families who were initially anxious to be supportive later become resentful and angry at their changed lifestyle. A great deal of time and effort is needed to counsel these families, and frequent referral to other social agencies is a necessary additional support. Eleven males and two females were derelict and lived alone in substandard accommodations. Constant efforts were made to rehabilitate these patients without success. Eight of this group became terminal and depended entirely on the care provided by the Head and Neck Cancer Team.

The Preoperative Phase

Patients are admitted to the ward, usually four days prior to surgery, for the necessary medical assessment and psychosocial work-up. In addition to this, there is the physical familiarisation program during which patients are able to see all the areas of the hospital in which they will be cared for and have the opportunity to meet the staff involved.

The Early Postoperative Phase

The first three weeks are the most stressful for the patient because of: (1) the inability to communicate, especially in those patients with a tracheostomy, (2) the presence of intravenous and nasogastric tubes, and (3) frequent lengthy dressing periods necessary to care for wounds, flaps, and skin grafts.

This stage is characterised by a severe reactive depression in all patients, which is made more distressing by lack of sleep due to unavoidable intervention by the nursing staff. During this time they display antisocial reactions and become irritable. Management is based on the preoperative counselling, which attempts to explain the finite period of this stage, together with intensive support from all members of the team. The technique is reassurance with constant reference to previous discussion of problems that the patients are now experiencing. The greatest single fear is one of isolation from members of the medical and nursing staff because of the communication barriers. There is no place for the treatment of this reactive depression by drug therapy. Where there is an endogenous element, a psychiatrist should be involved in the management. This was the case with ten patients of the 151 studied.

The watershed in the postoperative phase appears to be when the patient sees progress being made—for example, when the tracheostomy is closed or at the division and insetting of flaps. All patients make considerable advances at this time. The team needs to encourage support by the immediate family members, and such support is extended to the wider family and friends as the patient recovers. One phenomenon observed during this time is the initial enthusiasm of relatives to actively facilitate the patient's efforts at written communication and sign language. However, both parties soon tire. The family members feel guilt at their desire to withdraw, and the patient becomes depressed at this additional isolating factor.

The Later Postoperative Phase

Problems occurring in the later postoperative phase include the emerging awareness of change in body image (Fig. 2), difficulties with speech, dribbling, and swallowing. As progress is made, the withdrawal of intensive nursing facilities is often associated with a feeling of rejection, because of the established dependence on these services. At this time, parallel efforts should be made to prepare the home to receive the patient. This involves the immediate family's becoming aware that they will be required to take over where the hospital leaves off in the ongoing patient care. The multidisciplinary team prepares them in the skills necessary to support the patient; care of wounds, preparation and delivery of food, timing of rest periods, mobilisation, and emotional support.

FIG. 2. A. *and* **B.** *The change in facial appearance in a 70–year old woman after excision of the left side of the tongue, floor of mouth, and left mandible, and incontinuity neck dissection. The intraoral defect has been repaired by a forehead flap.*

The Postdischarge Period

A formal postoperative assessment is made approximately three months after the patient has been discharged from hospital. The social worker coordinates contact between the community team, patient and family, and the hospital team. The patient regularly attends a Head and Neck Follow–up Outpatient Committee, where the members of the hospital team encourage the patient and family to report any problems. There emerges an understanding that the team is always available for consultation, without developing in the patient a sense of overdependence and guilt.

Problems with Speech. Distorted speech results from a combination of the excisional surgery affecting vital organs, such as the tongue, and reconstructive efforts, which may change the dimensions and sensitivity of the oral cavity. All patients from the high socioeconomic group were well motivated to pursue normality through continued speech therapy. Verbal communication played a major role in their lifestyle. On the other hand, 22 patients with oral cancer from the lower and middle socioeconomic groups had continuing problems with speech and lacked motivation to improve. Examination of this group showed them to be chronic alcoholics, had minimal or no family support, and lacked any prior dependence on verbal skills.

Problems with Eating and Drinking. Changes in the ability of the patient to eat and drink in a socially acceptable manner caused long-term problems. Those patients undergoing major intraoral reconstruction are principally affected, and the degree of functional impairment depends on the nature of excision and repair. When the patient is first removed from the protective environment of the hospital to the home, the time required for special food preparation and eating puts a strain on the family. The difficulties and increased duration of food consumption becomes an embarrassment, resulting in humiliation and sometimes withdrawal from the family group at meals. In one study, for example, four out of six males in the upper income group who had major intraoral reconstruction separated themselves from the ritual of the family meal. All patients who had composite resections and intraoral flaps required an altered diet, which was "blended" or "nonchew" because of the changed physiology of the oral cavity. The prospect of eating this food forever is depressing, as the food is often unpalatable and ultimately becomes boring.

Those patients who need to be fitted with tooth-bearing prostheses, supported on flaps, find them cosmetically acceptable but functionally inadequate and tend not to use them at all, except when they visit the doctor in Hospital. However, when prostheses are needed for obturating palatal fistulae, these are usually found to be useful.

Family Stress. The ability of families to cope with a member suffering from head and neck cancer varies immensely. The problem begins at the time the initial diagnosis is made when the family begins a grief reaction, and their ability to cope with this during the various stages determines the degree of stress. Lengthy hospitalisation completely disrupts family life and often raises feelings of anger in the wider family. The visual aspects of the excision and reconstruction, particularly in the early phases, often produce a sense of repugnance. If the relationships were conflicting prior to diagnosis of the cancer, these early stresses often make the situation worse. As the hospitalisation becomes longer and the visible impairments become obviously permanent, feelings of rejection toward the patient may develop.

The loss of communication through the excisional surgery involving the tongue, the necessary tracheostomy, and the subsequent inability of patients to communicate well in writing is also very stressful. A consistently observed early phenomenon is that the family becomes frustrated, the patient senses this frustration, and both parties withdraw. This situation is amenable to therapy aimed at producing a venting of feelings, and ultimately mutual tolerance.

Disruption of normal social behavior such as eating and drinking is a heavy burden on the family, especially when the affected person feels obliged to eat in another room, and the family is forced to make radical adjustments to socialisation in the home. There is often a deliberate physical placement of the patient around the table where he or she cannot be seen as easily by guests or children. This change of roles creates anxiety, grief, and loss of self-esteem, and may produce depression.

The situation may improve, however, the longer the patient survives. But with recurrent tumor, both patient and head and neck cancer team are plunged into a new depressive phase, and the cycle starts all over again.

Adaptation and Adjustment. Emotional adjustment becomes easier the longer the patient survives without recurrence. Such patients are gradually able to achieve a level of acceptance. Those patients, however, who suffer a recurrence of their disease have associated reactive depression. This is a particularly difficult phase for the patient and the team; all experience guilt, and the family feels let down and angry. A renewed fear of further loss of body parts is often encountered. Secondary surgery strikes a particular fear in the patient because he has previous knowledge of what he has to go through.

All patients who had forehead flaps initially complained that the residual defect worried them. It was the noticeable loss of contour of the face which provoked negative reactions and comment. The change in the facial appearance is one of the biggest problems encountered and has stimulated the surgeons in the Royal Adelaide Hospital Team to spend every effort to obviate those defects. All patients interviewed preferred a scar on the shoulder or chest wall to a scar on the forehead.

In adjusting and adapting, the emotional is intimately bound up with the physical, especially with loss of function, such as speech and swallowing, which situation is often seen as a forced return to childhood status. Some patients require long-term therapy. Ambulation often poses a problem, and many patients require a rest period during the day. Those who have had radical neck dissections show a reduction in neck movement and limitation of shoulder movement and may require physiotherapy for up to a year.

Seventy patients came from the country areas of South Australia and lived up to 500 miles from the treating hospital. These patients had a fear of isolation from the treating team. The regular review involved long journeys, and the need to throw themselves on the mercy of the wider family to provide support and temporary accommodation. This produces anxieties for the patient and stress for the family. They often need the help of voluntary agencies to assist with financial aid for this travel and accommodation.

Sexual Adjustment. Of the 93 patients with oral cancer, 27 male and three female patients had sexual problems arising out of alcoholism, which preceded the onset of the oral cancer. These problems were well established at the time of the initial diagnosis of cancer. These were the people who admitted that they had marital problems. This marital breakdown was identified by the statement that the patient had ceased to cohabit. Seven males and one female were divorced at the time of presentation. The divorced patients did not have sexual attachments, and the nondivorced patients had ceased to cohabit. Four couples who were prepared to discuss this area of their lives indicated that they had problems associated with the change in facial appearance and oral function after surgery for oral cancer. They all complained of the prevalence of odor that usually accompanies altered oronasal physiology, which placed an additional stress on their relationship.

Employment and Income. The majority of patients were not working when they developed their cancer and were already on pensions. Of those who had been working when it became manifest, about half returned to their former occupation. Initially, almost all of them returned to work in a reduced capacity because they required considerable time to build up their physical endurance.

In the Australian community there is a reluctance for employers to take people back to work who have visible signs of having had cancer. There are many real problems with patients whose speech is affected, especially if they have to answer telephones or deal with the general public. There are also many problems contrived by employers to get rid of a person who is afflicted by cancer, because of the social stigma attached to this disease. The head and neck cancer team, and especially the surgeon, is often required to intervene with employers to assure a proper return to employment of patients who are capable. Employers prefer, if possible, to dismiss patients with facial cancer or have them pensioned off. Most patients suffer a degree of financial hardship because of their cancer, which not only involves a reduced income but also shortens the working lifetime.

Psychological Trauma Caused by Fear of Cancer and Facial Mutilation. The initial interviews are of vital importance in setting the scene. Despite the full explanation with the statistical facts, indicating percentage survival and some knowledge of the proposed facial mutilation, there is always the fear of the unknown, "Will I be the one who gets the recurrence?" Almost all

patients initially say that they are not worried about disfigurement, if only the cancer can be cured.

However, those patients who do well from the point of view of the cancer refocus their attention on the deformity, thus stimulating the surgical team to strive for better results. Patients from the higher socioeconomic group were all found to be very fastidious about appearance (Fig. 3). Their demands for improved function and form have led to changes in surgical techniques.

Free bone grafts and local flaps have been supplanted by the transfer of bone and skin flaps from the hip, to reconstruct the mandible and floor of mouth using microvascular techniques. It is common for patients to be anxious about leaving the hospital, especially with regard to their changed facial appearance, a factor that contributes to feelings of social isolation. It is the role of the hospital and community team to facilitate the education of relatives and friends in understanding and supporting the disfigured patient.

FIG. 3. *A 60–year old man who had an angle–to–angle resection of the mandible, floor of mouth and anterior tongue, which was reconstructed by a composite bone and skin "free" tissue transfer from the hip, using microvascular anastomosis.*

Management of the Terminal Patient

There has been an upsurge in the emphasis on managing the dying patient in medical practice. This has been pioneered by Dr. Elisabeth Kubler-Ross.[3] Terminal care as a part of cancer therapy is vital because of the high percentage of patients who become terminal and die.

The team approach outlined previously can be extended to those patients who enter the terminal phase. Such care can extend into the home environment, or the hospital team can make special arrangements to deliver this care in the general ward setting. Patients dying from head and neck cancer suffer particular problems: (1) The disease and treatment often affects the function and appearance of the person's face. (2) Patients who die from head and neck cancer usually do so from local disease, which is often drawn out and the cancerous tissue is frequently visible, thus complicating the dying process for the patient, family, and medical attendants (Fig. 4).

The management of those patients who become terminal has been based on the knowledge of the stages of dying, formulated and described in detail by Dr. Kubler-Ross and summarised as follows:

1. *Denial* ("No, not me"). It helps cushion the impact of a patient's awareness that death is inevitable.
2. *Rage and Anger* ("Why me?"). The patient resents the fact that others will remain alive and in health. For example, God is a special target and is regarded as imposing the death sentence, arbitrarily.
3. *Bargaining* ("Yes me, but"). Patients accept the fact, but bargain for more time, mostly with God.
4. *Depression*.

   (a) ("Yes, me")—reactive talk about losses they have experienced.

   (b) Withdrawal—stage of preparatory grief: For example, ("Don't bother coming"), this affects all who have helped during stage (a) and is the precursor of peace and acceptance.
5. *Acceptance* ("My time is very close now and it is all right"). Neither a happy nor an unhappy stage, it is devoid of feelings but it is not resignation...it is really a victory.

FIG. 4. *A patient with terminal cancer. The fungating ulcerating lesion distorts his facial features.*

These stages are only a guide to understanding, and not every person goes through every stage. Many patients fluctuate between denial and acceptance throughout the course of illness; some never go beyond denial.

In accepting that the dying process can be described in this way, it is reasonable to adopt the policy of frankness with the patient and family as far as the diagnosis and prognosis is concerned. This is a continuation of the frankness that was necessarily expressed prior to the institution of any surgery, and the groundwork has usually been laid well before the patient comes into the terminal phase. After this, it depends on the patient's reaction as to how they are managed.

It has been our experience that it is better to support as much reality as the patient and family can tolerate. Whatever the level, there must be a commitment to standing by them, which gives them the confidence they need. It is here that the essential challenge comes. In practical terms, the patient must be offered all the facilities available. There is need to plan for the living stage even though the patient is dying, and the patient must be offered all the practical help possible in attending to his day-to-day affairs. He must be given the opportunity to explore his feelings, which necessitates that every member of the head and neck cancer team is made available to the patient. In particular, patients value a continuing relationship with their surgeons, thus risking eventual rejection. The surgeon has feelings of failure and inadequancy, and the patient feels guilty because he has in fact failed his surgeon by dying.

There needs to be a flexible relationship between the home, the outpatient clinic, and the hospital ward, so that the terminal patient can be managed at any time by the same group of people in a chosen situation. One of the great fears that patients have is an inability to cope at home and abandonment. This fear is relieved by a short stay in hospital, and perhaps returning home with the knowledge that they can always be readmitted on short notice. A policy of an around-the-clock service with surgeon and social worker, available to allay the patients' fears, has been found to be effective. Although this is a heavy personal commitment, it has never been abused in any way by the patients.

There are a number of aspects of the management of these dying patients which need attention.

Pain. The basis of management of the terminal phase is adequate pain relief. This is often difficult to achieve, while simultaneously maintaining a lucid conscious stage. It often becomes necessary to overcome rigid nursing procedures that are organised against the sympathetic administration of narcotics, a situation that thus highlights the necessity for close team work.

Odor. Local disease of the mouth and face is particularly offensive to the patient and people caring for them. The natural history of untreated or recurrent local disease of the mouth is one of the most unpleasant processes. The tremendous social disability makes the normally difficult dying process even more difficult, because of the complicated relationships between the person, his family, and the medical staff. The nursing care is arduous, often requiring heroic efforts on the part of the nursing staff to keep the patient in a suitable state to relate to other people. Senior nursing staff have to carefully choose those members of the nursing complement capable of withstanding the pressure. Such a situation involves mutual support so necessary in a head and neck cancer team. It is very tempting for the medical staff to reject the patient, to walk past the door, and to become depressed themselves.

Speech. Carcinoma affecting the oral cavity especially gives rise to difficulties with speech, which complicate the problems of communication. It means that attendants need to be supportive and to spend time inventing and encouraging other ways of improving communication for the patient.

Swallowing and Nutrition. These are intimately bound up with the problems of intraoral cancer and pose great challenge to the nursing staff. Each case demands individual treatment and a team that is informed of problems as they arise, so that care is consistent and continual.

Loss of Body Image. The patient who emits strong odors, is in pain, and has a fungating tumor of the face or mouth has a severe loss of self-worth. He may be repulsive not only to his family and the medical staff, but to himself as well. Such a situation requires an almost spiritual approach by those individuals charged with maintaining the dying patient's dignity.

Conclusion

The psychological implications of head and neck cancer surgery are vast. They affect not only the patient but also the family, the wider community, and indeed, the treating professionals as well. The delivery of this care involves a multidisciplinary team approach, with the hospital team extending its influence into the community. Such a team must be capable of dealing with the many and variable situations with which it is confronted.

The unpredictability of cancer, with the constant threat of recurrent disease, which produces a renewed crisis, casts its shadow over the whole scene. Whether the course of head and neck cancer results in recovery or death, it is possible to help people to preserve their self-respect and to give them a greater opportunity to control those aspects of their lives that are important to them, even perhaps to help them to develop rewarding relationships they were unable to achieve in their predisease state.[2]

The attending professionals are also given the opportunity for learning and growth, as new problems, both technical and psychological arise.

References

1. David, D. J., and Barritt, J. A.: Psycho–social aspects of head and neck cancer surgery. Aust. N. Z. J. Surg., 47: 584, 1977

2. Kaplan, B. E., and Hurley, F. L.: Head and neck cancer: A threat to life and social functioning. Social Work in Health Care, 5:51, 1979.

3. Kubler-Ross, E. K.: On Death and Dying. New York, Macmillan Publishing Company, 1969.

4. Liggett, J.: The Human Face. London, Constable and Company Ltd., 1974.

5. Macgregor, F. C., Able, T., Bryt, A., et al.: Facial Deformities and Plastic Surgery: A Psychosocial Study. Springfield, Illinois, Charles C Thomas 1953

c/o 326 South Terrace
Adelaide, South Australia 5000

Malignant Schwannoma of the Inferior Dental Nerve

By D. J. David[1], B. Speculand,[2] B. Vernon-Roberts,[3] and R. P. Sach[1]
[1]Plastic Surgery Unit, Royal Adelaide Hospital, [2] Department of Oral Pathology and Oral Surgery, The University of Adelaide and [3] Professor of Pathology, The University of Adelaide, and Head of Division of Tissue Pathology, The Institute of Medical and Veterinary Science, Adelaide.

Malignant schwannomas arise *de novo* or in patients with von Recklinghausen's neurofibromatosis, of which 10 to 15 per cent experience malignant change (De Vore and Waldron, 1961). The benign neurilemoma is believed not to undergo malignant change (D'Agostino *et al.*, 1963; Harkin and Reed, 1969). In a series of 155 cases of malignant schwannoma, 30 cases (26 per cent) were associated with von Recklinghausen's disease. This association is thought to carry a poorer prognosis since only 30 per cent of those cases associated with von Recklinghausen's disease survived 5 years in contrast to 66 per cent for the whole group (Ghosh *et al.*, 1973). Economou *et al.* (1958) have commented on the risk of venous spread of malignant schwannoma and also suggested that the ability to travel along a nerve may be due to multicentric origin simulating metastasis.

We found 11 previously reported cases of malignant schwannoma of the inferior dental nerve (Table I). Four began with a lip ulcer or tumour which was excised. In 1 instance the initial histopathology report indicated squamous cell carcinoma and this was not queried until 3 years later when the true nature of the lesion was revealed (De Vore and Waldron, 1961). The delay between initial excision of lower lip lesions and more obvious development of malignant schwannoma of the inferior dental nerve ranged from 6 months to 5 years. Seven cases were not preceded by an initial lip lesion.

The radiological findings also present 2 varieties; there may be either a cystic lesion of the mandible or a more obvious cylindrical enlargement of the inferior dental canal.

Nine other oral cases of malignant schwannoma have been reported and are listed in Table 2.

We present here 2 new cases of malignant schwannoma of the inferior dental nerve which illustrate the 2 varieties of clinical presentation and radiological findings.

Case 1. A 55-year-old man had a left mental nerve anaesthesia and a non-ulcerated swelling of his left mandible involving the buccal sulcus of the premolar area. Some 5 years previously he had received irradiation to his lower lip for a lesion diagnosed elsewhere as a squamous cell carcinoma, and on recurrence of the tumour 1 year later, had a wedge excision of his lip.

No neck nodes were palpable, but X-ray of his mandible showed a marked cylindrical enlargement of the left inferior dental canal from foramen to mandibular foramen (Fig. 1). A biopsy revealed the presence of a malignant tumour with extensive growth along a nerve trunk. The tumour was made up of spindle cells with scanty cytoplasm, arranged in interlacing fascicles and exhibiting numerous mitotic figures. Occasional multinucleate cells were also present. The appearances were those of a malignant schwannoma (Fig. 2).

Address for Reprints: B Speculand, Department of Oral Pathology and Oral Surgery, The University of Adelaide 5000, South Australia.

TABLE I

Malignant schwannoma of the inferior dental nerve

	Age	Sex	VRD	History	Treatment	Outcome
A: INITIAL LOWER LIP LESION (4)						
De Vore and Waldron	65	M	No	1. "V" excision for lip ulcer — "SCC" 3 years previously 2. Numbness and shooting pains mental foramen and ID canal (Diabetic)	Irradiation	AR 20 mo
Economou *et al.*	56	M	No	1. Excision lump lip 2 yrs previously. 2. Mental foramen and ID canal	Hemimandibulectomy	AW 9 yr
Lewis and Hart	41	M	No	1. Multiple enucleations of lip tumour 5 yrs previously. 2. Mental foramen and ID canal intracranial spread	Hemimandibulectomy	D 5 yr
Wise and Asbury	31	M	No	1. "V" excision lip sarcoma 6 months previously 2. Mental foramen and ID canal to Gasserian ganglion	Lip excision Hemimandibulectomy, Craniotomy	AW 6 mo
B: NO INITIAL LIP LESION (7)						
Bell	65	F	No	Premolar region mandible	Surgical removal and cautery	—
Cuneo and Rand	37	M	No	Burning numbness lip and chin. Mental foramen ID canal to Gasserian ganglion	Excision Cautery Craniotomy	AR 3 mo
De Larue *et al.*	30	M	No	Premolar region mandible and ID canal	Excision	AR 6 mo
Haywood	14	F	No	Mental foramen and ID canal to Gasserian ganglion	Hemimandibulectomy	D 1 yr
Ingram	4½	F	No	Decidous molar region and lingual penetration	Resection	AR 10 mo
Villa and Bunag	23	F	No	Mass	Surgical removal	—
Wilson and Walsh	2	F	No	Mandible	—	—

AW = alive and well
AR = alive and recurrence
D = died
VRD = von Recklinghausen's disease

The whole of the left half of his mandible from midline to temporomandibular joint was excised and the inferior dental nerve was sectioned as high as possible. A simultaneous block dissection of the left side of the neck was also performed. The excised mandible was decalcified and opened along the inferior dental canal. The inferior dental nerve was markedly thickened by a homogeneous grey-white tumour (Fig. 3). The tumour cells were arranged in interlacing coarse bundles, whorls and occasional herring-bone patterns (Fig. 4a). The plump spindle cells had moderate nuclear pleomorphism (Fig. 4b) and there were occasional bizarre giant multinucleate cells; mitoses were frequent in many areas. There was also a polyhedral epithelioid component with the cells arranged in solid rounded nests (Fig. 4c).

These microscopic appearances were considered to be those of a malignant schwannoma with areas of epithelioid differentiation. On electron microscopy of formalin fixed paraffin embedded material we found the frequent presence of extracellular basement membrane type material with varying amounts of collagen between the tumour cells (Fig. 5). This was considered to support the view that the tumour was of Schwann cell origin. Tumour was present in the proximal end of the inferior dental nerve at the line of surgical resection and also at the anterior line of surgical resection of the mandible at the midline where the tumour was infiltrating cancellous bone via the medial neural elements. There was no tumour present in lymph nodes or any other part of the specimen.

TABLE II

Other oral cases of malignant schwannoma

	Age	Sex	VRD	History	Treatment	Outcome
Blankenship *et al.*	52	F	Yes	Maxilla-metastasis to lungs	Irradiation	AR 6 wk
Cutler and Gross	32	F	No	Cystic maxillary and palatal lesion	Irradiation	AR 6 mo
Economou *et al.*	50	M	No	Nodule right commissure mouth	Excision	AW 2 yr
	59	M	No	Tumour upper lip	Excision	D 5yr (other causes)
	20	M	No	Left buccal mucosa	Excision	AW 3 yr
	14	M	No	Left upper lip	Excision (recurred with intra-cranial spread)	D 5 yr
	6	F	No	Submandibular mass	Hemimandibulectomy and submandibular dissection	AW4
Eversole *et al.*	47	M	No	Periosteum of mandible	Excision and hemi-mandibulectomy	AW 15 mo
Millard and Busser	42	F	No	Maxilla	Irradiation	D 4 mo

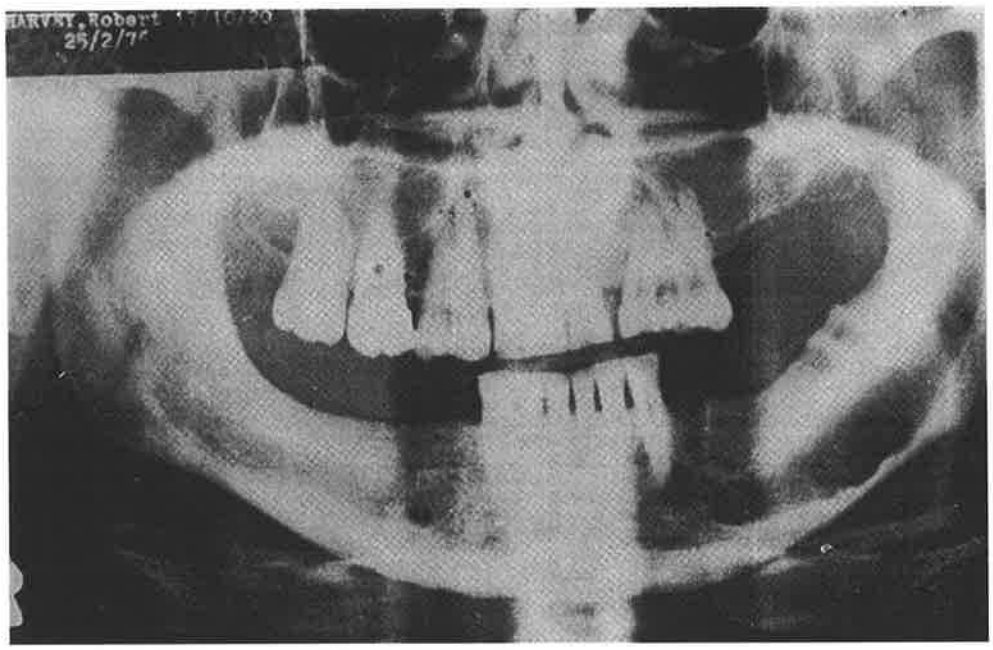

FIG. 1. *Orthopantomogram showing cylindrical enlargement of inferior dental canal and enlarged left mental foramen.*

During convalescence he had a grand-mal fit. Although no radiological or brain-scan evidence of intracranial tumour was detected, tumour was found in the trigeminal ganglion after a transcranial approach. Further surgery was futile. His cerebral function slowly but progressively deteriorated in association with intracranial tumour spread and he died 18 months after his mandibulectomy.

Slides of the previously excised "carcinoma" of the lip were reviewed; the appearances were very similar to those of the alveolar tumour and were consistent with a diagnosis of malignant schwannoma (Fig. 6).

Case 2. A 59-year-old obese alcoholic diabetic presented to his general dental practitioner with loose mandibular teeth associated with a cyst-like lesion of the anterior mandible (Fig 7a). The loose anterior teeth were removed. He returned 4 weeks later with right mental nerve anaesthesia and a swelling involving the healing sockets. A biopsy confirmed malignant schwannoma.

Radiology now showed an irregular expansion of the mandible from the left central incisor to the right canine. The margins were less well defined with superior and anterior cortical expansion. The anterior margin clearly showed irregularity due to new bone spicules (Fig. 7b).

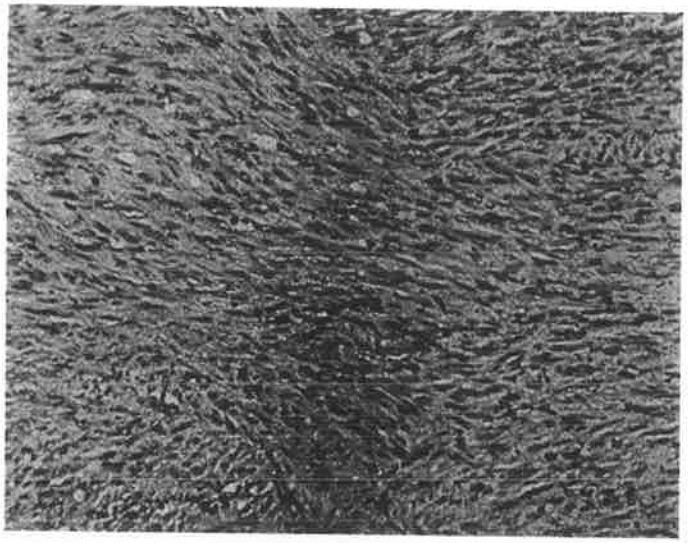

FIG. 2. Case 1. *Medium power view of tumour removed at initial biopsy. Tumour composed of spindle cells arranged in interlacing fascicles. H & E x 200.*

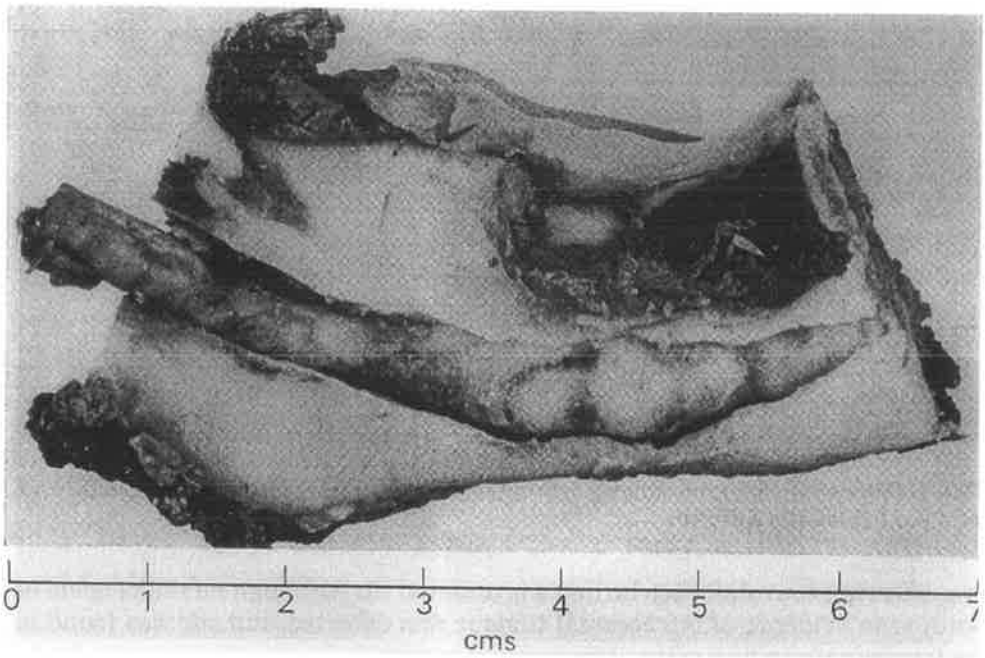

FIG. 3. Case 1. *Bisected mandible showing generalised enlargement of the inferior dental nerve with a marked nodular expansion in one area.*

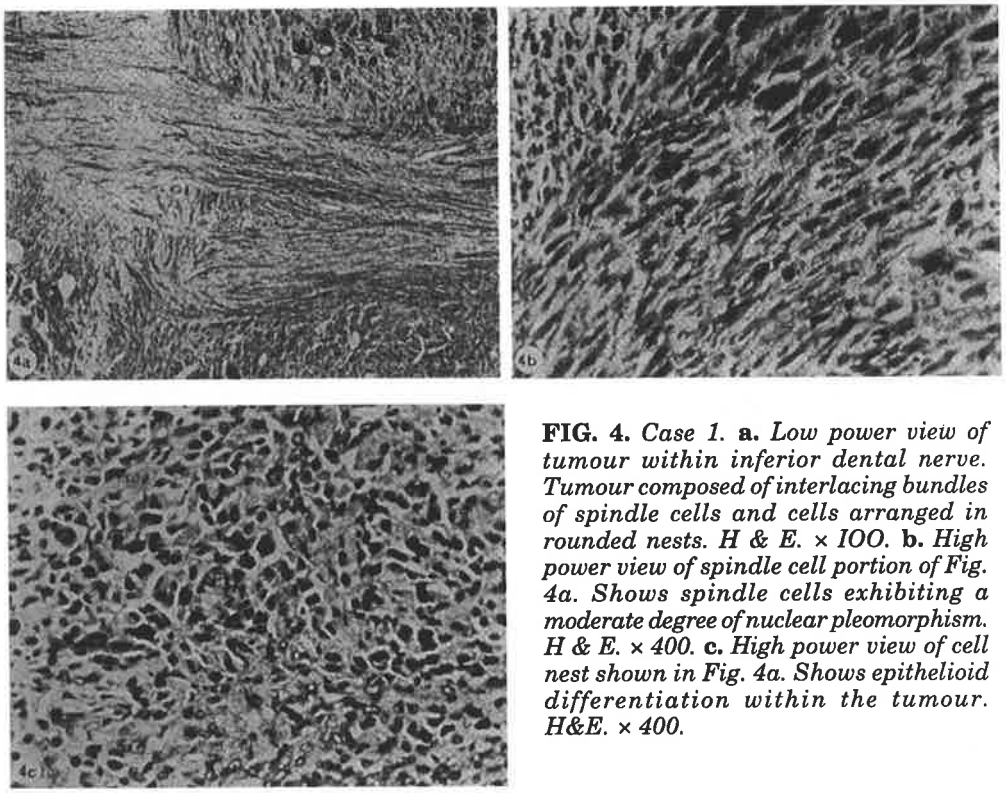

FIG. 4. *Case 1.* **a.** *Low power view of tumour within inferior dental nerve. Tumour composed of interlacing bundles of spindle cells and cells arranged in rounded nests. H & E. × IOO.* **b.** *High power view of spindle cell portion of Fig. 4a. Shows spindle cells exhibiting a moderate degree of nuclear pleomorphism. H & E. × 400.* **c.** *High power view of cell nest shown in Fig. 4a. Shows epithelioid differentiation within the tumour. H&E. × 400.*

At operation, a frozen section of the right inferior dental nerve at the lingula was obtained via an Obwegeser sagittal split approach. This was free of tumour, as was a frozen section of the mental nerve. The mandible, from right angle to left canine, was resected by a combined intra- and extra-oral approach. Immediate frozen section and subsequent paraffin section established complete excision and the patient is free of disease some 3 months postoperatively.

When the excised mandible was bisected the right inferior dental nerve was found in continuity with tumour tissue (Fig. 8), which histologically had a spindle cell growth pattern, the cells arranged in whorls and interlacing fascicles and with frequent mitotic figures (Fig. 9) consistent with a diagnosis of malignant schwannoma. The presence of extracellular basement membrane material on electron microscopy supported the view that the tumour was of Schwann cell origin.

Tumour cells were found along the incisive branch of the inferior dental nerve 5 mm from the main tumour (Fig. 10).

Discussion

The rarity of malignant schwannoma of the inferior dental nerve is supported by the absence of other recorded cases in South Australia and the total of only 13 cases now reported in the literature. Ghosh *et al.* found 115 cases of malignant schwannoma form the records of the Memorial Sloan-Kettering Cancer Center between 1920 and 1970; 16 (14 per cent) involved the head and neck. Economou *et al.* reported 14 cases of malignant schwannoma of cranial nerve origin, of which I affected the inferior dental nerve. Thus approximately 1 per cent of all malignant schwannomas may affect the inferior dental nerve.

The wide age distribution of those with inferior dental nerve lesions accords with the findings of Ghosh *et al.* for malignant schwannoma in general. However, the 13 inferior dental nerve cases and the 9 other oral cases show a sex distribution of 2M:1F in contrast to that of IM:1.4F recorded by Ghosh *et al.*

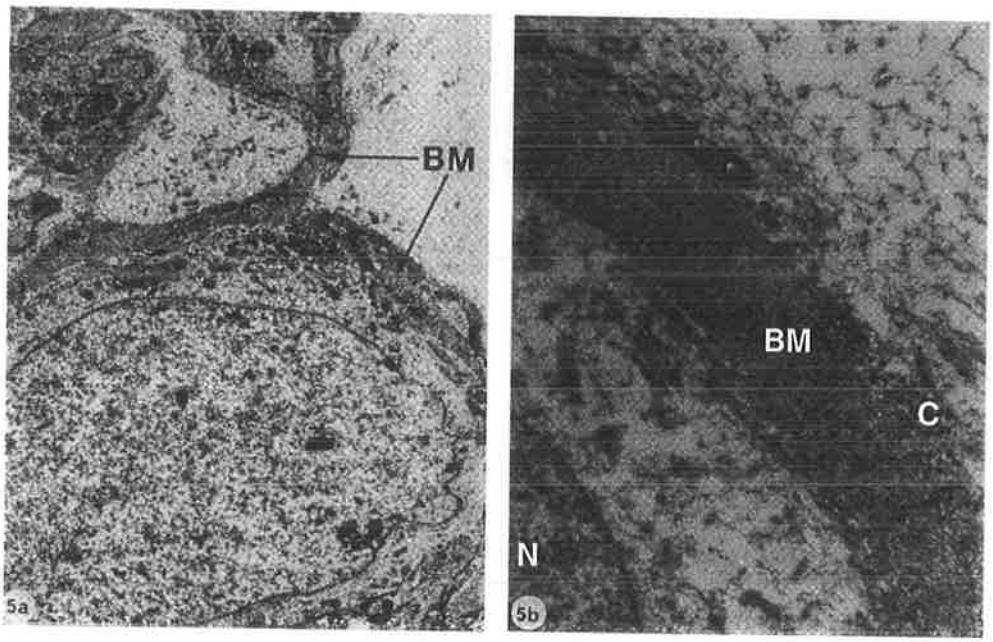

FIG. 5. Case 1. a. *Electron micrograph of formalin-fixed paraffin embedded material. Shows extracellular basement membrane type material (BM) with varying amounts of collagen between the tumour cells. × 12,000.* **b.** *Electron micrograph showing relationship between thick layer of extracellular filamentous basement membrane type material (BM), collagen fibres (C) and tumour cell nucleus (N) × 39,000.*

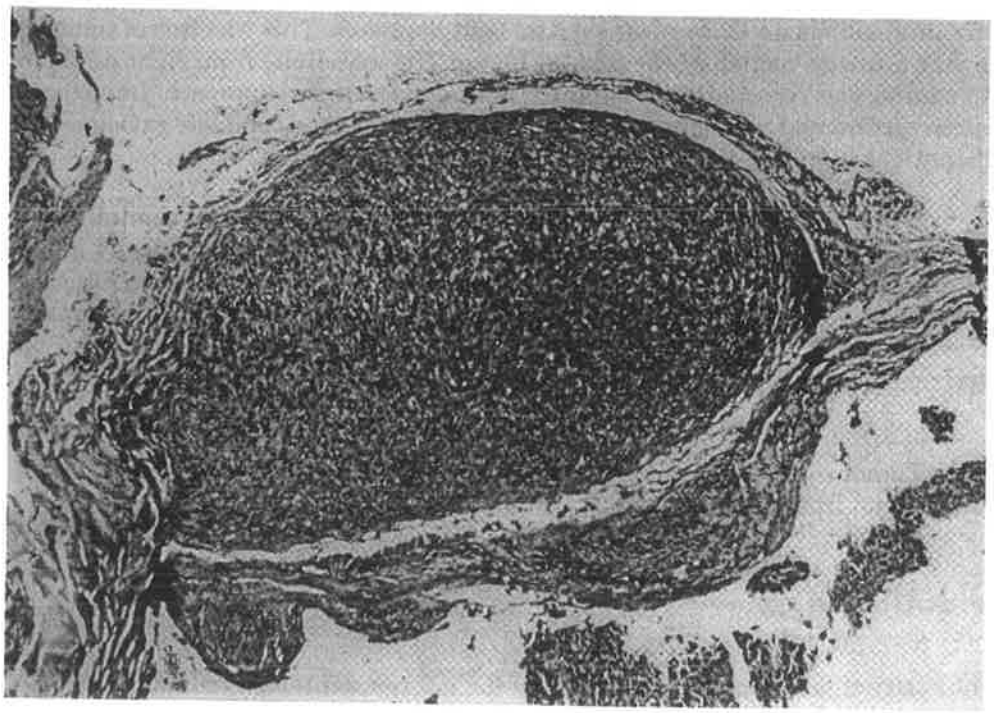

FIG. 6. Case 1. *Low power view of tumour removed from left lower lip 5 years previously. Shows a spindle cell tumour extending along a nerve trunk. H & E. × IOO.*

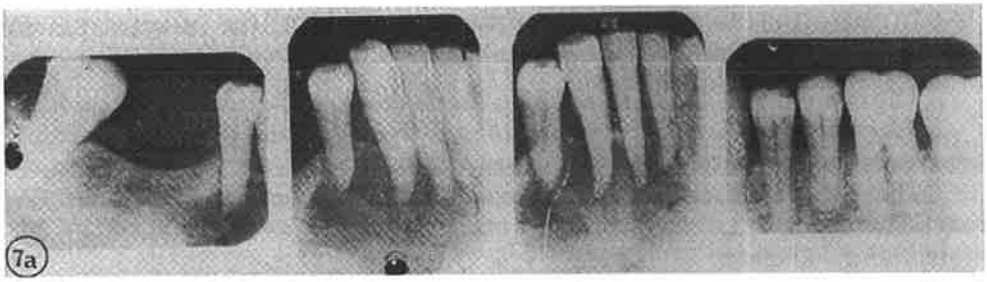

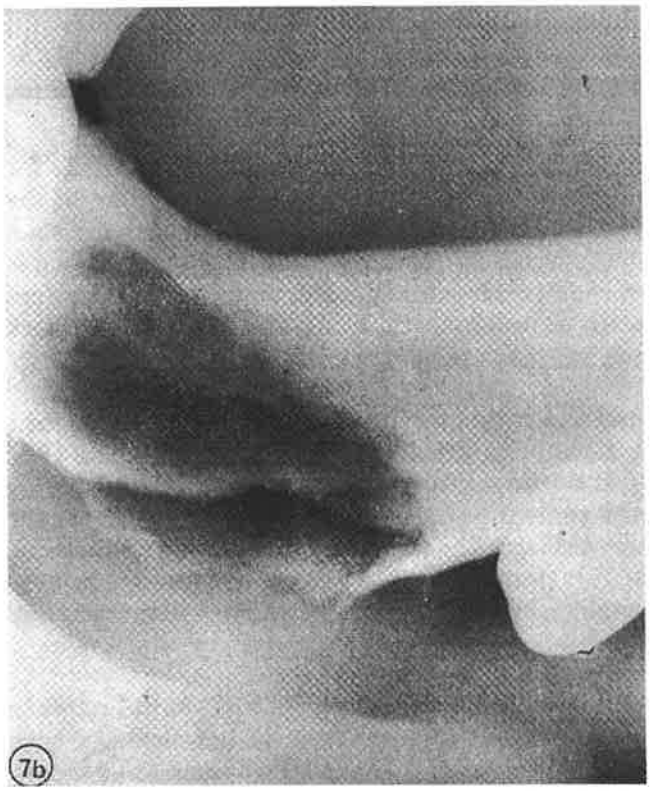

FIG. 7. Case 2. a. *Periapical radiographs of loose anterior teeth at presentation to general dental practitioner.* **b.** *4 weeks after removal of loose anterior teeth.*

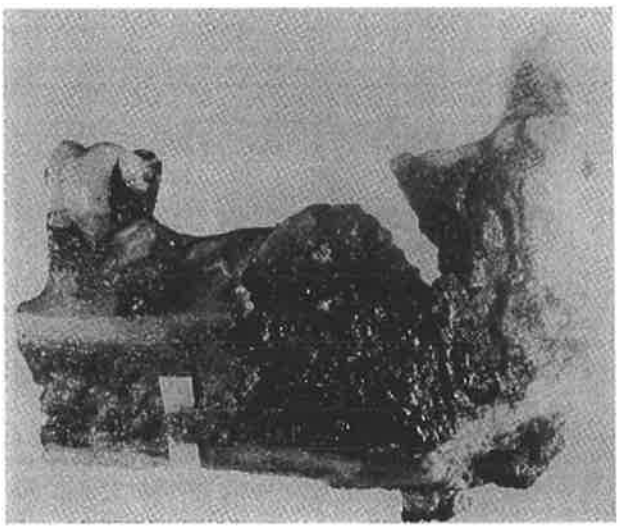

FIG. 8. Case 2. *Bisected mandible showing inferior dental nerve (elevated by white marker) in continuity with tumour contained in the biopsy cavity in the mandible.*

In each of the cases described here, the tumour fulfilled the following criteria for the histopathological diagnosis of malignant schwannoma:

The tumour was situated within a nerve trunk and extending along it;

There was unequivocal evidence of malignancy within the tumour with invasion of the epineurium;

There was electron microscopic evidence for the origin of the tumour from Schwann cells, i.e. extracellular basement membrane material and intercellular collagen.

There were some epithelioid features in Case 1 but in neither case was there any evidence of pre-existing plexiform neurofibroma, rhadbomyosarcomatous differentiation, cartilaginous metaplasia or necrosis as has been described in malignant schwannoma in other sites (Harkin and Reed; Ghosh *et al.*).

Malignant schwannoma of the inferior dental nerve may extend as far proximally as the trigeminal ganglion and distally across the midline of the mandible via intra-osseous nerve fibres supplying the mandibular incisors. Distant metastasis is by venous spread, particularly to the lungs (Economou *et al.*). Therefore an initial chest radiograph is mandatory. Since the tumour does not metastasise via lymphatics, a prophylactic block dissection of the neck probably has little place in surgical management.

The 2 cases reported and the review of the literature suggest a specific surgical approach. Frozen sections of biopsies from the mental nerve and the proximal inferior dental nerve at the lingula should first be studied. The excision can be extended anteriorly until tumour free tissue is found. If the biopsy at the lingula is positive, it is necessary to biopsy the trigeminal ganglion by craniotomy. If the ganglion is tumour free, it is possible to resect a core of tissue containing the involved nerve up to the ganglion, by a combined intracranial and extracranial approach.

The prognosis of malignant schwannoma of the inferior dental nerve is poor Only 1 case was alive and well beyond 5 years (Table 1). In contrast, Ghosh *et al* report 66 per cent 5-year survival for malignant schwannoma in general. Nineteen of their 103 cases available for follow-up study subsequently developed recurrence such that the 10-year survival rate dropped to 58 per cent Clearly when dealing with the mandibular nerve, excision is wasted if the route to the brain is not inspected at the beginning.

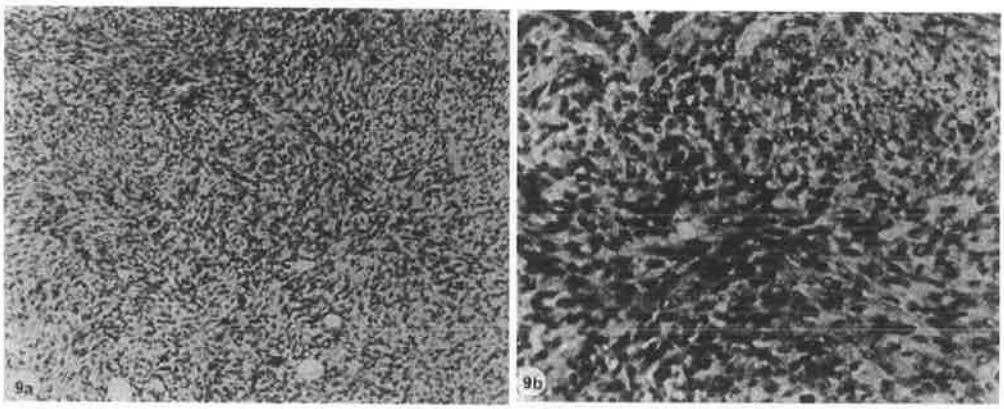

FIG. 9. Case 2. a. *Low power view of section through tumour removed from right mandible. Shows tumour composed of spindle cells arranged in whorls and interlacing fascicles with some degree of palisading. H & E × 100. b. High power view of portion of Fig. 9a. Tumour composed of slender and plump spindle cells with moderate nuclear pleomorphism and scattered mitotic figures. H & E × 400*

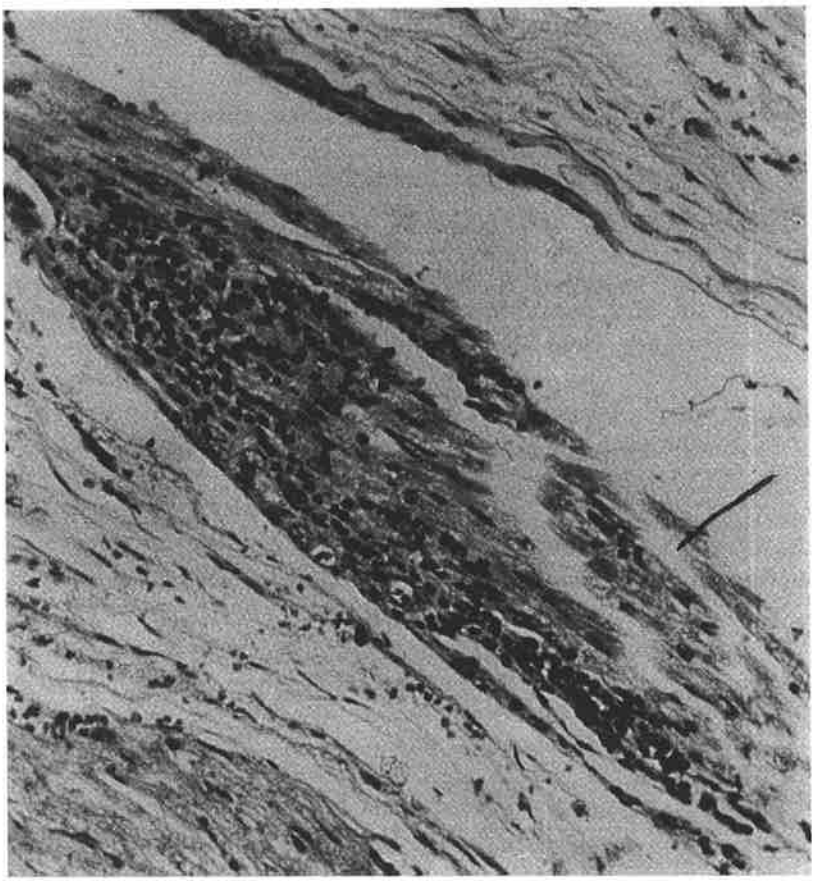

FIG. 10. Case 2. *High power view of section through inferior dental nerve showing tumour cells extending along a nerve 0.5 cm distal to the main tumour mass. H & E. × 400.*

We wish to thank Mr D. N. Robinson, Director, Plastic Surgery Unit, Royal Adelaide Hospital, for his helpful criticism of the manuscript; Dr. N. D. M. Harvey, Director, Radiotherapy Unit, Royal Adelaide Hospital, for referring Case 1; Dr. B. N. Fitzpatrick, 79 Pennington Terrace, North Adelaide, for referring Case 2; and Miss S. Williamson for the typing.

References

1 D'agostino, A.N., Soule, E.H. and Miller, R.H. (1963). Primary malignant neoplasms of nerves (malignant neurilemomas) in patients without manifestations of multiple neurofibromatosis (von Recklinghausen's disease). Cancer, 16, 1003.

2 De Vore, D.T. and Waldron, C.A. (1969). Malignant peripheral nerve tumours of the oral cavity: Review of the literature and report of a case. Oral Surgery, Oral Medicine, and Oral Pathology, 14, 56.

3 Economous, S.G., Southwick. H.W. and Slaughter, D.P.(1958). Neurofibrosarcomas of cranial nerve origin. Archives of Surgery, 77, 271.

4 Ghosh, B.L., Ghosh, L., Huvos, A.G. and Fortner, J.G. (1973). Malignant schwannoma: A clinicopathologic study. Cancer, 31, 184.

5 Harkin, J.L. and Reed, R.J. (1969). Malignant primary nerve sheath tumours. In "Tumours of the peripheral nervous system", p. 107. Atlas of Tumor Pathology, Second Series. Washington, D.C.: Armed Forces Institute of Pathology.

Experience with Surgery for Head and Neck Cancer in a Geriatric Population

J. A. Trott,[1] D. J. David[2] and R. M. Edwards[3]
Royal Adelaide Hospital, South Australia.

Twenty–five patients with head and neck cancer aged seventy years or older and who were treated surgically by the Plastic Surgery Unit at the Royal Adelaide Hospital over a six year period were reviewed. This study allowed us to formulate definitions of the terms "old age" and "debility" as contraindications to surgery in otherwise operable cases. Our management programme for patients having head and neck cancer surgery is described in detail.

Old age and debility have often been cited as high risk factors mitigating against surgery in the treatment of oral cancer and other advanced cancer of the head and neck[1].

Our experience in the Head and Neck Section of the Plastic Surgery Unit at the Royal Adelaide Hospital has led us to believe that very few patients have been rejected for surgery on these grounds alone. It was also our impression that patients fitting the category of "old and debilitated" have tolerated surgery extremely well.

Our study was designed to look at this group of patients and assess their clinical course. In addition we have tried to define the terms "old age" and "debility" in the context of these disorders.

Patients and Methods

Since 1973 all head and neck cancer patients referred for treatment at the Royal Adelaide Hospital have been assessed by a consultative Head and Neck Committee. This Committee is composed of a Radiotherapist, a Plastic Surgeon, an E.N.T. Surgeon and a Social Worker; and recommends a treatment programme for each patient referred.

The files of all patients seen by the Committee between 1973 and 1979 were examined. Those patients 70 years of age or older presenting with oral, parotid or neck cancer were selected for further study. Sixty–eight patients fitted this category. The committee judged twenty-nine cases to be inoperable on grounds of tumour pathology alone.

Thirteen had surgery recommended but performed by other specialties. One patient with an operable lesion was rejected for surgery because of intractable congestive cardiac failure. Twenty-five patients had their definitive surgical treatment performed by the Plastic Surgery Unit and these are the cases studied. All of these patients had surgery performed by the Senior Surgical Author, while all anaesthetics were given by the anaesthetic author.

1 Visiting Plastic Surgeon Royal Adelaide Hospital.
2 Senior Visiting Plastic Surgeon, Royal Adelaide Hospital
3 Director of Anaesthesia and Intensive Care, Modbury Hospital

Reprints: Mr J. A. Trott, 303 South Terrace, Adelaide 5000, South Australia

Results

Age at Operation

The age range was from 70 to 89 years with an average of 76 years. This has been broken down further as shown in Table 1.

Pathology

The overall pathology is shown in Table 2. Fifteen patients had squamous cell carcinoma of the oral cavity anterior to the fascial pillars. Eight patients had secondary deposits of squamous cell carcinoma in the neck and/or parotid gland from regional skin or an unknown primary lesion. One patient had gross recurrence of a malignant mixed tumour of the parotid. One patient had a primary squamous cell carcinoma of the floor of the maxillary antrum.

A further breakdown of squamous carcinoma of the oral cavity is shown in Table 3.

TABLE 1

*Age range: 70 to 89 years **

70 to 75 years	13
76 to 80 years	6
81 to 85 years	3
86 to 90 years	3

*Average 76 years

TABLE 2

Pathology

Primary squamous cell carcinoma of oral cavity.	15
Secondary squamous cell carcinoma in neck or parotid.	8
Squamous cell carcinoma of antrum.	1
Malignant mixed tumour of parotid..	1

TABLE 3

Squamous cell carcinoma of oral cavity

	No neck disease clinically	Ipsilateral lymph node disease—not fixed	Total
T1	4	-	4
T2	5	2	7
T3	4	-	4
Total	13	2	15

Clinical Features

The operations performed are described in Table 4. The intention in each case was a curative procedure

The preoperative general status of these patients is shown in Table 5.

The time in hospital ranged from eight to 72 days with an average of 31 days.

The postoperative complications are listed in Table 6.

Haematoma was listed only where operative release was required. Postoperative survival times and modes of death are shown in Tables 7a, 7b and 8. Five patients died from their disease. These deaths occurred between eight months and three and a half years following surgery with the age at death ranging from 72 to 91 years.

Seven patients died from disease other than their cancer or factors relating to their surgery. These deaths occurred between two months and five years from the time of surgery, with an age range from 74 to 89 years. Interestingly, one patient with carcinoma of the coral cavity subsequently developed carcinoma of the caecum with multiple liver metastases.

At the time of review, 13 patients were alive and well. The time from operation varied from ten months to five years and their ages ranged from 72 to 91. Only one patient was found to have a recurrence although he was otherwise well ten months after surgery.

The tour surviving patients with squamous cell carcinoma of the oral cavity were assessed to determine oral function and these results are shown in Table 9.

Discussion

We believe that these results confirm the place of surgery in the treatment of head and neck cancer in the elderly. The surgeon and anaesthetist are the apex of the head and neck cancer team and we believe that this team approach has contributed to minimising surgical morbidity. There are many points which are important in managing these patients and these are discussed in detail below.

Once it has been decided that the patient's tumour is operable, the patient's ability to tolerate the intended procedure is assessed. While the decision to proceed must rest with the surgeon and the anaesthetist, when general systemic disease exists consultation with an appropriate physician is arranged. The answers to the following questions are required: 1. What is the nature of pathology? 2. How much does it affect normal physiological function? 3. Can the disease be alleviated by medical treatment and if so, by what means and what time span will be required. The following investigations are required as a routine: complete blood screen; chest X–ray examination; electrocardiograph; biochemical screen; coagulation studies; arterial blood gas analysis.

Investigations occasionally required include: culture of coloured sputum; pulmonary function studies; serum digoxin for patients on therapy.

TABLE 4

Operations performed

A. Oral Cancer Group	
1. Excision with direct closure/local mucosal flap split skin graft.	5
2. Excision with direct forehead or delto-pectoral flap repair	6
3. Excision with in-continuity neck dissection and immediate flap repair.	4
B. Secondary Deposits in Neck and/or Parotid Gland	
1. Radical neck dissection.	5
2. Superficial parotidectomy with incontinuity neck dissection.	3
C. Malignant Primary of Parotid Gland	
1. Total parotidectomy including external ear with large scalp rotation flap.	1
D. Antral SCC	
1. Maxillectomy and orbital exenteration	1

TABLE 5

Preoperative General Status

*Fit for age	10
Ischaemic heart disease including hypertension and previous myocardial infarction	8
Mild congestive cardiac failure	1
Chronic obstructive airway disease	4
Diabetes	1
Chronic renal failure	2

*No systemic disease

TABLE 6

Postoperative Complications

Chest infection	5
(One patient required IPPV and treatment for septicaemia)	
Oral Fistula	1
Jaundice	1
Renal failure	1
Haematoma	2
Septicaemia from UTI	1
Non-malignant sinus	1

TABLE 7A

Postoperative Survival Times

death from disease [5]

Age at death [years]	Time from operation [years]	Cause of death
75	11 months	Broncho pneumonia and cachexia
74	8 months	Malignant cachexia
80	9 months	Trismus cachexia and pneumonia
91	3 years 7 months	Gross local recurrence and pneumonia
72	18 months	Trismus and broncho-pneumonia

TABLE 7B

Postoperative Survival Times
death from other causes [7]

Age at death [years]	Time from operation [years]	Cause of death
81	5 years	Myocardial Infarction and Congestive Cardiac
77	2 years	Myocardial Infarclion
81	15 months	Carcinoma of caecum with multiple metastases
75	2 months	Cardio Vascular Accident
82	3 months	Pneumonia
74	22 months	Chronic airways disease/ respiratory insufficiency
89	11 months	Broncho-pneumonia

TABLE 8

Postoperative Survival Times
Alive and Well [13]

Age at Review	Time from operation
91	2½ years
81	4 years
72*	10 months
76	5 years
76	26 months
72	2 years
77	2½ years
82	4½ years
76	4 years
76	3 years 10 months
72	15 months
75	15 months
77	2 years

The following problems require attention:

Hypertension

Aggressive therapy for hypertension is not carried out in this age group.

Cardiac failure

Those patients who do not respond to diuretics and bed rest are digitalised.

Pulmonary Function

Exercise tolerance, the ability to cough and the amount and nature of sputum are the main determinants of satisfactory pulmonary function.

Physiotherapy and appropriate antibiotic therapy are necessary to reduce the amount of infected sputum. These patients will tolerate surgery quite well in the presence of marked reduction in the usually accepted pulmonary function measurements such as vital capacity and forced expiratory volume. An elevated arterial carbon dioxide tension is of bad prognostic significance.

Liver Function

Abnormal liver function as detected by a biochemical screen does not contraindicate surgery if these parameters return towards normal when alcohol is prohibited and a nutritious diet provided. A prolonged prothrombin time may respond to Vitamin K therapy.

Cerebral Function

Apart from routine neurological examination a social work assessment provides valuable insight into the patient's ability to cope with his surroundings.

Airways

Mobility of tongue, jaw and neck is assessed. During this investigative phase the patient is discouraged from smoking, prohibited from taking alcohol and encouraged to take a nutritious diet. Vitamins, particularly thiamine are given. As these patients usually have a long history of smoking, alcoholism and malnutrition, this is most important.

Induction of Anaesthesia

Difficulty in intubating the trachea in these patients is quite common. Tumour in the mouth, previous surgery and radiotherapy may be the cause of intubation problems, though in practice there seems no reliable method of determining whether or not this will be so in the individual patient. However severe trismus will occasionally but not reliably relax during anaesthesia.

In some patients intubation difficulty increased with the passage of time due to increasing rigidity in the floor of the mouth. That a patient was easily intubated on one occasion was no guarantee this would be so weeks or months later.

As the result of intubation failure may be catastrophic in the paralysed anaesthetised patient it is wise to expect problems in every case.

A simple and safe solution is to pass the endotracheal tube under local anaesthesia in a sedated but cooperative patient. The method is to inject four mls of four per cent lignocaine into the airway through the cricothyroid or cricotracheal membrane after diazepam 10 mg has been given slowly intravenously. After a few minutes the patient is instructed to open the mouth wide and breathe deeply. The warmed and lubricated laryngoscope is inserted as gently as possible and the tube passed using the sound of air washing back and forth as a guide to the appropriate direction should vision be obscured. If nasotracheal intubation is required the nose can be anaesthetised by painting

with 10% cocaine paste.

During intubation, gentleness and words of encouragement are required. There has been no recall of these events in elderly patients when diazepam has been used. If general anaesthesia is now induced with narcotic drugs, nitrous oxide and halothane, an assessment can be made of the dosages required to produce adequate depth. This varies markedly in the elderly alcoholic.

All patients having major cancer procedures involving the floor of the mouth and the mandible, have a tracheostomy performed as a first step. The stoma is placed below the first or second tracheal ring, a Bjork flap is constructed and the tracheostomy tube used is the largest which will fit comfortably. Postoperatively tracheostomy patients are nursed in an intensive care situation for 24 hours.

Maintenance of Anaesthesia

Maintenance of anaesthesia is achieved by means of a nitrous oxide, narcotic drugs, curare sequence and mechanical ventilation. Halothane and droperidol increase the depth of anaesthesia and aid in the production of a modest degree of deliberate hypotension. A reduction of mean pressure by one third can readily be achieved and this usually results in a reduction of blood pressure in elderly hypertensive patients to 100-110 mm Hg systolic. Direct arterial monitoring is useful but not essential. In particularly frail patients deliberate hypotension is confined to those parts of the dissection associated with heavy blood loss allowing the pressure to rise in between. The social worker assessment is repeated after convalescence is complete. This assessment has proved a most reliable indicator of any cerebral damage resulting from deliberate hypotension. None of the group studied was found to have increased cerebral impairment. Blood loss estimation is inaccurate as losses on numerous wet packs and swabs is difficult to measure. In addition, blood may be hidden on drapes, under the patient or may find its way into the stomach. Adequacy of transfusion is confirmed by central venous and arterial pressure measurements. The development of cardiac failure in elderly patients with a history of heavy alcohol ingestion is a likely event and may be heralded by a rise in central venous pressure, a fall in pulmonary compliance and a drop in arterial oxygen tension before there is a fall in arterial pressure. Continuous central venous monitoring will allow detection at an early stage. Calcium chloride is an extremely useful cardiotonic agent. Occasionally cardiac glycosides may be required.

A normal body temperature is maintained by warming fluids for infusion and by means of a warm water mattress. Hypothermia is to be avoided. Regular arterial blood gas analysis will confirm the adequacy of ventilation. Arterial oxygen tension is best kept in the region of 35-40 torr. The development of a metabolic acidosis suggests that tissue perfusion is poor and that the blood pressure is too low.

Penicillin 3g intravenously is given to non allergic patients at the time the bone is divided and continued after the operation for seven days.

Postoperative Management

These patients are nursed in an intensive care situation for at least 24 hours after tracheostomy or for as long as a nasotracheal tube is used. Attention to the following problems is required:

Respiratory Infection

Hypoxia resulting from atelectasis and infection is common and occurred in five patients. The presenting symptom is usually restlessness and confusion. These both warrant an immediate chest X-ray examination and blood gas analysis.

TABLE 9
Assessment of Oral Function of Four Surviving Patients with Squamous Cell Carcinoma of Oral Cavity

	Age	Operation	Eating	Speech	Saliva
T3 SCC retromolar	70	Hemimandibulectomy Hemiglossectomy Innervated Deltopectoral flap	Good	Good	Good
T3 SCC Floor of Mouth	77	Hemimandibulectomy Hemiglossectomy Innervated Deltopectoral flap	Excellent	Excellent	Good
T1SCC Side of Tongue Nib neck	73	Hemiglossectomy and Neck dissection	Fair	Fair	Good
T1 SCC Side of Tongue	80	Hemiglossectomy	Excellent	Excellent	Excellent

Atelectasis may be transient and recurrent so that confusion and restlessness may be intermittent. Repeated examination may be required for its detection and appropriate physiotherapy will usually solve the problem. The misdiagnosis of atelectasis as delirium tremens and the consequent use of sedatives may be disastrous.

Blood Volume Replacement

Frequent haemoglobin estimations and "top up" transfusions may be required.

Septicaemia

Septicaemia is more likely to develop with the presence of raw surfaces. It is prevented by good surgical technique which allows early closing of the wound.

Liver Dysfunction

A transient rise in liver enzymes is common. Jaundice occurred in one patient. Further surgery is not contraindicated, especially if it results in the closure of open surfaces.

Surgical Principles

We believe the following to be important.

Adequate Tumour Excision

While not always guaranteeing cure this gives the best chance of survival plus uncomplicated healing. Malignant sinus and fistula formation will follow rapidly if excision is incomplete.

Reconstructive Details

Maximum function and rapid primary healing are the aims. These shorten the hospital stay, decrease the postoperative complication rate and facilitate psycho-social rehabilitation. Expertise in flap surgery is mandatory with attention to sculpturing the flap into the mouth to allow easy cleaning, improve tongue mobility and prevent salivary and food pooling. We believe that an innervated flap is of considerable help in oral lining reconstructions and whenever possible the pedicle of such a flap is de-epithelialised to avoid fistula formation and a second stage operation. The composite free flap will solve many of the problems of anterior mandibular resection. The four surviving oral cancer cases reviewed showed no functional problems of note and all achieved complete psycho-social adjustments as judged by our social worker.

Conclusions

Meaningful survival figures cannot be deduced from a series of this size. The operative mortality in the group studied was zero. It is well accepted that the most important factor in deciding the form of treatment for head and neck cancer is the tumour pathology.[3] However, surgeons may decline to operate on old or debilitated patients in whom surgery offers the best chance of cure, because of a fear of operative mortality or functional disability.

From our experience presented above, we believe that old age per se is not a contraindication to surgery. We have defined debility as being either physical or mental, the latter being assessed by our social worker.[4]

We define mental debility as existing in those elderly patients in whom, because of their mental state, the nursing problems following surgery can be predicted to be greater than those of nursing the patient with his disease.

We define physical debility as being gross failure of a single body system or mild failure of multiple body systems which will not respond to preoperative medical measures. In our experience these contraindications are fairly rare and surgery, when indicated, is extremely well tolerated in the over seventy age group.

References

1 Gaisford JC. Tumours of the head and neck—the who, when and how treatment. Plast Reconstr Surg 1965; 36: 447–453

2 David DJ. use of innervated delto-pectoral flap for intra oral reconstruction. Plast Reconstr Surg 1977; 60: 377–380.

3. Fleming WB, Long RM, Kerr RC. The management of squamous cell cancer of the mouth and throat Aust NZ J Surg 1978; 48: 607–610

4. David DJ, Barritt JA. Psychosocial aspects of head and neck cancer surgery Aust NZ J Surg 1977;47: 584–589

SURGICAL TECHNIQUES

Technical Aspects of the Cranio-facial Approach to Tumours of the Orbit and Skull Base

David J. David,[1] Donald A. Simpson,[2] Tor G. Henrikkson[3] and Mark H. Moore[4]
South Australian Cranio-Facial Unit, Adelaide Children's Hospital and Royal Adelaide Hospital, Adelaide, South Australia

During the period July 1980-August 1987, 21 patients required cranio-facial extension of conventional neurosurgical osteotomies for tumours of the skull base and orbit. Five different types of combined osteotomies are described. Their applications to the treatment of various tumours and the subsequent reconstructions are presented and discussed.

Key words: anterior cranial fossa, cranio-facial osteotomies, infra-temporal compartment, malignancy, middle cranial fossa, orbit, skull base, surgical approaches, surgical treatment, tumour.

Introduction

Many lesions of the skull base can be approached by the standard craniotomies evolved by neurosurgeons over the last century. However some areas remain inaccessible when approached through conventional neurosurgical exposures.[1-3]

Cranio-facial surgery offers the advantage of extending osteotomies into the facial skeleton to assist tumour resection. The temporary removal of cranio-facial structures provides better surgical access and facilitates subsequent reconstruction.[4-7]

There are a number of indications for a combined cranio-facial approach: tumours in regions where access is difficult; tumours adjacent to vital structures which require clear visualisation; tumours requiring *en bloc* resection with a margin of normal tissue; and tumours requiring good exposure to define deep extensions.

The objects of this review are to present the application of cranio-facial techniques which are complementary to established neurosurgical techniques in the management of skull base and orbital tumours, and to discuss five different osteotomy patterns, illustrating the exposure provided and the subsequent reconstructions.

[1]FRCS. FRCS(E), FRACS; Head, SACFU. [2]D. Univ., FRCS, FRACS: Neurosurgeon, SACFU. [3]MD Past Cranio-facial Fellow SACFU. Present address: University Hospital of Uppsala, Sweden. [4]MB, ChB; Cranio facial Fellow, SACFU.

Correspondence: Dr M. H. Moore, South Australian Craniofacial Unit, North Adelaide 5006, South Australia, Australia.

Accepted for publication 26 November 1987.

Methods

A retrospective review of all skull base and orbital tumour resections performed during the period July 1980-August 1987 at the Adelaide Children's Hospital and the Royal Adelaide Hospital revealed 21 patients who required a combined cranio-facial approach for their tumour resection. The types of cranio-facial osteotomies required in these 21 patients were: unilateral fronto-orbital flap osteotomy; fronto-orbital crown osteotomy; fronto-orbitomalar osteotomy; naso-orbito-maxillary osteotomy; and temporo-malar-mandibular osteotomy.

Unilateral Fronto-orbital Flap Osteotomy

After turning down a bicoronal scalp flap, the temporalis muscle is detached and subperiosteal dissection of the orbital roof performed. Burrholes are placed in the temporal fossa just behind the lateral orbital margin; just above the medial end of the supraorbital rim and in the midline of the frontal hairline.

The unilateral bone flap containing the frontal bone, superior orbital margin and the adjacent roof of orbit can then be osteotomized and removed in one piece (Fig. 1).

Extradural dissection of the floor of the anterior cranial fossa allows piecemeal removal of the remainder of the orbital roof, including the roof of the optic canal. This allows exposure of tumours of the deep medial compartment of the orbit, the orbital apex, and orbital tumours with an intracranial extension.

After tumour removal, wound closure requires a water-tight dural repair, replacement and fixation of the bone flap, and if necessary, a free bone graft to reconstruct the orbital roof.

Fronto-orbital Crown Osteotomy

After raising a bicoronal scalp flap and a bifrontal bone flap, the extradural dissection of the orbital roof is performed. The fronto-orbital crown is then osteotomized, comprising the supra-orbital margins, the bases of the frontal processes of the zygomatic bones and the anterior orbital roof and laterally as far as needed (Fig. 2).

If the olfactory nerves are divided at the level of the cribriform plate, and extradural dissection carried posteriorly, in combination with removal of such midline structures as the clivus, the potential exists for exposure of the skull base in the midline compartment from the nasion anteriorly to the anterior edge of the foramen magnum posteriorly. This provides access to the cribriform plate, olfactory groove, ethmoidal roof and labyrinth, medial orbital walls, spheroid and clivus areas and the pituitary gland. Traditionally, some of these areas have been regarded as surgically inaccessible and there has been a tendency to avoid operating on tumours within them, or to carry out piecemeal removal.[7]

Simultaneously the dura from the floor of the two lateral compartments of the anterior and middle cranial fossae is elevated, providing access to the optic canals, spheroidal ridges and fissures.

Wide tumour resection will remove most of the tissue between the sub-arachnoid space and the nasopharynx. Closure of this communication between the intracranial cavity and nasopharynx requires the transfer of galeal frontalis muscle flaps and pericranial flaps,[7] the bony defects being closed with split calvarial bone grafts or rib grafts (Fig. 3).

Fronto-orbito-malar Osteotomy

The bicoronal scalp flap is extended down to the tragus on the side of the lesion, and subperiosteal dissection of the supra-orbital margin and the orbital roof is

FIG. 1. *Fronto-orbital flap osteotomy, where the frontal bone, the superior orbital margin, and the immediately adjacent roof of the orbit are mobilised.*

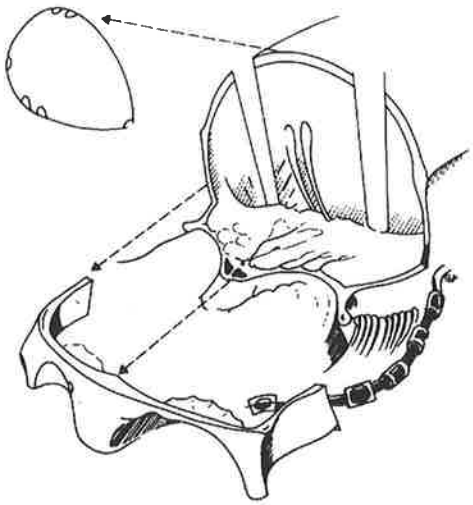

Fig. 2. *Fronto-orbital crown osteotomy mobilizes the lateral and anterior aspect of the anterior fossa as well as the anterior part of the orbital roofs.*

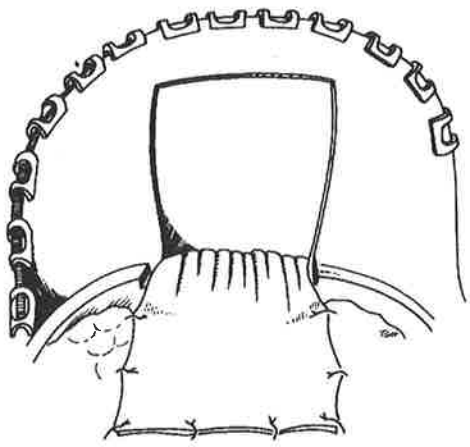

FIG. 3. *A pericranial and galeal frontalis flap can be designed from the reflected bicoronal skin flap. It is sutured over the bone grafts, thus bridging the defect in the anterior fossa.*

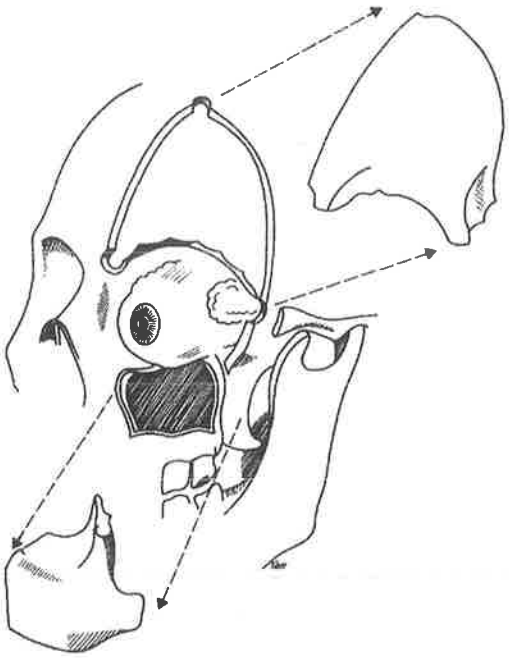

FIG. 4. *A fronto-orbito-malar osteotomy removes both the fronto-orbital flap and the malar body.*

performed, exposing the temporal fossa, lateral orbital wall, and the zygomatic region.

A fronto-orbital-malar free bone flap can now be fashioned and removed in one or two pieces, providing access to the orbit and the pterygo-maxillary fossa (Fig. 4). In some instances the malar may be left attached to the masseter muscle

Extradural dissection allows the middle fossa and foramen rotundum to be approached. The lachrymal gland and postero-lateral aspect of the orbit are accessible and the orbital dissection can be extended towards the infra-orbital nerve and orbital fissures.

Via the infra-temporal fossa, the pterygomaxillary region can be exposed and this provides access to the infra-temporal portion of the spheroid bone, the pterygoids and the posterior aspect of the maxilla. A further extension into the parapharyngeal region then becomes possible.

Complete tumour resection is performed under direct vision. The bone flap can be replaced but an additional bone graft is often needed.

Naso-orbital-maxillary osteotomy

After the standard bicoronal scalp flap and dissection of the pericranium down to the orbits, a frontal bone flap is raised. The dura is elevated from the floor of the anterior fossa and the cribriform plate. If possible, one half of the cribriform plate and its olfactory filaments are left, avoiding total anosmia. Extra-dural dissection is carried back to the lesser wing of spheroid and the anterior wall of the middle fossa.

The front wall of the maxilla is exposed by a Weber-Ferguson incision, but in cases with advanced skin malignancy, a wide skin excision may be required.

The osteotomies pass along the anterior fossa floor and include midline structures such as the cribriform plate, the lateral mass of the ethmoid bone and the orbital apex. If necessary, lateral extension may include the roof of the temporal fossa and a segment of the fronto-temporal vault. Anteriorly the orbital framework including the nasal bone is resected with the osteotomy extending down into the maxilla and passing just above the dental apices (Fig. 5).

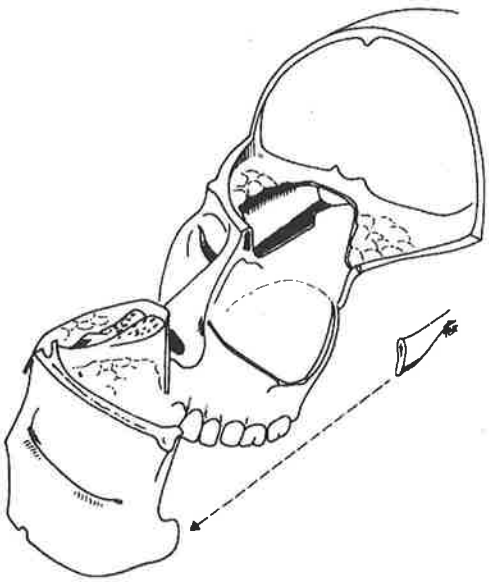

FIG. 5. *A naso-orbito-maxillary osteotomy of the central face includes the nasal skeleton, the orbital cone, the maxilla and midline structures.*

Subsequent reconstruction may be extensive and is dependent upon the type of tumour resected and the amount of soft tissue available. It is imperative again that the naso-pharyngeal area is carefully separated from the anterior fossa, using local fascial and muscle flaps to prevent intracranial spread of infection from the nasopharynx.[7]

Temporo-malar-mandibular osteotomy

A face lift incision is extended into a coronal incision to provide access. The skin flap is raised in the sub-cutaneous layer and the facial nerve dissected free to permit total parotidectomy. The temporal fossa is then cleared down to the malar arch which is osteotomized (Fig. 6). The mandibular ramus dissected and cut horizontally just above the mandibular foramen. After detaching the lateral and medial pterygoid muscles from the lateral pterygoid plate and the greater wing of spheroid, the pterygomaxillary and infra-temporal vascular and neural structures can be identified.

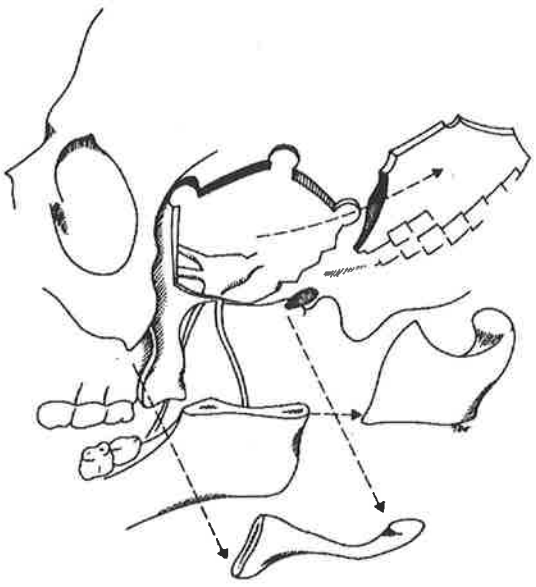

FIG. 6. *A temporo-malar-mandibular osteotomy includes the zygomatic arch, the ascending ramus of the mandible and a temporal bone flap.*

If the tumour has invaded the mandibular or maxillary branches of the trigeminal nerve, they are sacrificed to allow complete tumour removal. However the most critical structure to preserve from injury is the internal carotid artery.

After removing a temporal bone flap the middle fossa dura is elevated and the dissection carried medially to the foramen spinosum and the foramen ovale in the greater wing of spheroid. This enables the surgeon to protect the trigeminal nerve and the internal carotid artery.

Although the trigeminal nerve is at risk in this approach, many of the skull base tumours are benign and such excellent exposure assists complete tumour resection. This approach also provides access to the nasopharynx and maxillary sinus for deeper tumour extensions.

Results

Fronto-orbital Flap Osteotomy

This approach was used in five patients during the 7-year period. In four of these patients, lesions were localised to the orbital contents. Their diagnoses included neurofibroma, non-Hodgkin's lymphoma, meningioma and squamous cell carcinoma. The fifth patient had fibrous dysplasia with orbital wall involvement which required reconstruction with a composite micro-vascular iliac graft including bone. In the other cases however, the osteotomized portion of bone was replaced with interosseous wire fixation.

One patient had a minimal cerebrospinal fluid leak for 12 weeks which only required antibiotic prophylaxis.

Fronto-orbital Crown Osteotomy

There were six patients with extensive tumours exposed by this procedure.

One patient had an aesthesio-neuroblastoma occupying the central anterior fossa region and the ethmoids. Another patient suffered from an aggressive juvenile fibroma involving the whole of the maxilla, ethmoids, lesser wing of spheroid and orbit.

One teenager presented with a large nasopharyngeal angiofibroma, with computer tomography and magnetic resonance imaging scan evidence of involvement of the ethmoids and spheroid sinuses with extension into the cavernous sinus. This exposure both confirmed the extensive nature of this lesion, and demonstrated the non-involvement of the cavernous sinus, thus allowing complete resection.

A fourth patient had this approach employed in the exposure of an extensive meningioma of the floor of the anterior cranial fossa.

In all cases, pericranial and galeal muscular flaps were used to cover the bone grafts reconstruction and separate the intracranial cavity from the nasopharyngeal space (Fig. 3).

The two remaining patients in this group developed communications between the extra-dural space and the nose. One patient with extensive fibrous dysplasia developed an infection which involved the bone grafts, some of which sequestrated, requiring surgical removal 15 weeks after the initial procedure. The dead space under the frontal lobes was then filled with a latissimus dorsi free muscle flap with good result.

The fourth patient had a recurrent seller chordoma and she died 11 months after operation from continued tumour growth.

Fronto-Orbital Malar Osteotomy

This approach was used in six cases. Three had orbital tumours, two had extensive fibrous dysplasia involving the greater wing of the spheroid and petrous temporal bones and the last had a well differentiated orbito-maxillary teratoma. No intra-operative or postoperative complications were recorded.

Naso-Orbital Maxillary Osteotomy

One patient with a poorly differentiated squamous cell carcinoma involving the orbit and nasal sinuses required this osteotomy. The complete orbital cone with adjacent midline structures were removed *en bloc* with overlying skin measuring 140 x 90 mm^2. The tumour was found to infiltrate the optic nerve and excision was not complete. The patient died 12 months after the procedure.

Temporo-Malar-Mandibular Osteotomy

A patient with a chondrosarcoma of the left infratemporal fossa required a large *en bloc* resection combined with a radical neck dissection. The operative specimen included the temporalis muscle, the proximal fragment of the mandible with its attached masseter muscle, the deep portion of the parotid gland and the temporomandibular joint. The mandibular branch of the trigeminal nerve was divided and the external carotid artery ligated and divided. The excision was complete. The adjacent sterno-mastoid muscle was divided distally and rotated upwards as a flap to fill the cavity. The post-operative course was uneventful.

A similar approach was adopted in a patient who required palliation for a recurrent ulcerated adenocystic carcinoma of the retromolar trigone which extended through the infratemporal fossa, pterygomaxillary fissure to the base of the skull. Mandibular and intra-oral reconstruction was performed using a split iliac free flap, the temporal calvaria being reconstituted with split rib grafts.[8]

The excision was incomplete, but 6 months postoperatively he remains free of pain and macroscopically recurrent disease.

The final case was a young girl with a Ewing's sarcoma of the infratemporal fossa, recurrent after full dose chemotherapy and radiotherapy. Having employed this approach, intra-operative frozen section confirmed extensive tumour involvement of the trigemonal ganglion and a decision was made not to proceed further.

Discussion

It has been suggested that good exposure promotes *en bloc* tumour resection and thus a greater possibility for a wide free margin and radical extirpation.[7] On the other hand piecemeal removal may be appropriate, as many skull base tumours are known to be benign.[9] Both procedures however are facilitated by a wide exposure.

Cranio-facial extensions of established neurosurgical osteotomies give wide exposure which offers better visualisation of the vital structures traversing the skull base, better mechanical advantage to the surgeon and facilitates the use of the operating microscope. Any danger to the dura or communication with the nasopharynx can similarly be safely repaired under direct vision, using the galeal frontalis muscle flap, a vascularized tissue barrier interposed between the sub-arachnoid space and the nasopharynx.[7]

Acceptable cosmesis is possible even after such major tumour resections. Reconstructions of the bony framework is possible by replacing those osteotomized fragments of the cranial and facial skeleton, achieving stable fixation with interosseous wires, or more recently miniplates. Where extensive bony resection is necessary, skeletal reconstruction is achieved with split calvarial, rib or iliac

bone grafts. Functional mandibular reconstruction in these instances most frequently requires a free osteo-cutaneous flap. [8]

Similarly soft tissue contour restoration, and the obliteration of the large potential spaces generated by thc resections, with their attendant infection risk, demand vascularized soft tissue transfer, either local (temporalis, sternomastoid, etc.,) or distant (latissimus dorsi, rectus abdominis, etc.).

Functional, aesthetic and socially unacceptable disfigurement no longer is a necessary accompaniment of these wide tumour exposures and resections.

Although the application of a combined craniofacial approach to tumours involving the orbit and skull base allows wider exposure and facilitates more complete tumour excision, the question of improvement in overall survival remains as yet unanswered.

For the neurosurgeon, this is of particular importance in relation to such locally massive tumours as chordoma and meningioma: their propensity to recur is well known, and more radical resections deserve very careful consideration.[10]

Conclusion

The cranio-facial approach to tumours involving the orbit and skull base has the advantages of: wider surgical exposure; extensive tumour resection; repair of difficult dural and nasopharyngeal mucosal damage under direct vision; less brain retraction required; improved ability to reconstruct large deficits; and improved cosmetic appearance.

Acknowledgments

The authors wish to thank Mr P. Carney and Mr P. Reilly for permission to report their cases.

References

1. Hybels R. L. & Freidbert S. R. (1980) Combined otolaryngologic and neurosurgical approaches to tumours of the temporal bone and skull base. Surg. Clin. North Amer. 60, 609–28.

2. Kumar A. & Fisch U. (1983) The infra–temporal fossa approach for lesions of the skull base. Adv. Tech. Stand. Neurosurg. 10, 188–220.

3. Kumar A., Valvassori G., Jafar J. & Mafee M. (1986) Skull base lesions: A classification and surgical approaches. Laryngoscope 96, 252–63.

4. Derome P. J. & Guiot G. (1979) Surgical approaches to the spheroidal and clival areas. Adv. Tech. Stand. Neurosurg. 6, 101–36.

5. Derome P. J. (1985) Surgical management of tumours invading the skull base. Can. J. Neurol. Sci. 12, 345–7.

6. Johns M. E. (1984) Supra-orbital rim approach to the anterior skull base. Laryngoscope 94, 1137–9.

7. Jackson I. T., Marsh W. R., Bite U. & Hide T. A. H. (1986) Cranio–facial osteotomies to facilitate skull base tumour resection. Br. J. Plast. Surg. 39, 153–60.

8. David D. J., Tan E., Katsaris J. & Sheen R. Mandibular reconstruction with vascularised iliac crest: a ten year experience. Plast. Reconstr. Surg. (in press).

9. Goldenberg R. A. (1984) Surgeons view of the skull base from the lateral approach. Laryngoscope 96, 1–21.

10. Simpson D. A. (1957) The recurrence of intracranial tumours after surgical treatment. J. Neurol. Neurosurg. Psychiat. 20, 22–39.

Mandibular Reconstruction with Vascularized Iliac Crest: A 10 – Year Experience

David J. David, F.R.C.S., F.R.A.C.S., Eugene Tan, F.R.A.C.S., James Katsaros, F.R.A.C.S., and Robert Sheen, M.B., M.S.
North Adelaide, South Australia

Since 1978, 35 patients have undergone mandibular reconstruction with vascularized iliac crest. During this time, the technique of raising and shaping the iliac crest has undergone a series of modifications. Initially, osteocutaneous segments based first on the superficial circumflex iliac system and later on the deep circumflex iliac system were used. More recently, only the inner table of the ilium has been employed, and where intraoral lining is required, an ulnar forearm free flap has been added.

Thirty-two patients were reconstructed successfully. Of the three anastomotic failures, one bony segment was able to survive as a free graft. There were no donor-site complications. With continued experience, operative morbidity has been minimised, while the technique has been modified to tailor the reconstruction to the specific requirements of the patient. It is concluded that vascularized iliac crest provides the most appropriate mandibular reconstruction for a range of congenital and acquired defects.

In recent years, vascularized iliac crest transfer has been accepted by plastic surgeons as the method of choice for achieving a satisfactory reconstruction of the mandible[1-5]. A healthy blood supply to the bone leads to prompt healing, which, in turn, influences mortality, morbidity, and function. This contrasts with the inadequacies of previous attempts using implants or nonvascularized tissue.

This report details the indications for surgery, operative techniques, and long-term functional results. In particular, the evolution of our technique of raising and shaping the iliac crest over the last 10 years is discussed.

Evolution of Operative Techniques

The technique employed for raising, shaping, and fixing the vascularized iliac crest has evolved since 1978.

Stage A

In our initial experience with microvascular jaw reconstruction, segments of iliac crest based on the superficial circumflex iliac artery (SCIA) system were used. These vessels anastomose with perforators emerging in the line of the external oblique attachment. When raising the composite SCIA flap, the initial dissection is the same as that used for raising a free groin skin flap. Attachments of the skin to fascia within 1 cm on either side of the iliac crest are preserved to retain a periosteal blood supply to an estimated 2-cm segment of bone. The thigh muscle facia and external and internal oblique fibers are then incised to expose the desired height of iliac crest.

This technique was used in two patients whose diagnosis was hemifacial microsomia[6] and in one patient with squamous cell carcinoma. Bone fixation in these patients was achieved by interosseous wiring with intermaxillary fixation for 6 weeks.

Reprinted from PLASTIC AND RECONSTRUCTIVE SURGERY
Plastic and Reconstructive Surgery 82(5) :792-803

Stage B

With the advent of the deep circumflex iliac artery (DCIA) flap, it became possible to provide a large amount of vascularized iliac crest for reconstruction of extensive defects. The technique of raising the flap has been described in detail by Taylor et al.[2,3]

Efforts are made to reduce the bulk of soft tissue taken with the flap. With increasing experience and competence, the amount of muscle attached to the bone can be kept to a minimum. After detachment of the flap, it is transferred to a side table, where it is shaped into the desired configuration. The resected tumor specimen serves as a model for shaping the bone graft; in congenital abnormalities, a preformed template is used. To reconstruct the symphysis, a subperiosteal osteotomy is performed, removing a wedge of bone in the sagittal plane. After stabilization with an interosseous wire, final shaping is performed with a burr (Fig. 1). Step osteotomies, with interosseous wiring, are sufficiently strong to preclude the need for intermaxillary fixation in these patients.

Stage C

In the next stage in the evolution of the technique, only the inner table of the ilium was taken.[7] In raising the "split" iliac crest bone graft, the deep circumflex iliac artery vessels are dissected laterally to the anterosuperior iliac spine. The ilium is then split along the crest, taking care not to breach the inner cortex. This osteotomy is usually performed with the long blade of the sagittal saw after the pattern of the graft has been marked out on the bone (Fig. 2). The desired shape of the hemimandible is achieved more easily by taking the contralateral iliac crest. The split ilium is not too bulky and is useful in congenital and acquired problems where there is adequate soft tissue.

Stage D

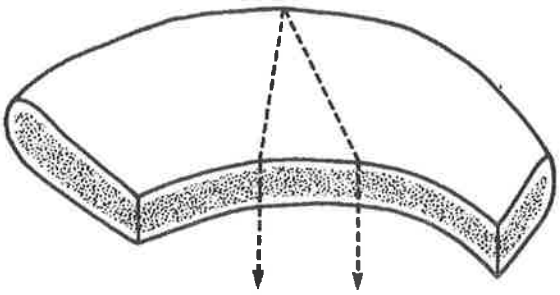

Wedge Osteotomy

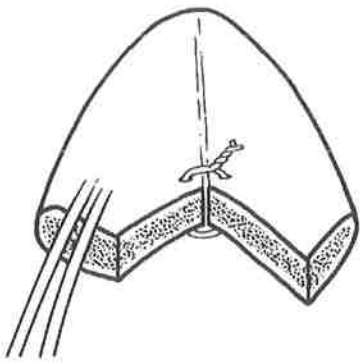

Completed osteotomy for symphysis reconstruction

FIG. 1. *Method of symphysis reconstruction using the full thickness DCIA flap showing closing wedge osteotomy.*

To recreate the symphysis with this thin bone graft, vertical subperiosteal osteotomies are performed at appropriate sites. A strip of the iliac crest, taken as a nonvascularized graft, is onlayed over the outer aspect of the new jaw using miniplates and lag screws (Fig. 3). This firmly secures the osteotomized segments and augments the chin prominence. No intermaxillary fixation is necessary.

Stage E

When intraoral lining is required, the split iliac crest graft is combined with a free forearm flap. Our preference has been the ulnar rather than radial forearm flap, since this tends to provide hairless skin and a donor site that is less conspicuous.[8] This thin flap helps to recreate the contours of the floor of mouth, labial sulcus, and alveolar margin, which may facilitate the fitting of dentures.

Materials and Methods

From 1978 to 1987, 35 patients have undergone iliac crest reconstruction of the mandible. There were 24 males and 11 females, with ages ranging from 11 to 81 years (mean 45 years). The indications for mandibular resection are divided into three major categories (Table I).

In the congenital group, all six patients suffered from hemifacial microsomia. Three patients were operated on primarily, while the other three had undergone previous attempts at reconstruction. The principle of treatment in all patients was centralisation of the facial skeleton by bimaxillary osteotomy and filling the resultant mandibular and soft-tissue gap with vascularized iliac crest and soft tissue.[9]

Of 26 patients in the tumor group, 20 were treated for squamous cell carcinoma. Three of these patients had undergone previous irradiation and were referred for residual or recurrent tumor. Eleven patients underwent planned radiotherapy as soon as the wounds had healed. Both patients with ameloblastoma had been treated in overseas hospitals where nonvascularized bone grafts had been used for repair. These patients presented a number of years later for definitive reconstruction. Of two patients with mocoepidermoid carcinoma, one was reconstructed as part of his definitive treatment, while the other had undergone palliative resection following a recurrence involving the base of skull. The patient with fibrous dysplasia had been managed conservatively for 2 years prior to radical mandibular surgery. The single patient with the primordial cyst had undergone hemimandibulectomy and presented for secondary reconstruction of the residual deformity.

In the trauma category, all patients had self-inflicted gunshot injuries affecting the maxilla and orbits as well as the mandible.

TABLE I
Indications

Congenital:	
Hemifacial microsomia	6
Tumor:	
Squamous cell carcinoma (SCC)	20
Ameloblastoma	2
Mucoepidermoid carcinoma	2
Fibrous dysplasia	1
Primordial cyst	1
Trauma:	
Shotgun injury	3

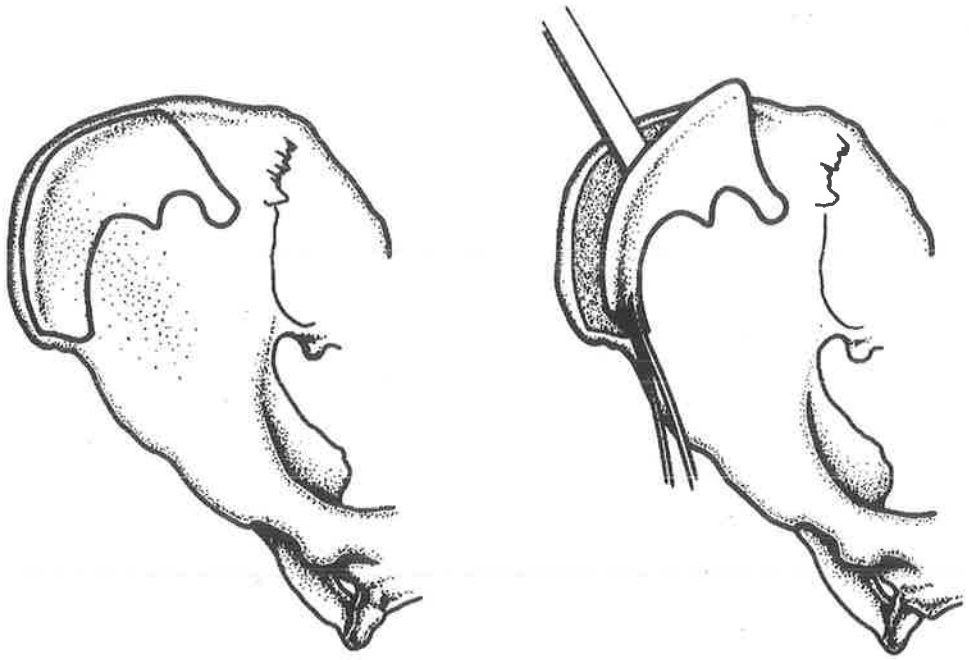

FIG. 2. *Using the contralateral iliac crest, a template of the mandible is outlined before osteotomies are made to split the inner table with preservation of the DCIA vessels.*

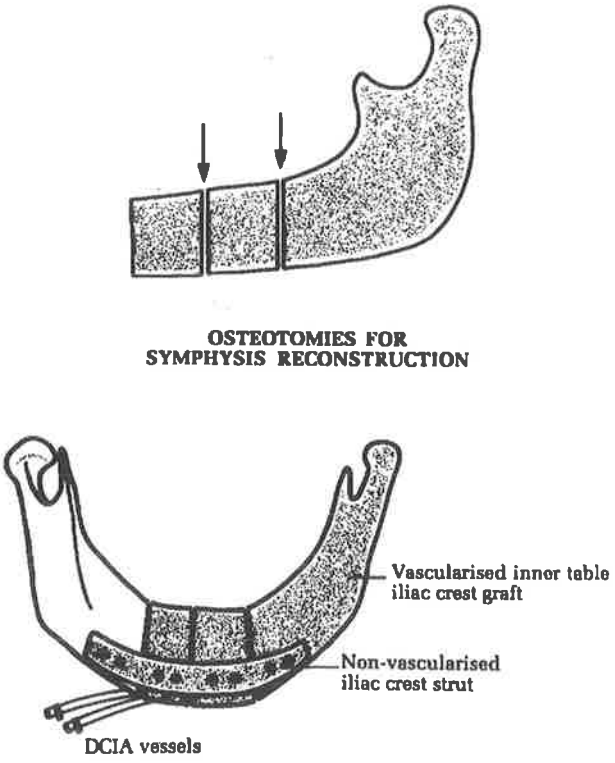

FIG. 3. *Reconstruction of the symphysis is achieved with vertical osteotomies preserving the periosteum on the lingual side. A strut of nonvascularized iliac crest secures all segments and augments the chin prominence. The cancellous surface of the inner table faces outward.*

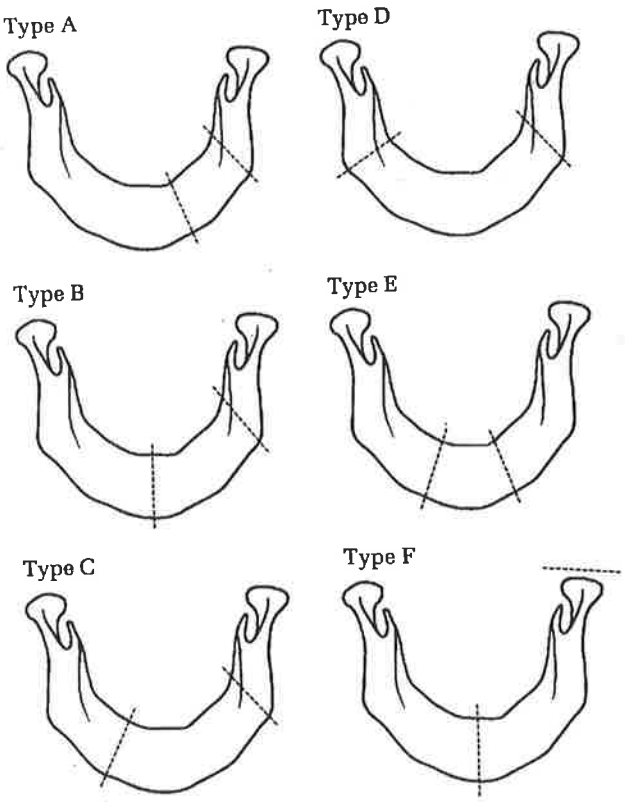

FIG. 4. *Classification of mandibular reconstruction according to the segment of bone resected.*

Classification

Patients have been classified according to the segment of mandible reconstructed (Fig. 4):

Type A: Short segment confined to one side (O patients)

Type B.: Unilateral angle to symphysis (4 patients)

Type C: Between the angle and body of the other side (12 patients)

Type D: Angle to angle (5 patients)

Type E: Symphysis (4 patients)

Type F: Hemimandible, including the mandibular condyle (10 patients)

Results

The basic data, type of reconstruction, and outcome (including complications) are presented in Table II. All patients with hemifacial microsomia were reconstructed successfully. They all required secondary sculpturing of the soft-tissue element of the composite flap.

In the tumor group, three flaps were unsuccessful. In one case, vascularization failed because of unrecognised trauma to the vessels.

Another case involved secondary reconstruction of a previous angle-to-angle resection for ameloblastoma. In retrospect, this patient was unsuitable for reconstruction with the full-thickness DCIA flap because the bulk of the muscle,

skin, and bone could not be fitted into the defect without kinking and compression of the vessels. The third case was a young woman with fibrous dysplasia in whom part of the bone died because of anastomotic failure. However, the large cancellous surface in contact with the soft-tissue bed allowed survival of most of the bone as a free graft.

Of the 20 patients with squamous cell carcinoma, 6 have died of their disease. The remaining patients have been followed from 6 months to 7 years.

In the gunshot injury group, a DCIA flap with soft tissue and bone was used in two patients. In the third patient, a similar flap was raised in combination with vascularized jejunum to resurface not only the oral cavity, but also the lining of the nose and maxillary sinus. The definitive result has been achieved in one patient, but the other two will require further surgery.

Graft viability was assessed clinically, in the majority of patients, by observing the soft tissue. Bone healing was assessed clinically by the absence of pain and mobility on stressing and radiologically by the loss of osteosynthesis lines and the presence of connecting trabeculae. All surviving grafts showed excellent union.

All patients who had previous radiotherapy were successfully reconstructed, and there was no difficulty with bone healing. Eleven patients with squamous cell carcinoma received radiotherapy in the early posthealing phase with no untoward results. Small areas of dehiscence with exposure of bone or metal occurred in two patients. These healed by secondary intention.

Although five patients are able to wear dentures, none can chew food effectively. However, in those patients with teeth present on the contralateral side, masticatory function has been preserved. Two patients have been scheduled for implantation of osseointegrated prosthetic teeth.

There were no significant donor-site complications.

Case Reports

The following cases demonstrate milestones in the evolution of our method of mandibular reconstruction.

Case 1. Stage A: SCIA Osteocutaneous Flap

A 14-year-old girl was referred for definitive reconstruction of left-sided hemifacial microsomia. She had been treated in infancy by a variety of methods, including metatarsal transfer, and later by the insertion of a Bowerman's prosthesis. Included in her reconstruction was the prior fashioning of a temporomandibular joint using costal cartilage. This was followed by transfer of a composite SCIA osteocutaneous flap. This provided bone for the left hemimandible and a deepithelialized skin flap for soft-tissue augmentation. Interosseous wiring was performed in this case, and because of the mandibular osteotomy, intermaxillary fixation was required for 8 weeks. A further operation was required for soft-tissue contouring. It is interesting to note from the three-dimensional reconstruction that the mandible is alive and well, but the nonvascularized reconstructed zygomatic arch has resorbed (Fig. 5).

Case 2. Stage B: DCIA Osteocutaneous Flap

A 70-year-old man with a T_3 squamous cell carcinoma of the floor of mouth eroding the anterior mandible underwent resection of the anterior half of the tongue, angle-to-angle resection of the body of the mandible and bilateral suprahyoid

TABLE II
Patient Summaries

Patient	Age	Sex	Diagnosis	Classification	Type of Reconstruction	Radiotherapy	Outcome
1	15	F	Hemifacial microsomia	F	SCIA		Facial symmetry achieved
2	70	F	SCC	C	DCIA	Postoperative	Alive and well
3	16	F	Hemifacial microsomia	F	SCIA		Facial symmetry achieved
4	64	F	SCC	F	DCIA	Postoperative	Died of multifocal tumor
5	11	M	Hemifacial microsomia	F	DCIA		Facial symmetry achieved
6	58	M	SCC	D	DCIA	Preoperative	Alive and well
7	67	M	SCC	C	DCIA	Postoperative	Died of recurrent tumor
8	41	M	Shotgun injury	D	DCIA	Satisfactory result	
9	34	F	SCC	C	DCIA	Preoperative	Alive and well
10	63	M	SCC	E	DCIA		Alive and well
11	37	M	Shotgun injury	B	DCIA + jejunum		Requires further surgery
12	81	F	SCC	C	DCIA		Alive and well
13	78	M	SCC	C	DCIA	Postoperative	Alive and well
14	61	F	SCC	B	Split DCIA + forearm flap	Postoperative	Alive and well
15	59	F	SCC	C	DCIA		Alive and well
16	63	M	SCC	B	DCIA	Postoperative	Died of local recurrence, anastomic failure
17	72	M	SCC	C	DCIA	Postoperative	Alive and well
18	28	M	Ameloblastoma	D	DCIA		Alive and well
19	18	F	Primordial cyst	F	Split DCIA		Alive and well
20	34	M	Hemifacial microsomia	F	DCIA		Facial symmetry achieved
21	18	M	Hemifacial microsomia	F	Split DCIA + forearm flap		Facial symmetry achieved
22	16	F	Hemifacial microsomia	F	DCIA		Facial symmetry achieved
23	23	F	Fibrous dysplasia	F	Split DCIA		Partial bone loss
24	68	M	SCC	C	DCIA	Preoperative	Alive and well
25	29	M	Mucoepidermoid carcinoma	B	DCIA	Alive and well	
26	52	M	SCC	C	DCIA		Died of recurrent tumor
27	55	M	SCC	D	DCIA	Postoperative	Died of recurrent tumor
28	61	M	SCC	E	DCIA	Postoperative	Alive and well
29	33	M	Shotgun injury	E	DCIA		Requires further surgery
30	47	M	Ameloblastoma	D	DCIA		Anastomic failure
31	38	M	SCC	C	DCIA	Postoperative	Died of recurrent tumor
32	24	M	SCC	E	Split DCIA + forearm flap		Alive and well
33	31	M	Mucoepidermoid carcinoma	F	DCIA	Preoperative	Alive and well
34	54	M	SCC	C	DCIA		Alive and well
35	54	M	SCC	C	SCIA	Postoperative	Alive and well

neck dissection. A deep circumflex iliac artery (DCIA) flap was transferred with soft-tissue fitting into the floor of the mouth between tongue and lip. The muscle of the graft was attached to the suprahyoid muscles. Bony fixation was by step osteotomy and interosseous wiring. No intermaxillary fixation was required. A further operation was needed to resculpture the soft tissues. Although speech and oral competence are good, this patient has been able to wear a denture for cosmetic purposes only (Fig. 6).

Case 3. Stages D and E: "Split" Osteotomized DCIA Flap with Vascularized Forearm Flap

A 61-year-old woman presented with a squamous cell carcinoma of the alveolus and left body of the mandible.

Composite body-to-angle resection was reconstructed with a vertically osteotomized deep circumflex iliac artery (DCIA) flap. The iliac crest was secured

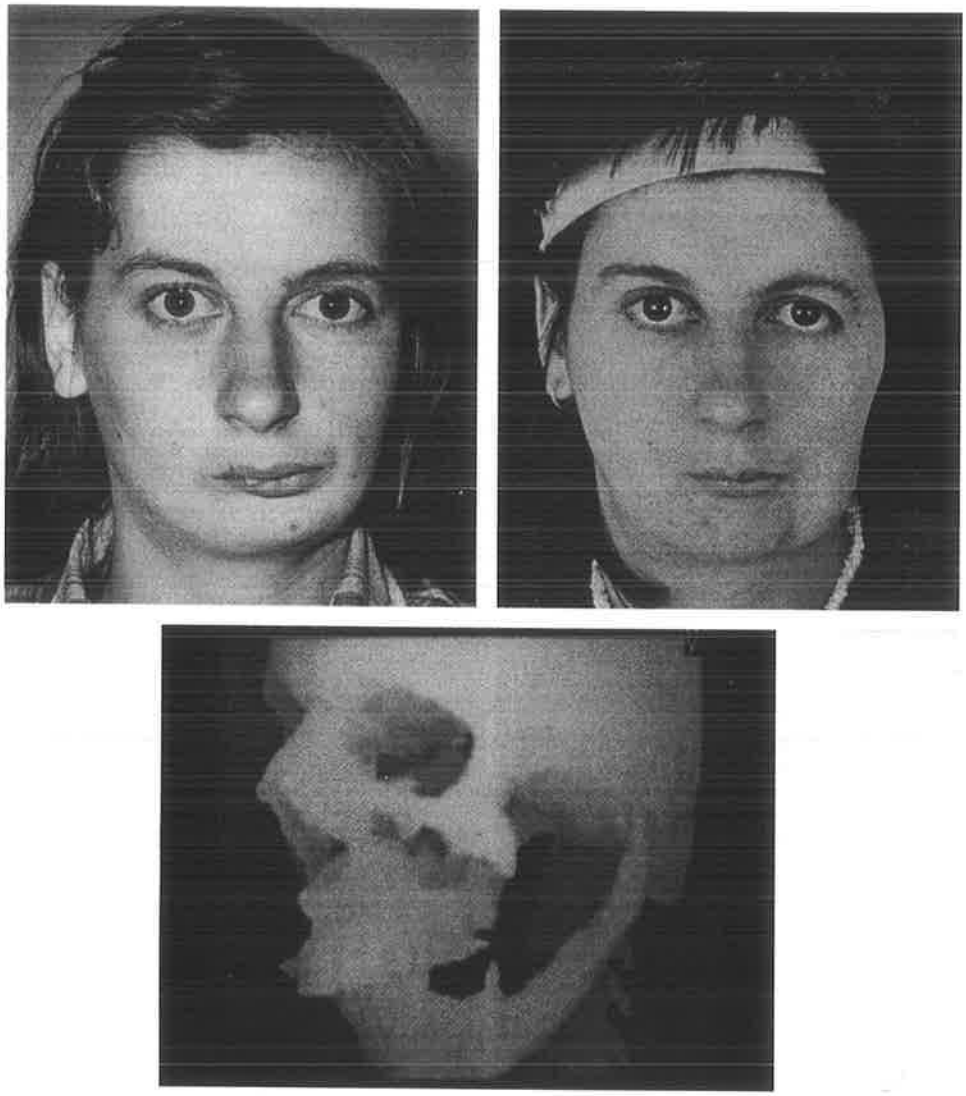

FIG. 5. Case 1. *A 14-year-old girl with hemifacial microsomia showing preoperative (above, left) and postoperative (above, right) appearance and three-dimensional CT scan (below) of the reconstructed left hemimandible 10 years later.*

to the mandibular remnants, while a nonvascularized bony strut gave stability to the new mandibular arch. Inset of a forearm flap completed reconstruction of the lining (Fig. 7).

Case 4

A 24-year-old man with a squamous cell carcinoma of the alveolus invading the floor of mouth at the symphysis required an angle-to-angle resection of the mandible with part of the tongue and floor of mouth. A split deep circumflex iliac artery (DCIA) iliac bone graft was shaped with two verticle subperiosteal osteotomies to recreate the symphysis. The height of the graft matched that of the normal alveolar margin. A strip of nonvascularized bone was onlayed with lag screws to secure the shape of the graft and to add bulk to the chin. The graft was rigidly fixed into position with two miniplates on each side. An ulnar forearm flap provided a smooth, thin lining over the alveolus and floor of mouth (Fig. 8).

Discussion

In recent years, many reports of jaw reconstruction using free vascularized tissues have been published. The prevailing opinion in international forums is that the

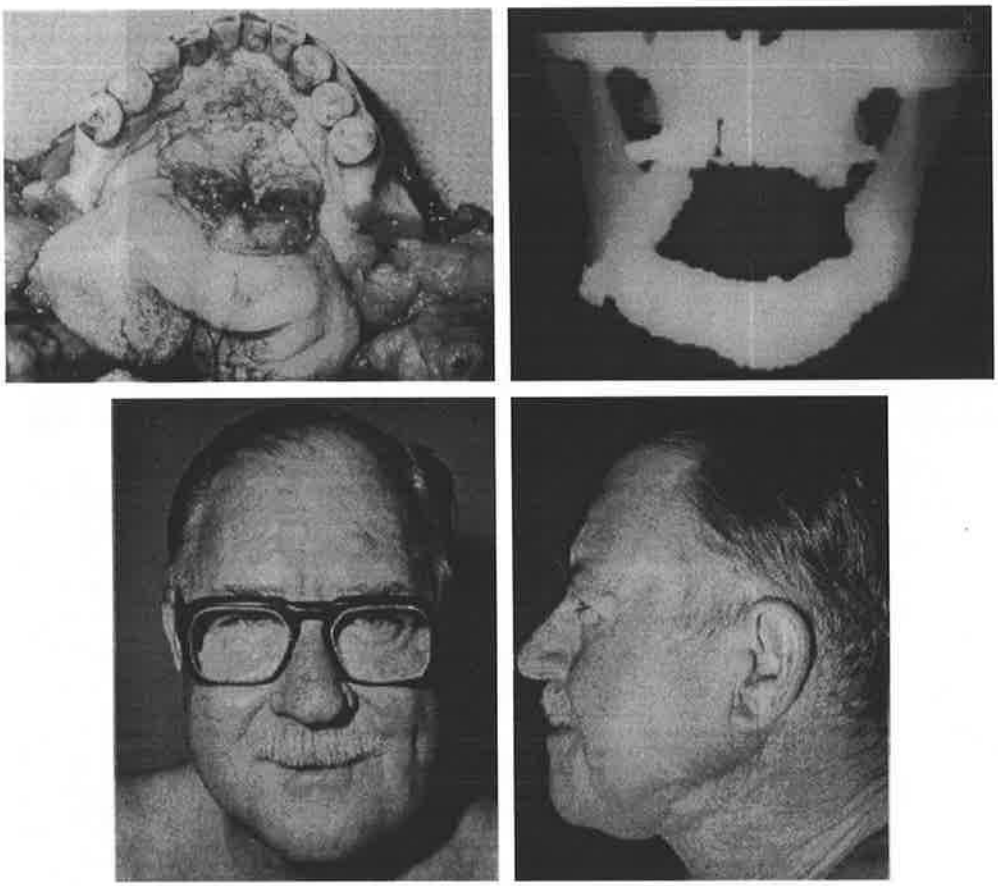

FIG. 6. Case 2. *(Above, left) A 70 year old man with a squamous cell carcinoma of the floor of the mouth invading the mandible. (Above ,right) The angle to angle reconstruction 6 years later. (Below) The post operative appearance.*

iliac crest is the most popular form of such reconstruction. Other free tissue transfers, such as the dorsalis pedis,[10] radial forearm,[11] and scapulars[12] osteocutaneous flaps, have their proponents. The authors, having undertaken this prospective trial of iliac crest reconstruction 10 years ago, have limited experience with the latter methods, which on theoretical and practical grounds do not have the same appeal.

The dorsalis pedis flap has not been used mainly because of the well-known donor-site problems. Also, the amount of bone that can be taken is limited in length, being suitable only for symphyseal or short-segment reconstruction. The potential for a radius fracture has been the major dissuading factor in adopting the radial osteocutaneous flap. It is also felt that an inadequate thickness of bone is available for reconstructing the height of the mandible, especially in younger patients with teeth. We have not used the scapular osteocutaneous flap because in the past we have found the skin to be thick and it does not match the properties of forearm skin as a substitute for intraoral lining. Only 10 cm of the lateral border of the scapula can be taken easily, and this is therefore more suited to straight-segment reconstructions of the mandible.

Although these other methods give good results in certain situations, it is felt that vascularized iliac crest transfer in conjunction with a free forearm flap is the one technique that can provide appropriate tissues for most mandibular defects. Moreover, it was considered desirable to attain proficiency with one method, since this is more likely to give an increasingly higher success rate, lower morbidity, and improved function through constant modification of technique.

Following Taylor's description of the deep circumflex iliac artery (DCIA) system,[2, 3] it became possible to harvest large segments of bone based on more

FIG. 7. Case 3. *(Above, left) A 61-year-old woman with a squamous cell carcinoma of the alveolus and left body of mandible. Following body-to-angle resection, reconstruction was performed with a "split" DCIA flap. (Above, right) Miniplates, lag screws; and a nonvascularized iliac crest strut were used for bony fixation. (Below, left) A free forearm flap provides lining. (Below, right) The result at 6 months.*

reliable vessels. However, it was found that the soft-tissue attachments were often excessively bulky and the bone too thick. This problem was overcome by splitting the ilium in those cases in which lining was not required. A natural progression has been to combine this with a free forearm flap to provide the most appropriate tissue for both bony and soft-tissue replacement. Recent use of miniplate fixation, lag screws, and onlay bone grafting has resulted in a very accurate reproduction of the mandible. In particular, the contour of the lower border of the mandible and the chin point are faithfully recreated.

The natural consequence of refining the method of reconstruction has been a reduction in morbidity. This was particularly evident in those patients who had been previously irradiated. In addition, the rapid healing of well-vascularized tissues has eliminated the complications of infection and fistula formation. This has permitted the early administration of postoperative radiotherapy to those patients with T_2 and T_3 squamous cell carcinomas, thereby improving their prognosis.[13] This represents a significant advance in the management of intraoral malignancy.

Although one patient ultimately had a good result following "split" DCIA reconstruction, anastomotic failure in this patient resulted in considerable postoperative morbidity. Partial necrosis of the graft resulted in a persistent sinus necessitating sequestrectomy at 6 months. Such problems were not encountered in the remaining four patients reconstructed with a Split" DCIA flap, all of whom had positive bone scans at 3 days (see Fig. 8).

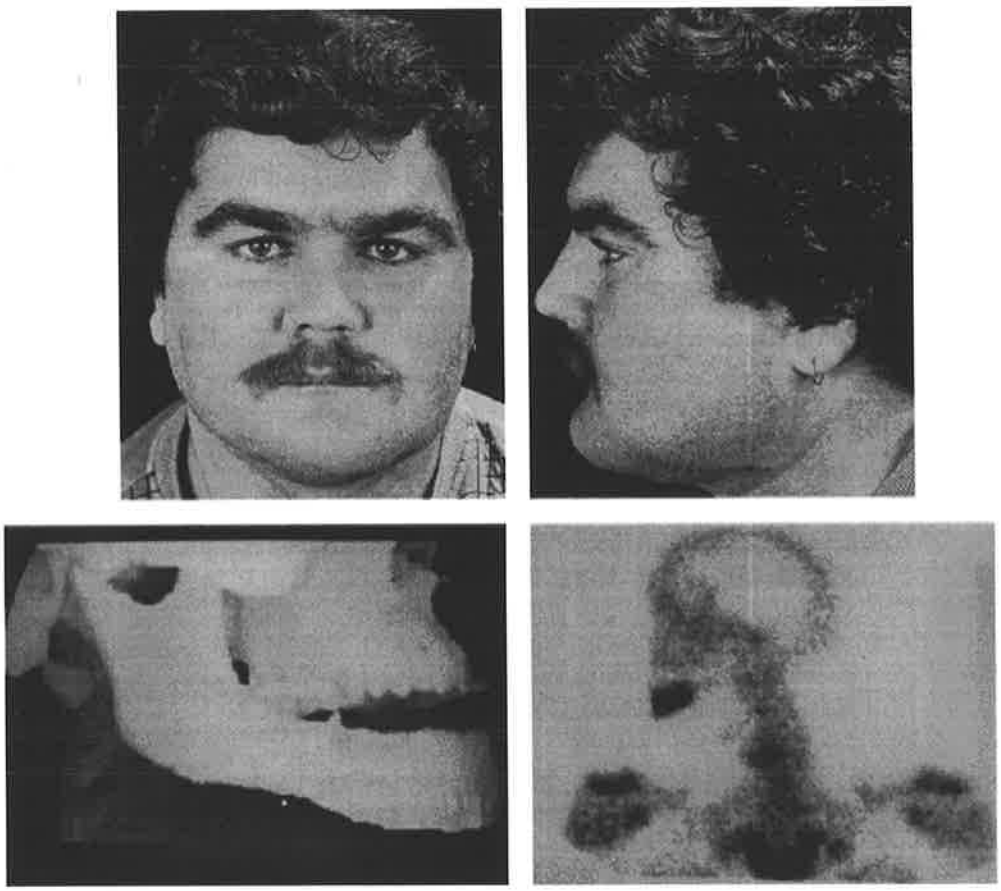

FIG. 8. Case 4. *A 24-year-old man with a squamous cell carcinoma of the alveolus showing the postoperative result (above) and the three-dimensional CT scan (below, left) of the angle-to-angle mandibular reconstruction at 6 months. (Below, right) The bone scan at 3 days shows good uptake of the isotope.*

Refinements in surgical technique have been accompanied by better functional and cosmetic results. Better jaw function is reflected in the quality of chewing and speaking, while an improved appearance permits more effective psychosocial rehabilitation. The ultimate objective of reconstruction of the mandible is to have osseointegrated prosthetic teeth, and this is the direction in which our prospective development of these techniques will be aimed.

David J. David, F.R.C.S., F.R.A.C.S. South Australian Craniofacial Unit
Adelaide Children's Hospital
King William Road
North Adelaide, S. A. 5006
Australia

References

1 O'Brien, B. Mc.C, Morrison, W. A., MacLeod, A. M., and Dooley, B. J. Microvascular osteocutaneous transfer using the groin flap and iliac crest and the dorsalis pedis flap and second metatarsal. Br. J. Plast. Surg. 32: 188, 1979.

2 Taylor, G. I., Townsend, P., and Corlett, R. Superiority of the deep circumflex iliac vessels as the supply for free groin flaps: Experimental work. Plast. Reconstr. Surg. 64: 595, 1979.

3 Taylor, G. I., Townsend, P., and Corlett, R. Superiority of the deep circumflex iliac vessels as the supply for free groin flaps: Clinical work. Plast. Reconstr. Surg. 64: 745, 1979.

4 Taylor, G. I. Reconstruction of the mandible with free composite iliac bone grafts. Ann. Plast. Surg. 9: 361, 1982.

5 Salibian, A. H., Rappaport, I., and Allison, G. Functional oromandibular reconstruction with the microvascular composite groin flap. Plast. Reconstr. Surg. 76: 819, 1985.

6 David, D. J., and Tan, E. Microvascular surgery in maxillofacial reconstruction. Ann. Acad. Med. Singapore 8: 481, 1979.

7 Taylor, G. I., and Daniel, R. K. Aesthetic aspects of microsurgery: Composite tissue transfer to the face. Clin. Plast. Surg. 8: 333, 1981.

8 Lovie, M. J., Duncan, G. M., and Glasson, D. W. The ulnar artery forearm free flap. Br. J. Plast. Surg. 37: 486, 1984.

9 David, D. J., Tan, E., and Cooter, R. D. Composite Free Flap Reconstruction for Severe Hemifacial Microsomia. In D. Marchac (Ed.), Craniofacial Surgery: Proceedings of the First International Congress of The International Society of Cranio-Maxillo-Facial Surgery, Cannes-La Napoule, 1985. Berlin: Springer-Verlag, 1987.

10 MacLeod, A. M., and Robinson, D. W. Reconstruction of defects involving the mandible and floor of mouth by free osteocutaneous flaps derived from the foot. Br. J. Plast. Surg. 35: 239, 1982.

11 Soutar, D. S., Scheker, L. R., Tanner, N. S. B., and McGregor, I. A. The radial forearm flap: A versatile method for intraoral reconstruction. Br. J. Plast. Surg. 36: 1, 1983.

12 Swartz, W. M., Banis,J. C., Newton, E. D., Ramasastry, S. S., Jones, N. F., and Acland, R. The osteocutaneous scapular flap for mandibular and maxillary reconstruction. Plast. Reconstr. Surg. 77: 530, 1986.

13 Robertson, A. G., McGregor, I. A., Flatman, G. E., Soutar, D., and Boyle, P. The role of radical surgery and postoperative radiotherapy in the management of intaoral carcinoma. Br. J. Plast. Surg. 38: 314, 1985.

CLINICAL NOTES

Craniofacial Deformation in Cystic Hygroma

Mark H. Moore, F.R.A.C.S.*
David J . David , A.C. , F.R.C.S. , F.R.C.S. (E), F.R.A.C.S.†
Adelaide, Australia

Mandibular and dentoalveolar deformities associated with cystic hygroma of the head and neck have previously been described. This small series has identified changes involving the entire craniofacial skeleton, attributable to both the local and distant effects of massive facial lymphangiomas, without evidence of any actual soft tissue ingrowth into bone.

In view of the inability to excise such lesions and normalise the soft tissue anatomy, the surgical approach to the craniofacial skeletal abnormality should be to reserve the required osteotomies or ostectomies until the completion of facial growth.

Key Words: cystic hygroma, craniofacial growth, lymphangioma

The soft tissue features of the cystic hygroma are well described.[4,6] Such cystic hamartomatous growths of lymphatic origin most commonly involve the face and neck.[4] Ranging in diameter from several millimeters to cover 15 centimeters, they are characteristically infiltrative of fascial planes and extend into adjacent muscles and nerves.

Vascular hamartomas, e.g., hemangiomas and lymphangioma of the face, however, infrequently involve the underlying facial skeleton. Where skeletal changes are noted, these being more common with hemangiomas, they have been attributed to direct growth of the lesion into the bone, pressure of the lesion growing adjacent to the bone or secondary to the circulatory effect of the lesion on the neighbouring periosteum.[7] Inhibition or diminution of growth of elements of the facial skeleton may similarly follow the use of radiotherapy or surgery in the treatment of such lesions.

Isolated reports have described dental malocclusions, dentoalveolar abnormalities, and apparent mandibular overgrowth occurring in association with large cystic hygromas that have extensive intraoral involvement.[2,3,5] These dental and skeletal changes are a consequence of a combination of one or both of the local mechanisms described above.

The review of a small series of patients with large cystic hygromas involving the face and neck has revealed patterns of skeletal deformation both locally in the lower third of the face and also at a distance in the middle and upper thirds of the craniofacial skeleton.

Method

A review of The Australian Craniofacial Unit's records identified a group of patients with extensive cystic hygromas involving the face, oral cavity, and neck.

Reprint requests: Mark H. Moore, F.R.A.C.S., The Australian Craniofacial Unit, Adelaide Children's Hospital, 72 King William Road, North Adelaide, South Australia 5006
*Assistant Craniofacial Surgeon; †Head, The Australian Craniofacial Unit, Adelaide Children's Hospital, North Adelaide, South Australia

Clinical examination and radiographic assessment, including complete 2D and 3D computerised tomographic scans, revealed patterns of craniofacial skeletal distortion, in addition to the soft tissue abnormalities and contributed significantly to the overall detection of craniofacial deformation.

Case reports that describe the pattern and extent of craniofacial bony disorganisation are reviewed.

Patient 1

This patient presented in infancy with an extensive lymphangioma involving the cheek, lower face, and neck with an intraoral extension to involve the tongue.

Surgical soft tissue debulking performed at age 14 months and 16 months was followed by an exacerbation of his upper respiratory obstruction, which required tracheostomy at age 21 months. Examination at age 6 years reveals a persistent soft tissue mass involving the lower face and upper neck bilaterally with continuing intraoral extension (Fig. 1). The calvarium, orbits, and midfacial skeleton are normal. The mandible is asymmetrical in size, somewhat thinned out on the right side in the region of the angle and ascending ramus. There is almost no gonial angle and the mandibular growth pattern is unfavourable with an anterior open bite (Figs. 2 and 3). The occlusion is Class 1.

Patient 2

This 14-year-old girl presented with a large previously operated lymphangioma of the left face extending into the floor of her mouth and the left side of her tongue (Figs. 4 and 5).

The soft tissue mass extends from the level of the supraorbital margin above to the lower border of the mandible on the left below. Deeply the lesion is limited by the underlying bony skeleton, which is distorted but not infiltrated. Posteriorly the cystic hygroma extends around behind the naso- and oropharynx and above into the infratemporal fossa. The left eye is proptosed and displaced upward by 6 mm (Fig. 4). The external nose is deviated to the right, as is the chin. The left angle of the mouth is depressed.

The calvarium and midline cranial base structures are automatically undisturbed. The left orbital floor and infraorbital rim are elevated, with the latter markedly anteriorly displaced. The left zygomatic arch was inferiorly dislocated and distorted in shape (Fig. 6). The nasal septum is deviated to the right anteriorly.

The posterior maxillary height on the left is markedly reduced, the interposed soft tissue mass producing a severe posterior open-bite deformity on this side (Fig. 5).

From the front and right side the occlusal plane is level. There is very poor tooth root structure and development in the left posterior maxilla and mandible.

The posterior mandibular height is increased on the left, which in combination with the maxillary deformity contributes to the left buccal open bite (Fig. 6).

Surgical intervention to correct the skeletal anomalies has been planned when growth is complete.

Patient 3

This 5-year-old presented with a massive, previously operated cystic hygroma of the left side of the face and neck. Having had a tracheostomy inserted at the age of 14 days, he subsequently underwent partial excision of the neck and left facial mass at age 14 months and again at 2 years, with preservation of the facial nerve.

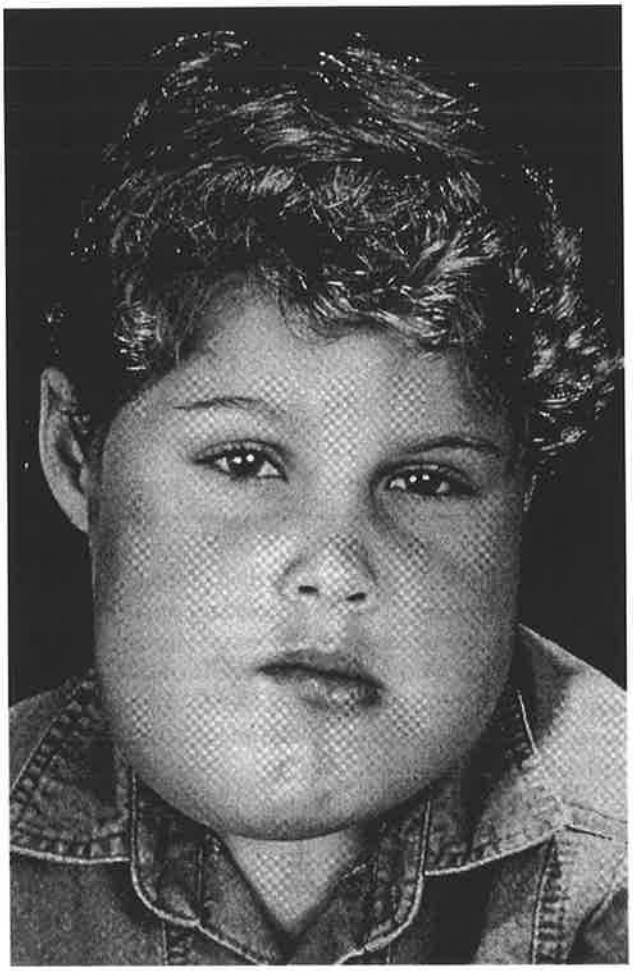

FIG. 1. *6-year-old with extensive cystic hygroma involving the lower face and upper neck bilaterally.*

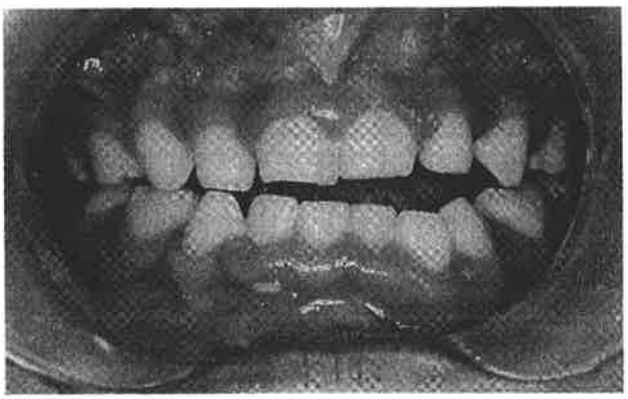

FIG. 2. *Occlusal view demonstrating the anterior open-bite deformity and Class 1 occlusion.*

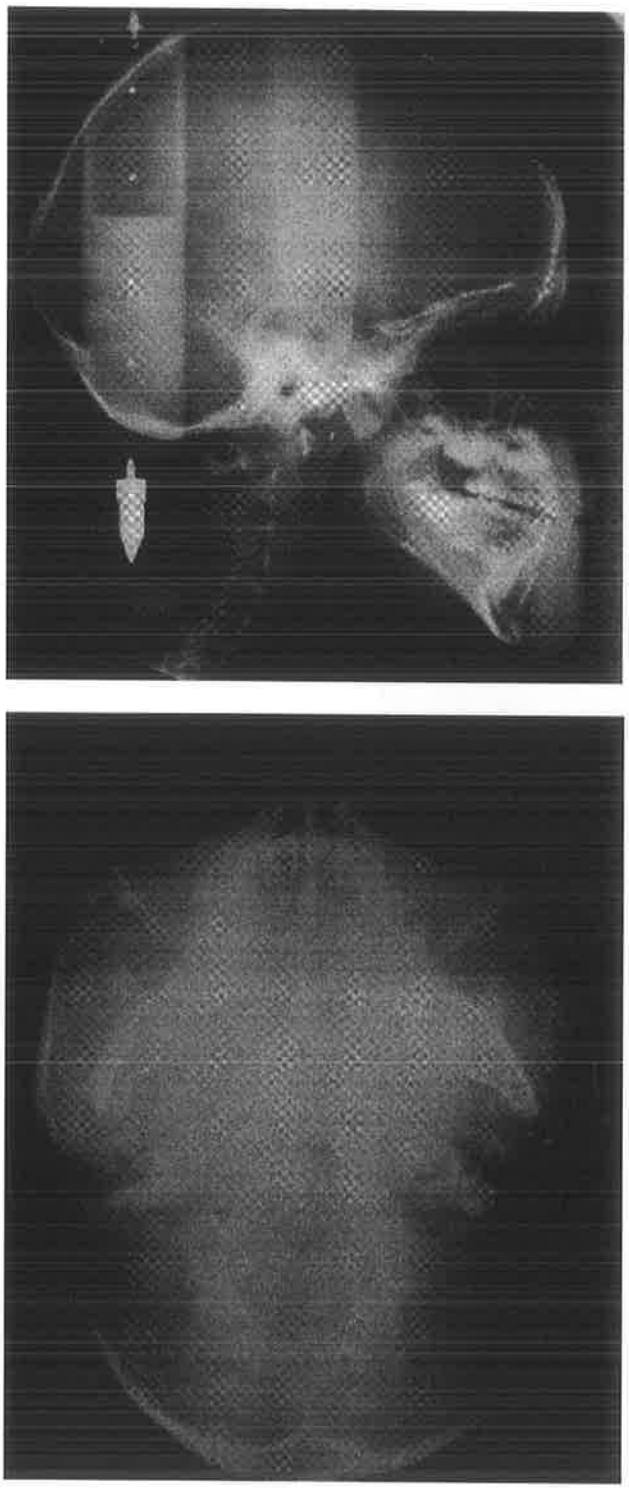

FIG. 3. A. *Lateral and* **B.** *basal cephalometric views showing the mandibular asymmetry and poorly developed gonial angle.*

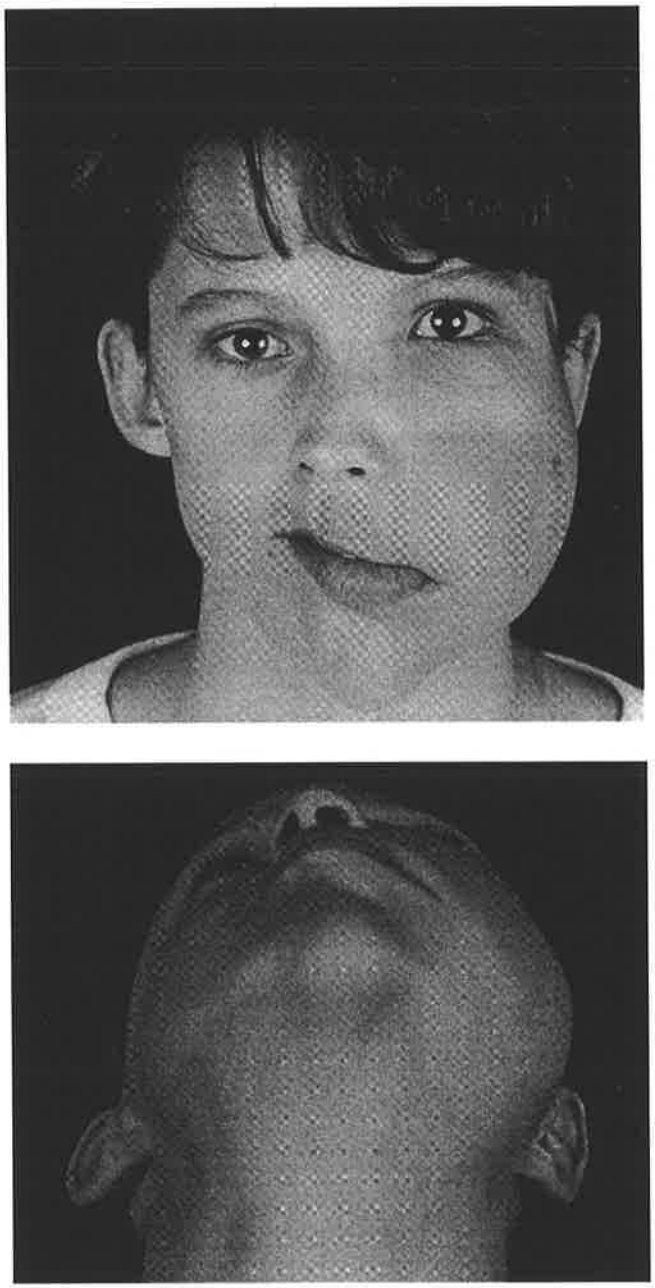

FIG. 4. A. *and* **B.** *14-year-old with a cystic hygroma of the left side of the middle and lower thirds of the face, producing very obvious left orbital dystopia and proptosis of the left globe.*

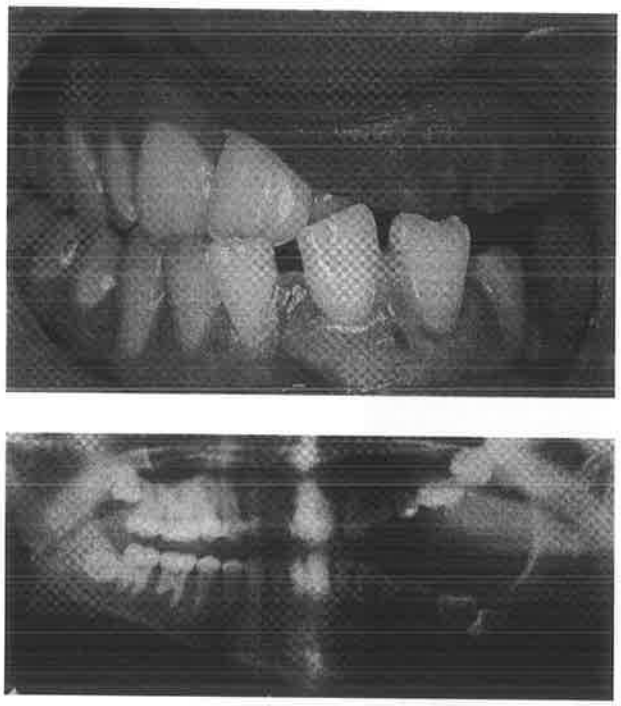

FIG. 5. *Occlusal view confirming the intraoral extension, with the corresponding skeletal changes in the maxilla and mandible manifest on the orthopantomogram.*

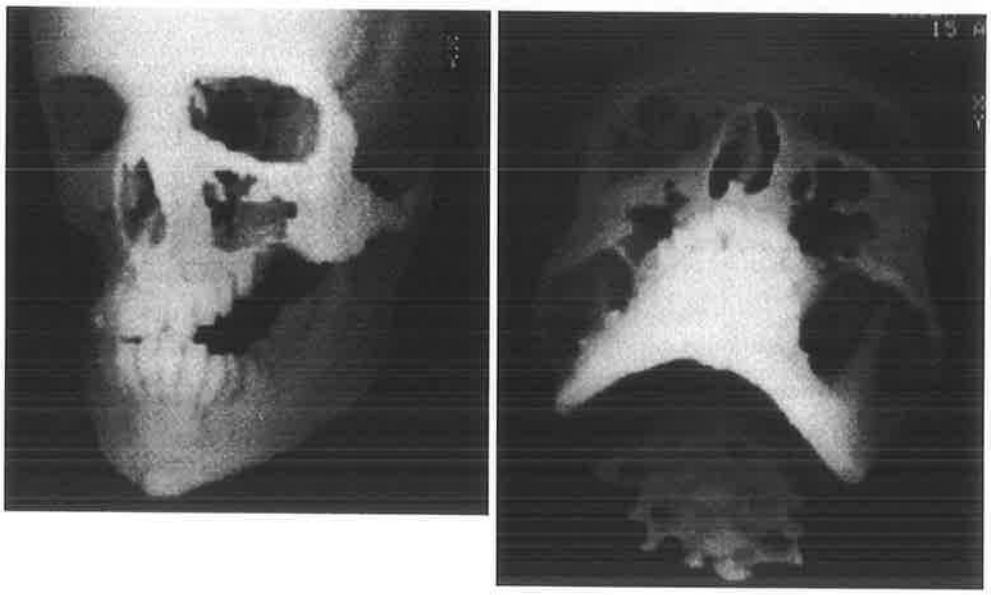

FIG. 6. A. *Oblique and* **B.** *worms eye 3-D CT reformats expose the skeletal anatomy of the orbitozygomatic, midface, and mandibular deformities.*

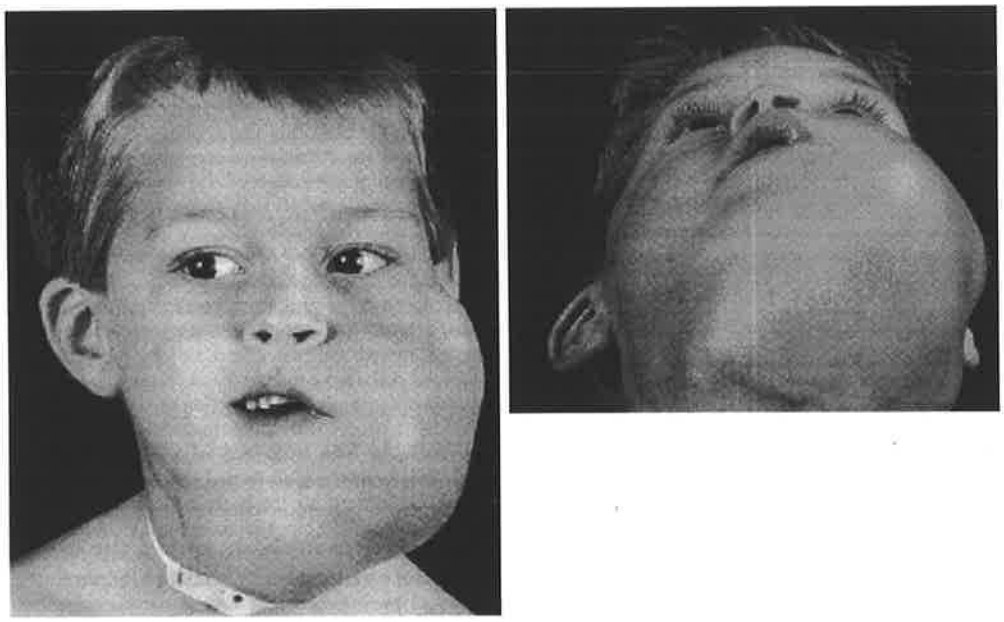

FIG. 7. A. *and* **B.** *5-year-old with massive lymphangioma of the face and neck with tracheostomy in situ.*

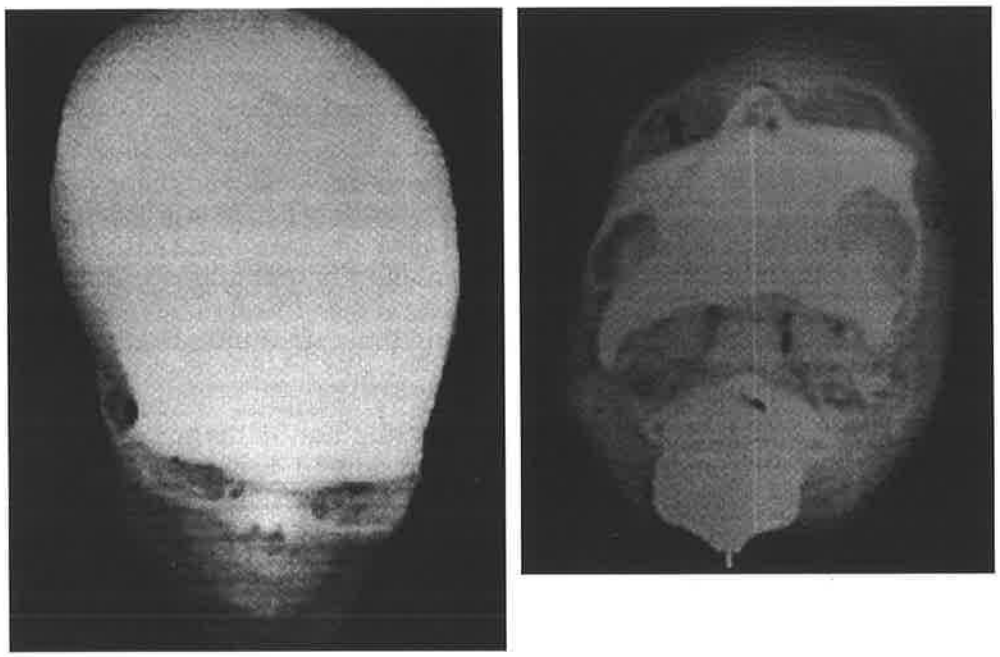

FIG. 8. A. *Bird's-eye and* **B.** *worm's-eye 3-D CT reformats reveal the marked parallelogram plagiocephaly above and the obvious orbitozygomatic asymmetry below.*

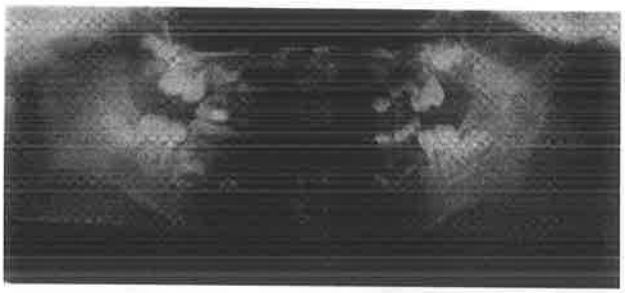

FIG. 9. *Orthopantomogram exposes the maxillary and mandibular asymmetries and associated open-bite deformities.*

Examination confirms massive soft tissue swelling on the left side of the face, from the level of the zygomatic arch above, to become continuous with the thyroid cartilage below. Posteriorly the mass extends to the mastoid region, with involvement and narrowing of the external auditory meatus. In the face it extends as far medially as the alar base of the nose, with some involvement of the upper lip. There is full thickness involvement of the left cheek with infiltration of the soft palate, floor of the mouth, and tongue (Fig. 7).

In the neck, the soft tissue mass crosses the midline to the level of the contralateral external ear. The skeletal deformation begins above with severe parallelogram plagiocephaly, marked right frontal flattening, right occipital bossing, and posterior displacement of the right external ear in relation to the left (Fig. 8). There is no evidence of premature fusion of the coronal or fronto-sphenoidal suture complexes.

The left orbit is elevated some 3 mm in relation to the right orbit, with the lateral orbital wall on the left being shorter, thicker, and anteromedially rotated. The left infraorbital margin is similarly anteriorly displaced, and the zygomatic arch is flattened (Fig. 8). The anterior vertical maxillary height is greater on the left side, with tilting of the occlusal plane and open-bite deformities anteriorly on the right and posteriorly on the left. The mandible is similarly asymmetrical, displaced to the right with apparent lengthening of the vertical ramus on the left, an increase in the posterior facial height, and prominent antegonial notching bilaterally (Fig. 9).

Two-dimensional cephalometric analysis added little in terms of quantification of this severe three-dimensional skeletal disorder. Further soft tissue surgery has been performed, reserving the major skeletal interventions until the completion of facial growth.

Discussion

The clinically overt and surgically challenging soft tissue derangement associated with large lymphangiomatous masses of the head and neck has contributed to the masking of the underlying skeletal abnormalities. Comprehensive clinical assessment, examination, and the advent of more refined radiologic techniques have identified the extent and severity of the associated craniofacial bony disturbances.

Previous isolated reports documented dental malocclusion and mandibular skeletal abnormalities in large cystic hygromas.[2, 3, 5, 6] All such cases manifested large lesions with extensions into the floor of the mouth and tongue. The occlusal and mandibular skeletal growth disturbances were attributed to local distortions of the mandibular body and dentoalveolar process, induced by the locally deforming forces of the cystic hygroma. Hence involvement of the floor of the mouth and tongue, with their concomitant enlargement and protrusion, produces anteriorly directed forces against the dentoalveolar process and mandibular symphysis.

Alternatively, such soft tissue masses may produce forward subluxation of an otherwise anatomically normal mandible.[5]

The three cases presented here, demonstrate disturbances in craniofacial anatomy considerably more extensive than previously noted. The first case, with its relatively symmetrical soft tissue involvement of the lower face, tongue, and neck, has skeletal anomalies confined to the mandible with an anterior open-bite deformity.

With extension of the soft mass into the midface, dentoalveolar and skeletal anomalies of the maxilla are manifest. Orbitozygomatic deformities with bony overgrowth zygomatic body and arch and clinically significant vertical orbital dystopia may accompany the large cystic hygroma.

In the presence of massive soft tissue distortion, twisting of the cranial base has been noted, reflected above as a marked parallelogram plagiocephaly, and manifest below as a bony facial scoliosis with involvement of the total height of the face. These skeletal abnormalities occur far beyond, and at some distance from, the primary soft tissue problem.

The weight of soft tissue exerts such tractional forces on the cranial base that asymmetries are manifest of both calvarium above and face below, just as in the plagiocephaly of untreated torticollis, without evidence of associated craniosynostosis. The presence during the neonatal period of the abnormal soft tissue functional matrix potentially exerts its deforming influence on the growing pediatric craniofacial skeleton. Indeed the presence at birth, and persistence through the early years, of the cystic hygroma ensures that such massive soft tissue distortions exert maximal distorting effects on the cranial base. In such cases then, in addition to the local direct effects on skeletal growth, these distant influences may play an important part in producing craniofacial dysmorphology.

The qualification of the anatomy of this growth disturbance remains troublesome. Complex two-dimensional cephalometric and pattern profile analysis in these asymmetric skeletal distortions is both difficult and adds little to that which can be appreciated by clinical examination. Only the application of a reliable technique of three-dimensional craniofacial analysis will allow complete qualification of the skeletal deformity, the changes produced by our surgery, and the long-term stability of the results.[1]

Only Osborne et al[5] have approached the surgical correction of the mandibulofacial deformity accompanying large head and neck cystic hygromas. Performing corrective mandibular surgery during the phase of mixed dentition and in the presence of unresolved soft tissue deformity as in their cases does not produce lasting stable correction of the mandibular skeletal disturbances and risks damage to the developing dental follicles. The influence of subsequent facial growth and the ongoing abnormal soft tissue functional matrix contributing to the virtual complete skeletal relapse. Similarly, attempts at correction of the calvarial asymmetry in infancy or childhood, as would be done for a sutural synostosis, are doomed to failure in the presence of persisting major soft tissue disturbances. Indeed in the clinical setting where such major soft tissue deformity remains largely un-correctable, no logical rationale exists for early orbital or maxillofacial skeletal corrective surgery. Leaving both the correction of the orbital dystopia and the malocclusion until the completion of facial growth should ensure a stable predictable skeletal outcome despite the persisting soft tissue mass. The period of both mixed and adult dentition prior to the completion of facial growth must be best employed to minimise the soft tissue problem.

The understanding and definition of the skeletal problems that accompany large cystic hygromas should permit more refinement in the surgical sculpturing of these most difficult faces.

References

1. Abbott AH. The acquisition and analysis of craniofacial data in three dimensions. Ph.D. Thesis. University of Adelaide, 1989.

2. Farman AG, Katz J, Eloff J, Cywes S. Mandibulo-facial aspects of the cervical lymphangioma (cystic hygroma). Br J Oral Surg 1978–79; 16:125.

3. Knowles CC. Malocclusion associated with an extensive lymphangioma of the face. Trans Br Soc Orthod 1971; 57:101.

4. Ninh TN, Ninh TX. Cystic hygroma in children; a report of 126 cases. J Pediatric Surg 1974; 9:191.

5. Osborne TE, Levin LS, Tilghman DM, Haller JA. Surgical correction of mandibulofacial deformities secondary to large cervical cystic hygromas. J Oral Maxillofac Surg 1987; 45:1015.

6. Paletta FX. Lymphangioma. Plast Reconstr Surg 1966; 37:269.

7. Williams HB. Facial bone changes with vascular tumours in children. Plast Reconstr Surg 1979; 63:309.

Basal encephalocoele: imaging and exposing the hernia

M. H. Moore, M. L. Lodge and D. J. David
Australian Craniofacial Unit, Women's and Children's Hospital, North Adelaide, Australia

Summary

Basal encephalocoeles are rarely reported anomalies. Eight cases seen by one unit manifested external facial features and internal cerebral anomalies characteristic of the individual encephalocoele subgroups. CT and MR imaging delineates the anatomy of the skeletal defect and the associated cerebral abnormalities. Such imaging of cases of median cleft face syndrome may identify previously unsuspected basal encephalocoeles.

Transcranial correction with increased exposure, if needed, by the technique of facial bipartition has been performed in five cases.

Basal encephalocoele, a developmental herniation of cerebral and meningeal tissue through a defect in the cranial base, has long been identified as a rare cause of soft tissue protrusion into the orbit, nasal cavity, nasopharynx or paranasal sinuses. Classification of basal encephalocoeles into subtypes based on the anatomical point of exit—trans-ethmoidal (TEE), spheno-ethmoidal (SEE), spheno-maxillary, spheno-orbital, and trans-sphenoidal (TSE) — is well accepted.[1] Similarly, the pattern of associated craniofacial, cerebral and ophthalmic anomalies with particular subtypes is documented and provides some opportunity to speculate on aetiology.[2-6] Theories ranging through failure of ossification centres in the sphenoid,[7] persistence of the craniopharyngeal canal and failure of closure of the anterior neuropore,[8] and anomalous induction of mesenchymal tissues or failure of fusion of the neural folds into a neural tube at this point have all been postulated as causative of basal encephalocoeles.[9]

The concealed, occult location and apparently recondite nature of the basal encephalocoele has also provided a continuing challenge to both diagnosis and management. The advent of complex techniques of three dimensional imaging and surgical exposure of this region has largely overcome these problems, permitting earlier accurate diagnostic delineation and the potential for definitive correction of both the primary encephalocoele and the secondary growth disturbances it may induce.

This study reviews the experience of the Australian Craniofacial Unit in managing basal encephalocoeles between 1986 and 1992.

Patients

A review of the records of the Australian Craniofacial Unit revealed eight patients with the diagnosis of basal encephalocoele. Six underwent a detailed multidisciplinary assessment in the unit before proceeding to surgical correction, while the remaining two were reviewed in overseas clinics but declined further treatment.

TABLE 1
Distribution of basal encephalocoele type (n = 8)

Trans-ethmoidal (TEE)	3
Spheno-ethmoidal (SEE)	1
Spheno-maxillary	0
Spheno-orbital	0
Trans-sphenoidal	4

Complex radiologic investigation included cephalometric radiography, axial and coronal 2-D CT scanning with 3-D CT reconstruction and, in the last four patients, MRI scanning.

Transcranial correction, performed at the earliest opportunity so as to minimise any distorting influence on craniofacial growth, has been favoured in this unit.

Results

In this series the distribution of encephalocoele type is recorded in Table 1. The TEE tended to present later in life, when compared to the TSE. The associated facial anomalies in the TEE group were minimal, with one case demonstrating mild hypertelorism and another a cleft lip. The patient with SEE (Figs 1, 2) and three of the TSE group all had marked hypertelorism, cleft lip and palate, these features of the median cleft face syndrome precipitating their early diagnosis (see Table 2).

Agenesis of the corpus callosum (see Table 3) was only seen in the spheroidal encephalocoeles, conforming to the view that only TSE are seen in association with the median cleft face syndrome.[2, 6] CT scan and MRI scan revealed a small TSE in one case with multiple rare craniofacial clefts, bilateral nasal probosci and unilateral microphthalmus, thought to be an example of the amniotic band sequence. At the time of transcranial correction of the craniofacial clefts, no encephalocoele was identified, although dissection may not have been carried sufficiently posteriorly to identify brain herniation in the region of the spheroid sinus and pituitary fossa (Table 4).

Presentation in the TEE group in two cases was to an otorhinolaryngologist for persistent rhinorrhoea. One had experienced several episodes of meningitis since a neonate, with eventual insertion of a ventriculoperitoneal shunt for treatment of hydrocephalus. The remaining case of TEE presented with symptoms of panhypopituitarism (see Table 2).

Prior to surgery, hypothalamic-pituitary function was assessed by hormone assays. This was repeated postoperatively and found to be unchanged. One patient with SEE was found to have panhypopituitarism 18 months post surgery and is responding well to replacement therapy. Surgical correction of the encephalocoele was performed in five cases (Table 4). The TEE were approached via a bifrontal craniotomy with reduction of the herniated brain and meningeal coverings and bone grafting of the cranial base defect.

The more posteriorly placed SEE and TSE were approached using a combination of the above transcranial approach and facial bipartition. This permitted concomitant correction of both the encephalocoele and the hypertelorism in patients as young as 4 months of age, with an uncomplicated postoperative course. In these cases bone graft and a galeofrontalis flap was interposed in the region of the defective cranial base (Figs 3, 4).

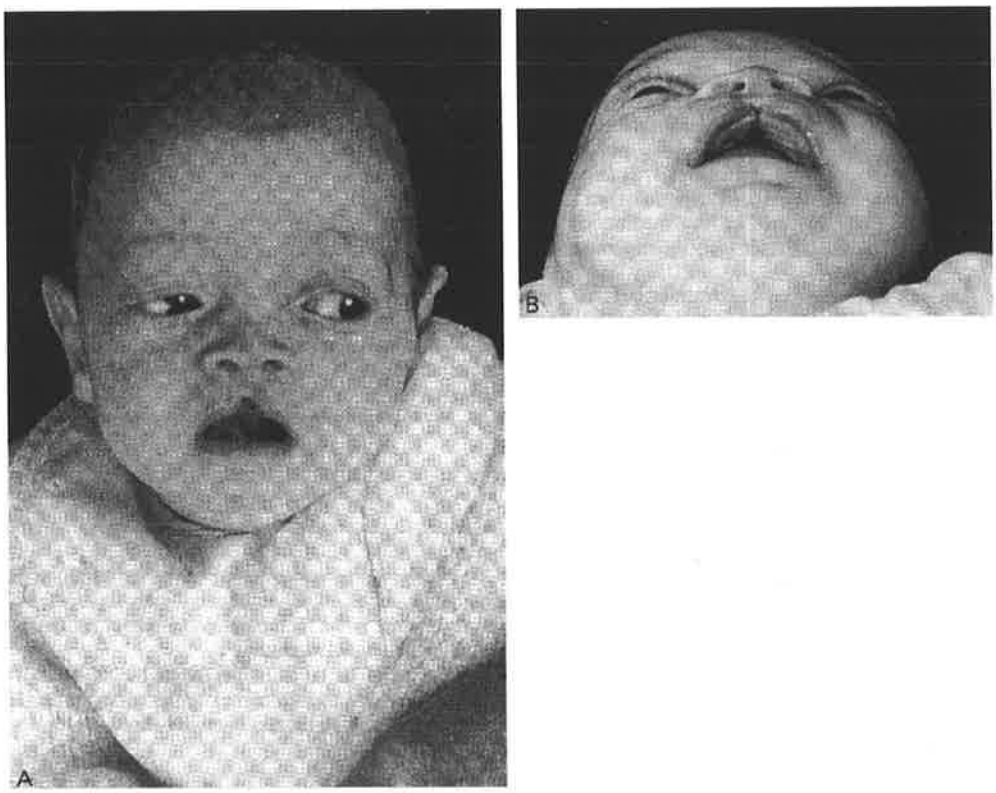

FIG. 1.— A. *Four month old child with a spheno-ethmoidal meningo-encephalocoele demonstrating median cleft lip and* **B.** *median cleft alveolus.*

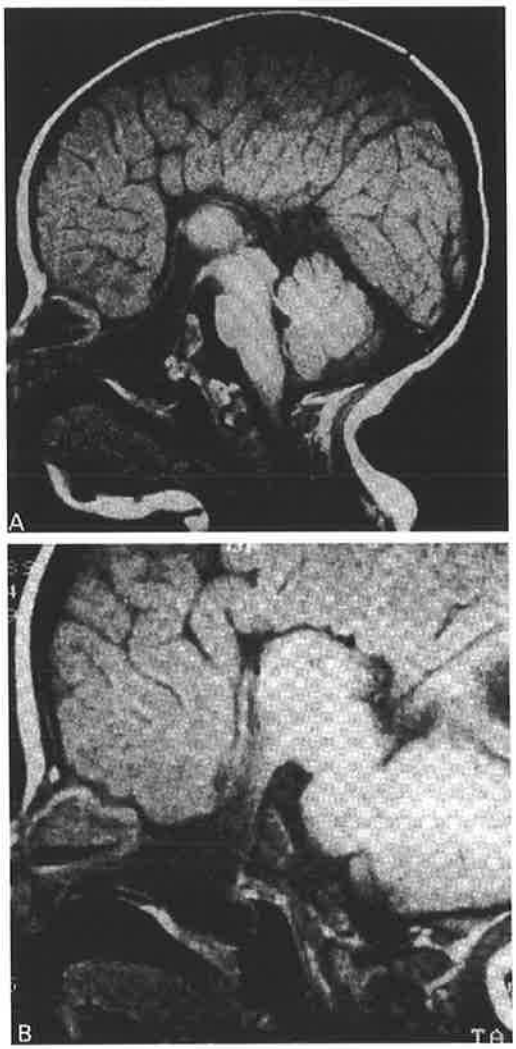

FIG. 2.— A. B. *MRI scan of four month old child with a sphenoethmoidal meningo-encephalocoele, sagittal views*

TABLE 2
Patient characteristics

Case	Encephalocoele type	Age at presentation and reason	Facial morphology	Panhypopituitarism
1.	TEE	6 years (Panhypopituitarism)	Cleft lip	Yes
2.	TSE	Birth (Median cleft face)	Cleft lip, palate Hypertelorism	Yes
3.	TEE	10 years (Rhinorrhoea)	Hypertelorism	No
4.	TSE	Birth (Median cleft face)	Cleft lip, palate Hypertelorism	No
5.	SEE	Birth (Median cleft face)	Cleft lip, palate Hypertelorism	No
6.	TEE	3 years (Rhinorrhoea)	Normal	No
7.	TSE	Birth (Median cleft face)	Cleft lip, palate Hypertelorism	Yes
8.	TSE	I year (Incidental finding on MRI)	Tessier clefts Hypertelorism	No

TABLE 3
Neurological features

Case	Encephalocoele type	Corpus Callosum	Meningitis	Mental retardation
1.	TEE	Present	No	No
2.	TSE	Absent	Post-op	Yes
3.	TEE	Present	Prior to diagnosis	No
4.	TSE	Present	No	No
5.	SEE	Absent	No	Develop-mental delay
6.	TEE	Present	Prior to diagnosis	Yes
7.	TSE	Unknown	No	No
8.	TSE	Present	No	No

TABLE 4
Surgical intervention in basal encephalocoele

Case	Encephalocoele type	Surgery	Age at surgery
1.	TEE	No surgery	-
2.	TSE	Transcranial correction (not at ACFU)	6 years
3.	TEE	Transcranial correction	10 years
4.	TSE	Facial bipartition Transcranial correction	2 years
5.	SEE	Facial bipartition Transcranial correction	4 months
6.	TEE	Transcranial correction	3 years
7.	TSE	Transcranial correction	1 year
8.	TSE	Transcranial correction of Tessier clefts Exploration for basal encephalocoele	1 year

Discussion

Basal encephalocoeles occur at a reported rate of 1 in 35,000 live births. Their occult location, and past difficulties in both imaging and exposing this area, have undoubtedly contributed to underdiagnosis. Whilst localisation to involvement of either the ethmoid or spheroid bones may help in determining the symptomatology of how the Encephalocoele will present, it does not necessarily prevent confusion with more common conditions, and thus misdiagnosis.

Heinecke in 1882 was reported by Fenger[10] to have originally classified basal encephalocoeles as sphenopharyngeal, spheno-orbital or spheno-maxillary in type. Subsequently Gisselson[1] expanded the classification, by labelling them according to the position of exit of the encephalocoele.

The TEE presents the more challenging diagnostic dilemma as associated facial and cerebral anomalies, which may act as a marker for the encephalocoele, are much less frequent. The presence of an intranasal tumour, which pulsates synchronously with the pulse or respiration, with symptoms of nasal obstruction from birth, requires appropriate assessment and imaging with MRI to exclude a TEE. Failure to consider this diagnosis risks the initiation of inappropriate treatment complicated by cerebrospinal fluid leak and meningitis. [11-13]

In contrast, the encephalocoeles which are transmitted through the spheroid bone will most commonly have co-existing anomalies of the face, optic system and brain, corresponding to the median cleft face syndrome.[14] The facial manifestations, hypertelorism, broad nasal root, median cleft nose, median cleft lip and maxilla and cranium bifidum occultum frontale are much more arresting and when seen require exclusion of an associated basal encephalocoele. This is particularly so where transcranial correction of the hypertelorism is envisaged. In this group there is also an increased incidence of anomalies of the optic disc, optic nerves, lipomas or agenesis of the corpus callosum and concomitant widening of the lateral ventricles. These associated findings all add to the speculation and uncertainty regarding aetiology.

Importantly, these more posteriorly located basal encephalocoeles may be associated with hypothalamic-pituitary dysfunction[15] and indeed knowing whether these regions are part of the herniated cerebral tissue is essential prior to any surgical intervention.

Detailed 3-D CT reconstruction of the cranial base allows one to view the skeletal outlines of the hernia. Bony marginal hypoplasia is not evident—all bony elements are present, although displaced, where the encephalocoele is of significant size. These techniques, when used routinely in the major midline craniofacial anomalies, such as median cleft face syndrome, will reveal the hitherto unsuspected basal encephalocoele. Visualising the anatomy of these disturbances in the cranial base then provides the opportunity to plan surgical correction appropriately, whether this be by hernia reduction and bone graft alone, or in combination with extensive craniofacial osteotomies.

Quantitative analysis, particularly in those late presenting cases, may in the future allow assessment of the growth disturbing influence of the encephalocoele on midfacial growth.

Conventional exposure by frontal craniotomy has been successful for ethmoidal encephalocoeles, presenting as they do in the older age group. In the light of the potential for earlier diagnosis, with the advent of improved imaging, there are no contraindications to definitive early correction. Reduction of the anomalous cerebral tissue via this route then permits closure and sealing of the cranial base defect with bone graft and a vascularised galeofrontalis flap. Any inadvertent penetration of the nasal cavity is then separated by vascularised tissue from direct communication with the intracranial space.

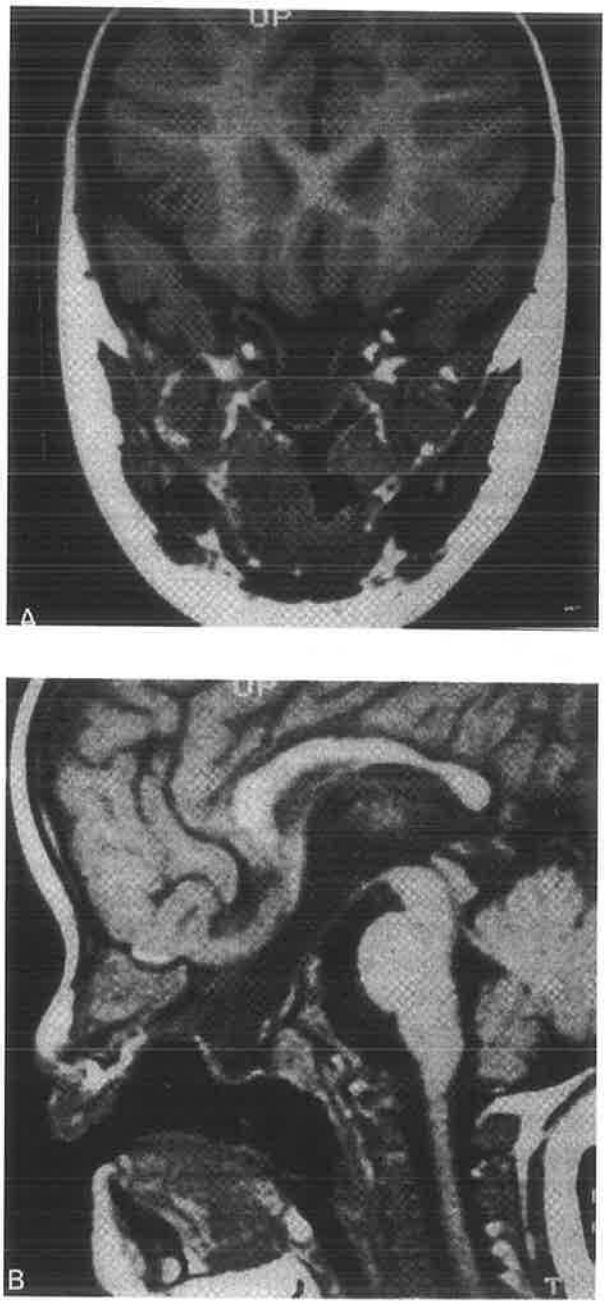

FIG. 3. A. *MRI scan of 2 year old child with a trans-sphenoidal meningo-encephalocoele, coronal view.* **B.** *MRI scan of 2 year old child with a trans-sphenoidal meningo-encephalocoele, sagittal view.*

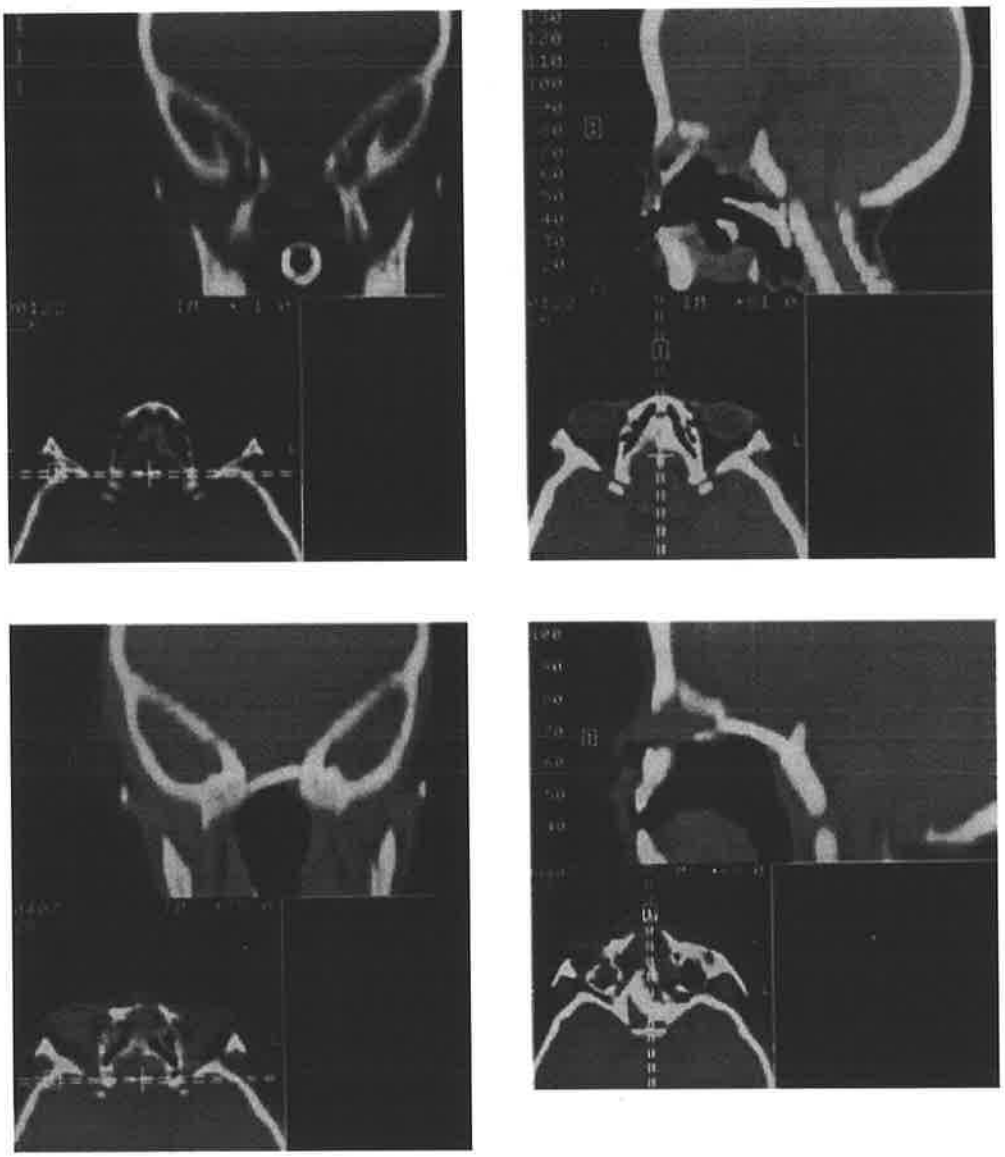

FIG. 4. A. *CT scan of 2 year old child with a trans-sphenoidal meningo-encephalocoele, coronal view.* **B.** *CT scan of 2 year old child with a trans-sphenoidal meningo-encephalocoele, sagittal view.* **C.** *CT scan of 2 year old child after correction of trans-sphenoidal meningoencephalocoele, demonstrating the bone graft* in situ, *coronal view.* **D.** *CT scan of 2 year old child after correction of trans-sphenoidal meningo-encephalocoele, demonstrating the bone graft* in situ, *sagittal view.*

Encephalocoeles originating in the region of the spheroid bone are more taxing both in terms of exposure and requirements for preservation of vital functional cerebral tissue the pituitaryhypothalamic axis. Additionally, their association with the median cleft face syndrome introduces the extra dimension of hypertelorism correction. Facial bipartition, performed by convention at approximately five years of age, facilitates both encephalocoele exposure and correction of hypertelorism, with minimal risk of damage to the midfacial unerupted secondary dentition. Where the extra mobilisation necessary for hypertelorism correction is not required, facial bipartition may be employed even earlier—in this series as young as four months of age. Mini- or microplate fixation provides precise stable reconstruction of the face, and calvarial bone the ideal donor site for graft material to occlude the cranial base defect.

Future observations of facial growth following cranial base reconstruction in these cases are planned.

References

1. Gisselson L. Intranasal forms of encephalomeningocele. Acta Octolaryngol 1947; 35: 519–31.

2. Yokota A, Matsukado Y, Fuwa I, Moroki K, Nagahiro S. Anterior basal encephalocele of the neonatal and infantile period. Neurosurgery 1986; 19: 968–78.

3. Naidich TP, Osborn RE, Bauer B, Naidich MJ. Median cleft face syndrome: MR and CT data from 11 children. Journal of Comp Assisted Tomog 1988; 12: 57–64.

4. Grubben C, Fryns JP, De Zegher F, Van den Berghe H. Anterior basal encephalocele in the median cleft face syndrome. Comments on nosology and treatment. Genetic Counselling 1990; 1: 103–9.

5. Temple IK, Brunner H, Jones B, Burn J, Baraitser M. Midline facial defects with ocular colobomata. Amer J Med Genet 1990; 37:23–7.

6. Soyer P, Dobbelaere P, Benoit S. Transalar spheroidal encephalocele. Clin Radiology 1991; 43: 65–7.

7. Elster AD, Branch CL. Transalar spheroidal encephaloceles: a review of clinical and roentgen features in 8 cases. Radiology 1989; 170: 245–7.

8. Pollock J, Newton TH, Hoyt WF. Transsphenoidal and transethmoidal encephaloceles: a review of clinical and roentgen features in 8 cases. Radiology 1968; 90: 442–53.

9. Barkovich A. Anomalies of the corpus callosum: correlation with further anomalies of the brain. Amer J Roentgenology 1988; 151: 171–9.

10. Fenger C. Basal hernias of the brain. Amer J Med Science 1895; 109: 519–31.

11. Lumsden A, Wilson JA, McLaren K, Maran AG. Unusual polypoidal tumours of the nasal cavity: a clinicopathological review of 18 cases. Clin Otolaryngol 1986; 11: 31–6.

12. Chen J. Antra-choanal polyp: a 10 year retrospective study in the podiatric population with a review of the literature. J Otolaryngol 1989; 18: 168–72.

13. Albernaz MS. Intrasphenoidal encephalocele. Otolaryngol Head and Neck Surg 1991; 104: 279–81.

14. De Myer W. The median cleft face syndrome. Neurology 1967; 17: 961–71.

15. Lieblich JM, Rosen SW, Guyda H, Reardon J, Scheff M. The syndrome of basal encephalocele and hypothalamic pituitary dysfunction. Annal Int Med 1978; 89: 910–6.

Chapter 7
Research and Technical Development

We shall not cease from exploration
and the end of all our exploring
will be to arrive where we started
and know the place for the first time.

T.S. Eliot

7. Research and Technical Development

The idea of developing and defining tools of investigation to throw light on the pathology and pathogenesis of craniofacial deformity has been central to the author's research strategy for the ACFU.

The technique for direct viewing of the velopharyngeal sphincter in speech was refined with synchronised colour viewing, split screen video fluoroscopy and speech sound and is described in Nasendoscopy:Significant Refinements of a Direct-Viewing Technique of the Velopharyngeal Sphincter, 1982[1]. This then very modern and effective technology is now widely available in many formats.

The author's Chapter in McCarthy's textbook Velopharyngeal Incompetence, 1990[2], sets out the clinical application of this tool of investigation.

The papers Three-Dimensional Reconstruction of the Facial Bones Utilizing Computerised Tomography for Craniofacial Surgery, 1983[3] and Three-Dimensional Reconstruction of Craniofacial Deformity Using Computed Tomography, 1983[4] represent the early involvement of the author and colleagues in this important advance in imaging and its implications for the study and treatment of craniofacial deformity.

Craniofacial Computer Modelling, 1986[5] outlines a parallel stream of study in the ACFU using biplanar cephalometric data.

The introduction to Craniofacial Deformities: Atlas of Three Dimensional Reconstruction from Computed Tomography, 1990[6] is an overview of the techniques developed thus far.

Effective use of this radiological and computer technology was made in the study Helmet-Induced Skull Base Fracture in a Motorcyclist, 1988[7].

■

The practical application of these three-dimensional analyses is addressed in Application and Comparison of Techniques for Three-Dimensional Analysis of Craniofacial Anomalies, 1990[8]. Progress to a position whereby landmarks can be determined, from which mathematical models are produced, is outlined in Craniofacial Osseous Landmark Determination from Stereo Computer Tomography Reconstructions, 1990[9].

Craniofacial Imaging, Models and Prostheses, 1994[10], describes some of the practical outcomes of this work.

Clinical and Radiological Findings in a Large Kindred and Exclusion of the Gene from 7p21 and 5qter, 1994[11] is another example of the value of multidisciplinary cooperation within the ACFU.

Apert Syndrome Results from Localised Mutations of FGFR2 and is Allelic with Crouzon Syndrome, 1995[12], is an example of inter-unit cooperation on an international scale, the Author's contribution being that of collecting data and making it available for a multi-centre study.

Central Nervous System Imaging in Crouzon Syndrome 1995[13], demonstrates advances being made in understanding the underlying pathology using modern radiology.

Papers

1. David DJ, White J, Sprod R, Bagnall A 1982 Nasendoscopy: Significant Refinements of a Direct-Viewing Technique of the Velopharyngeal Sphincter. Plast Reconstr Surg 70(4):423–428

2. David DJ, Bagnall AD 1990 Velopharyngeal Incompetence — Chapter 58. Plastic Surgery Vol. 4 — Cleft Lip & Palate & Craniofacial Anomalies 2903–2921

3. Hemmy DC, David DJ, Herman GT 1983 Three-Dimensional Reconstruction of the Facial Bones Utilizing Computerised Tomography for Craniofacial Surgery. Proceedings 8th Int Cong of Plastic and Reconstructive Surg 275–276

4. Hemmy DC, David DJ, Herman GT 1983 Three-Dimensional Reconstruction of Craniofacial Deformity Using Computed Tomography. Neurosurgery 13(5):534–541

5. Travan GR, Brown T, Townsend SC, David DJ 1986 Craniofacial Computer Modelling. Proc. 4th Australasian Conference on Computer Graphics 195–199

6. David DJ, Hemmy DC, Cooter RD 1990 Craniofacial Deformities: Atlas of Three Dimensional Reconstruction from Computed Tomography. Springer-Verlag, New York

7. Cooter RD, David DJ, McLean AJ, Simpson DA 1988 Helmet — Induced Skull Base Fracture in a Motorcyclist. The Lancet 84–85

■

8. Abbott AH, Netherway DJ, David DJ, Brown T 1990 Application and Comparison of Techniques for Three-Dimensional Analysis of Craniofacial Anomalies. Jnl Craniofacial Surg 1(3): 119–134

9. Abbott AH, Netherway DJ, David DJ Brown T 1990 Craniofacial Osseous Landmark Determination from Stereo Computer Tomography Reconstructions. Annals Academy of Med. 19(5): 595–604

10 Abbott J, Netherway DJ, Wingate P, Abbott AH, David DJ 1994 Craniofacial Imaging, Models and Prostheses. Aust J Otolaryng 1(6): 581–587

11 Ades LC, Mulley JC, Senga IP, Morris LL, David DJ, Haan EA 1994 Clinical and Radiological Findings in a Large Kindred and Exclusion of the Gene from 7p21 and 5qter. American Jnl of Med Genetics 51:121–130

12 Wilkie AOM, Slaney SF, Oldridge M, Poole MD, Ashworth GJ, Hockley AD, Hayward RD, David DJ, Pulleyn LJ, Rutland P, Malcolm S, Winder RM, Reardon W 1995 Apert Syndrome Results from Localised Mutations of FGFR2 and is Allelic with Crouzon Syndrome. Nature Gen 9:165–171

13 Proudman TW, Clark BE, Moore MH, Abbott AH, David DJ 1995 Central Nervous System Imaging in Crouzon Syndrome.Jnl Craniofacial Surg 6(5):401–405

■

Nasendoscopy: Significant Refinements of a Direct-Viewing Technique of the Velopharyngeal Sphincter

D. J. David, F.R.C.S., F.R.A.C.S., J. White, M.B., B.S., R. Sprod, A.I.M.B.I., and A. Bagnall, L.C.S.T., M.A.A.S.H.
North Adelaide, Australia

The velopharyngeal sphincter is formed by the posterosuperior part of the soft palate anteriorly, the posterior wall of the nasopharynx posteriorly, and the palatopharyngeal arches laterally. These structures define the pharyngeal isthmus. A number of other structures lie in close proximity, including the nasopharyngeal tonsils or adenoids and the pharyngeal opening of the auditory or eustachian tube.

The sphincter is a dynamic three-dimensional structure intimately involved in swallowing and speech. Incompetence of this sphincter during speech will result in a variety of speech abnormalities, the precise pattern of which will depend not only on the degree and type of velopharyngeal sphincter malfunction, but also on the degree and type of other anatomic and neurologic deformities involved in speech and on the individual's speech training. However, the velopharyngeal sphincter exerts a powerful effect on speech, and abnormalities of its function will often result in marked speech abnormalities not remediable by speech therapy alone. Thus numerous surgical procedures have been designed over the years to improve sphincter function.

Because of the complex anatomy and function of this sphincter, objective assessment of the benefits of surgery is dependent on direct viewing of the sphincter during unhindered continuous speech. Since the sphincter operates in three dimensions, viewing must incorporate visualisation of this three-dimensional movement.

Pigott and Makepeace first reported the use of combined nasendoscopy and lateral cinefluoroscopy to- allow such a three-dimensional assessment in 1975. Their technique used a black and white split-screen videotape recording of the two images to provide a permanent record of sphincter function, allowing objective assessment of the results of surgery.

The South Australian Craniofacial Unit, since its formation in 1975, has seen a considerable number of patients with velopharyngeal sphincter problems, either preoperatively or as a result of midface advancement. This has necessitated the routine use of nasendoscopy to assess sphincter function. We have developed significant refinements of the technique reported by Pigott and Makepeace,[1,2] and these refinements have allowed the technique to become a routine procedure at our unit.

Equipment

The success of our technique depends on high quality equipment. The nasendoscope is a 4-mm Storz-Hopkins 27015 C with a 70-degree viewing angle (rod length 113 mm) (Fig. 1). Illumination must be of high intensity for an adequate

From the South Australian Craniofacial Unit at the Adelaide Children's Hospital.

video image. We use a Storz xenon 487 cold light source, with light transmitted through a 5-mm flexible fiberoptic bundle. The nasendoscope image is transmitted to the camera through a Storz Wittmozer articulated Hopkins optic arm with a 50/50 to 10/90 beam splitter (Figs. 2 and 3). This instrument provides an optically "true" image to the colour television camera.

The video equipment must be of high resolution and sensitivity. The nasendoscope image is received by an Ikegami 2400 colour camera, with a Canon TV Macro 10- to 100-mm lens (J10 x 10B). The videofluoroscopy image is recorded from a high-resolution x-ray monitor by an Ikegami 2300 colour camera with a Canon V10 X 15E zoom lens.

Control equipment for both cameras is housed in a separate control console (Fig. 3) which includes a Shintron 370 series video switching and effects generator, an Electronics visuals waveform monitor EV4030, a Sony PVM 1300 AS high-resolution colour video monitor, and a Teac Tascam 3 balanced-line audio mixer. To this control unit are connected both colour video cameras and an IVC871 P open-reel l-in. colour videotape recorder/reproducer.

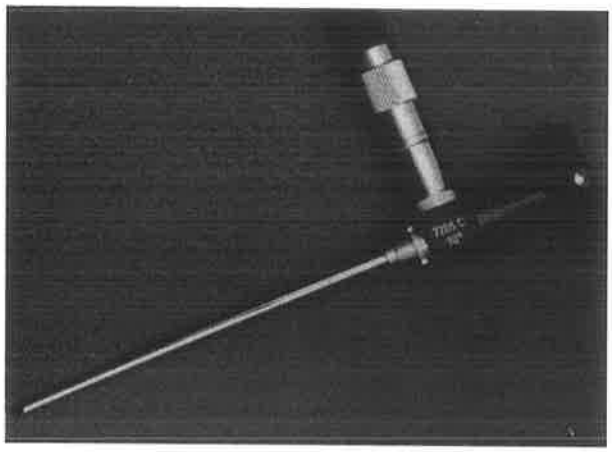

FIG. 1. *Storz-Hopkins 4-mm nasendoscope with 70-degree viewing angle.*

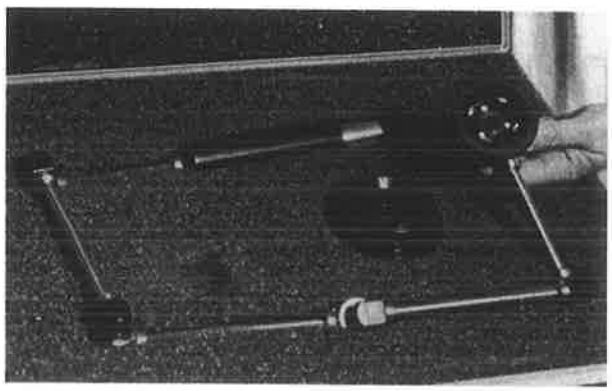

FIG. 2. *Storz-Wittmozer articulated Hopkins optic arm with 50/50 to 10/90 beam splitter.*

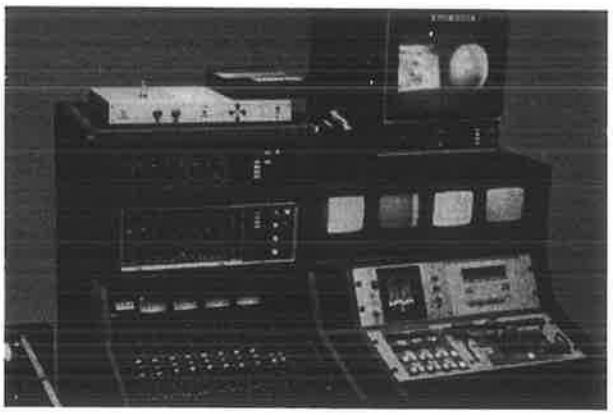

FIG. 3. *Video and audio control console, with a high-resolution colour video monitor and the 1-in. videotape recorder/reproducer on the left. The special processing unit is placed on the top of the control console.*

To allow adequate size and placement of the circular nasendoscope image, a special processing unit was designed and built. This unit, which sits on the control console, duplicates the drive-pulse signals of the nasendoscope camera (2400) and allows vertical and horizontal phase to be adjusted so that the image can be shifted to any part of the screen. This allows both the fluoroscopy and the nasendoscopy images to be side by side and of maximum size within the television format.

The patient's speech is recorded with a tie-clip Marantz EC-15P balanced electret microphone placed on the patient's collar. This will pick up the patient's and nasendoscopist's speech, but little of other sounds in the room. The audio signal is processed by the Tascam mixer.

The split-screen video image and the audio are recorded synchronously on the l-in. videotape recorder. Because the videotapes are later edited and dubbed to 3/4-in. U-MATIC format for use within the craniofacial unit, 1-in. recorders are used to maintain maximum picture detail and quality.

The layout of the system is shown in Figure 4. A schematic for the video section is shown in Figure 5. It is essential that the layout of equipment permits all personnel to see the final video monitor, including the nasendoscopist, who should be able to look up directly from the nasendoscope viewpiece to see the video images.

Technique

All patients referred to our unit with craniofacial anomalies will first be assessed by a craniofacial surgeon, who will organize further referrals and assessment by other team members. In the majority of cases this will include assessment by a speech pathologist on the team, who will then make a recommendation for nasendoscopy, if this is indicated. The second source of patients for nasendoscopy is direct referral by plastic surgeons, otorhinolaryngologists, and speech pathologists outside the unit. In all cases presenting for nasendoscopy, the referring speech pathologist is encouraged to attend the investigation

Patients have the procedure carefully explained to them prior to commencement, often several weeks or even months beforehand, especially for children. Such prior preparation has enabled us to successfully investigate children as young as 5 years of age, and occasionally even younger.

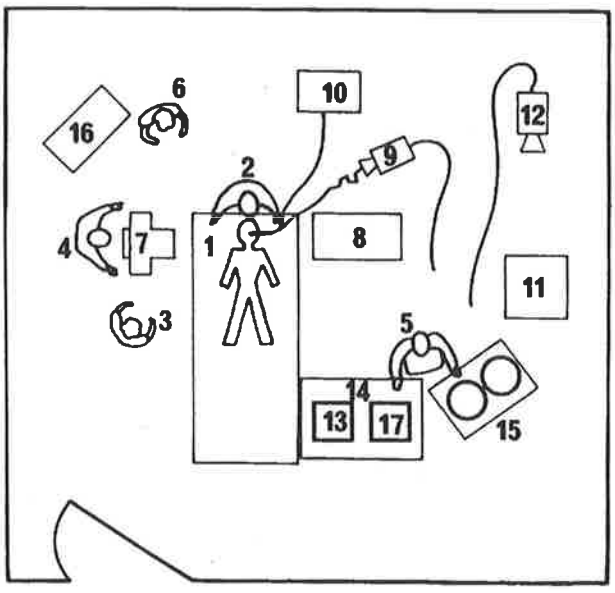

FIG. 4. *Schematic layout of the nasendoscopy room:* **1.** *patient,* **2.** *nasendoscopist,* **3.** *speech pathologist,* **4.** *radiographer,* **5.** *television operator,* **6.** *nurse,* **7.** *x-ray source,* **8.** *fluoroscopy unit,* **9.** *colour TV camera to receive nasendoscope image,* **10.** *cold light source,* **11.** *lateral fluoroscope monitor,* **12.** *TV camera to receive fluoroscopy monitor image,* **13.** *split-screen colour master monitor,* **14.** *TV and audio control unit,* **15.** *videotape recorder,* **16.** *trolley with local anesthetic and emergency equipment, and* **17.** *video image shifter.*

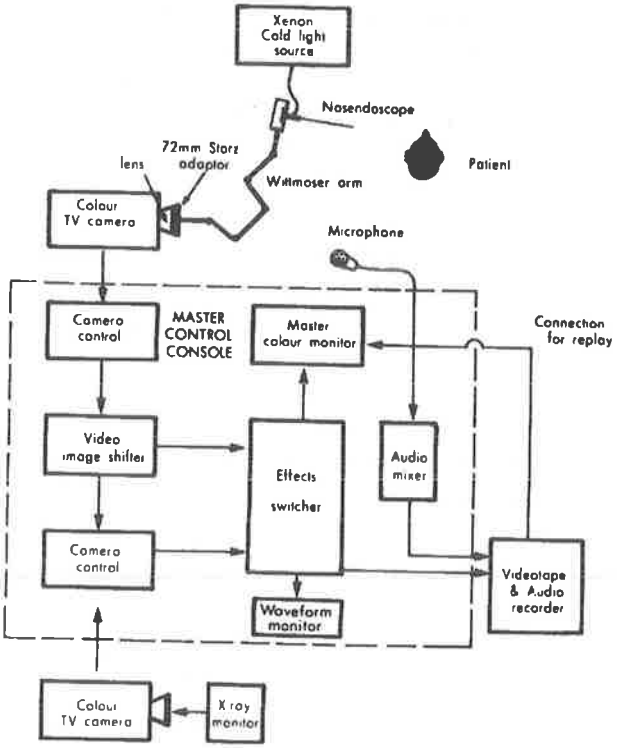

FIG. 5. *Schematic layout of video equipment.*

The patient has anesthesia of the nasal mucosa, induced by a spray of 10% cocaine, introduced at the nares. This is followed by the introduction of 25% cocaine paste on cotton buds, which are successively placed farther and farther down the nose, until the posterior wall of the nasopharynx is reached. This must be done slowly and gently to avoid the sharp pain that will occur with less delicate administration. Such pain will inevitably reduce the effectiveness of the investigation, especially in children, but also in some adults. Anesthesia along the whole track of the nasendoscope having been achieved, the patient is asked to wait 5 to 10 minutes prior to investigation. This delay allows time for contracture and drying of the nasal mucosa, thus allowing optimal viewing conditions.

The patient is then brought into the examination room and lies supine on the x-ray table, which is locked into position (Fig. 6). The patient's head is placed in a soft ring as close to the end of the table as possible, and the neck is extended slightly. The videofluoroscopy equipment is positioned by the radiographer to show a lateral view of the velopharyngeal sphincter and the tongue.

The microphone is placed as close as possible to the patient to record speech. Anesthesia of the nasal mucosa is rechecked and extended, if necessary, and after further explanation of the procedure, the nasendoscope is introduced through the nares under direct vision. An initial view of the sphincter is made; then the Hopkins optic arm is connected to the nasendoscope.

The patient is asked to recite a standard script, which allows analysis of all velopharyngeal movements during speech and direct comparison preoperatively and postoperatively. During the investigation, the personnel present have a real-time view of sphincter function, both from above by means of the nasendoscope and from the side by means of the fluoroscopy (Fig. 7), combined side by side on a video monitor. Immediately on completion of the procedure, the videotape is replayed to check the quality of recording, to explain findings to the patient or parent, and for a dictated report. Both the report and the videotape are kept as a permanent record.

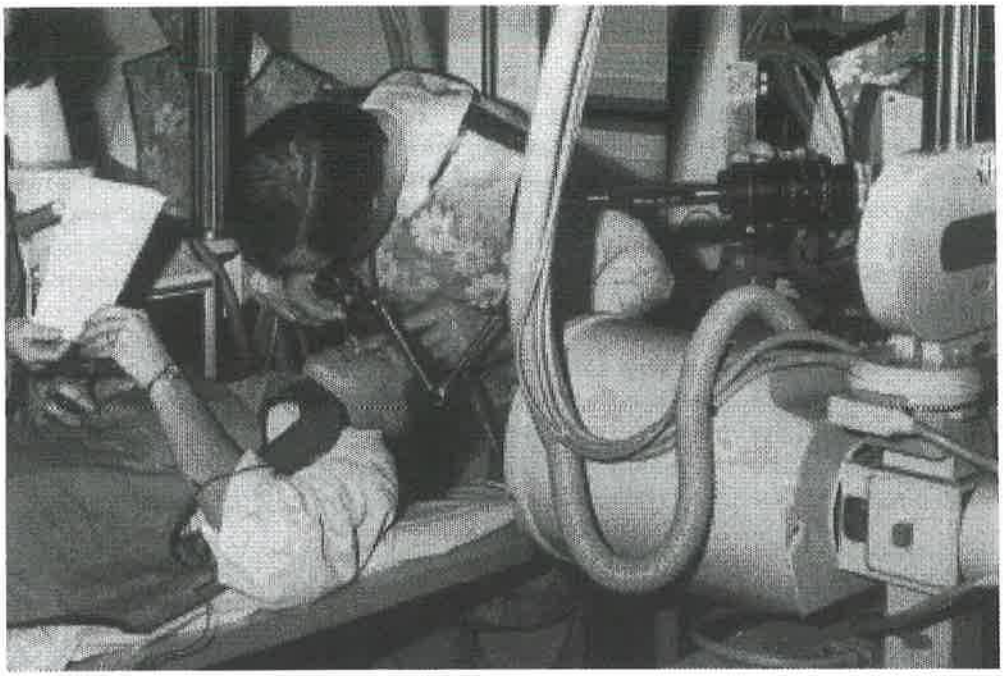

FIG. 6. *Patient in examination position, supine on x-ray table, head in a soft ring with neck slightly extended. The nasendoscope is being introduced with the Wittmoser arm attached and connected to the colour TV camera. The patient is holding the standard script.*

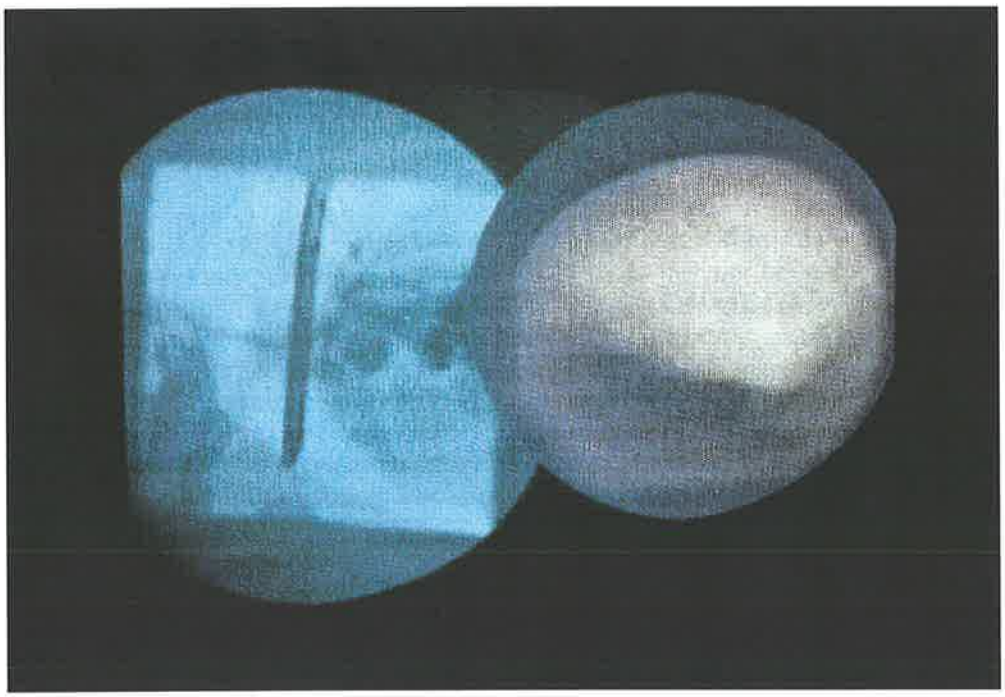

FIG. 7. *Combined split-screen colour nasendoscopy image and lateral videofluoroscopy image photographed on the monitor.*

Facilities are maintained for immediate treatment of cocaine reactions, should these occur. However, we have not had any such reactions to date.

Usually, six persons are required for our nasendoscopies. These consist of the nasendoscopist (usually a craniofacial surgeon), a second medical officer, who applies the topical anesthesia, the speech pathologist, the television operator, a radiographer, and a nurse.

Discussion

The advantages of split-screen video recording of the nasendoscope view and lateral videofluoroscopy over other techniques of investigation of velopharyngeal sphincter function have been discussed elsewhere.[1,2] Our refined technique allows greater flexibility of positioning of the two elements in the split screen to produce a much enhanced image of greater diagnostic value. The use of high-quality colour cameras and videotape recorders has further enhanced image quality.

The compactness and relative ease of operation have allowed this nasendoscopy technique to be used on a wide range of patients as a regular diagnostic tool. The video equipment is used for production of teaching material as a regular medical television education unit when not used for nasendoscopy, thus allowing reasonable amortisation for the original capital outlay.

Previously reported methods of split-screen video nasendoscopy require the patient to be in a sitting position.[1,2] This may allow completely normal movement of the velopharyngeal sphincter under the effects of gravity, but it also requires the nasendoscopist to be some distance from the patient, whose head is not fixed. This method does not give good control of the nasendoscope position. We have persisted with the original technique used by Pigott, with the patient supine, which gives good control of the patient, whose head is in a relatively fixed position, and allows the nasendoscopist to be close to the patient. Precise control of the nasendoscope position over extended time periods is thus achieved, allowing a high-quality image to be recorded.

The greater control of the patient and nasendoscope also allows the procedure to be less traumatic, with a consequently increased rate of successful examinations. The potential problem with this position is possible aberrations of sphincter function as a result of posture. In our experience this is not a problem.

This technique has enabled us to evaluate velopharyngeal sphincter function in a wide variety of clinical conditions, including patients with cleft deformities, especially cleft lip and palate; craniosynostosis syndromes such as Crouzon syndrome; patients with facial microsomia syndromes; and the effects of midface advancement on sphincter function. A study of these problems is underway, and an initial report on craniosynostosis syndromes has been given.[3]

We believe our refinement of the split-screen nasendoscopy technique offers major advantages over previous techniques and is invaluable for:

1. Viewing defects of the velopharyngeal sphincter
2. Predicting which patients will benefit from pharyngoplasty
3. Observing changes in sphincter function after midface surgery and predicting preoperatively those patients likely to need pharyngoplasty postoperatively

Summary

The need for a three-dimensional record of velopharyngeal sphincter function in patients with craniofacial anomalies and speech problems is discussed. A refined split-screen video technique using colour nasendoscope image, lateral videofluoroscopy, and synchronous speech recording with the patient awake and in a supine position is described. A special signal processor is used to position the colour nasendoscopy image. The examination is recorded on l-in. videotape. The technique allows three-dimensional appraisal of sphincter function with direct viewing and enables assessment of a range of abnormalities, assessment of the effectiveness of pharyngoplasties, and prediction of speech deformities and their management following midface craniofacial surgery.

Dr. J. White
South Australian Craniofacial Unit Adelaide Children's Hospital
King William Road
North Adelaide, S.A. 5006 Australia

Acknowledgments

We gratefully acknowledge the support of our colleagues in the craniofacial unit and the Adelaide medical community. Dr. Lloyd Morris, Director of Diagnostic Radiology at the Adelaide Children's Hospital, has kindly made his equipment and staff available for our nasendoscopy clinics. Mr. Barry Grieger, Director of Medical Illustration at the Adelaide Children's Hospital, has assisted with clinics and has made his staff and video equipment available to us. Messrs. Brian Lord, Chief Radiographer, Jack Wirth, Senior Radiographer, and Hans Kannussaar, Senior Radiographer, have provided expert help with these procedures and we are most grateful to them as well.

References

1. Pigott, R. W., and Makepeace, A. P. W. The technique of recording nasal pharyngoscopy. Br. J. Plast. Surg. 28: 26, 1975.

2. Pigott, R. W. The development of endoscopy of the palatopharyngeal isthmus. Proc. R. Soc. Lond. [Biol.] 195: 269, 1977.

3. Bagnall, A. Speech Problems in Crouzon Syndrome. Paper presented at the International Cleft Palate Congress, Acapulco, Mexico, May 1981.

Velopharyngeal Incompetence

David J. David, A. D. Bagnall

Key to Symbols

[æ]	as in c<u>a</u>t	[k]	as in <u>c</u>at
[ϵ]	as in g<u>e</u>t	[f]	as in <u>f</u>un
[i]	as in s<u>ee</u>	[θ]	as in <u>th</u>in
[p]	as in <u>p</u>ie	[s]	as in <u>s</u>un
[t]	as in <u>t</u>ie		

Anatomic and Functional Considerations

A competent velopharyngeal sphincter is essential for intelligible speech. The palate is part, but not the whole, of the sphincter, and a cleft palate is but one of the abnormalities affecting the velopharyngeal sphincter and speech. Modern concepts demand that the function of the velopharyngeal sphincter be seen in the context of the function of the whole vocal tract. The object of any surgery performed on the velopharyngeal sphincter is to provide an apparatus that permits the development of normal speech.

"Velopharyngeal incompetence" is the term used when the patient is diagnosed as being unable to close the sphincter completely. The sphincter is situated between the oral and nasal cavities and permits the speaker to separate the nasal from the oral cavity. Closure is achieved by tension in the velum and its elevation toward the posterior pharyngeal wall. At the same time, closure is assisted by the posterior and lateral pharyngeal walls, which move toward the rising velum, thus diminishing the lumen of the pharynx. As the person prepares to speak, the velum is partially raised and held at the ready position before speech begins; it then moves to the closed position as phonation starts. For nasal sounds (i.e., [m], [n], and [ŋ], the sphincter remains open. Complete closure does not always occur on non-nasal sounds, e.g., vowels. However, the ability to close the sphincter is essential for compression of air behind the point of constriction so that the consonants, especially plosives (e.g., [p], [t], and [k]) and fricatives (e.g., [f], [θ], and [s]) can be released with sufficient strength. In general terms, slight opening of the sphincter does not necessarily result in hypernasality. However, for a voice that has quality, richness, and carrying power, and consonants that are clear and precise, the ability to close the sphincter is essential. After normal function is understood, deviation from normal can be analyzed more effectively.

The raising and tensing of the velum, with or without full closure of the sphincter, plays a large part in the production of clear vowels. The size and shape of the pharynx, the degree of opening of the sphincter, and the various degrees of tension in the pillars of fauces and the soft palate are also important variables. The changes that appear in the velopharyngeal sphincter and vocal tract for the vowels [æ], [ϵ], and [i] are demonstrated in Figure 58-1.

Estill (1986) and others have suggested that the precise closure of the velopharyngeal sphincter ensures the efficiency of vocal cord action. Firm closure of the velopharyngeal sphincter makes possible the development of a negative

pressure in the pharynx, which, acting as a "back pressure," assists and maintains firm closure of the vocal cords. This ensures adequate compression of the air stream by closely approximated margins of the vocal cords, assisting the production of a clear, strong vocal note. The breathy, weak vocal note emanating from the larynx of the speaker with velopharyngeal incompetence demonstrates this finding. In addition, a speaker who is unable to close this sphincter is handicapped as a communicator. The voice lacks carrying power, richness, warmth, subtlety of light and shade, and above all, esthetic quality. If the vocal note has access to the nasal cavity in excess of what is required for a pleasing tone, hypernasality or excessive nasality result.

The velopharyngeal sphincter has an essential part to play in the production of speech sounds. If air escapes into the nose through an open velopharyngeal sphincter, consonants lack precision and clarity. They may become distorted, may be associated with nasal snorting, or may be substituted for by pharyngeal or glottal sounds. The speaker may develop compensatory habits: excessive tension of the vocal tract; increased breath flow, or articulators substitutes, which are maladaptive patterns of vocal behavior that further detract from the clarity and quality of speech.

Analysis of the workings of the velopharyngeal sphincter has shown it to be a highly complex and, as yet, only partially understood mechanism. The cerebral cortex, lower neurologic systems, and auditory perceptual monitoring ability of the speaker result in a subtlety of action of the sphincter, which ensures a truly efficient and pleasing voice. It follows, therefore, that the expectations of surgery may be unduly high, considering the complexities of the vocal instrument. It is not yet possible to match the surgery, however sophisticated and skillful, to the intricacies of the instrument. Progress is being made slowly as the ever more objective tools of investigation are employed to throw more light on the nature and function of the velopharyngeal sphincter. More precise understanding, not only of the mechanism as it presents to the investigator, but also of the changes that result from surgery, subsequent healing, and voice and articulation therapy will ensure the development of more sophisticated and effective treatment. For the present, treatment must be based on precise evaluation of the sphincter deficiency followed by conservative and/or surgical intervention.

Speech analysis is also discussed in Chapter 54.

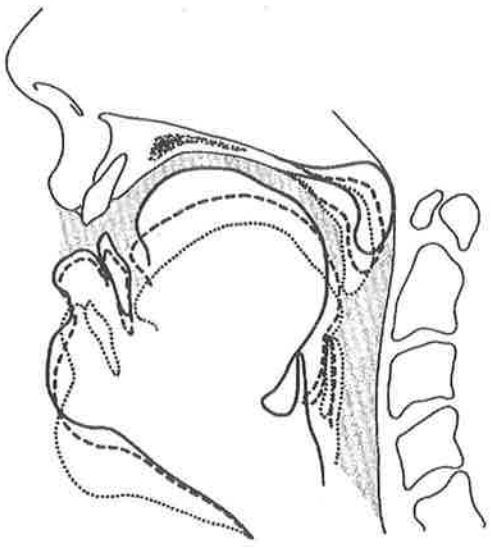

FIG. 58. 1. *Velar elevation. Tracings taken from xero-radiographs in which the velum and tongue are seen in different positions for different cardinal vowels. [æ] = ... [ϵ] = -----, [i]= —*

Causes of Velopharyngeal Incompetence

The patient with hypernasal speech or demonstrable nasal air escape may have an incompetent velopharyngeal sphincter. This may have several causes:

1. *Idiopathic insufficiency of the musculature,* in which all elements of the sphincter are working, but a tight seal, i.e., one sufficiently strong to withstand the positive air pressures built up in the oral cavity during speech, is not possible. On oral examination, no obvious signs of abnormality appear. Patients often complain of vocal fatigue and accusations of mumbling from their family or friends. On closer examination they have some element of excessive hypernasality or nasal air escape. Nasendoscopy and synchronous lateral videofluoroscopy may reveal a slight deficiency in closure of the sphincter. A slit may be seen where the velum approaches the posterior pharyngeal wall but does not quite close the aperture. Conversely, where one or the other lateral wall is not sufficiently active, a gap is seen either unilaterally or (sometimes) bilaterally. These patients may not require surgery. Speech therapy to develop firmer closure may resolve the problem.

2. *Congenital palatal insufficiency is* a condition in which the velum is too short to reach across to the posterior pharyngeal wall. This has been variously termed a short soft palate (Kaplan, Jobe, and Chase, 1969), congenital short palate (Greene, 1964; Morley, 1973), and regional growth and development disturbances (Fletcher, 1960). Conversely, the pharynx has been considered too capacious for the size of the velum. This has been variously described as a "box pharynx" or a congenital large pharynx (Calnan, 1971a). In these cases all elements of the sphincter are working but are disproportionate.

3. *Submucous cleft palate is* a condition in which the soft palate muscles fail to unite in the midline, although the mucous membrane is intact. As the palate elevates, the levators can be seen lifting and pulling the segments of the cleft apart, forming a central furrow or area of translucency *(zona pellucida).* The patient speaks with hypernasality, which may be mild, moderate, or excessive. Submucous cleft palate has been described in various ways, but most investigators agree that it is usually characterised by a bifid uvula, a bony notch in the hard palate, and diastasis of the palatal muscles (Calnan, 1954). In 1977 this concept was supported by Pruzansky (Peterson-Falzone, 1985). However, patients with hypernasal speech without the observable stigmata of submucous cleft palate, as described above, have been reported by Kaplan (1975) as presenting with "occult submucous cleft palate." Kaplan (1975) described the unusual muscle insertions similar to those seen in classic submucous cleft palate, even though oral examination revealed no evidence of submucous cleft palate. Subsequently, Croft and associates (1978) described the use of nasopharyngoscopy to assist the diagnosis of submucous cleft palate in 20 patients. An absence of the musculus uvulae on the nasal surface of the palate, resembling a V-shaped depression or concavity resulting in a central deficiency on attempted palatal closure, has been described as "occult submucous cleft palate" (Shprintzen, 1979). This lack of muscle bulk is not obvious upon visual inspection or palpation of the oral surface of the velum. Clearly, however, this muscle bulk is essential for velopharyngeal competence. Peterson-Falzone (1985) emphasised that there is considerable disagreement between investigators regarding their criteria when making the diagnosis of submucous cleft palate, and that nasendoscopy can reveal muscular deficiency when other "intraorally visible stigmata" are absent.

4. *Following repair of cleft palate,* velopharyngeal incompetence can occur as a result of anomalies in the movement of the various elements of the closure pattern. Surgery to close the soft palate has, as its major aim, the provision of palatal length, bulk, muscle arrangement, and movement potential sufficient to provide the speaker with full closure of the velopharyngeal port during speech

(Morris, 1984). With the nasendoscope, it is sometimes noted that the speaker with a repaired cleft palate has a shortened velum that can never reach the posterior pharyngeal wall. Other patients have satisfactory velar elevation and stretch, but the posterior and lateral pharyngeal walls do not move adequately, leaving a deficit on closure. Yet others close with approximately equal movement of all elements of the sphincter, but there is a central deficit, circular in shape. The shortness of the palate following surgery has been attributed to the original inadequacy of palatal tissue rather than to the inadequacies of the surgery (Greene, 1964).

5. *After pharyngeal flap or pharyngoplasty* a patient may still have velopharyngeal incompetence and hypernasality owing to inadequate flap width, i.e., air escaping on either side. If a pharyngeal flap is so narrow that the lateral ports remain open during speech, there are surgical procedures designed to manage this difficult problem (Cosman and Falk, 1975; Owsley, Lawson, and Chierici, 1976). If a flap is situated too low in the pharynx, beneath the point where the lateral pharyngeal walls can effect closure, it creates two funnels that aerodynamically promote nasal air escape (Osberg and Witzel, 1981).

6. *After adenoidectomy* a patient may present with velopharyngeal incompetence. Before surgery, he may have been closing the velum against the pad of lymphoid tissue. After adenoidectomy, the velum is unable to close against the posterior pharyngeal wall. Greene (1964) hypothesised a failure in movement of the palate probably due to lack of use, which gradually resolves, although this may take as long as three months. However, Calnan (1971b) stated that speech therapy for this group was without effect, and recommended surgery by a cartilage implant behind the posterior wall of the pharynx to return the speech to normal. Hypernasality that occurs following adenoidectomy has been thought to resolve over time, variously reported as six months to one year (Massengill, 1972) and two to six months (Goode and Ross, 1972). After this time, if speech remains hypernasal, careful evaluation and surgical management may be necessary.

7. *Enlarged tonsils* have also been considered as a cause of velopharyngeal incompetence. When the tonsils restrict the airway in the oropharynx because of their size, the speaker may develop a degree of hypernasality. This results from his awareness of a restricted airway that causes him to open the sphincter (Bloch, 1979). In this situation, a patient may develop a forward tongue carriage in an additional effort to increase the size of the airway. When greatly enlarged, the tonsils may add sufficient weight to the palatopharyngeal arch, such that the speaker has difficulty achieving full closure. In this way, they inhibit velar elevation (Bzoch and Williams, 1979). It is thought that enlarged tonsils interfere with the access of the vocal note to the oral cavity. This impedance leads to the diversion of sound energy into the nasopharynx and nasal cavities, increasing the perceived hypernasality (Subtelny and Koepp Baker, 1956). In this way, enlarged tonsils can have a detrimental effect upon speech, but their precise role, especially with regard to velopharyngeal incompetence, is not fully understood.

8. *After midface advancement,* velopharyngeal incompetence can occur. Patients at risk in this way are those with previously repaired cleft palate and/or those who had demonstrable nasal air escape and hypernasality before surgery. The advancement of the face clearly stresses the sphincter, which subsequently is unable to make full closure (Schwarz and Gruner, 1976; Witzel and Munro, 1977; Schendel and associates, 1979; McCarthy and associates, 1979). It is also important to note that in other cases of midface advancement the sphincter may be disrupted temporarily by the surgery, e.g., subcranial Le Fort III osteotomies in Crouzon's or Apert's syndrome. However, the craniosynostosis patients (with Crouzon's or Apert's syndrome) are generally not at risk of developing velopharyngeal incompetence after Le Fort III advancement osteotomy (McCarthy and associates, 1979).

9. *Neurogenic* conditions give rise to problems of weakness, incoordination, and fatigue affecting the pattern of closure. These include some cases of hemifacial microsomia with unilateral weakness, peripheral neuritis, myasthenia gravis, nuclear lesions, bulbar poliomyelitis, and supranuclear paresis, which is usually congenital and typified by the child with cerebral palsy. Upper and lower motor neuron lesions result in dysarthria, which may include the velopharyngeal sphincter. Velopharyngeal incompetence is a significant element contributing to the speech disturbance of the patient with spastic, flaccid, or mixed dysarthria. The movements of the velopharyngeal sphincter for swallowing are usually affected. Evaluation and management of velopharyngeal incompetence in dysarthria require careful analysis and cooperation between surgeons and speech pathologists (Dworkin and Johns, 1980).

10. *Lack of velopharyngeal sphincter movement for speech.* Some children present with velopharyngeal incompetence of a gross nature, and on nasendoscopy the sphincter has been seen to be immobile. On swallowing, the sphincter appears to be normal. This problem requires further investigation and research, since pharyngoplasty does not resolve their hypernasal speech. In the same way, therapeutic management has also been found to be ineffective. Little is known of this condition, but wide, superiorly based pharyngeal flaps have been performed in order to provide some obturation for these patients (Huskie, 1985).

11. *Functional/hysterical hypernasality* has been found in the presence of a competent speech mechanism. This has been attributed to emotional disturbance (Greene, 1964). In the absence of any organic abnormality, hypernasality does occur (Crikelair and associates, 1964); Porterfield and associates, 1966). Hypernasality can appear in the absence of organic or physiologic abnormalities, e.g., when the individual imitates the speech he perceives in his environment. On nasendoscopy, normal movement and closure of the velopharyngeal sphincter is seen, usually on the production of consonants, a maneuver that requires the development of intraoral air pressure for their precise release. However, the vowels are produced with an open sphincter, imparting hypernasal tone to the voice. Hypernasality is commonly found in the deaf speaker, owing to an inappropriate use of the sphincter. The perception of hypernasality by the listener is dependent on the characteristics of the entire vocal tract and not only on the use of the velopharyngeal sphincter (Curtis, 1968). Hence, *pseudohypernasality,* or *functional hypernasality* presents the greatest challenge in the diagnosis of velopharyngeal incompetence. Just as no two individuals close their velopharyngeal sphincter in precisely the same way, or position their articulatory organs in precisely the same way, no two individuals have precisely the same voice quality. Issues related to voice quality and the degree of nasality found in the language environment of the speaker, especially in the family, must also be taken into account when deciding when, or if, the velopharyngeal sphincter is incompetent. This understanding is essential when surgery is being considered, as, by definition, the patient with pseudohypernasality does not have velopharyngeal sphincter incompetence, and surgery is, therefore, contraindicated.

History of Surgery

Surgery aimed at correcting velopharyngeal incompetence is not new. In the sixteenth century, Pierre Franco (1561) indicated an awareness of the connection between cleft palate and poor speech. During the nineteenth century, surgical procedures were developed that are still being used in modified forms. Following primary cleft palate surgery, secondary techniques for the correction of velopharyngeal incompetence include palatal lengthening procedures; pharyngeal flaps; augmentation of the posterior pharyngeal wall with soft tissue or implants; sphincter reconstruction; and prosthetic obturators.

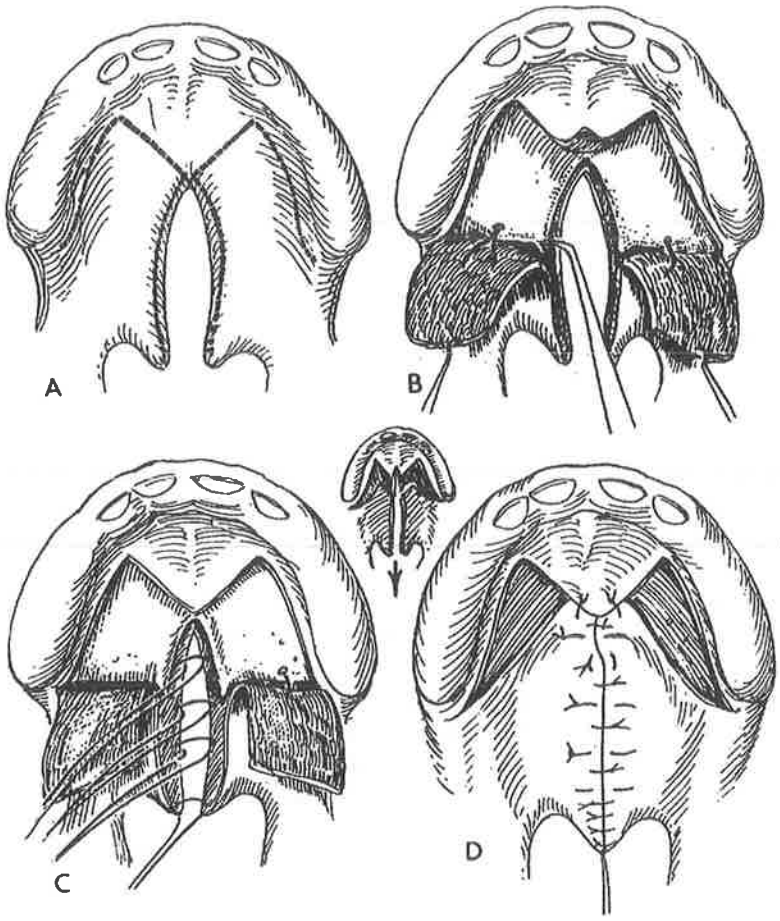

FIG. 58–2. *The Veau-Wardill-Kilner operation for repair of a cleft of the secondary palate.* **A.** *Outline of the incision.* **B.** *The flaps are raised.* **C.** *Suture of the mucous membrane on the nasal aspect of the palate.* **D.** *Position of the flaps at the completion of the operation.*

Palatal Lengthening Procedures
(Fig. 58–2)

Palatal pushback procedures with anterior obturation were reported by Suersen (1869), Passavant (1878), Garel (1894), Kingsley (1897), and Gillies and Fry (1921). These techniques involved dividing the hard and soft palates and placing an obturator in the intervening space. Veau and Ruppe (1922) introduced a technique designed for closure of the hard palate using widely undermined mucoperiosteal flaps that were dependent for their survival solely on the posterior palatine vessels. Ganzer (1917) reported similar flaps, and those operations were subsequently modified by Wardill (1937) and Kilner (1937). This technique may be effectively combined with the intravelar veloplasty of Braithwaite (1964) (Fig. 58–3).

These surgical innovations made possible retrodisplacement and lengthening of the soft palate, which could be used in patients in whom primary palate closure failed to achieve sufficient palate length for competency. Dorrance (1930) had emphasized this point and had also suggested the use of the pushback procedure as a secondary operation. Limberg (1927) advocated removal of the bony posterior palatine shelf to allow greater retrodisplacement of the palate. Many procedures based on the technique have since been described.

Pharyngeal Flaps

The posterior pharyngeal flap was introduced by Passavant (1865). The procedure consisted of the creation of adhesions between the soft palate and the pharyngeal

wall, rather than a formal elevation of a full thickness pharyngeal flap, which was then attached to the palate. Schonborn (1876) and Shede (1889) employed a formal, inferiorly based flap of the posterior pharyngeal wall. Other authors reported such techniques subsequently. Bardenheuer (1892) first suggested a superiorly based pharyngeal flap, which has since been advocated by Sanvenero-Rosselli (1935), Conway (1951), and Stark and DeHaan (1960). Other authors have described variations on this principle.

Augmentation of Posterior Pharyngeal Wall
(Fig. 58–4)

The first operation to correct velopharyngeal incompetence by building up the posterior pharyngeal wall was described by Passavant in 1862, when he developed techniques to accentuate production of the posterior pharyngeal wall muscle ridge. Gersuny (1900) and Eckstein (1904) injected paraffin behind the pharyngeal wall to displace it anteriorly. Perthes (1912) and Hill and Hagerty (1960) inserted cartilage; Halle (1925) and von Gaza (1926) employed fascia implants in the same retropharyngeal site. Blocksma (1963) used Silastic as a retropharyngeal implant, and Ward (1968) used injectable Teflon. Extrusion of the implanted material was common and the level at which it was placed was often ineffective owing to migration, or indeed, to the various levels over which the sphincteric closure takes place, a variable that is dependent on the individual's use of the sphincter. Brauer (1965) advocated seamless Silastic pillows. All these techniques may be used when the deficit in closure is small (less than 0.5 cm).

Reconstruction of Velopharyngeal Sphincter

Browne (1935) attempted to reconstruct the velopharyngeal sphincter anatomically, by placing a constricting suture around the entire oronasal port at the level of Passavant's ridge. McCutcheon (1954) dissected the pharyngeal wall and transposed flaps to the midline from both sides. Braithwaite (1968) reported a technique for the dissection of the medial pterygoid muscles from their origin, allowing them to reorganise more inferiorly and medially. Hynes (1950) transferred the lateral salpingopharyngeal muscles, reflecting them as flaps (Fig. 58–5). The authors, by the use of nasendoscopy, have seen such cases functioning effectively when the lateral wall muscle was maintained in the flap. Orticochea (1968, 1983) advocated the construction of a dynamic muscle sphincter of the pharynx in which the lateral musculo-mucosal flaps are set into a small posterior pharyngeal flap. Modifications were suggested by Jackson and Silverton (1977) (Fig. 58–6) whereby the constructed sphincter provides dynamic and static obturation of the velopharyngeal isthmus. This popular technique awaits long-term assessment of its efficacy compared with the pharyngeal flap technique.

Other Approaches

Combinations of the above procedures have been advocated, including a combined palatal pushback and an inferiorly based flap (Padgett, 1930; Conway, 1951), or a combined pushback operation with a superiorly based flap (Broadbent and Swinyard, 1959; Edgerton, 1962, Buchholz and associates, 1967; Honig, 1968). In 1954, Hynes reported the combination of his pharyngoplasty with primary palatal repair. Dalston and Stuteville (1975) advocated primary nasopalatal pharyngo-plasty.

Prosthetic Obturation
(see Chap. 72)

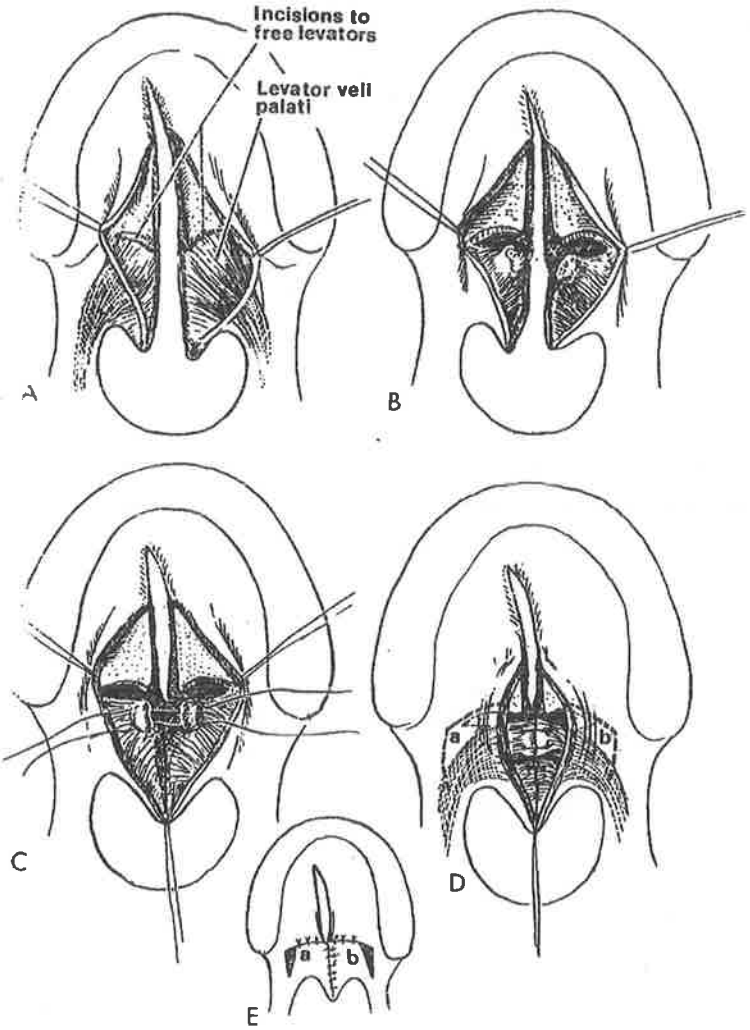

FIG. 58–3. *Levator transplant procedure (Braithwaite).* **A.** *In a cleft of the secondary palate, the levator muscles fail to insert into the nominal position across the midline. Note the insertion on the posterior maxillary spine. In reconstruction of the soft palate, incisions are made along the posterior border of the hard palate to release the aponeurosis of the levator, allowing it to move posteriorly.* **B.** *With the incision of the levator aponeurosis and its liberation from the posterior maxillary spine, the levator moves posteriorly and forms a round muscular bundle on each side.* **C.** *The levator muscle is joined in the midline by suture. Overlap of the muscles at this point, as originally recommended by Braithwaite, may also be performed.* **D.** *The sutured, reconstructed levator muscle. The levator sling has been re-established.* **E.** *When the levator suture is combined with soft palate closure as a primary procedure, there may often be deficiency of mucosa on the soft palate. Small flaps (a, b) are formed in closing the midline to aid a difficult soft palate closure.*

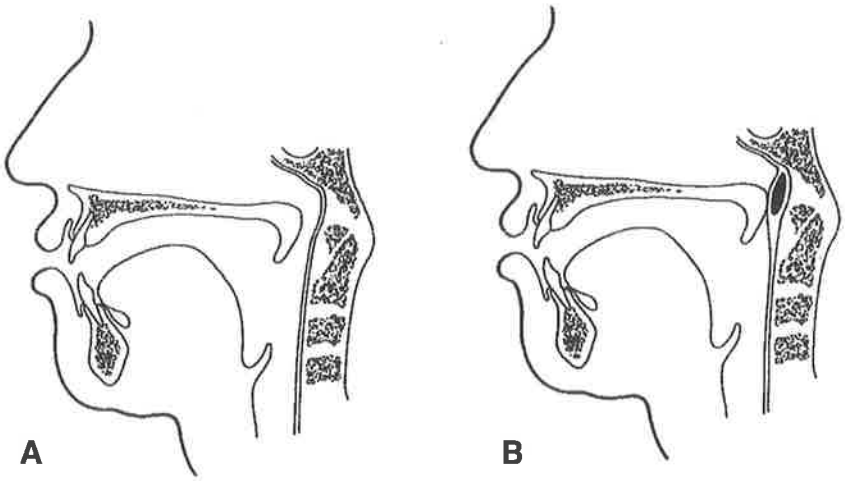

FIG. 58-4. A. *The relative position of the soft palate and the atlas of the spine.* **B.** *The preferred positioning of the retropharyngeal implant in order to obtain velopharyngeal competence.*

Management

Management of velopharyngeal sphincter incompetence involves:

1. Evaluation and measurement of the underlying deficiency of the velopharyngeal sphincter and the associated contributing abnormalities.

2. Surgery and/or therapeutic management of the sphincter inadequacy.

3. Modification of the secondary superimposed compensatory habits.

In this way, the speaker with velopharyngeal incompetence can be provided with the potential for normal, acceptable speech.

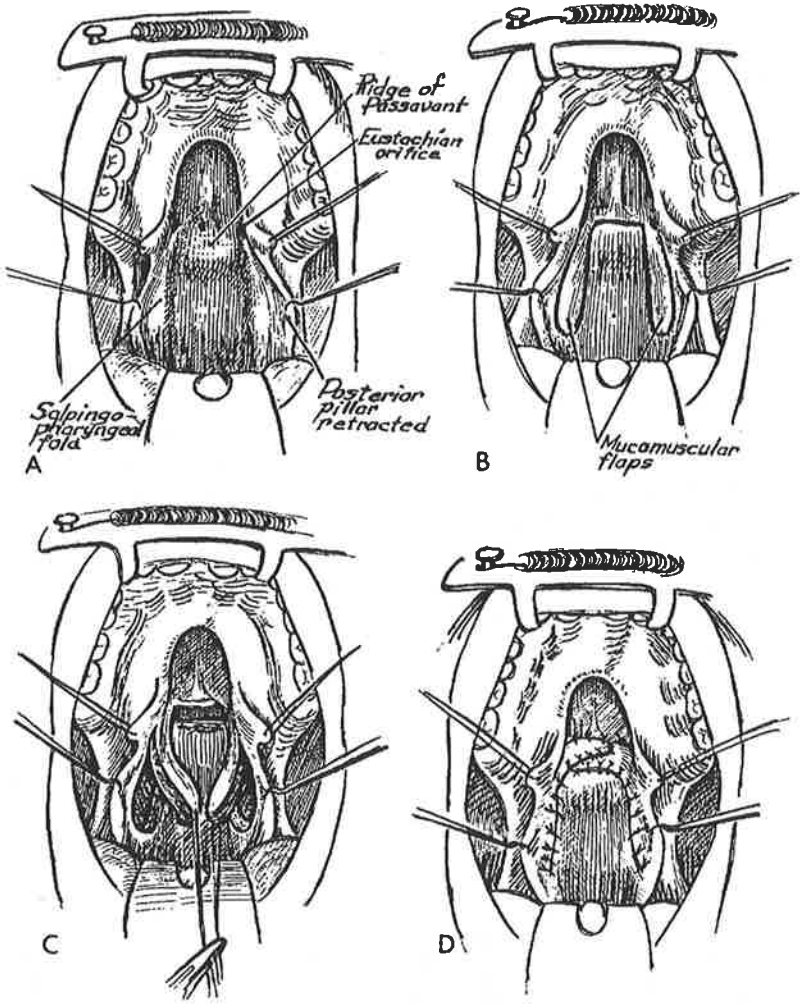

FIG. 58–5. *The Hynes pharyngoplasty. This procedure, performed as a primary as well as a secondary operation, consists of elevating two superiorly based flaps that envelop most of the salpingopharyngeus muscles. Closure of the donor defects narrows the pharynx, while a medial interpolation and crosslapping of the two flaps produces a horizontal shelf above Passavant's edge, which brings the posterior pharyngeal 'target" closer to the velum. (After Hynes, 1950.)*

Evaluation and Measurement

Management of velopharyngeal incompetence and the associated speech distortion involves several choices. Thorough assessment of velopharyngeal incompetence is essential, to avoid inappropriate treatment methods. Initially, it must be determined that the speech distortion is due to the sphincter being unable to close. Second, after it is determined that the sphincter is inadequate in some way, three decisions are possible:

1. The young patient can be observed, reassured at intervals, and, hopefully, with maturity and with satisfactory hearing and speech patterns in his environment, his speech may improve and the velopharyngeal sphincter may eventually be found to be competent. In this way, surgery can be avoided.

2. The patient may receive speech therapy designed to produce firmer, consistent closure of the sphincter and the development of more acceptable speech.

3. The patient may be scheduled for surgery, with or without speech therapy subsequently to develop optimal use of the new mechanism.

As both speech therapy and surgery are costly in terms of time, money, and emotional energy, such decisions must not be made hurriedly. A caring approach to the needs of the individual; thorough investigation; detailed informed discussion with patient, parents, and family; and sensitivity to the specific requirements of the individual speaker are essential. Therapy based on inadequate evaluation of the potential of the velopharyngeal sphincter for change is doomed to failure and can cause much distress. In the same way, careful evaluation before surgery is essential. It follows that for effective treatment, every effort must be made to achieve as objective an analysis of the problem as possible.

Traditionally, the ear of the speech pathologist or surgeon has been the most frequently used assessment tool. Auditory impressions or perceptual measures or ratings are no measure of velopharyngeal incompetence, but they can lead and lend weight to more objective measures. Audio recordings over time can also provide comparisons of gains or changes from surgery or other forms of therapy. There have been attempts to validate auditory perceptual impressions by spectrographic analysis. However, although nasality is immediately perceived by the human ear, the acoustic correlate is difficult to describe and (considering the complexity of the vocal instrument) is of little use as a test of velopharyngeal sphincter competence (van den Berg, 1962). The measurement of oral and nasal sound intensity as a method of analyzing hypernasality was attempted by Fletcher and Bishop (1970). They developed an instrument called TONAR, which is sometimes used to measure velopharyngeal function, but support for this application is lacking (McWilliams, Morris, and Shelton, 1984). The benefits to be gained from TONAR depend on its demonstrated ability to correlate its results with reliable ratings of hypernasality. Although hypernasality related to the individual's ability to close the velopharyngeal port is discussed in relation to TONAR, most of the studies completed with this instrument have been directed toward nasality, rather than to analysis of sphincter closure.

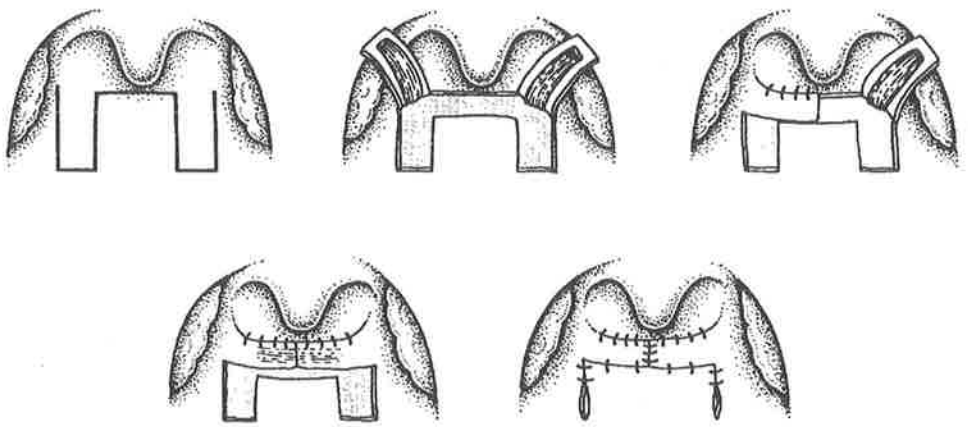

FIG. 58–6. *The sphincter pharyngoplasty as described by Orticochea and modified by Jackson (1983). The similarity to the Hynes technique is noted.*

Nasal air flow measures of various types have been used over the years, including pneumotachometers and warm wire flow meters (McWilliams, Morris, and Shelton, 1984). Of particular interest is Warren's PERCI (palatal efficiency rating computed instantaneously) (Warren, 1979). This aeromechanical system was designed to give information concerning the velopharyngeal mechanism during speech. It displays and records the difference in air pressure in the mouth and in the nose during speech. Differential pressure readings are used to compute the size of the velopharyngeal orifice area. As PERCI is not sensitive to minimal openings in the velopharyngeal sphincter, its use is limited.

Oral/nasal air flow measures have been used by speech pathologists for many years to determine the competence of the velopharyngeal sphincter. A variety of devices, which are indirect methods of assessment, have been used to investigate the sphincter, but do not give detailed analysis of the workings of this mechanism. They range from "cardboard or plastic paddles" (Bzoch, 1979) to a small mirror or mirrored surface, such as the Floxite Detail Reflector (Bloch, 1979). Testing for nasal air emission can also be carried out with a stethoscope held under the nose or against the nares during production of consonants (Bloch, 1979). The Seescape detects nasal air emission during speech; with the tip inserted into the nares, any emission of air causes a float to rise in a rigid plastic tube. In the same way, U-tube manometers, water manometers, ultrasound, and accelerometers provide pressure/flow information concerning nasal air escape. From these data, deductions can be made as to the effectiveness of velopharyngeal closure, but the precise nature of the working of the sphincter cannot be revealed by such devices (McWilliams, Morris, and Shelton, 1984).

Articulation tests have been specifically designed to elicit words containing speech sounds that require oral pressure for correct production. In this way, they assist the speech pathologist to discriminate between speakers who have adequate velopharyngeal closure and those who do not. Such a test is the Iowa Pressure Articulation Test (Morris, Spriestersbach, and Darley, 1961). An articulation test that aims to facilitate identification of articulation errors based on research findings of the characteristic articulation of children 3 to 6 years of age with repaired cleft palate has been designed by Bzoch (Bzoch Error Pattern Diagnostic Articulation Test, 1978). This test aims to delineate the type of substitution or distortion used by these children owing to their difficulty in developing normal articulation related to velopharyngeal incompetence. However, the test makes no objective assessment of velopharyngeal sphincter closure but deduces velopharyngeal incompetence from articulation errors.

Electromyographic studies utilising hooked wire electrodes inserted into the velopharyngeal mechanism may give additional information regarding patterns of movement and potential for sphincter closure (Fritzell, 1969; Lubker, Fritzell, and Lindqvist, 1970). When combined with cineradiographic investigation of velar function, additional information is provided (Lubker, 1968). However, this method of investigating velopharyngeal sphincter function can be criticised on the basis that precise placement of the electrodes is difficult, especially for the inexperienced. As the technique is both invasive and somewhat painful, it requires a considerable degree of cooperation from the subject. It is, therefore, problematic for young children. Nevertheless, such studies provide useful information concerning the use of the velopharyngeal sphincter and may throw additional light on its normal function (Bell-Berti), 1983).

More objective information about the velopharyngeal sphincter has been provided by radiology and endoscopy (Pigott, 1979). Lateral pharyngeal radiographs were used to demonstrate the height and position of the velum in relation to the posterior pharyngeal wall, but only in two dimensions. This technique could not provide information concerning the movements of the lateral pharyngeal walls. Cinefluorography and videofluoroscopy followed. It was recognised that there was a need to gather more information from videofluoroscopy than could be provided from the midsagittal view. Multiview

videofluoroscopy, a technique that adds a base view to the traditional lateral and frontal projections, was developed by Skolnick (1970). These views, obtained consecutively, are thought to complement each other and are interpreted together. The ability of the observer to retain and recall on observing each of these views what he has gained from the previous one provides the investigator with a three-dimensional understanding of the velopharyngeal sphincter. Clearly, the visual perceptual abilities of the observer and the experience of the radiographer and investigating team play a large part in the usefulness and objectivity of this system. The timing of the speech event, its replication by the patient, and accurate positioning of the patient are crucial to the validity of this system. However, both cine and videofluoroscopy have added to the understanding of the velopharyngeal sphincter, and have a role in the diagnosis and choice of treatment for the patient with velopharyngeal incompetence (McWilliams, Morris, and Shelton, 1984).

Endoscopy permits observation of the essential elements of the velopharyngeal sphincter as they move in relationship to one another. Over the years, several types of endoscopes have been utilised, but there is general agreement that an endoscope that does not interfere with the movements of the articulatory organs or of the velopharyngeal sphincter is the instrument of choice. At the present time, both flexible and rigid endoscopes are used. The flexible nasopharyngoscope has advantages in respect to its ease of insertion, but many prefer the superior optics of the rigid nasopharyngoscope. For example, the Storz-Hopkins 4.2 x 3.5 mm overall diameter nasopharyngoscope has an angle of 70 degrees, which corresponds closely to the plane of isthmus closure or presumptive plane of closure of the velopharyngeal sphincter in most individuals. Its particular optic system permits more light transmission and greater clarity than other lens or fiberoptic systems. It has an extremely wide field of view encompassing the entire isthmus (Pigott, 1979). However, the nasopharyngoscope provides only a two-dimensional image. The third image, i.e., vertical height of closure, can be provided by a synchronised lateral videofluoroscopic image. When these two images are displayed side by side on a split screen and synchronised with the speech recording, a dynamic view of the changing positions of the various components of closure during different speech events is provided (David and Bagnall, 1984). This technique enables the investigating team to review the examination at will and to compare pre- and post-treatment examinations of the sphincter.

Some concern has been expressed regarding the ease with which a patient, especially a young child, can tolerate and cooperate with the nasendoscopy procedure, especially when the rigid nasopharyngoscope is used. At the South Australian Cranio-Facial Unit, over 1000 nasendoscopies have been performed during the past decade. The Storz rigid nasopharyngoscope with its preferred optical characteristics is used routinely coupled with simultaneous lateral videofluoroscopy and speech recording (David and associates, 1982). The two adjacent images are set on a split screen, permitting instantaneous viewing and video recording. Sixty-five per cent of the nasendoscopies are of adults and adolescents, and 35 per cent of children under 10 years of age. Nasendoscopy of the adults has been almost 100 per cent successful. Of the total patient group, 92 per cent of nasendoscopies were successful, with the patient able to cooperate fully and a precise, clear video recording being obtained for future reference. Twenty-two per cent of nasendoscopies are examinations of younger children, 4 to 6 years of age. This group of children receive one session of orientation to the procedure. It frequently involves the use of a tangible behavior reinforcement game, the child proceeding through each stage of the game, which corresponds with a particular stage of the nasendoscopy procedure. With the use of this tangible reward technique and with careful and thorough preparation, often including some "roleplay," 80 percent of nasendoscopies in this age group are successful at the first attempt. A calm and confident parental attitude, an atmosphere of mutual trust, and an unhurried approach are also essential elements of this success.

CT scans have been proposed as a further investigative tool, especially

when combined with endoscopy (Honjo and associates, 1984). Considering the intricacies of sphincter movement and the variable height of closure, the use of 3 mm cuts, as suggested by these researchers, would not provide tomograms capable of delineating the subtleties of closure.

From this overview of the various instruments available for evaluation of the velopharyngeal sphincter, it is apparent that each has its advantages and disadvantages. With more objective diagnostic information, the choice of appropriate patient management is simplified. It is important to remember that impressions gained from evaluating the action of the sphincter during speech production that is in any way contrived have limited value. The most objective investigation results from analysis of movements of the velopharyngeal sphincter during spontaneous speech. Any instrument that permits the patient sufficient freedom to speak at will, while allowing the investigator to observe and analyze every component of the sphincter in view, paves the way for effective treatment.

Choice of Surgery

With the increase of objective, quantitative, preoperative, and postoperative evaluation data, it is possible to approach the problem of treatment choice more rationally. In particular, the information gained from direct viewing with the nasendoscope, together with synchronised lateral videofluoroscopy, provides information to aid the proper choice of surgical technique.

The range of defects of sphincter closure may include:

1. A central defect, small or large, in the velopharyngeal sphincter with satisfactory palatal elevation and lateral wall movement.

2. A flaplike action of the palate with a weak lateral wall component, producing a transverse, slitlike defect in the sphincter. Occasionally a significant posterior pharyngeal wall ridge is observed with this pattern of closure.

3. Poor palatal movement with satisfactory lateral pharyngeal wall movement.

4. Asymmetric gaps with lack of elevation of the palate on one side more than the other, or asymmetric lateral pharyngeal wall movement, as commonly seen in unilateral craniofacial microsomia.

5. Gross failure of all elements of the sphincter.

The challenge presented to the clinician by the use of modern tools of objective assessment is to design the appropriate treatment for the observed deformity. It is clear that *small central defects* with good function of all elements of the sphincter may well respond to a number of different procedures. Such small defects are amenable to treatment by posterior wall implant, or a small, centrally placed superior pharyngeal flap, although the latter treatment also renders the palate immobile. In such cases, the nasendoscope view demonstrates a central muscular deficiency on the upper surface of the palate. Re-repair of the palate with retroposition of the levator mechanism may also be appropriate. Pigott (1986) has suggested that a central augmentation of the area of the musculus uvulae by a local musculomucosal flap, taken from the substance of the oral side of the soft palate and transposed into the midline of the dorsum of the palate, may help.

In cases in which there is *gross failure of all elements of the sphincter,* the situation is much more difficult. Some surgeons use palatal appliances and others prefer a large pharyngeal flap. It is the authors' experience that this rare but unhappy situation cannot be effectively treated by surgery using currently available techniques.

The *asymmetric defects* of the sphincter, which are associated with a lack of elevation of the palate on one side or with an asymmetric lateral pharyngeal wall movement, may be treated by an offset, superiorly based pharyngeal flap or by a unilateral sphincter pharyngoplasty.

If there is a *deficiency in elevation of the palate, but satisfactory lateral wall movement,* the situation is theoretically ideal for a superiorly based pharyngeal flap. The lateral wall movement closes the lateral ports and the tethering of the already deficient palate does not constitute a significant loss of function to the palatal element of the sphincter.

The most common situation in the authors' experience is the finding of a weak lateral wall movement with a stronger palatal function, although there is a great range of variation in the degrees of function of the individual elements of the sphincter. The less prominent the movement of the lateral pharyngeal wall, the less effective is the superiorly based flap. The palate is tethered by the flap and there is incomplete obturation as a result of the limited lateral wall movement. Efforts to overcome this situation have been directed toward adding a pushback procedure to the flap, or making the flap very wide, thus running the risk of nasopharyngeal obstruction or even sleep apnea. It is in this situation (poor lateral pharyngeal movement) that the sphincter pharyngoplasty may be of more use as a dynamic, or even static, mechanism.

The argument concerning the relative advantages of the superior versus the inferior pharyngeal flap has developed into a challenge to choose the most appropriate operation for the defect based on the findings of videofluoroscopy and nasendoscopy. Jackson (1985) suggested an appropriate matching of surgical procedures to the pattern of sphincter deformity. He preferred to use the sphincter pharyngoplasty to solve the difficult problem of the weak lateral wall movement, as suggested above. Such a procedure allows the dynamic palate to continue moving and it augments the posterolateral aspects of the sphincter with a dynamic mechanism.

In the authors' experience, a vast majority of cases do not show definite lateral wall movement without palatal elevation, or definite failure of lateral wall movement with satisfactory palatal elevation, but a variable mix of relative deficiencies of sphincter components. It is in this group that much energy needs to be expended in evaluating the respective results of the sphincter technique and the superiorly based pharyngeal flap. It is not known how often the palatopharyngeus muscle transposed in the sphincteric operation functions as an integral part of the velopharyngeal sphincter in speech. However, the point is well taken that sphincter pharyngoplasty is not an "end of the line" operation. It is capable of being adjusted and even combined with pharyngeal flap procedures.

Operative Technique

For a superiorly based, lined pharyngeal flap, a videotape of the nasendoscopy and synchronous lateral fluoroscope is viewed before surgery so that the flap can be tailored to suit the defect as closely as possible (Fig. 58–7).

The operation is begun with oroendotracheal intubation, and an appropriate mouth gag is used to expose the palate and oropharynx. The surgeon sits at the head of the table; a fiberoptic head lamp is a useful aid to visualisation. The midline of the palate is injected with 1/80,000 epinephrine in solution of 2 per cent lidocaine, and a small amount of the solution is injected into the posterior pharyngeal wall. The soft palate is divided in the midline, the incision not quite reaching the hard palate. The nasal lining is divided transversely on each side, leaving a fringe attached to the posterior part of the hard palate. The nasal lining distal to the transverse incision is elevated from the underlying musculature. A trapdoor flap is marked on the posterior pharyngeal wall and, within limits, the width of the flap can be tailored to the defect as visualized; e.g., in unilateral

craniofacial microsomia, with a unilateral defect in the sphincter, the flap can be constructed mostly on the side of the defect. The flap is elevated from the transverse incision toward the head, separating the mucosa and pharyngeal musculature from the underlying prevertebral fascia. One must be careful not to damage the base of the flap, as the mucosa becomes friable in the area of the adenoids.

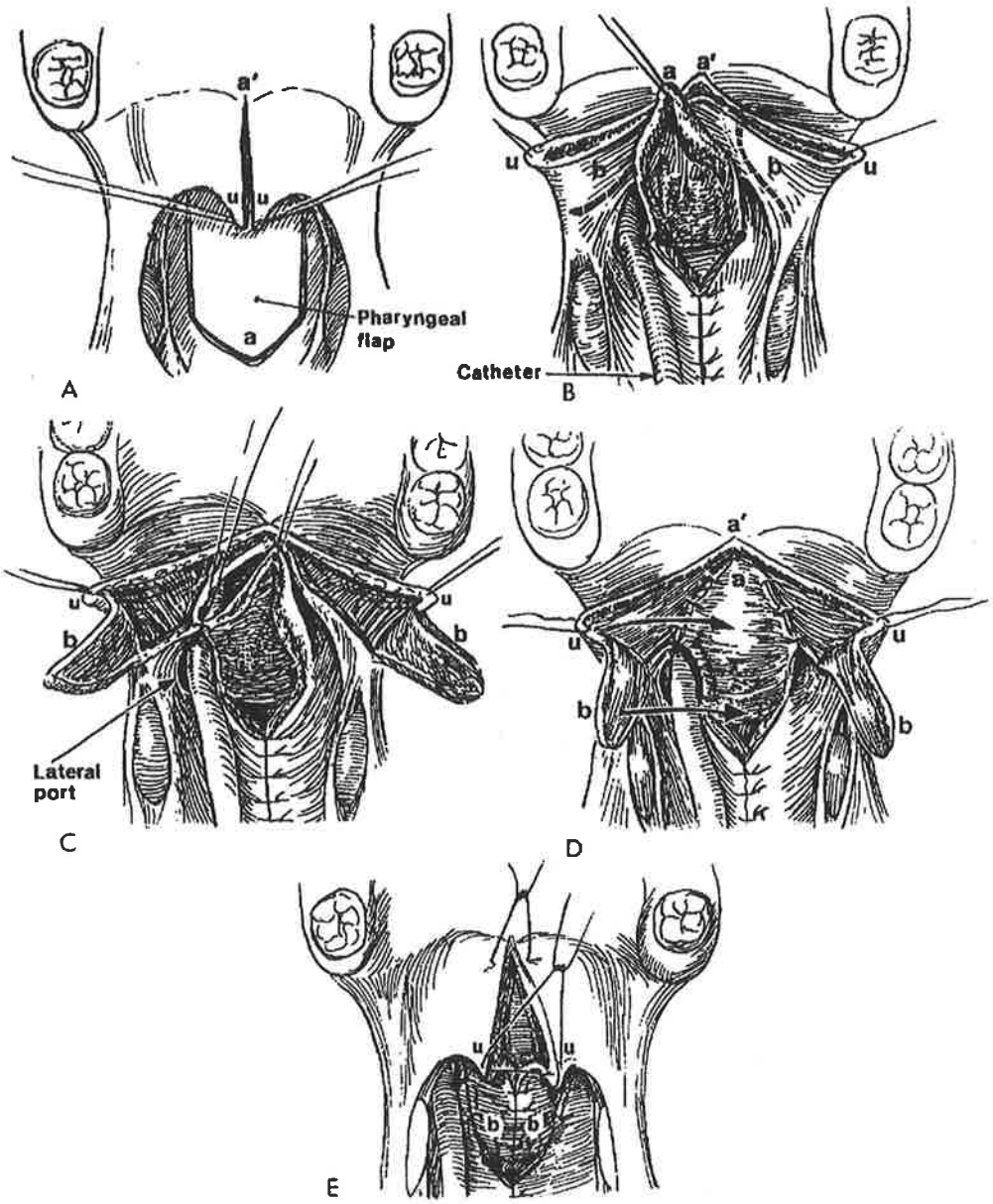

FIG. 58–7. *Lateral port control pharyngeal flap.* **A.** *The soft palate is divided and a superiorly based pharyngeal flap is designed, extending the full width of the posterior pharyngeal wall. It is elevated from the prevertebral fascia.* **B.** *The posterior pharyngeal wall has been closed in the midline with catgut sutures. Closure of the posterior wall should not extend fully to the base of the pharyngeal flap or this will result in a narrowing or tubing of the flap. Alternatively the posterior wall defect can be left open. Development of lining flaps* (b) *on the nasal surface of the soft palate is illustrated.* **C.** *The lining flaps in the soft palate* (b) *have been elevated and retracted laterally. The catheter is placed in the lateral port on one side of the pharyngeal flap. Suturing of the pharyngeal flap into the mucosa of the soft palate has begun.* **D.** *The pharyngeal flap has been sutured to the nasal surface of the soft palate; suturing has extended toward the pharyngeal wall snugly around 14 French catheters. The lining flaps* (b) *are about to be rotated over the raw surface of the pharyngeal flap.* **E.** *The lining flaps have been sutured over the raw surface of the pharyngeal flap in the midline. The oral side of the soft palate is closed, beginning at (u) and proceeding anteriorly. (From Hogan, V. M.: A clarification of the surgical goals in cleft palate speech and the introduction of the lateral port control (L.P.C.) pharyngeal flap. Cleft Palate J.,* 10:331, 1973.)

The pharyngeal flap, once elevated, is sutured into the fringe of the nasal lining left on the posterior margins of the hard palate. The corners are sutured laterally as far as possible, and one additional suture of 3-0 or 4-0 chromic catgut in the midline is ample. Using finer suture material (4-0 or 5-0 catgut), the nasal lining flaps developed from the dorsal aspect of the soft palate are sutured to the raw surface of the pharyngeal flap. If the pharyngeal flap is relatively narrow, the pharyngeal defect can be closed. Rarely, it is left to heal spontaneously; the posterior wall heals rapidly and the scar contracts the pharyngeal mucosa quickly. The soft palate is closed meticulously in two layers with 4-0 chromic catgut sutures.

The superiorly based pharyngeal flap pharyngoplasty depends on lateral pharyngeal wall movement that is able to close the residual ports. Experience with over 1000 nasendoscopies in ten years has led the authors to the conclusion that the superiorly based flap needs to be positioned sufficiently high to be effective in the area of the pharynx at which the sphincter is operating. The authors have observed a number of flaps that have been of the proper size but malpositioned, so that the pharynx is endeavoring to close at another level. Jackson (1983) made the same point about the Orticochea sphincteric pharyngoplasty, explaining the need to have the flaps inserted higher in the pharynx. Unlined flaps tend to tube and become cordlike and ineffective.

In patients with severe deficiency of the velopharyngeal sphincter, the superiorly based, lined pharyngeal flap can be combined with pushback procedures. The nasal lining attached to the posterior palatal shelf is divided to give additional pushback effect and the lining is used to cover the pharyngeal flap.

Postoperative management involves careful resuscitation and extubation. An intravenous line is maintained for the first 12 hours and intravenous ampicillin is given for this period. Clear fluids only are given for the next 12 hours and the patient may have a soft diet for the next three weeks. Postoperative evaluation follows the preoperative assessment regimen. The results of surgery are evaluated by repeat speech assessment and nasendoscopy with synchronous lateral videofluoroscopy. This evaluation is performed at three months, a period that gives time for adequate healing and permits full evaluation of the capacity of the sphincter.

The pharyngeal flap operation is not without its negative aspects. Some patients develop hyponasality. During the first few weeks after surgery, there is an incidence of snoring that may persist, and a few patients may suffer from sleep apnea. A small number of patients experience an unpleasant taste. Some report halitosis, which may result from retained secretions on the upper surface of the pharyngeal flap; these are often seen during nasendoscopy. In addition, there may be persistent velopharyngeal incompetence.

Postoperative Speech Therapy

Following pharyngoplasty or any surgical procedure to provide a patient with a competent sphincter, it cannot be assumed that a patient will automatically speak clearly without residual resonance or articulation distortion. This is certainly true of a patient who has articulatory distortion or substitution patterns before surgery. After surgery, some patients demonstrate improved or near-normal vocal quality with no need for additional therapeutic intervention (Shprintzen, 1979). However, speech patterns that have been developed in the presence of velopharyngeal incompetence may not automatically change after surgery. Owing to the effect of the speaker's auditory perceptual monitoring, the patient may reproduce the speech he is used to hearing from himself. The pattern of voice use that a speaker favors has been described as the "vocal image" (Cooper, 1971). The speaker with long-standing velopharyngeal incompetence may have identified with the hypernasal vocal tone for so long that after surgery he may reproduce

his habitual supralaryngeal adjustments to retain and maintain previous resonant voice quality.

Therapy, after surgery, is begun only after the capacity of the pharyngeal flap or other surgical procedure to provide a competent sphincter has been evaluated. Again, the need is for careful assessment using, if possible, the same measures and instrumentation employed before surgery. After surgery, nasendoscopy and synchronised lateral videofluoroscopy, with the patient duplicating the speech produced at the initial investigation, can determine the need for, and potential success of, speech therapy. After it has been ascertained that the sphincter is capable of closure, sufficient for the production of normal vocal tone and for the necessary development of intraoral air pressure, therapy can be instigated to optimise the results of surgery. Utilizing the techniques of voice therapy, developing the patient's auditory discrimination ability, and encouraging relaxed and slightly more forward tongue carriage, the therapist encourages vocal tone placement or focus to use the supraglottic resonating system in a balanced way. Compensatory habits need to be addressed, such as excessive breath flow, the onset of phonation without firm closure of the vocal cords, tense and constricted laryngopharynx, and retraction of the tongue. The patient learns how to produce his voice without nasal tone, possibly through the use of negative practice, i.e., purposely making the "old" followed by the "new" vowel quality (Van Riper, 1963). He may experience, for the first time, the ability to speak with an efficient vocal tract, in which satisfactory air pressures can be maintained above the level of the larynx, ensuring assistance to the vocal cords in their compression of the air stream. Sucking through a straw closed at its distal end and simultaneously voicing from a nasal phoneme onto a high close vowel, e.g., [i], he may experience the effects of a closed nasopharynx in the form of a bright, clear, ringing voice quality. Modifying the vocal technique in this and other ways, the patient sheds his previous identity as a nasal speaker and adopts the clear esthetic vocal quality of the speaker with a competent velopharyngeal sphincter. In addition, articulation therapy to eradicate glottal stops and pharyngeal articulation may be required to correct the production of speech sounds.

Long-term Results

The aim of management of velopharyngeal incompetence is to provide the speaker with acceptable speech. To be acceptable, speech must be clearly intelligible. It does not require effort on the part of the speaker and does not have any distortion in its quality that attracts attention to itself.

Speech results after surgery to improve hypernasal speech have been variously reported. Bronsted and associates (1984) reported: "In Copenhagen as in most other cleft palate centers, satisfactory speech results are found in about 80 per cent of cleft palate cases as a result of primary palatoplasty. Another 16 per cent achieve acceptable speech with the aid of speech therapy. The remaining 5 per cent require secondary management because of insufficient velopharyngeal closure." Dalston and Stuteville (1975), who advocated the use of primary nasopalatal pharyngoplasty, found that adequacy of speech varied from less than 50 per cent to 95.8 per cent. Lewin, Heller, and Kodak (1975) reported that after surgical management, 60 per cent of patients presenting without cleft, but with velopharyngeal incompetence, achieved acceptable speech.

However, opinions on what constitutes acceptable speech seem to vary. Speech is variously termed "perfect," "normal," "satisfactory," and "adequate." Different researchers assess the adequacy of speech in various ways. Some have their patients read to them (Bronsted and associates, 1984), some have them perform a variety of speech tasks (Musgrave, McWilliams, and Matthews, 1975), and some make empirical judgments only (Hotz and Gnoinski, 1976). Spontaneous speech is sometimes, but rarely, used (Lewin, Heller, and Kodak, 1975).

In most studies, speech pathologists skilled in the area of cleft palate management assessed the adequacy of speech. A study by Podol and Salvia (1976) threw doubt on the ability of the speech pathologist to remain objective. These authors found that the judgment of unacceptable hypernasality and of the need for speech therapy was made more frequently when listeners (speech pathology students) were presented with visible evidence of cleft palate. A recent study at the South Australian Cranio-Facial Unit addressed the issue of speech acceptability of children with repaired cleft palate, and found that the judgments of untrained naive listeners were in marked variance with those made by a speech pathologist skilled in the treatment of hypernasality. This study used recordings of spontaneous speech elicited at each child's school, and two different modes of assessment. The speech pathologist clearly had a lower expectation of the children's speech. She found that 48 per cent of the cleft subjects were inadequate speakers. In marked contrast, naive listeners, using a rank order, found that 71.5 per cent of the subjects spoke less acceptably than their peers.

Rating scales were the measuring device most commonly favored in most studies. Lewin, Heller, and Kojak (1975) used a five point scale, 1 being normal voice quality and 5 representing severe hypernasality. The ratings were based sometimes on acceptability, sometimes on a variety of parameters. A rating scale, however, cannot give information as to how the speaker functions in his or her everyday setting. It relates only to an arbitrary standard in the mind of the speech pathologist. Speech standards vary from place to place, from region to region, and certainly across socioeconomic groups. Speakers have to be provided with speech that compares well with that of their peers. Studies of speech acceptability that isolate the speakers from their social and cultural milieu may be less than realistic. Additionally, the judgments of speech acceptability may be more objective if made by those without knowledge of the speaker's history or surgical management.

References

1 Bardenheuer, D.: Vorschlage zu plastischen Operationen bei chirurgischen Eingriffen in der Mundhohle. Arch. Klin. Chir., 43:32, 1892.

2 Bell-Berti, F.: The velopharyageal mechanism. An Electromyographic study. A preliminary report. Haskins Laboratories, New Haven, 1983.

3 Bloch, P. J.: Clinical evaluation for the cleft palate team setting. In Bzoch, K. R. (Ed.). Comm. Disord. Re Cleft Lip & Palate, 2:230, 1979.

4 Blocksma, R.: Correction of velopharyngeal insufficiency by Silastic pharyogeal implant. Plast. Reconstr. Surg., 31:268, 1963.

5 Braithwaite, F.: In Gibson, R. (Ed.): Modern Trends in Plastic Surgery. London, Butterworth, 1964.

6 Braithwaite, F.: The importance of the levator palati muscle in cleft palate closure. Br. J. Plast. Surg.,21:60, 1968.

7 Brauer R. O.: Push-back repair of the cleft palate with nasal mucosal flaps to prevent late contracture; follow up results of the Cronin procedure. Plast. Reconstr. Surg., 36:529, 1965.

8 Broadbent, T. R., and Swinyard, C. A.: The dynamic pharyngeal flap: its selective use and electromyographic evaluation. Plast. Reconstr. Surg., 23:301, 1959.

9 Bronsted, K., Liisberg, W., 0rsted, A., Prytz, S., and Fogh-Andersen, P.: Surgical and speech results following palatopharyagoplasty operations in Denmark 1959-1977. Cleft Palate J., 21:170, 1984.

10 Brown, J. B.: Elongation of the partially cleft palate. Surg. Gynecol. Obstet., 63:768, 1936.

11 Browne, D.: An orthopaedic operation for cleft palate. Br. Med. J., 20:1093, 1935.

12 Buchholz, R. B., Chase, R. A., Jobe, R. P., and Smith, H.: The use of a combined palatal pushback and pharyngeal flap operation: a progress report. Plast. Reconstr. Surg., 39:554, 1967.

13 Bzoch, K. R.: Bzoch Error Pattern Diagnostic Articulation Test. Comm. Disord. Re Cleft Lip & Palate, 2:168, 1978.

14 Bzoch, K. R.: Measurement and assessment of categorical aspects of cleft palate speech. Comm. Disord. Re Cleft Lip & Palate, 2:169, 182, 1979.

15 Bzoch, K. R., and Williams, W. N.: Introduction, rationale, principles and related basic embryology and anatomy. Comm. Disord. Re Cleft Lip & Palate, 2:16, 1979.

16 Calnan, J. S.: Submucous cleft palate. Br. J. Plast. Surg., 6:264, 1954.

17 Calnan, J. S.: Congenital large pharynx. A new syndrome with a report on 41 personal cases. Br. J. Plast. Surg., 24:263, 1971a.

18 Calnan, J. S.: Permanent nasal escape in speech after adenoidectomy. Br. J. Plast. Surg., 24:197, 1971b.

19 Conway, H.: Combined use of the pushback and pharyngeal flap procedures in the management of complicated cases of cleft palate. Plast. Reconstr. Surg., 7:214, 1951.

20 Cooper, M.: The vocal image and vocal suicide. Voices: The Art & Science of Psychotherapy, 6:26, 1971.

21 Cosman, B., and Falk, A. S.: Pharyngeal flap augmentation. Plast. Reconstr. Surg., 55:149, 1975.

22 Crikelair, G. F., Kastein, S., Fowler E. P., Jr., and Cosman, B.: Velar dysfunction in the absence of cleft palate. N.Y. J. Med., 64:263, 1964.

23 Croft, C. B., Shprintzen, R. J. Daniller, A., and Lewin, M. L.: The occult submucous cleft palate and the musculus uvulae. Cleft Palate J., 15:150, 1978.

24 Curtis, J. F.: Acoustics of speech production and nasalisation. In Spriestersbach, C. (Ed.): Cleft Palate and Communication. New York, Academic Press, 1968.

25 Dalston, R. M., and Stuteville, O. H.: A clinical investigation of the efficacy of primary nasopalatal pharyngoplasty. Cleft Plate J., 12:177, 1975.

26 David, D. J., and Bagnall, A. D.: Evaluation of velopharyngeal closure by CT scan and endoscopy—Honjo et al. Discussion. Plast. Reconstr. Surg., 74:626, 1984.

27 David, D. J., White, J., Sprod, R., and Bagwall, A.: Nasendoscopy: significant refinements of a direct-viewing technique of the velopharyngeal sphincter. Plast. Reconstr. Surg., 70:423, 1982.

28 Dorrance, G. M.: Congenital insufficiency of the palate. Arch. Surg., 21:185, 1930.

29 Dworkin, J. P., and Johns, D. F.: Management of velopharyngeal incompetence in dysarthria—a historical review. Clin. Otolaryngol., 5:61, 1980.

30 Eckstein, H.: Paraffin for facial and palatal defects. Dermatol. Ztschr. (Basel) 11:772, 1904.

31 Edgerton, M. T.: Surgical lengthening of the cleft palate by dissection of the neurovascular bundle. Plast. Reconstr. Surg., 29:551, 1962.

32 Estill, J.: Voice Scientist: PhD. program in speech and hearing, The Graduate Center, City University of New York. Personal communication, 1986.

33 Fletcher, S. G.: Hypernasal voice as indication of regional growth and development disturbances. Logos, 3:3, 1960.

34 Fletcher, S. G., and Bishop, M. E.: Measurement of nasality with TONAR. Cleft Palate J., 7:610, 1970.

35 Franco, P.: Traité des Hernies. Lyon, Thibauld Payan, 1561.

36 Fritzell, B.: The velopharyngeal muscles in speech. An electromyography and cineradiographic study. Acta Otolaryngol., 250:1, 1969.

37 Ganzer, H.: Neue Wege des plastischen Verschlusses von Gaumendefekten. Berl. Klin. Wochenschr., 54:209, 1917.

38 Garel, J.: Deux cas d'anomalie congénitale des piliers antérieurs du voile du palais. Rev. Laryngol. (Bordeaux), 14:489, 1894.

39 Gersuny, R: Ueber eine subcutane prosthese. Ztschr. Heilk., 21:199, 1900.

40 Gillies, H. D., and Fry, W. K.: A new principle in the surgical treatment of "congenital cleft palate" and its mechanical counterpart. Br. Med. J., 1:335, 1921.

41 Goode, R. L., and Ross, J.: Velopharyngeal insufficiency after adenoidectomy. Arch. Otolaryngol., 96:223, 1972.

42 Greene, M. C. L.: The Voice and its Disorders. London, Pitman Medical Publishing, 1964, pp. 190, 193.

43 Halle, M.: Gaumennaht und Gaumenplastik. Arch. Ohr. Nas. Kehlkopfheilk., 12:377, 1925.

44 Hill, M. J., and Hagerty, R. F.: Efficacy of pharyngoplasty for speech improvement in postoperative cleft palates. Cleft Palate Bull., 10:66, 1960.

45 Hogan, V. M.: A clarification of the surgical goals in cleft palate speech and the introduction of the lateral port control (L.P.C.) pharyngeal flap. Cleft Palate J., 10:331, 1973.

46 Hönig, C. A.: Treatment of velopharyngeal insufficiency after palatal repair. Plast. Reconstr. Surg., 41:93, 1968.

47 Honjo, I., Mitoma, T., Ushiro, K., and Kawano, M.: Evaluation of velopharyngeal closure by CT scan and endoscopy. Plast. Reconstr. Surg., 74:5, 1984.

48 Hotz, M., and Gnoinski, W.: Comprehensive care of cleft lip and palate in children at Zurich University: a preliminary report. Am. J. Orthod., 70:481, 1976.

49 Huskie, C. F.: Chief speech therapist, West of Scotland Regional Plastic and Oral Surgery Unit, Canniesburn Hospital, Glasgow, Scotland. Personal communication, 1985.

50 Hynes, W.: Pharyngoplasty by muscle transplantation. Br. J. Plast. Surg., 3:128, 1950.

51 Hynes, W.: The primary repair of clefts of the palate. Br. J. Plast. Surg., 7:242, 1954.

52 Jackson, I. T.: A review of 236 patients treated with dynamic muscle sphincter. Discussion. Plast. Reconstr. Surg., 71:187, 1983.

53 Jackson, I. T.: Sphincter pharyngoplasty. Clin. Plast. Surg., 12:711, 1985.

54 Jackson, I. T., and Silverton, J. S.: Sphincter pharyngoplasty as a secondary procedure in cleft palates. Plast. Reconstr. Surg., 59:518, 1977.

55 Kaplan, E. N.: The occult submucous cleft palate. Cleft Palate J., 12:356, 1975.

56 Kaplan, E. N., Jobe, R. P., and Chase, R. A.: Flexibility in surgical planning for velopharyngeal incompetence. Cleft Palate J., 6:166, 1969.

57 Kilner, T. P.: Cleft lip and palate repair technique. St. Thomas Hosp. Rep., 2:127, 1937.

58 Kingsley, N. W.: Surgery or mechanism in the treatment of congenital cleft palate. N.Y. Med. J., 29:484, 1897.

59 Lewin, M. A., Heller, J. C., and Kodak, D. J.: Speech results after Millard island flap repair in cleft palate and other velopharyngeal insufficiencies. Cleft Palate J., 12:263, 1975.

60 Limberg, A.: Neue Wege in der radikalen Uranoplastik bei angeborenen Spaltendeformationen: Osteotomia interlaminaris und pterygomaxillaris, Resectio Marginis Foraminis palatini und neue Plattschennabt. Fissura ossea occulta und ihre Behandlung. Zentralbl. f Chir., 54:1745, 1927.

61 Lubker, J. F.: An electromyographic-cinefluorographic investigation of velar function during normal speech production. Cleft Palate J. 5:1, 1968.

62 Lubker, J. F., Fritzell, B., and Lindqvist, J.: Velopharyngeal function. An electromyographic study. R. Inst. Technol. STL-QPSR, 4:9, 1970.

63 Massengill, R., Jr.: Hypernasality. Considerations in Causes and Treatment Procedures. Springfield Charles C Thomas, 1972.

64 McCarthy, J. G., Coccaro, P. J., Schwartz, M., WoodSmith, D., and Converse, J. M.: Velopharyngeal function following maxillary advancement. Plast. Reconstr. Surg., 64:180, 1979.

65 McCutcheon, G. T.: Modified Passavant technic of cleft palate repair. Ann. Surg., 139:613, 1954.

66 McWilliams, B. J., Morris, H. L., and Shelton, R. L.: Instrumentation for assessing the velopharyngeal mechanism. In McWilliams, B. J., Morris, H. L., and Shelton, R. L. (Eds.): Cleft Palate Speech. St. Louis, MO, C. V. Mosby Company, 1984, p. 152.

67 Morley, M. E.: Cleft Palate and Speech. Edinburgh & London, Churchill Livingstone, 1973.

68 Morris H. L.: Surgical management of clefts. In McWilliams, B. J., Morris, H. L., and Shelton, R. L. (Eds.): Cleft Palate Speech. St. Louis, MO, C. V. Mosby Company, 1984, p. 64.

69 Morris, H. L., Spriestersbach, D. C., and Darley, F. L.: An articulation test for assessing competency of velopharyageal closure. J. Speech & Hearing Res., 4:48, 1961.

70 Musgrave, R. R., McWilliams, B. J., and Matthews, H. P.: A review of the results of two different surgical procedures for the repair of clefts of the soft palate only. Cleft Plate J., 12:281, 1975.

71 Orticochea, M.: Construction of a dynamic muscle sphincter in cleft palates. Plast. Reconstr. Surg., 41:323, 1968.

72 Orticochea, M.: A review of 236 cleft palate patients treated with dynamic muscle sphincter. Plast. Reconstr. Surg., 71:180, 1983.

73 Osberg, P. E., and Witzel, M. A.: Physiologic basis for hypernasality during connected speech in cleft palate patients—a nasendoscopic study. Plast. Reconstr. Surg., 67:1, 1981.

74 Owsley, J. Q., Jr., Lawson, L. I., and Chierici, G. J.: The re-do pharyngeal flap. Plast. Reconstr. Surg., 57:180, 1976.

75 Padgett, E. C.: The repair of cleft palates after unsuccessful operations, with special reference to cases with an extensive loss of palatal tissue. Arch. Surg., 20:453, 1930.

76 Passavant, G.: Ueber die Operation der angeborenen Spalten des harten Gaumens und der damit complicierten Hasenacharten. Arch. Ohr. Nas. Kehlkopfheilk., 3:196, 1862.

77 Passavant, G.: Ueber die Beseitigung der naeselnen Sprache bei angeborenen Spalten des harten und weichen Gaumens (Gaumensegel, Schlundnaht und Ruecklagerund des Gaumensegels). Arch. Klin. Chir. 6:333, 1865.

78 Passavant, G.: Ueber die Verbesserung der Sprache nach der Uranoplastik. Dtsch. Gesellsch. Chir., 7:128, 1878.

79 Perthes, H.: Reported by Hollweg, E. Beitrag zur Behandlung von Gaumenspalten. Dissertation Tübingen, 1912.

80 Peterson-Falsone, S. J.: Velopharyngeal inadequacy in the absence of overt cleft palate. J. Craniefac. Genet. Dev. Biol. [Suppl.], 1:97, 1985.

81 Pigott, R. W.: Some physical characteristics of instruments used to investigate palatopharyngeal incompetence. Diag. & Treat. Palatoglossal Malfunction, Monograph 2. London, College of Speech Therapists, 1979.

82 Pigott, R W.: Personal communication, 1986.

83 Podol, J., and Salvia, J.: Effects of visibility of a prepalatal cleft on the evaluation of speech. Cleft Palate J., 13:361, 1976.

84 Porterfield, H. W., Trabue, J. C., Stimpert, R. D., and Terry, J. L.: Hypernasality in noncleft palate patients. Plast. Reconstr. Surg., 37:216, 1966.

85 Sanvenero-Rosselli, G.: Divisione palatine e sua cura chirurgica. Atti Cong. Int. Stomatol., 391, 1935.

86 Schendel, S. A., Oeschlaeger, M., Wolford, L. M., and Epker, B. N.: Velopharyngeal anatomy and maxillary advancement. J. Maxillofac. Surg., 7:116, 1979.

87 Schönborn, D.: Ueber eine neue Methode der Staphylorrhaphie. Arch. Klin. Chir., 19:527, 1876.

88 Schwarz, C., and Gruner, E.. Logopaedic findings advancement of the maxilla. J. Maxillofac. Surg., 4:40, 1976.

89 Shede, J.: Zur operativen Behandlung der Gaumensplaten. In Predoehl, A. (Ed.) Jahrb. d. Hamburg. Staatskrankenan sta 274, 1889.

90 Shprintzen, R. J.: Velopharyngeal insufficiency in the absence of overt or submucous cleft palate. The mystery solved. Diag. & Treat. Palatoglossal Malfunction Monograph 2. London, College of Speech Therapists, 1979.

91 Skolaick, M. L.: Videofluoroscopic examination of the velopharyngeal portal during phonation in lateral and base projections—a new technique for studying the mechanics of closure. Cleft Palate J., 7:803, 1970.

92 Stark, R. B., and DeHaan, C.: The addition of a pharyngeal flap to primary palatoplasty. Plast. Reconstr. Surg., 26:378, 1960.

93 Subtelny, J. D., and Koepp Baker, H.: The significance of adenoid tissue in velopharyngeal function. Plast. Reconstr. Surg., 17:235, 1956.

94 Suersen, W.: Ueber die Herstellung einer dentlichen Aussprache durch ein neues System kunstlicher Gaumen bei angeborenen und erworbenen Gaumendefecten. Klin. Wochenschr., 6:110, 1869.

95 van den Berg, J. W.: Modern research in experimental phonetics. 12th Int. Cong. Logopaedics and Phoniatrics. Folia Phoniatr. (Basel), 14:81, 1962.

96 Van Riper, C.: Speech Correction. Principles and Methods. Englewood Cliffs, NJ, Prentice-Hall, 1963, p. 296.

97 Veau, V., and Ruppe, C.: Les résultats anatomiques et foncionnels de la staphylorraphie par les procédés classiques. Rev. de Chir., 60:81, 1922.

98 von Gaza, W.: Transplanting of free fatty tissue in the retropharyngeal area in cases of cleft palate. Lecture German Surgical Society, April 9th, 1926.

99 Ward, P. H.: Uses of injectable Teflon in otolaryngology. Arch. Otolaryngol., 87:637, 1968.

100 Wardill, W. E. M.: Technique of operation for cleft palate. Br. J. Surg., 25:117, 1937.

101 Warren, D. W.: PERCI: a method of rating palatal efficiency. Cleft Palate J., 16:279, 1979.

102 Witzel, M. A., and Munro, I. R.: Velopharyngeal insufficiency after maxillary advancement. Cleft Palate J., 14:176, 1977.

Three–Dimensional Reconstruction of the Skull and Facial Bones Utilising Computed Tomography in Craniofacial Surgery

D.C. Hemmy, G.T. Herman, D.J. David*

X-ray techniques are utilised by the physician to gain information about most structures in the body. Conventional x-rays, contrast studies, complex motion tomography and computed tomography (with and without contrast) are utilised to examine anatomic structures. Information gained permits pathologic diagnoses and is used to plan surgical procedures. Common radiographic procedures with images in different projections require that the physician assimilate multiple images and mentally reconstruct these images to obtain a 3-dimensional image of the exact spatial relationships and extent of a lesion. This mental reconstruction of images is many times erroneous and often misleading particularly when examining patients with complex structural abnormalities.

Radiation exposure is critical to the lens of the eye and the gonads. Conventional tomograms have a relatively high radiation dose to the eye (during skull tomography). The skin dose from polytomography may be as high as 50 to 75 rads. Positive contrast cisternography substitutes a decreased radiation dose for a slightly increased risk of contrast reaction and catheter complications, and radiation dose to the eye is high especially if AP magnified films are taken. All of these tests require the physician to mentally compare two-dimensional images to determine the three-dimensional anatomy.

During axial CT scanning the x-ray beam is tightly collimated so that critical organs receive significant irradiation only if they are in the x-ray beam. Scans through the skull base may pass through the eye, however. Skin dose from contagious 1.5 mm CT scans has been measured at 5 rads per scan utilising the General Electric CT/T 8800 body scanner. However, the same body area normally is scanned only once, so the dose is not cumulative as it would be for conventional tomography. Furthermore, low dose techniques using reduced mA in osseous examination can reduce the skin dose to 1 to 2 rads per scan. With conventional CT, images in multiple planes can be created by the physician. A 4-dimensional image of the skull and facial bones allows the clinician to precisely define normal and pathologic anatomy. This is particularly true in appreciation of the complex anomalies encountered in craniofacial surgery.

In many 3-dimensional imaging applications the 3-D scene is represented by a 3-D array of volume elements (voxels). Computerised tomography provides the values assigned to voxels which are abutting parallelepipeds a portion of the 3-D space occupied by the human body.

Each CT slice obtained contains 320 x 320 picture elements or pixels of size 0.8 mm x 0.8 mm. The accuracy of the cross sectional slices is reflected, among other things, by the thickness of the slice. The lower limit of the thickness is 1.5 mm. Utilising techniques called subregioning and interpolation, 1 a portion of the CT slice is selected and a binary cubic scene voxel size 0.8 mm x 0.8 x 0.8

*The Med. Coll. of Wisconson, U.S.A., Hosp. of the Univ. of Pennsylvania, U.S.A., Adelaide Children's Hosp., Australia

FIG. 1. *Child with fronto-naso-orbital dystopia and unilateral hypertelorism.*

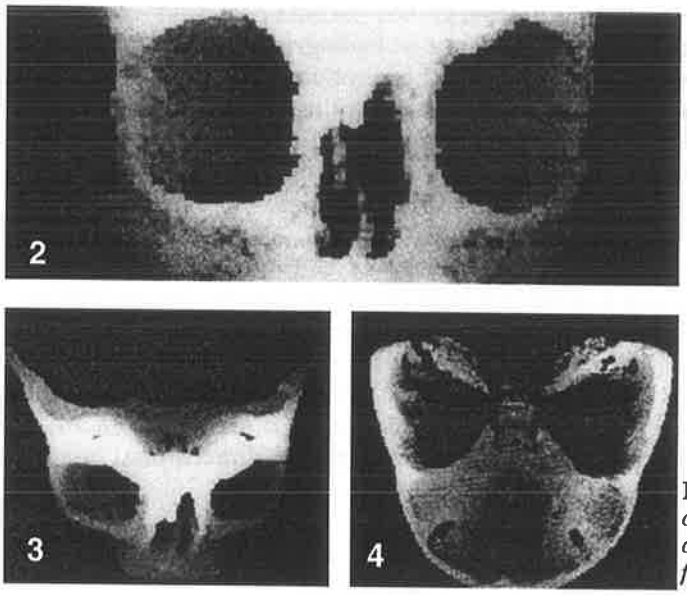

FIG. 2–4. *Examples of 3–dimensional reconstruction of a portion of the skull and facial bones of child in Fig. 1.*

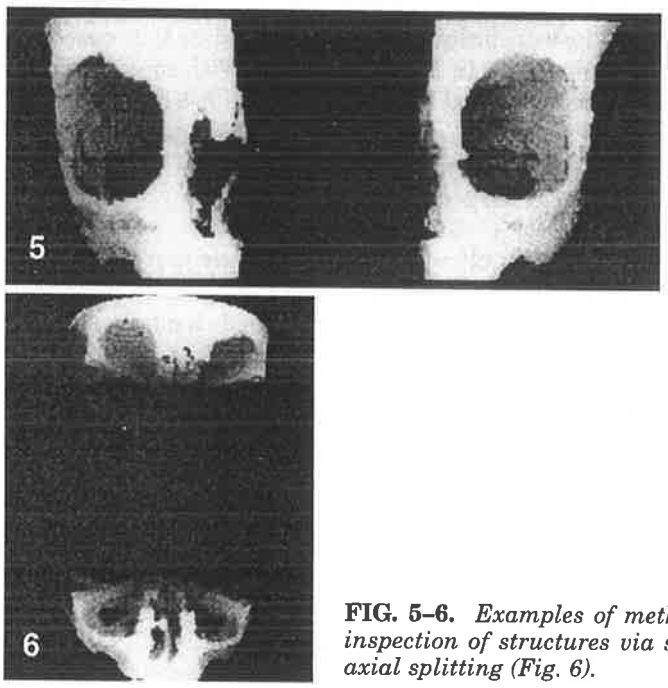

FIG. 5–6. *Examples of method which permits internal inspection of structures via sagittal splitting (Fig. 5) or axial splitting (Fig. 6).*

mm is created. By thresholding, a value of 1 is assigned to a voxel the density of bone or greater. A 0 indicates its absence. The voxel size is in a 1.5 mm thick CT slice is 0.8 x 0.8 x 1.5 mm. The desire to have a cubic scene requires the creation of an interpolated new voxel or 0.8 x 0.8 x 0.8 mm whose densities are estimated based on the densities of the original voxels. The surface of the bony objects in the binary scene is then detected by a surface detection algorithm.

Efficient computer procedures are then utilised to approximate surfaces and construct the 3-dimensional image. 1 The object of study may then be displayed from various angles and a movie made by displaying sequential angular images. Furthermore, computer guided dissection of the object may be performed to permit removal or reconfiguration of a portion in preoperative planning or, in the case of the bilateral structures, comparison by means of counterrotation of the two objects.

In summary, three-dimensional reconstruction appears to be a useful tool utilising data acquired through conventional CT permitting accurate analysis of complex anatomic structures and precise preoperative planning allowing the surgeon to select the necessary remedial procedure.

Reference

1 Herman, G.T.: Surfaces of objects in discrete 3-dimensional space. Computer Graphics 80:287–300, August, 1980.

THE MEDICAL COLLEGE OF WISCONSIN
8700 WEST WINCONSIN AVENUE
MILWAUKEE, WISCONSIN
53226

Three-Dimensional Reconstruction of Craniofacial Deformity Using Computed Tomography

D. C. Hemmy, M.D., D. J. David, M.B.B.S., and Gabor T. Herman, Ph.D.
Department of Neurosurgery, Medical College of Wisconsin, Milwaukee, Wisconsin (D.C.H.), South Australian Craniofacial Unit, Adelaide Children's Hospital, Adelaide, Australia (D.J.D.): and Section of Medical Imaging, Department of Radiology, University of Pennsylvania, Philadelphia, Pennsylvania (G.T.H.)

The computed tomographic studies obtained routinely in the examination of patients with congenital or acquired defects of the skull and facial bones can be utilized as a substrate to provide an accurate three-dimensional representation of osseous abnormalities. The total dose of x-irradiation is reduced as other means of radiological examination are eliminated. Osseous structures are faithfully reproduced. Complete inspection of the reproduced structure can be made from any viewpoint, including internal inspection. *(Neurosurgery* 13:534-541, 1983)

Key words: Computed tomography, Craniofacial anomaly. Facial trauma. Irradiation. Osseous abnormality. Skull defect

X-ray techniques are utilized by the physician to gain information about most structures in the body. Conventional x-ray filming. contrast studies, complex motion tomography, computed tomography (CT) (with and without contrast), and nuclear magnetic resonance are utilized to examine anatomic structures. The information gained permits pathological diagnosis and is used to plan surgical procedures. Common radiographic procedures with images in different projections require that the physician assimilate multiple images and mentally reconstruct these images to obtain a three-dimensional concept of the exact spatial relationships and extent of the lesion. This mental reconstruction of images is many times erroneous and often misleading, particularly when patients with complex structural abnormalities are examined. Furthermore, such mental reconstruction does not remain a permanent record, and time and imagination are required to reinterpret the x-ray films on each occasion.

Radiation exposure is critical to the lens of the eye and the gonads. Conventional tomograms expose the eye to a relatively high dose of radiation during skull tomography. The skin dose may be as high as 50 to 75 rads. Angiography also exposes the eye to a high radiation dose (especially if anteroposterior magnifying films are taken), as well as carrying the risks of reaction to the contrast agent and catheter complications. Both of these tests require the physician to compare two-dimensional images mentally to determine three-dimensional anatomy.

During axial CT scanning, the x-ray beam is tightly collimated so that critical organs receive significant irradiation only if they are in the x-ray beam. Scans to the skull do however, pass through the eye. The skin dose from contiguous 1.5-mm CT scans has been measured at 5 rads per scan using the General Electric CT/T8800 body scanner (General Electric Medical Systems, New Berlin, Wisconsin). However, the same body area normally is scanned only once so the dose is not cumulative as it would be for conventional tomography or angiography. Furthermore, low dose techniques using reduced milliamperes in an osseous

examination reduce the skin dose to I to 2 rads per scan. With conventional CT, images in multiple planes can be created by the computer, but the three-dimensional effect must still be inferred by the physician. Three-dimensional images of the skull and facial bones allow the clinician to define precisely normal and pathological anatomy. This is particularly true in cases of congenital abnormalities and facial trauma in which many bizarre and uncommon anatomical variations occur. Such problems occur in cases of complex craniofacial fractures where fracture lines extend from the cranial base to the face and also in the sometimes unusual three-dimensional nature of the bony defects associated with frontoethmoidal encephaloceles. The faithful representation of structures permits precise preoperative planning, avoiding surgical pitfalls that are not disclosed by other examinations. In a similar fashion. the foreknowledge imparted by these images permits the reduction of operating time in complex craniofacial surgery. thus reducing morbidity.

TABLE 1

Patient Data

Diagnosis		No. Patients Studied
Frontonasal encephalocele		8
Craniofacial clefts		5
Midface hypoplasia		1
Craniosynostosis syndromes		9
Apert's syndrome	5	
Crouzon's syndrome	2	
Bicoronal synostosis	2	
Orbital dystopia		4
Craniofacial trauma		3
Hemicraniofacial microsomia		1
Fibrous dysplasia		1
Orbital neurofibromatosis		2
Total		**34**

Material

Material for this study was collected from the institutions represented by the authors (D.C.H. and D.J.D) in the United States and Australia, respectively. Table 1 indicates the number and types of deformities studied. In each of these cases, the study was obtained as a part of the preoperative planning and forms a part of the patient's permanent medical record.

Methods

Outpatients admitted to our units undergo CT examinations as part of their assessment. Because motion during the examination is not permitted, appropriate sedative or anesthetic agents are used. If information is required about both the soft tissue structures and the osseous structures, standard scanning techniques are utilized. If information about osseous structure is all that is desired, low milliampere techniques are utilised. For precise and faithful reproduction, abutting slices 1.5 mm thick are obtained. Slices of greater thickness may be used, but this will result in less precision. In scanning the face, usually 45 slices are obtained. Scanning usually begins at the alveolar ridge of the maxilla and proceeds in a cephalad direction. The teeth are generally not scanned to prevent

the production of an artifact from metallic restorations. As can be readily determined by the thickness of the slice and the number of slices permitted, reconstruction of an axial distance of 6.75 cm is made. If an examination of more of the skull and facial bones is desired, additional slices can be obtained, again of uniform thickness. Forty-five slices have generally been satisfactory to display the skull base, orbits, and midface, which are the areas of greatest interest and attention in craniofacial surgery.

In many three-dimensional imaging applications, the three-dimensional scene is represented by a three-dimensional array of volume elements (voxels). CT provides the values assigned to voxels, which are abutting parallelepipeds filling a portion of the three-dimensional space occupied by the human body.

With the GE CT/T 8800, each CT slice obtained contains 390 x 320 picture elements (pixels) each 0.8 x 0.8 mm in size. The accuracy of the cross sectional slice is reflected. among other things. by the thickness of the slice. The lower limit of the slice thickness is 1.5 mm. With this slice thickness. the size of a voxel is 0.8 x 0.8 x 1.5 mm.

With a technique called subregioning, a portion of the CT slice is selected by electronically outlining a box on the screen of the General Electric independent physicians display console (IPDC) (General Electric Medical Systems) (Fig. 1). The output slices from the CT scanner are then reviewed to determine whether all objects of interest on all of the CT slices lie within the box. It is only these

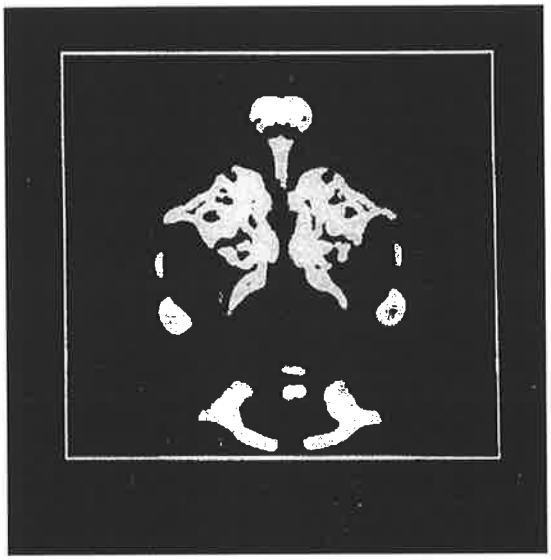

FIG. 1. *CT slice showing the subregion of interest.*

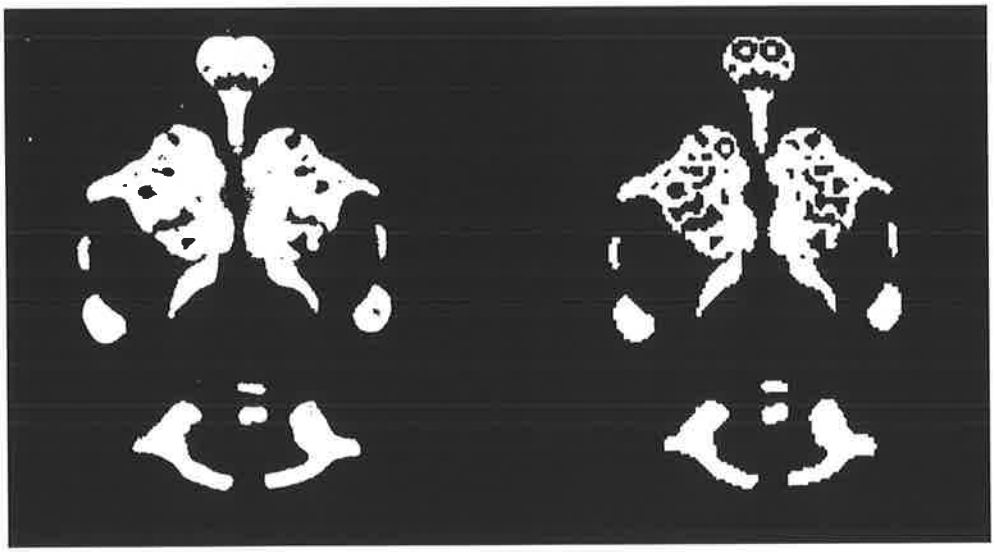

FIG. 2. *Right, image formed after the bone threshold was determined.*

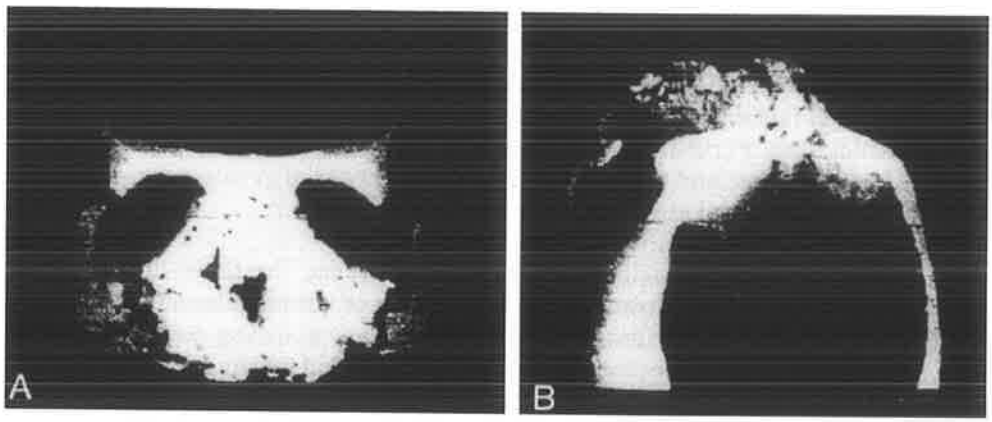

FIG. 3. A. *anteroposterior (AP) view of severe facial fracture demonstrates disruption of the orbits with lateral displacement of the zygomatic bones and complex nasoethmoidal maxillary fractures. The skull above the orbits, behind the interaural line, and below the maxilla has been eliminated because it is not of interest.* **B.** *a superior rotational view of the same patient shows the cranial fossa and the cribriform plate demonstrating that the anterior cranial fossa and the posterior wall of the frontal sinus are intact. The cribriform plate on the left is clearly normal. This view also demonstrates disruption of the zygomatic complex bilaterally and the fact that the fractures are entirely subcranial (The defect in the floor of the middle cranial fossa is artifactual because the last CT slice was obtained above this level).*

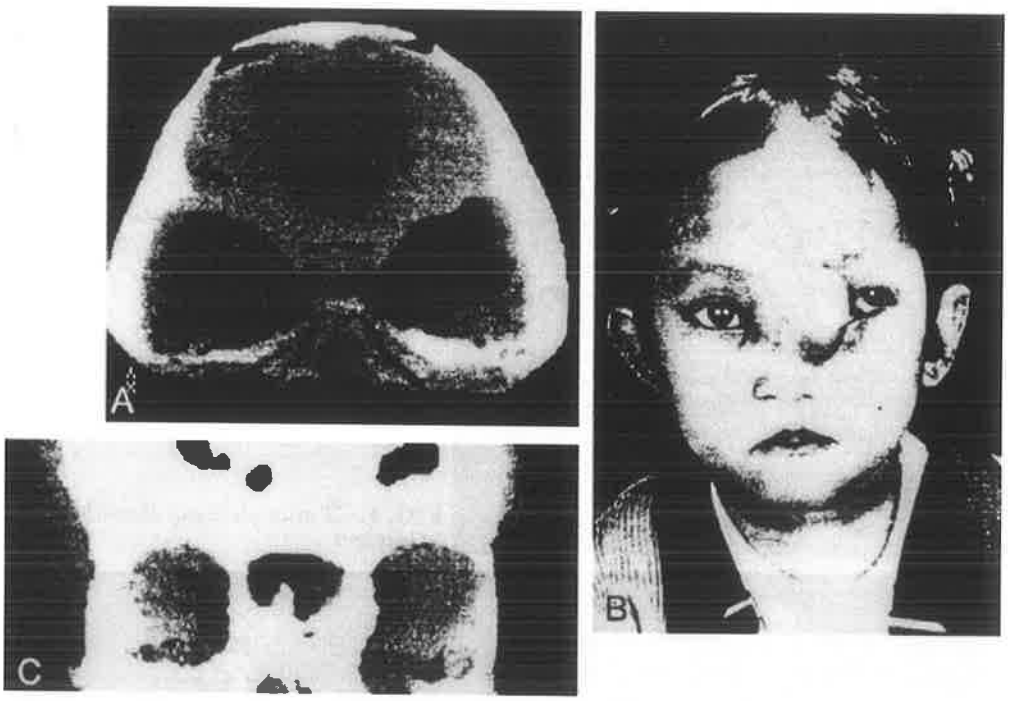

FIG. 4. A. *superior view shows a frontoethmoidal meningoencephalocele of the nasofrontal type with a massive opening at the anterior margin of the cribriform plate at the site of the foramen caecum extending toward the face.* **B.** *face of the patient* **C.** *AP view shows the large defect with the nasal bones inferior to the opening the nasal and pyriform margin depressed downward and the medial orbital walls shifted laterally. (Note the old frontal craniectomy).*

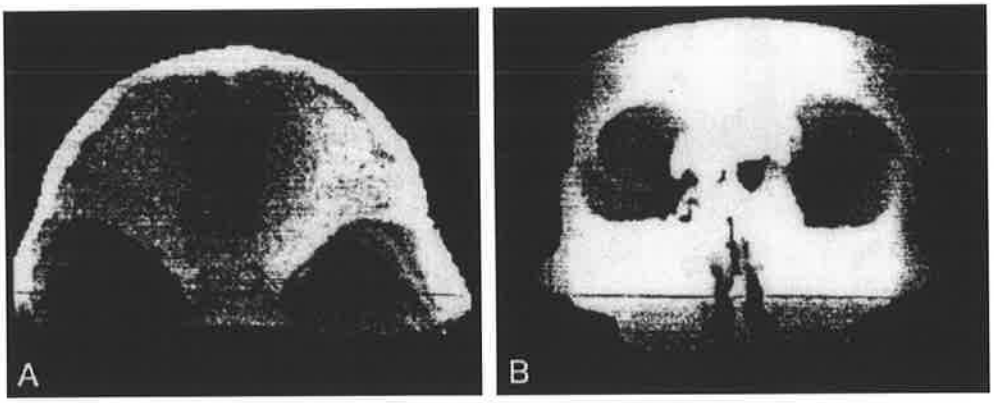

FIG. 5. A. *superior view of a patient with a frontoethmoidal meningoencephalocele of the nasoethmoidal type with the defect at the site of the foramen caecum.* **B.** *AP view of the same patient shows the defect beneath the splayed out nasal bones above the pyriform aperture expanding laterally to erode the anterior margins of the medial orbital wall, which produces telecanthus, hypertelorism, and elongation of the face.*

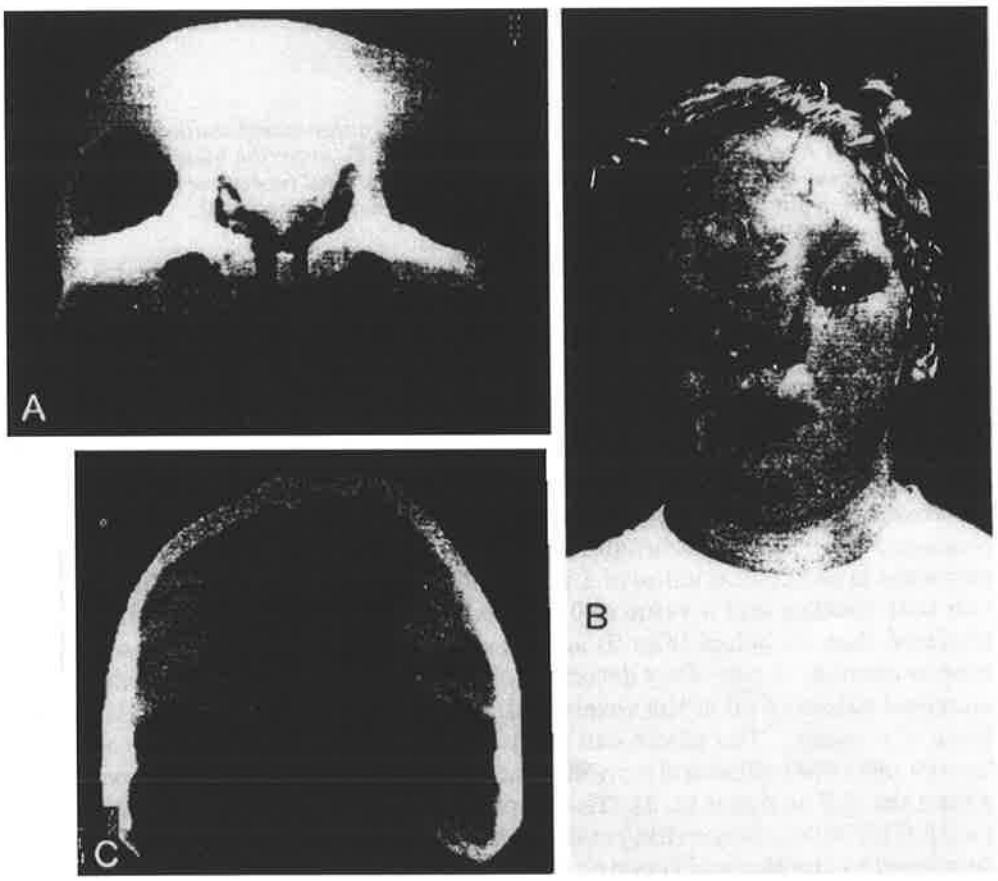

FIG. 6. A. *skull of a patient with a frontal teratoma that was excised at birth. The resulting shortened face and gross hypertelorism are seen.* **B.** *face of the patient.* **C.** *note the widened, depressed anterior cranial fossa. Once again, the defect in the floor of the middle cranial fossa is artifactual because this area was not scanned.*

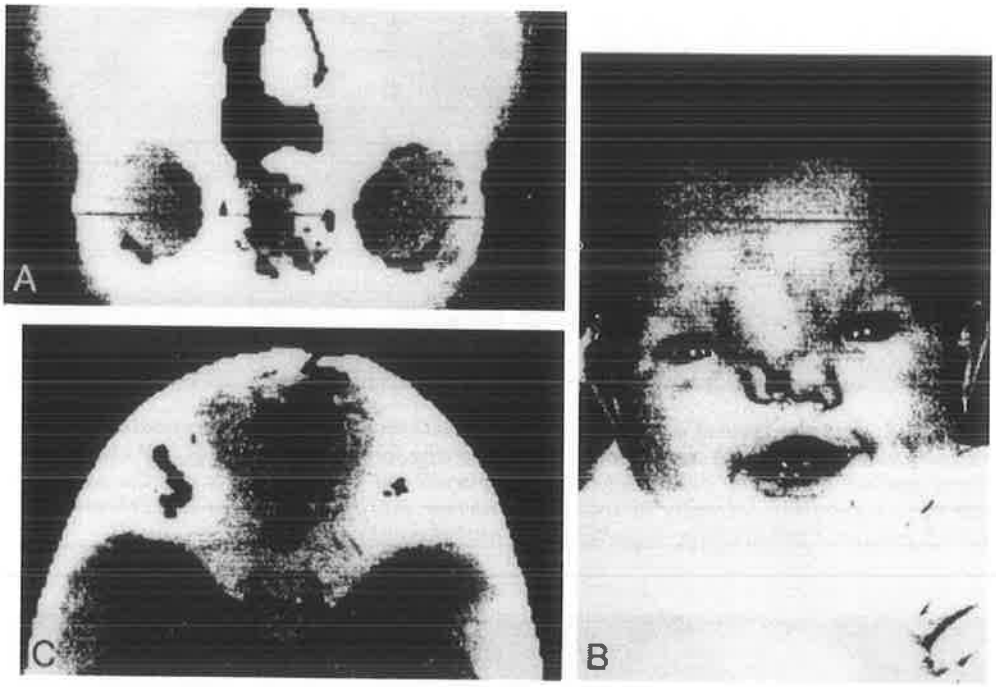

FIG. 7. A. *AP view of a Tessier 13 cleft shows extensive frontonasoethmoidal involvement and subsequent hypertelorism.* **B.** *face of the patient.* **C.** *superior view demonstrates involvement of the anterior cranial fossa. (Defects in the orbital roof are artifactual due to thinness of the orbital roof and subsequent computer-generated artifact).*

picture elements that will be used as the substrate for three-dimensional reconstruction. The objects outside the box will not be included. In most cases, the posterior limit of the box is positioned at the anterior aspect of the foramen magnum or just behind the interaural line.

Interpolated slices are then created, based on the densities of the original slices. The desire to produce a cubic scene requires the creation of interpolated new voxels of size 0.8 x 0.8 x 0.8mm and therefore a new CT slice 0.8 mm in thickness. After this, a technique called thresholding is used. A density on the gray scale is selected: a value of 1 is assigned to a voxel with a density greater than that number and a value of 0 is given to a voxel with a lesser value. The threshold that we select (Fig. 2) is that of bony density. Thus, a binary cubic scene is created. A boundary detection algorithm is then used to determine the connected subset of all of the voxels with a binary value of 1 that constitute the object of interest. The object can then be displayed with shading to confer a three-dimensional effect and a preselected rotation at various angular increments around the X.Y or Z axis (2, 3). These operations are permitted from the output of a GE CT/T8800 scanner that provides the input for the program entitled "3D82" (developed by the Medical Imaging Processing Group. Department of Radiology. Hospital of the University of Pennsylvania for General Electric Medical Systems). The images can be displayed on the IPDC unit to be viewed singly from various angles or as a rotating "movie". Furthermore, "hard copy" can be made through the use of 35-mm film or standard x-ray sheets. We have found it useful to rotate the image 360° about two axes the X axes: which is parallel to the interaural line, and the Z axis, which is parallel to the spinal axis.

Twelve 30° incremental displays are made along each axis. These 12 images placed together on the screen are then photographed as a "contact" print. From the 24 images that have been created in this fashion 7 or 8 images are selected to be displayed as larger images on x-ray film to become part of the patient's permanent record and to be utilized in the operating room.

Results

Determination of the extent and pattern of facial fractures and also of the possible involvement of the cranial base is indeed a difficult problem for the surgeon. Involvement of the cranial base has added significance in both the management and the prognosis of a patient with facial trauma. (Fig. 3). Modern concepts of the management of craniofacial fractures require a team approach of neurosurgeons and plastic surgeons working together during the same surgical operation. The presence or absence of defects in the anterior cranial fossa and the need for repair of dural defects or fixation of frontal bone fractures will dictate different courses of surgical management. Correct information obtained before operation leads to a confident operative plan, reduces unnecessary surgery, and makes prognostication more accurate.

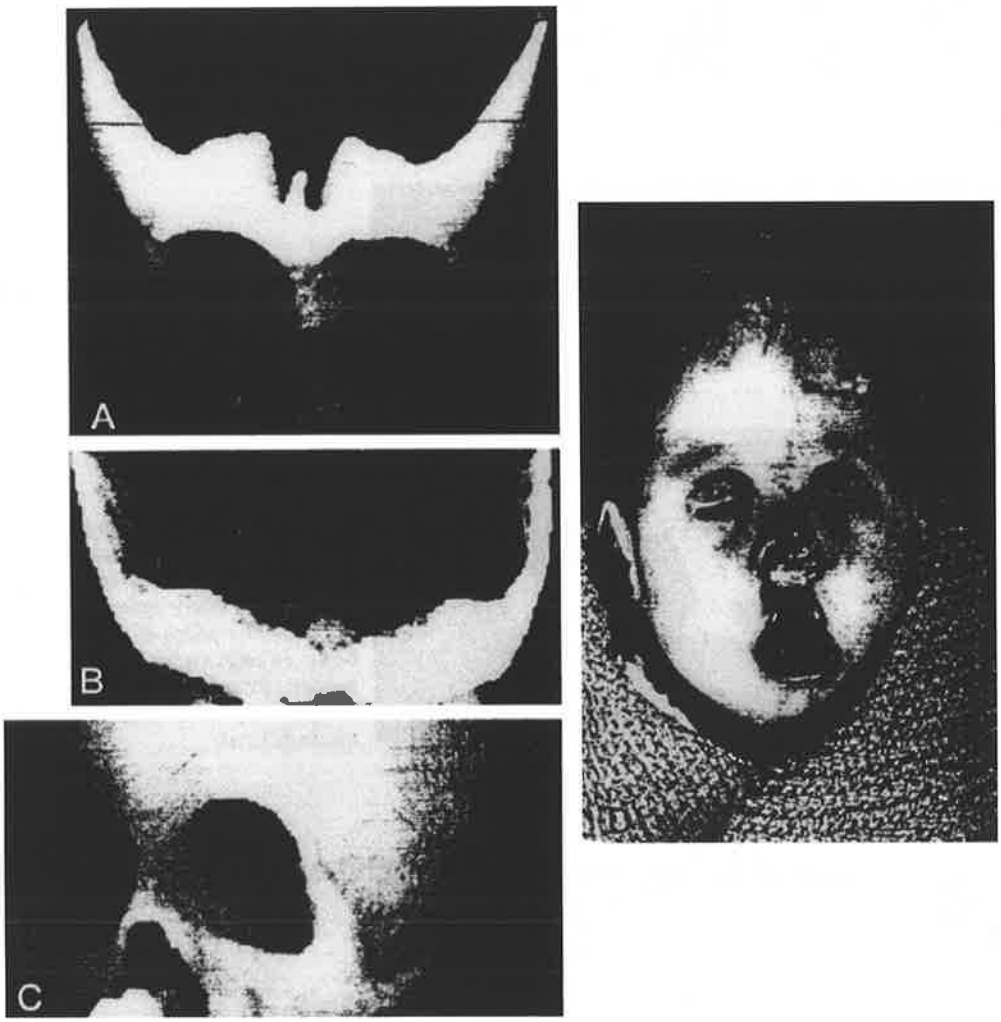

FIG. 8. *AP* **A.** *posterior* **B.** *and oblique* **C.** *views and photograph* **D.** *of a 6-month-old patient with craniosynostosis, hypotelorism, bilateral cleft lip and palate, and projecting premaxilla. Note the elevated sphenoid wings. The abnormalities in this patient do not correspond to any presently recognised syndrome.*

The method has permitted us to determine the precise classification of sincipital meningoencephaloceles preoperatively according to anatomic involvement (Figs. 4 and 5). Subclassification is easy to perform and facilitates operative management. Furthermore, we believe that we are now able to classify craniofacial clefts with greater accuracy (Figs. 6 to 8).

In craniosynostosis syndromes, the cranial base is easily inspected and subsequent variations in craniofacial anatomy can be correlated (Figs. 9 to 11). Furthermore, the extent of an iatrogenic defect in patients previously operated is easily determined, once again reducing operating time (Figs. 4C and 10).

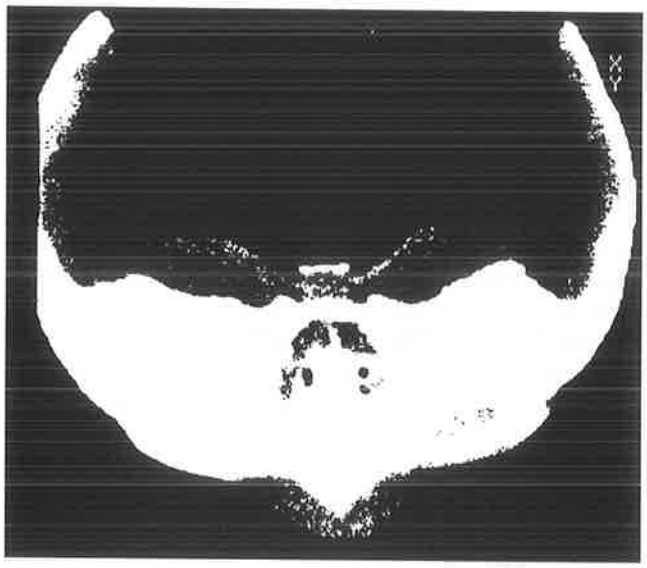

FIG. 9. *Superior view. Apert's syndrome, shows distortion of the cranial base with foreshortened anterior cranial fossa, depressed cribriform plate, widened ethmoid producing consequent hypertelorism, and forward position of the middle cranial fossa. The relationship of the small face to the superior structures is also demonstrated.*

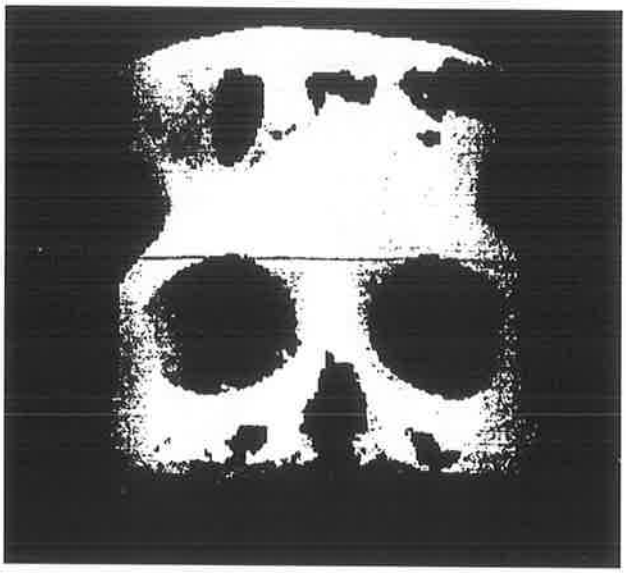

FIG. 10. *Previously operated case of turricephaly demonstrates defects in the frontal bone and ingrowth of bony spicules from the posterior plate of the frontal bone invaginating the dura mater. Foreknowledge of the complex permits safe surgical management.*

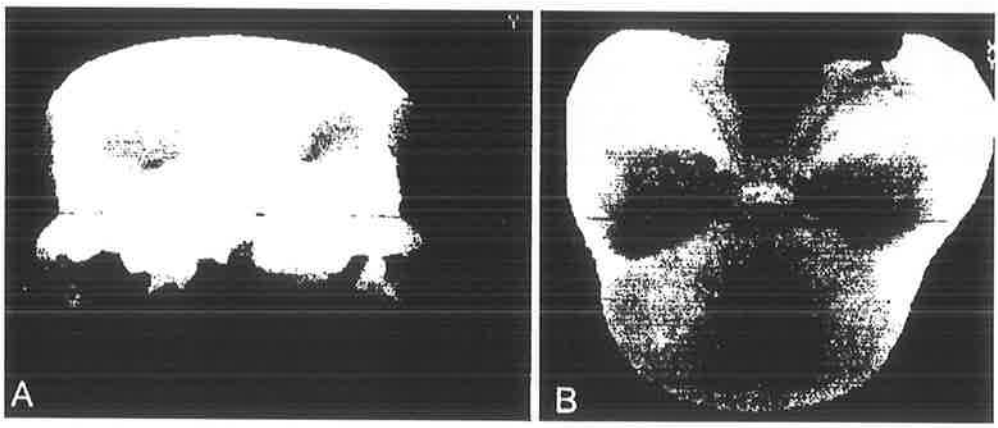

FIG. 11. *AP* **A.** *and superior* **B.** *views of a patient with craniofacial microsomia demonstrate the distortion of the cranium and the face with a small enophthalmic orbit and a maxillary cleft.*

Discussion

We believe that the use of this method provides precise anatomical data previously unobtainable from living subjects. The information obtained from the scan has been found to be remarkably accurate when checked at operation. The method is economically feasible because it uses data that are routinely obtained through the use of a CT scanner and because the reconstruction program operates on existing equipment, namely the IPDC. This method has simplified the preoperative assessment of craniofacial abnormalities by the very nature of the image that is produced, the fact that it can be kept as a permanent record and that it does not require reinterpretation when viewed by different individuals. The method required less radiation exposure than is necessary with conventional methods of assessment. The knowledge obtained serves to reduce operating time and hence reduce operative morbidity because there are many pitfalls in this complex surgery that can be predicted and remedied when using three-dimensional reconstruction.

The ability to "extract" the skull and facial bones electronically from living subjects permits the possibility of arriving at more precise classifications of craniofacial anomalies. Furthermore, we envisage the possibility of a central repository of data. Such a repository would permit the concentration and classification of rare anomalies. Hitherto, such information has depended upon conventional radiographic techniques and the occasional postmortem examination, as well as findings at operation.

Volume can be assessed through this method. Changes in cerebral volumes after manipulative techniques can be determined. Furthermore, ventricular volume can be computed. Further developments will include the ability to perform a simulated osteotomy and skeletal shifts (1) as foreshadowed before the time of the actual operation to determine the result of operative manipulation and subsequently to perform the operation with precision. A number of additional capabilities are being developed. One of these is relating the soft tissue conveniently and accurately to the bony configuration. The problem of metallic artifact resulting from certain types of dental restorations and metallic sutures reduces the capacity of the technique to cope with the postoperative situation. Other artifacts that pose problems are the pseudoforamina appearing in areas of very thin bone, which result from the limitations of the resolution obtained by the scanner.

Acknowledgments

Supported in part by NIH Grant No. HI 28438.

The authors thank Dr. Julian White of the South Australian Craniofacial Unit for his assistance in coordinating the studies presented here.

Received for publication. April 14, 1983; accepted July 8, 1983.

Presented at the 51st Annual Meeting of the American Association of Neurological Surgeons. Honolulu, Hawaii, April 25–29 1982.

Reprint requests: David C Hemmy, M.D. Department of Neurosurgery, 8700 West Wisconsin Avenue, Milwaukee, Wisconsin 53226.

References

1. David DJ. Poswillo D. Simpson D: The Craniosynostoses. Berlin. Springer-Verlag. 1982. P 86.

2. Herman GT, Liu HK: Three-dimensional display of human organs from computed tomograms. Comput Graphics Image Processing 9:1–21. 1979

3. Udupa JK: Display of 3D information in discrete 3D scenes produced by computerized tomography. Proc IEEE 71: 420–431. 1983.

Craniofacial Computer Modelling

G.R. Travan, B.Sc., B.Sc.(Hons), M.Sc
T. Brown, D.D.Sc. F.R.A.C.D.S.
S.C. Townsend, B.D.S, B.Sc.Dent(Hons), Ph.D.
D.J. David, M.B.B.S., F.R.A.C.S., F.R.C.S, F.R.C.S.(E)
Department of Dentistry. The University of Adelaide and The South Australian Cranio-Facial Unit, Adelaide Children's Hospital, Adelaide, South Australia

Summary

A system for the generation, display and manipulation of 3D colour models of the face is described, together with the results of NC machining. Data for the techniques were derived from stereophotogrammetry. Applications of the methods to the study of facial morphology and also for pre-surgical planning are considered.

Introduction

The generation, manipulation and display of three-dimensional images is a well-developed area of computer science and an essential feature of computer-aided design, drafting and manufacture (CAD/CAM). The application of the algorithms and techniques to medical imaging is a relatively new area which has stimulated widespread interest, especially in relation to pre- and post-operative surgical planning and in the fabrication of prostheses.

Generally, medical images are 'surfaces' reconstructed from imaged serial sections. The surfaces are projected onto an image plane where suitable 'rendering' has been applied to the selected form of representation used to model the three dimensional scene. This medical imaging process has been applied clinically, in craniofacial surgery, (Vannier, Marsh, Warren and Barbier, 1983) and in the display of intra-cranial soft tissue structures (Vanneir, Gado, and March, 1983). Herman (1978) has developed a 'cuberille' approach to the 3D reconstructions from CT scan data which has been utilized for radiation therapy and surgical planning (Bloch and Udupta, 1983). Furthermore, Parviti, Wood, Young and Duncan (1983) have investigated an interactive system for planning reconstructive surgery, a feature of which was the NC (Numeric Control) milling of a skull from a reconstructed CT scan. More recently, 3D reconstruction schemes have been extrapolated to other imaging modalities, such as magnetic resonance imaging (Vannier, Butterfield, Jordan, Murphy, Levitt and Gado, 1985) and ultrasound (Greenleaf, 1982). The importance of a 3D colour-range method to image CT scan data for normal and pathologic intra-cranial conditions has been emphasized (Farrell et al. 1984).

While there are technical problems associated with the display, manipulation and machining of biological replicants, it would seem that the tools and techniques are well established, at least in principle. Using stereophotogrammetry, computer tomography or magnetic resonance imaging, data bases can be established as an initial step of primary importance, enabling subsequent development and analysis.

It must be appreciated however, that unlike other CAD/CAM applications, there have been few attempts to quantify complex 3D surfaces such as faces, other than by simpler dimensioning. This is largely due to the nature of human surface anatomy which is difficult to describe readily, even by higher order equations.

In our own research we have been interested in the analysis of shape, particularly in the quantification of facial appearance. We are especially interested in the quantification and localization of shape differences on twins as part of a wider genetic analysis of dentofacial growth. Most investigations of facial morphology have been based on two-dimensional data and attempts to demonstrate asymmetries have generally relied on the construction of arbitrary mid-line axes. Our computer-based approach provides the opportunity to visualize facial morphology in three-dimensions in any orientation. It also enables the generation of normal and reversed facial images which can be compared to assess asymmetry without the need to define a mid-line. We aim to compare facial morphology, including asymmetry, in monozygous and dizygous twins in an attempt to clarify the role of genetic factors on facial appearance. The techniques developed also have implications for surgeons who are seeking more accurate and informative approaches to the pre- and post-operative assessment of patients with craniofacial abnormalities. The potential for the development of an interactive system exists which would ultimately allow surgeons to view and manipulate computer-generated facial models of their patients prior to actual surgery.

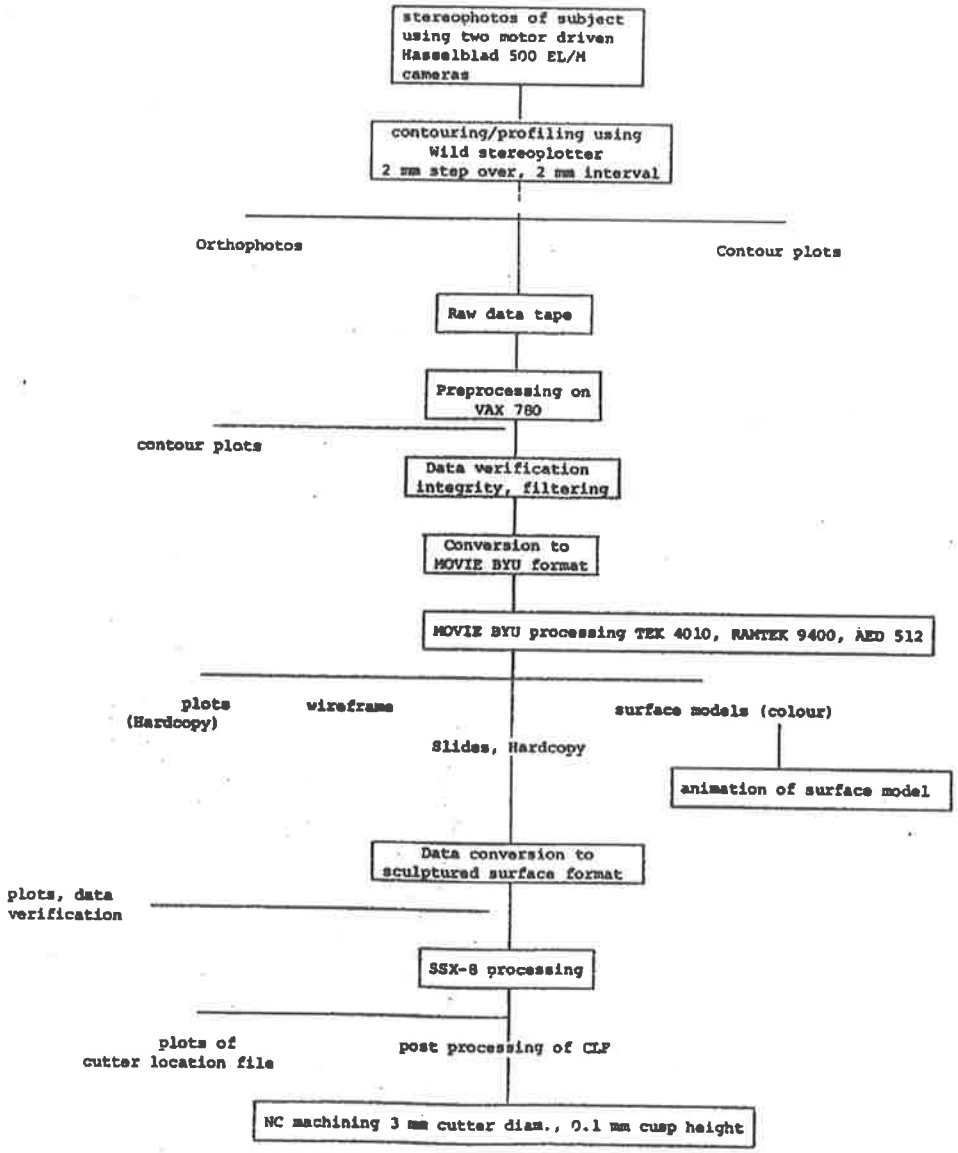

FIG.1. *Flow Chart of Craniofacial Computer Modelling Scheme*

We here describe a technique that utilizes stereophotogrammetry to establish a data base, and a computer system that enables the display of 3D facial models. The overall scheme is reflected in Figure 1. To date the procedure has been applied to three facial models including a craniofacial patient and the faces of a pair of identical twins. The preliminary results of NC machining are also described.

Stereophotogrammetry

The technique of reconstructing 3D cartesian coordinates from 2D stereophotogaphs, known as photogrammetry, has been used extensively in mapping from aerial photographs. It has also been successfully applied to the reconstruction of surface topology with great accuracy (0.1 mm) in engineering and in the biomedical engineering of sculptured surfaces. Savara (1985) indicated its importance to surgical planning and referred to other applications in the study of teeth, the assessment of facial swelling and contouring, somatotyping, and in the calculation of body surface area and volume. Duncan and Mair (1983) have described such a system for the milling of sculptured surfaces from photogrammetric data, indicating the suitability of the technique in the biomedical sciences.

The essential features of our potogrammetric process are stereophotographs produced by two calibrated and motor-driven Hasselblad cameras, model 500 EL/M. By knowing the focal lengths and viewing dimensions, the 3D co-ordinates (X,Y,Z) can be obtained from simple geometric principles. In our particular case the process of data collection is automated through stereoplotters and digitizers used in aerial photography by the Mapping Branch, South Australian Department of Lands. These 3D cartesian co-ordinates can be plotted subsequently using computer graphic principles. An example of our earlier work is demonstrated in Figure 2.

Recently, a more suitable method has been adapted which enables better post-processing and machining of the raw data. By 'profiling' across the face in a horizontal plane, an automatic system has been used to register the nodal co-ordinates at 1 mm intervals and at 2 mm contour intervals. These profile scans typically resulted in 30,000 nodes recorded over 50 contour levels for each face. The profiles could them be plotted in any view or orientation.

Movie-BYU

The 3D cartesian co-ordinates reconstructed from the stereophotographs were preprocessed and 'realized' as a surface by MOVIE-BYU, a general purpose computer graphics package, often used as a pre/post processor in finite element analysis. Mosaic and display programs within the package enable the generation of a surface from contour data by a polygonal rendering scheme. The Fuchs algorithm was used to form triangular patches between successive contour layers by mapping adjacent contours onto a unit square and selecting the minimal diagonal distance. Hidden-line removal, smoothing, and shading with multiple light sources are features of the subsequent rendering process which enables the visualization of colour models with perspective. The reconstructed planar surface can be regarded as a simple model which maintains approximate boundary representations and the surface an aesthetic surface.

The profiling procedure generated contours that were mutually centered thus minimizing the need for manual intervention when decisions were required on complex branching. MOVIE-BYU was particularly effective for this type of contouring. After preprocessing of the raw contour data (MOVIE-BYU version

5.2 allows only 8192 polygons), the entire surface formation becomes automatic within the movie scheme. PLATE 1 demonstrates the wire frame model generated by mosaic on a Ramtek 9400 connected to VAX 750. There are 8100 polygons in the model. PLATE 2 contains the flat element shading while PLATE 3 demonstrates Gouraud shading. All pictures were taken by a 'matrix' system.

In all cases the generation time was significant and many orders of magnitude greater than desirable. The computation of the surface patches with the rendering scheme where surface normals are determined with light squares, hidden-line removal, and viewer direction with perspective calculations represents a major computational problem. Nevertheless, a 16 mm animated movie was produced in order to enhance depth perception through the cues associated with movement.

NC Machining

The ability to manufacture biological replicants via computer control has direct consequences in the area of prosthetics. Therefore, as an extension to the capability of displaying 3D surfaces, machining of the surface was attempted. Preprocessing of the movie data base was necessary due to the constraints of surface formation within the heavily apt based sculptured surface package SSX-8. A restriction of 36 points per contour and 4 mm intercontour interval for spline formation enabled the direct NC machining (3 axis) after generation of cutter location data with SSX-8 for 14 splines. A 3 mm cutter diameter was utilized with a cusp height set at 0.1 mm. The few reentrants were edited manually from the data base. Machining was carried out through a direct buffered NC link after post processing of he CLD (Cutter Location Data) file to the appropriate machine code. The mastif used was a blue hard wax used industrially for die casting. The resultant replicant is demonstrated in PLATE 4 and required almost no hand finishing, demonstrating the feasibility of machining complex sculptured surfaces such as those present in biology and medicine.

Conclusions

A technique has been described to generate 3D colour representations of facial models and to NC machine the resultant surface using techniques that are well established in computer graphics and CAD/CAM. Because numerous data points are required to adequately represent a complex anatomical surface such as a human face, the computation time required to generate the models is excessive. Although the procedures are therefore not feasible for real time surgical simulation at present, the potential for further development, particularly in relation to the metric analysis of facial shape, is apparent.

Furthermore, it is hoped to extend this work to a CAD/CAM environment which would offer the benefit of interactive graphics, more versatility in terms of surface generation, metric analysis and direct NC link within a graphic environment. This would enable a quantitative examination of facial shape, an appraisal of craniofacial growth and development, and it could also have ramifications for pre- and post-surgical analysis and the design and fabrication of prosthetic appliances.

Acknowledgements

The authors wish to thank Greg Marsh and the CAPS group at the Defence Research Centre Salisbury for permission to use the facilities of the CAP group, including MOVIE-BYU and SSX-8.

Particular thanks to Steve Mellor for help with MOVIE-BYU images and Rob Aitchison for the milling of the facial models. Thanks are also extended to Ron McLeod from the South Australian Department of Lands for profiling the stereophotographs.

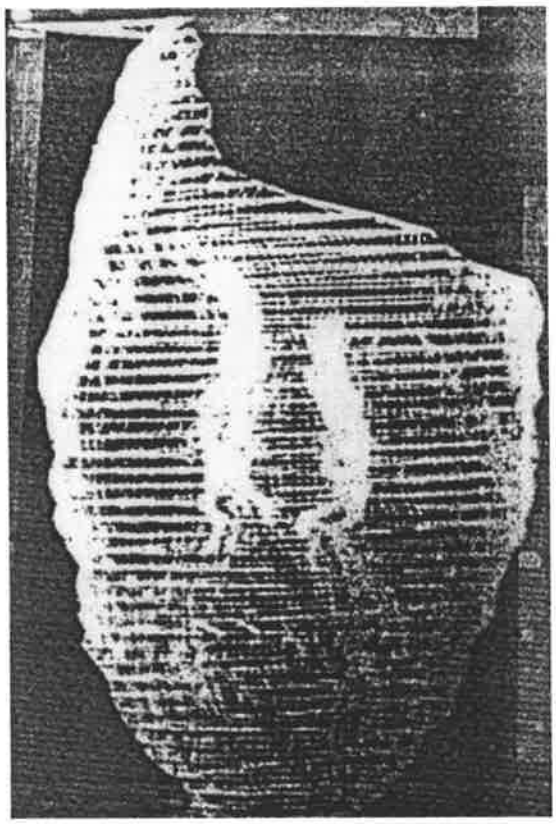

PLATE 1. *Wireframe model of cranio-facial patient.*

FIG.2. *A plot of an early contouring method*

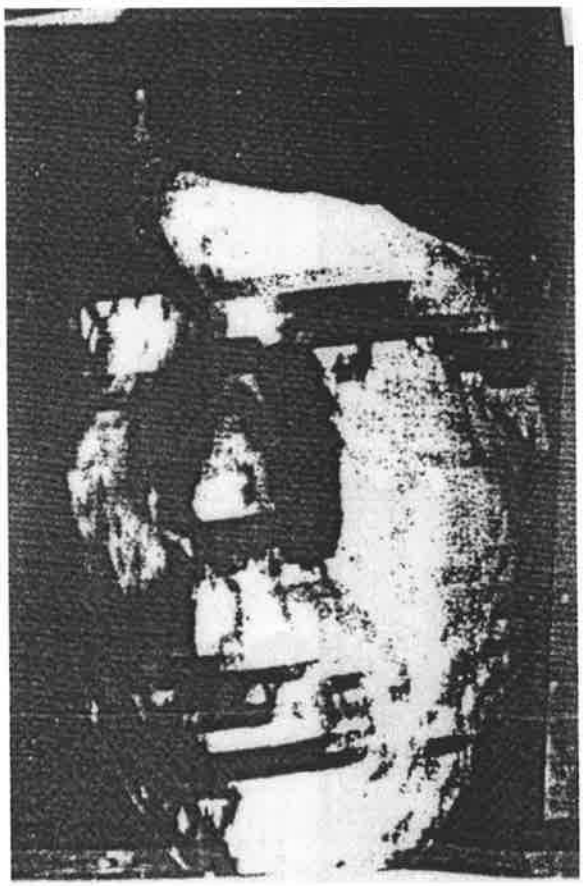

PLATE 2. *Flat element shading of cranio-facial patient.*

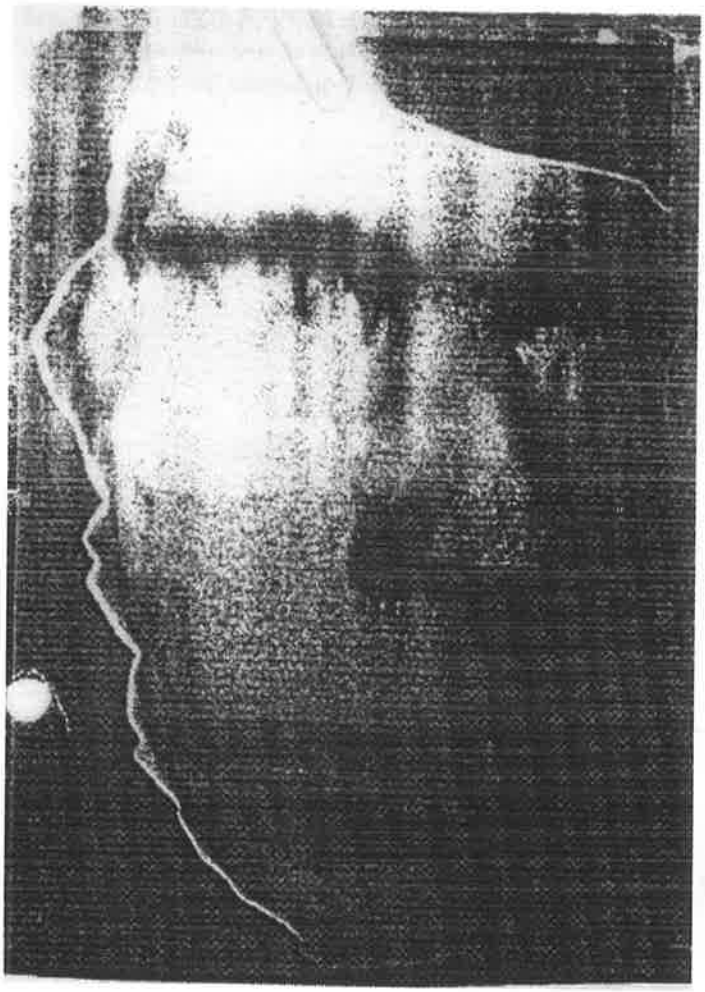

PLATE 3. *Gouraud shaded model.*

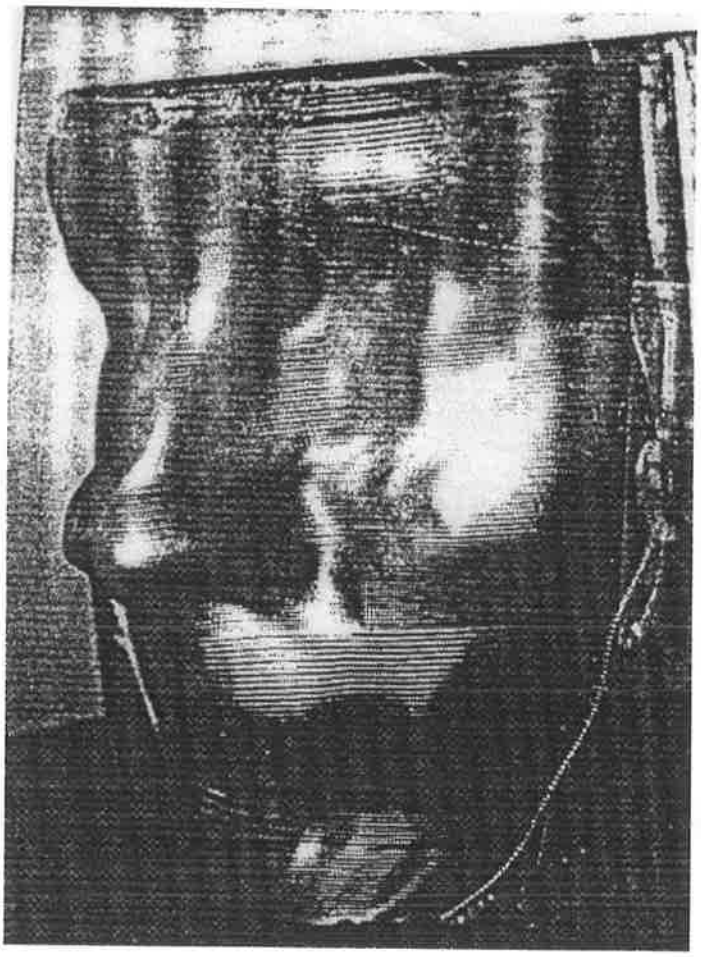

PLATE 4. *NC machined model.*

References

1 Parviti , D., Wood, S., Young, S.W. and Duncan, J.P. (1983). An Interactive Graphics System for Planning Reconstructive Surgery. Proc, Nat. Comp. Graphics Association, Chicago, June.

2 Vannier, M.W., Gado, M.H. and Marsh, J.L. (May/June 1983). Three dimensional Display of Intracranial Soft Tissue Abnormalities. Am. J. Neuroradiology, 4:520–521.

3 Vannier, M.W., Marsh, J.L., Warren, J.O. and Barbier, J. (1983). Three dimensional CAD for Craniofacial Surgery. Electron Imaging, 2:48–54

4 Herman, G.T. and Liu, H.K. (1978). Three dimensional Display of Human Organs from Computed Tomograms. Computer Graphics and Image Processing, 7:130.

5 Greenleaf, J.P. (1982). Three dimensional Imaging in Ultrasound. Journal of Medical Systems, Vol.6, pp.579–589

6 Savara, B.S., Miller, S.H. Demuth, R.J. and Kawamoto, H.K. (1985). Biostereometrics and Computer Graphics for Patients with Craniofacial Malformations, Diagnosis and Treatment Planning. Journal of Plastic and Reconstructive Surgery, 75:495–499.

7 Duncan, J.P. and Mair, S.G. (1983). Sculptured Surfaces in Engineering and Medicine. Cambridge University Press.

8 Bloch, P. and Udupta, J.K. (1983). Application of Computerized Tomography to Radiation Therapy and Surgical Planning. Proc. I.E.E.E. 71:351.

9 Vannier, M.W., Butterfield, R.L., Jordan, D., Murphy, W.A. Levitt, R.G. and Gado, M. (1985). Multispectoral Analysis of Magnetic Resonance Images. Radiology, Vol. 154, No. 1, pp221–224.

10 Farrell, E.J., Zappulla, R. and Yang, W.C. (1984). Color 3-D imaging of normal and Pathologic Intracranial Structures. IEEE Computer Graphics and Applications, Vol. 4, No. 9, pp5–17.

History of Three-Dimensional Imaging of Craniofacial Disorders

The ultimate understanding of the deranged anatomical state is derived by studying postmortem specimens. However, the craniofacial disorders, which are rare and predominantly nonfatal, provide a paucity of material for collection, study, and classification. Investigation of craniofacial disorders must then, by necessity, be directed to the living patient using the investigative tools at hand (chiefly noninvasive but occasionally invasive), relying on limited intraoperative photography and the keen memory of the surgeon.

Since the time of Roentgen we have been able to delineate the macroscopic structure of hidden organs. The two-dimensional superimposition of organs using standard x-ray techniques results in anatomical obscuration of both normal and pathological structures, limiting the accuracy of this modality. The use of polytomography, which requires that the tube and cassette move about the patient as well as the addition of contrast agents, aids in distinguishing one structure from another. However, these methods still fall prey to the valid criticisms of lack of tridimensionality (as one perceives objects in the surrounding milieu by means of binocular vision) and necessary interpretation by an experienced individual. Furthermore, interpretations are recorded verbally, are often imprecise, and vary from observation to observation.

The introduction of computed tomography (CT) by Hounsfield in 1973 provided a sophisticated method for examining the internal structure of the body on a macroscopic level without obscuration by overlapping structures. Computed tomograms provide information about "slices" of the human body. If the CT slices are obtained in an abutting or overlapping fashion, a set of measurements are obtained that, if displayed correctly, can provide three-dimensional anatomical information. This fact was first recognized by Herman and Liu in 1977.

Hemmy et al. suggested in 1979 that rendered three-dimensional images would be useful to the understanding of paediatric craniofacial and spinal anomalies. They believed that the three-dimensional image stood as a permanent graphic assembly of CT slice data in contradistinction to the often erroneous mental assimilation and reconstruction of multiple CT slices, which also has the disadvantage of error among interpreters.

The method of Gabor Herman was introduced to the South Australian Craniofacial Unit by David Hemmy in 1980. The introduction was met with some skepticism, as technically sophisticated polytomographic equipment was already situated and used by the group at Adelaide Children's Hospital. Furthermore, the large-aperture, high resolution scanner was just being introduced. The nearest site capable of providing this service was Hobart, Tasmania—well over 1100 kilometers away. Nonetheless, through research funding and persistence, several patients were scanned in Hobart. Image processing, limited in the number of slices that could be processed and therefore incapable of presenting the full anatomical context, was carried out at the State University of New York in Buffalo in the laboratories of Gabor Herman. Technical problems were solved by long distance telephone. Needless to say, a considerable time elapsed between scanning and presentation of the rendered images in Adelaide (Fig. 1.1). In a few cases, the images arrived after the surgery had been completed. In addition to the great physical distances involved in this project, image processing was slow, requiring 8–12 hours for batch image processing.

Craniofacial Deformities : Atlas of Three Dimensional Reconstruction from Computed Tomography

Over the next year the utility of the three dimensional presentation of CT data was realized. Confidence in the accuracy of the image as well as the usefulness of having available a nearly infinite number of possible views served to eliminate polytomography as a major investigative tool. By 1982, CT and reconstructed views were the major radiographic tool at the South Australian Craniofacial Unit. Reconstruction of three dimensional data was carried out for two more years as an experimental protocol at the laboratories of David Hemmy. In 1984, commercial prototype software became available, making the Adelaide unit self-sufficient.

By 1983, case material had been collected and examined and the clinical efficacy determined. Publications by Hemmy et al. (1983) and Marsh and Vannier (1983) attested to the usefulness of this modality. Both of these clinical reports used a three-dimensional display similar to the method of Herman and Udupa (1981). By this time three-dimensional display of Craniofacial data was routine at the Medical College of Wisconsin, the South Australian Craniofacial Unit, and Washington University (St. Louis).

Computed tomography and the reconstruction of CT data in three dimensions has, over a period of 7 years, completely eliminated many conventional radiographic examinations and now is beginning to seriously threaten radiocephalometry. The recent reduction in the cost of both hardware and software systems supporting three-dimensional reconstruction makes these systems an economic reality.

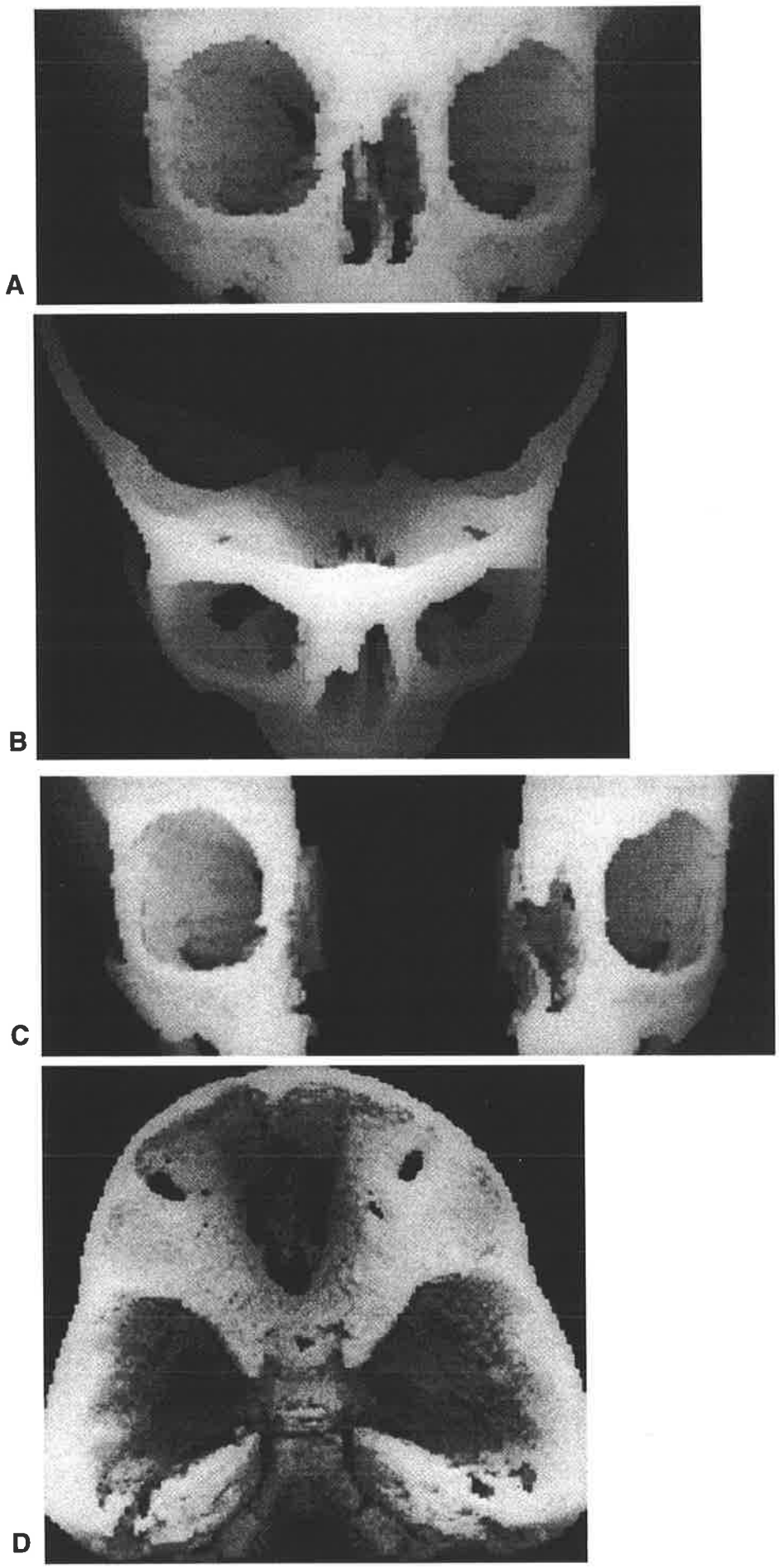

FIG. 1.1. *Three-dimensional image of patient with midfacial cleft and orbital hypertelorism acquired in Hobart, processed in Buffalo, and used in Adelaide.*

Recommended Reading

1 Hemmy DC, David DJ, Herman GT: Three dimensional reconstruction of Craniofacial deformity using computed tomography. Neurosurgery 13:534–541, 1983.

2 Hemmy DC, Herman GT, Millar EA, Haughton VM: Three-dimensional reconstruction of the spine and calvarium in children utilising computed tomography. In: Proceedings of the Second International Child Neurology Congress, Sydney, Australia, p 81, 1979.

3 Herman GT, Liu HK: Display of three-dimensional information in computed tomography. J Comput Assist Tomogr 1: 155–160, 1977.

4 Herman GT, Udupa JK: Display of three-dimensional discrete surfaces. Proc SPIE 283:90–97, 1981.

5 Hokayem N: The investigation and information drawn from dry skulls. In Caronni EP (ed): Craniofacial Surgery. Little, Brown, Boston, p 12, 1985.

6 Hounsfield GN: Computerized transverse axial scanning (tomography). I. Description of the system. Br J Radiol 46:1016–1022, 1973.

7 Marsh JL, Vannier MW: The "third" dimension in Craniofacial surgery. Plast Reconstr Surg 71:759–767, 1983.

8 Tessier PL, Hemmy DC: 3-D imaging in medicine ... a critique by surgeons. Scand J Plast Reconstr Surg 20:3–11, 1986.

Three-Dimensional Imaging Techniques

Currently, there are a number of software programs designed to provide three-dimensional reformatting of computed tomography (CT) and to operate on computer equipment supplied with CT acquisition systems. These programs, unless operating on an independent work station, are subordinate to the reconstruction programs necessary for slice display. This method facilitates handling of the great volume of data to be processed. Consequently, when reference is made to a work station, it is a dedicated work station, currently the IIS (Dimensional Medicine, Inc., Minnetonka, Minnesota).

Generation of a three-dimensional image may be divided into a number of steps, including CT scanning, data selection, and data processing.

CT Scanning

It must be emphasized a priori that the acquisition and production of a high quality, high fidelity three-dimensional study begins with scrupulous attention to detail. It is important that the personnel of the radiology department understand the purpose of the study, with stress placed on the fact that these studies are used to comprehend, with great detail, anatomical variance rather than to make a diagnosis or place a particular pathology "label" on the anomaly. With this requirement in mind, the wishes of the surgeon (which sometimes seem excessive to the radiologist) are followed.

The patient must remain motionless during the study. It is an absolute requirement such that the patient should be sedated or anesthetized. To date, there is no easy correction for misregistration of CT slices. The patient's head is restrained in a head holder with the orbitomeatal line perpendicular to the floor.

The surgeon designates the area to be scanned (Fig. 2.1). Ideally, this information is conveyed to the radiographer by means of a drawing or marks on a photograph of the patient. The areas of extreme interest are scanned, obtaining the thinnest slices possible (usually 1.5 mm), whereas areas of lesser interest but necessary to provide an anatomical context are scanned to allow a slice thickness of 3–5 mm (Fig. 2.2). The ordinary craniofacial study requires 100–150 slices.

Optimum scan factors should include the soft tissue technique (particularly the first time a patient is scanned) to highlight associated soft tissue anomalies, an image matrix of 512 x 512, and a narrow field of view. Using a phantom we have determined that, provided abutting (rather than overlapping) slices are used, the total radiation delivered to the area scanned is, at maximum, 5 rad, as the x-ray beam is tightly collimated. Although newer programs permit correction for tilt of the CT gantry, tilting should be avoided unless it is necessary to avoid the inaccuracies produced from metallic dental restorations or appliances. Lastly, a reasonable amount of time (45–75 minutes) should be set aside for the scan. Nearly all problems result from a poorly performed scan.

Data Selection

Data selection implies an observer interaction. CT slices are reviewed sequentially, if necessary. Slices at either extreme of the sequence may be rejected if they are not germane to reconstruction. Because the CT slices are composed of picture elements (pixels) having grey values proportional to the attenuation of the x-ray

beam by the tissue represented, and because the three-dimensional object is to be a "dissection" of the object scanned, tissues or grey values must be removed through a process called segmentation, or thresholding, in order that only the values of interest are included. Furthermore, by a process called subregioning, only those areas of the entire CT slice that are of interest are selected for economy of computation. At this time, if the surgeon has a protocol of predetermined views, or "pose angles," only those views of interest are selected.

Threshold selection is an important step. There is a reasonable amount of information loss, both intentional and unintentional, that occurs between acquisition of the CT scan and provision of the rendered three dimensional image (Fig. 2.3). Incorrect thresholding can render the displayed image inaccurate, permitting the inclusion or exclusion of data and causing a false representation (Fig. 2.4).

Image Processing

It is necessary to obtain a natural and correct perception of the full three-dimensional spatial relations of often complex patient anatomy. As noted, the processing of a set of original CT images into a rendered three-dimensional image (or a pseudo three-dimensional object) typically removes a significant amount of information. There is the possibility that this gain in perception may introduce some ambiguity. Therefore certain image criteria must be met to satisfy clinical criteria.

A number of alternative models for generating a two-dimensional image of a three dimensional object may be considered. In essence, such models define how a final image is to be formed, typically by simulating transmission and reflection of light by objects of interest. One possible approach is to generate an image in which the brightness of a pixel is related to the total thickness of the object along a given ray (such as a transmission radiograph). This approach, however, is insensitive to surface irregularities, which may be clinically important. Accordingly, we use the alternative of computing rendered images based on a surface shading model. With this approach, the brightness of a pixel is based on computation of diffusely reflected light from the surface, which depends on both the depth of a surface element (surfel) and its attitude (surface normal direction) with respect to the incident light and viewing directions (Fig. 2.5).

The surface shading approach permits varying the number and location of simulated light sources that can be used and the rate at which reflected brightness may drop off with increasing depth and angles of incidence and reflection of the light. Using interactive control of surface normal and depth shading along with arbitrary three-axis rotations permits subtle details to be seen.

The image quality of shaded surface images is affected by the relative strengths of the depth shading and surface normal shading. Although to some extent the judging of these images is a subjective matter, those images that are relatively restricted in their edge darkening are most suitable for anatomical display.

Occasionally it is desirable to view more than one surface at a time. In such cases, multiple surfaces can be exhibited using transparency and color to facilitate viewing (Fig. 2.6).

Typical computer graphics methods fit curves or patches to relatively sparsely defined data and subsequently render images from these smooth curves or patches. However, high resolution CT data are far from sparsely defined; moreover, a fracture or foramen as narrow as one pixel in a 512 x 512 image matrix may be clinically significant, requiring that it be visible on the final image. Therefore a volume element (voxel) data representation making use of a regular

three-dimensional array called a binary volume is used. The binary volume has a granularity that is typically less than the size of the resolution elements of the original data and is not based on any assumptions of object smoothness, orientation, or the contiguous relations of elements, called *connectivity*. This representation simply assigns a binary value of 1 to each element included after segmentation or thresholding and a binary value of 0 to elements not fulfilling the criterion.

In many cases of clinical importance, segmentation is normally accomplished by applying a threshold criterion to the original CT pixel values. Pixel values between specified minimum and maximum values are considered "bone" and are assigned a binary value of 1. In most of these cases, the object contrast and signal-to-noise ratio are high, requiring no special data preparation or conditioning prior to thresholding. In certain scanned areas where representative tissues are thin or small and surrounded by tissues that have markedly different CT values (e.g., ethmoid bone and the air-containing sinus), the reconstructed CT image presents a third value (*partial volume average)* not representative of either tissue. Thresholding procedures applied to this value result, generally, in exclusion of bone in the rendered object, giving the appearance of a hole where one, in actuality, does not exist. In order to avoid these errors, two dimensional image processing can be applied to the original CT slices to enhance some characteristic prior to segmentation. A problem seen with "dropout" of the ethmoid bone in many of the earlier images can now be corrected by applying a combined linear and nonlinear filter to enhance the thin bone without increasing background noise (which could be included as "bone" and therefore cause an error in appearance) (Fig. 2.7).

Prior to computing an binary value for the original CT pixel values based on thresholding, it is often appropriate to compute interpolated pixel values on a three dimensional mesh of points that provides even finer spacing than the original pixel data. It provides a voxel (like a pixel, a voxel has an X and a Y dimension, but because it is a volume element it also has a third, or Z. dimension) smaller than the original data resolution element dimensions (Fig. 2.8). No error is created, as this interpolation does not add information to the original data but simply allows the original grey scale pixel data to be optimally used. It is clear that fidelity in the rendered images requires at least as many voxels as there were pixels in the original CT data. Consider CT data consisting of individual slices formed with a pixel matrix of 512 x 512 (512 rows of pixels and 512 columns of pixels). One hundred contiguous slices have been obtained, which results in a voxel volume of 512 x 512 x 100 voxels. After thresholding is applied, a binary volume is created that has these same dimensions (512 x 512 x 100). Interpolating these data could result in a binary volume having dimensions of 1000 x 1000 x 1000 elements or 512 x 512 x 512 elements. Not surprisingly, there is not a significant difference in the final rendered images using these two volumes, as resolution of the original 512 x 512 x 100 data presents the same fundamental limitations in both cases.

Gabor Herman and the Medical Image Processing Group presently located at the University of Pennsylvania developed an algorithm for computing a boundary surface comprised of voxel faces that are interfaces between 1 (present) and 0 (not present) voxels; they are mutually connected and also connected to a user-prescribed "seed point" on the boundary surface of interest. This technique uses connectivity criteria to build six lists of voxel surface elements, which correspond to the six possible directions of a voxel face (a voxel being a parallelepiped, which may be cubic). An important characteristic of this algorithm is that objects not connected to the surface of interest are automatically eliminated, a feature of utility in the elimination of an extraneous object of bone density such as the head holder or tape applied to the patient's forehead. A drawback to this processing method is the possible exclusion of anatomical parts that are not connected to one another, such as a bone sequestrum or the parietal bone as a portion of the skull in an infant.

A second surface extraction algorithm, not based on connectivity of voxels is also available. This method is several times faster than the connectivity method and is capable of handling large binary volumes (1000 x 1000 x 1000), as random access to the entire volume at once is not required. This method has the limitation that unwanted objects, such as the CT head holder, must be removed or "disarticulated" by the operator. However, disconnected portions of bone are always faithfully represented. Furthermore, "neighbor' codes, which define the orientation of the four faces connected to the displayed voxel face, are not generated, which affects some of the shading algorithms.

When a voxel surface has been generated by either of the methods, its elements (surfels) are projected onto a display matrix. The work station uses a depth buffer algorithm that, in a given display pixel, retains only the projected surfel that comes closest to the viewer. A surfel is projected orthographically into only those pixels whose centers lie within the bounds of the projected surfel.

Shading of the object can be based on surface neighbor codes (if a seed point has been defined) or on gradients in the depth image generated during projection into the display space. In the case of gradient shading, a small modulation from the discrete projected voxel face orientations is retained to provide the viewer with a subtle contouring effect, which serves as a depth cue. Using either the neighbor code-based or gradient-based choices for image rendering, the operator may select the relative amount of depth shading and surface normal shading to be used (Fig. 2.9).

The dedicated work station offers flexibility in the design of the anatomical object to be displayed. An "interactive" mode permits arbitrary three-axis rotation of the object. Furthermore, the permitted use of one or two binary volumes and a third "gray" volume containing complete 12-bit original pixel data permits internal inspection of an object from any desired viewpoint, displaying soft tissue alongside bone (Fig. 2.10).

Measurements can be made by determining three-dimensional coordinates (because there is a unique depth coordinate for the most frontal voxel along any ray). The distance between these coordinates can easily be computed and displayed. The definition of three consecutive points permits angular determination at the second, or vertex, point. Furthermore, volumetric measurements can be made by assessing the number of voxels contained in a defined space and converting this total to cubic centimeters (Fig. 2.11).

The speed required for interactive three-dimensional image processing is provided by a flexible image/graphics processing "engine," which works in conjunction with its own high speed memory, and a "supermicro" UNIX based host computer, which is coupled to the interactive devices ("mouse" and trackball) of the work station. The database is stored on two large-capacity Winchester disks. The work station in a large craniofacial unit is a surgical tool dedicated to the tasks of the unit, permitting day-today image processing dictated by the case load of the unit as well as investigative study of the collected cases of the unit (Figs 2.12–2.15).

Work Station Products

The permanent record of work station production comprises rendered images stored on a selected type of medium. That medium may be magnetic tape in the form of a video tape record of manipulation of images that occurred during the work session. It may also take a form suitable for storage and later review of archived images on magnetic tape suitable for review on the work station. Images may be captured by means of a 35-mm camera to record output. An experimental mode of transmission of images to a remote electronic terminal is also in evolution.

Lastly, the most common form of work product is presently displayed on transparency film using a laser imager (Fig. 2.16). This medium has the advantage of portability.

Recommended Reading

1 Hemmy DC, Tessier PL: CT of dry skulls with craniofacial deformities: accuracy of three-dimensional reconstruction. Radiology 157:113–116, 1985.

2 Hemmy DC, Tessier PL, David DJ: Methods for and pitfalls in the acquisition of computed tomographic data for faithful three-dimensional reconstructions. In Marchac D (ed): Craniofacial Surgery (pp. 9–11). Springer-Verlag, Berlin, 1987.

3 Herman GT, Udupa JK: Display of three-dimensional discrete surfaces Proc SPIE: 283:90–97, 1981.

4 Tessier PL, Hemmy DC: 3-D Imaging in medicine ... a critique by surgeons. Scand J Plast Reconstr Surg 20:3-11, 1986.

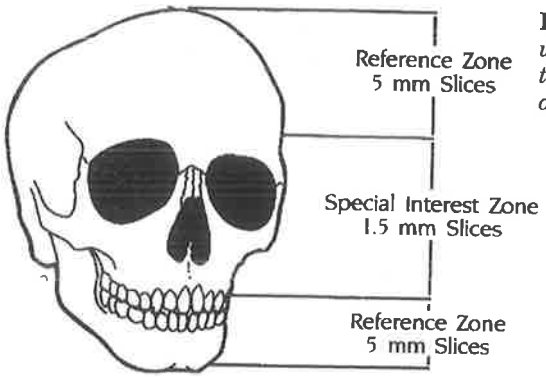

FIG. 2.1. *Method of specifying CT scans with thin slices in the area of interest and thicker slices in reference area or area of anatomical context.*

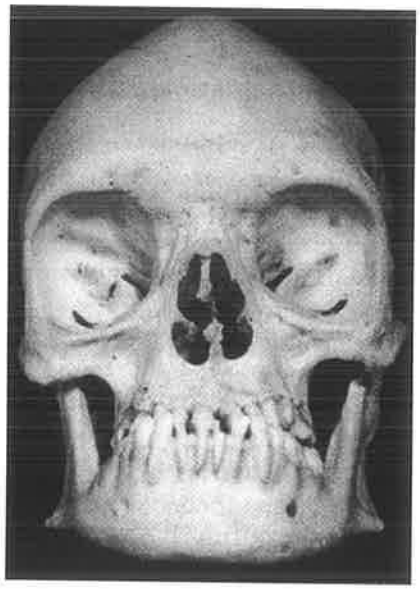

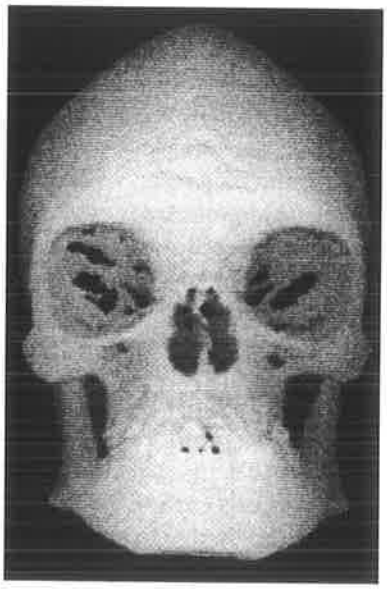

FIG. 2.2. *Dry skull with Crouzon syndrome* **A.** *scanned using 1.5 mm thick slices* **B.** *and 5.0 mm thick slices* **C.** *Note the lack of detail with thicker slices and the uniform appearance of the posterior orbits. Note also the appearance of holes in the posterior orbits on 1.5 mm thick slices due to partial volume averaging.*

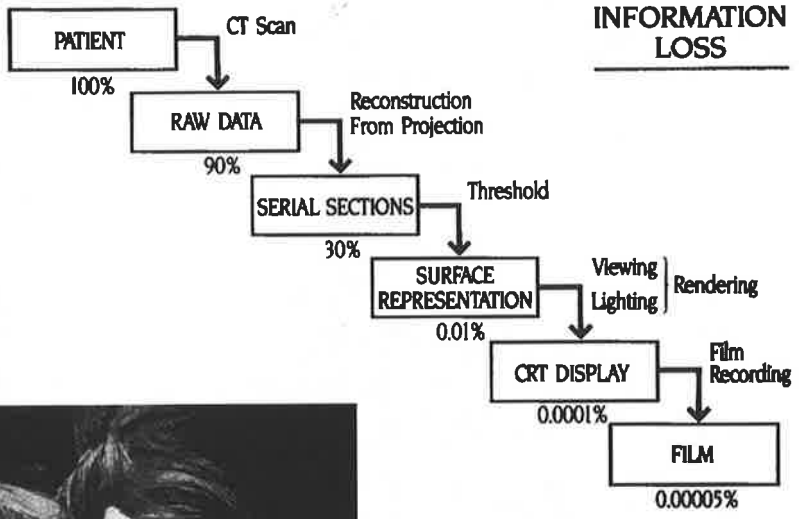

FIG. 2.3. *Sequential map of information loss* **A**. *that may occur from acquisition of data from patient* **B**. *to rendered image* **C**. *[(A) From Michael Vannier, MD, Mallinckrodt Institute, St. Louis, MO.]*

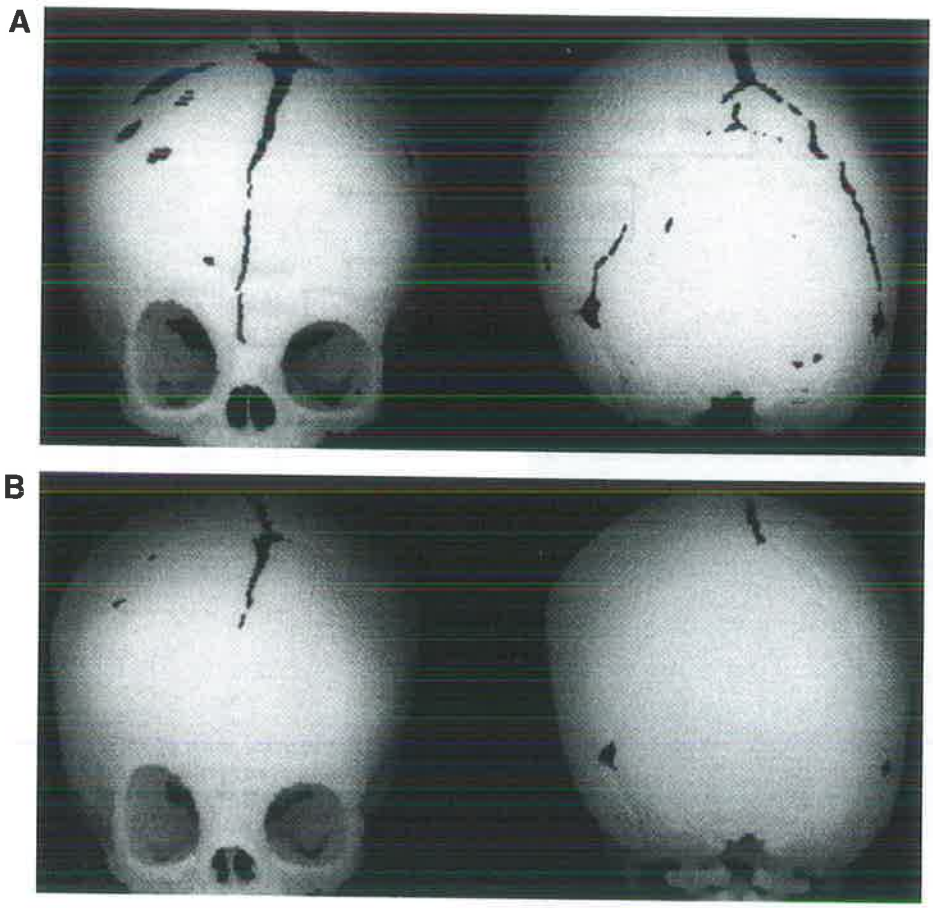

FIG. 2.4. *Error that may occur because of incorrect threshold.* **A.** *Incorrect image.* **B.** *Correct image.*

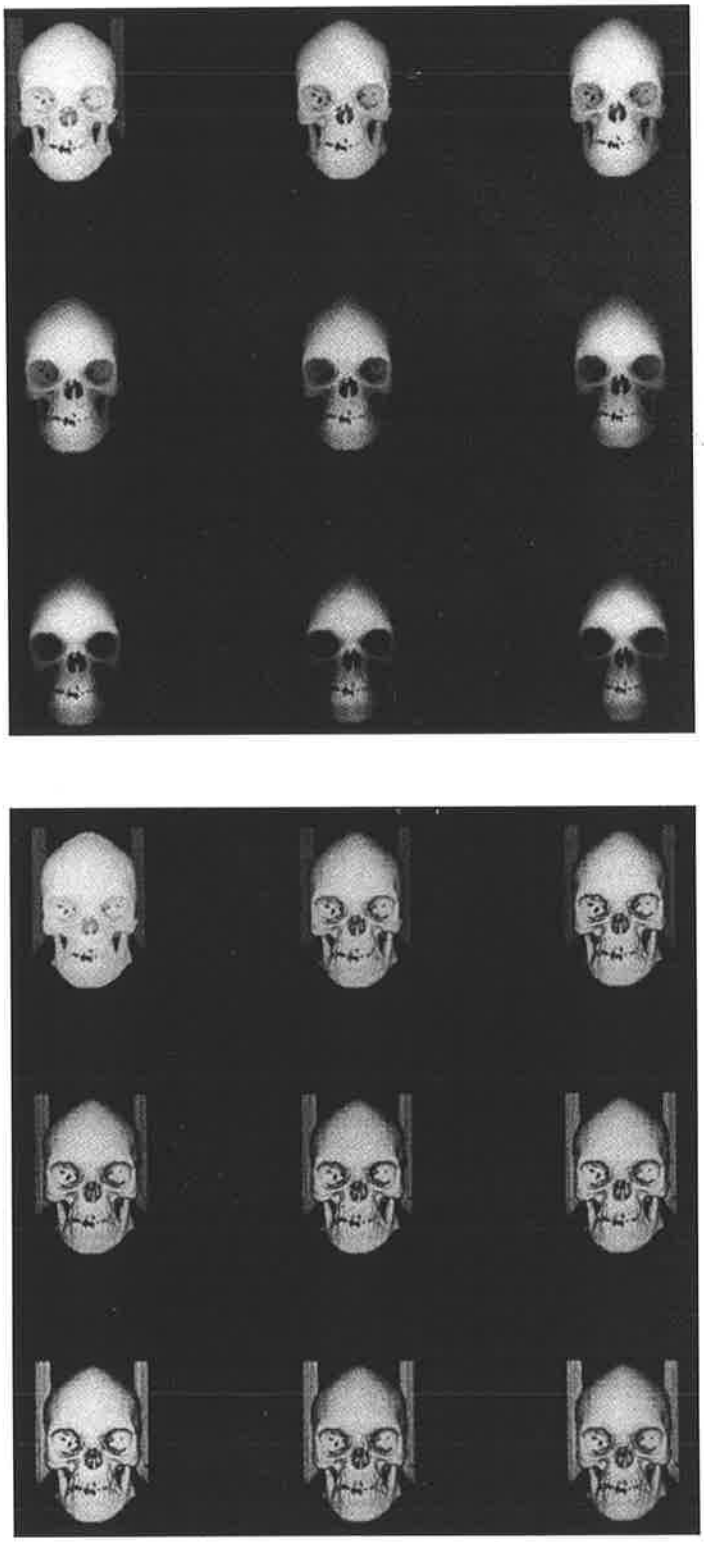

FIG. 2.5. A. *Images resulting from changes in depth shading.* **B.** *Images resulting from changes in surface normal shading.*

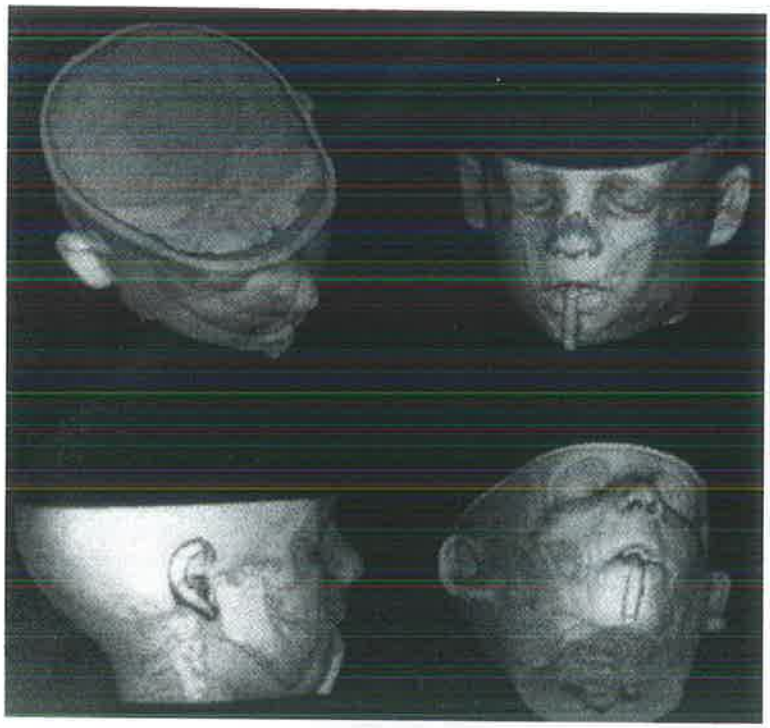

FIG. 2.6. *Image created using transparency for simultaneous display of two tissues.*

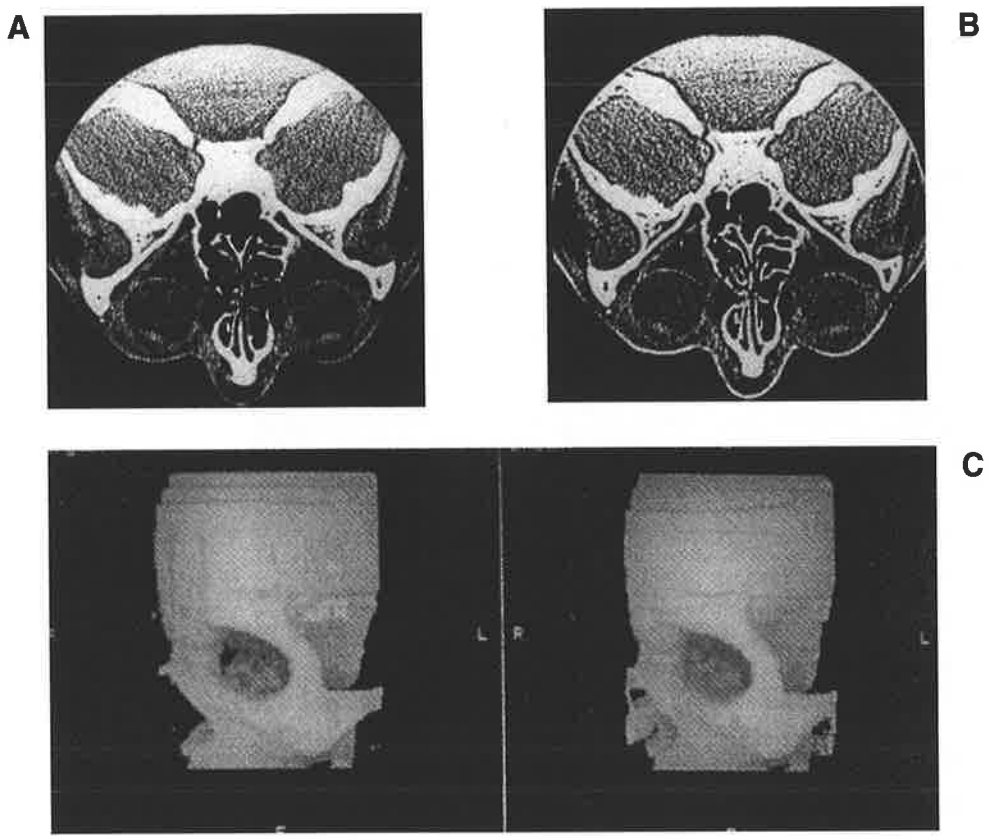

FIG. 2.7. *Use of combined linear and nonlinear filtering to improve detection of papyraceous ethmoid bone.* **A.** *Original CT slice.* **B.** *Filtered CT slice.* **C.** *Three-dimensional images before (left) and after (right) filtering to reduce "pseudo-foramina".*

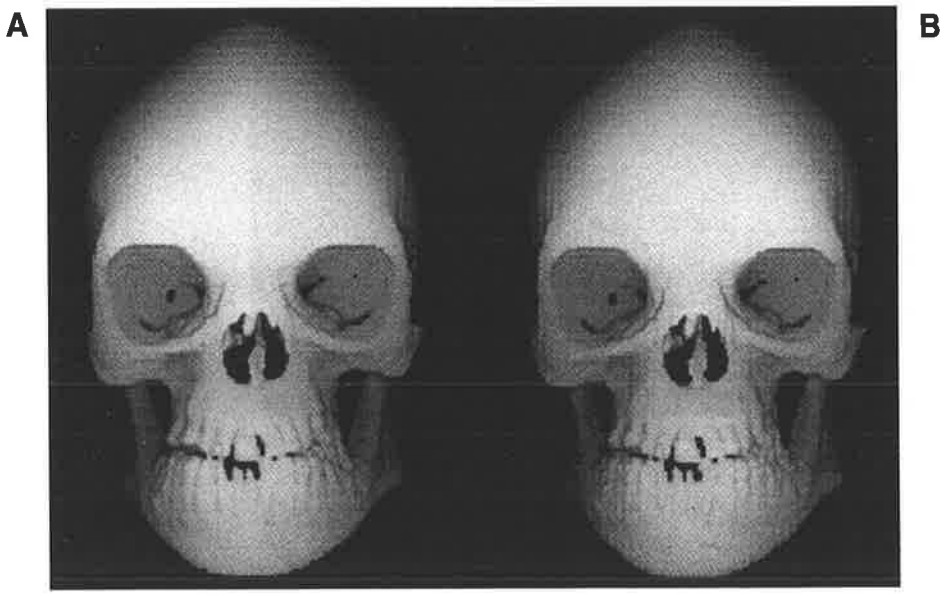

FIG. 2.8. *Images resulting from use of voxels larger* **A.** *and smaller* **B.** *than original data.*

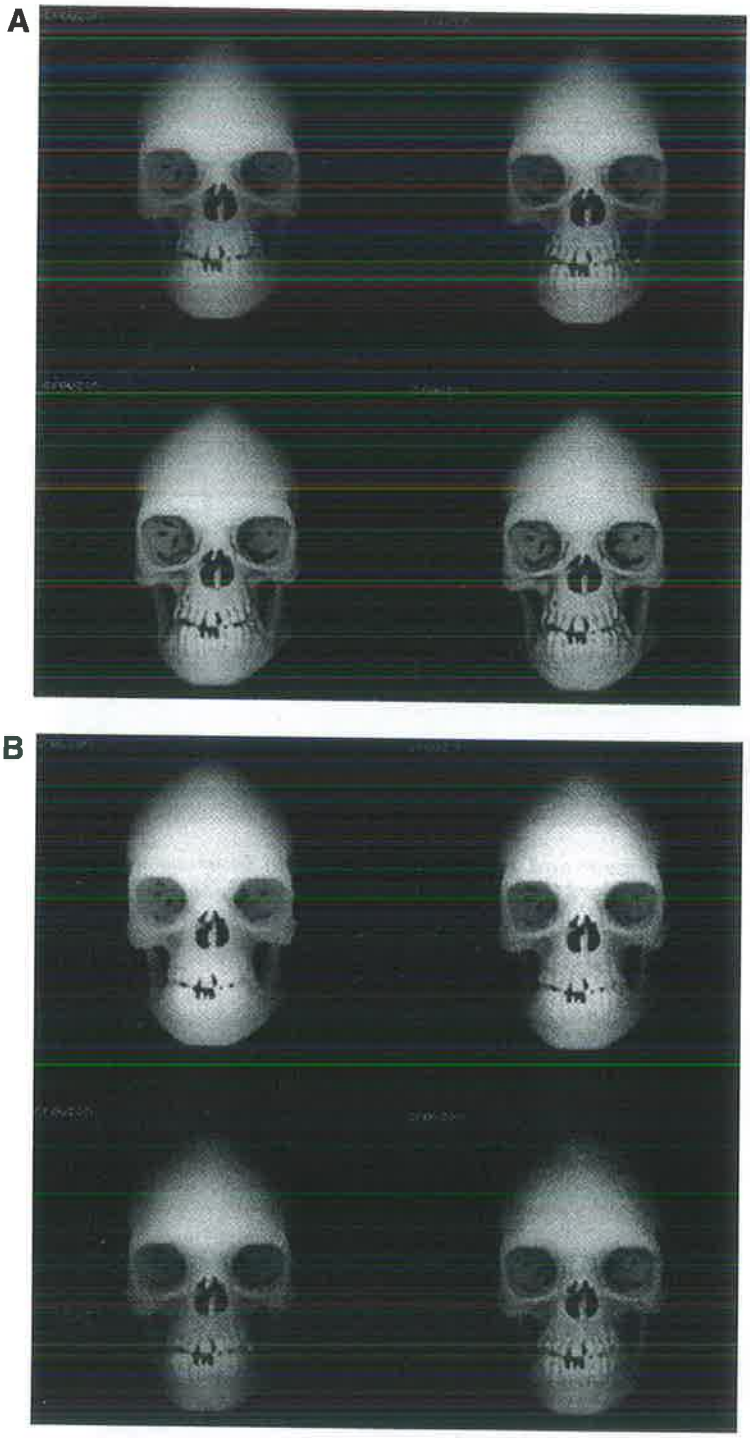

FIG. 2.9. A. *Gradient-based rendering.* **B.** *Neighbor-based rendering.*

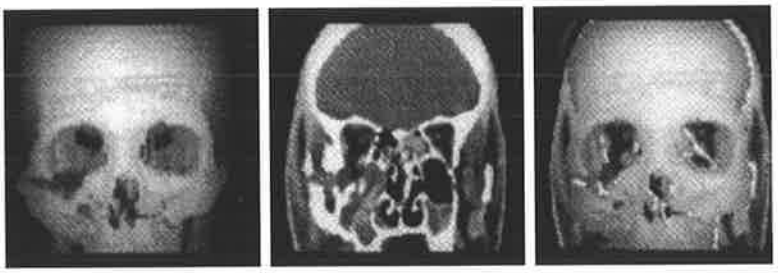

FIG. 2.10. *Use of the 12-bit gray volume to display soft tissue along with bone.*

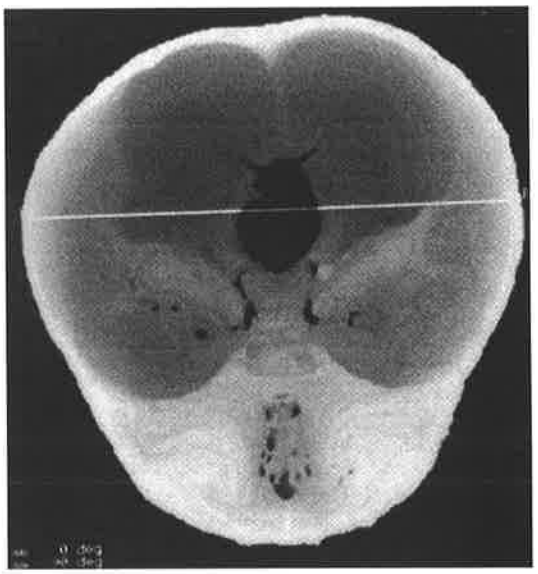

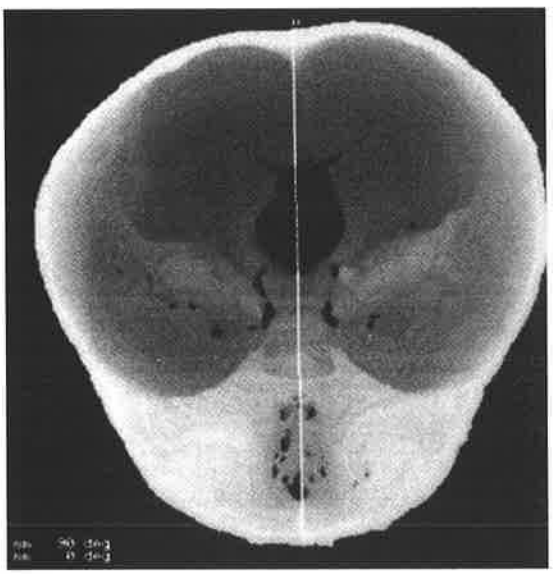

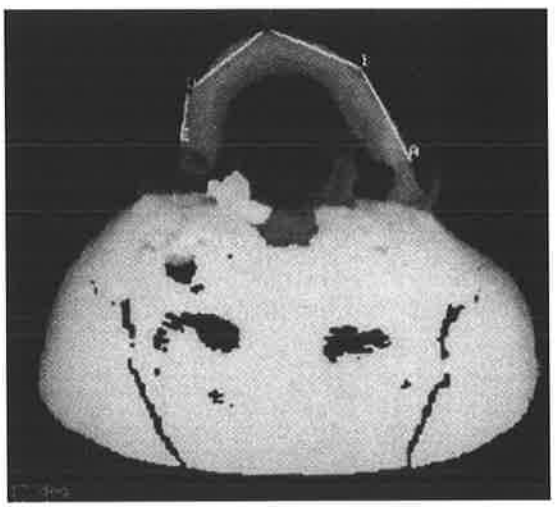

FIG. 2.11. *Linear and angular measurements.*

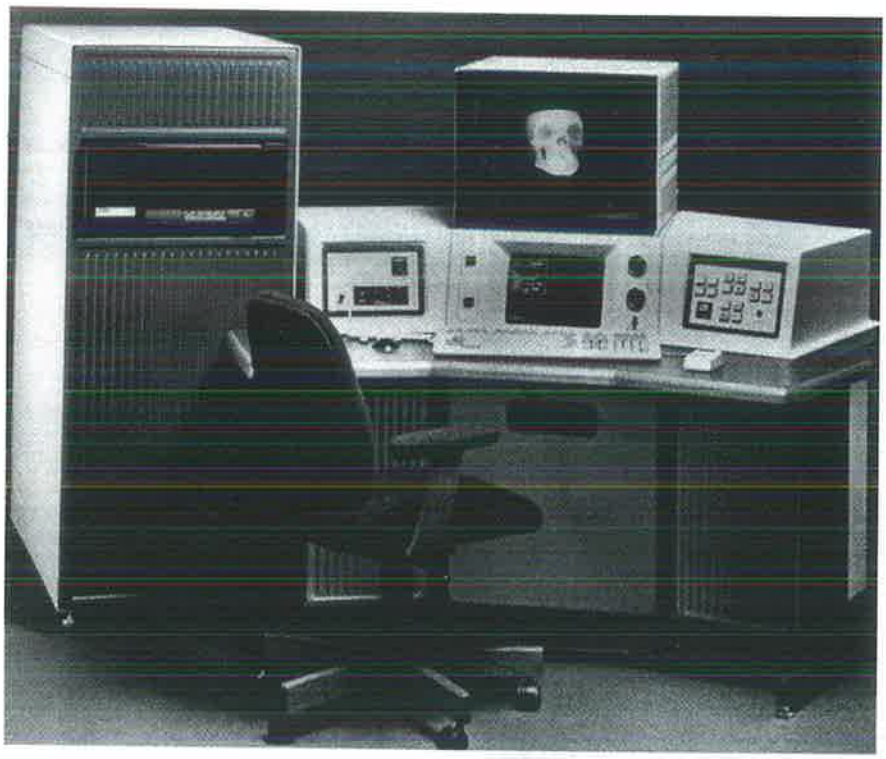

FIG. 2.12. *Dedicated work station.*

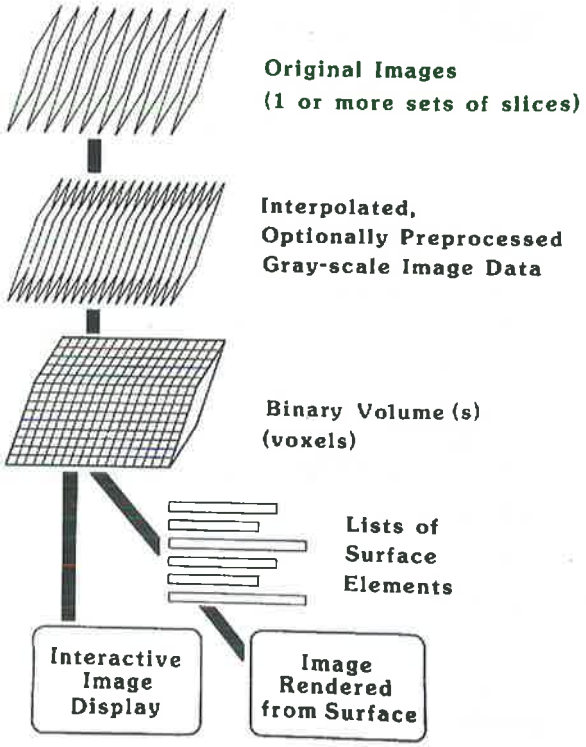

FIG. 2.13. *Data flow in work station.*

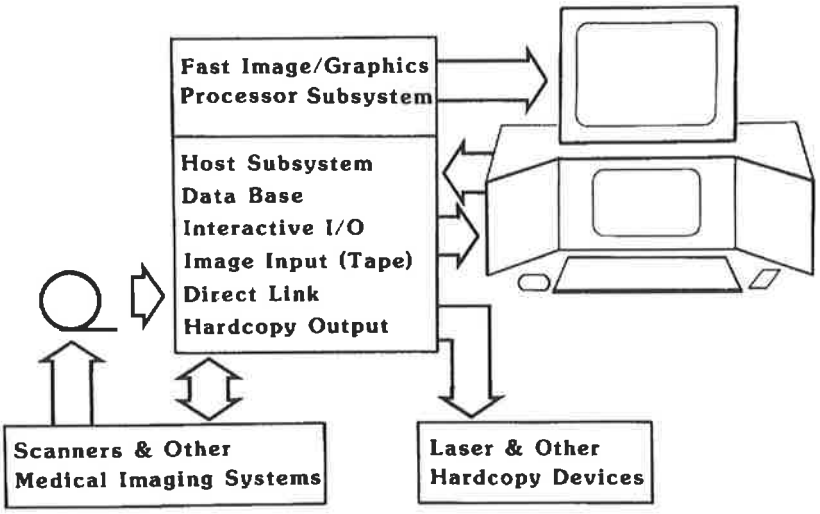

Fig. 2.14. Work station hardware components.

FOREGROUND (Interactive):	BACKGROUND:
Data Management	Data Input & Conversion
3-D Preparation	Batch MPR Computation
Interactive 3-D/MPR	Volume Computation
Image Review	Surface Computation
Snapshot Review	Batch Rendering
PRIMITIVES:	
Imaging	Interactive devices
Graphics	Menus
Data Base	
Unix Operating System	
Custom Microcode	
Device Drivers	

FIG. 2.15. *Work Station software components.*

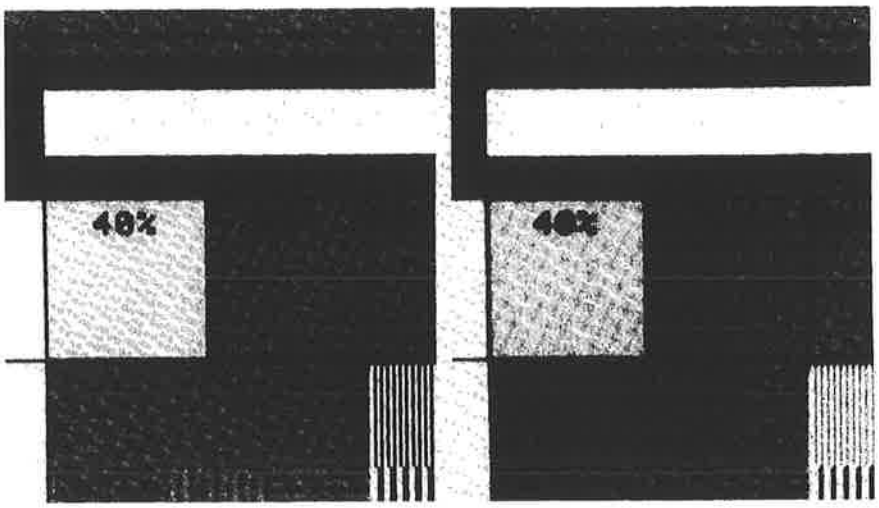

FIG. 2.16. Left: *Image produced using laser imager. (Courtesy 3M Company.)*
Right: *Image produced using standard multiformat camera.*

Helmet-induced skull base fracture in a motorcyclist

Rodney D. Cooter, David J. David, A. Jack Mclean, Donald A. Simpson
South Australian Cranio-Facial Unit, Adelaide Children's Hospital and Royal Adelaide Hospital and NH & MRC Road Accident Unit, University of Adelaide, South Australia

Summary

Observations after a fatal motorcycle accident suggested that the face bar of a full-face helmet may transmit an impacting force to the skull base via the chin strap and the mandibular rami and condyles, bypassing the energy-absorbing facial bones. If this mechanism is confirmed, the structural properties of these face bars will need to be reassessed.

Introduction

Helmets are widely advocated as a proven means of reducing head injury in motorcyclists.[1,2] The traditional open-face helmet has been modified by addition of a face bar to form the popular full-face helmet which reduces the risk of facial injury.[3] This, however, may not be wholly advantageous if the impact energy is redirected to more vital areas.

Scant attention has been paid to helmet-induced injuries sustained after craniofacial impacts.[4,6] An association of face bar impacts and skull base injuries has been observed by Harms[7], who suggested "an indirect blow via the mandible" as a possible mechanism in the generation of skull base trauma. In a consecutive necropsy series of 132 motorcycle and moped riders killed in 1977-83 in southern Sweden, Krantz[6] reported eleven ring fractures of the skull base in 38 motorcyclists with full-face helmets but only six such fractures in 64 riders wearing open-face helmets. Krantz suggested three mechanisms of generating skull base trauma — traction, torsion, and displacement of the atlas. We report here a case encountered during a multidisciplinary prospective study of both fatal and non-fatal craniofacial injuries to motorcyclists in Adelaide in 1986. The method included computed tomographic (CT) scanning of the head and face and also, in motorcyclists, of the helmet.

Case-report

A 19 year-old male motorcyclist and pillion passenger fell from a 500 cc motorcycle at a suburban intersection. The rider slid along the road and struck the front of his helmet on the edge of a concrete kerb. The pillion passenger was not injured and damage to the motorcycle was slight.

The motorcyclist was unconscious when found by the kerbside. When a bystander gave mouth-to-mouth resuscitation the blood flow from the ear canals was observed to increase. He did not regain consciousness and was pronounced dead on arrival at hospital. On examination there was blood in both external ear canals and a graze on the right cheek but no other overt signs of injury; in particular, there was no obvious chin trauma, all facial structures were palpably intact, and there was no abnormal midfacial mobility.

Results of Investigations

Radiology

A CT head scan 12h post mortem revealed a large volume of intracranial air. The underlying brain was radiologically normal, with no obvious intracranial haemorrhage. A fracture in the skull base extended across the posterior third of the middle cranial fossa bilaterally and traversed the clivus. Reformatted images through the skull base in oblique and sagittal planes were employed to examine the proximity of the mandibular condyles to the middle fossa fracture and to assess the degree of midline disruption (fig 1). The facial bony skeleton appeared intact.

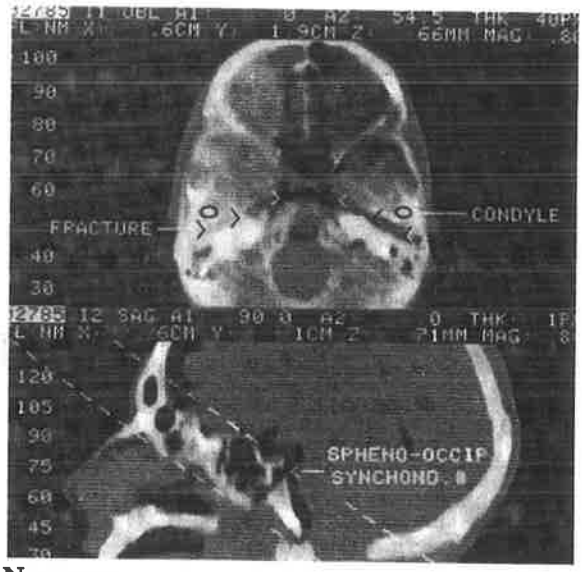

FIG. 1. *Reformatted CT scan of skull base.*

Above, a close physical relation is apparent between the underlying mandibular condyles (encircled) and the basal fracture (arrowheads). Disruption of the spheno-occipital synchondrosis is clearly shown on the mid-line sagittal reformat (below).

Necropsy

At necropsy the skull base fracture was found to have resulted in massive haemorrhage in to the pharynx, probably causing death by asphyxia. There was minor patchy subarachnoid haemorrhage over the right temporal lobe and serial sections revealed evidence of recent haemorrhage in the choroid plexus and both occipital horns. Microhaemorrhages were seen in the midbrain, pons, medulla, and cerebellum.

Helmet Study

The helmet, which was of full-face design and fibreglass construction, was retained on the rider's head during impact. There was a vertical fracture through the face bar on the right side about 60mm from the midline. At the fracture site there was 7mm vertical displacement, the larger portion of the face bar arc being displayed upward relative to the smaller portion. Two smaller undisplaced fractures were found in the helmet shell, in the upper edge of the facial aperture directly above the fracture in the face bar. There was no external evidence of any other impact to the helmet. The comfort padding was displaced rearwards on the inner right side of the helmet.

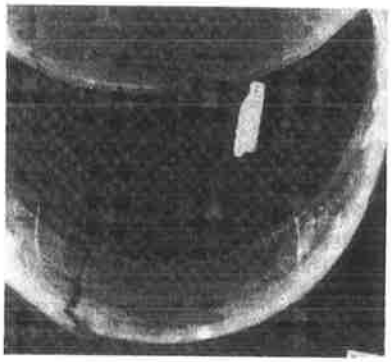

FIG. 2. *Plain radiograph showing face bar fracture on right (viewed from above).*

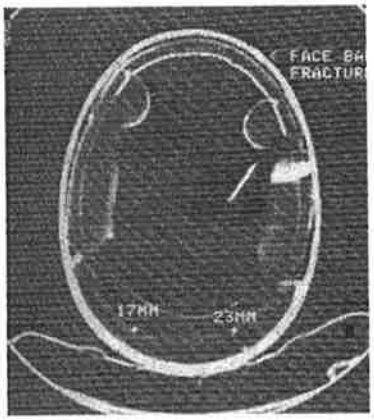

FIG. 3. *Axial CT scan of helmet.*

Note compressive deformation of the energy-absorbing liner at the left rear.

Various plain radiographic views were used to display helmet deformation; of these, a tangential view best demonstrated the fractures in the face bar and the upper facial component of the helmet (fig 2). A CT scan was then performed at 5 mm axial slice intervals. This revealed compressive deformation of the energy-absorbing liner to the left of the midline at the back of the helmet, diagonally opposite to the face bar disruption. (fig 3)

Proposed Mechanism of Injury

The force of a frontal impact to the face bar of a full-face helmet is transmitted through the shell of the helmet to the chin-strap. We postulate that a component of the impacting force is transmitted to the skull base by the chin-strap via the mandibular rami and condyles (fig 4). The subsequent impact on the skull base by the mandibular condyles fractures the floor of the middle cranial fossa.

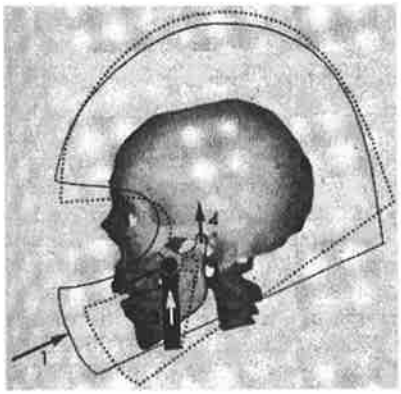

FIG. 4. *Proposed mechanism of injury.*

A three-dimensional CT reconstruction of the skull has been superimposed on a line diagram of the helmet worn. At impact, displacement and rotation (as shown by the dotted lines) would reduce the angle between vector 2 and vector 3 which would further contribute to chin-strap loading.

Discussion

A motorcyclist who receives an anterior chin impact while wearing an open-face helmet is likely to sustain mandibular fractures that will allow some dissipation of forces before they are transmitted to the skull base. Indeed, in a study of 210 patients with severe facial fractures Lee et al[8] concluded that facial structures absorb the energy of an impact and thereby prevent injury to the brain. Such natural protection is limited, of course, by the potentially fatal complications of facial fractures.[9]

In the case described here, the helmet's energy-absorbing liner overlying the left occipital region was deformed. There was no evidence of an external occipital impact, so the findings are consistent with a forward rotation of the top of the helmet about the chin-strap attachment points when the frontal impact on the right side of the face bar forced the lower part of the helmet backwards. Since there was no evidence of a substantial direct impact to the face, the

compression of the foam in the left occipital region is unlikely to have resulted from in-bending of the face bar driving the head back into the helmet. In any event, the impact on the face bar would have tended to displace the entire helmet to a greater degree than the head. The close proximity of the mandibular condyles to the fracture in the middle cranial fossa — well shown with the reformatted CT images — lends further support to the proposed sequence of face-bar → chin-strap → mandibular-condyle force transmission to the skull base.

If the postulated mechanism is confirmed the structural properties of the face bar of full-face helmets will need to be reassessed. A compromise might be necessary between facial protection and energy dissipation, since facial injuries can themselves cause death. The face bar could be redesigned so that it has more energy-absorbing capacity or so that it fragments or shears off at a critical loading.

We are grateful for the cooperation and assistance of Mr KB Ahern (State Coroner), Dr C. Manock (Forensic Science Centre, Adelaide) and Sergeant P. Cooling (Coroner's Sergeant) and his staff. We also thank Prof. T. Brown and Dr. A. Abbott (South Australian Cranio-Facial Research Unit), Dr P. Blumbergs (Institute of Medical and Veterinary Science) and Mr K McCaul and Dr G A Ryan (NH & MRC Road Accident Research Unit, University of Adelaide) for their help and advice. Financial assistance for this project was provided by a Royal Australasian College of Surgeons Foundation Johnson and Johnson Research Scholarship, the Neurosurgical Research Foundation of South Australia Inc, and the Australian Cranio Maxillo Facial Foundation.

Correspondence should be addressed to R.D.C South Australian Cranio-Facial Unit, Adelaide Children's Hospital, 72 King William Road, North Adelaide, South Australia 5006.

References

1 Aldman B, Thorngren L. The protective effect of crash helmets — a study of 96 motorcycle accidents. Proceedings of IRCOBI Conference, Goteborg 1979, 63–74

2 Cairns H. Head injuries in motor cyclists — the importance of the crash helmet Br Med J 1941, ii 465–71

3 Vaughan RG. Motor cycle helmets and facial injuries. Med J Aust 1977, P 125–27

4 Hoekstra HJ, Kingma LM. Bilateral first rib fractures induced by integral crash helmets. J Trauma 1985, 25: 566–67

5 Yates C. Injury associated with wearing a crash helmet incorporating facial protection. Br J Oral Surg 1976, 14: 163–64

6 Krantz KPG. head and neck injuries to motorcycle and moped riders — with special regard to the effect of protective helmets. Injury 1985, 16: 253–58

7 Harms PL. A study of motorcyclist casualties with particular reference to head injuries. Proceedings of IRCOBI Conference, Delft, 1984, 91–97

8 Lee KF, Wagner I.K, Lee YE, Suh JH, Lee SR. The impact absorbing effects of facial fractures in closed-head injuries — an analysis of 210 patients. J Neurosurg 1987, 66; 542–47

9 Arajarvi E. Lindqvist C, Santavirta S, Tolonen J, Kiviluoto O. Maxillofacial trauma in fatally injured victims of motor vehicle accidents. Br J Oral Maxillofac. Surg ,1986, 24: 251–57

Application and Comparison of Techniques for Three-Dimensional Analysis of Craniofacial Anomalies

Amanda H. Abbott, B.D.S., B.Sc.Dent.(Hons), Ph.D.
David J. Netherway, B.Sc.(Hons), Ph.D.
David J . David, A.C., M.B., F. R.C.S.(Edin), F.R.C.S., F.R.A.C.S.
Tasman Brown, M.D.S., D.D.Sc.
North Adelaide, South Australia

Traditionally, cephalometric analysis has been limited to data determined from two-dimensional (2-D) cephalograms. With imaging facilities such as CT and biplanar radiography now available, the natural extension has been towards the use of three-dimensional (3-D) coordinate positions of landmarks for comparative purposes. While these data have been potentially available for several years, the accurate and reproducible extraction of anatomic landmarks suitable for comparative purposes has been limited.

This paper presents results of the application of traditional comparative techniques to well determined 3-D coordinate data acquired from biplanar radiography and CT for a patient with Treacher Collins syndrome and further provides a comparison with the technique of strain analysis, often referred to as finite element analysis, which has been applied recently to craniofacial data.

Comparisons of distances and angles between landmarks, landmark coordinate positions, and strains of the patient relative to experimental reference standards reveal that the essential skeletal features of Treacher Collins syndrome have been identified and quantified by the analysis techniques. Further, a measure of the significance of the deviations has been determined by comparisons with the experimental reference standards.

Key Words: craniofacial complex, CT, biplanar radiography, 3-D quantification, experimental standards, Treacher Collins syndrome, landmark alignment, strain analysis, distances and angles

The study of craniofacial deformities is a complex problem. Craniofacial deformities display a vast range of characteristics, varying in type and severity with time. Traditional techniques for quantifying skeletal deformities are based on the identification of key osseous landmarks, which provide an immediate basis for homology between subjects, thus facilitating size and shape comparisons.

The most common method for obtaining craniofacial diagnostic data for humans has been from cephalograms. However, analysis of data from a single cephalogram is limited, due to the inherent distortion resulting from the projection into two dimensions. While extraction of three-dimensional (3-D) landmark data from biplanar (lateral and coronal) or stereo cephalograms has been investigated[3, 4, 9, 14, 24, 25] the techniques have not gained wide acceptance because of the difficulty in accurately locating the same landmark on both cephalograms. More recently, Brown and Abbott[7] described a technique, based on computer-aided point or landmark location, that reduces the difficulty in determining 3-D coordinates from biplanar cephalograms.

The Australian Cranio-Facial Unit, Adelaide Medical Centre for Women and Children, North Adelaide, South Australia, Australia
Reprint requests: Amanda H Abbott, Ph.D., The Australian Cranio-Facial Unit, Adelaide Medical Centre for Women and Children, 72 King William Road, North Adelaide, 5006, South Australia, Australia

In addition, 3-D landmark coordinate data can be obtained from 3-D CT reconstructions, although only a few quantitative results have been published[10,11,17,18] and then, only little information is available on the selection of landmarks, their coordinate locations, and their replicability. By utilising multiple sets of stereo images of 3-D CT reconstructions, Abbott[1] has obtained 3-D coordinate data of some 80 landmarks with well determined accuracies. While this off-line technique of multiple stereo images has allowed landmarks to be well identified and is suitable when additional CT computing facilities are not available, the technique will be superseded in the near future by the availability of cheaper and more powerful computing facilities for online interactive 3-D data collection.

With the availability of 3-D data collection techniques, it is now possible to proceed with the quantification and analysis of craniofacial morphology in three dimensions.

The simplest basis for size and shape comparison is that of distances and angles between specified landmarks or reference lines, and these can be determined readily from 3-D coordinate data.

Another method for the quantification of size and shape differences is the direct comparison of constellations of landmarks. This requires the constellations to be aligned in some specified manner. In this way, differences between two subjects are highlighted. Two homologous constellations of landmarks can be aligned for superimposition, using a minimum number of predetermined landmarks associated with a particular feature. However, the best features for alignment are not always known and, because of landmark location errors, it is often preferable to apply more general techniques that use a larger number of landmarks, such as those based on least squares or repeated median[1] criteria. This latter alignment technique is an extension into three dimensions of Siegel's[26,27] two-dimensional alignment technique.

Finite element or strain analysis can also be utilized to give another means of representing size and shape differences between subjects [1,2,5,6,8,20,22,23] in terms of principal stretch ratios and principal directions.

While distances and angles derived from 2-D cephalometric data for a patient can be compared with the appropriate population standards quite readily, the collection of 3-D data is rare and no 3-D standards exist. For this reason experimental reference standards have been developed by the authors against which the significance of deviations of an individual from the standards could be determined. Although these experimental standards are well suited for the development of analytic procedures, they are not adequately representative for regular clinical use. Nonetheless, the four skulls selected for the standard provided a useful 'normal' morphologic base to demonstrate how deviant structures in a patient that are obvious when examined clinically can be highlighted and quantified mathematically.

In this paper, the relative sensitivity and usefulness of distances and angles, alignment and superimposition, and strain analysis for describing and quantifying size and shape differences are assessed by their application to the quantification of the characteristic features[13] of a patient with Treacher Collins syndrome.

Method

Three methods were employed for size and shape comparison of the patient data with the experimental reference standards. These were (1) comparison of distances and angles, (2) comparison of landmark coordinate positions after alignment, and (3) strain analysis of homologous triangular elements.

Comparison of Distances and Angles

Distance and angle variables are determined directly from the landmark coordinate data.

Comparison of Landmark Coordinate Positions After Alignment

Alignment of two sets of landmark coordinate positions can be achieved using the least squares criterion, which fits one set of landmarks to the other by minimising the sum of the squared distances between homologous landmarks. Alignment can also be achieved by using the repeated median technique and this has recently been extended from two dimensions[26,27] to three dimensions.[1] Both alignment techniques can be performed with or without scaling. In the former case, the computed scale factor provides a measure of size difference and the resulting residuals tend to reflect the shape differences to a greater extent.

Repeated median alignment positions one landmark constellation relative to the other by calculating the median translation vector, repeated median scale factor, and repeated median orientation. The scale factor and orientation are based on the relative scale factor and orientation of all homologous line segments respectively. The repeated median is calculated by first determining a median scale factor and orientation for each landmark from all line segments associated with that landmark. The repeated median scale factor and orientation are then given by the median of the median values determined for each landmark. By using repeated medians, the technique has the potential for exact alignment on those landmarks that do not differ between the homologues, provided they number more than 50 percent of the landmarks. Frequently the repeated median technique is preferred over least squares alignment because of its robustness, and in this paper only results using repeated median alignment are reported.

Strain Analysis of Homologous Triangular Elements

In order to apply the techniques of strain analysis to the craniofacial complex, an homology must be defined between the structures being compared. Homologous landmarks can be used as a basis for subdividing the skull into a number of elements of finite size. The strain analysis technique describes the shape difference between homologous elements in terms of a uniform strain within the finite elements. For these elements to be sensitive to subtle differences of biologic significance the elements should

(1) be small enough to describe, or be contained within, a single biologic unit, but large enough such that the influence of the landmark location errors on the vertex positions does not adversely affect the analysis;

(2) not overlap, so that each describes a unique environment, otherwise the description of areas of overlap would become more complicated; and

(3) have angles at vertices not too small (say approximately $\geq 15°$).

Many of the bones of the craniofacial complex are relatively thin, and it is more appropriate for these structures to be described by their external surfaces using triangular, rather than tetrahedral, elements. The vertices of the triangular elements are still determined in 3-D space but two-dimensional (or planar) strain analysis is used to describe their deformation. Some structures, particularly cavities, are biologic regions that have a significant depth component and therefore are more appropriately analysed using tetrahedral elements and 3-D strain analysis. The finite elements shown in Figure 1 (Table 1 and the Appendix list and define the landmarks used, together with their abbreviations) give a sufficiently good representation of the bones for this initial investigation of the merits of strain analysis applied to the craniofacial complex.

In the fields of engineering, physics, and mathematics, strain analysis is applied to continua to describe deformation due to applied forces or stresses. In

the context of shape comparison of biologic subjects, strain analysis is used simply to describe the mathematical transformation of one element to its homologue, without any suggestion of a biologic mechanism related to the actual stresses on bones.

The transformation from one element to its homologue can be understood by considering the components of the "material deformation gradient" matrix, F. assuming a uniform strain within the element. The material deformation gradient, F, can be interpreted (Fig. 2) as:

(1) a rotation, R_1^T, of an element in the first subject to align the principal directions with the coordinate axes;

(2) dilations and/or contractions, Λ, along these directions to produce the shape of its homologous element in the second subject; and

(3) a rotation,R_2, to orient the element with its homologous element in the second subject.

The diagonal matrix, Λ, contains the principal stretch ratios, which are the ratios of lengths along the principal directions between the homologous elements. The principal stretch ratios are independent of the orientation of either subject. The rotation matrix, R_1, describes the orientation of the principal directions associated with the element in the first subject while the matrix, R_2^T, describes the orientation of the principal directions associated with its homologue in the second subject. These principal directions are fixed relative to the elements—if the elements are differently oriented before performing the strain analysis, while R_1 and R_2 are different, the principal directions are the same relative to coordinate frames attached to the respective elements.

The coordinates of the vertices are used to directly calculate the material deformation gradient, F.[1,19] The decomposition of F into the components R_2, Λ, and R_1^T can be achieved using the technique of singular value decomposition [12,15,16].

An example of strain analysis is given to illustrate the concepts involved. Figure 3 and Table 2 show the results of a strain analysis on a triangle that has been deformed simply by extension along both the X and Y-axes. Strain analysis showed that the major (thick line) and minor (thin line) principal directions were along the X-axis and the Y-axis respectively. The major and minor principal stretch ratios are 1.25 and 1.0667 respectively. This corresponds to percentage stretches of +25 percent and +6.67 percent. The percentage area change associated with the deformation is an increase of 33.3 percent. The percentage stretch is defined as:

$$\% \text{ stretch} = (\text{principal stretch ratio} - 1) \times 100$$

and percentage area/volume change is defined as:

$$\% \text{ area/volume change} = (\text{product of principal stretch ratios} - 1) \times 100.$$

The strain analysis shows clearly that the deformation is simply described by dilations parallel to the two orthogonal sides of the triangle.

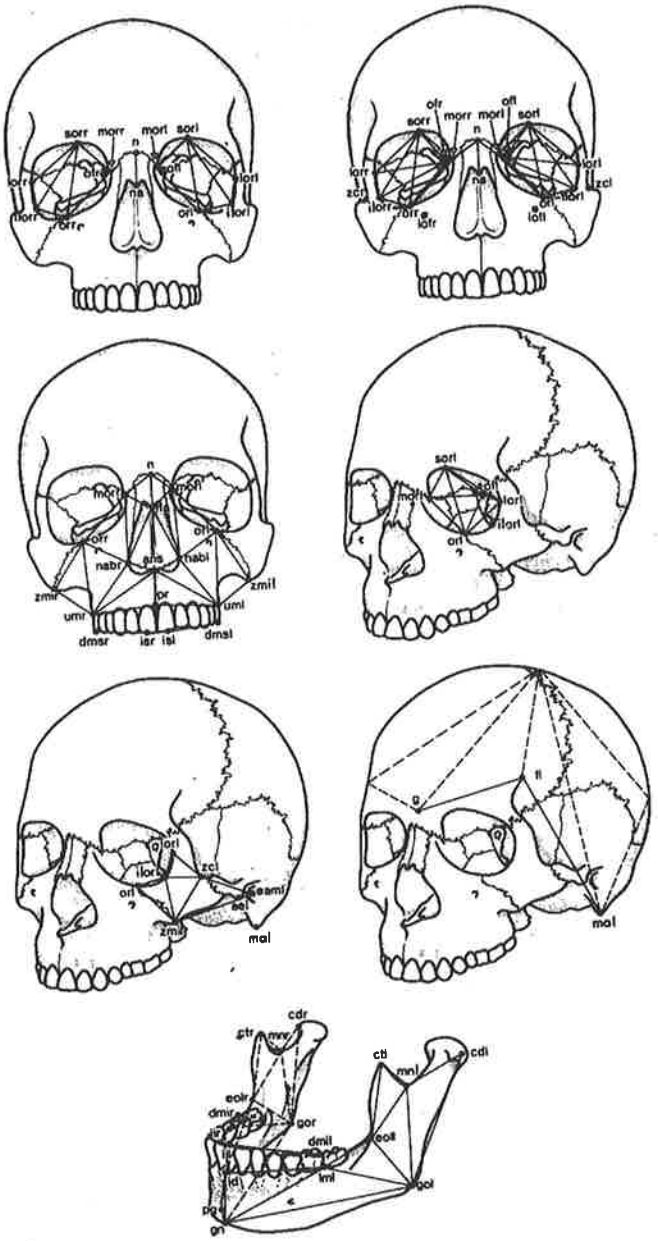

FIG.1. *Division of the craniofacial complex into a number of triangular and tetrahedral elements for strain analysis.*

TABLE 1

List of Osseous Landmarks and Their Associated Abbreviation

Landmark Name	Landmark Abbreviation	Landmark Name	Landmark Abbreviation
95		med ant clinoid L	macl
96		med ant clinoid R	macr
97		med f ovale L	mfol
98		med f ovale R	mfor
99		med f spinosum L	mfsl
100		med f spinosum R	mfsr
101		medial orbitale L	morl
102		medial orbitale R	morr
ant clinoid L	acl	nasal breadth L	nabl
ant clinoid R	acr	nasal breadth R	nabr
ant nasal spine	ans	nasale	na
articular emin L	ael	nasion	n
articular emin R	aer	naso-lacrimal inf L	nlil
articulare L	arl	naso-lacrimal inf R	nlir
articulare R	arr	odontoid	odp
asterion L	asl	opisthion	o
asterion R	asr	opisthocranion	op
auriculare L	aul	optic foramen L	ofl
auriculare R	aur	optic foramen R	ofr
basion	ba	obitale L	orl
bregma	br	orbitale R	orr
condylion laterale L	cdl	palatine tubercle L	pltl
condylion laterale R	cdr	palatine tubercle R	pltr
coronoid tip L	ctl	petrous anterius L	pal
coronoid tip R	ctr	petrous anterius R	par
disto-molare inf L	dmil	petrous posterius L	ppl
disto-molare inf R	dmir	petrous posterius R	ppr
disto-molare sup L	dmsl	pogonion	pg
disto-molare sup R	dmsr	porion L	pol
euryion L	eul	porion R	por
euryion R	eur	post nasal spine	pns
ext audit meat L	eaml	posterior clinoid L	pcl
ext audit meat R	eamr	posterior clinoid R	pcr
ext oblique line L	eoll	pre-articulare L	parl
ext obique line R	eolr	pre-articulare R	parr
f mag lateralis L	fmll	prosthion	pr
f mag lateralis R	fmlr	pterygo-lateralis L	ptll
foramen caecum	fc	pterygo-lateralis R	ptlr
glabella	g	pterygo-orbitale L	ptol
gnathion	gn	pterygo-orbitale R	ptor
gonion L	gol	pterygo-superius L	ptsl
gonion R	gor	pterygo-superius R	ptsr
hamular notch L	hnl	sella	s
hamular notch R	hnr	sphenoidale ant L	spal
hormion	h	sphenoidale ant R	spar
incision infer L	iil	sphenoidale lat L	spll
incision infer R	iir	sphenoidale lat R	splr
incision sup L	isl	subspinale	ss
incision sup R	isr	superior orbitale L	sorl
infero-frontale L	ifl	superior orbitale R	sorr
infero-frontale R	ifr	supero-lat orbitale L	slorl
infero-lat orbitale L	ilorl	supero-lat orbitale R	slorr
infero-lat orbitale R	ilorr	supramentale	sm
infradentale	id	upper molar L	uml
infraorbital for L	iofl	upper molar R	umr
infraorbital for R	iofr	vertex	v
lambda	l	zygion L	zgl
latero-frontale L	lfl	zygion R	zgr
latero-frontale R	lfr	zygo corner L	zcl
lateral orbitale L	lorl	zygo corner R	zcr
lateral orbitale R	lorr	zygo-frontale L	zfl
lower molar L	lml	zygo-frontale R	zfr
lower molar R	lmr	zygomaxillare inf L	zmil
mandibular notch L	mnl	zygomaxillare inf R	zmir
mandibular notch R	mnr		
mastoidale L	mal		
mastoidale R	mar		

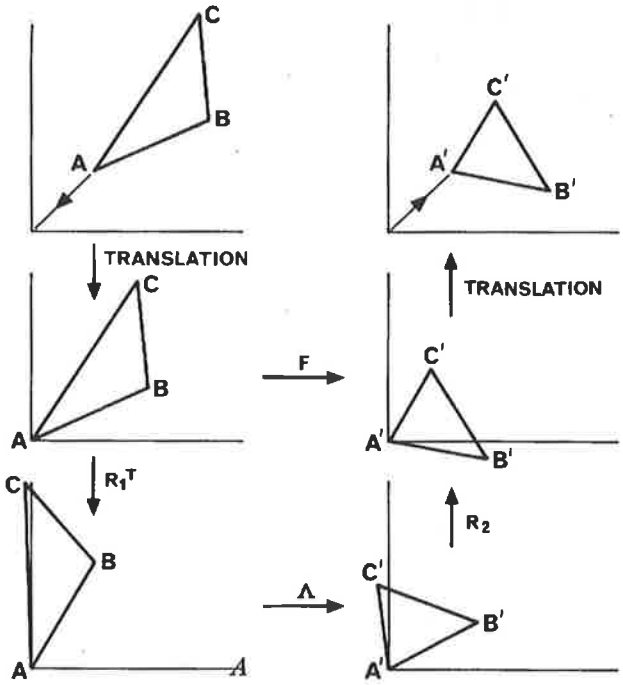

FIG. 2. *Pictorial representation of the decomposition of the material deformation gradient, F (= $R_2 \Lambda R_1^T$), into a rotation, R_1^T, dilations and / or contractions, Λ, along the coordinate axes and a rotation, R_2*

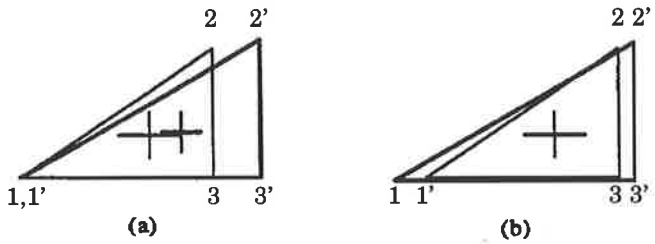

FIG. 3. *Shape comparison of two triangles using strain analysis. The thick triangle was generated by extension of the thin triangle in the X and Y directions. The principal directions are plotted at the centroids of the triangles and indicate the direction in which contraction or dilation would change the shape of one triangle to match the shape of the other triangle, but not necessarily match its orientation. The major and minor principal directions are shown in thick and thin respectively, for the first (thin) triangle and vice versa for the second triangle (thick). In* **a.** *the triangles are oriented with vertices 1 and 1', coincident and the line segments 13 and 1'3' coincident in direction to illustrate the generation of the thick triangle from the thin triangle. In* **b.** *alignment is on the centroids of the triangles and on the principal directions.*

Experimental Reference Standards

Experimental reference standards were derived from four adult female skulls of Australian Aboriginal origin, each with intact cranium and mandible. Coordinates, representing 80 osseous landmarks, were determined by integrating data derived from biplanar radiographs and 3-D computed tomography reconstructions.[1,2] Although the sample size for creation of the experimental reference standards was inadequate for statistical significance, it was considered sufficient for the initial evaluation of various methods for the generation of standards and methods of 3-D size and shape analysis. The experimental reference standards are used for these purposes in exactly the same way as population standards drawn from large samples.

TABLE 2

Comparison of a Triangle (Thick Line) Deformed Simply by Stretching Along the X and Y Axes, With the Initial Triangle (Thin Line) Using Strain Analysis, Illustrated in Figure 3

Thin Triangle			Thick Triangle		
Vertex No.	Coordinate		Vertex No.	Coordinate	
	x	y		x	y
1	0.000	0.000	1	0.000	0.000
2	40.000	30.000	2	50.000	32.000
3	40.000	0.000	3	50.000	0.000

Strain Analysis		
	Minor	Major
Principal strain	0.0689	0.2813
Principal stretch ratios	1.0667	1.2500
Percentage stretches	6.67	25.00

	Homologue 1		Homologue 2	
	X	Y	X	Y
Minor principal stretch Dns	0.000	1.000	0.000	1.000
Major principal stretch Dns	-1.000	0.000	-1.000	0.000
Area	600.00mm^2		800.00mm^2	

Percentage area change = 33.33%

The following four sets of standards were created from the landmark coordinate data:[1]

(1) distance and angle standards;

(2) 3-D coordinate standards for individual bones;

(3) 3-D coordinate standards for the whole skull; and

(4) strain standards.

Distance and angle standards were created in the usual way by calculating for each variable the mean and variance using the skull data base. Both individual bone and entire skull landmark coordinate standards were generated, using an alignment procedure based on the repeated fitting of all bones or skulls with each other until the coordinates for the average bone or skull converged. By alignment of each bone or skull of the data base with the average bone or skull form, the mean and standard deviation of the coordinates for each landmark were calculated. For each skull, a strain analysis was performed with each of the bone standards. The strain standards were produced by calculating the mean and standard deviation of the resulting percentage stretches and percentage area changes.

Quantification of the Deviation of an Individual From a Population Mean in Terms of the Population Standard Deviation

Population statistics can be used to test whether an individual is likely to belong to that population. If the population mean and standard deviation for a particular variable are known, the deviation of that variable from the mean can be expressed in terms of the standard deviation. This facilitates comparison of analytic techniques.

For distance and angle analysis, the Z-score[28] is the appropriate test statistic to determine the significance of the deviation of the variable from the mean. In the case of a single 3-D coordinate measurement (x,y,z), a a d/σ-score and a $\chi^2(3)$ distribution are used[21] to determine the significance of the distance of a coordinate position from a mean coordinate position. With respect to strain analysis, the probability distributions of the percentage stretches and percentage area/volume changes are non-Gaussian; therefore, it was useful to apply a criterion of significant deviation when the percentage stretch and/or percentage area/volume change exceeded an arbitrary level of 20 percent. Levels of significance could be calculated, if required, from the determined probability density functions.

Results

Comparison of Analysis Techniques With Qualitative Description

Treacher Collins syndrome (TCS) is used to illustrate the techniques of 3-D analysis of size and shape differences. In this paper, the results for the mandible and the zygoma are presented, as these bones display some of the typical features of TCS. The reader is referred to Abbott[1] for a complete description of the analytic findings of the patient's entire craniofacial complex.

To illustrate the efficiency of the analytic procedures, the key skeletal features of Treacher Collins syndrome for the mandible and the zygoma as described by Gorlin et al[13] are examined. Each feature is listed below, together with a summary of the corresponding quantitative results (Tables 3 to 8 and Figs. 4 to 9) found for a patient with TCS using (1) comparison of patient landmark coordinates with those of the specific bone standards, (2) comparison of patient landmark coordinates with those of the skull standard, (3) comparison of patient distances and angles with the distance and angle standards, and (4) strain analysis between elements defined in the patient and the corresponding elements in the bone standards.

Mandible

Key Feature: Hypoplasia

Alignment With Bone Standard (Table 3 and Fig. 4)
The scale factor, 8.4 percent, indicates that the patient's mandible is smaller than the standard, but not outside the normal population variance. The superimposed wire frame diagrams show, and the residuals quantify, the following features:

- smaller ramus height bilaterally;
- smaller mandibular body length bilaterally; and
- less developed condylar process.

Alignment With Skull Standard (Table 4 and Fig. 5)
This alignment accentuates genial angle and chin differences.

Distance and Angle Comparison (Table 5 and Fig. 4)
Most of the distance Z-scores are negative, indicating the patient's smaller mandibular size. Fifteen of the distances are significantly smaller at the 95 percent confidence level than those of the standard:

- total mandibular length an (left and right—note both gnathion and pogonion were used to define the chin giving another set of measurements)
- posterior ramus height (left and right)
- gonion right to coronoid tip right
- condylion laterale left to mandibular notch left
- lower border of the mandible (left and right-note both gnathion and pogonion were used to define the chin giving another set of measurements)
- dental arch length (left)
- dental arch breadth

TABLE 3

Nonscaled and Scaled Repeated Median Comparisons of the Patient's Mandible With the Repeated Median Experimental Reference Mandible Standard Using the d / σ-Score.

Landmark Name	Nonscaled Residual	d/σ Score	Scaled† Residual	d/σ Score	SD	LE
condylion laterale (R)	12.397	3.094*	11.425	2.852*	4.01	1.72
condylion laterale (L)	11.238	3.046*	8.369	2.269*	3.69	2.39
gonion (R)	12.873	3.629*	14.542	4.100*	3.55	1.16
gonion (L)	10.763	2.611*	11.139	2.702*	4.12	1.78
gnathion	8.991	2.811*	6.578	2.057*	3.20	0.76
pogonion	10.770	2.746*	8.325	2.123*	3.92	1.50
infradentale	7.509	3.689*	3.044	1.495	2.04	.51
lower molar (R)	6.892	2.934*	5.883	2.504*	2.35	.80
lower molar (L)	8.419	5.315*	6.486	4.095*	1.58	.87
coronoid tip (R)	5.157	1.116	9.940	2.152*	4.62	.89
coronoid tip (L)	6.420	1.747*	10.631	2.893*	3.67	1.72
mandibular notch (R)	-	-	-	-	3.74	0.41
mandibular notch (L)	1.848	0.578	5.658	1.770*	3.20	1.20
ext oblique line (R)	-	-	-	-	2.38	1.12
ext oblique line (L)	4.795	1.473	6.662	2.047*	3.26	3.15

*†Patient is 8.4% smaller than the standard with scale factor Z-score = -1.713. Scale factor standard deviation for this standard = 0.0493. *Significant at the 5% level; - = landmark not measured for patient; SD = standard deviation; and LE = landmark location error.*

Strain Analysis (Table 6 and Fig. 6)
The external surface of the patient's mandible is 8.8 cm^2 smaller than the standard based on the measured triangles in common between the patient and the standard. Individual triangles quantify the extent of hypoplasia in different parts of the mandible (seven triangles showed area decreases, two showed marginal area increases).

Key Feature: Obtuse Gonial Angle

Alignment With Bone Standard (Table 3 and Fig. 4)
Landmarks defining the left and right angle, condylion laterale, gonion, and gnathion differ in position to increase both the left and right angle of the mandible significantly.

Alignment With Skull Standard (Table 4 and Fig. 5)
As above, but the angular difference appears more evident due to orientation.

Distance and Angle Comparison (Table 5 and Fig. 4)
Quantified directly—significantly more obtuse (10 to 14° larger).

TABLE 4

Nonscaled and Scaled Repeated Median Comparisons of the Patient's Skull With the Repeated Median Experimental Reference Skull Standard Using the d/σ-Score.

Landmark Name	Nonscaled Residual	d/σ Score	Scaled† Residual	d/σ Score	SD	LE
sella	3.491	1.041	1.417	0.423	3.35	2.24
nasion	0.918	0.483	4.809	2.531*	1.90	1.01
glabella	20.543	4.599*	24.627	5.514*	4.47	2.11
vertex	25.639	4.203*	35.337	5.793*	6.10	2.76
opisthocranion	11.006	1.656*	22.422	3.373*	6.65	0.85
opisthion	4.905	1.646*	2.410	0.809	2.98	0.45
mastoidale (L)	11.483	2.056*	10.653	1.908*	5.58	1.61
mastoidale (R)	7.177	1.962*	7.936	2.169*	3.66	1.44
basion	7.585	1.210	5.970	0.952	6.27	2.66
ext auditory meatus (R)	3.462	0.759	5.121	1.122	4.56	1.72
ext auditory meatus (L)	9.250	1.966*	10.153	2.158*	4.70	2.37
condylion laterale (R)	7.391	1.953*	6.180	1.633*	3.78	1.72
condylion laterale (L)	10.036	1.946*	9.174	1.779*	5.16	2.39
gonion (R)	17.481	3.963*	14.200	3.219*	4.41	1.16
gonion (L)	19.011	4.300*	16.101	3.642*	4.42	1.78
gnathion	21.010	5.757*	18.065	4.950*	3.65	0.76
pogonion	20.817	4.314*	18.318	3.796*	4.83	1.50
infradentale	15.572	4.136*	11.734	3.117*	3.76	.51
prosthion	10.038	2.414*	6.570	1.580	4.16	1.87
ant nasal spine	3.035	0.619	1.940	0.396	4.91	1.09
post nasal spine	5.882	1.250	5.441	1.156	4.70	2.14
upper molar (R)	20.616	5.202*	17.415	4.394*	3.96	1.00
upper molar (L)	15.602	3.706*	12.607	2.994*	4.21	0.72
lower molar (R)	17.886	6.182*	14.674	5.072*	2.89	0.80
lower molar (L)	15.308	7.339*	12.187	5.843*	2.09	0.87
zygomaxillare inf (R)	-	-	-	-	5.21	0.89
zygomaxillare inf (L)	-	-	-	-	5.08	1.30
coronoid tip (R)	9.908	2.272*	11.621	2.665*	4.36	0.89
coronoid tip (L)	14.510	3.031*	16.376	3.421*	4.79	1.72
palatine tubercle (R)	-	-	-	-	3.63	2.38
palatine tubercle (L)	-	-	-	-	5.30	2.58
optic foremen (R)	7.615	3.645*	7.785	3.727*	2.09	0.77
optic foremen (L)	8.246	1.797*	7.641	1.665*	4.59	1.02
nasale	2.994	0.754	6.950	1.749*	3.97	0.91
bregma	9.624	15.624*	19.304	31.337*	0.00	0.62
medial orbitale (R)	3.863	1.787*	5.204	2.407*	2.16	1.40
medial orbitale (L)	-	-	-	-	1.74	1.39
superior orbitale (R)	8.462	2.436*	4.852	1.397	3.47	1.83
superior orbitale (L)	8.531	2.583*	6.521	1.974*	3.14	3.30
lateral orbitale (R)	12.073	3.325*	10.568	2.910*	3.63	0.81
lateral orbitale (L)	11.377	2.641*	9.556	2.219*	4.31	4.24
infero-lateral orbitale (R)	13.642	3.290*	11.648	2.809*	4.15	1.44
infero-lateral orbitale (L)	9.421	3.061*	7.899	2.567*	3.08	1.65
orbitale (R)	9.953	3.350*	7.660	2.578*	2.97	2.20
orbitale (L)	7.175	2.413*	4.654	1.666*	2.87	2.97
infraorbital for (R)	-	-	-	-	3.50	2.96
infraorbital for (L)	-	-	-	-	4.47	2.50

TABLE 4 cont'd

Nonscaled and Scaled Repeated Median Comparisons of the Patient's Skull With the Repeated Median Experimental Reference Skull Standard Using the d/σ-Score.

Landmark Name	Nonscaled Residual	d/σ Score	Scaled† Residual	d/σ Score	SD	LE
artic eminence (R)	-	-	-	-	4.58	1.74
artic eminence (L)	-	-	-	-	5.95	3.17
zygomatic corner (R)	14.899	4.768*	11.982	3.834*	3.12	0.77
zygomatic corner (L)	12.108	4.633*	10.038	3.841*	2.61	1.18
infero-frontale (R)	25.652	6.100*	23.837	5.668*	4.21	2.55
infero-frontale (L)	16.849	3.495*	16.223	3.365*	4.82	2.61
nasal breadth (R)	9.069	2.331*	6.042	1.553	3.89	1.43
nasal breadth (L)	3.730	1.121	2.491	0.749	3.33	2.61
mandibular notch (R)	-	-	-	-	3.74	0.41
mandibular notch (L)	14.113	2.877*	14.470	2.950*	4.91	1.20
ext oblique line (R)	-	-	-	-	2.87	1.12
ext oblique line (L)	15.380	4.666*	13.442	4.078*	3.30	3.15
for mag lateralis (R)	5.874	0.626	3.536	0.377	9.38	1.86
for mag lateralis (L)	7.991	0.882	5.105	0.564	9.06	1.22
incision superius (R)	-	-	-	-	0.00	1.75
incision superius (L)	11.137	6.563*	9.608	5.662*	0.00	1.70
anterior clinoid (L)	2.822	0.799	1.522	0.431	3.53	1.84
anterior clinoid (R)	1.873	1.005	4.141	2.222*	1.86	0.46
sphenoidale ant (L)	13.322	2.805*	17.246	3.631*	4.75	2.33
sphenoidale ant (R)	7.138	2.169*	11.130	3.383*	3.29	2.38
95	16.775	2.968*	16.311	2.886*	5.65	3.54
96	8.214	2.098*	10.442	2.667*	1.49	3.91
97	10.431	2.334*	7.903	1.768*	4.47	1.14
98	3.120	1.855*	3.917	2.329*	1.68	1.48
99	6.315	2.159*	4.252	1.454	2.92	0.53
100	2.222	2.709*	3.898	4.754*	0.19	0.82
101	12.630	2.412*	14.115	2.695*	5.24	3.01
102	7.642	2.331*	10.433	3.182*	1.58	3.28
med anterior clinoid (L)	2.692	0.988	3.086	1.133	2.23	2.72
med anterior clinoid (R)	3.410	1.012	4.025	1.194	2.32	3.37
posterior clinoid (L)	7.644	1.480	6.536	1.265	2.99	5.16
posterior clinoid (R)	4.494	1.284	3.829	1.094	2.93	3.50

†Patient is 8.6% smaller than the standard with scale factor Z-score = -1.888. Scale factor standard deviation for this standard = 0.0457.
**Significant at the 5% level; - = landmark not measured for patient; SD = standard deviation; and LE = landmark location error.*

Strain Analysis (Table 6 and Fig. 6)

The angle of the mandible is encompassed by the two triangles sharing the side gonion left to external oblique point left. The overall area change of the triangle goleoll-lml is small (+5.8 percent), compared with the large reduction along the minor principal stretch direction (20.3 percent), and the large expansion along the major principal stretch direction (32.8 percent). Inspection of Figure 6 for this triangle reveals that the direction of deformation of the major principal stretch direction was essentially a continuation, although more obtuse, of the major principal stretch direction of the middle ramus triangle. These results imply that while the area of the bone remains unaltered, the patient, relative to the standard, demonstrates a large deformation in the region of the angle of the left mandible. The direction of this deformation indicates that the patient has an increased ramus to body angle relative to the standard.

TABLE 5

Distance and Angle Comparison of the Patient's Mandible With the Experimental Reference Mandible Standard Using Z-Scores

Name	Value	Z-score	Mean	SD
cdr-gor	46.23	-4.84*	58.86	2.61
gor-gn	67.89	-1.73	82.03	8.15
gn-pg	7.82	- 1.81	10.87	1.69
pg-id	22.29	1.51	19.89	1.59
gn-gol	70.24	-2.04*	83.37	6.45
gol-cdl	43.48	-3.13*	56.49	4.16
cdl-mnl	13.98	-4.40	25.74	2.67
mnl-ctl	15.51	-0.07	15.65	2.09
ctl-eoll	27.11	-0.21	28.05	4.42
eoll-mil	28.14	-0.12	28.52	3.27
mll-id	32.56	-3.32*	40.36	2.35
id-mlr	39.04	-1.11	40.45	1.28
mir-eolr	-	-	28.03	4.21
eolr-ctr	-	-	30.33	4.62
ctr-mnr	-	-	13.70	1.66
mnr-cdr	-	-	27.03	2.41
mnr-gor	-	-	44.94	4.59
ctr-gor	46.33	- 2.04	-55.30	4.39
cdr-ctr	26.86	-1.87	35.52	4.62
eolr-id	-	-	66.95	3.66
cdr-gn	102.35	-2.35*	118.37	6.82
cdr-pg	104.10	-2.52*	118.62	5.77
mnl-gol	37.38	-1.08	42.34	4.60
ctl-gol	48.07	-1.64	54.37	3.84
cdl-ctl	24.66	-2.54*	34.85	4.01
eoll-id	58.98	-2.06*	65.95	3.38
cdl-gn	100.03	-2.85*	116.13	5.65
cdl-pg	101.50	-2.43*	118.45	6.96
gor-pg	71.87	-2.33*	86.48	6.26
gol-pg	73.87	- 2.09*	90.05	7.73
gor-gol	87.43	0.95	82.16	5.52
cdr-cdl	101.22	-0.21	101.94	3.35
mnr-mnl	-	-	84.65	3.26
ctr-ctl	93.33	2.08*	83.61	4.68
eolr-eoll	-	-	77.99	3.35
mlr-mll	46.95	-2.69*	55.44	3.16
cdr-gor-gn	126.44	2.58*	113.55	5.00
cdl-gol-gn	121.40	3.07*	110.98	3.39
gor-gn-gol	78.51	3.99*	59.79	4.69
gor-cdr-mnr	-	-	46.79	4.78
gol-cdl-mnl	55.50	2.96*	44.57	3.69
cdr-mnr-ctr	-	-	117.27	7.84
cdl-mnl-ctl	113.39	0.24	112.19	5.00
mnr-ctr-eolr	-	-	65.01	3.20
mnl-ctl-eoll	64.21	-0.43	66.79	6.05
ctr-eolr-mlr	-	-	108.28	6.61
ctl-eoll-mll	139.02	4.76*	112.66	5.54
eolr-id-eoll	-	-	71.99	3.80
mir-id-mll	81.42	-4.48*	86.88	1.22
cdr-gor-pg	122.11	3.04*	108.08	4.62
cdl-gol-pg	117.39	3.92*	105.72	2.98
gor-pg-gol	73.71	4.64*	55.58	3.91
ML(l)/NSL	57.82	6.89*	37.36	2.97
ML(r)/NSL	55.63	8.05*	38.56	2.12
NL/ML(l)	52.13	3.69*	34.86	4.68
NL/ML(r)	50.03	5.83*	34.52	2.66
CL/ML(l)	82.00	-0.18	83.64	9.19
CL/ML(r)	83.86	-1.15	89.48	4.90

**Significant at the 5% level. - Not determined due to nonmeasurement of one or more landmarks. Mean Z-score = 0.01; SD Z-score = 3.16; and RMS Z-score = 3.12.*

Key Feature: Deficient Ramus

Alignment With Bone Standard (Table 3 and Fig. 4)
Landmarks defining the rami, condylion laterale, coronoid tip, external oblique line, and "onion differ in position significantly, and the figures show the smaller size of the rami.

Alignment With Skull Standard (Table 4 and Fig. 5)
As above.

TABLE 6

Stretch Ratio and Area Change Comparison Between the Patient's Mandible and Zygoma and Their Respective Experimental Reference Bone Standards Using Strain Analysis

Area of Representation	Triangle Vertices			%Stretch Minor	%Stretch Major	%Area Change
Mandible						
post. ramus (R)	cdr	gor	mnr	-	-	-
middle ramus (R)	gor	mnr	eolr	-	-	-
ant. ramus (R)	mnr	eolr	ctr	-	-	-
jn.ramus-body (R)	gor	eolr	mlr	-	-	-
lower body (R)	gor	mlr	gn	-25.49	10.23	-17.86
upper body (R)	mlr	gn	id	-4.07	6.93	2.58
chin	gn	id	pg	-29.94	26.04	-11.71
post. ramus (L)	cdl	gol	mnl	-45.02	-7.30	-49.04
middle ramus (L)	gol	mnl	eoll	-15.75	-3.62	-18.80
ant. ramus (L)	mnl	eoll	ctl	-4.29	1.28	-3.06
jn. ramus-body (L)	gol	eoll	mll	-20.31	32.81	5.84
lower body (L)	gol	mll	gn	-20.64	-12.07	-30.23
upper body (L)	mll	gn	id	-18.26	3.07	-15.74
Zygoma						
medial body (R)	zmir	orr	ilorr	-	-	-
lateral body (R)	ilorr	zmir	zcr	-	-	-
frontal process (R)	ilorr	lorr	zcr	-68.95	4.75	-67.48
zygomatic arch (R)	zmir	zcr	eamr	-	-	-
medial body (L)	zmil	orl	ilorl	-	-	-
lateral body (L)	ilorl	zmil	zcl	-	-	-
frontal process (L)	ilorl	lorl	zcl	-39.56	-6.22	-43.31
zygomatic arch (L)	zmil	zcl	eaml	-	-	-

- Not determined due to nonmeasurement of one or more landmarks.

Distance and Angle Comparison (Table 5 and Fig. 4)
Both right and left posterior ramus heights are smaller (12.6 mm and 13.0 mm respectively).

Strain Analysis (Table 6 and Fig. 6)
Left anterior (Δ mnl, eoll, ctl), middle (Δ gol, mnl, eoll) and posterior (Δcdl, gol, mm) ramus triangles show progressive underdevelopment from anterior to posterior (that is, 3.1 to 18.8 to 49.0 percent area decreases).

TABLE 7

Nonscaled and Scaled Repeated Median Comparison of the Patient's Zygoma With the Repeated Median Experimental Reference Zygoma Standard Using the d / σ–Score

Landmark Name	Nonscaled Residual	d/σ Score	Scaled† Residual	d/σ Score	SD	LE
mastoidale (L)	15.768	2.714*	12.367	2.218*	5.81	1.61
mastoidale (R)	12.632	3.903*	11.415	3.527*	3.24	1.44
ext audit meat (R)	9.066	3.236*	9.117	3.254*	2.80	1.72
ext audit meat (L)	13.761	4.024*	12.982	3.796*	3.42	2.37
zygomaxillare inf (R)	-	-	-	-	4.93	0.89
zygomaxillare inf (L)	-	-	-	-	5.03	1.30
lateral orbitale (R)	6.079	2.210*	6.041	2.197*	2.75	0.81
lateral orbitale (L)	7.491	1644*	5.638	1.237	4.56	4.24
infero-lateral orbitale (R)	8.238	2.555*	6.687	2.074*	3.22	1.44
infero-lateral orbitale (L)	5.869	2.051*	4.297	1.502	2.86	1.65
orbitale (R)	6.021	2.740*	4.966	2.260*	2.11	2.20
orbitale (L)	4.080	1.372	2.355	0.792	2.66	2.97
infraorbital for (R)	-	-	-	-	2.67	2.96
infraorbital for (L)	-	-	-	-	4.70	2.50
artic eminence (R)	-	-	-	-	3.66	1.74
artic eminence (L)	-	-	-	-	5.33	3.17
zygom corner (R)	12.004	7.013*	7.605	4.443*	1.71	0.77
zygom corner (L)	12.191	6.296*	8.946	4.620*	1.94	1.18

†Patient is 11.2% smaller than the standard with scale factor Z-score = -4.468. Scale factor standard deviation for this standard = 0.0251.*
**Significant at the 5% level; - = landmark not measured for patient; SD = standard deviation; and LE = landmark location error.*

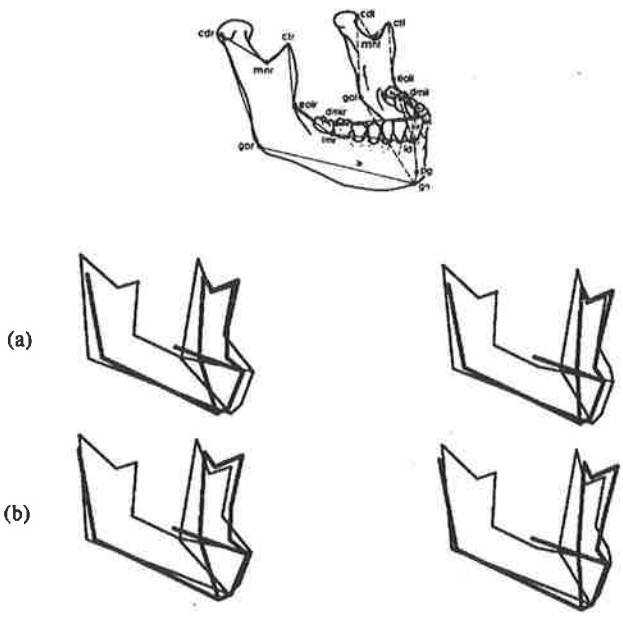

FIG. 4. *Stereo comparison of TCS patient (thick) with experimental mandible standard (thin) using* **a.** *nonscaled and* **b.** *scaled alignment. The left and right images of each stereo pair correspond to left and right eye views respectively. With practice stereo viewing can be achieved without special glasses and may be facilitated by placing a piece of paper vertically between the left and right eye views.*

TABLE 8

Distance and Angle Comparison of the Patient's Zygoma With the Experimental Reference Zygoma Standard Using Z-Scores

Name	Value	Z-score	Mean	SD
lorr-zcr	10.05	-5.41*	16.38	1.17
zcr-eamr	54.96	-1.87	58.49	1.89
eamr-aer	-	-	24.12	2.45
aer-zmir	-	-	43.08	2.87
zmir-orr	-	-	28.78	2.72
orr-ilorr	15.39	-0.99	18.00	2.63
ilorr-lorr	10.15	-0.12	10.35	1.65
lorl-zcl	13.83	-1.07	18.52	4.40
zcl-eaml	50.13	-3.39*	59.11	2.65
eaml-ael	-	-	24.38	3.96
ael-zmil	-	-	45.04	3.43
zmil-orl	-	-	27.24	3.45
orl-ilorl	14.04	-0.40	15.41	3.40
ilorl-lorl	10.70	-0.42	12.60	4.54
zmir-ilorr	-	-	22.28	4.36
zmir-zcr	-	-	22.65	4.77
zmir-eamr	-	-	65.07	3.47
zcr-ilorr	5.48	-6.20*	17.57	1.95
zmil-ilorl	-	-	23.16	5.27
zmil-zci	-	-	24.56	4.97
zmil-eaml	-	-	67.71	3.48
zcl-ilorl	11.66	-3.68*	19.32	2.08
zmir-zmil	-	-	91.68	1.57
aer-ael	-	-	107.43	5.18
eamr-eaml	101.40	2.19*	94.98	2.93
zcr-zcl	91.06	-10.40*	111.24	1.94
lorr-lorl	90.82	-1.19	95.96	4.31
ilorr-ilorl	82.20	-1.73	89.40	4.17
orr-orl	55.92	-0.90	59.27	3.70
lorr-ilorr-eamr	72.60	-0.13	73.78	9.32
lorl-ilorl-eaml	61.55	-0.86	77.69	18.71
lorr-zcr-eamr	96.73	-4.96*	125.79	5.86
zcr-eamr-zmir	-	-	20.05	3.07
eamr-zmir-orr	-	-	112.46	11.40
zmir-orr-ilorr	-	-	50.41	9.01
orr-ilorr-lorr	119.08	-0.26	121.17	7.95
ilorr-lorr-zcr	31.51	-7.02*	78.50	6.69
Iorl-zcl-eaml	108.27	-2.25*	127.59	9.47
zcl-eaml-zmil	-	-	20.75	3.40
eaml-zmil-orl	-	-	109.70	9.17
zmil-orl-ilorl	-	-	57.56	9.80
orl-ilorl-lorl	110.48	-0.91	122.82	13.49
ilorl-lorl-zcl	54.98	-1.38	74.05	13.78

**Significant at the 5% level. - Not determined due to nonmeasurement of one or more landmarks. Mean Z-score = -2.32; SD Z-score = 2.83; and RMS Z-score = 3.61.*

Key Feature: Flat or Aplastic Coronoid and Condyle

Alignment With Bone Standard (Table 3 and Fig. 4)
The relevant landmarks differ in position significantly and the figures show the direction of the differences to be consistent with Gorlin's description.[13]

Alignment With Skull Standard (Table 4 and Fig. 5)
As above.

Distance and Angle Comparison (Table 5 and Fig. 4)
A smaller, flatter condylar region is indicated by:

- shorter distance between condylion laterale left to mandibular notch left (11.8 mm);
- shorter distance between condylion laterale left to coronoid tip left (10.2 mm); and
- increased angle gonion left to condylion laterale left to mandibular notch left (10.9°).

Strain Analysis (Table 6 and Fig. 6)
The left posterior (Δ cdl, gol, mnl) ramus triangle shows a 49.0 percent area reduction, predominantly due to a 45 percent reduction parallel to a line joining the condylar head left to the mandibular notch left, resulting in a flatter condylar process.

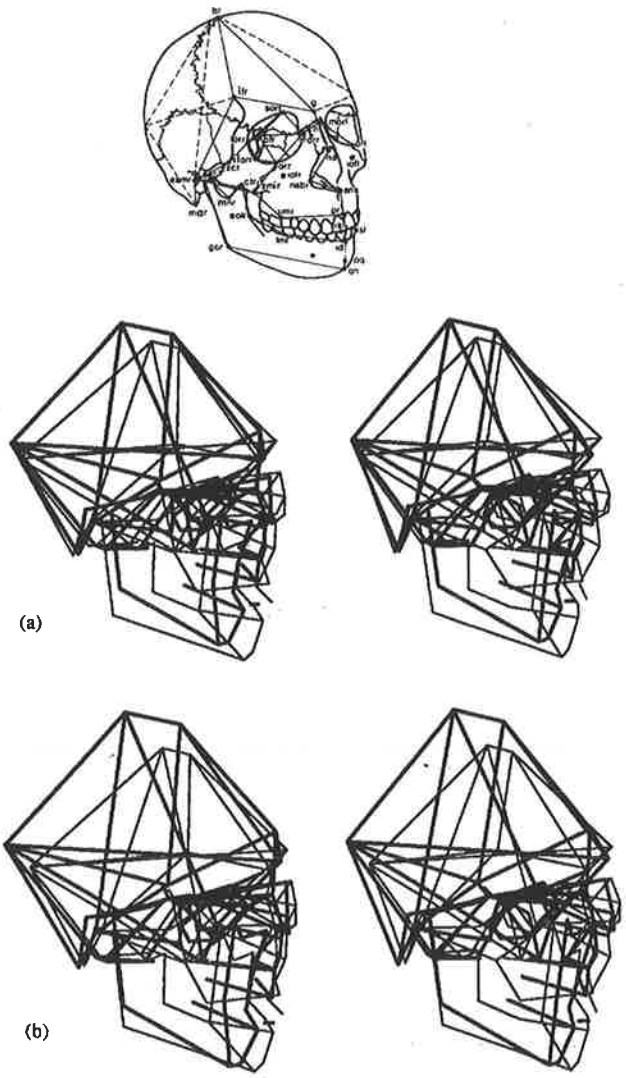

FIG. 5. *Stereo comparison of TCS patient (thick) with experimental head standard (thin) using* **a.** *nonscaled and* **b.** *scaled alignment.*

Key Feature: Receding Chin

Alignment With Bone Standard (Table 3 and Fig. 4)
The scaled figures show that profile of the patient's chin has a similar shape to the standard. However, the nonscaled figures show a receding chin due to the smaller mandible size and the increased ramus to body angle.

Alignment With Skull Standard (Table 4 and Fig. 5)
The patient's chin is very superoposteriorly displaced relative to the skull standard. For example, the gnathion is displaced by 21 mm after alignment without scaling.

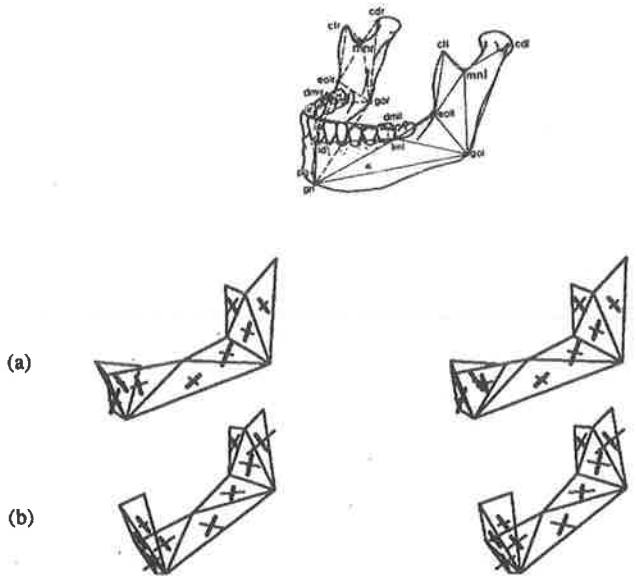

FIG. 6. *Shape comparison between the TCS mandible and the experimental mandible standard using strain analysis. The upper stereo pair* **a.** *show the principal stretches and directions (thin-minor, thick-major) required to deform the mandible standard to produce the shape of the TCS mandible. The lower stereo pair* **b.** *show the principal stretches and directions (thick-minor, thin-major) required to deform the TCS mandible to produce the shape of the mandible standard.*

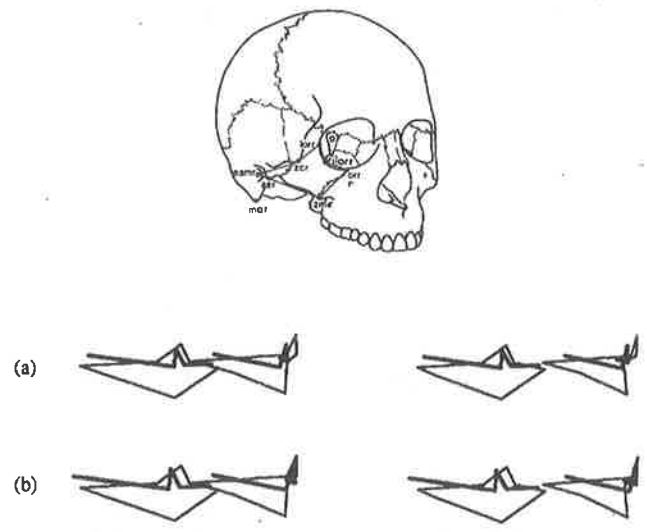

FIG. 7. *Stereo comparison of TCS patient (thick) with experimental zygoma standard (thin) using* **a.** *nonscaled and* **b.** *scaled alignment.*

Distance and Angle Comparison (Table 5 and Fig. 4)
The lower face heights do not differ significantly from those of the standard. However, the lower border of the mandible is significantly shorter-in length.

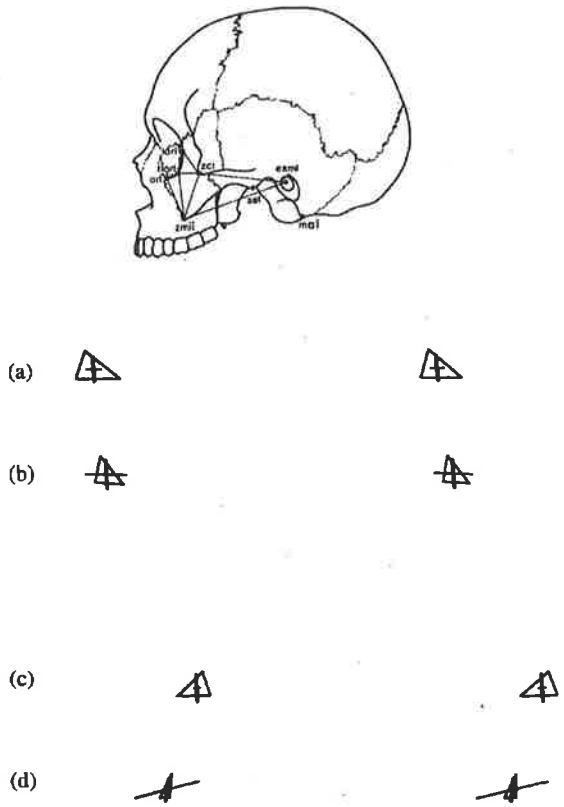

FIG. 8. *Shape comparison between the left* **a. b.** *and the right* **c. d.** *zygomas of the patient and the experimental zygoma standard using strain analysis. The upper stereo pairs a. and* **c.** *show the principal stretches and directions (thin-minor, thick-major) required to deform the zygoma standard to produce the shape of the TCS zygoma. The lower stereo pairs* **b.** *and* **d.** *show the principal stretches and directions (thick-minor, thin-major) required to deform the TCS zygoma to produce the shape of the zygoma standard. The triangles shown are: Δilorl, lorl, zcl and Δilorr, lorr, zcr. See text regarding absence of landmarks.*

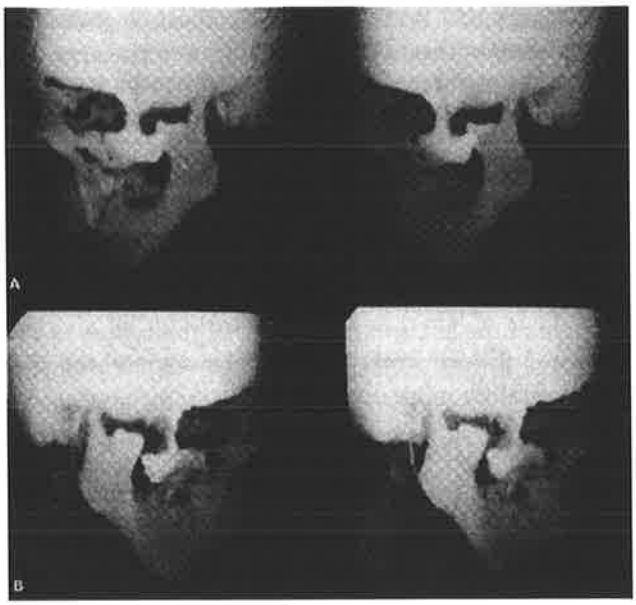

FIG. 9. *Near lateral* **a.** *left and* **b.** *right 3-D CT reconstructions showing in particular the severe hypoplastic nature of the patient's zygomas and absence of both zygomatic arches.*

Strain Analysis (Table 6 and Fig. 6)
The receding chin is associated with the smaller size of the triangles representing the body and ramus of the mandible.

Key Feature: Concave Lower Border of Mandible

This was not determined as no landmarks were located on the curve of bone between gonion and gnathion.

Other Quantified Results Not Described by Gorlin et al[13]

Alignment With Bone Standard (Table 3 and Fig. 4)
Residuals for landmarks defining the following regions are also significant when compared with the standard:

- dental arch (narrow in breadth);
- coronoid processes (tips more laterally displaced); and
- angle of the mandible (larger bigonial breadth).

The median residual is 8.4 mm (for both nonscaled and scaled alignment), indicative of considerable shape differences.

Alignment With Skull Standard (Table 4 and Fig. 5)
In addition to the above:

- the condylar heads are positioned more anterosuperiorly and medially;
- the patient's mandible relative to the skull standard is rotated to move the chin posteriorly and superiorly.

Distance and Angle Comparison (Table 5 and Fig. 4)
- The arch breadth and arch angle are 8.5 mm and 5.5° smaller respectively.
- The left dental arch length is smaller than the right, and significantly smaller than the standard by 7.8 mm.
- The coronoid tip width was significantly increased (9.7mm)
- The bigonial breadth was larger than the standard (5 mm), but this was not significant
- The lower border angle as measured from gonion right to gnathion to gonion left was significantly increased (18.7°).
- The angular relationship of the mandibular plane to the cranial base and the hard palate were also significantly more obtuse (16 to 21° larger). The angle of the lest anterior border of the ramus to the dental alveolar crest in the molar region was also significantly more obtuse.

Strain Analysis (Table 6 and Fig. 6)
- There was contraction along the left dental arch length (Δ lml, gnn, id) of 18.3 percent but no significant change in the right dental arch length.
- The area of the left body of the mandible was smaller by 25.3 percent, with a contraction along the right mandible body length of 25.5 percent.

Absence of Landmarks

Two landmarks on the patient's mandible were not identified: the patient's right coronoid tip had deviated laterally, obscuring the mandibular notch, and the patient's dysplastic right zygoma obscured the region of the external oblique line. Other views of the subject could have allowed identification of the two nonidentified landmarks.

Zygoma

Key Feature: Gross Hypoplasia of the Zygomas

Alignment With Bone Standard (Table 7 and Fig. 7)
The scale factor indicates that the patient's zygomas, as defined by the selected osseous landmarks, are significantly smaller by 11.2 percent. The superimposed wire frame diagrams show, and the residuals quantify, the following characteristics:

- marked narrowing of the frontal process of the zygomatic bone right and left (essentially the lateral orbital walls), as the zygomatic corners are located more anteriorly, while inferolateral orbitales more posteriorly, more so on the right than the left; and
- orbitale, right and left, are located more posteriorly.

Alignment With Skull Standard (Table 4 and Fig. 5)
As quantified by the residuals, the patient's Zygomas are much smaller, differently shaped and displaced in an inferolateral direction.

Distance and Angle Comparison (Table 8 and Fig. 7)
All of the distances used to define the Zygomas of the patient were smaller than those of the standard (Z scores all negative). The following measurements are indicative of the extent of the undevelopment of the patient's zygomas relative to the standard:

- Both the distances zygomatic corner right to lateral orbitale right and zygomatic corner right to inferolateral orbitale right reflect the reduced width of the right zygoma (smaller by 6.3 mm and 12.1 mm respectively) and therefore its underdevelopment. Consistent with these measurements is the significantly smaller angle at lateral orbitale (47° smaller).
- The width of the left zygoma was also significantly smaller than the standard (by 7.7 mm from inferolateral orbitale left to zygomatic corner left).
- The separation of the zygomatic corners was reduced by 20.2 mm relative to the standard.

Strain Analysis (Table 6 and Fig. 8)
Only the triangles representing the left (Δ ilorl, lorl, zcl) and right (Δ ilorr, lorr, zcr) frontal processes of the Zygomas could be determined for the patient due to the absence of some landmarks. Both of these triangles showed large area reductions of 67.5 percent, right, and 43.3 percent, left, leading to a total decrease of 1.2 cm^2 relative to the standard.

Key Feature: Non Fusion of the Zygomatic Arches (Fig. 9)

Inspection of the patient's radiographs revealed both zygomatic arches to be absent. Those landmarks associated with the zygomatic arch were accordingly absent.

Key Feature: Absent Zygomas (Fig. 9)

Zygomas were not totally absent for this patient.

Other Quantified Results

Alignment With Bone Standard (Table 7 and Fig. 7)
The median of the residuals for the zygoma was 8.7 mm (nonscaled) and 7.2 mm (scaled), indicative of the substantial shape and size differences between the patient and the standard.

Absence of Landmarks

Many of the landmarks of the zygoma for the patient could not be identified due to absence of the zygomatic arches. In this case, the absence of landmarks is a reflection of the particular pathologic condition and also provides information regarding the severity of the syndrome.

Discussion

The differences between an individual with Treacher Collins syndrome and a set of experimental reference standards have been described and quantified by three techniques:

- comparison of distances and angles;
- comparison of landmark coordinate positions after alignment; and
- strain analysis of homologous triangular elements.

As might be expected, each technique, being based on the same data, reveals the same structural differences and leads to the same interpretation and conclusion regarding the manifestation of the syndrome. However, the different approaches throw the data into a different perspective and while each reflects the same morphologic characteristics, the ease of interpretation varies depending on the feature.

That each technique leads to the same interpretation is easily seen using the example of the key qualitative feature "deficient ramus," which is characterized through distance comparison by reduced ramus height, through alignment and superimposition by landmark coordinate differences in a direction indicating the reduced height of the ramus, and through strain analysis by the direction and magnitude of principal stretches that indicate reduction in ramus height and width.

That the ease of interpretation varies depending on the feature can be seen from the discussion that follows. The traditional technique of distance and angle comparison is particularly useful, because it provides a readily interpretable measure of the departures from a population standard; for example, the angle of the mandible and total mandibular length are quantified directly by these measures. Comparison of landmark constellations after alignment quantifies size and shape differences through variations in coordinate positions. By plotting the landmark positions, along with lines between landmarks to represent bone edges, differences between the structures are also readily visible. For example, the key feature "receding chin" was most easily appreciated using this technique. Alignment using the entire skull tends to result in similar interpretations, as to alignment with specific bones, but it includes the effects of position and orientation of the individual bones relative to the rest of the patient's skull. Strain analysis quantifies the principal directions of size and shape change, and these succinctly describe the nature of the differences over relatively small bone regions. For example, strain analysis of the triangles comprising the "angle of the mandible" indicated that while the area differences were small (indicating approximately the same quantity of bone) the principal stretches showed dilations in directions to increase the angle of the mandible with concomitant contractions orthogonal to these directions.

A good representation of the bone surfaces was achieved through the use of a relatively large number of accurately located landmarks enabling appropriately sized triangular elements in three dimensions to be defined. The results from the strain analyses were, accordingly, readily interpretable in terms of the known characteristics of Treacher Collins syndrome.

The essential skeletal features of Treacher Collins syndrome as described by Gorlin et al[13] for the mandible and the zygoma were identified and quantified by the above analyses. Moreover, a measure of their significance was determined by comparison with the experimental reference standards.

With the development of practical and representative 3-D population standards, the techniques described have the potential to provide the surgeon with a quantitative description of the extent and nature of craniofacial anomalies.

Acknowledgements.

We are grateful for the cooperation and assistance of the Department of Radiology, Adelaide Children's Hospital campus, in particular Graham Truman, Marion Tregeagle, and Amanda Russell. We also thank Mr. Graham Pretty, Senior Curator in Archaeology and Anthropology, The South Australian Museum, for allowing access to the skeletal material used in this investigation.

Financial assistance was provided by the Australian CranioMaxillo-Facial Foundation; Dr. Abbott was supported by a postgraduate scholarship awarded by the National Health and Medical Research Council of Australia.

References

1. Abbott AH. The acquisition and analysis of craniofacial data in three dimensions. Ph.D. Research Thesis. Adelaide, Australia: The University of Adelaide, 1988.

2. Abbott AH, David DJ, Brown T. The acquisition and analysis of craniofacial data in three dimensions. The 2nd International Congress of the International Society of Cranio-Maxillo-Facial Surgery, in press.

3. Baumrind S, Moffitt FH, Curry S. Three-dimensional x-ray stereometry from paired coplanar images: a progress report. Am J Orthod 1983; 84:292–312.

4. Baumrind S, Moffitt FH, Curry S. The geometry of three-dimensional measurements from paired coplanar x-ray images. Am J Orthod 1983; 84:313–322.

5. Bookstein FL. Tensor biometrics for changes in cranial shape. Ann Hum Biol 1984; 11:413–437.

6. Bookstein FL. Describing a craniofacial anomaly: finite elements and the biometrics of landmark locations. Am J Phys Anthropol 1987; 74:495–509

7. Brown T, Abbott AH. Computer-assisted location of reference points in three dimensions for radiographic cephalometry. Am J Orthod Dentofacial Orthop 1989; 95:490–498.

8. Cheverud JM, Lewis JL, Bachrack W, Lew WD. The measurement of form and variation in form: an application of three-dimensional quantitative morphology by finite-element methods. Am J Phys Anthropol 1983; 62:151–165.

9. Cutting C, Bookstein FL, Grayson B, Fellingham L, McCarthy JG. Three-dimensional computer-assisted design of craniofacial surgery procedures: optimization and interaction with cephalometric and CT-based models. Plast Reconstr Surg 1986; 77:877–887.

10. Cutting C, Grayson B, Bookstein FL, Fellingham L, McCarthy JG. Computer-aided planning and evaluation of facial and orthognathic surgery. Clin Plast Surg 1986; 13:449–462.

11. Cutting C, Bookstein FL, Grayson B, Fellingham L, McCarthy JG. Three dimensional computed-aided design of craniofacial surgical procedures. In: Marchac D, ed. Craniofacial surgery. Berlin, Heidelberg: Springer-Verlag, 1987.

12. Golub GH, Reinsch C. Singular value decomposition and least squares solutions. Numer Math 1970; 14:403–420.

13. Gorlin RJ, Pinborg JJ, Cohen MM Jr. Syndromes of the head and neck. 2nd ed. New York: McGraw-Hill, 1976.

14. Grayson B, Cutting C, Bookstein FL, Kim H, McCarthy JG. The three-dimensional cephalogram: theory, technique, and clinical application. Am J Orthod Dentofacial Orthop 1988; 94:327–337

15. Klemma VC, Laub AJ. The singular value decomposition: its computation and some applications. IEEE Trans Automat Contr 1980; 25:164–176.

16. Lawson CL, Hanson RJ. Solving least square problems. Englewood Cliffs, NJ: Prentice-Hall, 1974.

17. Marsh JL, Gado MH, Vannier MW, Stevens WG. Osseous anatomy of unilateral coronal synostosis. Cleft Palate J 1986; 23:87–100.

18. Marsh JL, Vannier MW. The anatomy of the cranio-orbital deformities of craniosynostosis: insights from 3-D images of CT scans. Clin Plast Surg 1987; 14:49–60.

19. Mase GE. Schaum's outline series. Theory and problems of continuum mechanics. New York: McGraw-Hill, 1970.

20. Moss ML, Skalak R, Patel H. Sen K, Moss-Salentijn L, Shinozu ka M, Vilmann H. Finite element method modeling of craniofacial growth. Am J Orthod 1985; 87:453–472.

21. Papoulis A. Probability, random variables and stochastic processes. 2nd ed. New York: McGraw-Hill, 1984.

22. Richtsmeier JT, Cheverud JM. Finite element scaling analysis of human craniofacial growth. J Craniofac Genet Dev Biol 1986; 6:289–323.

23. Richtsmeier JT. Comparative study of normal, Crouzon and Apert craniofacial morphology using finite element scaling analysis. Am J Phys Anthropol 1987; 74:473–493.

24. Savara BS. A method for measuring facial bone growth in three dimensions. Hum Biol 1965, 37:245–255.

28. Savara BS, Tracy WE, Miller PA. Analysis of errors in cephalometric measurements of three dimensional distances on the human mandible. Arch Oral Biol 1966; 11:209–217.

26. Siegel AF. Geometric data analysis: an interactive graphics program for shape comparison. In: Launer RL, Siegel AF, eds. Modern data analysis. New York: Academic Press, 1982.

27. Siegel AF. Robust regression using repeated medians. Biometrica 1982; 69:242–244.

28. Sokal RR, Rohlf FJ. Biometry. 2nd ed. New York: WH Freeman, 1981.

Appendix: Osseous Landmark Definitions — By Region

MANDIBLE

articulare left/right (arl/arr): The intersection between the external contour of the cranial base and the dorsal contour of the mandibular neck or condyle.

Chin Line (CL): The line through infradentale and pogonion. (Sometimes determined as the tangent to the anterior border of the mandible in the mid-sagittal plane.)

condylion laterale left/right (cdl/cdr): The most lateral point on the condylar head.

coronoid tip left/right (ctl/ctr): The most superior point on the coronoid process.

disto-molare inferius left/right (dmil/dmir): The distobuccal cusp of the lower first molar.

external oblique line left/right (eoll/eolr): The minimum distance from gonion to the inferior limit of the anterior border of the coronoid process (usually located near or at the junction of the ramus with the body of the mandible).

gnathion (gn): The most inferior point on the mandibular symphysis in the mid-sagittal plane (sometimes referred to as mentor).

gonion left/right (gol/gor): A point on the angle of the mandible located by the bisection of the angle formed by the mandibular line and the ramus line.

incision inferius left/right (iil/iir): The mid-point of the incisal edge of the mandibular central incisor.

infradentale (id): The most anterosuperior point on the mandibular alveolar margin in the mid-sagittal plane.

lower molar left/right (lml/lmr): The mid-point between the mandibular first and second molars at the level of the buccal alveolar margin.

Mandibular Line left/right (ML(l)/ML(r)): The line through gnathion, tangent to the lower border of the mandible at the region of the angle.

mandibular notch left/right (mnl/mnr): The most inferior point of the mandibular notch (sigmoid notch).

pogonion (pg): The most anterior point on the mandibular symphysis in the mid-sagittal plane relative to the mandibular line.

Ramus Line left/right (RL(l)/RL(r)): The line through articulare, tangent to the posterior border of the mandibular ramus at the region of the angle.

MAXILLA

anterior nasal spine (ans): The apex of the anterior nasal spine. (Also known as spinal point, sp).

disto-molare superius left/right (dmsl/dmsr): The distobuccal cusp of the maxillary first molar.

hamular notch left/right (hnl/hnr): The deepest point of the hamular notch located centrally between the maxillary tuberosity and the pterygoid process of the spheroid.

hormion (h): The most posterior and medial point on the junction of the vomer and spheroid bones.

incision superius left/right (isl/isr): The mid-point of the incisal edge of the maxillary central incisor.

infraorbital foramen left/right (iofl/iofr): The center of the infraorbital foramen as it exits the maxilla.

medial foramen ovale left/right (mfol/mfor): The most anterior point on the margin of the foramen ovale.

medial orbitale left/right (morl/morr): The most medial point on the orbital margin in the region of the frontolacrimal suture. (Located near the craniometric point Dacryon).

nasal breadth (alare) left/right (nabl/nabr): The most lateral point on the anterior nasal aperture.

nasale (na): The tip of the nasal bone.

Nasal Line (NL): The line through anterior nasal spine and posterior nasal spine.

Nasion-Sella Line (NSL): The line through nasion and sella.

nasion (n): The most anterior point of the frontonasal suture.

orbitale left/right (orl/orr): The most inferior point on the infraorbital margin.

palatine tubercle left/right (pltl/pltr): The deepest point on the posterior curvature of the palatine tubercle immediately behind the hamular notch.

posterior nasal spine (pns): The apex of the posterior nasal spine.

prosthion (pr): The most anteroinferior point on the maxillary alveolar margin in the mid-sagittal plane.

pterygo-lateralis left/right (ptll/ptlr): The most posteroinferior point on the outline of the lateral pterygoid plates.

pterygo-orbitale left/right (ptol/ptor): The most superior point on the margin of the pterygomaxillary fissure.

On lateral radiographs this is recognised as the most superior point on the pear-shaped pterygomaxillary fissure.

Craniometrically and with CT this is recognised as the most posterosuperior point on the pterygomaxillary fissure where it becomes continuous with the infraorbital fissure.

pterygo-superius left/right (ptsl/ptsr): The posterosuperior extremity of the medial pterygoid plate, closest to the apex of the petrous temporal bone.

subspinale (ss): The most posterior point on the anterior contour of the upper alveolar process in the mid-sagittal plane. (Also known as Down's Point A).

supramentale (sm): The most posterior point on the anterior contour of the lower alveolar process in the mid-sagittal plane. (Also known as Down's Point B).

upper molar left/right (uml/umr): The mid-point between the maxillary first and second molars at the level of the buccal alveolar margin.

zygomaxillare inferius left/right (zmil/zmir): The most inferior point on the zygoma, usually just posterior to the craniometric landmark of zygomaxillare. *zygomaxillare* - the lowest point on the external suture between zygomatic and maxillary bones.

ORBITS

infero-lateral orbitale left/right (ilorl/ilorr): The point on the lateral orbital rim closest to the bony concavity at the junction of frontal and temporal processes of the zygomatic bone.

infraorbital foramen left/right (iofl/iofr): The centre of the infraorbital foramen as it exits the maxilla.

lateral orbitale left/right (lorl/lorr): The most lateral point on the orbital rim in the mid-region of the lateral orbital wall.

medial orbitale left/right (morl/morr): The most medial point on the orbital margin in the region of the frontolacrimal suture. (Located near the craniometric point Dacryon).

nasale (na): The tip of the nasal bone.

nasion (n): The most anterior point of the frontonasal suture.

naso-lacrimal inferius left/right (nlil/nlir): The most anteroinferior point on the margin of the nasolacrimal groove as it exits the orbit (usually this point is located at the small spicule of bone covering the lateral wall of the nasolacrimal groove and the inferior orbital rim).

optic foramen left/right (ofl/ofr): The renter of the anterior opening of the optic canal.

Orbitale left/right (orl/orr): The most inferior point on the infraorbital margin.

superior orbitale left/right (sorl/sorr): The most superior point on the supraorbital margin.

supero-lateral orbitale left/right (slorl/slorr): The intersection of the frontozygomatic suture with the lateral orbital rim (almost the intersection of the curve of the supraorbital rim with the lateral orbital rim.)

zygomatic corner left/right (zcl/zcr): The mid-point of the bony concavity formed between the frontal and temporal processes of the zygomatic bone.

ZYGOMA

articular eminence left/right (ael/aer): The most inferolateral point on the articular eminence of the zygomatic process of the temporal bone.

auriculare left/right (aul/aur): The point on the superior border of the zygomatic arch that is nearest to craniometric point porion.

external auditory meatus left/right (eaml/eamr): The center of the external auditory meatus.

infero-lateral orbitale left/right (ilorl/ilorr): The point on the lateral orbital rim closest to the bony concavity at the junction of frontal and temporal processes of the zygomatic bone.

infraorbital foramen left/right (iofl/iofr): The center of the infraorbital foramen as it exits the maxilla.

lateral orbitale left/right (lorl/lorr): The most lateral point on the orbital rim in the mid-region of the lateral orbital wall.

mastoidale left/right (mal/mar): The most inferior point on the mastoid process.

Orbitale left/right (orl/orr): The most inferior point on the infraorbital margin.

porion left/right (pol/por): The most superior point on the margin of the external auditory meatus.

pre-articulare left/right (parl/parr): The most superior point on the lower border of the zygomatic arch located anterior to point articular eminence.

zygion left/right (zgl/zgr): The most lateral point on the zygomatic arch.

zygo-frontale left/right (zfl/zfr): The point located at the posterior extremity of the frontozygomatic suture.

zygomatic corner left/right (zcl/zcr): The mid-point of the bony concavity formed between the frontal and temporal processes of the zygomatic bone.

zygomaxillare inferius left/right (zmil/zmir): The most inferior point on the zygoma, usually just posterior to the craniometric landmark of zygomaxillare. *zygomaxillare-the* lowest point on the external suture between zygomatic and maxillary bones.

CRANIUM

asterion left/right (asl/asr): The intersection between temporal, parietal, and occipital sutures on the surface of the cranial vault.

basion (ha): The mid-sagittal point on the anterior margin of the foramen magnum (determined as the point of maximum convexity on the clivus of the skull at the anterior margin of the foramen magnum).

bregma (br): The intersection of the sagittal and the coronal sutures on the surface of the cranial vault.

euryion left/right (eul/eur): The bilateral points of maximum convexity on the cranial vault between which maximum cranial breadth is recorded.

external auditory meatus left/right (eaml/eamr): The renter of the external auditory meatus.

foramen magnum lateralis left/right (fmll/fmlr): The most lateral point on the margin of the foramen magnum.

Frankfort Horizontal Plane (FHP): The plane through right and left porions and the left orbitale.

glabella (g): The most prominent point in the mid-sagittal plane between the eyebrow ridges. Glabella is located slightly superior to the frontonasal suture. This definition is suitable for both craniometric and CT measurement, but in biplanar radiographic measurement from the lateral radiograph, the eyebrow ridges are more prominent, obscuring this landmark. For this reason the most anterior point on the frontal bone on the lateral radiograph is used because it can be reproducibly identified. The biplanar measurement of the landmark glabella is therefore anterosuperior to the craniometric or CT measurement of that landmark.

infero-frontale left/right (ifl/ifr): The point on the superior temporal line where the ridge between the anterior and lateral surfaces of the zygomatic process of the frontal bone flattens.

lambda (1): The intersection between the lambdoid and sagittal sutures on the surface of the cranial vault.

latero-frontale left/right (lfl/lfr): The bilateral points located behind the lateral orbital margin on the frontal bone which define minimum frontal breadth.

mastoidale left/right (mal/mar): The most inferior point on the mastoid process.

nasion (n): The most anterior point of the frontonasal suture.

opisthion (o): The mid-sagittal point on the posterior margin of the foremen magnum. This landmark is difficult to locate in the living due to the presence of the spinal column, in which case a good knowledge of related anatomic features aids identification.

opisthocranion (op): The most distal point on the skull from glabella in the mid-sagittal plane, excluding the external occipital protuberance.

porion left/right (pol/por): The most superior point on the margin of the external auditory meatus.

sphenion left/right (spl/spr): The junction of the coronal suture and the spheroid bone.

superior orbitale left/right (sorl/sorr): The most superior point on the supraorbital margin.

vertex (v): The most superior point in the mid-sagittal plane when the skull is oriented along the Frankfort Horizontal.

zygo-frontale left/right (zfl/zfr): The point located at the posterior extremity of the frontozygomatic suture.

CRANIAL BASE

anterior clinoid left/right (acl/acr): The mid-point of the tip of the anterior clinoid of the lesser wing of the spheroid bone. In the cases of bridging between the anterior and posterior clinoid the point is determined mid-way along the bridge.

basion (ba): The mid-sagittal point on the anterior margin of the foramen magnum (determined as the point of maximum convexity on the clivus of the skull at the anterior margin of the foramen magnum).

foramen caecum (fc): The mid-point of the foramen caecum.

foramen magnum lateralis left/right (fmll/lfmlr): The most lateral point on the margin of the foramen magnum.

medial anterior clinoid left/right (macl/macr): The most lateral point on the tuberculum sella at the level of the inferior margin of the optic groove.

medial foramen ovale left/right (mfol/mfor): The most anterior point on the margin of the foramen ovale.

medial foramen spinosum left/right (mfsl/mfsr): The most anteromedial point of the foramen spinosum.

odontoid (odp): The apex of the odontoid process of the second cervical vertebra.

opisthion (o): The mid-sagittal point on the posterior margin of the foramen magnum. This landmark is difficult to locate in the living due to the presence of the spinal column, in which case a good knowledge of related anatomic features aids identification.

petrous anterius left/right (pal/par): The most anterior point on the crest of the petrous temporal bone at the margin of the foramen lacerum.

petrous posterius left/right (ppl/ppr): The most posterior point on the crest of the petrous temporal bone where it becomes continuous with the lateral wall of the posterior cranial fossa.

posterior clinoid left/right (pcl/pcr): The mid-point of the tip of the posterior clinoid of the dorsum sella. In the cases of bridging between the anterior and posterior clinoid the point is determined mid-way along the bridge.

sella (s): The center of the sella turcica.

sphenoidale anterior left/right (spal/spar): The most anterior point on the posterior margin of the lesser wing of spheroid (usually located near or at the mid-point of the posterior margin of the lesser wing of the spheroid).

sphenoidale laterale left/right (spll/splr): The most lateral point on the lesser wing of spheroid where the posterior margin becomes continuous with the lateral wall of the middle cranial fossa.

DERIVED CRANIAL BASE LANDMARKS

95 The intersection of the plane parallel to the mid-sagittal plane through the landmark "sphenoidale anterior left" with the superior margin of the temporal bone.

96 The intersection of the plane parallel to the mid-sagittal plane through the landmark "sphenoidale anterior right" with the superior margin of the temporal bone.

97 The intersection of the plane parallel to the mid-sagittal plane through the landmark "anterior clinoid left" with the superior margin of the temporal bone.

98 The intersection of the plane parallel to the mid-sagittal plane through the landmark "anterior clinoid right" with the superior margin of the temporal bone.

99 The mid-point between the landmarks "anterior clinoid left" and "97".

100 The mid-point between the landmarks "anterior clinoid right" and "98".

101 The mid-point between the landmarks "lesser wing of sphenoidale anterior left" and "95".

102 The mid-point between the landmarks "lesser wing of sphenoidale anterior right" and "96".

Craniofacial Osseous Landmark Determination from Stereo Computer Tomography Reconstructions

A H Abbott,* *BDS, BSc Dent(Hons), PhD,* D J Netherway,** *BSc (Hons), PhD,* D J David,*** *AC, FRCS, FRACS,* T Brown, **** *MDS, DDSc*

Abstract

The accurate and reproducible determination of the three dimensional (3D) co-ordinate positions of anatomical landmarks from computer tomography (CT) images has been limited even though potentially the data have been available for several years. This paper describes a method of acquisition of osseous landmark positions using an off-line computing technique based on multiple stereo images of 3D CT reconstructions. The use of stereo pairs greatly enhances the consistent identification of osseous landmarks. Further, the technique is of particular value where access to the CT scanner is restricted due to heavy clinical demand and separate high quality graphics facilities are unavailable.

Osseous landmark position data were determined for dried skulls and patients with craniofacial conditions. Accuracies of the order 1.7mm (median) were obtained. These results encourage the use of the technique for acquisition of landmark positions for the study of the craniofacial complex in three dimensions.

Key words: 3D reconstructions, Craniofacial complex, Stereoscopic viewing.

Introduction

The life-like appearance of three dimensional (3D) computer tomography (CT) reconstructions has created great interest amongst surgeons and anthropologists interested in human growth and development. These 3D reconstructions can facilitate surgically an appreciation of pathological conditions of patients and also allow ongoing anthropological study of valuable skeletal material currently being returned for burial.

Three dimensional CT images inspire the desire for their use in osseous landmark position determination. While three dimensional landmark positions have been obtained from 3D CT reconstructions, only a few quantitative results have been published[1-4] and then only little information is reported on the selection of landmarks, their co-ordinate locations and their replicability.

The CT scanner available to us has the software facility to obtain three dimensional co-ordinate data of landmarks specified by the position of a cursor, but some potential difficulties in using the CT scanner for landmark determination became apparent. These were:

(i) Time: The appropriate image of the 3D CT reconstruction is viewed by an operator who places the cursor over the osseous landmark in question. Its

* Research Scientist
** *Principal Research Scientist*
*** *Head*
**** *Consulting Research Director*
The Australian Cranio-facial Unit, Adelaide Children's Hospital Campus, Adelaide Medical Centre for Women and Children. Address for Reprints: Dr Amanda H Abbott, The Australian Cranio-facial Unit, Adelaide Medical Centre for Women and Children, 72 King William Road, North Adelaide 5006, South Australia, Australia.

position is reported via the use of a function key in terms of element (in pixels), line (in pixels), and image number (giving relative orientation). This information is recorded and the procedure repeated for all landmarks of interest. By feeding the recorded information into the programme available on the scanner, the distance between and/or the location of selected landmarks could be obtained. This operation was found to be extremely time consuming and was not practical on the Adelaide Children's Hospital's CT scanner as it was in heavy clinical demand.

(ii) Identification of many landmarks on the CT console were based on a traditional cephalometric approach: A lateral or near lateral CT image was chosen to identify many landmarks and it was found that frequently the designated position did not intersect the surface or was located on the surface behind the edge of the surface of interest. This meant that an orientation of the reconstruction should be chosen in which the landmark was not at the very edge of the reconstruction. This requirement necessitated increased interactive use of the CT scanner, which heavy clinical demand constrained.

(iii) Location of the landmarks from monoscopic images: The depth perception produced by stereoscopic viewing enhances the ability of the operator to identify landmarks. Stereoscopic viewing was not an option on the CT scanner employed and could only be achieved using hard copy images.

For these reasons, it was decided that for the initial evaluation of CT co-ordinate data, landmark determination would be using off-line computing facilities, employing a method based on multiple sets of stereo images of 3D CT reconstructions. This paper reports this off-line technique and also demonstrates that use of stereo CT images allows landmarks to be well identified and is suitable when additional CT computing facilities are not available.

Materials and Methods

It was the intention of this investigation only to produce test material for the validation of the off-line computing stereo method for collecting three dimensional osseous landmark positions. It was decided therefore, that five skulls would be an adequate number for this purpose. Five skulls of Australian Aboriginal origin with intact cranium and mandible were selected from the South Australian Museum's skeletal collection.

A General Electric (GE) CT/T 8800 Scanner (General Electric Company, Medical Systems Group, Wisconsin, USA) housed in the Department of Radiology, Adelaide Children's Hospital, in conjunction with a Data General Nova 5140 (Data General, USA) was used to generate axial scans according to the Hospital's routine operating protocol. The protocol employed for the dried skulls, and for the patients selected in this study, included a current of 80mA, 120KV, pulse width code of 3msec, slice thickness of 5mm and a table shift interval of 3mm. For the patients, a slice thickness and a table shift of 1.5mm through the orbits was used.

For each CT examination, care was taken to ensure that the subjects scanned did not move. It was necessary, however, to sedate or give general anaesthesia to children under seven years and other patients whose co-operation could not be assured. The dried skulls and the patients' heads were oriented so that the orbitomeatal line (Frankfort Horizontal Line) was perpendicular to the floor. This position was maintained by use of the head strap fixed rigidly to an acrylic head holder.

Only one 3D CT reconstruction per subject was available due to imposed time restrictions for non-clinical work. Therefore, the CT data file was sub-regioned to exclude information superior to the supra-orbital ridge and posterior to the foramen magnum. The rationale for this was to permit viewing of the otherwise non-visible cranial base landmarks.

The threshold level determines the minimum density of material to be included in the 3D CT reconstruction. For dried skulls, a level of - 550 to - 450 Hounsfields is suitable and for patients a level of 150 to 200 Hounsfields is appropriate.

The three dimensional reconstruction programme used in this study was Display82, developed by the Medical Image Processing Group of the University of Pennsylvania.[5] Display82 was accessed by the programme 3D83[6] for GE Medical Systems. Essentially, this programme simplifies the creation of three dimensional displays by reducing the number of interactions on the part of the user. Photographic images of the axial slices and 3D CT reconstructions were recorded with the GE multiformat camera using Agfa Scopix film (Agfa-Gevaert Ltd., West Germany) and developed in a Kodak M5 (90 second) processor (Kodak, USA) .

Data Acquisition Analysis Facilities
The computing equipment used for data collection from the CT films consisted of an Apple 11 plus (Apple Computer, Inc., California, USA), a Hewlett Packard (Hewlett Packard Company, Inc., Colorado, USA) digitising tablet (HP9874A) and a plotter (HP9872A). This 2D co-ordinate data was uploaded to a Vax 11/785 (Digital Equipment Corporation, Maynard, Massachusetts, USA) for the calculation of 3D co-ordination positions and subsequent analysis.

Method Of Double Determination
The authors use the term "double determination" to refer to the estimation of systematic and random errors by the replication of measurement. Systematic error is assessed by testing whether the mean difference between pairs of measurements differs significantly from zero. Usually this is determined using a t-test for one dimensional data (for example, length) but for the measurement of two or three dimensional co-ordinate data, tests based on $\chi^2(2)$ or $\chi^2(3)$ distributions respectively are more appropriate."[7,8] If the mean is not zero at some high confidence level (say 95%), a systematic error is likely and its cause and effect must be evaluated. If there is no systematic error, the single measurement variance is determined from one half of the variance of the difference between two measurements and gives a measure of reproducibility.

Method Of Co-ordinate Determination From Multiple Stereo Pairs Of 3D CT Reconstructions
The position of each landmark can be determined from two views in which the landmark is visible. The programme Display82 produces orthographic (projection by lines perpendicular to the plane of projection) views of 3D CT reconstructions and this simplifies the determination of the depth co-ordinates. Figures l(a) and (b) show the geometric situation as a marker is rotated through an angle θ about the Z-axis, with the Y-axis as the direction of projection. From the two views, the co-ordinates $(x_1,z_2,)$ and (x_2,z_2) can be measured for a particular landmark. As the angular separation of the views is known, the depths y_1 and y_2 can be calculated. A better estimate for the z component is the average of z_1 and z_2. From the geometry $x_2 = x_1 \cos\theta - y_1\sin\theta$ and $y_2 = x_1\sin\theta + y_1\cos\theta$. Therefore, $y_1 = (x_1\cos\theta - x_2)\sin\theta$, and substituting, $y_2 = x, \sin\theta + (x_1\cos\theta - x_2)/\tan\theta$. The larger the angle, the more reliable is the determination of the depth co-ordinate.

Method Of Determining Landmark Positions From 3D CT Reconstructions
From the 3D CT reconstruction for each subject, forty images separated by 9° about the X-axis and about the Z-axis were generated for the determination of seventy six osseous landmark positions. Between adjacent orientations (that is, 9° separation) stereo imaging was used to provide the depth perception which greatly facilitated the identification and location of landmarks.

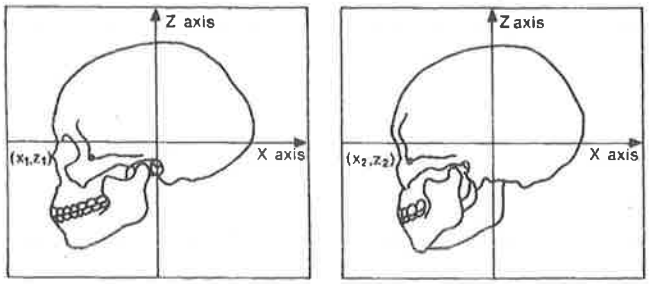

FIG.1a. *Tracings of two views of a 3D CT Construction with an angular separation θ about the Z-axis, with the projection down the Y-axis. The point (x_1, y_1, z,) projected at (x_1, z_1) in the left image 25 rotated to (x_2, y_2, z_2) and projected in the right image to (x_2, z_2).*

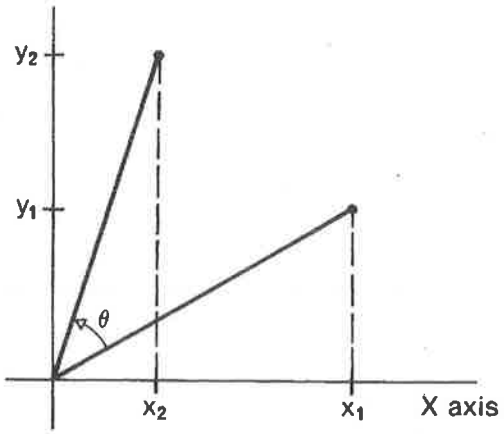

FIG. 1b. *Rotation of the point (x_1, y_1, z_1) to (x_2, y_2, z_2) viewed down the rotation axis.*

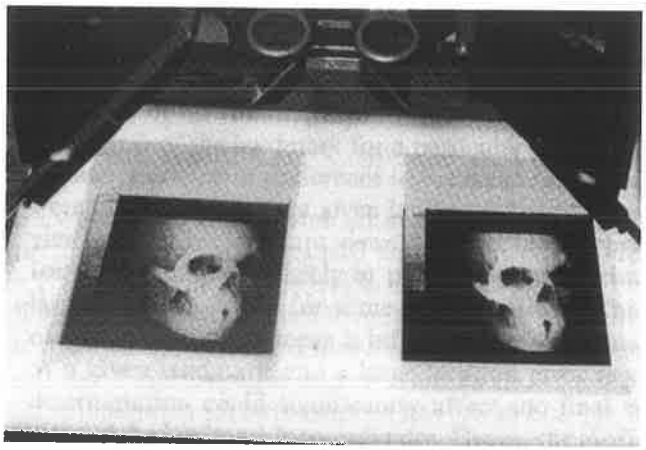

FIG. 2. *Stereo images facilitated identification of anatomical features and osseous landmarks.*

As the CT film could not be directly digitised, it was necessary to trace alignment marks, landmarks and their surrounding features. The images to be traced were overlaid with Acetate tracing film (General Aniline Film Corp., drafting film 0.05mm thickness), placed on a light box and traced in a darkened room using a 0.5mm H pencil. Opaque material was employed to mask areas of excess light. The stereo pairs were viewed using a Wild (Wild ST4—made by Wild in Singapore for Wild, Switzerland) stereoscope during tracing (Fig. 2). Unfortunately, tracing and marking the image in one view tended to impede stereo perception when attempting to trace and mark the associated pair. For this reason, only one image of a pair could be traced at one time. The errors associated with the subsequent digitising of marked osseous landmarks were negligible (~0.08mm) in comparison with landmark relocation errors. To reduce the potential problem of depth error associated with small errors in landmark relocation error, osseous landmark positions were generated from pairs of images

at intervals of at least 45°. For these reasons, only the left image of each stereo pair was traced and digitised. A stereo comparator of the kind employed by a cartographer, where a floating mark is used that does not impede depth perception and allows direct digitisation of the data, would have been preferable but one was not available for the present investigation.

The location of the centre of the image was determined from the cursor positioned at (0,0), the centre of the frame, and the rotation axes were taken to be parallel to the edges of the image. The orientation of the image about the rotation axis was displayed on the film. Initially, images of approximately 50% real size were used, but it was found that images of approximately 70% of real size gave more accurate results and all data in this paper are derived from images of this size.

After evaluation of all possible stereo pairs for, (a) ease of identification of osseous landmarks and, (b) number of osseous landmarks visible in each pair of stereo images (to reduce the number of tracings required to obtain the data), stereo pairs (two images 9° apart) at intervals of 45° were selected as follows (Fig. 3).

X-axis pairs: [27°, 36°], [72°, 81°], [117°, 126°], [225°, 234°], [270°, 279°], [315°, 324°);

Z-axis pairs: [18°, 27°], [63°, 72°], [108°, 117°], [234°, 243°], [279°, 288°], [324°, 333°]

For the 0°, the head is the anatomical position and facing the viewer. Angles are anti-clockwise looking down the X-axis of rotation and clockwise looking down the Z-axis of rotation. The axes are oriented as follows: with the origin at the centre of the head, the Z-axis is through the top of the head, the X-axis is through

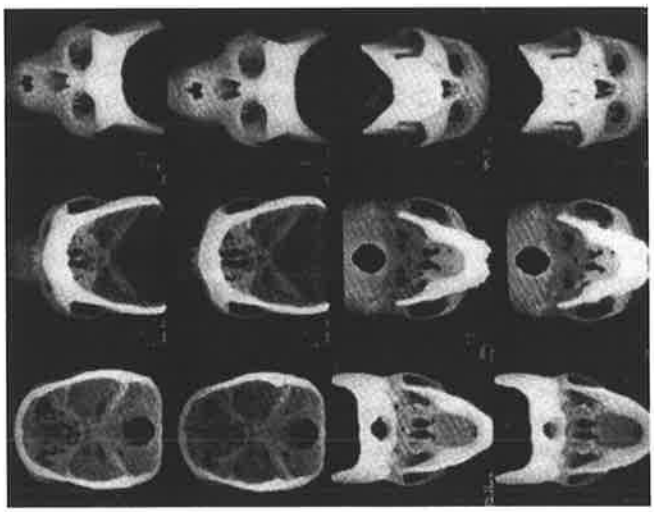

FIG. 3a. *Stereo images of a 3D CT reconstruction of a dried skull used for determination of osseous landmarks for rotations about the x-axis of [27°, 36°], [72°, 81°], [117°, 126°], [225°, 234°], [270°, 279°] and [315°, 324°] in order down the left pair of columns and up the right pair.*

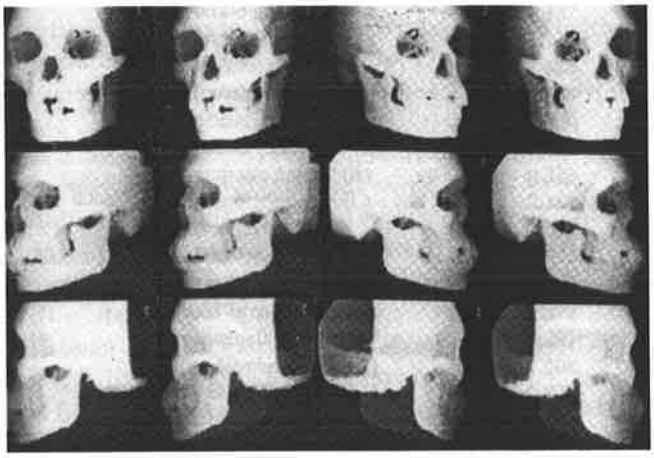

FIG. 3 b. *Stereo images of a 3D CT reconstruction of a dried skull used for determination of osseous landmarks for rotations about the Z-axis of [18°, 27°], [63°, 72°], [108°, 117°], [234°, 243°], [279°, 288°] and [324°, 333°] in order down the left pair of columns and up the right pair.*

the subject's left ear and the Y-axis is through the back of the head. All the landmarks could be located in more than one of the above stereo pairs.

For each rotation axis, many landmarks had been digitised on more than two images and this meant that their three dimensional co-ordinates could be calculated from any pair of images on which that landmark had been identified. The three dimensional co-ordinates calculated using any orientations about either axis were expressed relative to the frontal view (0°: subject facing viewer). The final three dimensional co-ordinates for each osseous landmark were taken to be the median co-ordinates of all determinations (from the multiple pairs of images) of the landmark for a particular subject. The median was used in preference to the mean, as attempts were made to identify a given landmark from as many views as possible; perhaps views that were inappropriate for the landmark possibly or potentially giving rise to larger location errors for some determinations. This is of importance as the mean is influenced by all estimates of a given landmark and a large location error in one determination could significantly affect the final estimate of the landmark's co-ordinates. Hence, the median, in this situation, was a more reliable estimate.

Results

Reproducibility of Osseous Landmark Identification For Dried Skulls

The anatomical osseous landmarks considered in this investigation have been detailed elsewhere.[9] Initially one hundred and eight osseous landmarks were considered for the study of reproducibility from which a final seventy-six were used.

An assessment of the landmark relocation error from CT data was made using the method of double determination. Due to limited access to the CT scanner, it was not possible to re-scan the five test skulls and then retrace their 3D CT reconstruction images. Thus, the double determination was based on the same CT stereo image pairs retraced after a time interval of one month. This time interval ensured that one did not remember non-image cues that would aid in identifying the same position on the film.

The co-ordinate data of the two determinations for the same skull were aligned using repeated median fitting,[8,10] and the resulting residuals were used for the determination of the landmark location errors. The mean residuals and standard deviations, across the five skulls for each landmark, are given in Table I. Significant average residuals, using the $\chi^2(3)$ test, are identified if their test statistic or $d\sqrt{n}/\sigma$ score exceeds 1.614 (95% confidence interval)[7,8]. For some landmarks, the $\chi^2(3)$ test indicated that the average residual is significantly different from zero (marked by an asterisk in Table I). This meant that the definition of the landmark (in the measurer's mind (AHA)) had changed in the one month period between determinations. This implied evolution of the landmark definitions and suggested that if the measurements were repeated again, with the more stable definitions, an even greater consistency and accuracy would be attained. Of the seventy-six osseous landmarks measured, twelve had changed significantly but for the most part, were displaced by less than 2mm (which is within the width of 2 to 3 voxels).

The last column in Table I lists the osseous landmark relocation errors. The relocation error is determined[11] as the root-mean-square difference divided by the square root of two. These errors are in the range of 0.411mm for the right coronoid notch to 5.165mm for left posterior clinoid. The median landmark relocation error is 1.7mm and this distance corresponds to approximately the width of 2 voxels in CT terms. When it is considered that the images used for landmark determination show only moderate contrast, were scanned 5/3 as opposed to 1.5/1.5, and the images were less than life size, the result reported for

the median landmark relocation accuracy is encouraging. Most of these deficiencies in the images can be minimised therefore, one can expect to further improve the accuracy of determination of the positions of osseous landmarks.

TABLE I:

Mean and standard deviation (SD) of the differences between the two CT determinations of the five skulls; test statistic ($d\sqrt{n}/\sigma$); number of observations (N); and osseous landmark relocation error for dried skull using CT

Landmark Name	Mean diff	SD	$d\sqrt{n}/\sigma$	n	Relocation error
sella	1.339	3.209	0.933	5	2.239
nasion	0.793	1.324	1.339	5	1.007
glabella	1.458	2.911	1.120	5	2.110
opisthion	0.588	0.361	2.307*	2	0.453
mastoidale (L)	1.228	2.214	1.109	4	1.610
mastoidale (R)	1.310	1.797	1.458	4	1.439
basion	1.715	3.748	1.023	5	2.663
ext auditory meatus (R)	0.897	2.534	0.792	5	1.724
ext auditory meatus (L)	0.669	3.671	0.408	5	2.369
condylion laterale (R)	1.894	1.703	2.486*	5	1.719
condylion laterale (L)	1.049	3.595	0.653	5	2.392
gonion (R)	0.471	1.752	0.601	5	1.157
gonion (L)	1.226	2.465	1.112	5	1.784
pogonion	1.951	1.199	2.301*	2	1.504
prosthion	2.645	0.000	0.000	1	1.870
ant nasal spine	0.938	1.420	1.321	4	1.094
post nasal spine	1.315	3.050	0.964	5	2.142
upper molar (R)	0.627	1.423	0.985	5	1.003
upper molar (L)	0.453	1.025	0.987	5	0.723
lower molar (R)	0.216	1.358	0.275	3	0.799
lower molar (L)	1.078	0.829	1.840*	2	0.868
zygomaxillare inferius (R)	0.301	1.405	0.429	4	0.886
zygomaxillare inferius (L)	1.274	1.533	1.662*	4	1.301
coronoid tip (R)	0.490	1.302	0.842	5	0.893
coronoid tip (L)	0.883	2.527	0.782	5	1.716
palatine tubercle (R)	1.503	3.480	0.864	4	2.381
palatine tubercle (L)	1.931	3.571	1.081	4	2.578
optic foramen (R)	0.382	1.434	0.377	2	0.766
optic foramen (L)	1.167	1.209	1.365	2	1.023
nasale	0.515	1.324	0.870	5	0.913
medial orbitale (R)	0.709	2.062	0.769	5	1.397
medial orbitale (L)	0.562	2.106	0.596	5	1.390
superior orbitale (R)	1.132	2.596	0.975	5	1.827
superior orbitale (L)	3.113	3.894	1.788*	5	3.303
lateral orbitale (R)	0.246	1.243	0.443	5	0.805
lateral orbitale (L)	2.726	5.963	1.022	5	4.235
infero-lateral orbitale (R)	1.192	1.852	1.439	5	1.443
infero-lateral orbitale (L)	0.878	2.416	0.812	5	1.649

TABLE I:

Mean and standard deviation (SD) of the differences between the two CT determinations of the five skulls; test statistic ($d\sqrt{n}/\sigma$); number of observations (N); and osseous landmark relocation error for dried skull using CT (con'd)

Landmark Name	Mean diff	SD	$d\sqrt{n}/\sigma$	n	Relocation error
orbitale (R)	1.137	3.233	0.786	5	2.197
orbitale (L)	2.178	4.022	1.211	5	2.973
infraorbital foramen (R)	2.628	3.765	1.396	4	2.961
infraorbital foramen (L)	2.208	3.196	1.382	4	2.503
articular eminence (R)	1.380	2.285	1.351	5	1.744
articular eminence (L)	2.156	4.401	1.095	5	3.174
zygomatic corner (R)	0.323	1.168	0.618	5	0.773
zygomatic corner (L)	0.364	1.819	0.448	5	1.179
infero-frontale (R)	0.991	3.877	0.571	5	2.550
infero-frontale (L)	2.832	2.649	2.391*	5	2.611
nasal breadth (R)	0.607	2.159	0.628	5	1.431
nasal breadth (L)	1.399	3.826	0.818	5	2.614
mandibular notch (R)	0.297	0.578	1.028	4	0.411
mandibular notch (L)	1.208	1.325	2.039*	5	1.197
ext oblique line (R)	0.737	1.621	0.909	4	1.121
ext oblique line (L)	1.687	4.767	0.708	4	3.154
medial foramen ovale (R)	2.203	4.040	0.944	3	2.805
medial foramen ovalue (L)	2.640	4.004	1.142	3	2.971
foramen magnum lateralis (R)	2.058	2.001	1.781	3	1.858
foramen magnum lateralis (L)	0.655	1.959	0.579	3	1.222
incision superius (L)	2.400	0.000	0.000	1	1.697
disto-molare superius (L)	0.832	0.000	0.000	1	0.588
anterior-clinoid (L)	2.474	1.153	3.035*	2	1.842
anterior clinoid (R)	0.372	0.760	0.02	2	0.462
sphenoidale anterior (L)	1.930	3.272	1.022	3	2.331
sphenoidale anterior (R)	2.122	3.211	1.145	3	2.385
95	2.759	5.124	0.932	3	3.544
96	3.414	5.337	1.108	3	3.915
97	1.567	0.534	4.149*	2	1.140
98	2.003	0.878	3.226*	2	1.483
99	0.683	0.432	2.239*	2	0.529
100	0.329	1.572	0.296	2	0.820
101	2.509	4.209	1.032	3	3.009
102	2.434	4.833	0.872	3	3.279
medial anterior clinoid (L)	3.271	2.881	1.606	2	2.725
medial anterior clinoid (R)	3.249	4.930	0.932	2	3.370
posterior clinoid (L)	2.231	8.518	0.454	3	5.165
posterior clinoid (R)	2.530	5.212	0.841	3	3.500

*probability less than 5%

Overall point location error = 2.144mm

Median point location error = 1.721mm

N.B. The number of significant figures given is not intended to convey the degree of precision but rather to allow numerical checking.

Comparison of Craniometric and CT Osseous Landmark Location for Dried Skulls

The distances between landmarks located using CT data were compared with the corresponding craniometric measurements to ascertain whether there were any significant landmark definition differences between the two methods of measurement. The median relocation error associated with craniometric determination of osseous landmark positions is 0.37mm,[8] significantly smaller than the CT landmark relocation error. The average and standard deviation of the differences for each distance were calculated to determine the significance of the average differences between CT and craniometric determination using t-tests (Table II).

Of the thirty-one distances compared, ten were found to be significantly different at the 95% confidence interval (marked with* in the lower portion of Table II). The results can be summarised as follows.

Apart from the two distance measurement differences due to thin bone exclusion arising from threshold selection (marked with a + in Table II), the distances that were significantly different from the craniometric measurement resulted from definition differences between the measurement systems. Recognition of these differences has led to a consistent set of landmark definitions applicable to both direct craniometric and CT determination.[9]

The average differences that were found to be non-significant between craniometric and CT data (upper portion of Table II) were in the range 0.180mm to 2.636 mm, with one rogue value of 5.590mm. This rogue value was for the bi-articular eminence distance for which the landmarks, articular eminence right and left, were ill defined for three of the five skulls due to flattened and/or worn eminences. Essentially, for two of the skulls here was no significant difference between the CT and craniometric measurements and it is only the impaired articular eminences on the remaining skulls that has led to a large variance being calculated. Similarly, the distance, nasion to basion, was found to have a relatively large standard deviation due to the influence of one observation.

The results of this section confirm that the 3D CT landmark co-ordinates derived using the multiple stereo imaging technique are consistent with craniometric measurement, provided that the same landmark definitions can be followed for the two measurement techniques.

The landmark determination accuracy for CT (median 1.7mm) is about twice that found using biplanar radiographic techniques [12] (median 0. 7mm). For patients with asymmetry, for example, the biplanar cephalometric images are difficult to interpret. So that, although the biplanar radiographic method has a greater accuracy when applied to normal anatomy the life-like appearance of the 3D CT reconstructions facilitates the confident identification of many more landmarks even in the presence of pathological conditions.

Reproducibility of Osseous Landmark Identification for Patients

To assess the influence of soft tissue and osseous abnormality on landmark identification, multiple stereo pairs of 3D CT reconstructions were generated and landmark co-ordinate data determined in a similar manner to that already described. The same number and orientation of stereo pairs were used for landmark determination on the dried skulls.

Three patients from the Australian Cranio-Facial Unit were selected—an adult and an eleven year-old, both with Treacher Collins Syndrome, and a twelve month old child with Apert's syndrome. Images from the 3D CT reconstructions for each patient were traced, digitised and the three dimensional co-ordinates of osseous landmarks determined (Fig. 4). One month later, the images were retraced, digitised and three dimensional co-ordinates again determined to

ascertain the reproducibility of landmark location using the technique of double determination.

The co-ordinate data of the two determinations for the same patient were aligned using the repeated median fitting approach.[8,10] This alignment revealed the average residual for each landmark ranged from 0.114mm to 5.673mm (Table III) with 88% (sixty-six out of seventy-seven) below 3mm.

TABLE II:

Statistics of the comparison of distances derived from CT Osseous Landmark positions with craniometric distance measurements for the five test skulls.

Distance	Mean diff	SD	t	n
right to left ext auditory meatus	-2.040	4.386	1.040	5
nasion to basion	2.596	4.644	1.250	5
right to left mastoidale	0.683	2.048	0.667	4
opisthion to basion	0.180	0.226	1.125	2
nasion to nasale	-0.874	1.258	1.554	5
zygo corner to infero-lateral orbitale (R)	1.788	1.973	2.026	5
med orbitale to lat orbitale (L)	-1.168	1.438	1.816	5
right to left infraorbital foramen	1.962	1.982	2.213	5
prosthion to ant nasal spine	-1.057	1.821	1.005	3
ant nasal spine to post nasal spine	0.438	2.571	0.381	5
upper molar to zygomax inf (R)	2.636	2.636	2.236	5
upper molar to zygomax inf (L)	2.052	1.811	2.533	5
right to left zygomaxillare inferius	1.652	2.750	1.343	5
right to left pterygo-orbitale	-0.370	0.856	0.864	4
right to left articular eminence	-5.590	5.472	2.284	5
right to left zygomatic corner	0.626	0.833	1.681	5
condylion laterale to gonion (R)	0.700	1.601	0.978	5
condylion laterale to gonion (L)	0.508	2.275	0.499	5
right to left mandibular notch	-1.492	1.571	2.124	5
right to left for magnum lateralis	0.657	0.692	1.643	3
right to left medial for ovale	0.777	2.158	0.623	3
superior orbitale to orbitale (R)	-3.620	1.912	4.234*	5
medial orbitale to lateral orbitale (R)	-0.992	0.445	4.983*	5
superior orbitale to orbitale (L)	-2.812	2.028	3.100*	5
zygo corner to infero-lateral orbitale (L)	2.204	1.769	2.785*	5
nasion to ant nasal spine	-2.134	0.872	5.475*+	5
right to left nasal breadth	1.430	0.784	4.076*+	5
right to left infero-frontale	2.612	1.483	3.939*	5
right to left condylion laterale	9.342	1.516	13.775*	5
right to left gonion	-3.196	1.657	4.312*	5
right to left coronoid tip	-1.700	1.072	3.546*	5

* probability less than 5%

\+ difference due to thin bone exclusion arising from threshold selection for the 3D CT reconstructions

SD standard deviation of the differences

t test statistic for the t-test

n number of observations

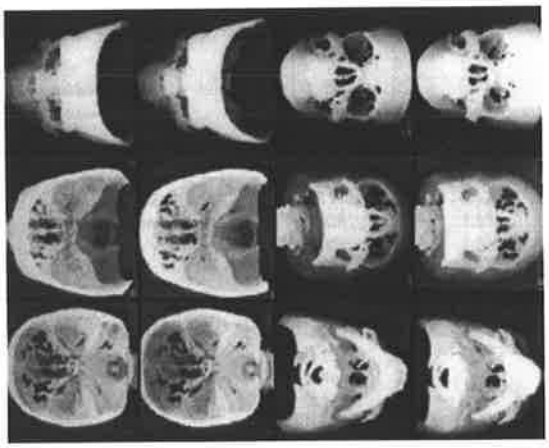

FIG. 4a. *Stereo images of a 3D CT reconstruction of an adult patient with Treacher Collins Syndrome used for determination of osseous landmarks for rotations about the X-axis of [27°, 36°], [72°, 81°], [117°,126°], [225°,234°], [270°, 279°] and [315°.324°] in order down the left pair of columns and up the right pair.*

FIG. 4b. *Stereo images of a 3D CT reconstruction of an adult patient with Treacher Collins Syndrome used for determination of osseous landmarks for rotations about the Z-axis of [18°, 27°], [63°, 72°], [108°, 117°], [234°, 243°], [279°, 288°] and [324°, 333°] in order down the left pair of columns and up the right pair.*

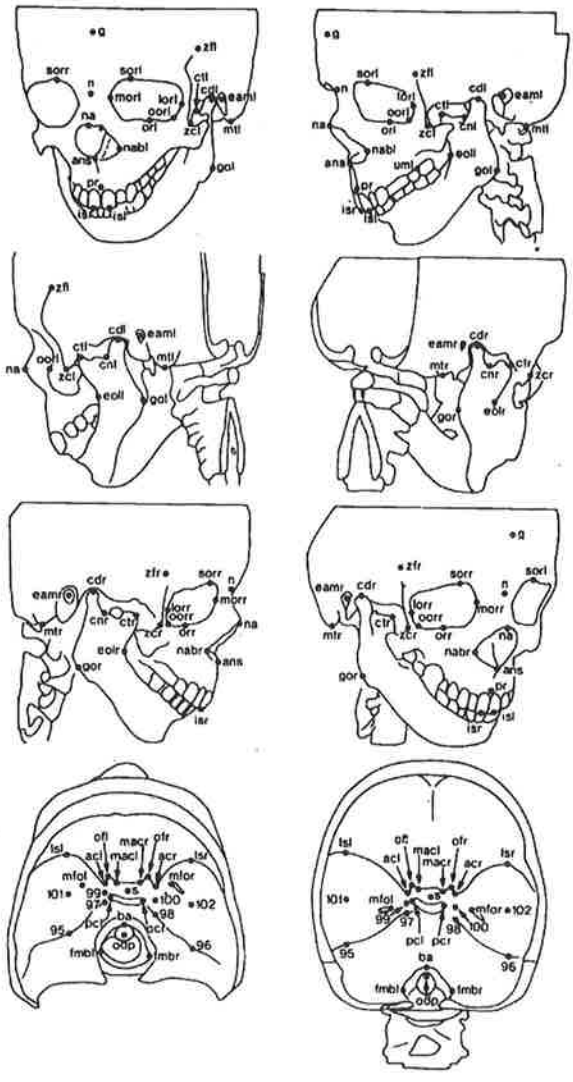

FIG. 4c. *Examples of tracings utilised for osseous landmark determination from the CT reconstruction for the adult patient with Treacher Collins syndrome. The landmark definitions and abbreviations are detailed elsewhere.*[9]

TABLE III:

Mean of the differences between the two CT determinations of the three patients and indicative CT Osseous landmark relocation errors.

Landmark Name	Mean diff	n	Relocation error
sella	0.790	3	1.364
nasion	0.625	3	0.860
glabella	1.191	2	1.152
mastoidale (L)	0.750	2	0.576
mastoidale (R)	0.996	2	0.952
basion	0.911	1	0.644
ext auditory meatus (R)	0.823	1	0.582
ext auditory meatus (L)	1.305	2	1.358
condylion laterale (R)	0.137	2	0.134
condylion laterale (L)	0.628	2	1.035
gonion (R)	1.069	3	1.813
gonion (L)	0.947	3	1.880
infradentale	2.384	1	1.686
prosthion	0.868	3	0.884
ant nasal spine	0.307	3	0.900
upper molar (R)	0.653	1	0.462
upper molar (L)	2.460	2	2.477
lower molar (R)	2.185	1	1.545
lower molar (L)	0.619	2	0.546
coronoid tip (R)	0.752	2	0.683
coronoid tip (L)	1.316	2	1.025
optic foramen (R)	1.173	1	0.830
optic foramen (L)	3.510	1	2.482
nasale	3.968	3	4.628
medial orbitale (R)	1.541	2	3.077
medial orbitale (L)	2.600	2	2.751
superior orbitale (R)	0.114	3	1.123
superior orbitale (L)	2.539	3	3.774
lateral orbitale (R)	0.560	3	0.577
lateral orbitale (L)	0.627	3	0.927
infero-lateral orbitale (R)	1.052	3	0.898
infero-lateral orbitale (L)	2.489	1	1.760
orbitale (R)	1.024	3	0.938
orbitale (L)	1.385	3	1.380
infraorbital foramen (R)	0.880	1	0.622
infraorbital foramen (L)	1.816	2	1.605
zygomatic corner (R)	1.387	3	1.389
zygomatic corner (L)	1.111	3	1.737
infero-frontale (R)	4.157	3	5.933
infero-frontale (L)	3.057	3	4.043
nasal breadth (R)	1.947	3	2.622
nasal breadth (L)	0.473	2	1.071

TABLE III:

Mean of the differences between the two CT determinations of the three patients and indicative CT Osseous landmark relocation errors, (con'd)

Landmark Name	Mean diff	n	Relocation error
mandibular notch (R)	1.268	2	1.531
mandibular notch (L)	1.398	3	1.951
ext oblique line (L)	0.704	1	0.498
medial foramen ovale (L)	2.072	1	1.465
foramen magnum lateralis (R)	1.413	2	1.627
foramen magnum lateralis (L)	5.673	2	4.565
incision superius (R)	0.452	3	0.977
incision superius (L)	0.372	3	1.504
incision inferius (R)	0.316	2	0.977
incision inferius (L)	0.506	2	0.568
disto-molare superius (R)	2.764	1	1.955
disto-molare superius (L)	0.1752	2	0.593
disto-molare inferius (R)	3.547	1	2.508
disto-molare inferius (L)	0.486	2	0.377
subspinale	1.768	2	1.398
odontoid peg	0.632	2	0.632
anterior clinoid (L)	0.695	3	0.799
anterior clinoid (R)	0.413	3	0.639
sphenoidale anterior (L)	0.941	3	1.219
sphenoidale anterior (R)	1.091	3	1.215
95	0.744	3	1.097
96	3.647	3	4.115
97	2.266	3	4.795
98	0.824	3	1.024
99	1.964	3	2.115
100	0.620	3	0.887
101	0.607	3	0.861
102	1.947	3	2.134
medial anterior clinoid (L)	1.458	3	1.749
medial anterior clinoid (R)	1.584	3	1.710
posterior clinoid (L)	1.255	3	1.269
posterior clinoid (R)	1.094	3	1.002

Overall point location error = 2.035mm
Median point location error = 1.244mm

Single landmark location errors are given in the last column of Table III. These should be considered indicative only, as there were only three (and sometimes less) patients contributing to their determination. In some cases, the 3D CT reconstruction images had not been generated according to the subregioning specifications and in these instances it was not possible to obtain all of the landmarks (for example, the patient with Apert's syndrome). Other missing landmarks were related to the presence of pathological conditions, resulting in the absence of bone and therefore, the associated landmarks could not be identified. The overall or pooled landmark location error taken over seventy-six landmarks was 2.0mm (approximately the width of 2.5 voxels) while

the median landmark location error was 1.2mm (approximately the width of 1.5 voxels). These results are comparable to those obtained for the landmark relocation errors calculated for the five dried skulls and indicate, for these patients, that soft tissue and osseous abnormality have had no apparent effect on landmark identification when the landmarks were in fact present.

Discussion

The availability of life-like 3D CT reconstructions has opened up a new world of analysis with the potential of providing insight into many conditions afflicting the human body. Presently these CT images are available to the vast majority of clinicians via the CT console or on radiographic film. Typically the clinician interacts only with the data in a qualitative sense—time constraints tend to limit his quantitative exploration of the available CT data.

To overcome the difficulties associated with the clinical time constraints on the CT equipment and associated with the translation of standard landmark definitions to the CT environment, an off-line computing method was developed to determine landmark co-ordinate positions from multiple sets of stereo images of 3D CT reconstructions. This had the advantage that stereoscopic viewing of these radiographs could be used, providing enhanced definition to the image being analysed and facilitating landmark location.

While the technique has been applied to only a limited data set, the results have provided an indication of individual landmark location accuracies and has led to the development of suitable landmark definitions applicable to both CT[9] and craniometry. This stereo technique has been applied to the craniofacial complex but clearly can be applied to other regions of the body provided appropriate landmarks can be defined.

The number of well determined landmark positions obtainable using this off-line computing stereo method encourages the next step, that is, the three dimensional analysis of individual patients and the concurrent accumulation of population data as a basis for statistical studies of craniofacial conditions.

While the off-line technique of multiple stereo images has allowed landmarks to be well identified with a median accuracy of approximately the width of two voxels and is suitable when additional CT computing facilities are not available, it is forecast the technique will be superseded in the near future by the availability of cheaper, higher powered computer workstations with suitable display facilties.

Conclusion

The reported method developed for three dimensional data acquisiton has enabled positions and relocation errors of a large number of osseous landmarks to be determined for dried test skulls and patients with craniofacial conditions. The known accuracy and reliability of these three dimensional co-ordinate positions facilitates the description of the craniofacial complex and provides the key to proceed with the analysis and quantification of craniofacial morphology in three dimensions.

Acknowledgements

We are grateful for the co-operation and assistance of the Department of Radiology, Adelaide Children's Hospital campus, in particular Graham Truman, Marion Tregeagle and Amanda Russell. We also thank Mr Graham Pretty, Senior Curator in Archaelogy and Anthropology, The South Australian Museum, for allowing access to the skeletal material used in this investigation.

Financial assistance was provided by the Australian Cranio-Maxillo-Facial Foundation; Dr Abbott was supported by a postgraduate scholarship awarded by the National Health and Medical Research Council of Australia.

References

1. Cutting C, Grayson B, Bookstein F L, Fellingham L, McCarthy J G. Computer-aided planning and evaluation of facial and orthognathic surgery. Clin Plast Surg 1986; 13:449–62.

2. Cutting C, Bookstein F L, Grayson B, Fellingham L, McCarthy J G. Three dimensional computed-aided design of craniofacial surgical procedures. In: D Marchac ed. Craniofacial Surgery. Berlin Heidelberg: Springer-Verlag, 1987:1 7–8.

3. Marsh J L, Gado M H, Vannier M W, Stevens W G. Osseous anatomy of unilateral coronal synostosis. Cleft Palate J 1986; 23:87–100.

4. Marsh J L, Vannier M W. The anatomy of the cranio-orbital deformities of craniosynostosis: insights from 3-D images of CT scans. Clin Plast Surg 1987; 14:49–60.

5. Udupa J K. Display82—A system of programs for the display of Three dimensional information in CT data. Technical report MIPG67, Department of Radiology, University of Pennsylvania, 1983.

6. Chen L S, Herman G T, Meyer C R, Reynolds R Y. Udupa J K. 3D83—An easy to use software package for three dimensional display from computed tomograms. Proceedings Society Photo-optical Instrumentational Engineers 1984; 515:309–16.

7. Papoulis A. Probability, random variables and stochastic processes. 2nd ed. New York: McGraw-Hill International Book Company, 1984: 187–8.

8. Abbott A H. The acquisition and analysis of craniofacial data in three dimensions. [Ph.D. Research Thesis]. Adelaide, Australia: University of Adelaide, 1988.

9. Abbott A H, Netherway D J, David D J, Brown T. Application and comparison of techniques for the 3D analysis of craniofacial anomalies. J Craniofac Surg (In press).

10. Siegel A F. Robust regression using repeated medians. Biometrica 1982; 69:242–4.

11. Dahlberg G. Statistical methods for medical and biological students. London: George Allen and Unwin Ltd., 1940:122–32.

12. Brown T, Abbott A H. Computer-assisted location of reference points in three dimensions for radiographic cephalometry. Am J Orthod Dentofacial Orthop 1989; 95:490–8.

Craniofacial Imaging, Models and Prostheses

John Abbott, David Netherway, Paul Wingate, Amanda Abbott and David David
The Australian Cranio-Facial Unit
Adelaide, South Australia

Patients with vast bony defects that cannot be accommodated by bone transplantation or traditionally manufactured prosthetic devices can be treated using custom designed prostheses based on solid, life-size models of the patient's bone in the region of the defect. This paper presents four cases where prosthetic devices have been designed using models, and discusses the CT data collection, imaging techniques and the construction of the life-size cranio-facial models. The model production techniques range from hand cutting to laser sintering. It is onto these models that titanium implant substructures can be fabricated for the prosthetic restoration of the patient.

Titanium implant substructures are indicated for patients suffering from severe trauma or other conditions where there is minimal bone present. Such substructures can form the basis for prosthetic restoration using artificial teeth, eyes and ears (Branemark et al 1984, Patrick et al 1989, Lesner and Huryu 1993). In the field of neurosurgery, titanium has also been used to cover cranial defects (Blair, Gordon and Simpson 1980).

Some patients presenting to the Australian CranioFacial Unit (ACFU) have vast bony defects affecting the mandible, maxilla and other craniofacial areas. Such patients may have suffered extensive tooth loss and require some form of prosthesis. For example, the 17 year old man shown in Figure 1 was struck in the mid-face by a large object entering through a motor vehicle windscreen three years prior to referral. The maxilla and all the maxillary teeth (except 26, 27 and 28) were removed as a single fragment (Figure 2). Reconstruction of such major composite tissue loss demands the provision of adequate external and intraoral soft tissue coverage in concert with restoration of mid-facial skeletal projection. Planned, complete, multidisciplinary clinical and radiological assessment is required in order to reconstruct such a patient. Prosthetic management may require the construction of models onto which custom made titanium implant substructures can be designed. Such implant retained prostheses significantly differ in design from the conventional titanium "screw" type implant, such as used to support a mandibular dental bridge (Figure 3).

Current practice is for large titanium implant substructures, such as those used for cranioplasties, to be produced using models made from alginate or silicone

J.R. Abbott B. Sc. Dent. (Hons), MDS, Ph.D., F.A.D.M.
Deputy Director, Craniofacial Research Unit
D.J. Netherway B.Sc. (Hons), Ph.D.
Principal Research Scientist, Craniofacial Research Unit
P. Wingate
Dental Technologist, Wingate's Laboratories
A.H. Abbott B.D.S., B. Sc. Dent. (Hons), Ph.D.
Senior Research Scientist, Craniofacial Research Unit
D.J. David AC, M.B.B.S., F.R.C.S.(Eng), F.R.C.S.(Edin), F.R.A.C.S. Head, The Australian Cranio-Facial Unit

Address:
The Australian Cranio-Facial Unit
Women's and Children's Hospital
72 King William Road
North Adelaide, South Australia, 5006

impressions of the defected region. Simple convex shapes of thin sheet titanium can be readily fashioned to fit the model using hydrostatic pressing techniques and/or traditional hand forming techniques. However, more complex contours involving orbital walls, zygomatic arch, maxilla and mandible require highly accurate models onto which a titanium substructure can be designed and constructed. Modern computer technology has made it possible to visualize anatomical structures in three dimensions and to produce the necessary life-size models of regions of interest.

In this paper, four cases are presented where models have been used to allow custom-designed prostheses or substructures for prostheses to be manufactured. The cases cover a cranioplasty plate for a motor vehicle accident victim, a war victim with insufficient bone for standard dental implants, a woman with a bone wasting disease and a patients with a cleft palate. The models were produced by hand cutting 0.75 mm acrylic sheets, numerically controlled milling devices and laser sintering.

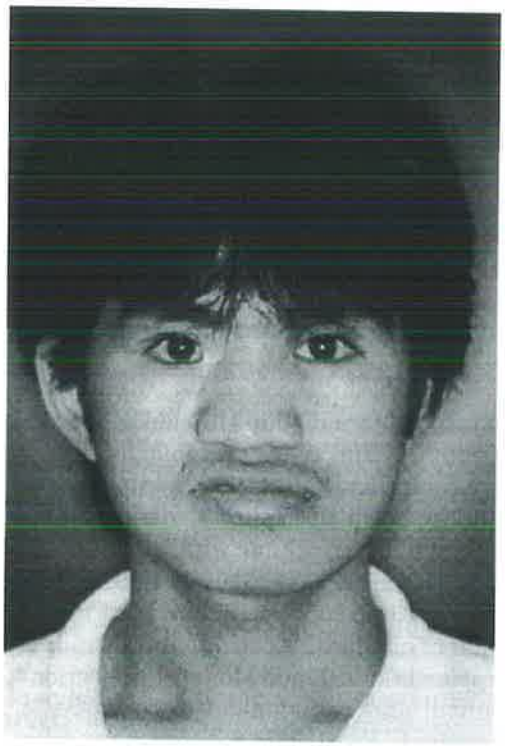

FIG. 1. *Motor vehicle accident victim with avulsed maxilla.*

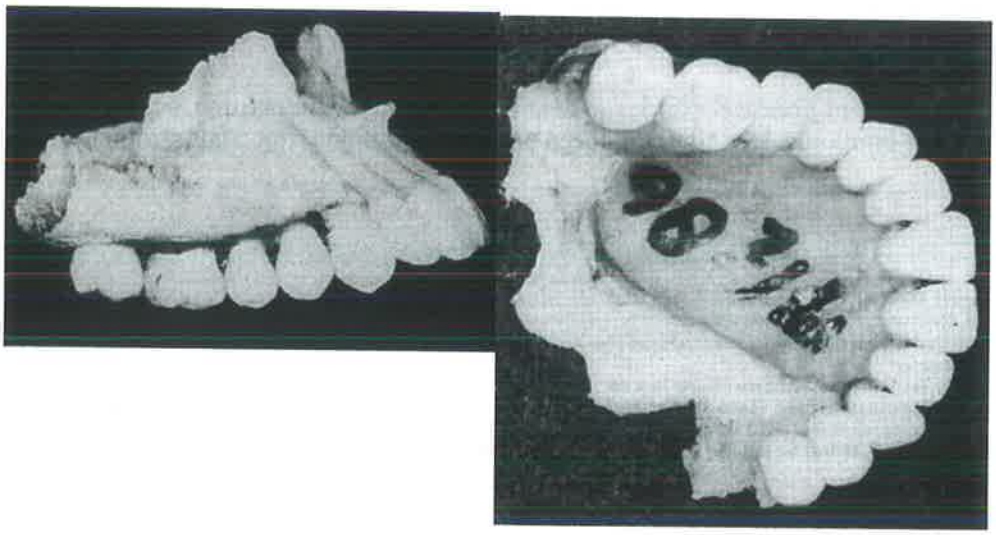

FIG. 2. *Avulsed maxilla of patient in Figure 1.*

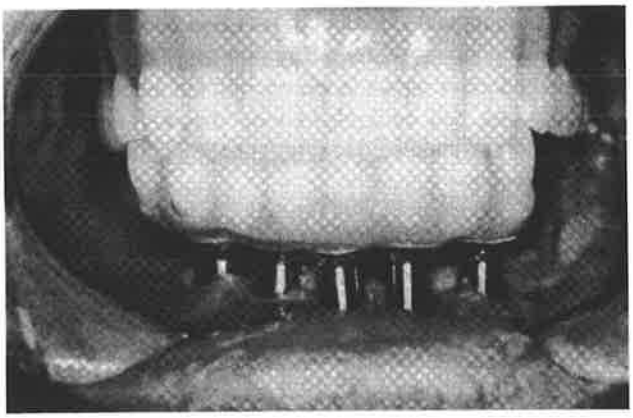

FIG. 3. *Standard titanium implants supporting a mandibular bridge.*

Method

Data Collection

The only method for collecting accurate enough information on the patient's craniofacial skeleton available to us is CT scanning. Typically, the highest resolution settings are used for the volume to be modelled, particularly if implants are to be custom-designed to fit exactly against the bone. See Table I for the parameters of the Scanners used to date.

TABLE 1

CT scanning parameters utilized to date for model production for prosthesis design.

CT Scanner	thickness/separation
GE8800, GE9800	1.5/1.5
Seimens Somatom	2/1
Toshiba TCT-900S	2/2, 2/1.5
GE High-Speed Advantage	1/1

Each slice is typically 512 by 512 pixels of 2 byte data. For a scan range of 100 mms and 1 mm steps the total data size is 50 Mb although some CT scanners compress the data, typically by a factor of two, for storage. For the accurate imaging and modelling of large defects, the data collected for processing is quite large and requires workstations with high speed and large capacities.

At the ACFU, Silicon Graphics workstations are networked to the GE High-Speed Advantage scanner so that the CT slice data can be transferred directly to the workstations for analysis. Data from other scanners is imported from ½" magnetic tape, QIK 150 tapes, Digital Audio Tapes, optical disks or even carried in via Laptop computer.

Imaging

The *Persona* software package (Maptek, 210 Glen Osmond Road Fullarton SA 5063) was used in order to render the CT data to provide 3D CT reconstructions for visualisation, measurement and selection of the region to be modelled. In planning the extent of the region to be modelled, the stereo 3D viewing capability enhances the visual perception of the information presented.

The 3D CT reconstructions are generated using a ray casting technique in order to detect the surface for each view of the data. A ray is sent through each pixel on the screen into the data volume and the pixel coloured according to various parameters, such as the surface gradient where the ray intersects a soft-tissue/bone threshold.

Typically, 60 images at 6 degree intervals are generated for axial and transporionic rotations of the data. Animation is achieved by viewing these images in rapid succession. Animated and stationary stereovision is achieved by displaying an adjacent pair of images as left and right eye views. The liquid crystal shutters of the glasses are synchronized to the frame rate of the monitor so that each eye sees only the image for that eye.

By displaying axial, sagittal, and coronal reformats simultaneously with the 3D CT reconstructions, and incorporating an "active marker" in each view of the data, points within the data volume can be accurately located for measurement of distances and angles between anatomic landmarks. Wireframe models of anatomic structures are displayed as the skeletal craniofacial landmarks listed in the *Persona* package (over 350) are identified.

Stacked Slice Models

Using *Persona,* contours for each slice can be produced through the region with a spacing equal to that of the thickness of acrylic sheet. These contours can be used to provide data for laser cutting or printed onto transparencies for use as templates for hand cutting. Fiducial markers are necessary to register the slices. Although hand cutting may seem antiquated when there are computer aided machining methods now possible, it is a relatively cheap and available method, and the plastic can be cut in a just few hours depending on the size of the job and the skill of the technician. Whether this method can be employed depends on how intricate and accurate the model needs to be. With the availability of models using the selective laser sintering process, the ACFU are no longer employing hand cutting techniques.

Iso-surface Construction

Computer aided milling/modelling machines are usually able to import triangulated surface meshes. These can be generated using a "Marching Cubes" algorithm (Lorensen and Cline 1987) or triangulated tetrahedral elements (Payne and Toga 1990). While the latter is relatively simple to code, it has the disadvantage that it produces perhaps twice as many triangles as the former type with similar fidelity. Both types have been utilised at the ACFU but the algorithm currently employed is based principally on the paper by Ake Wallin (1991) which is a variant of the Marching Cubes algorithm. The algorithm has the property of topological correctness (Ning and Bloomenthal 1993) at the resolution of the data and produces a high quality surface model with the least number of triangles. With high resolution CT scan data, the number of triangles generated even for just a section of the maxilla can be several hundred thousand which seriously impacts on display and manipulation time.

Decimation of Triangular Meshes

In order to reduce display, manipulation and modelling times, the triangular meshes are decimated - vertices are removed if their removal minimally affects the surface accuracy (Schroeder, Zarge and Lorensen 1992). For model production, the decimation algorithm has been used cautiously with minimal criteria for vertex removal, pending a study of the decrease in surface fidelity. Typically, the parameters are set to reduce the number of triangles by a factor of four in order to reduce the number of triangles to a level where the modelling time on the Sinterstation is tractable.

Selective Laser Sintering Models

The Sinterstation 2000 produces models by using the heat generated by a CO_2 laser in order to fuse powdered material layer upon layer. The fused powder has the same density as the surrounding powder so that it is not necessary to provide a support structure for parts that are not initially connected in the build process. This is unlike the stereolithography process where support structures are mandatory. The accuracy of the Sinterstation is of the order of 0.1-0.2 mms. The pixel size of the CT data is typically 0.3-0.5 mms within a slice and 1 mm thick,

so that the accuracy of the Sinterstation is slightly better than that of the intra-slice pixel resolution. The triangulation method employed interpolates between pixels and slices, improving the quality of the model.

Case Reports

Case 1

This 18 year old man was a passenger in a car involved in a motor vehicle accident. He was thrown from the car. Clinically, his pupils were reacting to light and he was noted to have CSF otorrhoea and bilateral CSF otorrhoea. There was a swelling of the right pterion and a complex fracture of the anterior cranial fossa and lateral orbital wall. A decompressive craniectomy and reduction of the pterional fracture was performed. At four weeks post injury, he was alert and oriented with a slight left hemi paresis and left-sided sensory inattention. A titanium cranioplasty plate was considered appropriate, given the large cranial defect shown in the 3D CT reconstructions of Figure 4.

The *Persona* module *Interrogate* allowed the region to be modelled and defined, and provided the axial contours for each slice required by the software interface to the computer controlled milling machine. The milled model shown in Figure 5 and Figure 6 shows the sheet titanium shaped to seat closely onto a plaster cast of the model. The plate was slotted in order to allow fine adjustments to be made at the margins during the operation. Screw holes were placed around the plate and several vent holes drilled into the main body of the plate. Figure 7 shows the clinical insertion of the plate.

Cranial defect repair may be accomplished using bone, acrylic or metal. Bone grafting is often less robust, may resorb and can be lumpy to feel. Acrylic

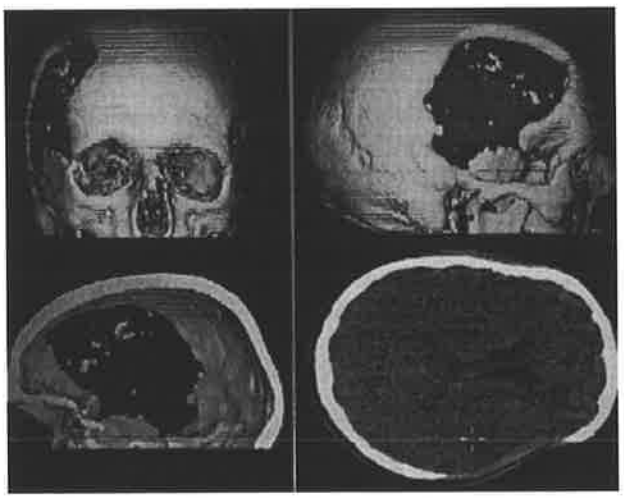

FIG. 4. *3D CT images the cranial defect,*

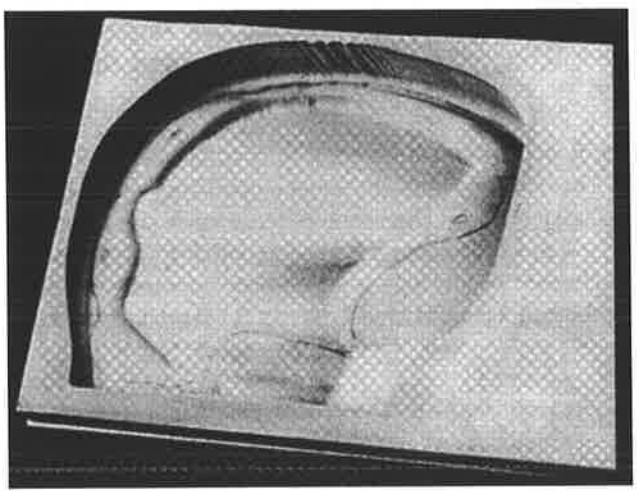

FIG. 5. *Milled model of cranial bone defect.*

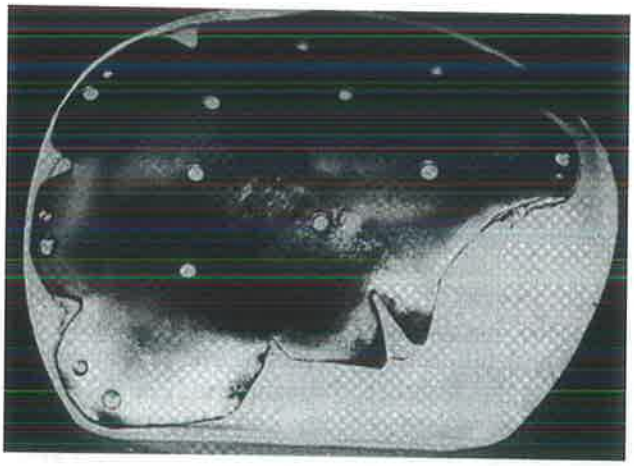

FIG. 6. *Titanium sheet which has been shaped to closely fit onto the model.*

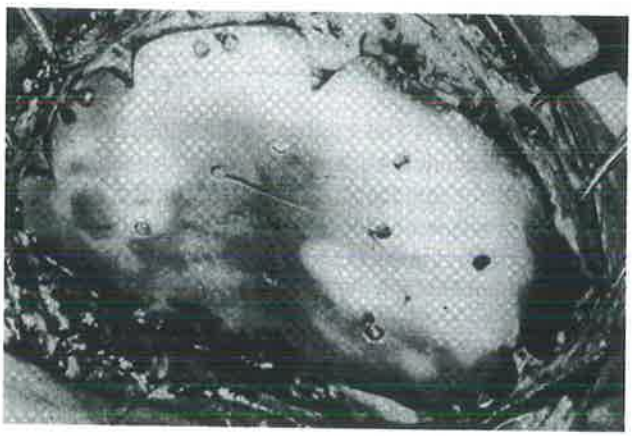

FIG. 7. *Clinical insertion of the titanium cranioplasty plate.*

may be an irritant and can break. Titanium, on the other hand, is strong, radio-opaque and inert. In the case described here, a titanium plate was also constructed using a conventional impression of the side of the patient's head for direct comparison in situ. This plate had the disadvantage that it was not well adapted to the underlying bone. Using a high quality model of the bone, based on the patient's CT scan, enables direct apposition of the plate against bone thus leading to a better fit and reduced operating time.

Case 2

A 38 year old male patient was the victim of a missile explosion. Amongst his many facial injuries was the complete loss of the left side of his maxilla. Deep scar tissue was present over the palate. His chief complaint was his lack of maxillary teeth. Figure 8 shows the defect remaining after many restorative operations. A solid model of the maxilla was constructed from stacked acrylic sheets based on contours from the CT scan data. A previous operation had placed a piece of rib bone into the defect region and it was onto this bone that a titanium substructure was designed in order to support a maxillary denture. Figures 9, 10 and 11 show the titanium substructure, the clinical insertion, and the post operative 3D CT reconstructions.

The strong radio absorption of most metals makes it difficult to obtain good CT images. For example, CT scans that include teeth containing amalgams generally have radiating high density streaks that severely degrade the images. While titanium is radio-opaque, it is not as dense as materials such as amalgams or stainless steel. By setting the threshold slightly higher than normal for bone, reasonable 3D CT reconstructions can be obtained (Figure 11), although thin bone may not be visible.

Unfortunately, extensive tight scar tissue on the palate resulted in exposure of the implant with subsequent migration of bacteria. Failure also occurred because the patient used the vertical retention rods to help his masticatory ability

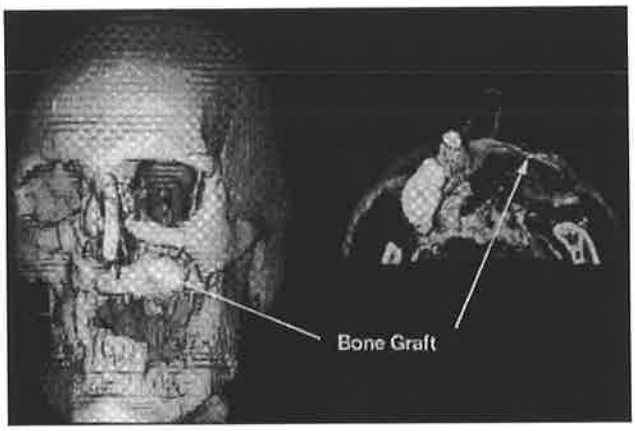

FIG. 8. *3D CT images of missile victim. The titanium substructure was designed to fit onto the rib graft.*

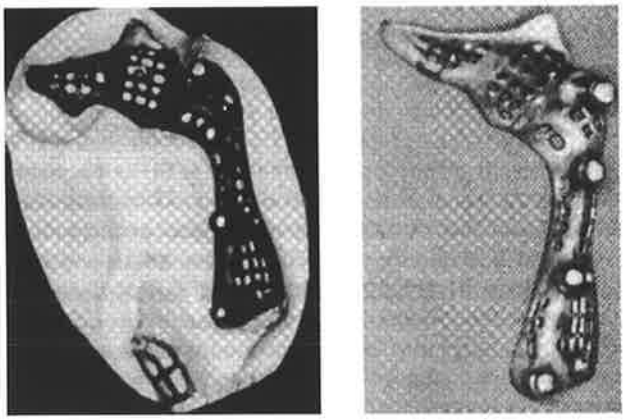

FIG. 9. *The cast titanium substructure incorporating vertical retention rods that will support an acrylic denture.*

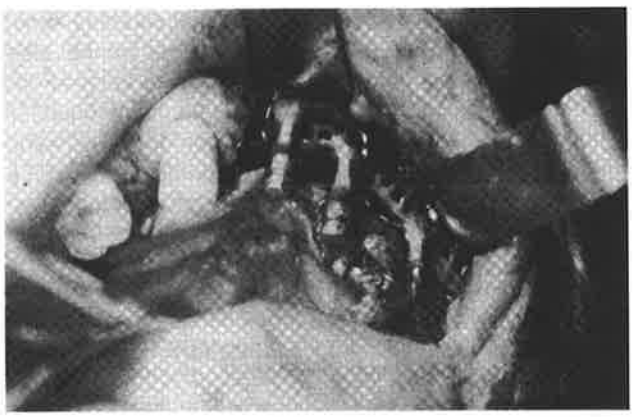

FIG. 10. *Clinical insertion of the titanium substructure.*

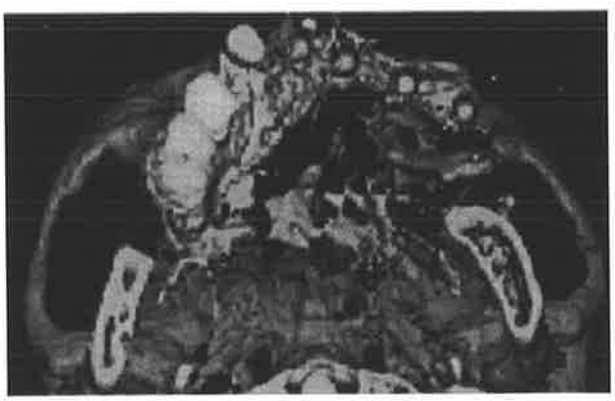

FIG. 11. *Post-operative 3D CT reconstructions showing the titanium substructure.*

prior to osseointegration. The surgery is being replanned and it is envisaged that there will be no retention rods on display. Instead, small hexagonal locking abutments will be incorporated into the titanium substructure (see case 4 below). This will allow for tissue to cover the implant and only after nine months will the substructure be exposed and prosthetic elements be secured into the hexagonal locking abutments.

Case 3

This is an example of a 20 year old female with Gorham disease or disappearing bone syndrome (Figure 12). The 3D CT reconstructions of her skull (Figure 13) showed a generalized osteolysis. The left side was more affected, with substantial loss of the spheroid, fronto-parietal and temporal bones. The left orbit was grossly bone deficient resulting in a proptosed eye. As a part of her treatment, it was decided that titanium prostheses could be manufactured in order to restore the left temporal region, left lateral and inferior orbital margin and left zygomatic arch.

From contours generated, based on the CT scan data, acrylic sheets were hand cut and stacked together to form a life-size 3D model (Figure 14). This model was duplicated in dental stone, and a titanium sheet for the temporal area was fashioned. This was welded to a titanium casting which was constructed to form a new orbital rim and zygomatic arch (Figure 15). Figure 16 shows the clinical insertion of the prosthesis while Figure 17 depicts the post-operative radiograph.

FIG. 12. *Twenty year old female with Gorham disease.*

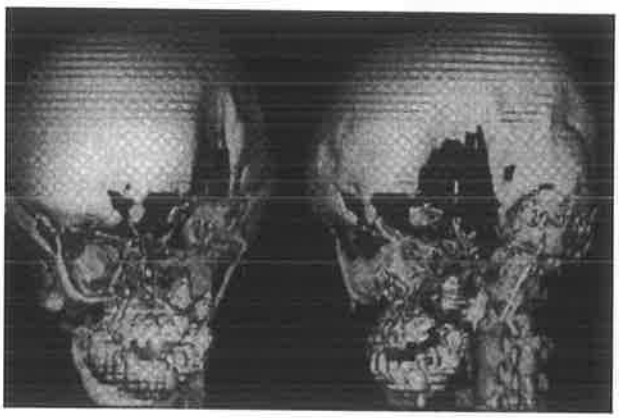

FIG. 13. *3D CT images displaying the extent of the osteolysis.*

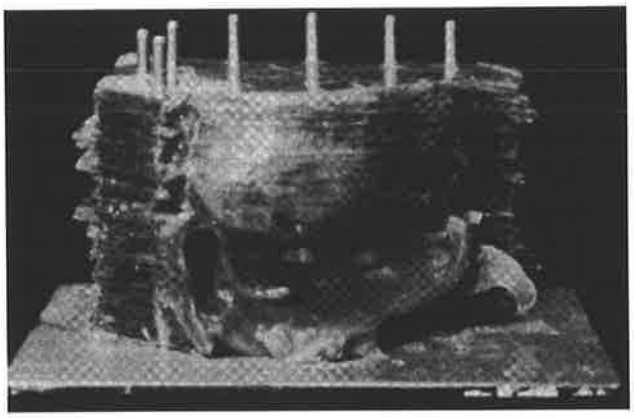

FIG. 14. *Laboratory working model showing the stacked acrylic slices.*

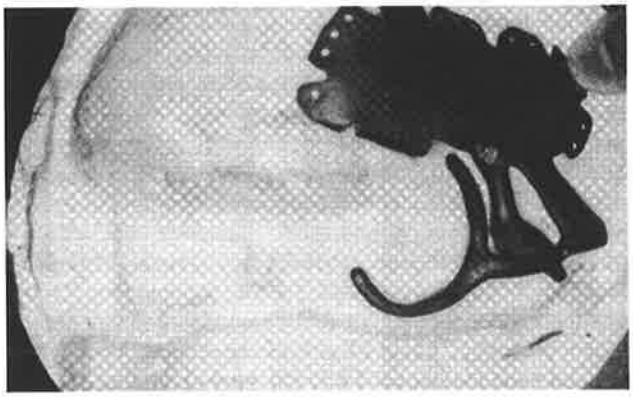

FIG. 15. *The titanium prosthesis seated on the dental stone model.*

Case 4

A young lady of 22 years of age, with left side cleft lip and palate, had an Angle Class III malocclusion and was treated orthodontically. Aesthetically, she wanted to have a tooth placed in the cleft site. Bone grafting to the maxilla was performed. However, subsequent resorption made it impossible to place a conventional 3.75 mm diameter implant.

The patient was CT scanned using abutting 1 mm slices and a nylon model constructed by laser sintering. A titanium substructure (Figure 18) incorporating an hexagonal locking abutment was cast onto a refractory model. This substructure was inserted over the cleft site (Figure 19) and screwed into place using a labial approach with specially made titanium screws. During the operation it was found that there had been further resorption of the bone graft since the CT scan taken eight months earlier. This meant that the lower part on one side of the titanium structure sat clear of the bone surface and some packing with hydroxylapatite was required.

After a healing period of nine months, the titanium screws should have osseointegrated. In second stage surgery, the hexagonal locking abutment will be exposed and a healing collar attached. Following three weeks of soft tissue healing, a titanium supra-mucosal element will be screwed into the hexagonal locking device. A porcelain crown can then be constructed in order to fit into the implant body.

FIG. 16. *Clinical insertion of the prostheses via a bicoronal scalp approach.*

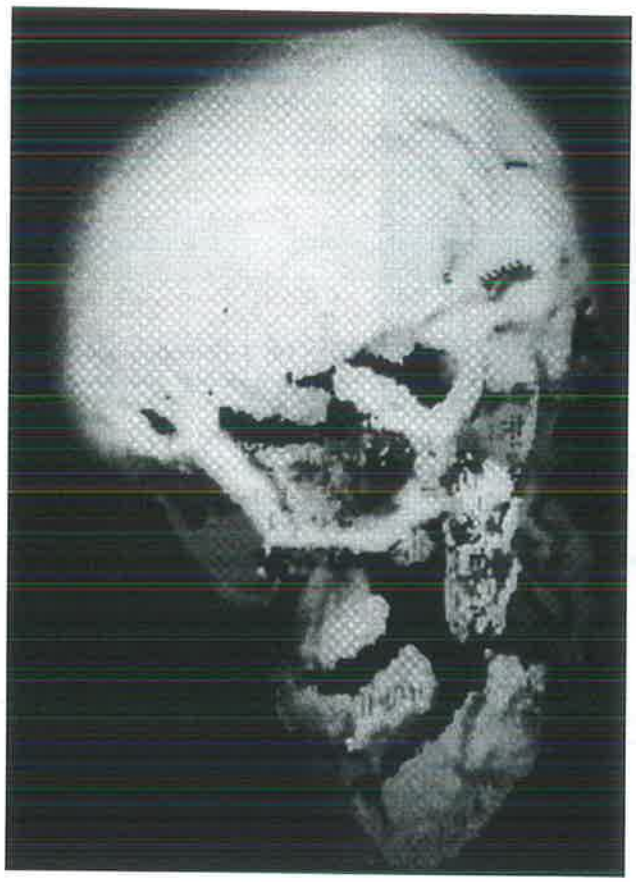

FIG. 17. *Post-operative 3D CT reconstruction showing the titanium implant*

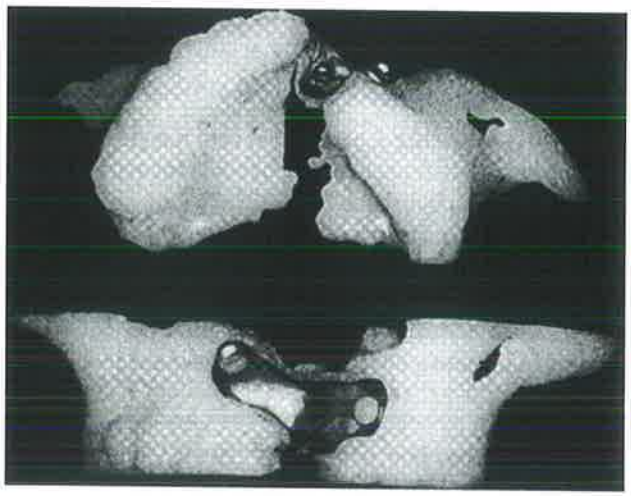

FIG. 18. *The nylon model and the titanium casting incorporating the hexagonal locking abutment.*

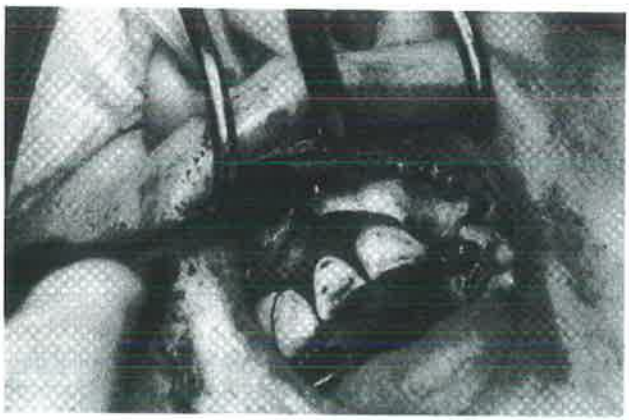

FIG. 19. *Clinical insertion.*

Discussion

In the past, various materials (ie. bone, acrylic, metal) have been used to repair defects in bone. It is generally the individual preference of the surgeon as to the choice, with bone being clearly preferred. However, each material has advantages and disadvantages. For example, prostheses constructed from polymethylmethacrylate are irritant because of the leaching of monomer and the fact that the low impact strength of acrylic makes it prone to shatter.

Titanium has properties which make it an excellent implant material. Besides its osseointegration capability, titanium is light-weight, non-corrosive, biocompatible, autoclavable, cost effective, and introduces minimal artefacts into post-operative CT scan images.

The production of life-size 3D models from CT data images has opened the way for a different approach to the management of large and complicated skull defects. Current indications suggest that such models not only allow for improved preoperative planning of cases but also superior fitting prostheses.

Acknowledgements

The authors thank the Australian Cranio-Maxillo Facial Foundation for financial support. This includes many contributing individuals and organizations, and in particular The Adelaide Bank Foundation which specifically funded resources for this project.

References

1 Blair G.A.S., Gordon D.S., Simpson D.A. (1980) Cranioplasty in children. Child's Brain 6(2), 82–91.

2 Branemark P., Adell R., Albrektsson T., Lekholm U., Lindstrom J., Rockier B. (1984) An experimental and clinical study of osseointegrated implants penetrating the nasal cavity and maxillary sinus. J. Oral Maxillofac. Surg. 42, 497–505.

3 Lesner T.H., Huryu J.M. (1993) Orbital prosthesis with a magnetically retained ocular component supported by osseointegrated implants. J. Prosthet. Dent. 69, 378–380.

4 Lorensen W.E., Clink H.E. (1987) Marching Cubes: A high resolution 3D surface construction algorithm. Computer Graphics 21(4), 163–169.

5 Ning P., Bloomenthal J. (1993) An evaluation of implicit surface tilers. IEEE Computer Graphics and Applications 13(6), 33–41

6 Payne B.A., Toga A.W. 91990) Surface mapping brain function on 3D models. IEEE Computer Graphics and Applications 10(5), 33–41.

7 Patrick D., Zosky J., Lubar R., Buchs A. (1989) The longitudinal clinical efficacy of Core-Vent dental implants: a five year study. J. Oral Implantology 15(2), 1–7.

8 Schroeder W.J., Zarge J.A., Lorensen W.E. (1992) Decimation of triangle meshes. Computer Graphics 26(2), 65–69.

9 Wallin A. (1991) Constructing isosurfaces from CT data. IEEE Computer Graphics and Applications 11(6), 28–33.

Experiment alone crowns the efforts of medicine, experiment limited only by the natural range of the powers of the human mind. Observation discloses in the animal organism numerous phenomena existing side by side, and interconnected now profoundly, now indirectly, or accidentally. Confronted with a multitude of different assumptions the mind must guess the real nature of this connection.

IVAN PAVLOV (1849–1936)

Jackson-Weiss Syndrome: Clinical and Radiological Findings in a Large Kindred and Exclusion of the Gene From 7p21 and 5qter

L.C. Adès, J.C. Mulley, I.P. Senga, L.L. Morris, D.J. David, and EN Haan
Department of Medical Genetics and Epidemiology, Centre for Medical Genetics (L.C.A., E.A.H.), Departments of Cytogenetics and Molecular Genetics (J.C.M., I.P.S.) and Organ Imaging (L.L.M.), and Australian Craniofacial Unit (D. J.D.), Women's and Children's Hospital, North Adelaide S.A., Australia

We describe the clinical and radiological manifestations of the Jackson-Weiss syndrome (JWS) in a large South Australian kindred. Radiological abnormalities not previously described in the hands include coned epiphyses, distal and middle phalangeal hypoplasia, and carpal bone malsegmentation. New radiological findings in the feet include coned epiphyses, hallux valgus, phalangeal, tarso-navicular and calcaneo-navicular fusions, and uniform absence of metatarsal fusions.

Absence of linkage to eight markers along the short arm of chromosome 7 excluded allelism between JWS and Saethre-Chotzen syndrome at 7p21. No linkage was detected to *D5S211*, excluding allelism to another recently described cephalosyndactyly syndrome mapping to 5qter. © 1994 Wiley-Liss, Inc.

Keywords: craniosynostosis, acrocephalosyndactyly, Jackson-Weiss syndrome, calcaneocuboid fusion, autosomal dominant, linkage analysis, gene mapping

Introduction

Jackson-Weiss syndrome (JWS; MIM No. 123150) [McKusick, 1992] is one of the dominantly inherited acrocephalosyndactylies (ACS). These are characterised by premature craniosynostosis in association with hand and/or foot abnormalities. Defined entities within the group are Apert syndrome (ACS I) [Blank, 1960], Saethre-Chotzen syndrome (ACS III) [Pantke et al., 1975; Kreiborg et al., 1972; Bianchi et al., 1985], Pfeiffer syndrome (ACS V) [Pfeiffer, 1969, 1964], Robinow-Sorauf type ACS [Robinow and Sorauf, 1975], and JWS [Jackson et al., 1976]. Several authors have discussed their classification and distinguishing manifestations [Bianchi, 1985; Saethre, 1931; Chotzen, 1932; Vogt, 1933; Waardenburg, 1934; Noack, 1959]. Apert syndrome has a distinct and consistent phenotype but there is overlap between the other acrocephalosyndactylies, with considerable phenotypic variability between and within families. This can complicate the diagnosis of sporadic cases. Some ACS types originally classified as discrete entities have been recognised subsequently to represent extremes of phenotypic expression of existing ACS types [Escobar and Bixler, 1977a].

Four separate reports have described three families with JWS. The initial report by Cross and Opitz [1969] suggested autosomal recessive inheritance, but

Received for publication August 13, 1993; revision received January 4, 1994.
Address reprint requests to Dr. L.C. Adès, Department of Medical Genetics and Epidemiology, Centre for Medical Genetics,
Women's and Children's Hospital, 72 King William Road, North Adelaide S.A. 5006, Australia.

further study of the family by Jackson et al. [1976] demonstrated autosomal dominant transmission with variable expression and incomplete penetrance. The findings in this large Amish kindred included craniosynostosis, midface hypoplasia, and abnormalities of the feet. The only consistent manifestation was some abnormality in the clinical or radiographic appearance of the feet. Minimal manifestations included short, broad first metatarsal, abnormally shaped tarsal bone, and calcaneocuboid fusion [Gorlin et al., 1990]. Some affected individuals had no clinical or radiographic abnormalities of the face or skull. No mentally retarded individuals were detected in this family. Robinow and Sorauf [1975] added valgus of the distal phalanx and partial duplication of the distal phalanges of the great toe to the known spectrum of radiographic foot abnormalities in JWS. Escobar and Bixler [1977a, b] described another kindred with traits similar to those of the JWS, though the absence of any radiographic abnormalities of the feet suggests that the condition they described may be caused by a different gene or could be allelic with JWS. Detailed clinical descriptions defining the phenotypic variability of JWS are scarce and few photographs have been published.

None of the genes for the ACS had been mapped prior to 1992 when Brueton et al. [1992] reported a linkage study involving 16 British families with autosomal dominant non-Apert ACS, almost with ACS III. They concluded that ACS III maps to chromosome 7 at 7p21. Greig cephalopolysyndactyly has been mapped to 7p13 by analysis of translocations [Tommerup and Nielsen, 1983; Pelz et al., 1986], deletions [Wagner et al., 1990], and linkage analysis [Brueton et al., 1988]. The zinc finger protein gene, GL13, has also been mapped to 7p13 [Ruppert et al., 1990] and mutation of the gene results in the Greig cephalopolysyndactyly syndrome [Vortkamp et al., 1991]. Recently, Warman et al. [1993] described a new craniosynostosis syndrome which maps to 5q34-ter [Müller et al., 1993]. Affected individuals had fronto-orbital recession, frontal bossing, turribrachycephaly, or clover-leaf skull deformity. All had normal intelligence, most had myopia but none had exophthalmos, hypertelorism, midfacial hypoplasia, malocclusion, broad thumbs or broad great toes, ear anomalies, or soft tissue syndactyly.

We have documented the clinical and radiological manifestations of a large kindred with JWS and have been able to exclude allelism with the genes for ACS III and the aforementioned new craniosynostosis syndrome at 5q34-qter.

Materials and Methods

Pedigree

The pedigree is shown in Figure 1 and demonstrates autosomal dominant inheritance, we identified 16 affected individuals in 3 generations. The family shows variability of clinical and radiological changes within and between generations.

DNA Analysis

DNA was extracted from duplicate 10 ml samples of EDTA anticoagulated blood. Marker studies were carried out using highly polymorphic PCR based dinucleotide repeat polymorphisms [Weber and May, 1989]. A Perkin Elmer-Cetus DNA thermal cycler was used to PCR-amplify DNA for the markers *D7S472, D7S513, D7S507, D7S493, D7S529, D7S516, D7S526, D7S528,* and *D5S211* (see Table III) using reaction conditions based on Kogan et al. [1987].

Primers for microsatellite and PCR polymorphisms were synthesized on an Applied Biosystems Model 391 PCR-MATE EP DNA synthesizer. Purification was by the n-butanol method of Sawadogo and Van Dyke [1991]. PCR incubations for all markers were performed in 10 µl volumes in a Perkin Elmer-Cetus thermal

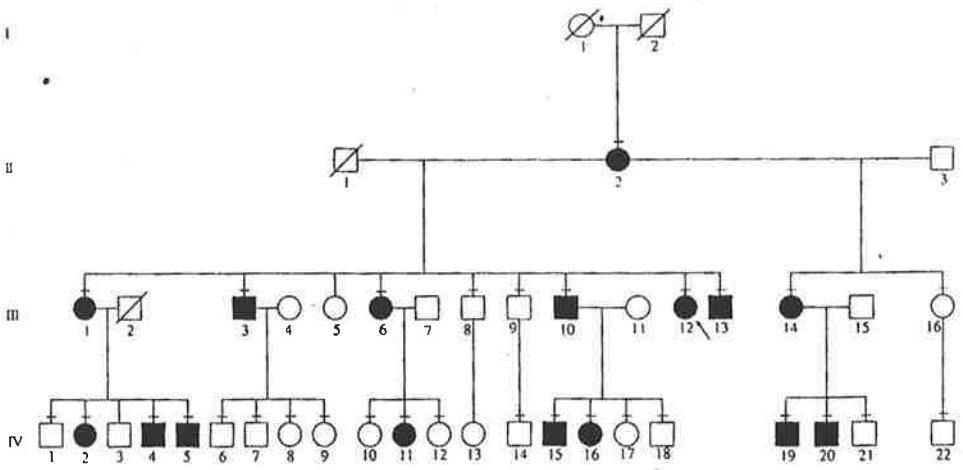

FIG. 1. *Pedigree of the kindred.*

cycler for 10 cycles at 94°C for 60 s, and at 72°C for 90 s, followed by 25 cycles at 94°C for 60 s, at 55°C for 90 s, and at 72°C for 90 s. The volume was adjusted to 40 µl with formamide loading buffer (95% formamide, 1 mM EDTA, 0.01% bromophenol blue, 0.01% xylene cyanol). After denaturation at 90°C for 3 min. 3 µl aliquots of each reaction mixture were subjected to electrophoresis in 5% polyacrylamide non-denaturing (7 M urea) gels. Genotypes were determined after autoradiography for 18-72 h.

Linkage Analysis

Linkage analysis was carried out using the MLINK program package [Lathrop and Lalouel, 1984] assuming 100% penetrance at the disease locus for individuals given full clinical and radiological examinations and 90% penetrance at the disease locus for three individuals who had clinical examinations alone (IV-6, IV-7, and IV-8). A gene frequency of } in 40,000 was assumed for the disease allele. A lod score of at least 3 demonstrates genetic linkage, and a lod score of -2 represents an exclusion [Morton, 1955].

Complete information was not available on 6 individuals within this kindred; III-5 was unavailable for examination but radiographs of the hands and feet were normal, IV-3 was unavailable for examination or radiographs, radiographs could not be obtained on IV-6, IV7, or IV-8 (all of whom were clinically normal), and although IV-18 was assessed clinically and radiologically, affectation status remains uncertain because of his young age. The two individuals IV-3 and IV-18 were assigned an unknown affectation status for the purpose of linkage analysis.

Results

Clinical Findings

Manifestations of affected individuals are presented in Table I with photographs of selected individuals in Figure 2. Most affected individuals in the kindred exhibited facial asymmetry, a broad forehead, and turricephaly. Craniosynostosis was not present in all, but when present involved the coronal sutures exclusively. Other craniofacial abnormalities observed included low anterior hairline, hypertelorism, ptosis, strabismus, nasal beaking, maxillary hypoplasia, and mandibular prognathism. Hearing loss was common with audiograms demonstrating conductive, sensorineural, or mixed deficits. No relatives had prominent ear crura, cutaneous syndactyly, or broad great toes. Two individuals,

III-1 and III-12, had a high arched palate. Two relatives, IV-16 and IV-19, were originally considered unaffected because of absence of craniofacial changes suggestive of the condition, but subsequently were classified as affected on the basis of abnormal radiographic findings.

Of the 16 affected individuals, all had facial asymmetry, 12 had craniosynostosis, 12 had deafness, 9 had hypertelorism, 8 had mental retardation which varied in severity from borderline to moderate, 7 had mandibular prognathism, 5 had brachydactyly of the hands and/or feet, 5 had a height at or below the third centile, 3 had a head circumference at or below the second centile, and 2 had had transcranial bilateral fronto-orbital reconstruction and advancement within the first three months of life.

Radiological Abnormalities

The radiological findings in the hands and feet of affected individuals are presented in Table II. There was carpal and/or phalangeal fusion in the hands of most but not all affected individuals, the pattern of fusion being variable. The most frequent defect was middle phalangeal hypoplasia of index, ring, and little fingers present in 8 of 16. Coned epiphyses and carpal bone segmentation abnormalities (congenital fusion of capitate and hamate bones, bipartite lunate) were less common. One individual had a separate ossific centre of the ulnar styloid.

The most common radiologic anomalies in the feet were congenital fusion of the cuboid and calcaneum present in 12 of 16, phalangeal fusion and hallux valgus. Less frequently seen were coned epiphyses and variable patterns of other tarsal and/or metatarsophalangeal fusions. None of the affected individuals had broad or bifid great toes, and none had fusion between metatarsals.

Intrafamilial variability of the radiologic findings was evident. II-2 had completely normal radiographs of the hands but multiple abnormalities of her feet. In contrast, IV-11 had many radiological abnormalities of the hands whilst the only positive finding in the feet was coned epiphyses. IV-19 and IV-20 had prominent abnormalities in both hands and feet. Calcaneo-cuboid fusion was not present in all individuals. Of the 8 obligate carriers, 4 demonstrated abnormalities in the feet alone and 4 had abnormalities in both hands and feet. There were no obligate carriers without radiological abnormalities in the feet, irrespective of whether calcaneo-cuboid fusion was present or not. Some parent-child pairs had similar radiological traits but discordance between parent and child was equally common. The clinical and radiological abnormalities of IV-19 are presented in Figure 3 to demonstrate that minimal clinical changes could still be associated with multiple radiological abnormalities. Figure 4 shows the radiographic appearance of calcaneocuboid fusion.

Diagnosis

On the basis of previously published reports, the clinical and radiological manifestations in this family are consistent with a diagnosis of Jackson-Weiss syndrome (see Discussion).

Linkage Results

Pairwise sex-averaged lod scores between JWS, eight markers on the short arm of chromosome 7 and one marker on the long arm of chromosome 5, are shown in Table III. JWS was clearly not linked to the markers examined on 7p and 5q. JWS was excluded from approximately 20cM either side of *D5S211*. The genetic background map for chromosome 7p (Fig. 5) excludes linkage of JWS to the region near *D7S10*. There was a suggestion of linkage to *D7S529;* however, the closely linked flanking markers *D7S493* and *D7S516* exclude linkage to the region between them using the lod –2 criterion.

TABLE I.

Clinical Manifestations

	II-1	III-1	III-3	III-6	III-10	III-12	III-13	III-14	IV-2	IV-4	IV-5	IV-11	IV-15	IV-16	IV-19	IV-20
Craniosynostosis[a]	+	+	+ C	+ C	-	+ C	-	-	-	-	+ C	+ C	+	-	-	+
Surgery	-	-	-	-	-	-	-	-	-	-	+	+	-	-	-	-
Orbitostenosis	-	+	+	-	-	+	+	+	-	-	-	-	+	-	-	+
Proptosis	-	-	+	-	-	+	-	-	-	-	-	-	+	-	-	+
Faciostenosis	-	-	+	+	+	+	+	-	-	-	+	-	+	-	-	+
Facial asymmetry	+	+	+	-	+	+	+	+	+	+	+	+	+	-	-	+
Orbital dystopia	+	-	-	-	-	+	+	-	-	-	+	+	-	-	-	+
Low anterior hairline	+	-	+	+	-	+	-	-	-	-	-	+	+	-	-	-
Hypertelorism	+	+	+	+	-	-	+	+	-	-	-	+	-	-	+	+
Ptosis	-	-	-	-	+	+	-	-	-	+	+	-	+	-	-	-
Strabismus	-	-	-	-	-	-	-	-	-	+	-	+	+	-	-	+
Nasal beaking	-	-	+	+	+	+	-	-	-	-	-	-	-	-	-	-
Micrognathia	-	-	-	-	-	-	+	-	-	-	-	-	-	-	-	-
Mandibular prognathism	+	-	+	+	+	+	-	-	-	-	-	+	+	-	-	-
Brachydactyly (fingers)	+	-	+	+	-	+	-	-	-	-	-	-	-	-	-	-
Brachydactyly (toes)	+	-	+	-	+	-	-	-	-	+	-	-	-	-	-	-
Hearing loss																
Conductive	-	-	+	+	+	-	-	+	+	-	+	-	-	-	-	+
Sensorineural	-	-	-	-	-	+	-	-	+	+	+	+	-	-	+	+
Intellect[b]	B	N	N	N	B	B	M	B	N	N	B	B	N	N	B	M
Height (centiles)	<3	10	3-10	<3	50	3-10	3	10-25	25-50	10-25	10-25	<3	<3	50-75	3-10	10
OFC (centiles)	<2	2	2-50	<2	50-98	50	>98	50-98	2-50	50-98	2-50	2-50	50	50	50	98

[a]C = coronal.
[b]N = normal, B = borderline, M = moderate retardation.

American Journal of Medical Genetics 51:121–130 (1994).

FIG. 2. *Photographs of affected family members II-2, III-3, III-6, III-10, III-12, III-13, IV-2 and IV-15.*

TABLE II.

Radiological Changes

	II-1	III-1	III-3	III-6	III-10	III-12	III-13	III-14	IV-2	IV-4	IV-5	IV-11	IV-15	IV-16	IV-19	IV-20
Hands																
Coned epiphyses	-	-	-	+	-	-	-	-	-	-	-	+	-	-	+	+
Distal phalangeal hypoplasia of 5th finger	-	-	-	-	-	-	-	-	-	-	-	-	+	+	+	+
Middle phalangeal hypoplasia of index /ring/little finer	-	-	-	+	-	+	-	+	-	-	-	+	+	-	+	+
Fusion of capitate and hamate	-	-	+	-	-	-	-	-	-	-	-	+	-	-	+	+
Bipartite lunate	-	-	-	-	-	-	-	-	-	-	-	+	-	-	-	-
Separate ossific centre of ulnar styloid	-	-	-	-	-	-	-	-	-	-	-	+	-	-	-	-
Feet																
Coned epiphyses	-	-	-	-	-	-	-	-	-	+	+	+	-	-	+	+
Calcaneo-cuboid fusion	+	+	+	-	+	+	+	+	+	+	-	-	-	+	+	+
Calcaneo-navicular fusion	-	-	-	-	+	-	-	+	-	-	+	-	-	-	-	+
medial cuneiform-navicular fusion	+	-	-	-	-	-	-	-	-	-	-	-	-	-	-	-
Fusion of phalanges of toes	+	-	+	+	-	-	+	+	-	-	-	-	-	+	-	+
Fusion between base of 1st metatarsals and medial cuneiform	+	-	-	-	-	-	-	-	-	-	-	-	-	-	-	-
Hallux valgus	+	+	+	-	+	-	+	-	+	+	+	-	-	-	-	-
Distal phalangeal hypoplasia of great/ 2nd/3rd/4th/5th toes	-	-	-	+	-	-	-	-	-	+	-	-	+	+	+	-

American Journal of Medical Genetics 51:121–130 (1994).

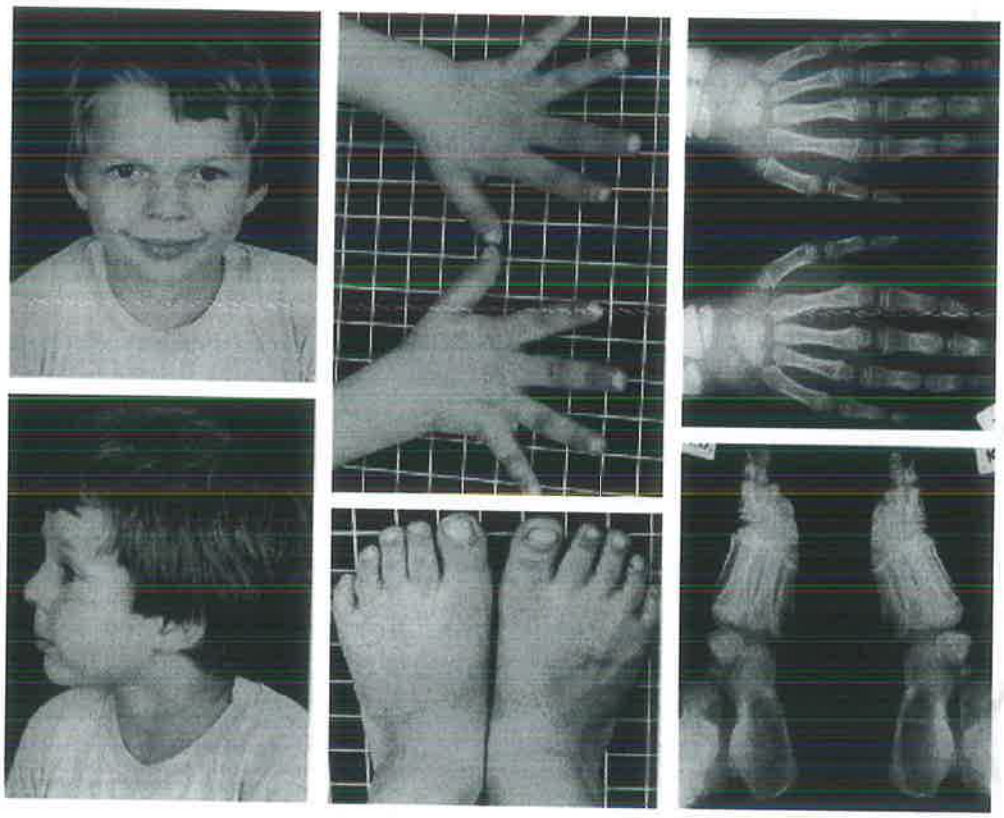

FIG. 3. *Clinical photographs and radiographs of IV-19. There are minimal craniofacial features but multiple radiologic abnormalities. In the hands these include coned epiphyses involving the middle phalanges of the index and fifth fingers bilaterally, associated shortness of the adjacent phalanges with premature fusion at the site of the coned epiphyses, and congenital fusion of the capitate and hamate. In the feet, abnormalities include coned epiphyses involving the proximal phalanges of the 2nd, 3rd, 4th, and 5th toes bilaterally, distal phalangeal hypoplasia of the 2nd toes, enlarged epiphyses at the base of the distal phalanx of the 3rd and 4th toes, and calcaneocuboid fusion.*

The highly polymorphic markers used were ideal not only for linkage analysis, but also paternity testing in the absence of a paternal DNA sample. Multiple non-paternity was detected as evidenced by the consistent presence of more than four alleles among the sibs in generation III. Analysis of duplicate samples excluded the possibility of sample confusion as an alternative explanation for this observation. On this basis, a highly conservative approach to linkage analysis was undertaken whereby none of the sibs in generation III were assumed to have the same father. The same approach was necessary for IV-1, IV-2, IV-3, IV-4, and IV-5. These modifications reduced the power of the analysis to detect linkage but eliminated the danger of generating false exclusions which might arise from undetected non-paternity.

Discussion

Jackson et al. [1976] reported an autosomal dominant syndrome consisting of craniosynostosis, midfacial hypoplasia, and abnormalities of the feet. Eighty-eight affected individuals were examined, and another 50 individuals were reliably report to be affected, making a total of 138. Penetrance was extremely high, and great variability in expression was observed. The variability of craniofacial abnormalities in this kindred was so marked that Jackson and Weiss considered there to be some individuals in the family who, seen in isolation, could be diagnosed to have ACS III, others with findings consistent with ACS V, and others again with anomalies consistent with Crouzon syndrome; not one individual resembled ACS I.

The only consistent extracranial manifestation was some abnormality in the clinical or radiological appearance of the feet. even in craniofacially normal affected individuals within the kindred. Minimal manifestation included short, broad first metatarsal, abnormally shaped tarsal bone, and calcaneocuboid fusion. In some instances, the first and second metatarsal) were fused, the second and third metatarsals were partially fused, the tarsal bones were abnormally shaped, and fusion of the navicular and first cuneiform bone occurred. Some affected individuals had mild cutaneous syndactyly of the second and third toes and broad great toes that deviated medially. No affected individual had broad thumbs.

Only one instance each of syndactyly between the third and fourth fingers, preaxial polydactyly of the feet, and fusion of the phalanges in the thumb was observed. Although the literature suggests that no thumb anomalies occur in JWS [Robinow and Sorauf, 1975; Jackson et al., 1976; Cross and Opitz, 1969], big thumbs with varus deformities were observed in the family reported by Escobar and Bixler [1977a, b].

Table III.

Pairwise Lod Scores Between JWS and Microsatellite Markers on Chromosomes 5 and 7

	Recombination fraction (θ)					
	0.01	**0.05**	**0.1**	**0.2**	**0.3**	**0.4**
Chromosome 7						
D7S472	-9.50	-5.40	-3.48	-1.64	-0.70	-0.20
D7S513	-9.08	-5.12	-3.07	-1.24	-0.44	-0.10
D7S507	-11.22	-6.14	-3.93	-1.85	-0.85	-0.36
D 7S493	-9.81	-4.45	-3.54	-1.74	-0.85	-0.34
D7S529	-1.13	0.66	1.17	1.23	0.86	0.34
D7S516	-9.22	-4.87	-2.99	-1.28	-0.52	-0.21
D7S526	-13.16	-7.23	-4.66	-2.26	-1.04	-0.35
D7S528	-6.39	-3.35	-1.66	-0.13	0.40	0.40
Chromosome 5						
D5S211	-13.54	-6.99	-4.30	-1.95	-0.85	-0.26

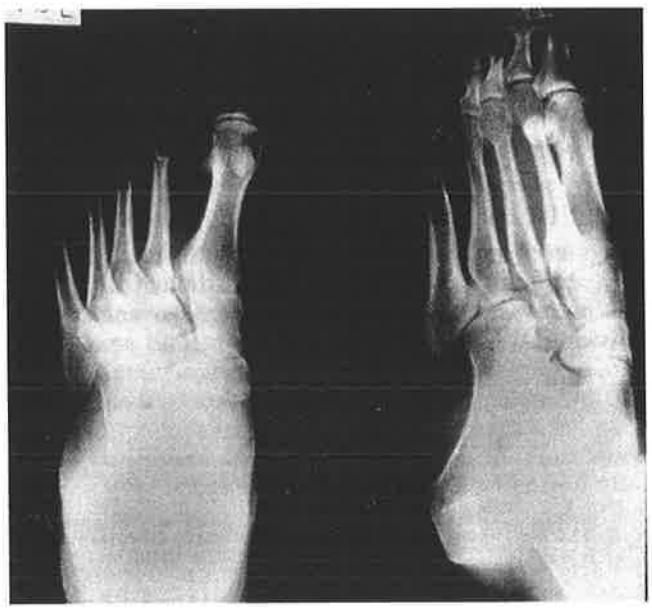

FIG. 4. *Foot radiographs of III-1, showing a composite bone involving cuboid and calcaneal bones articulating distally with the bases of the fourth and fifth metatarsals and minor hallux valgus.*

Some affected individuals showed no clinical or radiological abnormalities of the face or skull. No mentally retarded individuals were detected in this family.

Many of the manifestations in our kindred were the same as those seen in JWS (Table V). However, low frontal hairline, dental malocclusion, impaired hearing, and short stature were observed in our family but were infrequent in previously described families. Other traits sometimes seen in JWS include flat nasal bridge, cleft palate, cutaneous syndactyly, broad great toes, varus deformities of the great toes, and occasionally, large thumbs with varus deformities; none of these features was observed in our kindred.

Mental retardation of variable degree, present in 8 of 16 individuals within our kindred, has been reported in JWS [Cross and Opitz, 1969]. However, in our family, factors such as severe hearing loss in some individuals, marriages between individuals with intellectual disability, and poor socioeconomic circumstances in many made it difficult to determine whether or not mental retardation is part of the syndrome.

The diagnosis of JWS in our kindred was based on the radiological changes of the feet. The single most common finding was calcaneocuboid fusion, which is well recognised in JWS and to our knowledge, is not present in other dominant ACS. Yet there were differences between the feet of our patients and those of other reported individuals. First, short broad first metatarsals and abnormal tarsal bones occurred only once, each in a different individual and we did not find fusion between first and second, or second and third metatarsals. Second, we documented foot abnormalities not previously described in the JWS; these include coned epiphyses; hallux valgus; congenital fusion of the middle and distal phalanges of the third, fourth, and fifth toes and between tarsal and navicular bones; and calcaneo-navicular fusion.

Abnormalities noted in the hand radiographs of our family and not previously documented in JWS included coned epiphyses; middle phalangeal hypoplasia of the index, ring, and little fingers; congenital fusion of the capitate and hamate; bipartite lunate; and a separate ossific centre of the ulnar styloid. These abnormalities occurred infrequently.

This family clearly underscores the importance of performing radiographic studies of the hands and feet of individuals within ACS kindreds, even when cranio-facial, hand, and foot abnormalities are absent on clinical examination.

In Brueton's report [Brueton et al., 1992] demonstrating linkage of ACS III to distal chromosome 7p, 10 of the 16 families examined were thought to have findings of classic ACS III, 4 an ACS III-like syndrome, 1 JWS-type ACS, and 1 family had an ACS V-like syndrome. The failure to demonstrate linkage to distal chromosome 7p in our kindred using the 8 highly polymorphic markers *D7S472, D7S513, D7S507, D7S493, D7S529, D7S516, D7S526,* and *D7S528* in the region 7pter to 7pl5, suggests that ACS III and JWS are not allelic. Absence of linkage to *D5S211* also excludes allelism to the new cephalosyndactyly syndrome reported by Warman et al. [1993] and subsequently mapped to 5q34-qter by Muller et al. [1993]. Studies are continuing to assign the chromosomal location of the gene responsible for JWS as the first step toward discovery of a gene whose function is essential for normal development of the human skull, face, hands, and feet.

Acknowledgments

We wish to thank J. Spence for performing the DNA extractions, H. Phillips and A. Gedeon for laboratory assistance, H. Kozman for assistance with linkage analysis, C. Helps for secretarial assistance, E. Burton for arranging blood collections and radiological investigations, Professor D. Simpson for original referral of the family, and the families for their cooperation. This work was supported by the ACH Research Trust.

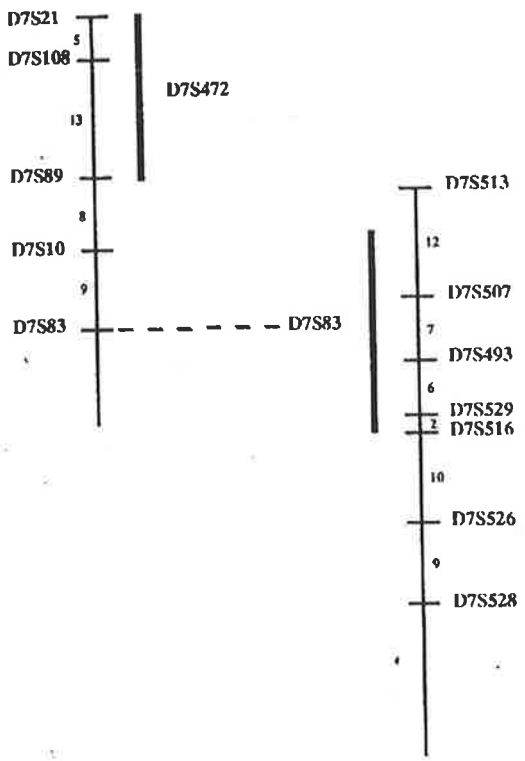

FIG. 5. *The background genetic map for chromosome 7p. Distances shown between markers are in centimorgans (cM). The relevant section of the NIH/CEPH Collaborative Linkage Map [1992] is shown on the left and the relevant section of the Weissenbach et al. [1992] maps shown on the right. These maps are tied together by* D7S83, *common to both maps. ACS III is closely linked to* D7S10 *[Brueton et al., 1992].*

TABLE IV.

Comparison of Clinical and Radiological Findings of Present Family and Jackson-Weiss Syndrome

	Present Family	Jackson-Weiss Syndrome
Clinical changes		
Craniosynostosis	+	+
Facial asymmetry	+	+
Low frontal hairline	+	-
Ptosis	+	+
Hypertelorism	+	+
Flat nasal bridge	-	+
Beaked nose	+	+
Maxillary hypoplasia	+	+
Dental malocclusion	+	-
Cutaneous syndactyly	-	+
Brachydactyly	+	+
Broad great toes	-	+
Impaired hearing	+	-
Short stature	+	-
Mental retardation	+	+
Radiological changes		
Hands		
Distal phalangeal hypoplasia	+	-
Middle phalangeal hypoplasia	+	-
Carpal bone malsegmentation	+	-
Coned epiphyses	+	-
Feet		
Hallux valgus	+	-
Short broad first metatarsal	+	+
Metatarsal fusion	-	+
Navicular-cuneiform fusion	+	+
Calcaneo-navicular fusion	+	-
Calcaneo-cuboid fusion	+	+
Coned epiphyses	+	-

References

1 Bianchi E, Arico M, Podesta AF, Grana M, Fiori P, Beluffi G (1985): A family with the Saethre-Chotzen syndrome. Am J Med Genet 22:649–658.

2 Blank CE (1960): Apert's syndrome (a type of acrocephalosyndactyly); observations on a British series of thirty nine cases. Ann Hum Genet 24:151–164.

3 Brueton LA, Huson SM, Winter RM, Williamson R (1988): Chromosome localllzation of a developmental gene in man: Direct DNA analysis demonstrates that Greig cephalopolysyndactyly maps to 7p13. Am J Med Genet 31:799–804.

4 Brueton LA, van Herwerden L, Chotai KA, Winter RM (1992): The mapping of a gene for craniosynostosis: evidence for linkage of the Saethre-Chotzen syndrome to distal chromosome 7p. J Med Genet 29:681–685.

5 Chotzen F (1932): Eine eigenartige familiäre Entwicklungsstörung. (Akrocephalosyndaktylie, Dysostosis craniofacialis und Hypertelorismus). Monatschr Kinderheilkd 55:97–122.

6 Cross HE, Opitz JM (1969): Craniosynostosis in the Amish. J Pediatr 75: 1037–1044.

7 Escobar V, Bixler D (1977a): Are the acrocephalosyndactyly syndromes variable expressions of a single gene defect? New York: Alan R. Liss Inc., for the National Foundation—March of Dimes BD:OAS X111(3C):139–154.

8 Escobar V, Bixler D (1977b): On the classification of the acrocephalosyndactyly syndromes. Clin Genet 12:169–178.

9 Gorlin RJ, Cohen MM, Levin LS (1990). "Syndromes of the Head and Neck", third ed. Oxford: Oxford University Press. Oxford monographs on medical genetics No. 19:529–531.

10 Jackson CE, Weiss L, Reynolds WA, Forman TF, Peterson JA (1976): Craniosynostosis, midfacial hypoplasia, and foot abnormalities in a large Amish kindred. J Pediatr 88:963–968.

11 Kogan SC, Doherty BS, Gitschier J (1987): An improved method for prenatal diagnosis of genetic diseases by analysis of amplified DNA sequences. N Engl J Med 317:985–990.

12 Kreiborg S, Pruzansky S, Pashayan H (1972): The Saethre Chotzen syndrome. Teratology 6:287–294.

13 Lathrop GM, Lalouel JM (1984): Easy calculations of lod scores and genetic risks on small computers. Am J Hum Genet 36:460–465.

14 Lathrop M (1992): A second-generation linkage map of the human genome. Nature 359:794–801.

15 McKusick VA (1992): "Mendelian Inheritance in Man," 10th ed. Baltimore: Johns Hopkins University Press.

16 Morton NE (1955): Sequential tests for the detection of linkage. Am J Hum Genet 7:277–318.

17 Müller U, Warman ML, Mulliken JB, Weber J (1993): Assignment of a gene locus involved in craniosynostosis to chromosome 5qter. Hum Mol Genet 2:119–122.

18 NIH/CEPH collaborative mapping group (1992): A comprehensive genetic linkage map of the human genome. Science 258:67–86.

19 Noack M (1959): Ein Beitrag zum Krankheitsbild der Akrocephalosyndaktylie (Apert). Arch Kinderheilkd 160:168–181.

20 Pantke OA, Cohen MM, Witkop CJ, Feingold M, Schaumann B, Pantke HC, Gorlin RJ (1975): The Saethre-Chotzen syndrome. New York: Alan R. Liss, Inc., for the National Foundation–March of Dimes. BD:OAS 11(2):191–225.

21 Pelz L, Kruger G. Gotz J (1986): The Greig cephalopolysyndactyly syndrome [lettter]. Helv Paediatr Acta 41:381–382.

22 Pfeiffer RA (1969): Associated deformities of the head and hands. New York: Alan R. Liss, Inc., for the National Foundation–March of Dimes. BD:OAS 5(3):18–34.

23 Pfeiffer RA (1964): Dominant erbliche Akrocephalosyndaktylie. Z Kinderheilkd 90:301–320.

24 Robinow M, Sorauf TJ (1975): Acrocephalopolysyndactyly, Type Noack, in a large kindred. New York: Alan R. Liss, Inc., for the National Foundation–March of Dimes. BD:OAS 11(5):99–106.

25 Ruppert JM, Vogelstein B, Arheden K, Kinzler KW. (1990). GL13 encodes a 190-kilodalton protein with multiple regions of GLI similarity. Mol Cell Biol 10:5408–5415.

26 Saethre H (1931): Ein Beitrag zum Turmschädelproblem. (Pathogenese, Erblichkeit und Symptomologie). Dtsch Z Nervenheilkd 117:533-555.

27 Sawadogo M, Van Dyke MW (1991): A rapid method for the purification of deprotected oligonucleotides. Nucleic Acids Res 19(3):674.

28 Tommerup N, Nielsen F (1983): A familial reciprocal translocation t(3;7)(p21.1;p13) associated with the Greig polysyndactyly-craniofacial anomalies syndrome. Am J Med Genet 16:313–321.

29 Vogt A (1933): Dyskephalie (dysostosis craniofacialis, maladie de Cronzon 1912) und eine neuartige Kombination dieser Krankheit mit Syndactylie der 4 Extremitäten (Dyskephalodaktylie). Klin Monatsbl Augenheilkd 90:441–460.

30 Vortkamp A, Gessler M, Grzeschik KH (1991): GL13 zinc finger gene interrupted by translocations in Greig syndrome families. Nature 352:539–540.

31 Waardenburg PJ (1934): Eine merkwürdige Kombination von angeborenen Missbildungen, doppelseitiger Hydrophthalmus verbunden mit Akrocephalosyndaktylie, Herzfehler, Pseudohermaphroditismus und anderen Abweichungen. Klin Monatsbl Augenheilkd 92:29–38

32 Wagner K, Kroisel PM, Rosenkranz W (1990): Molecular and cytogenetic analysis in two patients with microdeletion of 7p and Greig syndromes: hemizygosity for PGAM2 and TCRG genes. Genomics 8:487–491.

33 Warman ML, Mulliken JB, Hayward PG, Müller U (1993): Newly recognized autosomal dominant disorder with craniosynostosis. Am J Med Genet 46:444–449.

34 Weber JL, May PE (1989): Abundant class of human DNA polymorphisms which can be typed by the polymerase chain reaction. Am J Hum Genet 44:388–396.

35 Weissenbach J, Gyapay G, Dib C, Vignal A, Morissette J, Millasseau P, Vaysseix G, Lathrop M (1992): A second-generation linkage map of the human genome. Nature 359:794–801.

Apert syndrome results from localized mutations of *FGFR2* and is allelic with Crouzon syndrome

Andrew O.M. Wilkie[1, 2, 3], Sarah F. Slaney[1, 2, 3], Michael Oldridge[1], Michael D. Poole[3], Geraldine J. Ashworth[3], Anthony D. Hockley[4], Richard D. Hayward[5], David J. David[6], Louise J. Pulleyn[7], Paul Rutland[7], Susan Malcolm[7], Robin M. Winter[7] & William Reardon[7]

Apert syndrome is a distinctive human malformation comprising craniosynostosis and severe syndactyly of the hands and feet. We have identified specific missense substitutions involving adjacent amino acids (Ser252Trp and Pro253Arg) in the linker between the second and third extracellular immunoglobulin (Ig) domains of fibroblast growth factor receptor 2 (FGFR2) in all 40 unrelated cases of Apert syndrome studied. Crouzon syndrome, characterised by craniosynostosis but normal limbs, was previously shown to result from allelic mutations of the third Ig domain of FGFR2. The contrasting effects of these mutations provide a genetic resource for dissecting the complex effects of signal transduction through FGFRs in cranial and limb morphogenesis.

Apert syndrome[1] is a severe autosomal dominant malformation syndrome with a birth prevalence of 1 in 65,000 (ref. 2), that usually arises by new mutation. It is characterised by craniosynostosis (abnormal development and premature fusion of the cranial sutures, Fig. 1 a) and severe syndactyly (cutaneous and bony fusion of the digits, Fig. 1 b–d); a variety of abnormalities of the skin, skeleton, brain, and other internal organs occur at lower frequency[3–7]. Most patients have normal intelligence, often with specific learning difficulties, but a minority are mentally retarded[4, 8, 9]. Relatively few adults with Apert syndrome are known to have had children: 11 instances have been recorded[10]. The paucity of pedigrees has precluded a classical genetic linkage approach to the identification of the Apert gene. However, consideration of the two cardinal clinical features—craniosynostosis and syndactyly—suggests several potential candidate genes.

The molecular basis for four other craniosynostosis syndromes has been elucidated. A mutation of the homeobox-containing gene *MSX2* was identified in a single large family with variable, atypical ('Boston type') craniosynostosis[11]. However, mutations of *MSX2* were not found in Apert or other syndromes, so this may be a rare cause of craniosynostosis. Recently, mutations in two of the four fibroblast growth factor receptors (FGFRs), members of the receptor tyrosine kinase family, have been reported in three craniosynostosis syndromes. In Crouzon syndrome, characterised by normal hands and feet, eight different mutations of the alternatively spliced 'B' exon (exon 9) ofthe third immunoglobulin (Ig)-like domain in the extracellular portion of *FGFR2* were identified[12,13]. A different mutation of the same exon is present in a large kindred with Jackson-Weiss syndrome, in which broad big toes with tarsal-metatarsal fusions and occasional

[1]Institute of Molecular Medicine, John Radcliffe Hospital,Headington, Oxford OX3 9DU, UK
[2]Department of Clinical Genetics, Churchill Hospital, Oxford OX3 7LJ, UK
[3]Oxford Craniofacial Unit, The Radcliffe Infirmary NHS Trust, Oxford OX2 6HE, UK
[4]West Midlands Craniofacial Unit, Queen Elizabeth and Children's Hospitals, Birmingham B16 BET, UK
[5]Craniofacial Unit, Great Ormond Street Hospital for Children NHS Trust, London WC1N 3JH, UK
[6]Australian Craniofacial Unit, Women's and Children's Hospital, North Adelaide 5006, South Australia
[7]Mothercare Unit of Clinical Genetics and Fetal Medicine and Molecular Genetics Unit Institute of Child Health, London WC1N IEH, UK
Correspondence should be addressed to A.O.M.W.

syndactyly occur[13]. In Pfeiffer syndrome, characterised by broad thumbs and big toes and mild cutaneous syndactyly, a single missense mutation of exon 7 of *FGFR1* was identified in 5 unrelated families[14].

The identification of *MSX2, FGFR1* and *FGFR2* mutations in these craniosynostosis syndromes is intriguing in view of the severe bony syndactyly that distinguishes Apert syndrome. Recent studies of the vertebrate limb bud suggest that the interaction of molecules expressed in the apical ectodermal ridge (AER) with those in the underlying mesenchyme (progress zone) is essential for limb bud outgrowth (reviewed in ref. 15). Members of the MSX and FGF families appear to be critical players in this process. In the mouse and chick, *msx2* is expressed in the AER and both *msx1* and *msx2* are expressed in the immediately adjacent mesenchyme: transplantation experiments and studies of the chick *limbless* mutant indicate that continuing expression of these genes is dependent on a signal from the AER[16,17]. Candidate signalling molecules are fibroblast growth factors 2 and 4 (FGF2 and FGF4), which are both expressed in the AER and have been implicated in limb bud outgrowth[18–21]. Signal transduction of these FGFs is mediated by FGFRs and correspondingly, FGFR1 is expressed diffusely in the limb bud mesenchyme, while FGFR2 is predominantly expressed in the ectoderm including the AER[22,23]. The finding that the MSX and FGFR families of genes were implicated both in craniosynostosis and in the normal pattern formation and outgrowth of the developing limb, made them strong candidate genes for Apert syndrome. We included *FGFR3* in our study because although absent from the early limb bud, expression occurs in the skull and long bones[24] and mutations of *FGFR3* have recently been reported in achondroplasia[25,26]. We analysed the segregation of highly polymorphic genetic markers in four informative meioses and eliminated all but *FGFR2* from our initial list of candidates. We then identified mutations of the *FGFR2* gene by single strand conformation polymorphism (SSCP) analysis and DNA sequencing. Specific missense substitutions involving two adjacent amino acids in the linker between the second and third Ig domains account for all 40 patients examined. Our results provide genetic evidence for a role of FGFR2 in normal and abnormal limb patterning.

Exclusion of all candidate genes except FGFR2

We ascertained four new families in which an adult with Apert syndrome had children: in three there were at least two offspring, which contributed four informative meioses (Fig. 2). We analysed the segregation of microsatellite and minisatellite repeat markers closely linked to the MSX and FGFR genes. Two recombinants were identified at each of the gene-specific microsatellites for *MSX1, MSX2*, and *FGFR1*,excluding these loci (Fig.2). Similarly,*D4S115* and *D4S127,* which are separated by a 3 centiMorgan (cM) interval and flank the *FGFR3* gene[27,28] both showed recombinants in at least one individual in families A and C, excluding this locus with high probability. *FGFR2* has been mapped physically to chromosome 10q25.3-q26 (refs 29,30) and although it has not been mapped genetically, its position on the linkage map can be deduced from linkage studies in Crouzon and Jackson-Weiss syndromes[31,32]. The loci *D1OS190* and *D1OS217,* which encompass the genetic interval for these disorders, were non-recombinant in all four meioses. Thus *FGFR2* remained a candidate for the Apert mutation.

SSCP analysis of FGFR2

The main structural features of *FGFR2* are summarized in Fig. 3a. As the intron-exon structure and genomic sequence of human *FGFR2* are not fully documented, cDNA fragments were synthesised by the reverse transcription-polymerase chain reaction (RTPCR). We anticipated the likely position of introns in *FGFR2* from their corresponding positions in human *FGFR1* and murine *Fgfr2:* previous work suggested they would be conserved[33,34].

First strand cDNA or genomic DNA from individuals with Apert syndrome was amplified in 13 overlapping fragments extending between nucleotides 186 and 2376 (according to the numbering of ref. 35: see Box for explanation of

variations in terminology for denoting exons and cDNA sequence of *FGFR2),* and subjected to SSCP analysis. No consistently altered patterns of migration were observed for any fragments except for the 262 base pair (bp) 4F–7R primer combination (Fig.3*b*). With the 4F-7R fragment, all 35 unrelated patients screened showed additional bands not present in four controls, and these could be classified into two patterns. In type 1, comprising 21 patients, there were two faster migrating bands; in type 2, comprising 14 patients, there was a single slower migrating band (Fig. 4). These results suggested that the SSCP changes reflected mutation of this portion of *FGFR2* in all patients with Apert syndrome tested, and qualitatively that they comprised a limited mutational spectrum. As exons 8 and 9 are subject to alternative splicings[33,37], exon 8 would not be included in the 4F-7R product (see Fig. *3b).* Hence the mutations were likely to lie within exon 7.

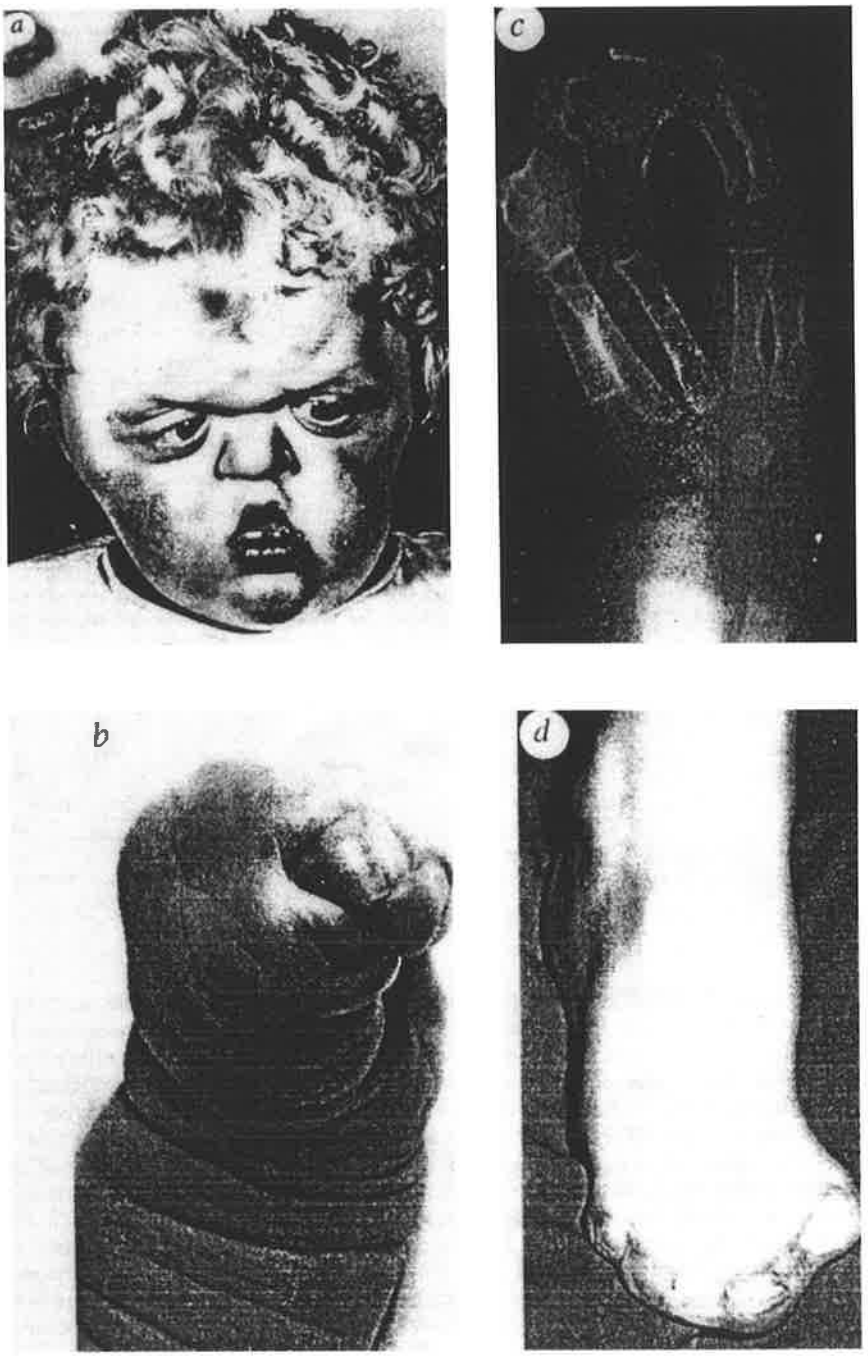

FIG. 1. *Clinical features of Apert syndrome.* **a.** *facial appearance;* **b.** *hand: severe syndactyly (type 3);* **c.** *radiograph of hand showing transverse phalangeal fusion;* **d.** *foot: severe syndactyly (type 3).*

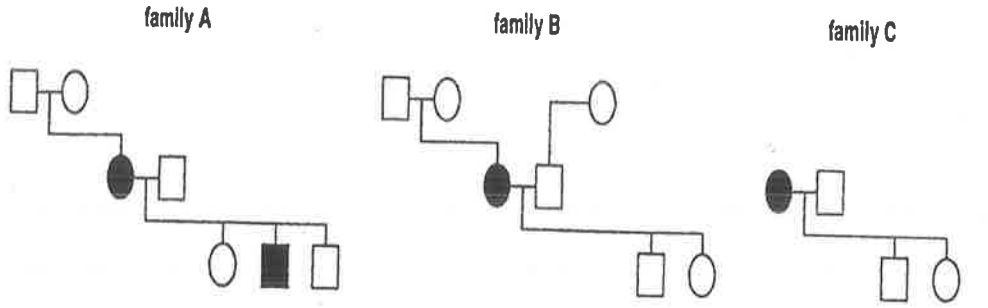

FIG. 2. *Analysis of MSX and FGFR genes as candidates for the Apert mutation. Genotypes (with arbitrary numbering of alleles) at seven loci are shown. The minimal number of recombinants (R), and the number of apparent non-recombinants (NR), are indicated on the right.*

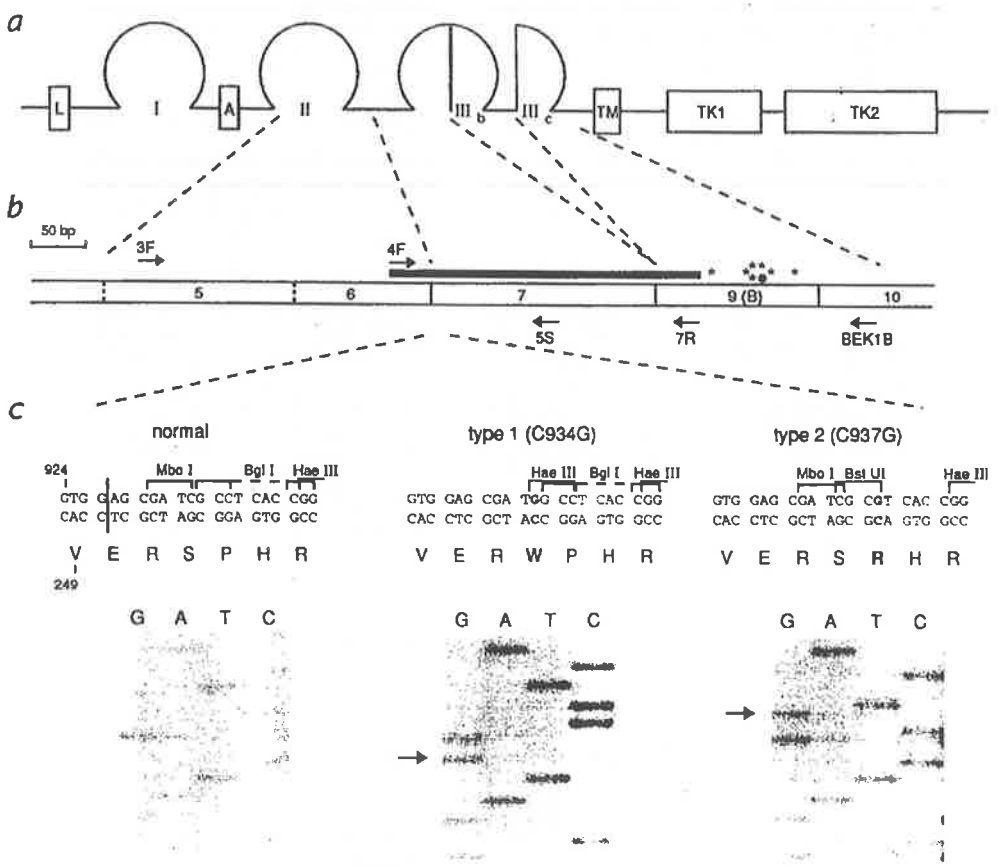

FIG. 3. *Structure of FGFR2 and analysis of mutations in Apert syndrome.* **a.** *Schematic diagram of FGFR2: note the hydrophobic leader sequence (L), three extracellular Ig-like domains (I-III), acidic domain (A), transmembrane region (TM), and intracellular tyrosine kinase domains (TK). The presence of domains III_b and III_c (KGFR and BEK forms, respectively) is mutually exclusive because of alternative splicing (adapted from ref.33)* **b.** *cDNA structure of the BEK form of FGFR2 encompassing the second and third Ig-like domains. The alternatively spliced exon 8 is absent in this form. Positions of introns confirmed by direct analysis of FGFR2 (refs 33,34,37) are shown as solid vertical lines; other intron positions and exon assignments are based on homology with FGFR1 structutre[33], with the exon numbering of ref.36. Additional features indicated are the positions of primers used for RT-PCR and sequencing (arrows); the 4F-7R fragment in which altered SSCP migration was observed (black bar); and the positions of mutations of exon 9 indentified in Crouzon syndrome (asterisks) and Jackson-Weiss syndrome (black dot)[12,13],* **c.** *comparison of DNA and protein sequence in the normal FGFR2 gene (left) and in the C934G and C937G mutations. Mutated nucleotides and amino acids (single letter code) are shown in bold. The position of the boundary between exons 6 and 7 is indicated by the vertical line through the normal sequence and is based on the murine fgfr2 sequence[34]. Diagnostic restriction enzyme sites for MboI, BglI, BstUI and HaeIII are shown. Below, sequence of cloned DNA demonstrating the mutations (arrows).*

Analysis of the 4F-7R fragment of FGFR2

To characterise the mutations at the DNA sequence level we chose initially to study two patients with the type 1 SSCP pattern, on whom fibroblast cell lines were available, and three patients with the type 2 pattern, on whom Epstein-Barr virus transformed (EBV) lines only were available. Whereas *FGFR2* was expressed at sufficient levels in fibroblasts to prepare pure 4F-7R fragment from a single round of PCR, two rounds were necessary for the EBV lines (see Methodology). The purified fragments were then DNA sequenced, either directly or after cloning into a plasmid vector.

Both type 1 patients showed the same C→G transversion at position 934 of the cDNA, corresponding to a serine→tryptophan substitution at amino acid 252. A different mutation ofthe adjacent 3' codon was present in the three type 2 patients. All showed a C→G transversion at position 937, resulting in an proline→arginine substitution at amino acid 253 (Fig. 3c). It is likely that these mutations, which are located in the linker region between Ig domains II and III (see Discussion), lie very close to the 5' end of exon 7; by analogy with the structure of murine Fgfr2, the first nucleotide in exon 7 is just 6 bp upstream of the C934G mutation (Fig. 3c). Attempts to obtain specific amplification between primer 4F and a primer in exon 7 were unsuccessful, suggesting that a sizeable intron lies between them. As the DNA sequence of the intron abutting the start of exon 7 has not been reported in the human, further characterisation of the mutation was performed on cDNA samples generated by RT–PCR.

Box Exon and cDNA nomenclature for *FGFR2*

A number of different numbering/lettering terminologies have been used both to identify individual exons and for the cDNA sequence of *FGFR2*. These are summarised here to facilitate comparison with other articles. Exon numbering. The complete genomic structure of *FGFR2* is not known; exon numbering systems are based on comparison with the structure of human *FGFR1* (ref. 33) and murine Fgfr2 (ref. 36). This approach is validatedby the high conservation of sequence/structure of those regions investigated in detail; until the full genomic structure of *FGFR2* is described, exon assignments must be regarded as provisional.

After the exon numbering of *FGFR1* was initially proposed[33], two additional exons were identified at the 5' end of murine *FGFR1* and *FGFR2* and a new numbering system was suggested[36]. In addition, lettering systems have been used to refer to exons in the alternatively spliced region of the gene[33,37]. Usage of the various notations may be compared as follows:

	Exon assignment			
	7	5	U	III_a
	8	6	K	III_b
	9	7	B	III_c
	10	8	D	
Original ref.	36	33	37	33
Also used in refs.	This paper	14, 72	12	13

cDNA sequence. Human cDNA sequences for the *BEK* form of *FGFR2* have been reported by Dionne *et al*[35] and Houssaint *et al*[38]. They differ in that the sequence in ref. 35 includes much longer 5' and 3' untranslated regions, and the sequence in ref 38 contains a 9 nucleotide duplication (residues 952-960), not confirmed by further studies. The present paper adopts the nucleotide numbering in ref 35 (accession number x52832). The numbering in ref 12 is based on red 38, with 9 subtracted from the number beyond residue 961. For exons 7-10, the nucleotide numbering in ref. 12 can be converted to the numbering in this paperbyadding 167. The amino acid numbering is the same.

Restriction enzyme analysis

To determine whether other patients having the same SSCP pattern also had identical mutations, we exploited the diagnostic pattern of altered restriction enzyme sites created by the two mutations characterised. The C934G mutation destroys an *Mbo*I site and creates a *Hae*III site; the C937G mutation destroys a *Bgl*I site and creates a *Bst*UI site (Fig. 3*c*). The three patterns observed when the 145 bp 4F-5S cDNA fragment (see Fig. 3*b*) was digested with these four enzymes are shown in Fig. 5*a*. All 21 patients having the type I SSCP change, and an additional 4 patients examined subsequently (62.5% of 40 patients), showed loss of the *Mbo*I site, the appearance of a second *Hae*III site, and no *Bst*UI site, diagnostic of the C934G mutation. The 14 patients having the type 2 SSCP change and one additional patient (37.5% of 40 patients) showed loss of the *Bgl*I site, the appearance of a *Bst*UI site, and a single *Hae*III site, diagnostic of the C937G mutation. Twenty-three unrelated normal or Crouzon syndrome individuals had a normal pattern of digestion for all four enzymes.

In three cases cDNA was available from both normal parents of patients with Apert syndrome. All six parents showed the normal pattern of digestion with *Mbo*I, *Bgl*I, *Hae*III and *Bst*UI, demonstrating that the mutations had occurred *de novo* in the offspring (Fig. 5*b*). cDNA was available from 6 children of affected parents (all the offspring in families A and B (Fig. 2), and the only (affected) offspring in a fourth family): only the two affected offspring had inherited the abnormal restriction pattern present in their affected parent. It was possible to trace the parental origin of the mutation in these latter families using linked chromosome 10 markers. In all three cases the mutations had arisen in the father of the affected parent, consistent with a paternal age effect for new mutations in Apert syndromes[3, 39].

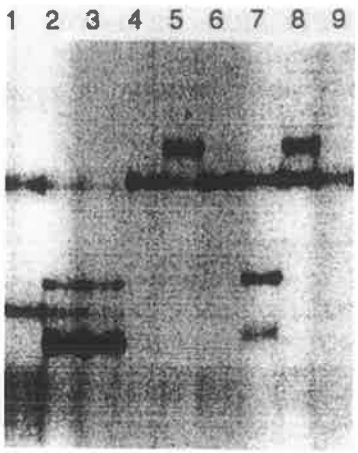

FIG. 4 *SSCP variation in the 4F-7R cDNA fragment observed in patients with Apert syndrome. Samples from lanes 1-3 are from fibroblast RNA; the remainder are from EBV cell lines. Lanes 1, 4, 6, 9, unrelated normal controls; lanes 2, 3, 5, 7, 8, patients with Apert syndrome. The type 1 variant SSCP pattern is present in lanes 2, 3 and 7; the type 2 variant in lanes 5 and 8.*

Correlation of syndactyly with genotype

A striking feature of Apert syndrome is that although the precise pattern of syndactyly varies between patients, in a single individual there is virtually always bilateral symmetry[3,40] (S.F.S., unpublished data). To determine whether the differences in the syndactylous pattern between individuals were related to the type of mutation in *FGFR2,* we classified the syndactyly using a modification of ref. 40, assigning the hands and feet (separately) three point scores from (1) mildest to (3) most severe involvement (see Methodology). The mean syndactyly severity score was greater for the C937G than the C934G mutation for both the hands and the feet. The difference in scores was not statistically significant for the hands alone, but was significant for the feet alone (G test of independence: G = 10.2, $P<0.005$) and for the hands and feet combined ($G_2=8.8$, $P<0.025$) (Fig. 6). Preoperative hand radiographs were available in 18 patients, and transverse fusions bridging between the middle/distal phalanges of the three central digits (Fig. 1*c*) were present in 3/11 and 6/7 patients with the C934G and C937G

mutations respectively, independently confirming a greater severity of syndactyly in the C937G mutation (G_1=5.8, P<0.025). Further analysis of the Apert phenotype will be required to determine whether there are other consistent differences attributable to the two mutations.

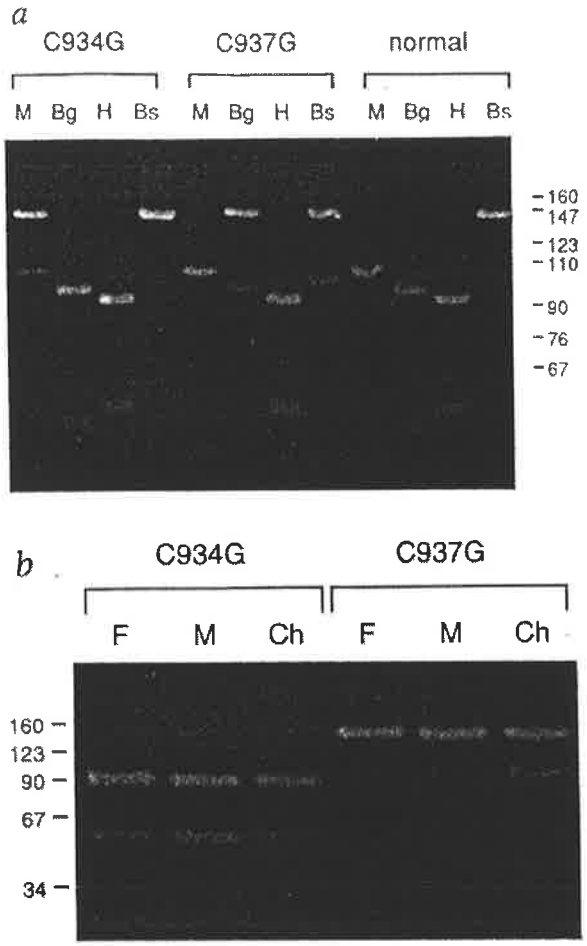

FIG. 5. *Detection of the C934G and C937G mutations in the 145 bp 4F-5S cDNA fragment by restriction enzyme analysis. a, Pattern of fragments observed on digestion with* MboI *(M), BBhlI (Bg), HaeIII (H) and BstUI (Bs). All restriction sites for these enzymes in the 4F-5S fragment are shown in Fig. 3c. In the normal individual (right), the predicted fragment sizes in bp are: M, 103 + 42; Bg, 95 + 50; H. 91 + 54; Bs, 145. In the patient with the C934G mutation (left), additional fragments are M, 145 and H, 45 + 9; with the C937G mutation (centre), additional fragments are Bg,145 and Bs, 100 + 45. Size markers (bp) are* MspI *cut pBR322 DNA;* b, *de novo occurrence of mutations in Apert patients born to normal parents. Digests of 4F-5S with (left) HaeIII, demonstrating Cg34G mutation; (right) BstUI, demonstrating C934G mutation. F. father; M, mother; Ch, affected child.*

Discussion

We have studied 40 unrelated patients with Apert Syndrome and identified missense mutations in *FGFR2* in all 40 patients, but in none of 23 normal controls or patients with Crouzon syndrome. In three families from which mRNA was available from both unaffected parents, we demonstrated that the mutation (C934G in one case, C937G in two) had arisen *de novo*. These observations indicate that specific non-conservative substitutions (Ser252Trp or Pro253Arg) of adjacent amino acids of FGFR2 cause the great majority of cases of Apert syndrome: different mutations may occur in occasional patients. This limited mutational spectrum could result from constraints at the nucleic acid or protein sequence level. At the nucleic acid level, both mutations are C→ G transversions, but the type 1 mutation (C934G) arises in a CpG dinucleotide, whereas the type 2 mutation (C937G)does not. CpG dinucleotides are hypermutable when the cytosine is methylated, but the usual mutation is a C→ T transition due to deamination[41]. Our failure to observe any C934T mutations (Ser252Leu) suggests that this would give a different phenotype. Analysis of the spectrum of mutations in the factor IX gene indicates that the rate of C→ G transversions may be enhanced at CpGs relative to other positions, although the mechanism of this is unknown[42]. This would be consistent with the ~1.7-fold higher frequency of the C934G mutation relative to C937G.

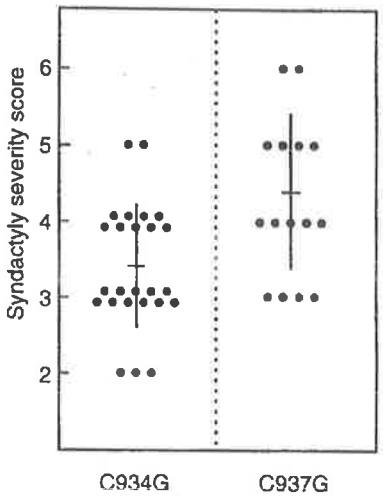

FIG. 6. *Correlation between syndactyly (hand and foot severity scores combined) and mutation. Individual data, the mean and standard deviation for each mutation are shown.*

Thus, although nucleic acid constraints may account for the greater frequency of the Scr252Trp substitution relative to Pro253Arg, the limited mutational spectrum probably arises from protein sequence constraints.

FGFR2 belongs to a complex intercellular signalling network that comprises at least nine FGFs and four FGFRs and whose binding is modulated by heparan sulphate proteoglycans[43]. The pleiotropic effects of this signalling pathway include the control of cell proliferation, differentiation, migration and survival in many different contexts, including embryonic development, angiogenesis, and malignancy. The biology of FGFR2 is itself very complex: alternative splicing involving the extracellular, transmembrane or intracellular regions creates many different isoforms of the protein[44]. In the extracellular region, the principal forms of alternative splicing are the inclusion or omission of the first Ig-like domain I, and the obligatory alternative use of either exon 8 or 9 to generate the IIIb and IIIc isoforms of the third Ig domain, respectively (Fig. 3a). The latter splice selection creates proteins (IIIb/KGFRand IIIc/BEK) with different binding affinities for FGF2 and FGF7 and the two forms are differentially expressed through development in different tissues[34,37,45,46]. Construction of chimaeric FGFRs by swapping domains shows that binding of FGFs to FGFRs requires both domains II and III, but that domain I is not essential[47, 48].

The Apert mutations occur in a region that is highly conserved amongst the different FGFRs. The target SerPro dipeptide is conserved in all vertebrate FGFRs examined so far, except for a Ser → Thr substitution in FGFR3 of the Iberian newt and a Pro → Ser substitution in FGFR2 of *Xenopus*(J.K. Heath, personal communication); in the human, the sequence identity of all four FGFRs extends over 16 amino acids in this region[44]. This suggests an essential function, but one that is common to all FGFRs rather than imparting them with individual biological properties. Although this local sequence conservation is not shared with other Ig superfamily members, alignment with more highly conserved features of the Ig domain (such as the paired cysteines) shows that the Ser-Pro dipeptide lies in the region linking Ig domains II and III together[49, 51]. The likely importance of this linker region in determining the relative orientation of these domains is highlighted by analysis of the crystal structure of a related Ig superfamily member, the soluble form of the adhesion molecule CD2 (ref. 52). Based on this and models of FGFR1/ligand interactions[50,51], we propose that the bulky Ser252Trp and Pro253Arg substitutions alter the relative orientation of domains II and III, and hence affect their binding to FGFs or dimerization with other FGFRs. The Pro252Arg mutation of FGFR1 identified in some cases of Pfeiffer syndrome[14] corresponds precisely to the Pro253Arg mutation of FGFR2 in Apert syndrome and further attests to the very specific nature of these amino acid substitutions. Studies of the effects of different substitutions of the Ser-Pro dipeptide on FGF binding and signal transduction in vitro, and construction of mouse models, will be required to delineate exactly how these mutations act.

The Fgfr2 gene was recently mapped to mouse chromosome 7 (ref. 53), but there is no obvious natural murine homologue of Apert syndrome.

Although there has been much recent interest in the role that FGF2 and/or FGF4 may play in limb bud outgrowth and maintenance of the zone of polarizing activity (ZPA)[18–21], less attention has been focused on the function of the various FGFRs in patterning. The mutations of FGFR2 in Apert syndrome described here, together with those recently identified in the Pfeiffer and JacksonWeiss syndromes (which have less dramatic limb phenotypes)[13,14], provide the first evidence from natural mutants for the involvement of the FGF/FGFR pathway in limb morphogenesis. Although initially it might appear that syndactyly is too subtle an abnormality to reflect a generalised disturbance of limb patterning, the classic studies by Gruneberg[54–57] of three syndactylous mouse mutants *(syndactylism / sm, Oligosyndactylism / Os,* and *shaker with syndactylism / sy),* argue otherwise. In all three, morphological abnormalities of the limb bud (thickening of the AER or narrowing of the antero-posterior width of the foot plate) were detectable between 10.5 and 12.5 days gestation, at or before the time of blastema formation of the skeletal elements. Thus syndactyly may reflect the end result of a relatively early disturbance of limb patterning. The high expressivity and striking symmetry of the syndactyly in Apert syndrome contrasts with the more variable, asymmetrical involvement of the limbs in some other genetically determined limb defects, for example ectrodactyly[58]. This implies that the mutant FGFR2 specifies an abnormal pattern that may be defined as precisely as is the normal pattern in the context of wild type FGFR2. Further evidence for a very specific role for FGFR2 in patterning is provided by our data indicating that the Ser252Trp and Pro253Arg mutations are associated with different severities of syndactyly (Fig. 6). We speculate, based on Gruneberg' s work, that the syndactyly of Apert syndrome is caused by a reduced antero-posterior length or thickening of the AER. As there is no evidence for a disturbance in antero-posterior identity of the digits, ZPA function[15] appears to be largely intact.

An intriguing question is why allelic mutations of *FGFR2,* which occur in Crouzon syndrome, are associated with entirely normal limb development. Although the Crouzon mutations initially reported were localized to the alternatively spliced exon 9 (111_c /BEK isoform)[12,13], we have recently identified mutations of exon 7 in several patients with Crouzon syndrome (A.O.M.W., S.M., unpublished data). These latter mutations are predicted to disrupt the third Ig domain in both the IIIb/KGFR and BEK isoforms, but there are no obvious phenotypic differences between Crouzon patients with exon 7 and exon 9 mutations. This suggests that abnormality of the BEK isoform is the main contributor to the Crouzon phenotype, and that this does not include a major effect on limb development. In Apert patients the mutant forms of both KGFR and BEK will be present, but whereas KGFR is abundantly expressed in the surface ectoderm during embryogenesis, BEK is only present more diffusely in the limb bud mesenchyme[45]. This suggests that the severe syndactyly of Apert syndrome may be caused by expression of mutant KGFR in the AER. As KGFR binds FGF4 with high affinity, but shows very poor FGF2 binding, any effect would probably have to be mediated through FGF4 (refs 34,37,45). Conversely, BEK expression exceeds KGFR in the skull and long bones[45], which could explain why craniosynostosis is present in both syndromes. Testing this hypothesis will require definition of the complete spectrum of mutations accounting for Crouzon syndrome and examination of the expression of the KGFR and BEK isoforms in the AER and cranial sutures. Additional questions are why Crouzon patients with exon 7 mutations have normal limbs, and why the exon 9 mutation in Jackson-Weiss syndrome is associated with mild limb abnormalities.

It is relatively unusual in human genetics to encounter unique phenotypes associated with specific mutations, sickle cell anaemia being the paradigm. Receptor tyrosine kinases are proving to be a rich source of dominantly inherited malformations associated with specific point mutations, examples including Pfeiffer syndrome (FGFR1)[14], achondroplasia (FGFR3)[25,26], and multiple endocrine

neoplasia type IIB (RET)[59,60]. Apert syndrome appears to represent the even more unusual situation of a disorder largely caused by two alternative mutations. It will be of great interest to determine the molecular basis of this, and whether further distinctive phenotypes associated with FGR2 mutation await discovery.

Methodology

Patients. Patients were ascertained through three UK craniofacial units (Oxford, London, Birmingham) and by enquiries through surgical and genetic colleagues. Appropriate ethics committee approval and informed consent was obtained. Each patient was interviewed and the clinical phenotype assessed: the severity of sydactyly was scored according to a modified version of a previous classification[40]. In the Apert hand, the central 3 digits are always sydactylous: in the least severe instance (type 1), the thumb and part of the little finger are separate from the syndactylous mass. In type 2, the little finger is not separate and in type 3 (Fig. 1b), the thumb and all the fingers are included. Similarly, syndactyly in the foot may involve mainly the 3 lateral digits (type 1), digits 2–5 with a separate big toe (type 2) or be continuous (type 3, Fig. 1d). Venous blood was taken from the patient for chromosome analysis (all G-banded karyotypes were normal), extraction of genomic DNA, and EBV transformation. In addition, fibroblast cultures were established from skin biopsies taken from two patients. Wherever possible, blood was also taken from the parents for genomic DNA extraction and in a few cases, EBV transformation and extraction of mRNA.

Canditate gene exlusion using genomic DNA. DNA extraction and Southern blotting and hybridization were perfomed by standard procedures[61]. Primers for analysis of polymorphic $(CA)_n$ microsatellites were purchased from Research Genetics. PCR reactions were perfomed in a volume of 15µl with 50 ng genomic DNA, 6 pmoles of each primer, and 0.4 U Thermostable DNA Polymerase(Advanced Biotechnologies) in a buffer containing 10 mM Tris HCl pH 8.3, 50 mM KCl, 1.5 mM $MgCl_2$ and 100 µM of each dNTP. All PCR was →performed in a Hybaid OmniGene Temperature Cycler on 96 well plates, using a 55°C annealing temperature. Products were separated on 6% polyacrylamide/ urea gels, blotted on to Hybond–N+ (Amersham), and hybridized to $(AC)_{10}$ end-labelled with α^{32}P dCTP using terminal transferase (Boehringer Mannheim), essentially as described in ref. 62. $(CA)_n$ microsatellite loci examined were MSX1 (ref. 63), MSX2 (ref. 11), FGFRI (ref. 64), D4S127 (ref. 65), D10S190 and D10S217 (ref. 66). The minisatellite locus detected by Southern blot analysis was D4S115 (ref. 67).

PCR and sequencing primers. Primers used for RT–PCR analysis of the Apert mutations (see Fig. 3b) were 3F (5'–AAAAGCGGCTCCATGCTG–3'), 4F(5"–GGGTCCATCAATCACTAC–3'), 5S (5'–GCTGGGCATCACTGTAAAC–3'), 7R (5'–CAATCTCTTTGTCCGTGGTG–3'), and Bek 1B (ref. 35). Primers 4F, 5S and 7R were also used as sequencing primers. A complete list of primer pairs and conditions used for the SSCP analysis of FGFR2 is available from A.O.M.W. on request.

RT–PCR analysis. RNA was extracted from EBV transformed cell lines, fibroblast cultures and venous blood[68]. 10 µg of total mRNA was employed in first strand cDNA synthesis in a total volume of 40 µl using 340 pmoles of random hexamer primers, 320 U RNase-Inhibitor (boehringer Mannheim) and 400 U MMLV reverse transciptase (Gibco BRL), as described in ref. 25. 4 µl of the first strand product (1µl if synthesized from fibroblast RNA) was used for PCR in a total of 25 µl, using the buffer in ref. 63, 40 mM each dNTP, 10 pmoles of each primer, 0.4 U AmpliTaq (perkin Elmer), and a hot start. 35 cycles consisting of 1 min denaturation (94°C), 1 min annealing (60°C for 4F–Bek1B and 64°C for 3F–7R and 4F–7R) and 30 s extension (72°C) were used for SSCP analysis and to obtain pure cDNA fragments from fibroblast RNA. The 4F–7R fragment was

made from EBV RNA by diluting the product from the 4F–Bek1B reaction by 1 in 400 and using 4 µl of this for a further round of PCR 920 cycles) with 120 mM each dNTP and the 4F–7R primers. As it provided difficult to obtain pure product in all cases, in later experiments the 4F–5S fragment was made using 1 µl of a 1 in 500 dilution of the first round 3F–7R product in a 25µl reaction including the 4F–5S primers and 120 mM each dNTP. Cycle conditions comprised 1 min denaturation (94°C) and 30s annealing (60°C), with the temperature shift up to the subsequent denaturation ramped at $1°Cs^{-1}$, for 20–24 cycles. PCR Products were digested with restriction enzymes according to the manufacturer's recommendations and analysed on 4.5% MetaPhor agarose gels (Flowgen).

SSCP analysis. Appropriate RT–PCR products were radiolabelled by including 0.1µlα^{32}P–dCTP per 25 µl reaction. 5 µl of product was detatured by addition of 10 µl 95% formamide, 20 mM NaOH, heated to 96°C for 3 min, and loaded onto a 7% polyacrylamide/0.5 x Tris borate EDTA gel with 2.6% cross-linking [69, 70]. Electrophoresis was performed in a cold room using a Strat Therm Cold Termperature Controller (Stratagene) to maintain a gel temperature of 10°C and maximum power output of 45 W. gels were dried down and autoradiographed.

DNA sequencing. PCR products were sequenced directly by including a single 5'–biotinylated primer, and immobilising the biotinylated PCR product to Dynabeads M–280 Streptavidin (Dynal), folowed by strand separation using fresh 0.15 M NaOhH[71]. Alternatively, PCR products were cloned into pCR-Script (Stratagene), and the plasmid sequenced using α^{35}S–dATP and the Sequenase kit (USB).

Acknowledgements

We thank B. Jones, D. Thompson, J. Budd, R. Hall, S. Lodge, T. Aziz, M. Briggs, M. Goldin, M. Wake, B. Vivian, J. Patterson, G. Suthers, R. Rossell (European Human Cell Bank, Porton Down), J. Sloane-Stanley, M. Fitchett, C.E. Blank, M. Carlton, J. Craig, R. Gibbons, P. Harris, S. Huson, B. Peral, S.L. Thein, C. Ward, J. Flint, J. Heath, D. Higgs, J. Hurst, E.Y. Jones, G. Morriss-Kay and D. Weatherall for their help and contribution to this work. We particularly thank all the patients and families, including the Apert Syndrome Support Group and the Craniofacial Support Group. This work was supported by Wellcome Trust awards to A.M.O.W. and S.F.S., and by the UK Medical Research Caouncil. The first two authors contributed equally to this work.

Central Nervous System Imaging in Crouzon Syndrome

Timothy W. Proudman, MB BS, Bruce E. Clark, FRACR, Mark H. Moore, FRACS, Amanda H. Abbott, DDS, PhD, David J. David, AC, FRACS
North Adelaide, South Australia, Australia

Although the need to prevent the secondary effects of craniosynostosis on the central nervous system is fundamental to the practice of craniofacial surgery, the detailed structural anatomy of the central nervous system in the syndromal craniosynostoses has become the subject of recent interest. A clinical and radiographic review of a population of 59 patients with Crouzon's syndrome determined the frequency of central nervous system deformities. Twelve percent of patients had evidence of decreased mental function. Ventriculomegaly on computed tomographic scan was present in 51% and found to be of three grades: mild, moderate, and severe (hydrocephalus). This was nonprogressive in 7 of the 11 patients with follow-up computed tomographic scans. Ten patients underwent surgical release to increase intracranial space; however, 6 of these patients showed no progression in ventricular size. Nonventricular anomalies were found less frequently (14%). Central nervous system findings show fewer nonventricular anomalies than in Apert's syndrome patients, with a corresponding higher mental function. The principal anomaly of ventriculomegaly is not directly related to suture defect and may represent a primary brain abnormality. Recommendations are made for the assessment and management of patients with Crouzon's syndrome with reference to these areas.

Key Words: Central nervous system, computed tomographic scan, ventriculomegaly, hydrocephalus

For centuries, as a result of both folklore and ignorance, an abnormal appearance has been assumed to imply reduced intelligence. Despite the potential for bony distortion interfering with neurological function, the majority of individuals with Crouzon's syndrome have normal intelligence. The most common intracranial problem is raised intracranial pressure (ICP) causing headaches and papilledema. This may lead to loss of eyesight and decreased intellectual performance in some, but not all, untreated patients.

In the past, autopsy examination, air ventriculography, and angiography provided the best information on the morphology of the central nervous system (CNS). Improvements in noninvasive imaging (computed tomography (CT) and magnetic resonance imaging (MRI) have allowed the structure and form of the CNS to be examined in greater detail.

Material and Methods

The clinical and radiographic CNS findings in a population of 59 patients with Crouzon's syndrome seen at the Australian Cranio-Facial Unit (ACFU) were examined. This population was composed of 36 females and 23 males ranging in age from 1 month to 38 years (median, 9 years). Clinical records were reviewed

From the Australian Cranio-Facial Unit, Women's and Children's Hospital, North Adelaide, South Australia,Australia.
Address correspondence to Dr Proudman, Australian Cranio-Facial Unit, Women's and Children's Hospital, 72 King William Rd, North Adelaide, South Australia 5006, Australia.

for neurological symptoms and signs. Specific features noted included intelligence, epilepsy, and evidence of raised ICP such as headaches. Many had undergone cranial vault or ventricular decompressive surgery as infants.

Thirty-eight CT scans of the brain are available for review. Some had been performed during CT examination of the craniofacial skeleton and the CT slices were taken parallel to the Frankfurt horizontal plane. One CT scan did not extend to the cranial vertex, giving an incomplete view of the ventricles. Brian scans were performed using 1-cm thick slices at 1-cm intervals, and the films were reviewed with an experienced neuroradiologist. The radiographs were examined for ventricular size. An increase in ventricular size was graded subjectively into three groups; mild ventriculomegaly, moderate ventriculomegaly, and severe ventriculomegaly. Asymmetry of the ventricles, change in ventricular size after surgery, and any other white and gray matter (nonventricular) findings were also reported. One patient had an MRI scan performed.

TABLE 1

Ventricular Abnormalities Found on Computed Tomographic Scan in 35 Patients with Crouzon's Syndrome

Abnormality	*No. Patients*
Lateral ventricular abnormality	
Ventriculomegaly	
Mild	18
Moderate	4
Severe/hydrocephalus	3
Lateral ventricle asymmetry	
Left	6
Right	1
Prominent ventricular horns	
Anterior	1
Posterior	1
Temporal	7
Enlarged third ventricle	16
Enlarged fourth ventricle	1

Results

Clinical

Neurological problems included epilepsy in three patients. Headaches were reported in eight patients, which was consistent with raised intracranial pressure in five children and related sinusitis, postoperatively, in two adults. No cause for intermittent headache was found in the last patient despite investigation, and the problem resolved spontaneously with time. Many patients (n=25) underwent neuropsychological testing and decreased intelligence (intelligence quotient less than 70) was found in only three. Many infants exhibited some degree of developmental delay related to poor feeding, obligatory mouth breathing, and recovery from surgery. Future assessment of mental function in this group will be of interest.

Computed Tomographic Scan

Ventricular Findings

Radiographic review demonstrated that six of the brain scans were within normal limits. Four other patients had been shunted before their initial examination at the ACFU and also had ventricular size within the normal limits. The lateral ventricular pattern was the most striking finding seen on the remaining CT scans (Table 1, Fig 1). Twenty five patients had some degree of ventricular enlargement.

This ranged in severity from mild nonprogressive ventriculomegaly in 18 patients to ventriculomegaly of a moderate degree in 4 and severe (hydrocephalus) in 3 (see Fig 1). Asymmetry of lateral ventrical dilatation was evident in 7 patients and in 9 patients, prominence was seen of the anterior (1), posterior (1), or temporal (7) horns. The third ventricle was enlarged in 16 patients whereas the fourth ventricle was abnormal in only one instance. Thirteen patients had both enlarged third ventricles and ventriculomegaly. A degree of cerebral aqueduct stenosis or a structural brain abnormality may be responsible for this. The extracerebral fluid space was prominent on 7 of the CT scans. Although it was uniformly enlarged in five patients, it was restricted to the cisterna magna in 1 and in the anterior temporal region in another.

Nonventricular Findings

Nonventricular deformities were not seen as frequently as ventricular abnormalities (Table 2). Schizencephaly in the left temporal region was seen in one patient (Fig 2). A wide arachnoid space adjacent to the pineal gland in another patient suggested the appearance of a possible arachnoid cyst or a dermoid. The septum pellucidum was not visualised in some slices of the scans of two patients (although the scans were of good quality), suggesting absence of this structure. Decreased cerebral mass was found in one patient.

TABLE 2

Nonventricular Abnormalities Found on Computed Tomographic Scan in 35 Patients with Crouzon's Syndrome

Abnormality	No. Patients
Schizencephaly	1
Wide arachnoid space adjacent to pineal	1
Partial absence septum pellucidum	2
Decreased cerebral mass	1

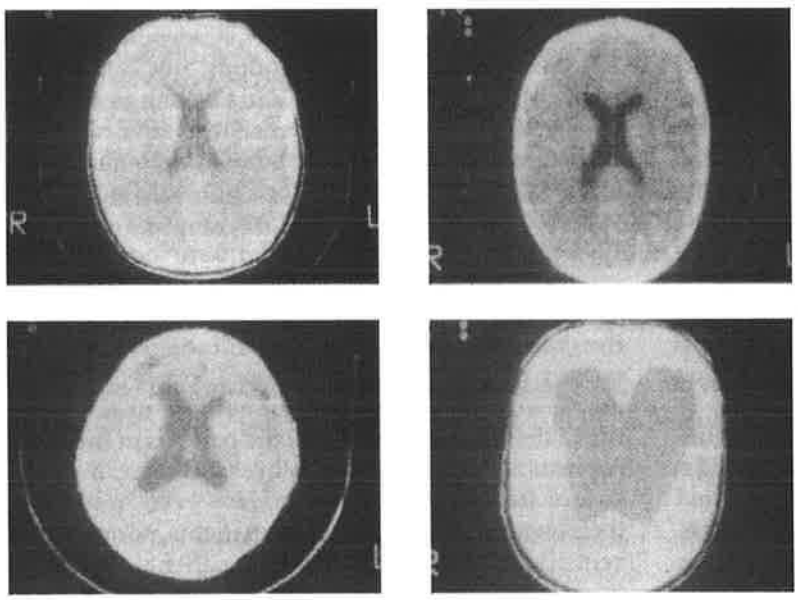

FIG. 1. *Ventricular patterns found on computed tomographic scan in Crouzon's syndrome: (top left) normal, (top right) mild ventriculomegaly, (bottom left) moderate ventriculomegaly, (bottom right) severe ventriculomegaly.*

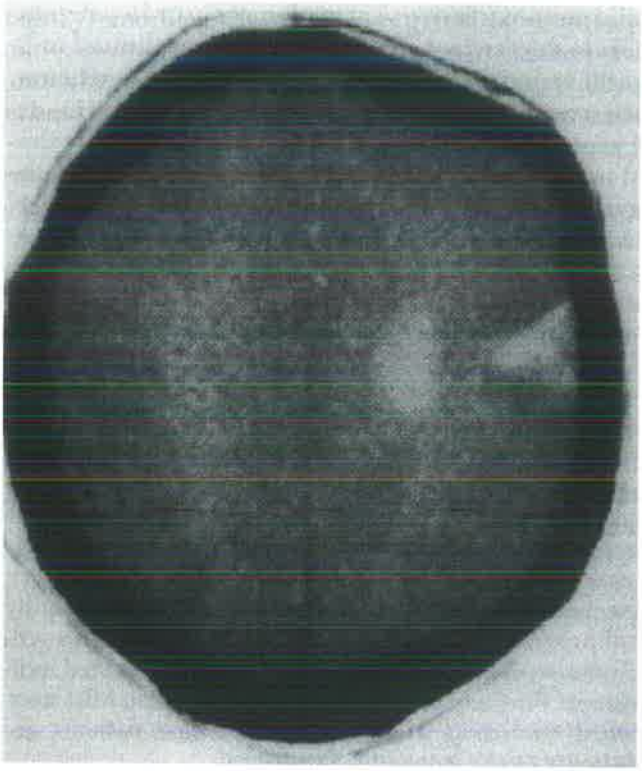

FIG. 2. *Computed tomographic scan showing schizencephaly in a patient with Crouzon's syndrome.*

Repeat Computed Tomographic Scans and Surgery

Follow-up CT scans were available in 11 patients. In 1 patient, gross hydrocephalus with raised ICP was evident at the time of presentation; the initial procedure was shunt decompression. On other occasions, hydrocephalus without raised ICP had been managed expectantly. Fronto-orbital advance and posterior craniectomy had been performed, allowing the dilated ventricles to assist the brain drive promoting calvarial growth [1]. After surgery, the patients were monitored by repeated clinical examination, cranial ultrasonography or CT scan. Three other infants required shunt insertion after surgery following progressive hydrocephalus.

On the other hand, seven patients (aged 2-28 years) had no change in their ventricular pattern on repeat CT scan (3 months to 4 years later). Six of these had decompressive surgery, such as fronto-orbital or frontofacial advancement, and one had no surgery at all. This finding suggests that the calvarial craniostenosis does not necessarily play a role in the development of the ventricular pattern. Ventricular shape is, therefore, most likely related to a primary brain deformity. The cranial base, which is not operated on , may locally influence the CNS development.

Clearly, some patients will experience progressive hydrocephalus and some will not; there do not appear to be any predictive factors seen on CT scan.

Magnetic Resonance Imaging

MRI was performed in one patient, aged 11 years, with failing eyesight as a result of raised ICP. MRI demonstrated optic nerve sheaths distended by subarachnoid fluid, consistent with the clinical picture. The ventricles were not grossly enlarged but showed mild ventriculomegaly with asymmetry. The corpus callosum and gyri appeared normal. The sella turcica appeared to be slightly larger than normal, and there was a suggestion that the pituitary was compressed by either the third ventricle or the suprasellar cistern extending into the fossa.

After bilateral decompressive craniotomies, repeat MRI showed improvement in the optic nerve distension; however, the pituitary fossa findings persisted. This method of investigation provides additional valuable information on CNS structure.

Discussion

The CNS is intimately related to the development of the cranial bones. Indeed, it was the disturbance in intellectual and visual function by the craniostenosis that prompted the development of surgical intervention described earlier. Headaches, deterioration in mental and visual function, along with radiographic evidence of craniostenosis are regarded as primary indications for surgery.

Early reports of brain disease in Crouzon's syndrome are autopsy case reports or larger studies that examine all the craniosynostoses together [2,3]. Findings include hypoplasia of the corpus callosum, microgyri, and features suggesting a change in proportion of the brain (i.e., decreased volume in the middle and anterior cranial fossae, stretch of the diencephalon, and firm, flattened gyri) [2,3]. They supported a concept that distortion of the cranial bones by the synostosis was responsible for the distortion of the brain.

Since these reports, patient management has improved, particularly in the areas of radiological investigation and surgical techniques. Attention has been directed to the relationship among mental retardation, hydrocephalus, raised intracranial pressure, and craniostenotic deformity.

Carmel and colleagues [4] reported the CT scans of 24 patients with simple craniostenosis and found distortion of the ventricular system associated with sagittal, unicoronal, and lambdoid synostosis. After surgical release, many of the distortions tended to correct themselves, and they suggested that the abnormalities indicated increased local pressure on the brain at the fusion side.

Renier and associates [5] measured the ICP in 92 patients with craniosynostosis (including 4 with Crouzon's syndrome) and found it to be elevated in one third, normal in one third, and borderline increased in one third. After surgery the ICP measurements reverted to normal. A statistically significant relationship between raised ICP and decreased mental level was identified, and they suggested that ICP measurement may be of help in determining optimal timing of surgical intervention.

Many studies have reported hydrocephalus in association with Crouzon's syndrome [1,6–10]. Noetzel and colleagues [9] prospectively performed CT scans on 50 patients with craniosynostosis, including 12 with Crouzon's syndrome. Of the 12 CT scans of Crouzon's syndrome patients, 6 were normal, 2 showed hydrocephalus, and the remaining 4 demonstrated nonprogressive ventriculomegaly, a moderate ventricular dilatation that did not progress over time and was not associated with raised ICP. Little if any change was seen after craniofacial surgery. In Crouzon's syndrome and other craniosynostosis conditions, they found that the dilatation was almost always asymmetric, with usually a normal appearance of the temporarl horns. They postulated that the ventriculomegaly was a distinct entity from hydrocephalus and that it resulted from abnormal development of the CNS and not from the local effects of the fused sutures.

Golabi and associates [10] reported three cases of Crouzon's syndrome with hydrocephalus in a series of 250 patients with craniosynostosis. This series reviews the features of the CNS in Crouzon's syndrome as well as in other related synostosis conditions, not differentiating between them.

A comprehensive review of the CNS findings in Apert's syndrome was reported by Cohen and Kreiborg [11]. Although the abnormalities in Apert's syndrome involve an apparently similar craniostenotic process, the CNS abnormalities reported differ from those seen in our series of Crouzon's syndrome patients. Cohen and Kreiborg combined their findings with all those described in the literature and did not give an indication of the frequency of each abnormality. It is also not clear in their article whether radiographic or autopsy examination of the CNS was carried out on all the patients in their group. A presumed lack of data in all patients accounts for the lack of frequency information. However, in examining their own 114 Apert's syndrome patients, nonprogressive ventriculomegaly was found in 2 patients and progressive hydrocephalus in none, although others have reported this finding. Agenesis of the corpus callosum was identified in 5 patients, but this has been reported infrequently in the literature in Crouzon's syndrome [12] and was not seen in our patients. Absent or defective septum pellucidum (which may be a marker for congenital anomalies) was seen in 3 of the Apert's syndrome group and in 2 of our Crouzon's syndrome group.

Many other abnormalities such as macrencephaly, gyral abnormalities, hippocampal abnormalities, encephalocele, apparent malformation of midline thalamic structures, hypoplasia of cerebral white matter, and heterotopic gray matter were reported in Cohen and Kreiborg's group. MRI provides greater detail of the cerebral matter and is, therefore, more sensitive to abnormalities in this region. Cohen and Kreiborg recommended that this investigation be performed on all patients.

The different trends in the CNS abnormalities of Crouzon's and Apert's syndromes that are emerging suggest that a primary developmental brain disorder is responsible. A more severe degree of brain matter abnormality in Apert's syndrome and greater incidence of mental retardation is contrasted with the predominantly nonprogressive ventricular deformity of Crouzon's syndrome, with a low proportion of mentally retarded individuals. Further clinical, CT, and, in particular, MRI studies of Crouzon's and Apert's syndrome patients are necessary to elucidate this further.

We are grateful for the assistance of Mrs Louise Netherway (research assistant, Australian Cranio-Facial Unit) and Dr David Netherway (principal research scientist, Australian Cranio-Facial Unit) in the preparation of this article.

References

1 Hanieh A, Sheen R, David DJ. Hydrocephalus in Crouzon's syndrome. Childs Nerv Syst 1989;5:188–189

2 Eshbaugh D. Relation of the changes in the brain to those in the skull of Crouzon's and similar diseases, with a report of a case. J Neuropathol Exp Neurol 1948;7:328–343

3 Gross H. Zur kenntnis der beqiehungen zwishchern gehirn und schadelkapsel bei den turricephalen, craniosynostischen dysostosen. Virchows Arch 1959;330:365–383

4 Carmel PW, Luken MG, Ascheri GF. Craniosynostosis:computed tomographic evaluation of skull base and calvarial deformities and associated intracranial changes. Neurosurgery 1981;9:366–372

5 Renier D, Saint-Rose C, Marchac D, Hirsch J-F. Intracranial pressure in craniosynostosis, J Neurosurg 1982;57:370–377

6 Fisherman MA, Hogan GR, Dodge PR. The concurrence of hydrocephalus and craniosynostosis J Neurosurg 1971;34:621–629

7 Hunter AGW, Rudd NL. Craniosynostosis: II. Coronal synostosis: its familial and associated clinical findings in 109 patients lacking bilateral polysyndactyly or syndactyly. Teratology 1977;15:301–310

8 Marsh JL, Vannier MW. Comprehensive care for craniofacial deformities. St Louis: CV Mosby, 1985

9 Noetzel MJ, Marsh JL, Palkes H, Gado M. Hydrocephalus and mental retardation in craniosynostosis. J Pediatr 1985;107:885–892

10 Golabi M, Edwards MSB, Ousterhout DK. Craniosynostosis and hydrocephalus. Neurosurgery 1987;21:63–67

11 Cohen MM, Jr, Kreiborg S. The central nervous system in the Apert syndrome. Am J Med Genet 1990;35:36–45

12 Kreiborg S. Crouzon syndrome: a clinical and roentgen cephalometric study. Scand J Plast Reconstr Surg (Suppl) 1981;18:11–198

Conclusion

Conclusion

This thesis has dwelt on the development of craniofacial surgery in the context of the Australian Craniofacial Unit over the last twenty years. Three interlocking circles of activity make up the overall unit function. They are delivery of health care; research and teaching.

These functions are carried out by an organisation that has been developed for the task, its essential element being that it is multidisciplinary.

The preceding chapters have described the progress that has been made in five different categories of craniofacial deformity by the ACFU and the author's contribution to that progress, together with the scientific and technical advances that have been necessary to measure outcome, understand disease, and improve treatment.

The five disease types included here are not the only ones managed by the ACFU, nor studied and written about by the author. They do however each illustrate in different ways the progress made over twenty odd years.

In all of the congenital problems and those others that may occur in childhood when growth is incomplete, the fourth dimension must be taken into account.

This realisation in itself has taken the focus away from the value of isolated surgical interventions and redirected it to understanding the disease process through growth. Only then can multidisciplinary protocol management be designed, delivered, assessed and the outcomes of the delivery of health care in this area evaluated.

The Craniosynostoses

At present the tools of investigation are being vigorously applied to

test the theories of causation, development and treatment of this type of deformity, using retrospective and prospective studies of the ACFU's large clinical data base. The future will bring more extensive and accurate gene mapping of the potentially severe deformities, and with it their earlier intrauterine diagnosis.

In the short term major problems such as craniostenosis, orbitostenosis and faciostenosis will be more easily dealt with by incorporating new techniques of bone distraction in the craniofacial region at the appropriate times during growth. The development of a suitable bone substitute to obviate extensive harvesting of the patient's own skeleton is taxing all centres seriously working on these problems.

The Rare Craniofacial Clefts

To date the ACFU has collected the largest group of patients with this deformity under study. It has been confirmed that these deformities involve the cranial base. Protocols of management based on the understanding that the cleft deformities continue to reassert themselves throughout growth have been established. Using this knowledge those protocols were designed to use all the relevant treatment methods at the most appropriate time in growth to produce a definitive result in late teenage.

An useful and predictive classification has been produced for cranio facial microsomia, and contributions made to the gene mapping of Treacher Collins Syndrome.

The future for study and management of rare craniofacial clefts lies in intense investigation of their causes; for this to occur adequate numbers of patients are needed for review and multi-centred studies are essential. The therapeutic effects of the currently available growth enhancing manoeuvres (orthodontic manipulation, bone lengthening, and tissue expansion of bone and soft tissue), need to

■

be studied over the next decade to determine their usefulness and place in treatment protocols.

Frontoethmoidal Meningoencephaloceles

Considerable progress has been made in the understanding of the pathological anatomy and hence the surgical treatment of this condition. On the other hand, apart from the early tentative postulation about its relation to advanced paternal age, no further progress has been made towards a theory of causation or about its curious geographical distribution.

Future studies should address this problem. The newly formed Asian Pacific Craniofacial Association is the best political and organisational structure through which this could possibly be achieved and it will do so by organising the necessary multicentre studies in the region.

Craniofacial Tumours

The technical advances made by the "craniofacial approach" have been passed on to neurosurgeons and head and neck surgeons, to access the depths of the craniofacial skeleton for tumour ablation.

There remain however the problems associated with the pathology and pathogenesis of two relatively common and difficult diseases, namely neurofibromatosis affecting the craniofacial skeleton and fibrous dysplasia.

Once again considerable literature exists on the operative techniques to "treat" various manifestations of these diseases, without there being sufficient knowledge of their pathology.

More knowledge is required about the variations within the disease called fibrous dysplasia. The author is currently involved in

■

examining the large database of the ACFU to clarify the different manifestations of this "disease" and the variations in the natural history.

Research And Technical Advancement

The progress from conventional radiology to the advanced three dimensional imaging of the present day has been dramatic. The further extension to produce real size nylon models of the skull has made model surgery possible and in some cases introduced new surgical possibilities. In the very near future real time surgery on the models together with accurately milled bone substitute replacements for the bone gaps will enable all cases to be "operated" in advance. Such complex "pre surgery" has already been achieved to reconstruct small pieces of jaw containing titanium implants.

The same technology is being used to produce normative data for cranial volume, orbital volume and facial bone shapes. In the foreseeable future they will be available for comparative studies, before during and after treatment.

Extension of the relationships between the ACFU and other international units will enable data to be pooled and protocols to be shared. This approach will also enable coordinated international programmes, to study and map the genes of the known genetically determined conditions, to develop further and be more productive.

Since the establishment of the then state of the art technology for the investigation of velopharyngeal incompetence in 1982, research continues to lay down normative data by relating what is being seen with the nasendoscope and via videofluoroscopy of the velopharyngeal sphincter with the nasometric pressure profile of speech. These data will enable an objective analysis to be made of changes in speech in patients with cranio facial deformity before, during and after treatment to the velopharyngeal sphincter.

■

Organisational Advancement

Two other aspects of the future development of craniofacial surgery warrant mention — formalisation of the new discipline of Craniofacial Surgery, and the development of training in the new discipline.

The new discipline has a recognisable name, an agreed area of scientific and therapeutic activity, and is being practised world wide. It is supported by an International Society founded in 1982, and has regional societies in USA, Europe, South America, and Asia-Pacific. There are national societies in some countries as well.

To date the Royal Colleges and equivalent standard setting and registering bodies have not recognised the specialty formally. This slow but inevitable process is being dogged by the tensions between, and the fluctuating fortunes of, some of the established surgical specialties.

The author has been at the forefront of the societies in which he is involved and in moves to widen membership away from purely plastic and reconstructive surgeons, to incorporate all of those specialties represented in the "team".

Training in craniofacial surgery has developed from an apprenticeship with Paul Tessier by a handful of individuals in the late 1960's and early 1970's, to a loose system of post specialist "fellowships". This system is progressing and developing rapidly towards more formal and measurable training. The implications of selecting and training the right people to work in a team without losing the flair of the individual is a challenge to the system. More important than the training of individual surgeons is the setting up of the whole unit to serve a particular community's health needs. This is a complex political, administrative, scientific and commercial task which has been successfully undertaken by the author, and

■

other members of the ACFU, in several countries.

The future holds the prospect of much demand for the transfer of this type of intellectual property. The central concept will continue to be the team approach.

Training in, understanding of, and successful involvement in team dynamics will become as essential for health units as it is in all other large modern organisations.

■